frontiers | Research Topics

Endophytic fungi: Secondary metabolites and plant biotic and abiotic stress management

Edited by
Mina Salehi, Essaid Ait Barka, Tünde Pusztahelyi and Naser Safaie

Published in
Frontiers in Microbiology

ISSN 1664-8714
ISBN 978-2-8325-4443-3
DOI 10.3389/978-2-8325-4443-3

About Frontiers

Frontiers is more than just an open access publisher of scholarly articles: it is a pioneering approach to the world of academia, radically improving the way scholarly research is managed. The grand vision of Frontiers is a world where all people have an equal opportunity to seek, share and generate knowledge. Frontiers provides immediate and permanent online open access to all its publications, but this alone is not enough to realize our grand goals.

Frontiers journal series

The Frontiers journal series is a multi-tier and interdisciplinary set of open-access, online journals, promising a paradigm shift from the current review, selection and dissemination processes in academic publishing. All Frontiers journals are driven by researchers for researchers; therefore, they constitute a service to the scholarly community. At the same time, the *Frontiers journal series* operates on a revolutionary invention, the tiered publishing system, initially addressing specific communities of scholars, and gradually climbing up to broader public understanding, thus serving the interests of the lay society, too.

Dedication to quality

Each Frontiers article is a landmark of the highest quality, thanks to genuinely collaborative interactions between authors and review editors, who include some of the world's best academicians. Research must be certified by peers before entering a stream of knowledge that may eventually reach the public - and shape society; therefore, Frontiers only applies the most rigorous and unbiased reviews. Frontiers revolutionizes research publishing by freely delivering the most outstanding research, evaluated with no bias from both the academic and social point of view. By applying the most advanced information technologies, Frontiers is catapulting scholarly publishing into a new generation.

What are Frontiers Research Topics?

Frontiers Research Topics are very popular trademarks of the *Frontiers journals series*: they are collections of at least ten articles, all centered on a particular subject. With their unique mix of varied contributions from Original Research to Review Articles, Frontiers Research Topics unify the most influential researchers, the latest key findings and historical advances in a hot research area.

Find out more on how to host your own Frontiers Research Topic or contribute to one as an author by contacting the Frontiers editorial office: frontiersin.org/about/contact

Endophytic fungi: Secondary metabolites and plant biotic and abiotic stress management

Topic editors

Mina Salehi — Tarbiat Modares University, Iran

Essaid Ait Barka — Université de Reims Champagne-Ardenne, France

Tünde Pusztahelyi — University of Debrecen, Hungary

Naser Safaie — Tarbiat Modares University, Iran

Citation

Salehi, M., Barka, E. A., Pusztahelyi, T., Safaie, N., eds. (2024). *Endophytic fungi: Secondary metabolites and plant biotic and abiotic stress management*. Lausanne: Frontiers Media SA. doi: 10.3389/978-2-8325-4443-3

Table of contents

frontiers | Frontiers in Microbiology

TYPE Editorial
PUBLISHED 29 January 2024
DOI 10.3389/fmicb.2024.1345210

OPEN ACCESS

EDITED AND REVIEWED BY
Jesús Navas-Castillo,
CSIC, Spain

*CORRESPONDENCE
Mina Salehi
✉ salehi.minasm@gmail.com
Naser Safaie
✉ nsafaie@modares.ac.ir

RECEIVED 27 November 2023
ACCEPTED 15 January 2024
PUBLISHED 29 January 2024

CITATION
Salehi M and Safaie N (2024) Editorial: Endophytic fungi: secondary metabolites and plant biotic and abiotic stress management. *Front. Microbiol.* 15:1345210. doi: 10.3389/fmicb.2024.1345210

Editorial: Endophytic fungi: secondary metabolites and plant biotic and abiotic stress management

Mina Salehi[1]* and Naser Safaie[2]*

[1]Department of Biotechnology and Plant Breeding, Faculty of Agriculture, Tarbiat Modares University, Tehran, Iran, [2]Department of Plant Pathology, Faculty of Agriculture, Tarbiat Modares University, Tehran, Iran

KEYWORDS

endophytism, mycorrhizae, bioactive compounds, biological control, sustainable agriculture

Editorial on the Research Topic
Endophytic fungi: secondary metabolites and plant biotic and abiotic stress management

Endophytes can live inside plant tissues without causing visible symptoms in their hosts (Hardoim et al., 2015). Endophytic fungi have gained remarkable attention in research, as they not only provide novel sources of bioactive secondary metabolites (SMs) that are the backbone of many drugs but can also protect the host plant from biotic and abiotic stresses that pose a serious threat to crop food safety and security. Hence, endophytic fungi have had a considerable impact on medicine, agriculture, and industry, and thus the economy. Previous studies (Torkamani et al., 2014; Tashackori et al., 2018; Salehi et al., 2019) presented the significant potential of fungal elicitors as well as co-cultivation of the endophytic fungus and plant cells for paclitaxel biosynthesis increment in a *Corylus avellana* cell culture. In this Research Topic, Zhang et al. showed that roots inoculated with endophytes promoted the production of polyphyllin, an antiviral, analgesic, antibacterial, and anti-inflammatory agent, in *Paris polyphylla* rhizomes, likely by the upregulation of downstream cytochrome P450 and UDP-glycosyltransferase genes involved in polyphyllin biosynthesis. Santra and Banerjee described endophytic *Curvularia eragrostidis* as a potent anti-microbial producer. This isolate produced volatile organic compounds (VOCs) that can be used as a tool for sustainable agriculture by preventing the growth of dangerous phytopathogens. In addition, bioactive metabolites produced by *Curvularia eragrostidis* can be a powerful alternative to traditional antibiotics and effectively curb the deadly diseases caused by multidrug-resistant gram-positive and gram-negative bacterial pathogens in the human population. Furthermore, numerous investigations have demonstrated that the majority of *Trichoderma* spp. can biosynthesize bioactive compounds and display antagonistic effects against nematodes and fungi that cause plant disease (Yao et al.). These bioactive compounds, which include cell wall-degrading enzymes and secondary metabolites, can effectively decrease plant disease, promote crop resistance, and enhance plant growth (Yao et al.). Gangaraj et al. showed that *Aspergillus niger* produced different antimicrobial metabolites and displayed high potential for the biocontrol of soil-borne diseases including guava wilt and others. Several

endophytic fungi have been isolated from *Brassica oleracea*, showing different advantages for the host, including cold tolerance, plant growth promotion, and induction of resistance to pests (*Mamestra brassicae*) and pathogens (*Xanthomonas campestris*; Poveda et al.). These endophytic fungi improved the growth of *B. carinata*, *B. rapa*, *B. nigra*, *B. napus*, and *B. juncea*, likely because of auxin and siderophore biosynthesis as well as P solubilization, or cellulase, amylase, or xylanase activity (Poveda et al.). SMs produced by endophytic fungi include phenols, alkaloids, polyketides, quinones, steroids, enzymes, and peptides, which display diverse biological activities such as anticancer, insecticidal, antioxidant, cytotoxic, antibacterial, antiviral, antifungal, and antimalarial properties (Hardoim et al., 2015). A microbial fermentation process would be the most favorable means for the production of bioactive secondary metabolites. Microorganisms are fast-growing, and their genetic manipulation is often relatively easy and can be scaled up to an industrial level (Salehi et al., 2018). The endophytic fungi of *Alisma orientale* produced numerous secondary metabolites with strong antibacterial and antioxidant activities (Shen et al.). Abo-Kadoum et al. reported that endophytic fungi in different plant species can offer an incredible way to supply a steady yield of resveratrol, a strong contender to treat a wide range of human diseases. Mulberry branch extracts promoted the mycelial growth and biosynthesis of bioactive compounds of *Sanghuangporus vaninii*, widely used in traditional medicine, by upregulating hydrolase family genes (Huo et al.).

Mycoendophyte "*Trichoderma* sp." displayed antioxidant, antifungal, and a-glucosidase inhibitory activities and also greatly inhibited the growth of plant pathogens including *Aspergillus niger*, *Fusarium* sp., and *Trichoderma viride* (Elfiati et al.). Ebrahimi et al. screened two effective endophytic fungal isolates, *Coniochaeta endophytica* and *Chaetomium globosum*, for the biocontrol of apple scab disease caused by *Venturia inaequalis*. Chemical control of plant disease can be destructive to the environment, and repeated use of chemical fungicides can lead to the prevalence of agrochemical-resistant strains. The application of endophytic fungi for enhancing tolerance or resistance to biotic stress is a greener alternative approach that could reduce the use of chemicals in agriculture, conferring benefits to both the environment and human health (Bhardwaj et al.). Using endophytic fungi for the protection of plants against abiotic stresses could additionally mitigate the detrimental effect of global climate change on agriculture. Under greenhouse conditions, the detrimental effects of salinity and drought stresses on barley were lessened by halotolerant endophytic fungi including *Neocamarosporium goegapense*, *N. chichastianum*, and *Periconia macrospinosa*, which were isolated from the roots of salt lake plants growing in the central desert of Iran. Indeed, such endophytic fungi have evolved various strategies to survive in harsh desert environments and are essential in providing their host plants with resistance against extreme environmental stress (Hosseyni Moghaddam et al.).

Mycorrhizal fungi are the other major class of endophytic fungi. They inhabit roots but spread out into the rhizosphere. Mycorrhizae can also enhance plant tolerance against different abiotic stresses related to global climate change, including heat, metals, salinity, drought, and extreme temperatures. Therefore, they can help plants to cope with the changing climate (Bonfante and Genre, 2010). Additionally, Zhao et al. reported that the inoculation of *Alkanna tinctoria* using arbuscular mycorrhizal *Rhizophagus irregularis* enhanced the production of shikonin and alkannin.

Author contributions

MS: Writing—original draft, Writing—review & editing. NS: Writing—original draft, Writing—review & editing.

Funding

The author(s) declare that financial support was received for the research, authorship, and/or publication of this article. MS and NS acknowledge Iran National Science Foundation (INSF, No. 4012798).

Acknowledgments

The guest editors sincerely appreciate the efforts of all authors, reviewers, and Frontiers in Microbiology Team who contributed to this Research Topic.

Conflict of interest

The authors declare that the research was conducted in the absence of any commercial or financial relationships that could be construed as a potential conflict of interest.

The author(s) declared that they were an editorial board member of Frontiers, at the time of submission. This had no impact on the peer review process and the final decision.

Publisher's note

References

Bonfante, P., and Genre, A. (2010). Mechanisms underlying beneficial plant–fungus interactions in mycorrhizal symbiosis. *Nat. Commun.* 1, 48. doi: 10.1038/ncomms1046

Hardoim, P. R., Van Overbeek, L. S., Berg, G., Pirttil,ä, A. M., Compant, S., Campisano, A., et al. (2015). The hidden world within plants: ecological and evolutionary considerations for defining functioning of microbial endophytes. *Microbiol. Mol. Biol. Rev.* 79, 293–320. doi: 10.1128/MMBR.00050-14

Salehi, M., Moieni, A., and Safaie, N. (2018). Elicitors derived from hazel (*Corylus avellana* L.) cell suspension culture enhance growth and paclitaxel production of *Epicoccum nigrum*. *Sci. Rep.* 8, 12053. doi: 10.1038/s41598-018-29762-3

Salehi, M., Moieni, A., Safaie, N., and Farhadi, S. (2019). New synergistic co-culture of *Corylus avellana* cells and *Epicoccum nigrum* for paclitaxel production. *J. Indust. Microbiol. Biotechnol.* 46, 613–623. doi: 10.1007/s10295-019-02148-8

Tashackori, H., Sharifi, M., Chashmi, N. A., Behmanesh, M., and Safaie, N. (2018). Piriformospora indica cell wall modulates gene expression and metabolite profile in Linum album hairy roots. *Planta* 248, 1289–1306. doi: 10.1007/s00425-018-2973-z

Torkamani, M. R. D., Jafari, M., Abbaspour, N., Heidary, R., and Safaie, N. (2014). Enhanced production of valerenic acid in hairy root culture of Valeriana officinalis by elicitation. *Cent. Eur. J. Biol.* 9, 853–863. doi: 10.2478/s11535-014-0320-3

frontiers | Frontiers in Microbiology

ORIGINAL RESEARCH
published: 20 May 2022
doi: 10.3389/fmicb.2022.906365

Inducing Tolerance to Abiotic Stress in *Hordeum vulgare* L. by Halotolerant Endophytic Fungi Associated With Salt Lake Plants

Mahdieh S. Hosseyni Moghaddam[1,2], Naser Safaie[1], Saleh Rahimlou[2,3] and Niloufar Hagh-Doust[2,3]*

[1] Department of Plant Pathology, Faculty of Agriculture, Tarbiat Modares University, Tehran, Iran, [2] Institute of Ecology and Earth Sciences, University of Tartu, Tartu, Estonia, [3] Center of Mycology and Microbiology, University of Tartu, Tartu, Estonia

A characteristic trait of plants living in harsh environments is their association with fungal endophytes, which enable them to survive under extreme stress. Abiotic stress resistance in agro-ecosystems, particularly in arid and semi-arid regions, can be increased by inoculating these fungal endophytes on plants other than their original hosts. The present study is therefore focused on the possible role of three halotolerant endophytic fungi, i.e., *Periconia macrospinosa*, *Neocamarosporium goegapense,* and *N. chichastianum,* isolated from roots of salt lake plants growing in the central desert of Iran, in alleviating the adverse effects of salinity and drought stresses on barley under greenhouse conditions. To perform this experiment, a randomized block design was applied with three factors: fungi (four levels including three halotolerant endophytic species and control), salinity (three levels including 8, 12, and 16 dS/m), and drought (four levels including 100, 80, 60, 40 percent field capacity). All plants were measured for growth characteristics, chlorophyll concentration, proline content, and antioxidant enzyme activities. A three-way analysis of variance indicated that all three fungal endophytes, to varying extents, induced the barley plants' resistance to salinity and drought, and their combined effects. Additionally, we found that fungal endophytes were more effective when the barley plants were subjected to higher levels of salinity and drought. Under the stress of salinity and drought, a strong relationship between inoculation of fungal endophytes and enhancement of biomass, shoot length, chlorophyll concentration, proline content, and activity of catalase, peroxidase, and superoxide dismutase was indicated. We discussed that increased root growth, proline content, and antioxidant enzyme activity are the main physiological and biochemical mechanisms causing stress resistance in barley plants inoculated with endophytes. Our research findings illustrate that fungal endophytes have a substantial potential for increasing abiotic stress tolerance in barley plants, which can be applied in agricultural ecosystems.

Keywords: crop production, environmental stress, halotolerant fungal endophytes, growth promotion, reactive oxygen species, stress tolerance

OPEN ACCESS

Edited by:
Md. Motaher Hossain, Bangabandhu Sheikh Mujibur Rahman Agricultural University, Bangladesh

Reviewed by:
Mehdi Ghabooli, Malayer University, Iran
Amr Fouda, Al-Azhar University, Egypt

***Correspondence:**
Naser Safaie
nsafaie@modares.ac.ir

Specialty section:
This article was submitted to Microbe and Virus Interactions with Plants, a section of the journal Frontiers in Microbiology

Received: *28 March 2022*
Accepted: *29 April 2022*
Published: *20 May 2022*

Citation:
Hosseyni Moghaddam MS, Safaie N, Rahimlou S and Hagh-Doust N (2022) Inducing Tolerance to Abiotic Stress in Hordeum vulgare L. by Halotolerant Endophytic Fungi Associated With Salt Lake Plants. Front. Microbiol. 13:906365. doi: 10.3389/fmicb.2022.906365

INTRODUCTION

Environmental challenges such as drought and salinity impose the greatest threat to plants growing on irrigated land which generates about 40% of the world's food (Chaves et al., 2003; Pimentel et al., 2004; Omar et al., 2009; Alikhani et al., 2013). Morphological changes, restriction of photosynthesis, growth reduction, disruption in the activities of the various enzymes, influence on the formation of reactive oxygen species (ROS), and performance imperfection are significant adverse effects of such environmental stress on crops (Yildirim et al., 2015; Sahin et al., 2018). Scientists around the world are searching for innovative methods to maintain crop yields in stressful conditions. Numerous studies have shown that plant-associated microorganisms increase plant resistance to environmental stress (Soussi et al., 2016; Bonatelli et al., 2021). The research to date has mainly focused on fungal and bacterial symbionts, such as mycorrhiza and nitrogen-fixing bacteria, and little is known about the potential benefits of other free-living endophytic microorganisms. However, some researchers have reported endophytes as one of the key plant-associated microorganisms involved in helping their hosts to increase growth and overcome biotic and abiotic stress (Khan et al., 2011; Piernik et al., 2017; Fouda et al., 2019; El-Sersawy et al., 2021).

Recent studies have indicated that endophytic microorganisms associated with plant species growing in harsh environments could induce significant abiotic stress tolerance in plants other than their original hosts (Redman et al., 2011; Moghaddam et al., 2021). These microorganisms increase environmental stress tolerance in their host plants by several mechanisms, such as raising water-use efficiency, enhancing antioxidant enzyme activity, the adjustment in ion transport and metabolic changes, modulation of phytohormones, etc. (Baltruschat et al., 2008; Lata et al., 2018). Bacterial endophytes associated with halophytic plants, i.e., *Arthrocnemum macrostachyum* and *Spergularia marina,* ameliorate salinity tolerance of *Vicia faba* by improvement of enzymatic and non-enzymatic antioxidant accumulation (Mahgoub et al., 2021). Endophytic ascomycete *Curvularia* sp. isolated from halophytic *Suaeda salsa* conveys salinity stress tolerance to poplar trees *Populus tomentosa* (Pan et al., 2018). Poplar trees inoculated with *Curvularia* sp. indicated higher levels of antioxidant enzymes and proline than non-inoculated plants. *Thermomyces* fungal endophyte isolated from extreme hot desert-adapted plants eliminates the adverse effects of heat stress on cucumber plants by increasing root length, improving photosystem II efficiency, photosynthesis rate, and water use efficiency relative to endophyte-free plants (Ali et al., 2018). In light of these studies isolating endophytic microorganisms associated with desert plants and studying their role in inducing tolerance to abiotic stress are of great biotechnological importance, especially in barren lands and saline environments.

Barley (*Hordeum vulgare*), as a monocotyledonous plant species, is the fourth most commonly produced cereal after maize, rice, and wheat. Therefore, studies on the methods of how to increase barley plants' resistance to abiotic stress are crucial for agricultural research. During the last decade, several studies have investigated the effect of fungal endophytes on barley plants' increasing resistance to salinity and drought stresses (Alikhani et al., 2013; Bagheri et al., 2013; Chen et al., 2018). Inoculation of *Epichloë*, an asexual endophytic fungus, significantly alleviated adverse effects of salinity stress on barley plants by promoting nutrient absorption and adjusting the ionic balance (Song et al., 2015). Improvement of ascorbic acid levels and antioxidant enzyme activity were observed in barley plants inoculated with *Piriformospora indica* under salinity stress (Baltruschat et al., 2008). Ghabooli et al. (2013) reported that *P. indica*, as a mutualistic root endophytic fungus, increases growth and salinity tolerance in barley plants by enhancing the K^+/Na^+ and Ca^{2+}/Na^+ ratios, sugars, and free amino acids. Endophytic fungus *Epichloë bromicola* significantly increased salinity stress in *H. brevisubulatum* by increasing the conversion of putrescine to spermidine and spermine as well as improving shift ability of free and soluble conjugated forms of polyamines to insoluble forms (Prema Sundara Valli and Muthukumar, 2018).

We previously indicated that three halotolerant endophytic fungal species, i.e., *Periconia macrospinosa*, *Neocamarosporium goegapense,* and *N. chichastianum,* isolated from the roots of Salt Lake plants growing in the central desert of Iran increase dicot plants' resistance to salinity and drought stresses (Moghaddam et al., 2021). This study aimed to investigate the potential benefits of these endophytic fungi in inducing the same abiotic stress tolerance in monocots. Fungal treatments including the three mentioned species and control plants (lacking endophytes) – under different salinity, drought, and their combination stress levels were applied to barley plants in a greenhouse experiment. For understanding the barley plant's reaction to different levels of salinity and drought stress, several important physiological and biochemical markers such as proline content of leaf and antioxidant enzymatic activities in the presence/absence of endophytic fungi were measured. Furthermore, growth parameters and leaf chlorophyll concentration were measured.

MATERIALS AND METHODS

Greenhouse Experimental Design

Hordeum vulgare L. (barley) was used as a model plant for salinity and drought stress tolerance assays. Salt-sensitive barley seeds (Reyhan 03, Iran) were surface-sterilized for 10 min in 0.25 percent sodium hypochlorite, followed by rinsing with water (Baltruschat et al., 2008). The surface-sterilized seeds were germinated at 24°C on sheets of Whatman filter paper, which were soaked in distilled water in sterile Petri dishes. After two days, the germinated seeds were transferred to pots containing 200 g of 2:1 autoclaved mixture of soil and peat (v/v) (pH = 6.7; EC = 1.1 dS/m). This experiment was conducted using a random block design, with 144 pots divided up into 36 pots for each fungal species treatment, and 36 pots for control treatments.

Three halotolerant fungal endophyte species, i.e., *Periconia macrospinosa*, *Neocamarosporium goegapense*, and *N. chichastianum,* isolated in our previous study (Moghaddam et al., 2021) were propagated in Potato Dextrose Broth (PDB;

Merck, Germany) for about ten days at 28°C, shaking at 180 rpm, in dark conditions. The pots were inoculated with fungal endophytes by mixing 200 g of the potting substrate with 2 g of fresh mycelium. The pots were maintained in a greenhouse at 27:19°C day: night cycle, 45–55% relative humidity, and a photoperiod of 16 h.

Barley plants were exposed to salinity and drought 10 days after inoculation. Salt lake water (31.4% Na^+; 0.3% K; 0.9% Mg; 0.3% Ca, 12.7% Cl; 0.8% SO_4; and 1.29% CO_3) from Hoz-e Soltan (35.00083333, 50.99250000) was used to induce salinity stress on endophyte-colonized plants as well as on the endophyte-free control plants. Salinity stress was applied at three levels of Electrical conductivity to the barley pots, including $S_1 = 8$ dS/m (without yield reduction), $S_2 = 12$ dS/m (25 percent yield reduction), and $S_3 = 16$ dS/m (50 percent yield reduction). In order to attain different salinity levels, the salt lake water was diluted with distilled water. Barley plants were exposed to drought stress at four different levels, including $D_1 = 100\%$, $D_2 = 80\%$, $D_3 = 60\%$, and $D_4 = 40\%$ of field capacity (FC). In order to determine the field capacity, soil samples of 200 g were taken at the time of filling plastic pots, stored in plastic bags, and transported to the laboratory. A 24-hour incubation at 105°C was then performed on these soil samples. By weighing and averaging these oven-dried samples, we determined the soil moisture content at the time of sowing the barley seeds. In order to estimate the saturation percentage of the oven-dried soil samples, distilled water was used to make a paste that was completely saturated.

The following equation was used to determine the field capacity:

$$\text{Field capacity} = \text{Saturation percentage}/2$$

A drought treatment was calculated as 100, 80, 60, and 40 percent field capacities. By using a balance, pots were weighed to determine the soil's field capacity. Plants were only watered if the capacity of the field decreased (Saeed et al., 2016). All experiments were applied in triplicates.

Confirmation of the Colonization of Barley Roots by Fungal Endophyte

We examined the roots and confirmed the internal plant colonization by the inoculated endophytic fungi as follows. Root samples were washed under tap water for 10 minutes and cut into 0.5-1 cm pieces. Root fragments were subjected to a three-step surface sterilization process including dipping in ethanol/water (70:30) for 2 min, followed by sodium hypochlorite/water (4:96) for 90 s, ethanol/water (70:30) for 2 min, and a final rinse in sterile distilled water for three times (1 min each). The inner layers of disinfected roots were cultured on PDA (Merck, Darmstadt, Germany), and incubated at 28°C (Hosseyni-Moghaddam and Soltani, 2014). A small amount of water from the final step was also spread on the same media. The control plants were treated in the same way. The isolated fungal species were identified either morphologically (**Supplementary Figure 1**) or by sequencing the ITS-rDNA region.

Measurements of Growth Parameters and Chlorophyll Concentration

Six weeks after planting the seeds, the root wet and dry weight and shoot length of the plants were measured. Using a SPAD-502 Chlorophyll meter, we measured the chlorophyll content of all leaf samples (Coste et al., 2010).

Antioxidant Enzymatic Activity and Proline Content of Leaf Measurements

Two weeks after the pots were stressed by salinity and drought, leaf samples were collected. Liquid nitrogen was used to crush 0.2 g of each leaf sample for homogenization. Then, 3 mL of HEPES-KOH buffer (pH 7.8) containing 0.1 mM EDTA was added to the leaf powder. Supernatants (enzyme extracts) were used for chemical analysis once the final solutions had been centrifuged at 4°C at 16,000 rpm for 15 min (Sahebjamei et al., 2007). A photochemical method was applied to measure superoxide dismutase (SOD) activity in the supernatant (Giannopolitis and Ries, 1977). First, a reaction mixture (3 ml) containing 300 μL enzyme extract, 75 μM nitroblue tetrazollium chloride (NBT), 1 μM riboflavin, 0.1 mM EDTA, 50 mM MHEPES-KOH buffer (pH 7.8), 12 mM L-methionine, and 50 mM Na_2CO_3 (pH 10.2), was prepared. Then, using a spectrophotometer (Cintra 6, GBC, Dandenong, Australia), one unit of superoxide dismutase activity was determined as the amount of enzyme needed to inhibit the 50% rate of NBT reduction measured at 560 nm. In a reaction mixture consisting of 500 μl of 10 mM H_2O_2, 1400 μl of 25 mM sodium phosphate buffer, and 100 μl of crude enzyme extract, catalase activity was measured. Following the decomposition of H_2O_2, absorbance at 240 nm declined. Catalase activity of the extract was expressed as CAT unit: min^{-1} mg^{-1} protein (Cakmak and Horst, 1991). A spectrophotometric measurement of the peroxidase activity was done by following the oxidation of guaiacol (2-methoxyphenol) to tetraguaiacol at 470 nm (Plewa et al., 1991). The reaction mixture (3 mL) contained 500 μl 28 mM guaiacol, 1900 μl 60 mM potassium phosphate buffer (pH 6.1), 500 μl 5 mm H2O2, and 100 μl crude extract. The enzyme activity was expressed as POX unit: min^{-1} mg^{-1} protein.

For the estimation of proline content, each leaf sample (0.2 g) was homogenized in 3 ml sulphosalicylic acid (3% w/v), and then centrifuged at 10,000 rpm for 15 min. A reaction mixture consisted of 2 ml supernatant, 2 ml freshly prepared acid ninhydrin solution, and 2 ml glacial acetic acid which was boiled at 100°C for 1 h. After completion of the reaction in an ice bath, the reaction mixture was extracted with 4 ml of toluene; absorbance was read at 520 nm (Bates et al., 1973).

Statistical Analyses

For each measured biological parameter of the barley plants, a three-way ANOVA was used to determine the effects of three factors, i.e., fungus, salinity, and drought. LSD tests were used to assess the significance of group differences at a $p \leq 0.05$ level. Analyses were conducted using statistical packages in R version 3.6.2 (R Core Team, 2021).

RESULTS

Colonization of Barley Roots by Halotolerant Endophytic Fungi

By using the same isolation technique, the isolated halotolerant fungal endophytes, i.e., *P. macrospinosa, N. goegapense,* and *N. chichastianum,* were re-isolated from the inoculated barley roots. However, these fungal species were not isolated from the control plants. The confirmation of colonization of barley roots by halotolerant endophytic fungi validated our results from this experiment.

Growth Promotion of Barley Plants Under Salinity and Drought Stress

A three-way analysis of variance revealed that halotolerant endophytic fungi significantly increased the tolerance of barley plants to salinity, drought, and their combined effects (**Tables 1**, **2**). Compared to the endophyte-free control plants, the barley plants' growth parameters were all improved ($p \leq 0.01$; **Table 1**). Six weeks after planting the seeds, inoculated barley plants indicated 27.6, 30.5, and 24.7% more biomass, root wet weight, and shoot length than their control counterparts, respectively. The results also indicated that the increasing drought or salinity levels negatively affect barley plants' growth characteristics ($p \leq 0.01$); however, the interaction effect of these abiotic stress was not significant (**Table 1**).

Barley plants' growth parameters were affected by the interaction between halotolerant endophytic fungi and drought stress ($P \leq 0.01$; **Table 1**). Under D_1, D_2, D_3, D_4 drought levels, the biomass of the inoculated barley plants was observed to be increased by 9.2, 23.1, 42, and 61.1 percent compared to the endophyte-free controls (**Figure 1**). Shoot length also increased by 7.2, 26.5, 34.7, and 41 percent compared to the control plants under D_1, D_2, D_3, D_4 drought levels ($p \leq 0.05$; **Figure 1**). In total, plants inoculated with *N. chichastianum* indicated greater biomass and shoot length than those inoculated with *P. macrospinosa,* and *N. goegapense* across all levels of drought stress ($p \leq 0.05$; **Figure 1**). Additionally, endophyte-colonized barley showed 7.4, 34.1, 47.1, and 50.9 percent greater root wet weight compared to endophyte-free controls, under D_1, D_2, D_3, D_4 drought levels, respectively (**Figure 1**). Overall, plants inoculated with *Neocamarosporium* species showed greater root wet weight than those inoculated with *P. macrospinosa* ($p \leq 0.05$; **Figure 1**).

Growth parameters of barley plants were affected by interactions between halotolerant endophytic fungi and salinity stress (**Table 1**). Under salinity levels of S_1, S_2, and S_3, the biomass of inoculated barley plants was increased by 17, 31.7, and 42.9 percent in comparison with endophyte-free control plants (**Figure 2**). The shoot length of the barley plants was observed to be increased by 17, 25.9, and 32.9 percent compared to the endophyte lacking controls under S_1, S_2, and S_3 salinity levels (**Figure 2**). Overall, *N. chichastianum*-inoculated plants indicated greater biomass and shoot length compared to the plants associated with *P. macrospinosa*, and *N. goegapense*, across all salinity stress levels ($p \leq 0.05$; **Figure 2**). Under salinities of S_1, S_2, and S_3, the endophyte-colonized barley plants indicated 18.9, 33.4, and 42.8 percent greater root wet weight

TABLE 2 | Three-way analysis of variance (ANOVA) of the effects of the halotolerant fungal endophytes, *P. macropinosa*, *N. goegapense*, and *N. chichastianum* on the activity of antioxidant enzymes including POX, CAT, and SOD, and leaf proline content of *Hordeum vulgare* L. (barley) under different levels of salinity and drought stresses.

Variables	DF[a]	POX	CAT	SOD	Leaf Proline content
Fungi	3	0.09***	0.10***	0.42***	1033***
Drought	3	1.20***	0.59***	2.65***	8044***
Salinity	2	0.10***	0.01***	0.24***	917***
Fungi:Drought	9	0.03***	0.01***	0.11***	464***
Fungi:Salinity	6	0.001***	0.001***	0.03***	49***
Drought:Salinity	6	0.001***	0.0006***	0.003***	4***
Fungi:Drought: Salinity	18	0.0003***	0.001***	0.01***	17***
Residuals	96	0	0.0001	0.0001	3

*Significant codes: 0 '***' 0.001 '**' 0.01 '*' 0.05 '.' 0.1 ' ' 1.*
a Degree of freedom.
The numbers presented in the table are the sum of squares of the fitted model.

TABLE 1 | Three-way analysis of variance (ANOVA) of the effects of the halotolerant fungal endophytes, *P. macropinosa*, *N. goegapense*, and *N. chichastianum* on the growth parameters and leaf chlorophyll concentration of *Hordeum vulgare* L. (barley) under different levels of salinity and drought stresses.

Variables	DF[a]	Biomass	Root wet weight	Leaf chlorophyll concentration	length shoot
Fungi	3	32.16***	58.03***	2325***	7013***
Drought	3	46.07***	109.83***	5349***	13187***
Salinity	2	12.30***	17.45***	389***	1844***
Fungi:Drought	9	4.60***	8.34***	391***	928***
Fungi:Salinity	6	1.60*	2.66***	45	226***
Drought:Salinity	6	0.02	0.02	0	2
Fungi:Drought:Salinity	18	0.06	0.10	0	6
Residuals	96	4.11	5.89	328	496

*Significant codes: 0 '***' 0.01 '*' 0.05 '.' 0.1 ' ' 1.*
a Degree of freedom.
The numbers presented in the table are the sum of squares of the fitted model.

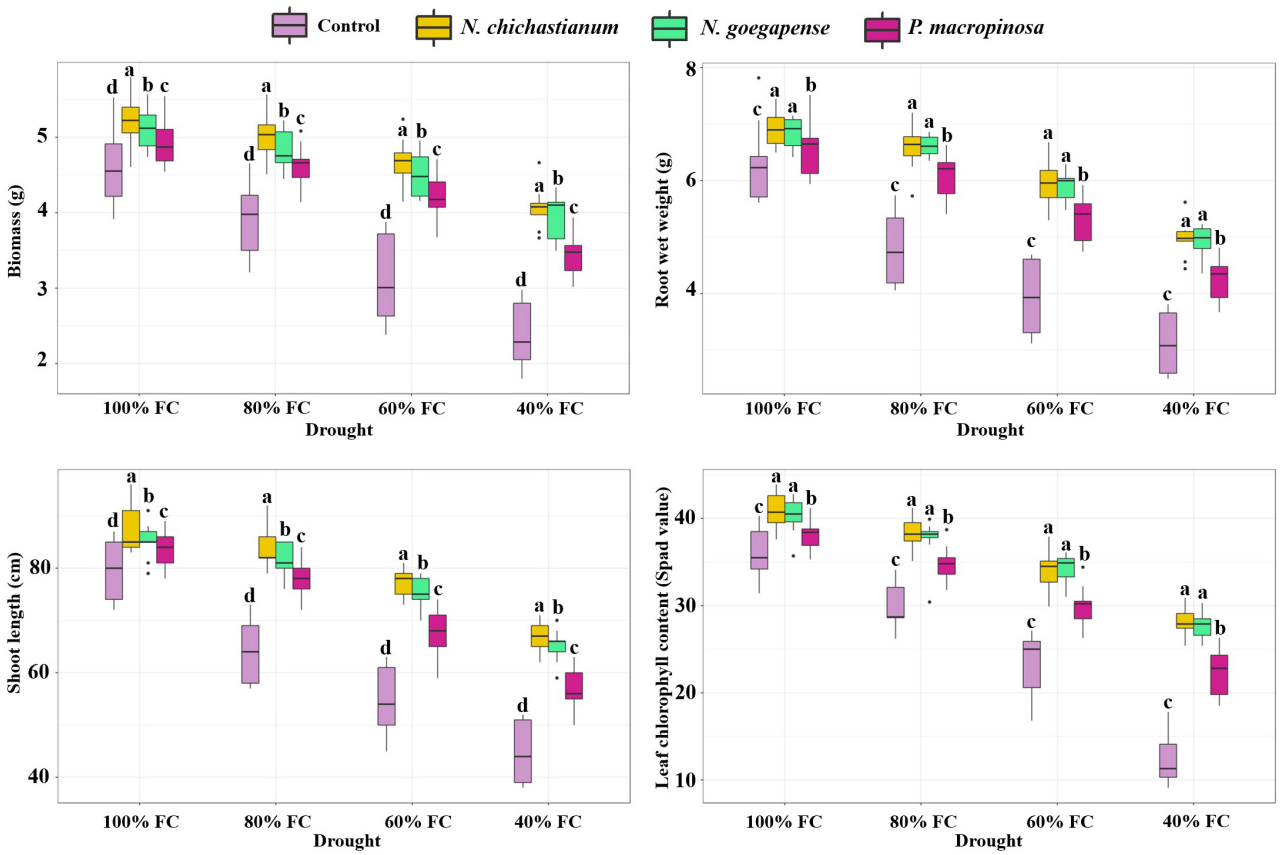

FIGURE 1 | The positive effects of halotolerant endophytic fungi species on drought stress resistance abilities of barley plants. Different levels of drought stress and different fungal treatment are shown on the horizontal axis and colorful boxes, respectively. Various letters on the top of bars display significant differences between mean values of different fungal treatments under the different levels of drought stress at $p \leq 0.05$.

than the endophyte-free plants, respectively ($p \leq 0.05$; **Figure 2**). The barley plants inoculated with *Neocamarosporium* species indicated greater root wet weight than those inoculated with *P. macrospinosa* at all levels of salinity stress ($p \leq 0.05$; **Figure 2**).

The outcomes indicated that a three-way interaction between drought, salinity, and fungus failed to significantly influence the growth characteristics of barley plants (**Table 1**). However, higher growth parameters were recorded in inoculated barley plants compared to the control plants. Additionally, the halotolerant endophytic fungi were more effective at improving barley plants' growth parameters when the plants were exposed to high levels of drought or salinity stress (**Figures 1**, **2**).

Effects of Halotolerant Endophytic Fungi on Leaf Chlorophyll Concentration of Barley Plants Under Salinity and Drought Stress

A three-way ANOVA study demonstrated that halotolerant endophytic fungi species significantly increased leaf chlorophyll concentration compared to the control plants lacking fungal endophytes ($P \leq 0.01$; **Table 1**). Six weeks after planting the seeds, plants colonized with halotolerant endophytic fungi indicated greater chlorophyll content in comparison with endophyte-free plants. The results also showed that increasing drought or salinity levels negatively affect barley plants' chlorophyll concentration ($p \leq 0.01$); however, the interaction effect of these abiotic stress was not significant (**Table 1**).

Chlorophyll content of leaves was positively affected by halotolerant endophytic fungi under different levels of drought stress ($p \leq 0.01$; **Table 1**). Compared to the endophyte-free barley plants, plants colonized with endophytes showed 10, 23, 42.8, and 110.4 percent higher chlorophyll contents at D_1, D_2, D_3, D_4 drought levels ($p \leq 0.05$; **Figure 1**). Contrary to our expectations, the presence of halotolerant endophytic fungi did not significantly affect chlorophyll concentrations in the leaves under salinity stress (**Table 1**). Nevertheless, plants inoculated with *Neocamarosporium* species had higher chlorophyll content than plants inoculated with *P. macrospinosa*, irrespective of the degree of drought stress ($p \leq 0.05$; **Figure 1**). Furthermore, results indicated that halotolerant fungal endophytes were more effective at improving leaf chlorophyll content when barley plants were subjected to a higher level of drought stress (**Figure 1**).

The effects of the three-way interactions between drought, salinity, and fungus on leaf chlorophyll concentration of barley plants were not significant (**Table 1**). However,

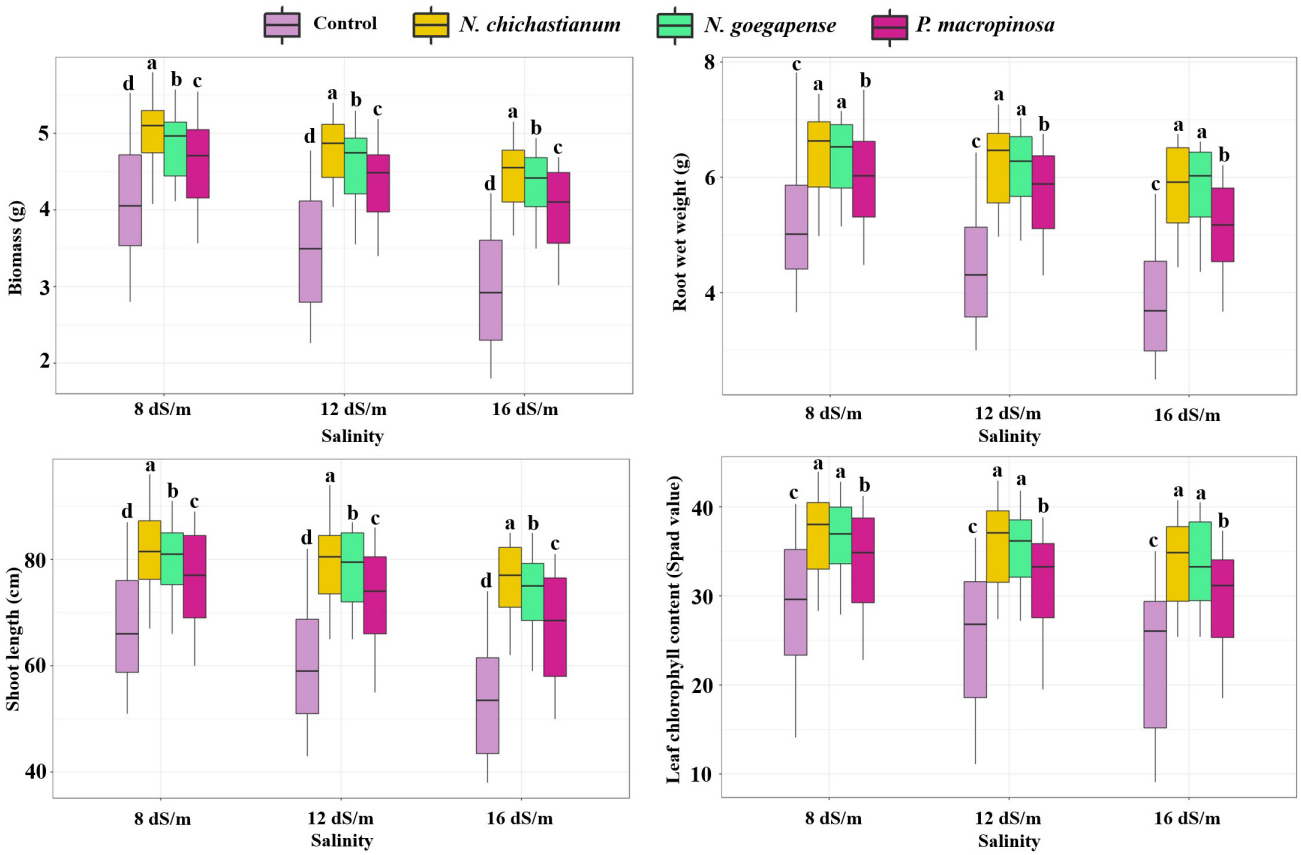

FIGURE 2 | The positive effects of halotolerant endophytic fungi species on salinity stress resistance abilities of barley plants. Different levels of drought stress and different fungal treatment are shown on the horizontal axis and colorful boxes, respectively. Various letters on the top of bars display significant differences between mean values of different fungal treatments under the different levels of salinity stress at $p \leq 0.05$.

endophyte-colonized plants had higher chlorophyll levels than endophyte-free plants.

Effects of Halotolerant Fungal Endophytes on Leaf Proline Content of Barley Plants Under Salinity and Drought Stress

Variance partitioning analysis indicated that halotolerant fungal endophytes significantly affected proline content of barley plants ($p \leq 0.01$, **Table 2**). Barley plants associated with *P. macrospinosa, N. goegapense,* and *N. chichastianum* showed 47.8, 35.9, and 32.8 percent higher proline levels than their endophyte-free counterparts (**Figure 3**). Moreover, increasing salinity increased leaf proline content of barley plants across the experiment. Similar patterns were observed in plants subjected to drought stress (**Table 2** and **Figure 3**).

Increasing salinity or drought stress levels significantly increased leaf proline content of barley plants across the experiment. Moreover, the interaction effects of salinity and drought stress had significant effects on proline content ($p \leq 0.01$, **Table 2**). Under S_1, S_2, and S_3 salinity levels, the proline content of inoculated barley plants was observed to be increased by 34.9, 36, and 43.9 percent compared to endophyte lacking controls, respectively. Further, interaction between halotolerant fungal endophytes and drought stress significantly affected the proline content of barley plants ($p \leq 0.01$, **Table 2**). When the endophyte-colonized barley plants were subjected to D_1, D_2, D_3, D_4 drought levels, their proline content was 17.8, 33.5, 43.2, and 46.7 percent higher than the endophyte-free controls, respectively ($p \leq 0.05$; **Figure 3**).

Outcomes indicated that the three-way interactions between salinity, drought, and fungus significantly impacted proline content ($p \leq 0.01$; **Table 2**). With increasing salinity and drought levels, the halotolerant fungal species were more effective on leaf proline content. Under the lowest levels of salinity and drought stress, inoculation of *P. macrospinosa, N. goegapense,* and *N. chichastianum* increased the proline content of leaf by 2.3, 15.9, and 14.3 percent, respectively, compared to the control plants ($p \leq 0.05$; **Figure 3**). While under the highest levels of drought and salinity, the barley plants colonized by *P. macrospinosa, N. goegapense,* and *N. chichastianum* showed a significant increase of proline content of leaf, by 48.4, 50.9, and 44.8 percent, respectively, compared to the control plants ($p \leq 0.05$, **Figure 3**). Overall, plants colonized with *N. goegapense* expressed the highest proline content of

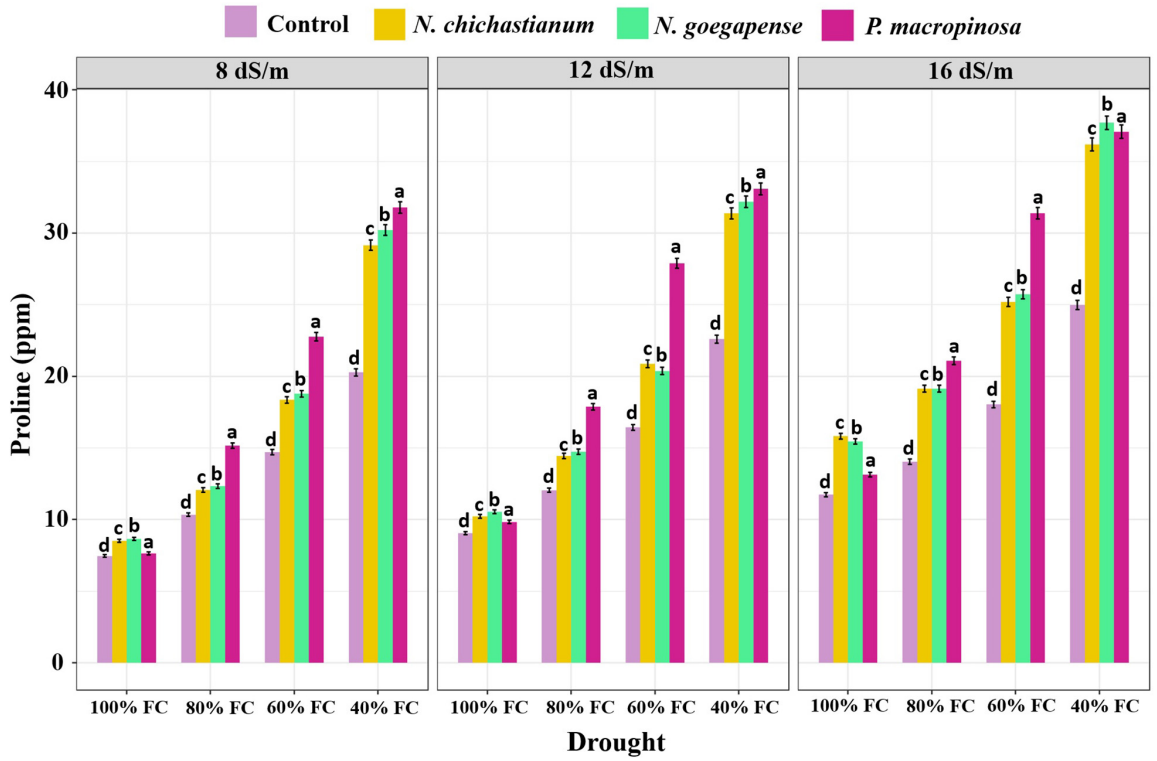

FIGURE 3 | The effects of halotolerant endophytic fungi species on leaf proline content of barley plants, under salinity and drought stress. Different levels of drought stress and different fungal treatment are shown on the horizontal axis and colorful bars, respectively. Various letters on the top of bars display significant differences between mean values of different fungal treatments under the different levels of salinity and drought stress at $p \leq 0.05$.

leaf under the lowest and highest salinity levels and drought stresses (**Figure 3**).

Effects of Halotolerant Fungal Endophytes on Antioxidant Enzymatic Activities of Barley Plants Under Salinity and Drought Stress

In barley plants, fungus, salinity, and drought treatments, and their interactions, significantly affected the activity of antioxidant enzymes including SOD, CAT, and POX ($p \leq 0.01$, **Table 2**).

As compared to the endophyte-free controls, plants inoculated with *P. macrospinosa*, *N. goegapense*, and *N. chichastianum* demonstrated 38.2, 25, and 22.6 percent greater CAT activity (**Figure 4**). The inoculations of P. macrospinosa, N. goegapense, and *N. chichastianum* also enhanced POX activity by 35, 25.8, and 25.9 percent, respectively (**Figure 5**). In addition, enhancement of SOD activity by 38.6, 29.9, and 35.4 percent, was observed in plants colonized with *P. macrospinosa*, *N. goegapense*, and *N. chichastianum* (**Figure 6**). The results also showed that increasing salinity or drought stress levels, as well as their interaction effects, significantly increased the SOD, CAT, and POX activities of barley plants ($p \leq 0.01$, **Table 2**).

Salinity and fungus interaction significantly affected SOD, CAT, and POX activities ($p \leq 0.01$; **Table 2**). Under S_1, S_2, and S_3 salinity levels, we respectively observed a 25.6, 30.9, and 46.4 percent increase in SOD activity among inoculated barley plants compared to endophyte-free control plants (**Figure 6**). Barley plants colonized with endophytes also showed 20.6, 25.9, and 33.2 percent greater CAT activity than those not colonized with endophytes, under S_1, S_2, and S_3 salinity levels ($p \leq 0.05$; **Figure 3**). Furthermore, under S_1, S_2, and S_3 salinity levels, endophyte-inoculated barley plants respectively indicated 24.9, 28.6, and 33.9 percent higher POX activities compared to the control plants ($p \leq 0.05$; **Figure 5**).

Drought and fungus interaction significantly affected SOD, CAT, and POX activities ($p \leq 0.01$, **Table 2**). Under D_1, D_2, D_3, D_4 drought levels, we respectively observed a 21.2, 32.1, 37.1, and 41.6 percent increase in SOD activity among inoculated barley plants compared to the endophyte-free control plants (**Figure 6**). Barley plants colonized with endophytes also indicated 18.6, 25.5, 30.3, and 34.6 percent greater CAT activity than those not colonized with endophytes, under D_1, D_2, D_3, D_4 drought levels ($p \leq 0.05$; **Figure 3**). Moreover, under D_1, D_2, D_3, D_4 drought levels, endophyte-inoculated barley plants respectively indicated 39.3, 31.9, 16.9, and 34.2 percent higher POX activities compared to the control plants ($p \leq 0.05$; **Figure 5**).

Three-way interactions between drought, salinity, and fungus had significant effects on SOD, CAT, and POX enzymes activity ($p \leq 0.01$, **Table 2**). Moreover, fungal endophytes were more influential on barley plants' antioxidant enzyme activities as

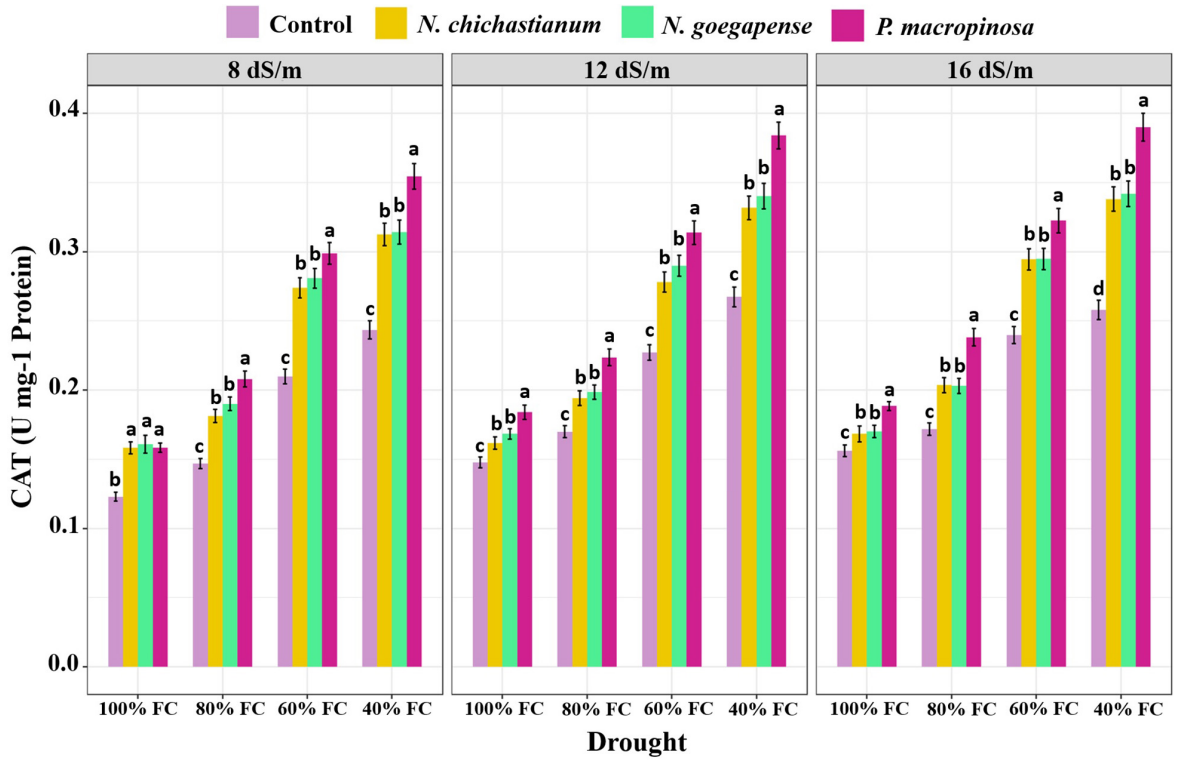

FIGURE 4 | The effects of halotolerant endophytic fungi species on CAT activity of barley plants, under salinity and drought stress. Different levels of drought stress and different fungal treatment are shown on the horizontal axis and colorful bars, respectively. Various letters on the top of bars display significant differences between mean values of different fungal treatments under the different levels of salinity and drought stress at $p \leq 0.05$.

salinity and drought increased (**Figures 4–6**). Under the lowest and highest levels of drought and salinity, barley plants colonized by *P. macrospinosa*, *N. goegapense*, and *N. chichastianum* showed higher SOD, CAT, and POX enzymatic activity than their control counterparts ($p \leq 0.05$). Under the lowest levels of salinity and drought stresses, *P. macrospinosa, N. goegapense,* and *N. chichastianum* increased the CAT activity by 28.9, 30.9, and 28.8 percent, SOD activity by 1.7, 1.2, and 4.9 percent as well as POX activity by 48.2, 64, and 73.5 percent compared to the controls, respectively ($p \leq 0.05$; **Figures 4–6**).

Under the highest levels of salinity and drought, *P. macrospinosa, N. goegapense,* and *N. chichastianum* significantly increased the CAT activity by 51.1, 32, and 30.9 percent, and SOD activity by 51.8, 40.2, 44 percent as well as POX activity by 34, 34.5, and 33.3 percent compared to the control plants, respectively ($p \leq 0.05$; **Figures 4–6**).

DISCUSSION

Drought and salinity threaten agricultural production, especially in arid and saline environments. Increasing food demand requires finding non-chemical ways to enhance plants' tolerance to salinity and drought. The evidence for endophytes as beneficial microbes has been growing in recent years, confirming their ability to confer certain benefits to their host plants under abiotic stress, such as persistent drought, extreme temperatures, high salinity, and heavy metal toxicity (Singh et al., 2011; Shahabivand et al., 2017; Lata et al., 2018; Alkahtani et al., 2020). In the meantime, the study of endophytes associated with plants living in harsh environments has gained increasing attention, with the hypothesis that these microorganisms are responsible for their host's tolerance of such conditions (Alkahtani et al., 2020; Mahgoub et al., 2021). Here we indicated that three halotolerant fungal endophytes, i.e., *P. macrospinosa, N. goegapense,* and *N. chichastianum*, isolated from roots of Salt Lake plants growing in the central desert of Iran, increase barley plant's tolerance to salinity, drought, and their combined effects. Furthermore, we found that these three fungal endophytes are more effective under high levels of drought and salinity stresses. This suggests that endophytic fungi might benefit plants more in adverse conditions. A similar result was observed when dicotyledonous plants inoculated with fungal endophytes were subjected to drought and salinity stress (Moghaddam et al., 2021).

Aiming to find out how these three halotolerant fungal endophytes impacted the establishment of salinity and drought stress tolerance, physiological and biochemical markers, such as biomass, root wet weight, shoot length, leaf chlorophyll concentration, proline content, and antioxidant enzymes activity were assessed. Under salinity and drought stress, barley plants inoculated with three studied fungal endophytes showed greater biomass, root wet weight and shoot length than endophyte-free

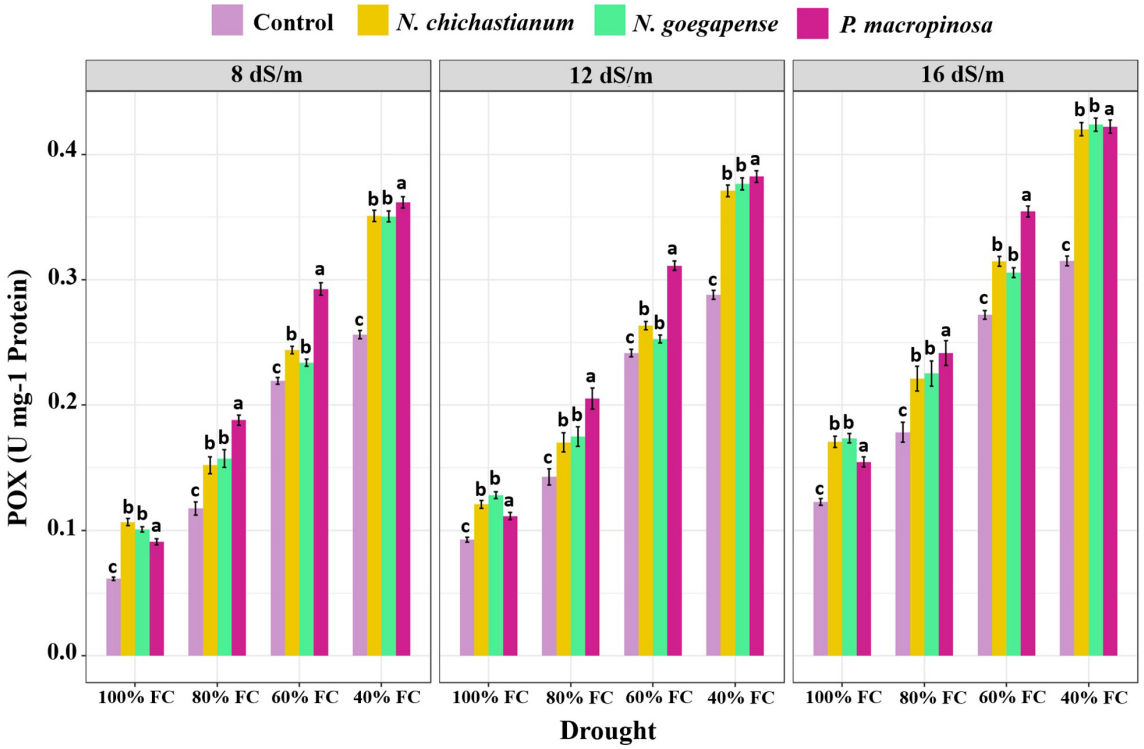

FIGURE 5 | The effects of halotolerant endophytic fungi species on POX activity of barley plants under salinity and drought stress. Different levels of drought stress and different fungal treatment are shown on the horizontal axis and colorful bars, respectively. Various letters on the top of bars display significant differences between mean values of different fungal treatments under the different levels of salinity and drought stress at $p \leq 0.05$.

barley plants. It may be consistent with endophyte-mediated habitat adaptive tolerance (Redman et al., 2011; Moghaddam et al., 2021). One of the main mechanisms of fungal endophytes for decreasing the adverse effects of salinity and drought stress on their host plants is increasing water absorption by increasing root growth (Lata et al., 2018).

Plants' ability to cope with abiotic stress can be assessed by evaluating leaf chlorophyll levels (Naumann et al., 2008). Salinity and drought stress by inhibiting chlorophyll biosynthesis cause nutritional starvation and suppressed enzyme activities. Under salinity and drought stress, a strong relationship between inoculation of fungal endophytes and enhancement of plant chlorophyll concentration has been indicated (Ghorbani et al., 2018). Here, under salinity and drought stress, barley plants associated with *P. macrospinosa*, *N. goegapense*, *and N. chichastianum* indicated more chlorophyll concentration than endophyte-free controls (**Figures 1**, **2**), suggesting that fungal endophytes have increased barley plants' tolerance to salinity and drought stress. Similar results were observed in tomato and cucumber plants inoculated with these fungal species (Moghaddam et al., 2021).

Under non-stressed conditions, ROS (Reactive Oxygen Species) are constantly produced in plants but maintained at a non-toxic level. However, ROS accumulation in plants exposed to abiotic stress, such as salinity, drought, high UV radiation, and extreme temperatures can cause significant damage to cell membranes, DNA molecules, and proteins (Elstner, 1991; Tsugane et al., 1999; Apel and Hirt, 2004). To prevent ROS accumulation and suppress their destructive effects, plants produce various anti-oxidative enzymes, such as superoxide dismutase, catalase, peroxidase, and ascorbate peroxidase (Foyer and Noctor, 2000; Bharti et al., 2016). Under environmental stress, endophytic fungi can increase the plant's antioxidant enzymatic activity to mitigate oxidative damage (Rodriguez and Redman, 2008; Jogawat et al., 2013; Sadeghi et al., 2020; Mahgoub et al., 2021). These compounds, combined with osmotic adjustment, stabilize cell components and eliminate free radicals. The current results show that halotolerant endophytic fungal species *P. macrospinosa* improved the antioxidant enzyme activity in barley under all levels of salinity and drought stress (**Figures 4**–**6**). These observations are in accordance with our previous study, indicating that *P. macrospinosa* is capable of increasing the activity of SOD, CAT, and POX enzymes in cucumber and tomato plants (Moghaddam et al., 2021). Barley plants inoculated with *N. goegapense* and, *N. chichastianum* indicated higher levels of antioxidant enzyme activity in comparison to endophyte-free plants under all levels of salinity and drought stress (**Figures 4**–**6**). However, these two fungal endophytes increased the activity of SOD, CAT, and POX enzymes of cucumber and tomato plants only in high levels of salinity and drought stress (Moghaddam et al., 2021). This finding suggests that although fungal endophytes improve

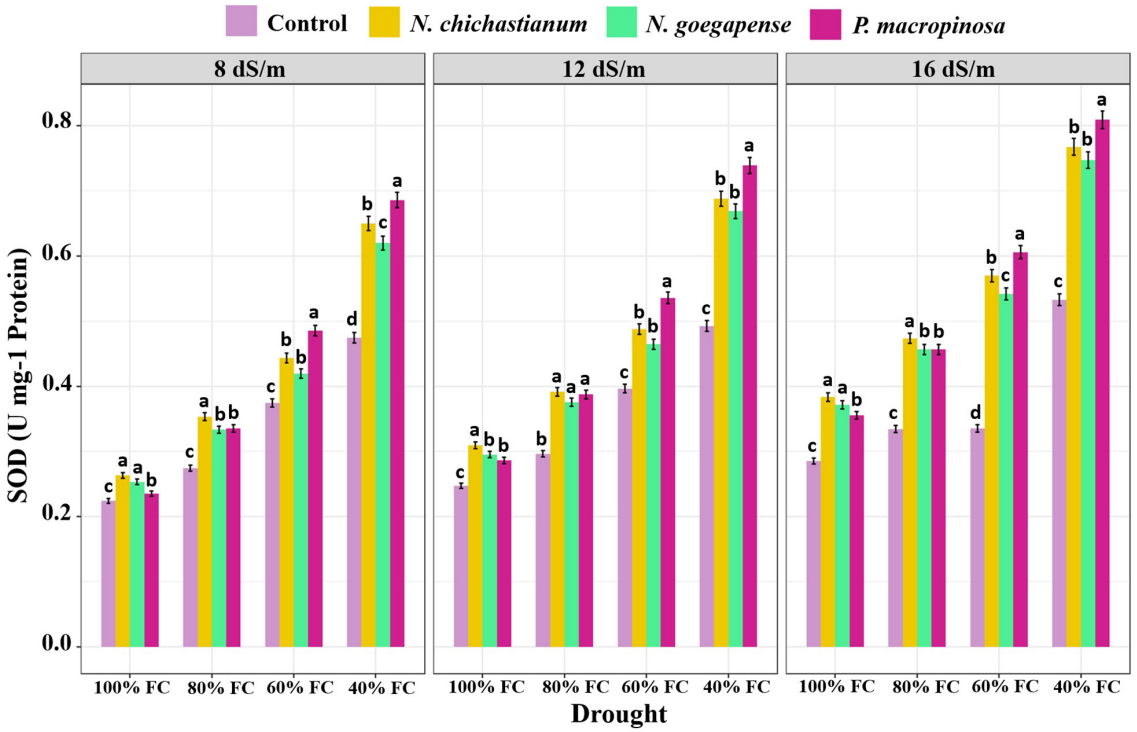

FIGURE 6 | The effects of halotolerant endophytic fungi species on SOD activity of barley plants under salinity and drought stress. Different levels of drought stress and different fungal treatment are shown on the horizontal axis and colorful bars, respectively. Various letters on the top of bars display significant differences between mean values of different fungal treatments under the different levels of salinity and drought stress at $p \leq 0.05$.

salinity and drought stress tolerance by increasing the POD, CAT, and POX enzymes activity in their host plant, the potential benefits of these microorganisms are dependent on the host plant's identity.

Different levels of abiotic stress increase the accumulation of proline in plant tissues (Fahramand et al., 2014; Hashem et al., 2015). Although the molecular role of proline in plant osmotolerance has not yet been demonstrated, it is believed that proline accumulation plays a significant role in plant abiotic stress tolerance via different mechanisms, including detoxification of ROS, osmotic adjustment, and conservation of membrane integrity (Heuer, 2010). Many studies have indicated that endophytic microorganisms can mitigate the destructive effects of salinity and drought stresses by increasing their host plant's proline content (Waller et al., 2005; Prasad et al., 2013; Mahgoub et al., 2021). In the current investigation, we observed a striking increase of leaf proline content in barley plant inoculated with *P. macrospinosa* under all levels of salinity and drought stress (**Figure 3**). An increase in proline content infers ionic influx reduction inside the cells and preserves plants by sustaining their osmotic balance. While our previous reports show that *Neocamarosporium* species increase the proline content of cucumber and tomato plants only in higher levels of salinity and drought stress (Moghaddam et al., 2021), here we observe that two halotolerant endophytic fungal species, *N. goegapense*, and *N. chichastianum,* improved the proline content of leaf under all levels of salinity and drought stress.

Overall, the current study and our previous study (Moghaddam et al., 2021) indicated that these three halotolerant endophytic fungi increase both monocot and dicot plant's resistance to salinity and drought stress across all levels. While *Periconia macrospinosa* increased the activity of antioxidant enzymes and proline content in both monocot and dicot plants under all levels of salinity and drought stress, two *Neocamarosporiun* species did not increase the levels of these biochemical markers in dicot plants under lower levels of the drought and salinity stress. It appears that identical fungal endophytes function differently in different plant species.

CONCLUSION

In the present study, three halotolerant endophytic fungal species, *P. macrospinosa, N. goegapense,* and *N. chichastianum,* increased several physiological and biochemical markers, including plant growth parameters, chlorophyll concentrations, antioxidant enzymes activity, and proline content in barley plants exposed to salinity and drought stress. Overall, we observed that these fungi significantly improved plant performance under these abiotic stresses. Such endophytic fungi associated with desert plants have developed some strategies to thrive in the harsh environment of the desert and play a fundamental role in conferring resistance to their host plants against extreme environmental stress. The results of our study show that fungal endophytes

might have the ability to increase the abiotic stress tolerance in plants other than their original hosts, which can be utilized in agricultural ecosystems. Different reactions were observed in two *Neocamarosporium* species in inducing tolerance to abiotic stress in dicotyledonous and monocotyledonous plants, highlighting the role of plant identity in such plant-microbe associations. We suggest studying the effects of endophytic fungal species on other major crops, especially in natural agricultural fields. Further in-depth studies are required to understand the molecular changes in the host plants induced by fungi under stressful conditions. Such studies are important regarding the future development of biofertilizers to reduce the excessive utilization of chemical compounds in agricultural fields.

DATA AVAILABILITY STATEMENT

The original contributions presented in the study are included in the article/**Supplementary Material**, further inquiries can be directed to the corresponding author/s.

AUTHOR CONTRIBUTIONS

MH performed the experiments, analyzed the data, and wrote the manuscript. NS designed and supervised the study. NH-D and SR helped with data analysis and improving the manuscript. This research manuscript was accomplished with the collaboration of all authors.

FUNDING

This research was supported by the Tarbiat Modares University of Iran.

ACKNOWLEDGMENTS

The authors express their gratitude to Mostafa Assadi (Research Institute of Forests and Rangelands, Tehran, Iran) for his valuable help with this project.

SUPPLEMENTARY MATERIAL

The Supplementary Material for this article can be found online at: https://www.frontiersin.org/articles/10.3389/fmicb.2022.906365/full#supplementary-material

Supplementary Figure 1 | Morphological characters of three fungal endophytes reisolated from barley plants. Seven-day colonies of *Neocamarosporium goegapense* **(A)**, *N. chichastianum* **(B)**, *Periconia macrospinosa* **(C)** on Potato Detrose Agar (PDA); Conidiomata and conidia of *N. goegapense* **(D–F)**, and *N. chichastianum* **(G,H)**; Conidiophore and conidia of *P. macrospinosa* **(I–K)**.

REFERENCES

Ali, A. H., Abdelrahman, M., Radwan, U., El-Zayat, S., and El-Sayed, M. A. (2018). Effect of Thermomyces fungal endophyte isolated from extreme hot desert-adapted plant on heat stress tolerance of cucumber. *Appl. Soil Ecol.* 124, 155–162. doi: 10.1016/j.apsoil.2017.11.004

Alikhani, M., Khatabi, B., Sepehri, M., Nekouei, M. K., Mardi, M., and Salekdeh, G. H. (2013). A proteomics approach to study the molecular basis of enhanced salt tolerance in barley (*Hordeum vulgare* L.) conferred by the root mutualistic fungus *Piriformospora indica*. *Mol. BioSyst.* 9, 1498–1510. doi: 10.1039/C3MB70069K

Alkahtani, M. D., Fouda, A., Attia, K. A., Al-Otaibi, F., Eid, A. M., Ewais, E. E.-D., et al. (2020). Isolation and characterization of plant growth promoting endophytic bacteria from desert plants and their application as bioinoculants for sustainable agriculture. *Agronomy* 10:1325. doi: 10.3390/agronomy10091325

Apel, K., and Hirt, H. (2004). Reactive oxygen species: metabolism, oxidative stress, and signal transduction. *Annu. Rev. Plant Biol.* 55, 373–399. doi: 10.1146/annurev.arplant.55.031903.141701

Bagheri, A. A., Saadatmand, S., Niknam, V., Nejadsatari, T., and Babaeizad, V. (2013). Effect of endophytic fungus, *Piriformospora indica*, on growth and activity of antioxidant enzymes of rice (*Oryza sativa* L.) under salinity stress. *Int. J. Adv. Biol. Biomed. Res.* 1, 1337–1350.

Baltruschat, H., Fodor, J., Harrach, B. D., Niemczyk, E., Barna, B., Gullner, G., et al. (2008). Salt tolerance of barley induced by the root endophyte *Piriformospora indica* is associated with a strong increase in antioxidants. *New Phytol.* 180, 501–510. doi: 10.1111/j.1469-8137.2008.02583.x

Bates, L. S., Waldren, R. P., and Teare, I. (1973). Rapid determination of free proline for water-stress studies. *Plant Soil* 39, 205–207. doi: 10.1007/BF00018060

Bharti, N., Pandey, S. S., Barnawal, D., Patel, V. K., and Kalra, A. (2016). Plant growth promoting rhizobacteria Dietzia natronolimnaea modulates the expression of stress responsive genes providing protection of wheat from salinity stress. *Sci. Rep.* 6, 1–16. doi: 10.1038/srep34768

Bonatelli, M. L., Lacerda-Júnior, G. V., dos Reis Junior, F. B., Fernandes-Júnior, P. I., Melo, I. S., and Quecine, M. C. (2021). Beneficial plant-associated microorganisms from semiarid regions and seasonally dry environments: a review. *Front. Microbiol.* 11:553223. doi: 10.3389/fmicb.2020.553223

Cakmak, I., and Horst, W. J. (1991). Effect of aluminum on lipid peroxidation, superoxide dismutase, catalase, and peroxidase activities in root tips of soybean (*Glycine max*). *Physiol. Plant.* 83, 463–468. doi: 10.1111/j.1399-3054.1991.tb00121.x

Chaves, M. M., Maroco, J. P., and Pereira, J. S. (2003). Understanding plant responses to drought—from genes to the whole plant. *Funct. Plant Biol.* 30, 239–264. doi: 10.1071/FP02076

Chen, T., Johnson, R., Chen, S., Lv, H., Zhou, J., and Li, C. (2018). Infection by the fungal endophyte Epichloë bromicola enhances the tolerance of wild barley (*Hordeum brevisubulatum*) to salt and alkali stresses. *Plant Soil* 428, 353–370. doi: 10.1007/s11104-018-3643-4

Coste, S., Baraloto, C., Leroy, C., Marcon, É, Renaud, A., Richardson, A. D., et al. (2010). Assessing foliar chlorophyll contents with the SPAD-502 chlorophyll meter: a calibration test with thirteen tree species of tropical rainforest in French Guiana. *Ann. For. Sci.* 67:607. doi: 10.1051/forest/2010020

El-Sersawy, M. M., Hassan, S. E.-D., El-Ghamry, A. A., Abd El-Gwad, A. M., and Fouda, A. (2021). Implication of plant growth-promoting rhizobacteria of *Bacillus* spp. as biocontrol agents against wilt disease caused by *Fusarium oxysporum* Schlecht. in *Vicia faba* L. *Biomol. Concepts* 12, 197–214. doi: 10.1515/bmc-2021-0020

Elstner, E. (1991). Oxygen radicals—biochemical basis for their efficacy. *Klinische Wochenschrift* 69, 949–956. doi: 10.1007/BF01645138

Fahramand, M., Mahmoody, M., Keykha, A., Noori, M., and Rigi, K. (2014). Influence of abiotic stress on proline, photosynthetic enzymes and growth. *Int. Res. J. Appl. Basic Sci.* 8, 257–265.

Fouda, A., Hassan, S. E. D., Eid, A. M., and El-Din Ewais, E. (2019). "The interaction between plants and bacterial endophytes under salinity stress," in *Endophytes and Secondary Metabolites*, ed. S. Jha (Cham: Springer), 1–18.

Foyer, C. H., and Noctor, G. (2000). Tansley Review No. 112 Oxygen processing in photosynthesis: regulation and signalling. *New Phytol.* 146, 359–388. doi: 10.1046/j.1469-8137.2000.00667.x

Ghabooli, M., Khatabi, B., Ahmadi, F. S., Sepehri, M., Mirzaei, M., Amirkhani, A., et al. (2013). Proteomics study reveals the molecular mechanisms underlying

water stress tolerance induced by *Piriformospora indica* in barley. *J. Proteomics* 94, 289–301. doi: 10.1016/j.jprot.2013.09.017

Ghorbani, A., Razavi, S. M., Ghasemi Omran, V. O., and Pirdashti, H. (2018). *Piriformospora indica* inoculation alleviates the adverse effect of NaCl stress on growth, gas exchange and chlorophyll fluorescence in tomato (*Solanum lycopersicum* L.). *Plant Biol.* 20, 729–736. doi: 10.1111/plb.12717

Giannopolitis, C. N., and Ries, S. K. (1977). Superoxide dismutases: I. Occurrence in higher plants. *Plant Physiol.* 59, 309–314. doi: 10.1104/pp.59.2.309

Hashem, A., Abd Allah, E. F., Alqarawi, A. A., Aldubise, A., and Egamberdieva, D. (2015). Arbuscular mycorrhizal fungi enhances salinity tolerance of *Panicum turgidum* Forssk by altering photosynthetic and antioxidant pathways. *J. Plant Interact.* 10, 230–242. doi: 10.1080/17429145.2015.1052025

Heuer, B. (2010). "Role of proline in plant response to drought and salinity," in *Handbook of Plant and Crop Stress*, ed. M. Pessarakli (Boca Raton, FL: CRC Press), 213–238.

Hosseyni-Moghaddam, M. S., and Soltani, J. (2014). Bioactivity of endophytic *Trichoderma* fungal species from the plant family Cupressaceae. *Ann. Microbiol.* 64, 753–761. doi: 10.1007/s13213-013-0710-1

Jogawat, A., Saha, S., Bakshi, M., Dayaman, V., Kumar, M., Dua, M., et al. (2013). Piriformospora indica rescues growth diminution of rice seedlings during high salt stress. *Plant Signal. Behav.* 8:e26891. doi: 10.4161/psb.26891

Khan, A. L., Hamayun, M., Kim, Y.-H., Kang, S.-M., and Lee, I.-J. (2011). Ameliorative symbiosis of endophyte (*Penicillium funiculosum* LHL06) under salt stress elevated plant growth of *Glycine max* L. *Plant Physiol. Biochem.* 49, 852–861. doi: 10.1016/j.plaphy.2011.03.005

Lata, R., Chowdhury, S., Gond, S. K., and White, J. F. Jr. (2018). Induction of abiotic stress tolerance in plants by endophytic microbes. *Lett. Appl. Microbiol.* 66, 268–276. doi: 10.1111/lam.12855

Mahgoub, H. A., Fouda, A., Eid, A. M., Ewais, E. E.-D., and Hassan, S. E.-D. (2021). Biotechnological application of plant growth-promoting endophytic bacteria isolated from halophytic plants to ameliorate salinity tolerance of *Vicia faba* L. *Plant Biotechnol. Rep.* 15, 819–843. doi: 10.1007/s11816-021-00716-y

Moghaddam, M. S. H., Safaie, N., Soltani, J., and Hagh-Doust, N. (2021). Desert-adapted fungal endophytes induce salinity and drought stress resistance in model crops. *Plant Physiol. Biochem.* 160, 225–238. doi: 10.1016/j.plaphy.2021.01.022

Naumann, J. C., Young, D. R., and Anderson, J. E. (2008). Leaf chlorophyll fluorescence, reflectance, and physiological response to freshwater and saltwater flooding in the evergreen shrub, *Myrica cerifera*. *Environ. Exp. Bot.* 63, 402–409. doi: 10.1016/j.envexpbot.2007.12.008

Omar, M., Osman, M., Kasim, W., and El-Daim, A. (2009). "Improvement of salt tolerance mechanisms of barley cultivated under salt stress using *Azospirillum brasilense*," in *Salinity and Water Stress*, eds M. Ashraf, M. Ozturk, and H. R. Athar (Cham: Springer).

Pan, X., Qin, Y., and Yuan, Z. (2018). Potential of a halophyte-associated endophytic fungus for sustaining Chinese white poplar growth under salinity. *Symbiosis* 76, 109–116. doi: 10.1007/s13199-018-0541-8

Piernik, A., Hrynkiewicz, K., Wojciechowska, A., Szymańska, S., Lis, M. I., and Muscolo, A. (2017). Effect of halotolerant endophytic bacteria isolated from *Salicornia europaea* L. on the growth of fodder beet (*Beta vulgaris* L.) under salt stress. *Arch. Agron. Soil Sci.* 63, 1404–1418. doi: 10.1080/03650340.2017.1286329

Pimentel, D., Berger, B., Filiberto, D., Newton, M., Wolfe, B., Karabinakis, E., et al. (2004). Water resources: agricultural and environmental issues. *BioScience* 54, 909–918.

Plewa, M. J., Smith, S. R., and Wagner, E. D. (1991). Diethyldithiocarbamate suppresses the plant activation of aromatic amines into mutagens by inhibiting tobacco cell peroxidase. *Mutat. Res.* 247, 57–64. doi: 10.1016/0027-5107(91)90033-K

Prasad, R., Kamal, S., Sharma, P. K., Oelmüller, R., and Varma, A. (2013). Root endophyte *Piriformospora indica* DSM 11827 alters plant morphology, enhances biomass and antioxidant activity of medicinal plant *Bacopa monniera*. *J. Basic Microbiol.* 53, 1016–1024. doi: 10.1002/jobm.201200367

Prema Sundara Valli, P., and Muthukumar, T. (2018). Dark septate root endophytic fungus *Nectria haematococca* improves tomato growth under water limiting conditions. *Indian J. Microbiol.* 58, 489–495. doi: 10.1007/s12088-018-0749-6

R Core Team (2021). *R: A Language and Environment for Statistical Computing*. Vienna: R Foundation for Statistical Computing.

Redman, R. S., Kim, Y. O., Woodward, C. J., Greer, C., Espino, L., Doty, S. L., et al. (2011). Increased fitness of rice plants to abiotic stress via habitat adapted symbiosis: a strategy for mitigating impacts of climate change. *PLoS One* 6:e14823. doi: 10.1371/journal.pone.0014823

Rodriguez, R., and Redman, R. (2008). More than 400 million years of evolution and some plants still can't make it on their own: plant stress tolerance via fungal symbiosis. *J. Exp. Bot.* 59, 1109–1114. doi: 10.1093/jxb/erm342

Sadeghi, F., Samsampour, D., Seyahooei, M. A., Bagheri, A., and Soltani, J. (2020). Fungal endophytes alleviate drought-induced oxidative stress in mandarin (*Citrus reticulata* L.): toward regulating the ascorbate–glutathione cycle. *Sci. Hortic.* 261:108991. doi: 10.1016/j.scienta.2019.108991

Saeed, N., Maqbool, N., Haseeb, M., and Sadiq, R. (2016). Morpho-anatomical changes in roots of chickpea (*Cicer arietinum* L.) under drought stress condition. *J. Agric. Sci. Technol.* 6, 1–9. doi: 10.17265/2161-6264/2016.01.001

Sahebjamei, H., Abdolmaleki, P., and Ghanati, F. (2007). Effects of magnetic field on the antioxidant enzyme activities of suspension-cultured tobacco cells. *Bioelectromagnetics* 28, 42–47. doi: 10.1002/bem.20262

Sahin, U., Ekinci, M., Ors, S., Turan, M., Yildiz, S., and Yildirim, E. (2018). Effects of individual and combined effects of salinity and drought on physiological, nutritional and biochemical properties of cabbage (*Brassica oleracea* var. capitata). *Sci. Hortic.* 240, 196–204. doi: 10.1016/j.scienta.2018.06.016

Shahabivand, S., Parvaneh, A., and Aliloo, A. A. (2017). Root endophytic fungus Piriformospora indica affected growth, cadmium partitioning and chlorophyll fluorescence of sunflower under cadmium toxicity. *Ecotoxicol. Environ. Saf.* 145, 496–502. doi: 10.1016/j.ecoenv.2017.07.064

Singh, L. P., Gill, S. S., and Tuteja, N. (2011). Unraveling the role of fungal symbionts in plant abiotic stress tolerance. *Plant Signal. Behav.* 6, 175–191. doi: 10.4161/psb.6.2.14146

Song, M., Chai, Q., Li, X., Yao, X., Li, C., Christensen, M. J., et al. (2015). An asexual Epichloë endophyte modifies the nutrient stoichiometry of wild barley (*Hordeum brevisubulatum*) under salt stress. *Plant Soil* 387, 153–165. doi: 10.1007/s11104-014-2289-0

Soussi, A., Ferjani, R., Marasco, R., Guesmi, A., Cherif, H., Rolli, E., et al. (2016). Plant-associated microbiomes in arid lands: diversity, ecology and biotechnological potential. *Plant Soil* 405, 357–370. doi: 10.1007/s11104-015-2650-y

Tsugane, K., Kobayashi, K., Niwa, Y., Ohba, Y., Wada, K., and Kobayashi, H. (1999). A recessive *Arabidopsis* mutant that grows photoautotrophically under salt stress shows enhanced active oxygen detoxification. *Plant Cell* 11, 1195–1206. doi: 10.1105/tpc.11.7.1195

Waller, F., Achatz, B., Baltruschat, H., Fodor, J., Becker, K., Fischer, M., et al. (2005). The endophytic fungus *Piriformospora indica* reprograms barley to salt-stress tolerance, disease resistance, and higher yield. *Proc. Natl. Acad. Sci. U.S.A.* 102, 13386–13391. doi: 10.1073/pnas.0504423102

Yildirim, E., Ekinci, M., Turan, M., Dursun, A., Kul, R., and Parlakova, F. (2015). Roles of glycine betaine in mitigating deleterious effect of salt stress on lettuce (*Lactuca sativa* L.). *Arch. Agron. Soil Sci.* 61, 1673–1689. doi: 10.1080/03650340.2015.1030611

Conflict of Interest: The authors declare that the research was conducted in the absence of any commercial or financial relationships that could be construed as a potential conflict of interest.

Publisher's Note: All claims expressed in this article are solely those of the authors and do not necessarily represent those of their affiliated organizations, or those of the publisher, the editors and the reviewers. Any product that may be evaluated in this article, or claim that may be made by its manufacturer, is not guaranteed or endorsed by the publisher.

frontiers | Frontiers in Microbiology

ORIGINAL RESEARCH
published: 23 June 2022
doi: 10.3389/fmicb.2022.920561

Broad-Spectrum Antimicrobial Action of Cell-Free Culture Extracts and Volatile Organic Compounds Produced by Endophytic Fungi *Curvularia Eragrostidis*

*Hiran K. Santra and Debdulal Banerjee**

Microbiology and Microbial Biotechnology Laboratory, Department of Botany and Forestry, Vidyasagar University, Midnapore, India

OPEN ACCESS

Edited by:
Mina Salehi,
Tarbiat Modares University, Iran

Reviewed by:
Suruchi Gupta,
University of Jammu, India
Kanika Chowdhary,
Indian Institute of Technology Delhi, India
Surendra Sarsaiya,
Zunyi Medical University, China

***Correspondence:**
Debdulal Banerjee
debu33@gmail.com

Specialty section:
This article was submitted to Microbe and Virus Interactions With Plants, a section of the journal Frontiers in Microbiology

Received: *14 April 2022*
Accepted: *30 May 2022*
Published: *23 June 2022*

Citation:
Santra HK and Banerjee D (2022) Broad-Spectrum Antimicrobial Action of Cell-Free Culture Extracts and Volatile Organic Compounds Produced by Endophytic Fungi Curvularia Eragrostidis. Front. Microbiol. 13:920561. doi: 10.3389/fmicb.2022.920561

Endophytes are the mutualistic microorganisms that reside within the host plant and promote plant growth in adverse conditions. Plants and their endophytes are engaged in a symbiotic relationship that enables endophytes to access bioactive genes of the ethnomedicinal plants, and, as a result, endophytes are constantly addressed in the sector of pharmaceuticals and agriculture for their multidomain bio-utility. The gradual increase of antimicrobial resistance can be effectively countered by the endophytic metabolites. In these circumstances, in the present investigation, endophytic *Curvularia eragrostidis* HelS1 was isolated from an ethnomedicinally valuable plant *Helecteris isora* from East India's forests. The secondary volatile and non-volatile metabolites are extracted from HelS1 and are found to be effective broad-spectrum antimicrobials. A total of 26 secondary metabolites (9 volatiles and 17 non-volatiles) are extracted from the isolate, which exhibits effective antibacterial [against six Gram-positive and seven Gram-negative pathogens with a minimum inhibitory concentrations (MIC) value ranging from 12.5 to 400 μg ml^{-1}] and antifungal (against seven fungal plant pathogens) activity. The secondary metabolite production was optimised by one variable at a time technique coupled with the response surface methodology. The results revealed that there was a 34% increase in antibacterial activity in parameters with 6.87 g L^{-1} of fructose (as a carbon source), 3.79 g L^{-1} of peptone (as a nitrogen source), pH 6.75, and an inoculation period of 191.5 h for fermentation. The volatile metabolite production was also found to be optimum when the medium was supplemented with yeast extract and urea (0.2 g L^{-1}) along with dextrose (40 g L^{-1}). Amongst extracted volatile metabolites, 1-H-indene 1 methanol acetate, tetroquinone, *N*, *N*-diphenyl-2-nitro-thio benzamide, *Trans* 1, 2-diethyl-*trans*-2-decalinol, naphthalene, and azulene are found to be the most effective. Our investigation opens up opportunities in the sector of sustainable agriculture as well as the discovery of novel antimicrobials against dreadful phyto and human pathogens.

Keywords: endophyte, broad-spectrum antimicrobial, volatile metabolite, sustainable agriculture, fungi

INTRODUCTION

Natural products, such as antibiotics, anti-fungal, anti-cancer, and other pharmaceutically valuable agents from plants and microbial sources, have always been the front warriors against dreadful infectious and non-infectious diseases (Tyrrell et al., 2006). The indiscriminate and irrational use of synthetic chemotherapeutic agents has led to intense and deleterious consequences of antimicrobial resistance (AMR) and the rapid development of multi-drug resistant strains (MRSA, methicillin-resistant *Staphylococcus aureus*; VRSA, vancomycin-resistant *S. aureus*; and PRSA, penicillin resistant *S. aureus,* etc.) (Deshmukh et al., 2022). Presently, the popular classes of antibiotics are losing their efficacy. The emergence of new and reemergence of old infectious diseases has made the situation difficult to combat those pathogens (Manganyi et al., 2019; Wang et al., 2019). The rising cases of AMR are roughly estimated to take the lives of 10 million people globally by 2050, and there might be an economic loss of a total of 100 trillion US$, affecting a number of 24 million global citizens (Sugden et al., 2016).

Fungal pathogens are a serious threat to domestic and commercial agrarian systems and largely affect the global food supply and economy. Fungal pathogens are reported to cause 70–80% of livestock and post-harvest infections in fruits, vegetables, cereals, and pulses, which ultimately affect the global demand-and-supply chain (Santra and Banerjee, 2020a). The increasing human population demands a simultaneous increase of 60–110% of the global food pool by 2050 to equilibrate the production-consumption ratio. But croplands are losing their fertility and productivity due to overuse of chemical fertilizers and fungal attacks, respectively (Edgerton, 2009; Liu-Xu et al., 2022). The use of chemical pesticides and systemic fungicides is the most popularly adopted solutions to tackle this problem but leads to detrimental side effects concerning human health due to the incorporation of xenobiotics in the food chain and the development of resistant micro-organisms. The situation demands the natural products derived from plants and microbes, which may be an alternative way to maintain sustainable ecosystem practices (Llorens et al., 2019). VOCs derived from endophytes are a very potent myco-fumigator and gaining interest in the agro-research industry (Saxena and Strobel, 2021).

Now, it is high time to switch on the search for novel anti-microbial compounds from biological entities; in recent times, endophytic microorganisms have had the most potent candidate in this field (Hussein et al., 2022; Maliehe et al., 2022; Sharma et al., 2022). Endophytes are hidden microbial entities that reside within the host plant and promote the growth of the plant under detrimental conditions and also possess immense pharmaceutical and biotechnological importance (Charria-Girón et al., 2021; Wolfe et al., 2022). They represent a wide range of microorganisms (bacteria, actinobacteria, fungi, mycoplasma) and are ubiquitous in their occurrence (Mishra et al., 2017, 2022; Yuan et al., 2022). It has been reported that plants harbor a wide spectrum of bioactive secondary metabolites (tannin, terpene, organic acids, aromatic volatiles, phenols, polysaccharides) for their existence. Endophytes are co-evolved partners with their host plants through horizontal gene transfer and can synthesize bioactive compounds similar to the host plant metabolites. The endophytic metabolites are pharmaceutically and agriculturally valuable and can be utilised for the development of antimicrobial products.

Our present investigational outcome has addressed the antimicrobial resistance and crop loss problems using endophytic secondary metabolites as a bio-weapon. In this study, an ethnomedicinally valuable plant *H. isora* from East Indian Forest is selected for an endophyte-related study, and an endophytic *Curvularia eragrostidis* HelS1 has been isolated from the leaf tissues of the host plant. *H. isora* as a whole or its different parts like stem-bark, leaves, fruits, seeds, and roots possess potent antimicrobial, anti-oxidant, hepato-protective, anti-plasmodial, anti-cancer, anti-nociceptive action and are randomly used as Ayurvedic and Unani medicines (Srinivasa et al., 2022; Tiwari and Bae, 2022). The secondary metabolites extracted from HelS1 endophyte are found to be effective anti-bacterial agents restricting the growth of pathogenic MRSA, and *Vibrio parahaemolyticus*, causing lethal leakage of necessary macromolecules, blocking bio-film formation, and hampering the central carbohydrate metabolism.

In this regard, the present study has been focused on the isolation, extraction, and testing of the antibacterial efficacy of endophytic fungi, which can lead to the discovery of new antimicrobial agents in controlling post-harvest decay/loss of standing crops and clinical infections, respectively.

MATERIALS AND METHODS

Collection of Plant Materials

Disease-free, healthy, and mature leaves of *Helicteres isora* (also called as an East India screw tree) were collected from forests near Burudhi lake areas of Ghatshila (22° 36′ 2″ N, 86° 26′ 47″ E), East Singhbhum district, Jharkhand, India, and brought to the Microbiology and Microbial Biotechnology Laboratory, Vidyasagar University in an icebox (Tarson, India) for further study endophytic fungal flora.

Isolation and Characterisation of Endophytic Fungi

Leaves were surface sterilised first in running tap water and then in sodium hypochlorite (4%)-NaOCl (HiMedia, India), H_2O_2 (3%)-hydrogen peroxide (HiMedia, India) solution for the removal of surface microorganisms (Schulz et al., 1993). Leaves were cut into small pieces (0.5 cm × 0.5 cm) by sterile blades and were flamed in a spirit burner for surface drying after emerging in 70% alcohol for 5–10 s. In total, 150 explants were placed on water agar Petri plates (Borosil, India) and incubated in a BOD incubator (SN Solutions, India) at 30°C for 3 to 5 days. The effectiveness of this sterilisation and isolation process was cross-checked by the explant imprintation technique described by Schulz et al. (1993). After 48 to 72 h of incubation, the endophytic fungal hyphae emerge from explant tissues. Agar blocks with fungal hyphae were transferred to a Potato Dextrose Agar (PDA; HiMedia, India) medium for further identification studies. Approximately, 150-μg ml^{-1} of streptomycin was mixed

with agar plates to avoid bacterial contamination. Isolates were characterised based on their morphology using light (Primo Star, Zeiss, Germany) and a stereo-microscope (Stemi 508, Zeiss, Germany). The colonisation frequency of each isolate, along with diversity indices like Shannon–Wiener, Simpson's dominance, Simpson's diversity, and species richness, was also calculated, following standard methods (Simpson, 1951; Hata and Futai, 1995; Gond et al., 2012).

Molecular Identification of the Most Potent Isolate

Endophytic fungi were subjected to rDNA-based molecular identification according to the standard protocols (Mahapatra and Banerjee, 2012). Partial sequencing of ITS1, a large subunit of ribosomal RNA gene along with a complete sequence of 5.8S ribosomal RNA and ITS2, was done. Further analysis was done using the 552-base pair of the consensus sequence. Sequences were submitted to GenBank. The sequences obtained in this study were compared to the GenBank database using BLAST. Fourteen sequences, including HelS1, were selected and aligned using the multiple alignment software program Clustal W, and the phylogenetic tree was constructed using MEGA 10 (Tamura et al., 2007).

Koch's Postulation Test for Confirmation of the Endophytic Nature of the Selected Isolate

Several *H. isora* plants were selected and transplanted to the Vidyasagar University greenhouse facility. Leaves were pinpricked two to three times in each of many leaves, and the leaf surfaces were inoculated with a fungal suspension of 10^8 spores ml^{-1}. Another set of uninoculated leaves was treated in the same manner but without the introduction of the endophytic fungal spore suspension. The plants were placed at 23°C in 100% relative humidity for 7–9 days and then checked for the occurrence of symptoms. Re-isolation of the putative endophyte was done in the same manner (from the surface-sterilised leaves) as described earlier for endophytic fungal isolation, and reisolated fungi were identified based on cultural and morphological characters (Strobel et al., 2011).

Antibacterial Activity of Cell-Free Supernatant of Endophytic Fungi

Screening of Endophytic Fungal Isolates for Production of Antibacterial Compounds

To detect the potent endophytic fungi with antibacterial activity, isolates were grown in 100 ml of PDB (Potato Dextrose Broth, HiMedia, India) for 5–8 days at 28°C, with a mild agitation of 125 rpm in dark conditions. Periodically, at an interval of 2 days, 10 ml of fungal culture broth was withdrawn, and cell-free supernatant (CFS) was prepared by filtering it using a muslin cloth, followed by centrifugation (10,000 rpm for 10 min) in a Remi R24 centrifuge, India. CFS was assessed for antibacterial activity by a disk diffusion technique against a wide range of both Gram-positive; *B. cereus* (ATCC, 14579), *B. subtilis* (ATCC, 11774), *Staphylococcus aureus* (ATCC, 29213), MRSA (ATCC, 33591), *Staphylococcus epidermidis* (MTCC, 2639), *Listeria monocytogenes* (MTCC, 657), and Gram-negative; *Shigella flexneri* (MTCC, 1457), *Shigella dysenteriae* (ATCC, 13313), *Klebsiella pneumoniae* (ATCC, 75388), *P. mirabilis* (ATCC, 12453), *P. aeruginosa* (ATCC, 9027), *V. parahaemolyticus* (ATCC, 17802), *E.* coli (MTCC, 4296) pathogenic microorganisms. Approximately, 5-mm diameter sterile disks were soaked with 50 μL of culture filtrate and were placed at the MHA (Mueller Hinton Agar, HiMedia, India) plates inoculated with test microorganisms and incubated at 37°C. After 24 h, zones of inhibition (in mm) were observed, and diameters were measured. Streptomycin, clindamycin, vancomycin, and ciprofloxacin (HiMedia) were used as standard antibiotics.

Physico-Chemical Characterization of Antibacterial Compounds

The cell-free supernatant (CFS) of the most potent antibacterial producer HelS1 was kept in a boiling water bath for 10 min to check its thermostability. Furthermore, to detect the proteinaceous nature of the antibacterial components, CFS- was treated with proteinase K (Thermo Scientific, United States) at a concentration of 1 mg ml^{-1} for 2 h at 37°C. The antibacterial activity of both heat-killed and proteinase-K-treated cell-free supernatant was studied against the pathogenic bacteria by the disk diffusion method with appropriate control (Fernandez-Garayzabal et al., 1992).

Extraction of Endophytic Fungal Metabolites

Based on the maximum antibacterial production, PDB was selected as the most suitable medium for fungal culture and solvent extraction. HelS1 was inoculated in 1 L of PDB in a 2-L Erlenmeyer flask at 28°C for 12 days, and CFS was obtained by filtering the broth with muslin cloth, followed by centrifugation (10,000 rpm for 15 min). For every 100 ml of the CFS, 200 ml of ethyl acetate (EA, HiMedia) was added and shaken vigorously for 30 min using a magnetic stirrer, and the EA layer was separated using a separating funnel. A Vacuum Rotary Evaporator (Bacca Buchi, Switzerland) was used to evaporate the excess EA. The remnants were suspended in DMSO (dimethyl sulphoxide, HiMedia, India) and stored for further bioactivity studies.

Determination of Minimum Inhibitory Concentrations and Minimum Bactericidal Concentration

Antibacterial activities of EA fraction of HelS1 CFS were determined against both Gram-positive and Gram-negative bacterial pathogens by a disk diffusion technique as described earlier (Bauer, 1966). EA fractions were dissolved in DMSO in different concentrations, and 15.62 μg ml^{-1} to 4 mg ml^{-1} of culture extract was prepared according to the broth micro-dilution method for the determination of MIC and minimum bactericidal concentrations (MBC) values in a 96-well round-bottom microtitre plate (Merck, Germany), following the guidelines of Clinical and Laboratory Standards International (CLSI). In the case of the MIC assay, 100 μL of fractions with varying concentrations

(0.195 μg ml^{-1} to 3.2 mg ml^{-1}) was added to 100 μL of MHB (1.5×10^8 CFU ml^{-1} prepared according to the 0.5 McFarland turbidity standard) in wells. Antibiotic ciprofloxacin and MHB (containing bacteria only) were selected as positive control and negative control, respectively. The plate was incubated at 37°C for 24 h. Quantification of the optical density in each well was carried out using a microplate reader (ROBONIK readwell Touch ELISA Plate Analyser, India). Wells showing zero growth on the plate were referred to as MBC.

Preparation of a Time-Kill Curve

The killing kinetics experiment was performed following the standard guidelines (Lorian, 2005). Fresh bacterial cultures of four pathogenic microorganisms; – MRSA, *S. epidermidis*, *V. parahaemolyticus*, and *S. flexneri* were prepared separately in MHB and were suspended in sterile saline water. The culture turbidity was adjusted at 0.5 McFarland's standard for inoculation. The suspension was diluted further to obtain an inoculum of 5×10^7 CFU ml^{-1}. DMSO that dissolved EA extract (HelS1 CFS) was prepared in different concentrations (MIC/2-half of MIC, MIC, MIC×2-double of MIC, MIC×4-four times of MIC) and was added to different flasks, containing a bacterial suspension of MRSA, *S. epidermidis*, *V. parahaemolyticus*, *S. flexneri* separately. In total, five sets of bacterial samples along with different concentrations of fungal EA were prepared for each bacterium. No addition of the fungal extract to a flask indicates the negative control. Bacterial cultures were harvested at different time intervals from the experimental setup and in total five-time points (0, 2, 4, 6, and 24 h) were selected for sampling, following centrifugation at 37°C at 110 rpm. The samples were serially diluted and re-cultured in the Muller Hinton agar and then incubated overnight at 37°C. To determine log CFU values, the plotted graph was defined as bactericidal or bacteriostatic based on the CFU reduction at various time intervals. The compounds were said to be bactericidal if they exhibited $\geq$ 3 log CFU (a colony forming unit) reduction and bacteriostatic if they exhibited <3 log CFU reduction.

Estimation of the Release of Intracellular Components From Pathogenic Cells

To check the effects of EA fraction of HelS1 on bacterial cell membrane permeability or cellular integrity, the release of intracellular macromolecules, i.e., protein, nucleic acid, and K+ ions on the extracellular environment, was checked. Gram-positive bacteria MRSA, *L. monocytogenes*, and Gram-negative bacteria *Pseudomonas aeruginosa* and *V. parahaemolyticus* were grown (OD620 nm = 0.5) in 250-ml MH broth, and bacterial cells were harvested by centrifuging the culture broth for 10 min at 6,000 rpm. The cell pellets were taken and washed two times with a 50-mM Na-P buffer (pH, 7.). The cell pellets were resuspended in 1 ml of the same 50-mM Na-P buffer. Then, the pellets were treated with EA extract of HelS1 at its MIC and MBC values. After 6 and 24 h of incubation, the complete solution was centrifuged at 10,000 rpm for 10 min to obtain the cell-free extracts. Protein and DNA concentrations in the mixture were determined following the methods of Lowry et al. (1951) and Burton (1956), respectively, using a Shimadzu UV 1800 spectrophotometer (Japan). K^+ ions concentration was calculated using a flame photometer (Elico, CL-378, India), with K_2HPO_4 (Merck, Germany) as a standard. The set that was only treated with DMSO was considered as a control.

Study of the Effect of Ethyl Acetate Fraction on Bacterial Key Enzymes

Four different Gram-positive and Gram-negative bacterial pathogens, MRSA, *L. monocytogenes*, *V. parahaemolyticus*, and *Pseudomonas aeruginosa*, were treated with the EA fraction of HelS1, respectively (MIC and MBC) for 24 h. The cells were harvested by centrifugation at 6,000 rpm for 10 min. Then, the harvested cells were washed with Na-P buffer solution (20 mM) and again suspended in 1 ml of the same buffer. After that, the cells were ruptured (using sonicator- Labsonic M) to obtain the cell-free extracts. Finally, the supernatants were collected by centrifugation at 10,000 rpm for 10 min and used as a crude enzyme. The most three physiologically valuable enzymes, FBPase (fructose-1,6-bisphosphatase), PFK (phosphofructokinase), and ICDH (isocitrate dehydrogenase), were assayed following the methods of Mandal and Chakrabarty (1993). Other necessary components, such as substrate, enzymes (cell-free extracts of individual bacterial pathogens), and co-factor, were mixed in a cuvette. The rate of NADP reduction was followed at 340 nm in a UV-Vis spectrophotometer (Shimadzu UV-1800). The specific activity was calculated as nanomoles of substrate consumed per minute per mole protein and compared to the untreated control.

Study of Inhibition of Biofilm Formation

Biofilm formation of the bacterial pathogens was tested using a 24-well polystyrene cell culture plate. One milliliter of MH broth was poured into each well and then inoculated with a 1% fresh culture of bacterial pathogens. The EA fraction of HelS1 (dissolved in 10% sterilised DMSO) was added at different concentrations to different wells. After an incubation of 48 h at 27°C, the broth was decanted from every well and then washed with sterilised distilled water without hampering the biofilm formation. After that, each well was dried and then washed gently with sterilised water without disturbing the biofilm. Next, the wells were stained with 1 ml of 0.1% crystal violet (SRL) and kept at room temperature for 10 min. The crystal violet stain was washed, and 1 ml of 33% acetic acid (SRL) was added to each well and then kept for 30 min at room temperature, providing mild agitation to extract the bound crystal violet from bacterial cells. The optical densities (OD) of acetic acid solution were then measured at 595 nm using a UV-vis spectrophotometer. The inhibition of the biofilm was determined according to the formula [60]% inhibition of biofilm formation = 100 – [(OD570 of sample/OD570 of control) * 100]. The biofilm formation was classified at three levels: the highest one (OD570 $\geq$ 1), intermediate (0.1 $\leq$ OD570 < 1), and no formation of biofilm (OD570 < 0.1).

Synergistic Activity of Ethyl Acetate Fraction of HelS1 and Antibiotic Ciprofloxacin

The synergistic antibacterial activity of the HelS1 EA fraction and broad-spectrum antibiotic ciprofloxacin against MRSA were tested, following the checkerboard method proposed by Orhan et al. (2005) with slight modifications. The EA fraction of the endophytic fungi HelS1 (0–1,000 $\mu g\ ml^{-1}$) and the most effective antibiotic ciprofloxacin (0–100 $\mu g\ ml^{-1}$) were used at variable combinations. A total of 1 ml of MH broth was taken to a 1.5-ml microcentrifuge tube and then inoculated with 1% MRSA culture (OD620 nm = 0.5). HelS1 EA extract and ciprofloxacin were mixed at variable combinations. The mixture was incubated at 28°C for 48 h. The cell pellets were drawn after centrifugation for 10 min at 6,000 rpm and washed thoroughly two times in a 50-mM Na-P buffer. Next, the bacterial cells were suspended in 1 ml of the same buffer, and the OD values were measured at 620 nm to quantify the cellular amounts. To calculate the ΣFIC (fractional inhibitory concentration), different OD values were placed on the checkerboard. ΣFIC was calculated by the following formula, ΣFIC = FIC of EA fraction + FIC of ciprofloxacin, where the FIC of the EA fraction or ciprofloxacin = MIC of the EA fraction or ciprofloxacin in combination/MIC of the EA fraction or ciprofloxacin alone. The combination of endophytic culture extract and ciprofloxacin was considered antagonistic when ΣFIC >4, synergistic when ≤ 0.5, and indifferent when >0.5 (Prinsloo et al., 2008).

Optimisation of Culture Conditions for the Production of Maximum Antibacterial Metabolites

The valuable growth parameters like incubation temperature, incubation time, medium p^H, additional carbon, nitrogen, and salt sources, and their most suitable concentration for optimum growth are measured using the OVAT (one variable at a time) system. Furthermore, the RSM (response surface methodology) technique was adopted by BBD (Box Behnken Design) to find out the most valid statistical model for maximum production of antibacterial components (Mahapatra and Banerjee, 2013).

The Anti-fungal Potential of Endophytic Fungi

Anti-fungal Action of Endophytic Fungal Volatile Organic Compounds

The isolates were further checked for their antifungal VOCs (volatile organic compounds) production against selected pathogens; *Rhizoctonia solani* (MTCC-4634), *Alternaria alternata* (MTCC-3793), *Fusarium oxysporum* (MTCC-284), *Geotrichum candidum* (MTCC-3993), *Botrytis cinerea* (MTCC-8659), *Cercospora beticola* (ATCC-12825), *Aspergillus fumigatus* (MTCC-3785), *Ceratocystis ulmi* (ATCC-32437), *Pythium ultimum* (ATCC-200006), following a bioassay method proposed by Strobel et al. (2001). Antifungal VOC production was checked at different time intervals (after 4th, 5th, 6th, and 7th days). A 1-cm wide strip of agar was cut off from the center of a standard Petri plate (100 mm × 15 mm) of PDA, forming two halves of agar. Endophytic fungi were inoculated onto one side of the plate (half-moon agar) and incubated at 24°C for 4–8 days for maximum production of bioactive VOCs. Test pathogenic fungi were inoculated on the other half-moon agar side of the Petri plate from the 4th until the 8th day. Petri plates were then wrapped for two-three times with parafilm and incubated at 24°C for 48–96 h. The growth of filamentous fungi was quantitatively assessed based on multiple measurement criteria of growth relative to control. Tests were conducted in triplicate.

Calculation of IC_{50} Values of an Artificial Mixture of Volatile Organic Compounds

The artificial mixture of authenticated VOCs was made by mixing the standards of volatiles purchased from Sigma in a particular ratio (following the relative ratio of VOCs emitted from endophytic *Curvularia eragrostidis* HelS1). The artificial mixture of VOCs was poured into a pre-sterilised micro cup (4–6 mm) and placed in the center of a PDA Petri plate. Agar blocks (5 mm × 5 mm × 5 mm) with pathogenic fungal hyphae were placed on the Petri plate at a 2.5-cm distance from the VOCs containing a micro cup, and they were wrapped with two layers of Parafilm. Mycelial growths were measured after 48 h of incubation. Control plates lack artificial mixtures. Tests on 2–40 μL of the artificial mixture per 50 ml of air space above the mycelial culture in the PDA plate were performed on four replicates, and IC50 values were calculated.

Optimization of Culture Media for Maximised Volatile Organic Compounds Emission

Endophytic fungi were grown on basal media with alterations in carbon and nitrogen sources to optimize the maximum production of VOCs. At first, a 5-mm fungal block was transferred to different media compositions like different nitrogen sources-beef extract, tryptone, peptone, yeast extract, and different carbon sources-cellulose, dextrose, and malt extract. The emission of naphthalene (the highest occurrence amongst other volatiles) was assessed qualitatively due to its moth ball-like odor. A rating of 0–5 has been assigned to each media composition based on olfactory observations of VOCs made by five different individuals [23]. The media compositions that were used for the VOC emission assay are as follows; -**1**- Beef extract, 0.2 g L^{-1} with salts; **2**- Tryptone, 0.2 g L^{-1} with salts; **3**- Peptone, 0.2 g L^{-1} with salts; **4**- Yeast extract, 0.2 g L^{-1} with salts; **5**- Yeast extract, 0.2 g L^{-1} with salts plus cellulose, 40 g L^{-1}; **6**- Tryptone with salts plus cellulose, 40 g L^{-1}; **7**- Yeast extract, 0.2 g L^{-1} with salts plus dextrose, 40 g L^{-1}; **8**- Tryptone, 0.2 g L^{-1} plus dextrose, 40 g L^{-1}; **9**- Yeast extract, 0.2 g L^{-1} plus malt extract, 40 g L^{-1}; **10**- Tryptone, 0.2 g L^{-1} plus malt extract, 40 g L^{-1}; **11**- Potato Dextrose Agar (PDA) (Hi-Media); **12**- Potato Carrot Agar (PCA) (Hi-Media); **13**- Oatmeal Agar (OA) (Hi-Media); **14**- instant smashed potato dextrose agar (potato, 4 g L^{-1}, dextrose-20 g L^{-1}); **15**- modified PDA (instantly smashed potato, 4 g L^{-1}; yeast extract and urea, 0.2 g L^{-1}; dextrose, 40 g L^{-1}); **16**- modified CDA (yeast extract and urea, 0.2 g L^{-1}; dextrose, 40 g L^{-1}); **17**- modified oatmeal (yeast extract and urea, 0.2 g L^{-1}; dextrose, 40 g L^{-1}). In each case, agar and salt

concentrations were maintained according to the modified M1-D medium (Pinkerton and Strobel, 1976). All the materials used for media preparation were purchased from SRL and HiMedia.

Identification of the Bioactive Compounds

Thin Layer Chromatographic Analysis of Ethyl Acetate Fraction

Partial purification of the bioactive metabolites of the HelS1 extract was performed using thin-layer chromatographic techniques. The dried fungal extract was resuspended in EA, maintaining a concentration of 20 mg ml^{-1}, and 10 μL of EA extract was loaded onto alumina–silica Thin Layer Chromatographic (TLC) plates (MERCK Silica gel F254) using capillary glass tubes. Acetone (HiMedia) and n-hexane (HiMedia) in a ratio of 2:8 were used as running solvent, and the retention factor was calculated for all the bands under UV light using a Camag UV Cabinet. The bioactive compounds corresponding to each band were scratched and collected and were finally dissolved in 1 ml of EA, which was centrifuged (7,000 rpm for 15 min) and evaporated to dryness. The dried components were then dissolved in DMSO at 100 μg ml^{-1} concentration, and antibacterial action was measured by disk diffusion technique (Wang et al., 2014).

Gas Chromatography-Mass Spectrometry Analysis of the Antibacterial and Antifungal Metabolites

The active fractions obtained from TLC analysis were analysed using Gas Chromatography (TRACE 1300)-Mass (ISQ QD Single Quadrupole) Spectrometry (GC-MS) system- Thermo Scientific (USA, Waltham, MA, United States) with an ESI mode. The instrument was configured with a DB-5 Ultra Inert column (30-m length and a 0.25 mm inner diameter) for a 22-min run of a 1 μL sample (a split-less flow) with an injector port and oven temperature of 240 and 50°C, respectively, having 10°C min^{-1} ramping time up to 260°C with helium as the carrier gas. Tri-plus RSH-based automated injection was done. The flow velocity of the carrier gas was set at 1 ml min^{-1}. The ionisation source was kept at 250°C with 70 eV of ionisation energy and 0.1 kV ionisation current. The mass fragmentation pattern was analysed by X-Calibur software. The identification of the various compounds was based on the SI and RSI value with the best-matched compound in the NIST library (Tomsheck et al., 2010).

Qualitative analyses of the volatiles emitted by the fungal endophyte were done using the Solid Phase Microextraction (SPME) fibre technique (Mitchell et al., 2009). The endophytic fungus was grown on a 50 ml gas vial (Thermo Scientific, United States), containing 5 ml of modified PDA (described previously) media, forming a slant and was incubated for 8 days at a temperature of 24°C. At first, the inoculated GC-Glass vial was heated at 40°C for 45 min in the incubation cabinet attached to the Tri-Plus RSH autosampler unit of the GC-MS instrument. The incubation cabinet was provided with mild agitation in clockwise and anti-clockwise orientations (five agitations per minute). Then, a baked SPME syringe (Supelco), consisting of 50/30 divinylbenzene/carburen on polydimethylsiloxane on a stable flex fibre, was injected into the GC-Gas vials through the magnet-based rubber cap and was exposed to the vapour phase for 45 min. The SPME fibre was then injected into the splitless injection port of the system, containing the ZB-Wax column (a 30 m diameter, a 0.25 mm inner diameter, 0.50 mm thickness). The column was set at 30°C for a 2-min hold, followed by an increase to 225°C at 5°C min^{-1}. Helium was used as the carrier gas with a flow velocity of 1 ml min^{-1}. Additionally, the column head pressure was maintained at 50 kPa. The SPME syringe was conditioned at a temperature of 240°C for 25 min under a flow of helium gas (1 ml min^{-1}). A 30 s injection time was used to introduce the sample fibre into the system. Bioactive components were identified following the NIST library databases and listed in the NIST terminology. The authenticity of the compounds was made according to the GC/MS of authentic standards (Sigma–Aldrich). Compounds that were not identified using the NIST library match were identified as the NIST library database only when they provide a quality score of 60 or better. Experiments were repeated two times.

Statistical Analysis

All experiments were performed in triplicate, and the results are presented as means ± standard errors (SE). Data were analysed by Prism GraphPad software version 9.2.0 (332) (San Diego, CA, United States). Minitab (version 20.2) statistical software was used for response surface methodology experiments (Box–Behnken design).

RESULTS

Identification of the Isolates and Selection of the Potent Endophytic Fungi

In total, eight endophytic fungi were isolated from the leaf samples of the *Helicteres isora* plant. The non-epiphytic nature of the fungal isolates was confirmed by the tissue fingerprinting method. Briefly, the aliquots with wash liquid of the explants were plated on PDA, and there was no occurrence of any endophytic fungi. The endophytes were non-pathogenic as they were isolated from healthy disease-free plants. Further confirmation was provided by Koch's Postulate results. There were no disease symptoms developed after inoculation of the endophytic fungi onto the *H. isora* host plant.

In total, 107 endophytic fungal taxa were obtained from the 150 samples (explants) of leaf tissues. Eight types of fungi were found, and isolates were identified as two species of Fusarium, one species of Pestalotiopsis, one species of Penicillium, two species of Aspergillus, and two different species of sterile isolates (HelS1 and HelS2). The two sterile isolates exhibited the highest colonisation frequency of 14 and 10.66%, respectively. The lowest colonisation frequency (4.66 and 6%) on the leaf tissues was shown by the two species of Aspergillus (**Supplementary Table 1**, **Supplementary Figure 1**). The diversity of the endophytic community of leaf tissues is represented in tabular form (**Supplementary Table 2**). The results of diversity indices indicate an acceptable range of endophytic fungal diversity in the leaf tissues of the explant.

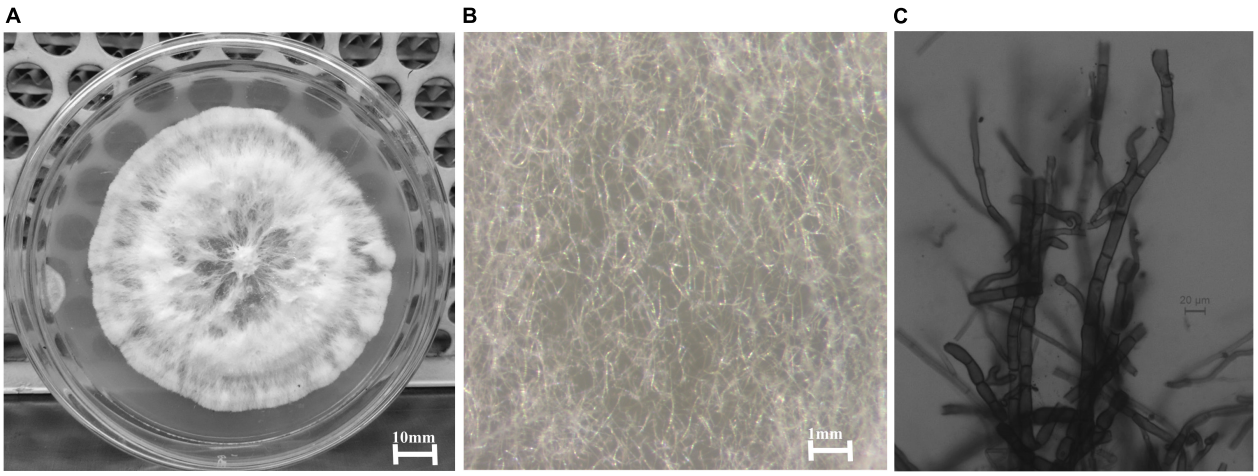

FIGURE 1 | (A) A 6-day old culture of *Curvularia eragrostidis* HelS1 grown on PDA. **(B)** Sterile mycelial hyphae of the isolate seen under a stereo-microscope. **(C)** Septate sterile hyphae seen under a light microscope.

The two isolates did not produce any reproductive structures and remained sterile even after inoculation in a leaf carnation agar medium and remained as unidentified. The isolates were tested for their antibacterial action, and one unidentified (isolate code-HelS1) isolate exhibited the highest antibacterial activity. The sterile isolate (HelS1) was identified as *Curvularia eragrostidis* HelS1 (Gen Bank Acc. No.-ON146362). Plate morphology, along with microscopic morphology, is recorded in **Figure 1**.

Molecular identification involving two primers ITS1 and ITS4, aiming at the conserved regions 28S rDNA and 18S rDNA, respectively, was utilised for the amplification of the ITS1-5.8S-ITS2 region of the endophytic fungal isolate HelS1. The gene products obtained through amplification were further sequenced, and derived results were assured by comparing the sequences against the available Genbank database of NCBI using the BLAST tool. Gaps and missing data were removed from the dataset. There were a total of 552 nucleotides in the final dataset. A phylogenetic tree was constructed to compare the sequence of HelS1 with the existing fungal nucleotide database in Genbank. Evolutionary distances were analysed by using the neighbour-joining method, and bootstrap analysis was performed to construct the phylogenetic tree, which is represented in **Figure 2** (Saitou and Nei, 1987; Tamura et al., 2004). The tree depicts that the endophytic fungal isolate is phylogenetically related to the *Curvularia eragrostidis*, and it is supported by high bootstrap values (72%). Five hundred bootstrapping repetitions were performed for the construction of cladograms. The phylogram constituted was divided into five groups (Felsenstein, 1985). The differentiation of the tree into five groups was based on different species of Curvularia utilised to set up the tree with a high-to-low similarity index. Different strains of five different species of Curvularia (Division-Ascomycota) were involved in constructing the phylogenetic tree, namely, *Curvularia eragrostidis*, *C. kusanoi*, *C. lunata*, *C. aeria*, *C. americana*, *C. pseudobrachyspora*. Another member of Mucoromycota-*Mucor* sp. was taken as the outgroup. The tree starts with *C. eragrostidis* strain T910 along with strains P1262, 195, and LZS52.2 and includes our endophytic isolate HelS1. All these strains are clustered into Group 1, with a high bootstrap value (72%). Groups 2 and 3 contain two species of *C. kusanoi* and *C. lunata*, respectively, whereas *C. aeria*, *C. americana*, and *C. pseudobrachyspora* constitute Groups 4 and 5, respectively. The total branch length of the phylogenetic tree was calculated as 0.73840605. The bioactive endophytic fungal isolate HelS1 evaluated in this study completely matches (a 100% query cover) with *C. eragrostidis* LZS 52.2 and, hence, can be concluded as *C. eragrostidis* HelS1.

Thermostable and Non-proteinaceous Nature of the Metabolites of HelS1

Heat-killed and proteinase K-treated extracts of HelS1 exhibited antibacterial action (in terms of a clear zone of inhibition in mm) same as the untreated one. The control sets containing uninoculated broth and proteinase K (1 mg ml^{-1}) did not exhibit any clear zone of inhibition.

Antibacterial Activity of HelS1 Metabolites

Isolate HelS1 exhibited the maximum antibacterial action and was selected for further antibacterial evaluation. PDB was selected as the most suitable medium for antibacterial production, and EA was selected as the most potent solvent for extraction of antibacterial metabolites. The EA extract of HelS1 exhibited broad-spectrum antibacterial action against 13 Gram-positive (6) and Gram-negative (7) pathogens. MIC and MBC values of EA extract against all the pathogenic microorganisms ranged from 12.5 to 100 µg ml^{-1} and 200 to 400 µg ml^{-1} for Gram-positive and Gram-negative pathogens, respectively (**Table 1**). The EA extract is found to be heavily effective against Gram-positive pathogens than the Gram-negative ones.

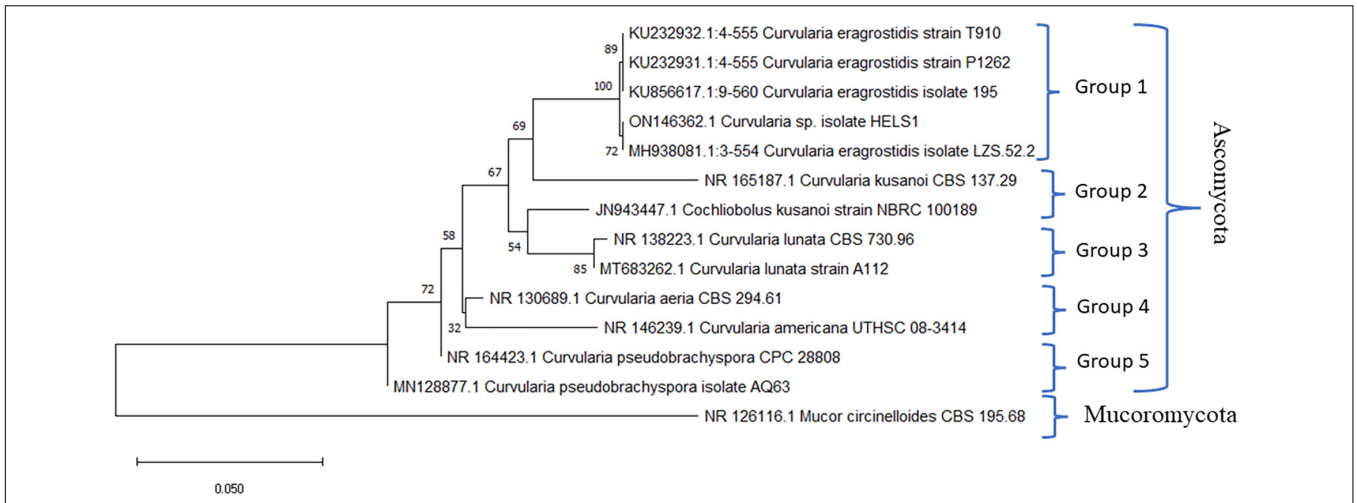

FIGURE 2 | A phylogenetic tree of the endophytic isolate *C. eragrostidis* HelS1.

TABLE 1 | Antibacterial activity-minimum inhibitory concentrations (MIC-μg ml^{-1}) and minimum bactericidal concentrations (MBC-μg ml^{-1}) of EA (ethyl-acetate) culture extract of HelS1 against pathogenic bacteria.

Pathogenic bacteria	MIC (μgmL^{-1})	MBC (μgmL^{-1})
Gram-positive pathogens		
B. cereus (ATCC-14579)	12.5	25
B. subtilis (ATCC-11774)	12.5	25
S. aureus (ATCC-29213)	50	100
Methicillin-resistant *Staphylococcus aureus* (MRSA; ATCC 33591)	100	200
S. epidermidis (MTCC 2639)	25	50
L. monocytogenes (MTCC657)	100	200
Gram-negative pathogens		
S. flexneri (MTCC 1457)	200	400
S. dysenteriae (ATCC 13313)	400	800
V. parahaemolyticus (ATCC 17802)	400	800
K. pneumoniae (ATCC 75388)	200	400
P. mirabilis (ATCC 12453)	400	800
P. aeruginosa (ATCC 9027)	200	400
E. coli (MTCC 4296)	400	800

Time-Killing Kinetics of Bacterial Pathogens Upon Treatment With HelS1 Metabolites

To determine the bacteriostatic or bactericidal nature of antimicrobial components, EA fraction of HelS1 was added into the active mid-log phase culture of MRSA, *S. epidermidis*, *S. dysenteriae*, and *K. pneumoniae* at different concentrations- MIC *O (control), MIC/2 (half of MIC), MIC, MIC*2 (double of MIC), MIC*4 (fourth times of MIC). The control set, which has not received any EA extract treatment, is considered the MIC*0. CFU counting at an interval of 2 h revealed that there was a rapid decline in microbial growth as a result of treatment with the fungal extract. The antimicrobial compounds exhibited 3 log CFU reduction at 100, 25, 400, and 200 μg ml^{-1}, respectively, against MRSA, *S. epidermidis*, *S. dysenteriae*, and *K. pneumoniae* after 12–18 h of treatment in all the cases. The <3 log CFU reduction denotes the MBC of the bioactive compounds. Detailed growth kinetics is represented in **Figure 3**.

Leakage of Intracellular Essential Molecules

Intracellular macromolecules like DNA, protein, and K^+ ions were found to be leaked in the extracellular environment after treatment with HelS1 EA extract, which specifies the cidal action of endophyte-derived bioactive compounds. The cell bursting effect was more massive in Gram-positive pathogens than in Gram-negative ones. There was a 1.5- to-2-fold increase ($p < .001$) of DNA, protein, and K^+ ion contents after 24 h of treatment in comparison to 6-h treatment (**Supplementary Figure 2**). The presence of K^+ ions on the extracellular fluid indicates that the bacterial cell integrity is disturbed upon treatment.

Biofilm Inhibition Potential of HelS1 Metabolites

UV-VIS spectrophotometric measurement of a biofilm after crystal violet staining revealed an inhibition ($p < 0.001$) of biofilm development of pathogenic strains as a result of treatment with HelS1 EA fraction. The pathogens formed a biofilm in the control situation in the absence of any HelS1 EA extract. The anti-biofilm action was maximum against *B. cereus*, *S. epidermidis*, and *S. dysenteriae* followed by other pathogens with an inhibition percentage of 79.08 to 93.09 (**Supplementary Figure 3**).

Ethyl Acetate Fraction of HelS1 Blocks the Energy Metabolism of the Pathogens

The EA fraction of HelS1 directly blocks the actions of necessary enzymes (PFK, ICDH, and FBPase) involved in the central carbohydrate metabolism of bacterial pathogens. Gram-positive pathogens face the worst effect in comparison to the Gram-negative ones. At lethal doses (MBC), the pathogens face a severe

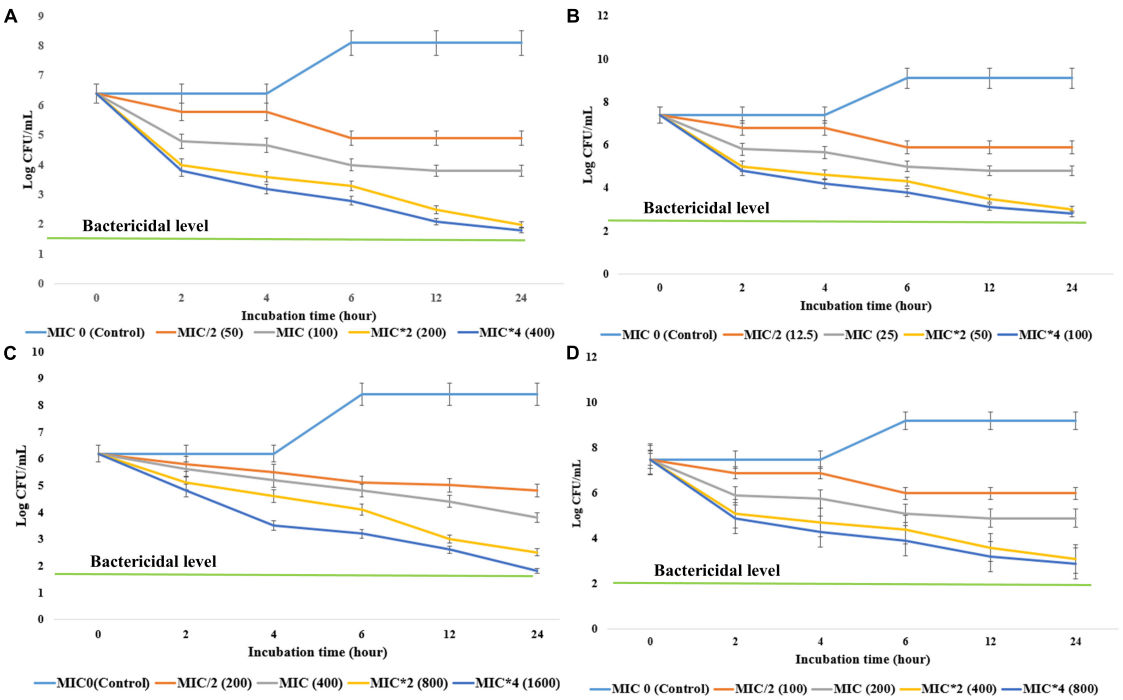

FIGURE 3 | The effect of different concentrations (minimum inhibitory concentrations: MIC/2, MIC, MIC*2, MIC*4) of antibacterial compounds of HelS1 on the growth of bacterial pathogens [**(A)** methicillin-resistant *Staphylococcus aureus* (MRSA), **(B)** *S. epidermidis*, **(C)** *S. dysenteriae*, **(D)** *K. pneumonia*] is represented here in the form of a time-kill curve. The CFUs (colony-forming units) are counted after 0, 2, 4, 6, 8, 10, 12, and 24 h of treatment. Values on the graphs are the means ± standard error (SE) of the three replicates.

stress situation (total blockage in energy metabolism), leading to a drastic reduction in enzymatic activity (**Figure 4**).

Synergistic Activity of Ethyl Acetate Fraction of HelS1 With Standard Antibiotic

Commercially available antibiotic ciprofloxacin, in combination with EA fraction of HelS1 in different concentrations, was tested for synergistic antibacterial action against MRSA. A checkerboard study elucidated that the combination of 6.25 μg ml^{-1} of EA fraction and 0.3 μg ml^{-1} of ciprofloxacin have synergistic activity against MRSA with ∑FIC of 0.425. The other higher combinations of 12.5 μg ml^{-1} (EA fraction) and 0.3 μg ml^{-1} (antibiotic-ciprofloxacin), 25 μg ml^{-1} (EA fraction), and 0.2 μg ml^{-1} (ciprofloxacin) were found to be synergistic too. No combinations were found to be antagonistic in this case. Different OD values in the checkerboard represent the growth of MRSA in different combinations of the two interacting agents (**Table 2**).

Optimisation of the Culture Conditions for the Enhancement of Antibacterial Productions

OVAT optimisation revealed that endophytic HelS1 exhibits maximum antibacterial action when grown on fructose concentration (a carbon source)-7 gm L^{-1}, peptone concentration (a nitrogen source)-4 g L^{-1}, MpH of 6.8 and fermentation time of 8 days, NaCl concentration, 0.5 g L^{-1} (**Supplementary Table 3**). After the OVAT optimisation, RSM technique was applied using a three-level BBD, which involved the most important four factors-peptone concentration, fructose concentration, MpH, and fermentation time to elucidate the optimum antibacterial production by the isolate. The statistical model predicted the maximum antibacterial production at five replicated center points (**Supplementary Table 4**). The following equation was suggested by the statistical design, which provides maximum antibacterial production with minimum utilisation of necessary nutrients. YZOI = $5.3389 - 1.2915x_1 - 1.3967x_2 - 1.0901x_3 - 1.3714x_4 - 1.2567x_1x_2 - 1.3698x_1x_3 + 1.1459x_1x_4 - 1.3789x_2x_3 + 1.3273x_2x_4 - 1.1336x_3x_4 - 1.6566x_1^2 - 1.6395x_2^2 - 1.5041x_3^2 - 1.8542x_4^2$. x_1, x_2, x_3, and x_4 are the coded factors of fructose concentration, peptone concentration, medium-pH, and fermentation time, respectively. The goodness of fit of RSM and experimental outputs were evaluated by regression analysis (**Supplementary Table 5**). Contour and 3D plots were created by Minitab to focus on the different variables for the optimum antibacterial action (**Supplementary Figure 4**). It was found that there was an ignorable marginal deviation between the observed 22.33 ± 0.58 (mm) and predicted 22.66 ± 0.58 (mm) antibacterial response, following the model's proposed fermentation conditions - fructose concentrations (6.868 g L^{-1}), peptone concentrations (3.791 g L^{-1}), M-pH-6.75, and fermentation time of 191.5 h.

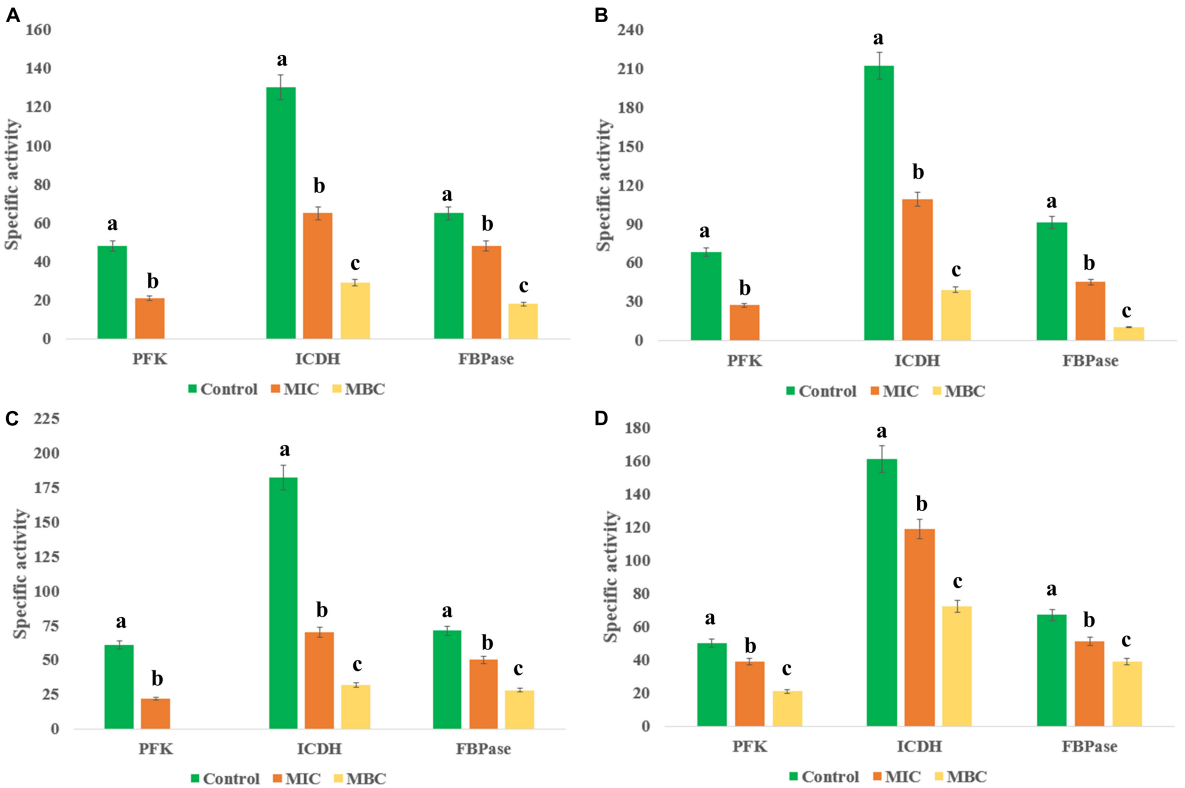

FIGURE 4 | Effect of different concentrations of HelS1 ethyl acetate (EA) extract on the essential enzymes of microorganisms (**A** MRSA, **B** *L. monocytogenes*, **C** *V. parahaemolyticus*, and **D** *P. aeruginosa*) involved in central energy (carbohydrate) metabolism. Values on the graphs are the means ± standard error (SE) of the three replicates. Tukey's multiple comparison test was performed. The different letters a, b, and c in each case [Control, MIC, minimum bactericidal concentrations (MBC)] represent a significant difference between them (At, $p < 0.05$).

Antifungal Activity of HelS1 Volatile Organic Compounds

Volatile Organic Compounds of HelS1 exhibited anti-fungal action against a variety of pathogenic fungi from broad taxonomic groups like ascomycetes, basidiomycetes, and oomycetes (**Table 3**). HelS1 derived-VOCs expressed varying degrees of inhibition in plate assays against eight fungal pathogens. Maximum inhibitory effect (varied between 31.9 and 70.9%) of the VOCs was detected after 7 days of growth of HelS1 endophytic fungi (**Figure 5**). Out of eight test fungi, *F. oxysporum* (70.9%) and *G. candidum* (67.1%) were found to be maximally inhibited by the VOCs. Other pathogens (*P. ultimum*, 61.1%; *B. cinerea*, 54.9%; *R. solani*, 51.1%) were also inhibited in a moderate range. There was no inhibition for *C. beticola*, and *C. ulmi*, and minimum inhibition against *A. fumigatus* and *A. alternata*. VOCs of HelS1 are found to be biologically selective.

TABLE 2 | Checkerboard-based representation of the cumulative effect of ethyl acetate (EA) fraction of HelS1 and antibiotic ciprofloxacin on the growth of methicillin-resistant *Staphylococcus aureus* (MRSA).

Ciprofloxacin (μgmL^{-1})	0.9	0.009	0	0	0	0	0	0
	0.7	0.059	0	0	0	0	0	0
	0.5	0.101	0	0	0	0	0	0
	0.3	0.4	0.32	0	0	0	0	0
	0.2	0.541	0.496	0.374	0.358	0	0	0
	0.1	0.689	0.598	0.402	0.376	0.296	0.198	0
	0	0.729	0.601	0.5	0.409	0.319	0.207	0
		0	3.125	6.25	12.5	25	50	100
		EA extract of HELS1 (μgmL^{-1})						

Effect of Substrate on Volatile Organic Compounds Production

Endophytic HelS1 was grown on several solid media (with changing nitrogen and carbon sources) to check the maximum production of bioactive volatiles. The VOCs were of characteristic odour due to maximum occurrence of naphthalene and azulene compounds, which smell like mothball. The increase in relative amounts of naphthalene and azulene emits a higher frequency of mothball-like odour, which is tested by five different lab-associated persons with a different olfactory score of 0–5. Finally, the most suitable media with a high olfactory score were designated as the most suitable VOC-emitting solid media for the selected isolate HelS1 (**Table 4**). Modified PDA (instantly smashed potato, 4 g L^{-1}; yeast extract; urea, 0.2 g L^{-1}; and dextrose, 40 g L^{-1}) with necessary salts was found to be the most suitable media composition for maximum VOCs emission.

TABLE 3 | Anti-fungal activity of an 8-day old endophytic fungus against selected fungal pathogens.

Fungal pathogens	Inhibition (%) after 168 h of treatment[a]	IC_{50} of artificial atmosphere after 72 h of treatment (μL 50 mL^{-1})	IC_{50} as μL mL^{-1} of air space needed for 50% inhibition[b]
Geotrichum candidum	67.1 ± 0.8	13.8 ± 0.7	0.276
Botrytis cinerea	54.9 ± 1.0	22.8 ± 0.5	0.456
Cercospora beticola	No inhibition	No inhibition	–
Rhizoctonia solani	51.1 ± 0.7	21.8 ± 0	0.436
Pythium ultimum	61.1 ± 0.9	13.6 ± 0	0.272
Fusarium oxysporum	70.9 ± 1.9	11.1 ± 0.1	0.222
Aspergillus fumigatus	33.39 ± 0.7	25.2 ± 0.6	0.504
Alternaria alternata	31.9 ± 1	29.2 ± 0.9	0.584
Ceratocystis ulmi	No inhibition	36.0 ± 1	0.72

[a]*Antifungal action was calculated as a percentage of pathogenic fungal growth inhibition relative to the growth of the same pathogenic fungi under control conditions.*
[b]*Concentration of VOCs' artificial mixture (prepared with standards) in microlitres per millilitre of air space required to produce a 50% reduction of the pathogenic test fungi.*

TABLE 4 | Effect of medium compositions on VOCs production by endophytic fungi with qualitative olfactory observations obtained from independent ratings of 0–5, 5 being the maximum.

Medium composition	Independent olfactory score (0–5)
Beef extract	1
Tryptone	1.5
Peptone	0
Yeast extract	1.5
Yeast extract + Cellulose	2.5
Tryptone + Cellulose	2.5
Yeast extract+ Dextrose	3
Tryptone + Dextrose	3
Yeast extract + Malt extract	2.5
Tryptone + Malt extract	2.0
PDA	3
CDA	3.5
Oatmeal	3
Instantly smashed Potato +dextrose agar	
Modified PDA	5
Modified CDA	4
Modified Oatmeal	3

Evaluation of IC_{50} Value of the Artificial Volatile Organic Compounds Mixture

Volatile organic compounds emitted by endophytic HelS1 were detected, and some of those selected chemicals were mixed in a proper ratio (as emitted by the endophyte and recorded by the GC-MS). Chemicals (whose standards were available) like 4-thujanol, naphthalene, 1,2-ethyl isobutyrate, undecane, azulene, and propionic acid were mixed in an exact ratio, and IC_{50} (in the complete air space of the test Petri plate) value of that artificial mixture was determined. The IC_{50} value was calculated, which ranged between 11.1 μg ml^{-1} and 36 μg ml^{-1} for 50% inhibition

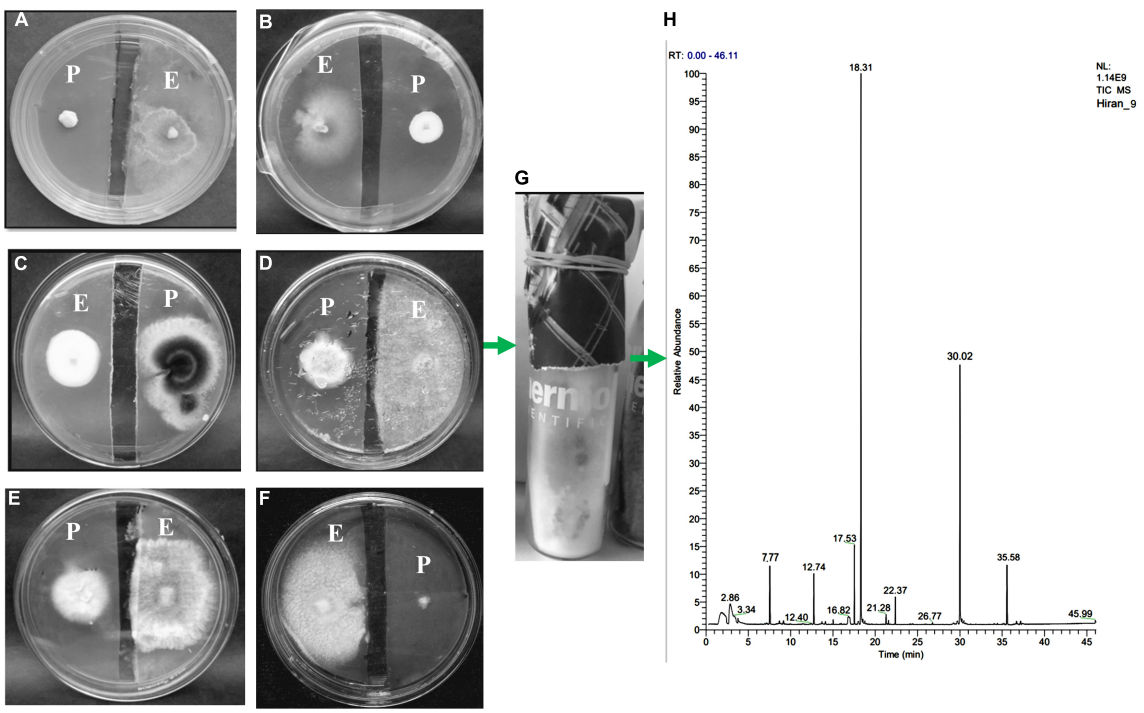

FIGURE 5 | An antifungal gas test performed by a split plate method **(A–F)**. The growth of pathogenic [**(A)** *Geotrichum candidum*, **(B)** *Botrytis cinerea*, **(C)** *Cercospora beticola*, **(D)** *Rhizoctonia solani*, **(E)** *Pythium ultimum*, **(F)** *Cercospora beticola*] fungi has been inhibited by the VOCs of endophytic fungi HelS1 (except in one case-C). **(G)** Represents how endophytic fungi are grown on GC-glass vials for VOC analysis. **(H)** GC-chromatogram of the VOCs produced by the endophytic HelS1.

of the pathogenic fungal growth (**Table 3**). There was complete inhibition of fungal growth (except *C. beticola*) when 65 μL of the artificial mixture was introduced. The requirement of an artificial mixture for 50% inhibition of mycelial growth varied from organism to organism. Growth of *G. candidum*, *P. ultimum*, and *F. oxysporum* was found to be 50% ceased at a concentration of 13.8, 13.6, and 11.1 μL, respectively, which represents the high sensitivity of the test pathogens toward the artificial mixture. Likewise, these three pathogens were also maximally sensitive to VOCs of HelS1. Another test fungi (*R. solani*, *B. cinerea*, and *A. fumigatus*) with moderate IC_{50} values of 21.8, 22.8, and 25.2 μL also exhibited moderate sensitivity to the VOCs of HelS1. But, in the case of *C. ulmi*, there was 50% inhibition of mycelial growth at 36 μL of artificial mixture, whereas the fungal VOCs were unable to inhibit its growth. Again, in the case of *A. alternata*, the fungal VOCs were found to be more efficient in comparison to the artificial mixture in terms of growth inhibition (high IC_{50} value). The fungal VOCs, as well as the artificial mixture, were ineffective against *C. beticola*.

Thin Layer Chromatographic Analysis and Antibacterial Action of the Active Fractions

Ethyl acetate fraction of HelS1 revealed six different bands under UV light (366 nm) after TLC analysis (**Figure 6**). Each fraction from six different bands was tested for antibacterial action, and bands A and B with an Rf value of 0.68 and 0.4, respectively, expressed antibacterial action against MRSA with a clear zone of inhibition of 17 and 21 mm.

Detection of Bioactive Components

Bioactive compounds present on both the bands (A and B) of TLC with antibacterial activity were identified by the GC-MS-NIST library (**Figure 6**). **Tables 5**, **6** represent all the compounds along with their respective RT (retention time), area percentage, quality score, MW (molecular weight), and chemical formula. The chemical structures of the bioactive compounds along with their mass spectra are represented in **Supplementary Figure 5**. The compounds present in the band A are 1-H-indene 1 methanol acetate (26.44% with an RT of 9.81 min and a quality score of 96), tetroquinone (15.29% with an RT of 8.77 min and a quality score of 91.29), eucalanone (12.39% with an RT of 6.82 min and a quality score of 95.08), etc. Other compounds are methyl benzoate, ethyl benzoate, 3-butyn-1-ol, cholan-16-one, and ethanol (**Table 4**).

Band B contains *N*, *N*-diphenyl-2-nitro-thio benzamide (18.25% with an RT of 19.48 min and a quality score of 98), *Trans* 1, 2-diethyl-trans-2-decalinol (17.11% with an RT of 19.36 and a quality score of 87), 1,2-benzene dicarboxylic acid diethyl ester (17.11% with an RT of 9.23, with a quality score of 97), etc. Other compounds are 2, 4-dimethyl benzaldehyde, ethyl decanoate, ethoxysympathol di PFP, and cholan-6-on, 23-methyl- (**Table 6**).

The SPME analysis revealed the occurrence of volatile compounds like naphthalene (47% with an RT of 18.31 min), azulene (22.54% with an RT of 30.02 min), 4-thujanol (7.04% with an RT of 17.53 min), propionic acid (5.63% with an RT of 35.58 min), benzene, 1, 3 dimethyl (4.7% with an RT of 12.74 min) (**Table 7**). Other compounds are undecane, 1,2-ethyl iso-butyrate, etc (**Figure 5**).

DISCUSSION

Antibacterial Activity of *Curvularia eragrostidis* HelS1 Metabolites Against Human Pathogenic Bacteria

In the modern world, antimicrobial resistance is one of the prime problems that need efficient handling strategies. The conventional antibiotics (like aminoglycosides, chloramphenicol, fluoroquinolones, macrolides, and tetracycline) are losing their efficacy; organisms are evolving as multi-drug-resistant strains, and it is high time to switch to something new and novel to tackle the situation (Ness, 2010; Villavicencio et al., 2021). Natural products from the plant, fungal, and bacterial secondary metabolites are the most prominent candidate in this respect. Here, our focus is especially on endophytic fungal metabolites. We have selected the ethnomedicinal plant *Helicteres isora* as the source of endophytic fungi due to its immense utilisation as an anti-microbial and anti-oxidative agent amongst the local ethnic tribes of Jharkhand, India (Kumar and Singh, 2014). Presently, we have isolated eight endophytic fungi from the leaf and stem tissues of the explant. The most potent antibacterial isolate is a true endophyte as it is sterile even after inoculation in a leaf carnation medium, and, also, there is no occurrence of disease symptoms when the isolate is re-inoculated onto leaf tissues of the healthy *H. isora* plant (following the methods of Koch's Postulate). The antibacterial activity of the mycelial EA extract of HelS1 is found to be lethal or bactericidal against six Gram-positive and seven Gram-negative human pathogens with MIC and MBC values of 12.5–400 μg ml^{-1} and 25–800 μg ml^{-1}, respectively. Maximum antibacterial action (in terms of lower MIC, MBC, leakage of macromolecules, inhibition of energy metabolism) is exhibited against Gram-positive pathogens than the Gram-negative ones. Gram-negative ones possess two protecting structures – thick outer membrane and periplasmic space, which makes it very difficult for the antibacterial principles to penetrate, whereas Gram-positive cells with only an outer peptidoglycan layer have a higher susceptibility toward antibacterial components (Duffy and Power, 2001). The enhanced permeability of the bacterial cell membrane can be achieved as a result of the insertion of fungal metabolites, which can restrict cell growth, cause leakage of vital cellular metabolites, and can eventually lead to cell death (Shin et al., 2007).

The extracted antibacterial metabolites are non-proteinaceous and thermostable, which makes them suitable for further *in vivo* experimentation. EA is selected as the most suitable extraction agent in comparison to other solvents (ethyl ether, petroleum ether, and *n*-hexane) as the EA fraction showed the highest antibacterial action. Non-proteinaceous nature and thermostability of antibacterial components obtained from endophytic fungi are also reported by Santra et al. (2022).

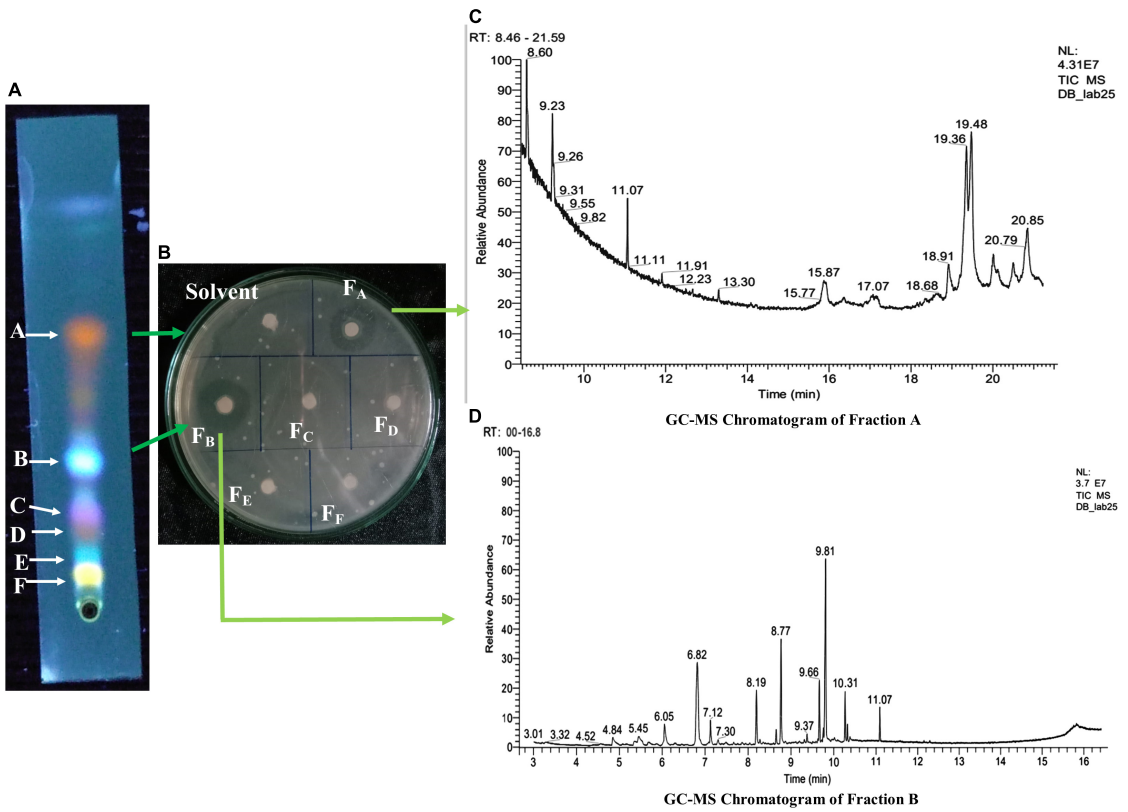

FIGURE 6 | (A) Thin-layer chromatographic (TLC) analysis of EA fraction of HelS1. **(B)** Zones of inhibition produced by bioactive compounds present in fractions (F_A–F_F) obtained from a TLC plate against pathogenic bacteria-MRSA. **(C)** GC-MS chromatogram of Fraction A showing the peaks of bioactive compounds. **(D)** GC-MS chromatogram of Fraction B, showing the peaks of bioactive compounds.

Malhadas et al. (2017) also reported the anti-bacterial action of the EA fraction of secondary metabolites of olive tree endophytes.

Our prime outcome of the study is an anti-MRSA activity of the fungal metabolites. MRSA is known to be a very fatal pathogen and causes a variety of disease in immune-compromised or healthy individuals (Zajmi et al., 2015). Extensive use of antibiotics and nosocomial infections has led to the development of such fatal strains (Doggrell, 2005). Anti-MRSA action of the EA fraction is further confirmed by the remarkable decrease in the number of CFUs paralleled to the higher increasing concentration of the anti-bacterial metabolites (as per the results of killing kinetics experiments).

The fungal metabolites disrupted the bacterial cell walls as there was leakage of intracellular macromolecules (DNA, protein, and K^+ ions) into the extracellular environment. So, the metabolites exhibit a cidal mode of action. A similar type of an outcome is also reported by the endophytic metabolites of *A. alternata* against bacterial pathogens (Chatterjee et al., 2019, 2020).

Time kill curves are the most reliable way to detect the bactericidal or bacteriostatic nature of the different concentrations of antibacterial principles (Guidelines, 2006; CLSI, 2017). This curve elucidates the kinetics of bacterial killing *in vitro* and, on the other hand, also provides us with qualitative and quantitative data on antibacterial principles for further investigations. Zajmi et al. (2015) detected the anti-MRSA and anti-Staphylococcal action of artonin by determining MIC and MBC values from the time-kill curve.

The necessary enzymes involved in central carbohydrate metabolism are also affected by the fungal metabolites, and there was a sharp inhibition of those enzymes involved in energy metabolism upon the increase of a treatment dose, i.e., MIC and MBC. A similar type of finding was made by Santra et al. (2022) and Chatterjee et al. (2019) where endophytic fungal metabolites inhibit the three main enzymes of potent bacterial pathogens involved in carbohydrate metabolism.

Development of antibiotic resistance and formation of a biofilm are the two main key features of methicillin-resistant *S. aureus* (MRSA) infections in both health care (infects implanted devices like urinary catheters, prosthetics, contact lens, and cause skin, heart valve, bone, soft tissue infections, pneumonia, septicemia) and community settings (Gordon and Lowy, 2008). More than 80% of human bacterial diseases are due to biofilm-forming bacteria (Davies, 2003). Biofilms are the aggregation of bacterial populations shielded in a matrix of exopolysaccharides, which provide the bacterial cells, enhanced resistance to antibiotic treatments, and it has been found that biofilm-incorporated cells are more virulent than the individual

TABLE 5 | A list of bioactive compounds present on the Spot A of the TLC plate identified by GC-MS analysis.

RT (min)	Total area (%)	Possible compounds	MW (g mol^{-1})	Chemical formula	Quality
8.60	11.40	Cholan-16-on, 23-methyl[a]	358	$C_{25}H_{42}O$	91
9.23	17.11	1,2-benzenedicarboxylic acid diethyl ester[a]	222.24	$C_{12}H_{14}O_4$	97
11.07	8.26	2,4-dimethylbenzaldehyde[a]	134	$C_9H_{10}O$	98
11.91	2.07	Ethoxysympathol di PFP[a]	487	$C17H_{15}F_{10}NO_4$	99
13.30	3.30	Unknown[b]	293	$C_{20}H_{37}O$	53
15.87	4.13	Ethyl decanoate[a]	200	$C_{12}H_{24}O_2$	90
18.91	3.72	Unknown[b]	282	$C_{19}H_{38}O$	41
19.36	17.11	*Trans* 1, 2-diethyl-trans-2-decalinol[a]	182	$C_{12}H_{22}O$	87
19.48	18.25	*N*, *N*-diphenyl-2-nitro-thio benzamide[a]	334	$C_{19}H_{14}N_2O_2S$	98
20.31	4.55	Unknown[b]	148	$C_{10}H_{12}O$	51
20.59	5.371	Unknown[b]	130	$C_8H_{18}O$	39
20.85	7.22	3 fluoro-5-[1-hydrox-2-(methyl amino) ethyl phenol][a]	185	$C_9H_{12}FNO_2$	92

Compounds detected in the control PDB liquid are not reported in the table.
[a]Compounds with a quality score ≥60 are identified with the spectral database of NIST.
[b]Compounds with a quality score less than 60 are considered as unknown.

TABLE 6 | A list of bioactive compounds present on the Spot B of the TLC plate identified by GC-MS analysis.

RT (min)	Total area (%)	Possible compounds	MW (g mol^{-1})	Chemical formula	Quality
4.84	2.07	Methyl benzoate[a]	136	$C_8H_8O_2$	68.23
5.45	1.66	Unknown[b]	296	$C_{21}H_{44}$	53
6.05	3.72	Unknown[b]	308	$C_{22}H_{44}$	58
6.82	12.39	Eucalanone[a]	390	$C_{22}H_{14}O_7$	89.79
7.12	4.13	Ethylbenzoate[a]	134	$C_9H_{10}O_2$	95.08
7.30	0.83	3-butyn-1-ol[a]	63.79	C_4H_6O	71.87
8.19	8.27	Unknown[b]	138	$C_8H_{10}O_2$	42
8.77	15.29	Tetroquinone[a]	172	$C_6H_4O_6$	91.29
9.37	0.83	Unknown[b]	320	$C_{20}H_{44}O_{12}$	43
9.66	9.50	Menthyl acetate[a]	198	$C_{12}H_{22}O_2$	69.04
9.81	26.44	1-H-indene 1 methanol, acetate[a]	188	$C_{12}H_{12}O_2$	96
10.31	8.68	Cholan-16-one, 3-(2-hydroxypropoxy)-cyclic 1, 2-propanedyl acetal[a]	358	$C_{25}H_{42}O$	88
11.07	6.20	Ethanol[a]	46	C_2H_5OH	92

Compounds detected in the control PDB liquid are not reported in the table.
[a]Compounds with a quality score ≥60 are identified with the spectral database of NIST.
[b]Compounds with a quality score of less than 60 are considered unknown.

TABLE 7 | GC/MS- SPME analysis of the volatile organic compounds (VOCs) emitted by an 8-day-old endophytic *Curvularia eragrostidis* HelS1 grown on a modified PDA medium.

RT (min)	Total area (%)	Possible compounds	MW (g mol^{-1})	Chemical formula	Quality
2.86	2.35	Azulene-1,2-dicarboxylate[b]	214.17	$C_{12}H_6O_4$	67
7.77	5.17	Diacetamide[b]	101.10	$C_4H_7NO_2$	65
12.74	4.7	Benzene, 1, 3 dimethyl[b]	106.17	C_8H_{10}	63
16.82	0.43	Unknown[c]	296	$C_{21}H_{44}$	53
17.53	7.04	4-thujanol[a]	154.25	$C_{10}H_{18}O$	94
18.31	47	Naphthalene[a]	128.17	$C_{10}H_8$	100
21.28	0.94	Unknown[c]	136	$C_8H_8O_2$	31
22.37	2.34	1,2-Ethyl iso-butyrate[a]	116.16	$C_6H_{12}0_2$	91
26.77	0.94	Undecane[a]	156.31	$C_{11}H_{24}$	96
30.02	22.54	Azulene[a]	128.17	$C_{10}H_8$	100
35.58	5.63	Propionic acid[a]	74.08	CH_3CH_2COOH	92

Compounds detected in the control PDA vial are not reported in the table.
[a]Denotes that the standard of those components was analysed, and mass spectra and retention time matched closely or completely with the respective fungal volatiles.
[b]Denotes that the components were identified according to the NIST library with a quality score of 60 or above, and no standards were used for comparison.
[c]Denotes that the components represent a quality score value less than 60.

cells (Akbari-Ayezloy et al., 2017; Piechota et al., 2018). Most of the ESKAPE (*Eetrococcus faecium*, *S. aureus*, *K. pneumoniae*, *Acinetobacter baumannii*, *Pseudomonas aeruginosa*, species of Enterobacter) pathogens are reported to develop a biofilm, which makes it very difficult to treat the infections (Mulani et al., 2019). Here, we have assessed the biofilm inhibitory action of fungal metabolites against three of the ESKAPE pathogens, and antibacterial metabolites of HelS1 successfully inhibited the biofilm formation (up to 79%) of those selected pathogenic bacteria.

The antimicrobial resistance can be, to some extent, tackled by administering excessively increased doses of antibiotics but that has some side effects and further worsens the situation. So, we have evaluated the synergistic action of antibiotics along with fungal metabolites by the checkerboard method, which elucidates the effective concentration of both the antibiotic and fungal metabolites at which maximum reduction in bacterial number takes place. It has been revealed that commercially available ciprofloxacin can inhibit bacterial growth at concentrations lower than its MIC when applied with HelS1 fungal metabolites. The cell wall-bursting action of antibacterial components promotes the better penetration of antibiotic ciprofloxacin to the pathogenic cells and the co-administration of both the drugs at specific concentrations (lower than their individual MIC values) can be an efficient disease management strategy. Co-administration of anti-fungal drug fluconazole and endophytic fungal metabolites also revealed the same result against *C. albicans* pathogenic cells (Chatterjee et al., 2019).

It is very necessary to keep any industrial-fermentation-based production line in a cost-efficient way, and optimisation of necessary growth parameters for the maximum production of the microbial product remains the primary target (Santra and Banerjee, 2021). To meet that criterion, we have optimised the fermentation parameters by the OVAT (one variable at a time) method coupled with RSM (response surface methodology) and

BBD (Box Behnken Design). Additional carbon and nitrogen sources, medium pH, and fermentation time are optimised in this study, and the model equation is found to be statistically valid (confirmed by regression analysis), as well as fruitful in fixing the optimum parameters on a trial-and-error basis. The large F value of 1472.53 indicates the model's significance. The higher value of R^2 adj (99.01%) confirms the high degree of correlation between the experimentally measured and statistically predicted data. A very low lack of fit *F* value of 11.67 indicated that the model has a very negligible amount of error. The model $p < 0.0001$ states that the model is appropriate for the evaluation of antibacterial production. The system accuracy was confirmed by the lack of fit *P*-value, which is 0.297 (higher than 0.05). The linear and quadratic effects of fructose concentration, peptone concentration, fermentation time, and medium pH were significant ($p < 0.0001$) in this model. Finally, the model predicted the most efficient antibacterial action of a 22.66 ± 0.58-mm clear zone of inhibition at FC, 6.868 g L^{-1}; PC, 3.791 g L^{-1}; MpH, 6.75; FT, 191 h; and 30 min, which suits with our experimental outcome of a 22.33- ± -0.58-mm clear zone of inhibition.

OVAT and RSM techniques were also adopted by several workers for the production of the antibacterial compound, and bioactive exopolysaccharides from endophytic fungal (*Fusarium* sp. SD5, *Pestalotiopsis* sp. BC55, *Colletotrichum alatae* LCS1, *Cochliobolus* sp. APS1) isolates (Mahapatra and Banerjee, 2013, 2016; Santra and Banerjee, 2022a,b; Santra et al., 2022).

The bioactive compounds were first separated using TLC, and then the most effective two bands were analysed for their composition. GC-MS-based identification revealed the occurrence of 12 antibacterial compounds in Fraction A (ethyl decanoate, *N, N*-diphenyl-2-nitro-thio benzamide, trans 1, 2-diethyl-trans-2-decalinol, etc.) and 13 bioactive compounds in Fraction B (methyl benzoate, ethanol, menthyl acetate, 3-butyn-1-ol, etc.) out of which four were unknown without any match of previously known compounds. Most of the components have not been previously reported from any endophytic fungi and are new reports from the present study.

An artificial mixture was prepared using the compounds available in the form of a standard (from Sigma), which mimicked the compositions of Bands A and B. All the components were not available, and the artificial mixture contained some selected available components in an appropriate ratio as produced by the endophyte. Finally, the antibacterial action of the artificial mixture was found to be inferior to the natural endophytic extract, and it could be concluded from the result that endophytic metabolites are genuinely unique and represent a wide array of unknown/new or novel bioactive metabolites that need further attention for broad-spectrum industrial and commercial exploitation.

Volatile Organic Compound-Mediated Anti-fungal Action

Volatile organic compounds represent a large group of diverse chemicals that possess a wide spectrum of biological activity (Santra and Banerjee, 2020b). Endophytic VOCs have been previously reported to be broad-spectrum antimicrobial in nature and also possess fuel potency (Strobel et al., 2010; Strobel et al., 2011). Endophytic *Muscodor albus* and several other species of Muscodor were isolated from different parts of the world along with *Phoma* sp., *Phomopsis* sp. and *Hypoxylon* sp., *Myrothecium innundatum*, which produces volatile antimicrobial and restricts the growth of severe phytopathogens (Daisy et al., 2002; Strobel, 2006; Mitchell et al., 2009; Banerjee et al., 2010a,b, 2014; Tomsheck et al., 2010; Saxena and Strobel, 2021). The present study also reports the anti-fungal action of bioactive VOCs emitted by the endophytic fungal isolate HelS1. The VOCs inhibit the growth of seven fungal pathogens, and the composition of VOCs has been identified using GC-MS. In total, nine compounds are detected in the HelS1-emitted VOC. The prime component was naphthalene, followed by azulene and 4-thujanol. Each of the components has its characteristic odour, but naphthalene being the most dominant one masks the other components' smell. So, the overall smell of the fungal VOCs largely mimics the mothball like a strong pungent odour masking the other smell. 4-thujanol (also known as sabinene hydrate) is a natural bicyclic monoterpene with the smell of spiciness of black pepper detected in the VOCs. Azulene (an isomer of naphthalene) is present as the second major component and bears a similar smell to naphthalene. Ethyl iso-butyrate with fruity aromatic odour and another bioactive compound undecane with faint odour is also produced by the isolate. Organic acid-propionic acid with a pungent, rancid unpleasant odour is emitted in minute amounts by the isolate. Earlier, naphthalene and sabinene monohydrates were reported by Daisy et al. (2002) and Singh et al. (2011) from *Muscodor vitigenus* and *Phomopsis* sp., respectively. The endophytic VOCs are majorly found to be bio-active, and our experimental outcomes support the same (Banerjee et al., 2010a,b; Kudalkar et al., 2012; Mao et al., 2019; Pena et al., 2019).

The maximum production of the major compound naphthalene is detected at a medium composed of PDA, which is supplemented with yeast extract and urea (0.2 g L^{-1}), dextrose (40 g L^{-1}). The maximum production of mothball-like odour is confirmed by the individual olfactory score of lab members. An artificial mixture is prepared, following the ratio of components present in the fungal VOC. The IC_{50} value of the artificial mixture against 9 phytopathogens ranged from 13.6 ± 0 μL 50 mL^{-1} to 36. ± 1 μL 50 ml^{-1}. Fungal pathogen *C. ulmi* is not at all inhibited by the endophytic VOCs but is inhibited with an IC_{50} value of 36 μL 50 ml^{-1} by the artificial mixture. In the case of *C. beticola*, both the fungal VOC and artificial mixture are unable to restrict its growth. In the case of fungal pathogens *F. oxysporum*, *G. candidum*, and *P. ultimum*, the maximum inhibition is found upon fungal VOC treatment, whereas the artificial mixture is most effective against *F. oxysporum*, *P. ultimum*, and *G. candidum*, respectively. So, there is a slight change in the mode of action between the fungal VOC and artificial mixture.

The findings suggest that, although, to some extent, the mimicry of the artificial mixture may yield similar results, but not in all the cases. It also elucidates that the presence of other compounds (either unknown or the not-detected ones) in the

original natural VOC mixture may trigger the fungal growth inhibition in some cases, but not for all. Similar types of outcomes were also reported by VOCs of endophytic *Phomopsis* sp. isolated from *Odontoglossum* sp. (Singh et al., 2011). Medicinal plants always serve as the pool of diverse endophytic fungi, and our present outcome also supports the same (Gond et al., 2012; Dhayanithy et al., 2019). *H. isora* leaf harbours eight different types of endophytic fungi, and the biodiversity indices declare the significant assemblage of endophytes, colonising the leaf tissues of the plant. Endophytes of medicinal plants regularly represent unique volatile with multidomain bioactivity (Banerjee et al., 2010a,b).

The antifungal activity of these endophytic volatiles opens up new scopes for sustainable agricultural practices and deep ecological approaches where the myco-fumigation technique can be applied to restrict the growth of phytopathogens in living stock feeds and in post-harvest disease management. In the recent past, use of endophytic fungal volatiles in the management of post-harvest decay has gained interest, and our present investigational outcome is just a new addition to that list (Saxena and Strobel, 2021).

The test organisms used in this study are a potential causal agent of several dreadful diseases and devastate the agro-economy. *G. candidum* causes soft root rot in *Ipomea batatas*, and *B. cinerea* (also called grey mold) causes necrotrophic lesions in over 200 plant species but, predominantly, in wine grapes (Holmes and Clark, 2002; Williamson et al., 2007). *R. solani* causes damping-off in a wide range of hosts, especially in rapeseed and wheat, whereas *P. ultimum* is the causal agent of root rot and damping-off in 100s of crops, especially corn, wheat, fir, soybean, and potato (Verma, 1996; Agrios, 2005). The other two pathogens *F. oxysporum* and *A. alternata* are known to cause fusarium wilt, foot, and root rot in hundreds of crops, and brown and black leaf spots in tomato, tangerine, tobacco, and strawberry, respectively (Michielse and Rep, 2009; Meena et al., 2017). Another human pathogen *A. fumigatus*, a causal agent of aspergillosis in immune-compromised patients, is also inhibited by the fungal VOCs (Dagenais and Keller, 2009). Millions of dollars are invested, and harmful-toxic chemical formulations are used on a large scale to control these pathogens (Aktar et al., 2009; Zubrod et al., 2019). So, instead of using xenobiotic antifungals with severe side effects, the fungal isolate can be used as a potential biocontrol agent to have a safe, green, and sustainable environment. It is the first investigation of VOCs emitted by an endophytic *Curvularia eragrostidis* HelS1 isolated from the medicinally valuable *Helicteres isora* plant from the forests of East India.

CONCLUSION

In a nutshell, endophytes are the all-square bioactive entities, and their volatile, non-volatile metabolites possess unique multi-domain bio-activity. Here, endophytic *Curvualria eragrostidis* HelS1 is found to be an effective anti-microbial producer. VOCs emitted by the isolate restrict the growth of dreadful phytopathogens and can be utilised as a tool for sustainable agriculture. The endophyte *C. eragrostidis* HelS1 can be commercialised as a myco-fumigator. This will be an alternative to synthetic anti-fungal and will act as a biocontrol agent in managing post-harvest diseases. In a world of dreadful diseases, it is the correct time to switch to the novel, non-toxic bio-metabolites, which will further support the concept of deep ecological movements. Not only in the arena of agriculture but also the isolate *Curvularia eragrostidis* HelS1 contributes to the field of pharmaceutical sciences where the bioactive metabolites can be a potent alternative to conventional antibiotics and may efficiently check the fatal diseases caused by multidrug-resistant Gram-positive and Gram-negative bacterial pathogens in the human population. Our outcomes open up rays of hope in the domain of novel, non-conventional bioactive product isolation from untapped biological sources, and endophytes from ethnomedicinal plants are found to be the major source in this respect.

DATA AVAILABILITY STATEMENT

The original contributions presented in this study are included in the article/**Supplementary Material**, further inquiries can be directed to the corresponding author.

AUTHOR CONTRIBUTIONS

HS and DB designed the research plan and prepared the manuscript. HS performed all the experiments and analysed the data statistically. DB coordinated the whole work and discussed the results. Both authors read the manuscript and approved it for submission.

FUNDING

HS gets Swami Vivekananda fellowship from Government of West Bengal.

ACKNOWLEDGMENTS

HS was thankful to Mr. Dipankar Mondal, a technical officer, USIC (University Sophisticated Instrumentation Centre), Vidyasagar University for the operation of the GC-MS instrument.

SUPPLEMENTARY MATERIAL

The Supplementary Material for this article can be found online at: https://www.frontiersin.org/articles/10.3389/fmicb.2022.920561/full#supplementary-material

REFERENCES

Agrios, G. N. (2005). *Plant Pathology*. Amsterdam: Elsevier Academic Press.

Akbari-Ayezloy, E., Hosseini-Jazani, N., Yousefi, S., and Habibi, N. (2017). Eradication of methicillin resistant *S. aureus* biofilm by the combined use of fosfomycin and β-chloro-L-alanine. *Iran. J. Microbiol.* 9, 1–10.

Aktar, M. W., Sengupta, D., and Chowdhury, A. (2009). Impact of pesticides use in agriculture: their benefits and hazards. *Interdisciplinary Toxicol.* 2, 1–12. doi: 10.2478/v10102-009-0001-7

Banerjee, D., Pandey, A., Jana, M., and Strobel, G. (2014). Muscodor albus MOW12 an endophyte of *Piper nigrum* L. (Piperaceae) collected from North East India produces volatile antimicrobials. *Ind. J. Microbiol.* 54, 27–32. doi: 10.1007/s12088-013-0400-5

Banerjee, D., Strobel, G. A., Booth, B., Sears, J., Spakowicz, D., and Busse, S. (2010b). An endophytic *Myrothecium inundatum* producing volatile organic compounds. *Mycosphere* 1, 241–247.

Banerjee, D., Strobel, G., Geary, B., Sears, J., Ezra, D., Liarzi, O., et al. (2010a). Muscodor albus strain GBA, an endophytic fungus of Ginkgo biloba from United States of America, produces volatile antimicrobials. *Mycology* 1, 179–186.

Bauer, A. W. (1966). Antibiotic susceptibility testing by a standardized single disc method. *Am. J. Clin. Pathol.* 45, 149–158.

Burton, K. (1956). A study of the conditions and mechanism of the diphenylamine reaction for the colorimetric estimation of deoxyribonucleic acid. *Biochem. J.* 62:315. doi: 10.1042/bj0620315

Charria-Girón, E., Espinosa, M. C., Zapata-Montoya, A., Méndez, M. J., Caicedo, J. P., Dávalos, A. F., et al. (2021). Evaluation of the antibacterial activity of crude extracts obtained from cultivation of native endophytic fungi belonging to a tropical montane rainforest in Colombia. *Front. Microbiol.* 12:716523. doi: 10.3389/fmicb.2021.716523

Chatterjee, S., Ghosh, R., and Mandal, N. C. (2019). Production of bioactive compounds with bactericidal and antioxidant potential by endophytic fungus *Alternaria alternata* AE1 isolated from *Azadirachta indica* A. Juss. *PLoS One* 14:e0214744. doi: 10.1371/journal.pone.0214744

Chatterjee, S., Ghosh, R., and Mandal, N. C. (2020). Inhibition of biofilm-and hyphal-development, two virulent features of Candida albicans by secondary metabolites of an endophytic fungus *Alternaria tenuissima* having broad spectrum antifungal potential. *Microbiol. Res.* 232:126386. doi: 10.1016/j.micres.2019.126386

CLSI (2017). *Performance Standards for Antimicrobial Susceptibility Testing, CLSI Suppl M100*, 27th Edn. Wayne, PA : Clinical and Laboratory Standards Institute.

Dagenais, T. R., and Keller, N. P. (2009). Pathogenesis of *Aspergillus fumigatus* in invasive aspergillosis. *Clin. Microbiol. Rev.* 22, 447–465.

Daisy, B. H., Strobel, G. A., Castillo, U., Ezra, D., Sears, J., Weaver, D. K., et al. (2002). Naphthalene, an insect repellent, is produced by *Muscodor vitigenus*, a novel endophytic fungus. *Microbiology* 148, 3737–3741. doi: 10.1099/00221287-148-11-3737

Davies, D. (2003). Understanding biofilm resistance to antibacterial agents. *Nat. Rev. Drug Discov.* 2, 114–122. doi: 10.1038/nrd1008

Deshmukh, S. K., Dufossé, L., Chhipa, H., Saxena, S., Mahajan, G. B., and Gupta, M. K. (2022). Fungal endophytes: a potential source of antibacterial compounds. *J. Fungi* 8:164. doi: 10.3390/jof8020164

Dhayanithy, G., Subban, K., and Chelliah, J. (2019). Diversity and biological activities of endophytic fungi associated with *Catharanthus roseus*. *BMC Microbiol.* 19:22. doi: 10.1186/s12866-019-1386-x

Doggrell, S. A. (2005). Rho-kinase inhibitors show promise in pulmonary hypertension: NAGAOKA T, FAGAN KA, GEBB SA et al.: inhaled Rho kinase inhibitors are potent and selective vasodilators in rat pulmonary hypertension. *Am. J. Respir. Crit. Care Med.* 171, 494–499. doi: 10.1164/rccm.200405-637OC

Duffy, C. F., and Power, R. F. (2001). Antioxidant and antimicrobial properties of some Chinese plant extracts. *Int. J. Antimicob. Agents* 17, 527–529. doi: 10.1016/S0924-8579(01)00326-0

Edgerton, M. D. (2009). Increasing crop productivity to meet global needs for feed, food, and fuel. *Plant Physiol.* 149, 7–13. doi: 10.1104/pp.108.130195

Felsenstein, J. (1985). Confidence limits on phylogenies: an approach using the bootstrap. *Evolution* 39, 783–791. doi: 10.1111/j.1558-5646.1985.tb00420.x

Fernandez-Garayzabal, J. F., Delgado, C., Blanco, M., Vazquez-Boland, J. A., Briones, V., Suárez, G., et al. (1992). Role of potassium tellurite and brain heart infusion in expression of the hemolytic phenotype of *Listeria* s on agar plates. *Appl. Environ. Microbiol.* 58, 434–438. doi: 10.1128/aem.58.1.434-438.1992

Gond, S. K., Mishra, A., Sharma, V. K., Verma, S. K., Kumar, J., Kharwar, R. N., et al. (2012). Diversity and antimicrobial activity of endophytic fungi isolated from Nyctanthes arbor-tristis, a well-known medicinal plant of India. *Mycoscience* 53, 113–121.

Gordon, R. J., and Lowy, F. D. (2008). Pathogenesis of methicillin-resistant *Staphylococcus aureus* infection. *Clin. Infect. Dis.* 46(Suppl._5), S350–S359.

Guidelines (2006). *Guidelines: Performance Standards for Antimicrobial Susceptibility Testing: Approved Standard M100- S16*. Available online at: https://clsi.org/media/wi0pmpke/m100ed32_sample.pdf

Hata, K., and Futai, K. (1995). Endophytic fungi associated with healthy pine needles and needles infested by the pine needle gall midge, *Thecodiplosis japonensis*. *Canadian J. Botany* 73, 384–390.

Holmes, G. J., and Clark, C. A. (2002). First report of *Geotrichum candidum* as a pathogen of sweetpotato storage roots from flooded fields in North *Carolina* and *Louisiana*. *Plant Dis.* 86, 695–695. doi: 10.1094/PDIS.2002.86.6.695C

Hussein, M. E., Mohamed, O. G., El-Fishawy, A. M., El-Askary, H. I., El-Senousy, A. S., El-Beih, A. A., et al. (2022). Identification of antibacterial metabolites from endophytic fungus *Aspergillus fumigatus*, isolated from *Albizia lucidior* leaves (Fabaceae), utilizing metabolomic and molecular docking techniques. *Molecules* 27:1117. doi: 10.3390/molecules27031117

Kudalkar, Strobel, G., Riyaz-Ul-Hassan, S., Geary, B., and Sears, J. (2012). Muscodor sutura, a novel endophytic fungus with volatile antibiotic activities. *Mycoscience* 53, 319–325.

Kumar, N., and Singh, A. K. (2014). Plant profile, phytochemistry and pharmacology of Avartani (*Helicteres isora* Linn.): a review. *Asian Pacific J. Trop. Biomed.* 4, S22–S26. doi: 10.12980/APJTB.4.2014C872

Liu-Xu, L., Vicedo, B., García-Agustín, and Llorens, E. (2022). Advances in endophytic fungi research: a data analysis of 25 years of achievements and challenges. *J. Plant Interact.* 17, 244–266.

Llorens, E., Sharon, O., Camañes, G., García-Agustín, and Sharon, A. (2019). Endophytes from wild cereals protect wheat plants from drought by alteration of physiological responses of the plants to water stress. *Environ. Microbiol.* 21, 3299–3312. doi: 10.1111/1462-2920.14530

Lorian, V. (ed.) (2005). *Antibiotics in Laboratory Medicine*. Philadelphia, PA: Lippincott Williams & Wilkins.

Lowry, O. H., Rosebrough, N. J., Farr, A. L., and Randall, R. J. (1951). Protein measurement with the Folin phenol reagent. *J. Biol. Chem.* 193, 265–275.

Mahapatra, S., and Banerjee, D. (2012). Structural elucidation and bioactivity of a novel exopolysaccharide from endophytic *Fusarium solani* SD5. *Carbohydrate Polymers* 90, 683–689. doi: 10.1016/j.carbpol.2012.05.097

Mahapatra, S., and Banerjee, D. (2013). Optimization of a bioactive exopolysaccharide production from endophytic *Fusarium solani* SD5. *Carbohydrate Polymers* 97, 627–634. doi: 10.1016/j.carbpol.2013.05.039

Mahapatra, S., and Banerjee, D. (2016). Production and structural elucidation of exopolysaccharide from endophytic *Pestalotiopsis sp*. BC55. *Int. J. Biol. Macromolecules* 82, 182–191. doi: 10.1016/j.ijbiomac.2015.11.035

Malhadas, C., Malheiro, R., Pereira, J. A., de Pinho, G., and Baptista. (2017). Antimicrobial activity of endophytic fungi from olive tree leaves. *World J. Microbiol. Biotechnol.* 33, 1–12. doi: 10.1007/s11274-017-2216-7

Maliehe, T. S., Mbambo, M., Nqotheni, M. I., Senzo, N. S., and Shandu, J. S. E. (2022). Antibacterial effect and mode of action of secondary metabolites from fungal endophyte associated with *Aloe ferox* mill. *Microbiol. Res.* 13, 90–101.

Mandal, N. C., and Chakrabarty, K. (1993). Succinate-mediated catabolite repression of enzymes of glucose metabolism in root-nodule bacteria. *Curr. Microbiol.* 26, 247–251. doi: 10.1016/j.jbiosc.2019.04.020

Manganyi, M. C., Regnier, T., Tchatchouang, C. D. K., Bezuidenhout, C. C., and Ateba, C. N. (2019). Antibacterial activity of endophytic fungi isolated from *Sceletium tortuosum* L.(*Kougoed)*. *Ann. Microbiol.* 69, 659–663.

Mao, L. J., Chen, J. J., Xia, C. Y., Feng, X. X., Kong, D. D., Qi, Z. Y., et al. (2019). Identification and characterization of new *Muscodor endophytes* from gramineous plants in Xishuangbanna, China. *Microbiol. Open* 8:e00666. doi: 10.1002/mbo3.666

Meena, M., Gupta, S. K., Swapnil, Zehra, A., Dubey, M. K., and Upadhyay, R. S. (2017). Alternaria toxins: potential virulence factors and genes related to pathogenesis. *Front. Microbiol.* 8:1451. doi: 10.3389/fmicb.2017.01451

Michielse, C. B., and Rep, M. (2009). Pathogen profile update: *Fusarium oxysporum*. *Mol. Plant Pathol.* 10:311.

Mishra, S., Bhardwaj, and Sharma, S. (2022). Metabolomic insights into endophyte-derived bioactive compounds. *Front. Microbiol.* 13:835931. doi: 10.3389/fmicb.2022.835931

Mishra, V. K., Passari, A. K., Chandra, Leo, V. V., Kumar, B., Uthandi, S., et al. (2017). Determination and production of antimicrobial compounds by *Aspergillus clavatonanicus* strain MJ31, an endophytic fungus from *Mirabilis jalapa* L. using UPLC-ESI-MS/MS and TD-GC-MS analysis. *PLoS One* 12:e0186234. doi: 10.1371/journal.pone.0186234

Mitchell, A. M., Strobel, G. A., Moore, E., Robison, R., and Sears, J. (2009). Volatile antimicrobials from *Muscodor crispans*, a novel endophytic fungus. *Microbiology* 156, 270–277.

Mulani, M. S., Kamble, E. E., Kumkar, S. N., Tawre, M. S., and Pardesi, K. R. (2019). Emerging strategies to combat ESKAPE pathogens in the era of antimicrobial resistance: a review. *Front. Microbiol.* 10:539. doi: 10.3389/fmicb.2019.00539

Ness, T. (2010). Multiresistant bacteria in ophthalmology. *Der Ophthalmologe: Zeitschrift der Deutschen Ophthalmologischen Gesellschaft* 107, 318–322. doi: 10.1007/s00347-009-2076-0

Orhan, G., Bayram, A., Zer, Y., and Balci, I. (2005). Synergy tests by E test and checkerboard methods of antimicrobial combinations against Brucella melitensis. *J. Clin. Microbiol.* 43:1. doi: 10.1128/JCM.43.1.140-143.2005

Pena, L. C., Jungklaus, G. H., Savi, D. C., Ferreira-Maba, L., Servienski, A., Maia, B. H., et al. (2019). Muscodor brasiliensis sp. nov. produces volatile organic compounds with activity against *Penicillium digitatum*. *Microbiol. Res.* 221, 28–35. doi: 10.1016/j.micres.2019.01.002

Piechota, M., Kot, B., Frankowska-Maciejewska, A., Grużewska, A., and Woźniak-Kosek, A. (2018). Biofilm formation by methicillin-resistant and methicillin-sensitive *Staphylococcus aureus* strains from hospitalized patients in Poland. *BioMed Res. Int.* 2018:4657396. doi: 10.1155/2018/4657396

Pinkerton, F., and Strobel, G. (1976). Serinol as an activator of toxin production in attenuated cultures of *Helminthosporium sacchari*. *Proc. Natl. Acad. Sci. U S A.* 73, 4007–4011. doi: 10.1073/pnas.73.11.4007

Prinsloo, A., van Straten, A. M. S., and Weldhagen, G. F. (2008). Antibiotic synergy profiles of multidrug-resistant *Pseudomonas aeruginosa* in a nosocomial environment. *South Afr. J. Epidemiol. Infect.* 23, 7–9. doi: 10.1080/10158782.2008.11441315

Saitou, N., and Nei, M. (1987). The neighbor-joining method: a new method for reconstructing phylogenetic trees. *Mol. Biol. Evol.* 4, 406–425.

Santra, H. K., and Banerjee, D. (2020a). "Natural products as fungicide and their role in crop protection," in *Natural Bioactive Products in Sustainable Agriculture*, eds J. Singh and A. Yadav (Singapore: Springer), 131–219.

Santra, H. K., and Banerjee, D. (2020b). "Fungal endophytes: a source for biological control agents," in *Agriculturally Important Fungi for Sustainable Agriculture*, (Cham: Springer), 181–216.

Santra, H. K., and Banerjee, D. (2021). "Microbial exopolysaccharides: structure and therapeutic properties," in *Microbial Polymers*, eds A. Vaishnav and D. K. Choudhary (Singapore: Springer).

Santra, H. K., and Banerjee, D. (2022a). Production, optimization, characterization and drought stress resistance by β-Glucan-Rich heteropolysaccharide from an endophytic fungi *Colletotrichum alatae* LCS1 isolated from clubmoss (*Lycopodium clavatum*). *Front. Fungal Biol.* 2:796010. doi: 10.3389/ffunb.2021.796010

Santra, H. K., and Banerjee, D. (2022b). Bioactivity study and metabolic profiling of *Colletotrichum alatae* LCS1, an endophyte of club moss *Lycopodium clavatum* L. *PLoS One* 17:e0267302. doi: 10.1371/journal.pone.0267302

Santra, H. K., Maity, S., and Banerjee, D. (2022). Production of bioactive compounds with broad spectrum bactericidal action, bio-film inhibition and antilarval potential by the secondary metabolites of the endophytic fungus *Cochliobolus sp*. APS1 isolated from the indian medicinal herb *Andrographis paniculata*. *Molecules* 27:1459. doi: 10.3390/molecules27051459

Saxena, S., and Strobel, G. A. (2021). Marvellous muscodor s: update on their biology and applications. *Microbial Ecol.* 82, 5–20.

Schulz, B., Wanke, U., Draeger, S., and Aust, H. J. (1993). Endophytes from herbaceous plants and shrubs: effectiveness of surface sterilization methods. *Mycol. Res.* 97, 1447–1450.

Sharma, A., Sagar, A., Rana, J., and Rani, R. (2022). Green synthesis of silver nanoparticles and its antibacterial activity using fungus *Talaromyces purpureogenus* isolated from *Taxus baccata* Linn. *Micro Nano Systems Lett.* 10, 1–12.

Shin, S. Y., Bajpai, V. K., Kim, H. R., and Kang, S. C. (2007). Antibacterial activity of eicosapentaenoic acid (EPA) against food borne and food spoilage microorganisms. *LWT* 40, 1515–1519. 12.005 doi: 10.1016/j.lwt.2006

Simpson, E. H. (1951). The interpretation of interaction in contingency tables. *J. R. Statistical Soc. Series B (Methodological)* 13, 238–241.

Singh, S. K., Strobel, G. A., Knighton, B., Geary, B., Sears, J., and Ezra, D. (2011). An endophytic *Phomopsis sp*. possessing bioactivity and fuel potential with its volatile organic compounds. *Microbial Ecol.* 61, 729–739. doi: 10.1007/s00248-011-9818-7

Srinivasa, C., Mellappa, G., Patil, S. M., Ramu, R., Shreevatsa, B., Dharmashekar, C., et al. (2022). Plants and endophytes–a partnership for the coumarin production through the microbial systems. *Mycology*. doi: 10.1080/21501203.2022.2027537

Strobel, G. (2006). Harnessing endophytes for industrial microbiology. *Curr. Opin. Microbiol.* 9, 240–244. doi: 10.1016/j.mib.2006.04.001

Strobel, G. A., Dirkse, E., Sears, J., and Markworth, C. (2001). Volatile antimicrobials from *Muscodor albus*, a novel endophytic fungus. *Microbiology* 147, 2943–2950.

Strobel, G. A., Knighton, W. B., Kluck, K., Ren, Y., Livinghouse, T., Griffin, M., et al. (2010). The production of myco-diesel hydrocarbons and their derivatives by the endophytic fungus *Gliocladium roseum* (NRRL 50072). *Microbiology* 156, 3830–3833. doi: 10.1099/mic.0.2008/022186-0

Strobel, G., Singh, S. K., Riyaz-Ul-Hassan, S., Mitchell, A. M., Geary, B., and Sears, J. (2011). An endophytic/pathogenic *Phoma sp*. from creosote bush producing biologically active volatile compounds having fuel potential. *FEMS Microbiol. Lett.* 320, 87–94. doi: 10.1111/j.1574-6968.2011.02297.x

Sugden, R., Kelly, R., and Davies, S. (2016). Combatting antimicrobial resistance globally. *Nat. Microbiol.* 1, 1–2. doi: 10.1038/nmicrobiol.2016.187

Tamura, K., Dudley, J., Nei, M., and Kumar, S. (2007). MEGA4: molecular evolutionary genetics analysis (MEGA) software version 4.0. *Mol. Biol. Evol.* 24, 1596–1599. doi: 10.1093/molbev/msm092

Tamura, K., Nei, M., and Kumar, S. (2004). Prospects for inferring very large phylogenies by using the neighbor-joining method. *Proc. Natl. Acad. Sci. U S A.* 101, 11030–11110. doi: 10.1073/pnas.0404206101

Tiwari, P., and Bae, H. (2022). Endophytic fungi: key insights, emerging prospects, and challenges in natural product drug discovery. *Microorganisms* 10:360. doi: 10.3390/microorganisms10020360

Tomsheck, A. R., Strobel, G. A., Booth, E., Geary, B., Spakowicz, D., Knighton, B., et al. (2010). *Hypoxylon sp*., an endophyte of *Persea indica*, producing 1, 8-cineole and other bioactive volatiles with fuel potential. *Microbial Ecol.* 60, 903–914. doi: 10.1007/s00248-010-9759-6

Tyrrell, K. L., Citron, D. M., Warren, Y. A., Fernandez, H. T., Merriam, C. V., Goldstein, E. J., et al. (2006). *In vitro* activities of daptomycin, vancomycin, and penicillin against *Clostridium difficile*, *C. perfringens*, *Finegoldia magna*, and *Propionibacterium acnes*. *Antimicrobial Agents Chemotherapy* 50, 2728–2731.

Verma, R. (1996). Biology and control of *Rhizoctonia solani* on rapeseed: a review. *Phytoprotection* 77, 99–111.

Villavicencio, E. V., Portero, C. E., and Narvaez-Trujillo, A. (2021). Antibacterial and antifungal activity of organic and peptidic extracts of ecuadorian endophytic fungi. *Adv. Microbiol.* 11, 266–282.

Wang, S. S., Liu, J. M., Sun, J., Sun, Y. F., Liu, J. N., Jia, N., et al. (2019). Diversity of culture-independent bacteria and antimicrobial activity of culturable endophytic bacteria isolated from different *Dendrobium stems*. *Sci. Rep.* 9:10389. doi: 10.1038/s41598-019-46863-9

Wang, Y., Yang, M. H., Wang, X. B., Li, T. X., and Kong, L. Y. (2014). Bioactive metabolites from the endophytic fungus *Alternaria alternata*. *Fitoterapia* 99, 153–158. doi: 10.1016/j.fitote.2014.09.015

Williamson, B., Tudzynski, B., Tudzynski, and Van Kan, J. A. (2007). Botrytis cinerea: the cause of grey mould disease. *Mol. Plant Pathol.* 8, 561–580. doi: 10.1111/j.1364-3703.2007.00417.x

Wolfe, E. R., Dove, R., Webster, C., and Ballhorn, D. J. (2022). Culturable fungal endophyte communities of primary successional plants on Mount St. Helens, WA, USA. *BMC Ecol. Evol.* 22:18. doi: 10.1186/s12862-022-01974-2

Yuan, Z. S., Liu, F., He, S. B., Zhou, L. L., and Pan, H. (2022). Community structure and diversity characteristics of rhizosphere and root endophytic bacterial community in different *Acacia species*. *PLoS One* 17:e0262909. doi: 10.1371/journal.pone.0262909

Zajmi, A., Mohd Hashim, N., Noordin, M. I., Khalifa, S. A., Ramli, F., Mohd Ali, H., et al. (2015). Ultrastructural study on the antibacterial activity of artonin e versus streptomycin against *Staphylococcus aureus* strains. *PLoS One* 10:e0128157. doi: 10.1371/journal.pone.0128157

Zubrod, J. P., Bundschuh, M., Arts, G., Brühl, C. A., Imfeld, G., Knäbel, A., et al. (2019). Fungicides: an overlooked pesticide class? *Environ. Sci. Technol.* 53, 3347–3365. doi: 10.1021/acs.est.8b04392

Conflict of Interest: The authors declare that the research was conducted in the absence of any commercial or financial relationships that could be construed as a potential conflict of interest.

frontiers | Frontiers in Microbiology

TYPE Original Research
PUBLISHED 05 October 2022
DOI 10.3389/fmicb.2022.981507

OPEN ACCESS

EDITED BY
Mina Salehi,
Tarbiat Modares University,
Iran

REVIEWED BY
Rouhallah Sharifi,
Razi University,
Iran
Surinder Banga,
Punjab Agricultural University,
India
Siamak Farhadi,
Tarbiat Modares University,
Iran

*CORRESPONDENCE
Jorge Poveda
jorge.poveda@unavarra.es
Pablo Velasco
pvelasco@mbg.csic.es

SPECIALTY SECTION
This article was submitted to Microbe and Virus Interactions With Plants, a section of the journal Frontiers in Microbiology

RECEIVED 29 June 2022
ACCEPTED 20 September 2022
PUBLISHED 05 October 2022

CITATION
Poveda J, Rodríguez VM, Díaz-Urbano M, Sklenář F, Saati-Santamaría Z, Menéndez E and Velasco P (2022) Endophytic fungi from kale (*Brassica oleracea* var. *acephala*) modify roots-glucosinolate profile and promote plant growth in cultivated *Brassica* species. First description of *Pyrenophora gallaeciana*. *Front. Microbiol.* 13:981507. doi: 10.3389/fmicb.2022.981507

Endophytic fungi from kale (*Brassica oleracea* var. *acephala*) modify roots-glucosinolate profile and promote plant growth in cultivated *Brassica* species. First description of *Pyrenophora gallaeciana*

Jorge Poveda[1]*, Víctor M. Rodríguez[2], María Díaz-Urbano[2], František Sklenář[3], Zaki Saati-Santamaría[3,4], Esther Menéndez[4] and Pablo Velasco[2]*

[1]Institute for Multidisciplinary Research in Applied Biology (IMAB), Universidad Pública de Navarra, Pamplona, Spain, [2]Group of Genetics, Breeding and Biochemistry of Brassicas, Mision Biologica de Galicia (MBG-CSIC), Pontevedra, Spain, [3]Laboratory of Fungal Genetics and Metabolism, Institute of Microbiology of the Czech Academy of Sciences, Prague, Czechia, [4]Microbiology and Genetics Department and Institute for Agribiotechnology Research (CIALE), University of Salamanca, Salamanca, Spain

Endophytic fungi of crops can promote plant growth through various mechanisms of action (i.e., improve nutrient uptake and nutrient use efficiency, and produce and modulate plant hormones). The genus *Brassica* includes important horticultural crops, which have been little studied in their interaction with endophytic fungi. Previously, four endophytic fungi were isolated from kale roots (*Brassica oleracea* var. *acephala*), with different benefits for their host, including plant growth promotion, cold tolerance, and induction of resistance to pathogens (*Xanthomonas campestris*) and pests (*Mamestra brassicae*). In the present work, the molecular and morphological identification of the four different isolates were carried out, describing them as the species *Acrocalymma vagum*, *Setophoma terrestris, Fusarium oxysporum*, and the new species *Pyrenophora gallaeciana*. In addition, using a representative crop of each *Brassica* U's triangle species and various *in vitro* biochemical tests, the ability of these fungi to promote plant growth was described. In this sense, the four fungi used promoted the growth of *B. rapa*, *B. napus*, *B. nigra, B. juncea,* and *B. carinata*, possibly due to the production of auxins, siderophores, P solubilization or cellulase, xylanase or amylase activity. Finally, the differences in root colonization between the four endophytic fungi and two pathogens (*Leptosphaeria maculans* and *Sclerotinia sclerotiorum*) and the root glucosinolate profile were studied, at different times. In this way, how the presence of progoitrin in the roots reduces their colonization by endophytic and pathogenic fungi was determined, while the possible hydrolysis of sinigrin to fungicidal products controls the colonization of endophytic fungi, but not of pathogens.

KEYWORDS

sinigrin, *Fusarium oxysporum*, *Setophoma terrestris*, *Acrocalymma vagum*, *Brassica* U's triangle, indoleacetic acid, glucosinolates

Introduction

Endophytic fungi live asymptomatically inside plant tissues. In agriculture, endophytic fungi have been isolated from roots and aerial parts of several crops, mostly cereals (barley, maize, rice, sugarcane, and wheat) and soybean (Rana et al., 2019). These fungi have important benefits for their host plants by increasing tolerance to abiotic stresses (Khan et al., 2015) and resistance to biotic stresses, through direct action or by activating plant defensive responses (Poveda et al., 2020a; Poveda and Baptista, 2021). Furthermore, endophytic fungi promote plant growth by increasing access to nutrients (nitrogen, phosphorus, potassium, iron, zinc, etc.), production of plant hormones, reduction of the plant ethylene concentration, or an increased water acquisition rate (Poveda et al., 2021a). However, the use of endophytic fungi in a directed way in agriculture requires knowledge of their biological capacities and their behaviors in different crops and environments, the development of a large-scale production system, and their release to the market (Murphy et al., 2018). In that sense, in recent years numerous patents have been filed (i.e., 185 patents between 1988 and 2019 [Al-Ani, 2019; Ortega et al., 2020]), on the use of isolates from genera such as *Neotyphodium*, *Muscodor*, *Curvularia,* and *Fusarium*.

Plant species within the genus *Brassica* include important crops both agronomically and economically worldwide (Francisco et al., 2017). The U's triangle classically explains the basic systematic relationship between the six major *Brassica* species (Nagaharu and Nagaharu, 1935). This system proposes that the three tetraploid species *B. juncea* (AABB genome), *B. napus* (AACC), and *B. carinata* (BBCC) are the derived allotetraploids of the diploid species *B. rapa* (AA), *B. nigra* (BB), and *B. oleracea* (CC), respectively, which arose by natural hybridization and chromosome doubling (Kim et al., 2018). Among the diploid species, kale (*B. oleracea* var. *acephala*) is a crop characterized by the formation of leaves along the stem, which are popular nowadays as a "superfood" as they contain phytochemicals beneficial to people's health (Šamec et al., 2020).

*Brassica*s represent a unique case for us to study due to the production of glucosinolates (GSLs). GSLs are a class of sulfur-containing compounds found predominantly in the Brassicaceae plant family (Wu et al., 2021). These secondary metabolites are involved in numerous plant physiological processes, including adaptation to environmental conditions (Poveda et al., 2021b) and defense against pests and diseases (Eugui et al., 2022), including pathogenic fungi (Poveda et al., 2020b). Therefore, pathogenic fungi need to develop tolerance mechanisms to GSLs that infect *Brassica* tissues (Vela-Corcía et al., 2019). In this sense, endophytic fungi from horseradish (*Armoracia rusticana*) (Brassicaceae family) have been described as colonizing the roots when GSLs are used as a nutrient resource (Szűcs et al., 2018).

Conversely, few studies have focused on the diversity of endophytic fungi and their role as plant stimulators in *Brassica* crops (Card et al., 2015; Poveda et al., 2022). A previous study described, for the first time, the diversity of root endophytic fungi in kale roots, and how some isolates could promote plant growth and resilience (Poveda et al., 2020c).

Against that background, the objectives of this work were to study the biological properties of the four endophytic fungi widely isolated in kale and determine the role of GSLs in the colonization of these fungi using the *Brassica* U's triangle.

Materials and methods

Biological material

The endophytic fungi used were isolated from *B. oleracea* var. *acephala* (kale) and identified by sequencing the internal transcribed spacer 1 (ITS1), 5.8S rDNA, and ITS2 as *Fusarium* sp. (MT628384), Pleosporales sp. A (MT628351), Pleosporales sp. B (MT628399), and *Acrocalymma* sp. (MT626728) (Vela-Corcía et al., 2019).

To test the role of GSLs in root colonization, two brassica root pathogenic fungi were used, *Sclerotinia sclerotiorum* and *Leptosphaeria maculans*. The *S. sclerotiorum* isolate MBG-Ss2 was originally isolated from naturally infected *B. napus* in an experimental field at MBG in January 2008 (Madloo et al., 2019). The *L. maculans* isolate CRD13/125/99 was provided by the Regional Diagnostic Center of the Regional Government of Castile and Leon (Salamanca, Spain), having been isolated from a *B. napus* field in Palencia (Spain) (Poveda, 2022).

The local kale (*B. oleracea* var. *acephala*) variety MBG-BRS0106 was utilized for *in planta* assays. Furthermore, for the growth promotion study of *Brassica* U's triangle crops, *B. oleracea* (MBG-BRS0462), *B. napus* (MBG-BRS0063), *B. rapa* (MBG-BRS0163), *B. juncea* (EXT-BRS0184), *B. nigra* (EXT-BRS0185), and *B. carinata* (EXT-BRS0219) were used.

Taxonomic study of endophytic fungi

DNA extraction, amplification, and sequencing

Fungal DNA was extracted from mycelium scraped from a PDA culture using a commercial kit (Phire Plant Direct PCR Kit,

Thermo Fisher Scientific). A ribosomal DNA region including the internal transcribed spacer 1 (ITS1), 5.8S rDNA, and ITS2 was amplified by PCR using primers ITS1 and ITS4 (White et al., 1990). The glyceraldehyde-3-phosphate dehydrogenase (GADPH) gene was amplified using the primer pair gpd-1 and gpd-2 (Berbee et al., 1999). The RNA polymerase II gene was amplified using RPB2-5 and RPB2-7c, and RPB2-7 and RPB2-11a (Liu et al., 1999). For large subunit rDNA (LSU), the LROR and LR5 primer pair was used (Vilgalys and Hester, 1990). Amplification conditions were 5 min at 98°C, 35 cycles at 98°C for 30 s, 54°C for 30 s, and 72°C for 60 s. PCR amplicons were purified following the manufacturer's instructions (MSB Spin PCRapace, Stratec Biomedical, Germany) and sequenced through the Genomics Service at CACTI, University of Vigo, Spain.[1] The GenBank accession numbers can be found in Supplementary Table S1.

DNA sequence analyses

The sequences obtained using the forward and reverse primers were assembled using the software package Seqman (v. 10.0.1) from DNAStar Inc. The resulting sequences were used for a BLAST search against the GenBank database. The datasets for phylogenetic analysis were obtained by downloading the sequences of accepted, closely related species from GenBank. Multiple sequence alignments were created in MAFFT v.7 (Katoh and Standley, 2013) using the G-INS-i method and edited in AliView v. 1.27 (Larsson, 2014). A suitable model of evolution for each alignment was selected in jModelTest v. 2.1.7 (Posada, 2008) using the BIC (Bayesian information criterion). The phylogenetic position of strains H22, H64, and H890 was demonstrated through maximum likelihood analysis of ITS (rDNA) in IQ-TREE v. 2.1.2 (Minh et al., 2020). The statistical support was determined by 1,000 standard bootstrap replicates. In the case of isolate H441, which is described as a new species in this study, single-locus maximum likelihood analysis was performed in the same way as mentioned above using DNA sequences of four loci, ITS (rDNA), LSU (rDNA), GAPDH, and RPB2. Furthermore, concatenated phylogenetic trees were calculated using partitioned analysis IQ-TREE v. 2.1.2 based on sequences of all four loci. The resulting phylogenetic trees were prepared in iTOL (Interactive Tree Of Life) (Letunic and Bork, 2021). Only significant bootstrap values (higher than 70) are presented in the final phylograms.

Fungal morphological study

Fungi were cultivated on potato dextrose agar (PDA) (Sigma-Aldrich, St. Louis, United States) at 25°C in a 12 h day/night cycle for 5 days. Morphologies of fungi structures were investigated using a Leica DM4500 microscope (Leica, Germany) equipped with a Retiga 2000R camera (QUIMAGING, Canada). At least 24 measurements per structure were taken.

1 https://cactiweb.webs.uvigo.es

In vitro plant growth promoting assays

Solubilization of insoluble phosphate (CaH_2PO_4) and potassium ($AlKO_6Si_2$) was performed using YED-P and Aleksandrov media, respectively (Hu et al., 2006; Jiménez-Gómez et al., 2020). If a clear halo around the mycelium appeared within 7 days of incubation at 28°C, it was considered a positive result. Auxins and siderophore production were analyzed by the colorimetric method (Khalid et al., 2004) and in M9-CAS-agar medium (Jiménez-Gómez et al., 2019), respectively. The production of siderophores was analyzed qualitatively, by means of the production of specific yellow halos. For the quantification of auxins produced, a standard line was made with the 3-indoleacetic acid (IAA) standard (I3750, Sigma-Aldrich, Missouri United States) by spectrophotometry at 530 nm.

Enzymatic activity assays

To detect cellulolytic, xylanolytic, or amylolytic activities, TSA medium was supplemented with 1% CMC (carboxymethyl cellulose), xylan, or starch, respectively (Garcia-Fraile et al., 2007). Briefly, a mycelium plug of each fungal isolate was placed on a different screening plate, which were incubated at 24°C for 7 days. Appearance of halos, which were observed after staining, indicated the degradation of the substrate. Cellulose- and xylan-supplemented plates were soaked in Congo Red and clarified with 1 M NaCl solution (Mateos et al., 1992). Starch-supplemented plates were soaked with lugol solution (potassium iodine, Panreac®) for a few seconds, until a halo appeared (Petzel and Hartman, 1986).

In planta growth promotion In *Brassica* U's triangle crops

For the *in planta* assays, a representative of each of the vertices and edges of the *Brassica* U's triangle was used: *B. napus*, *B. rapa*, *B. oleracea* var. *acephala*, *B. juncea*, *B. nigra,* and *B. carinata*. The plants were grown in 10 l pots with sterile (80°C, 24 h) peat substrate (Profi-Substract, Gramoflor, Valencia, Spain) and their roots inoculated with each endophytic fungus. Twelve plants were inoculated per fungus, leaving 12 plants uninoculated as a control. Fungal inoculation was performed as described by Poveda et al. (2019) for *B. napus*. At 4 weeks post-fungi inoculation, fresh and dry (48 h at 60°C) weights were taken from the aerial parts of the plants.

Root colonization assays with endophytic and pathogenic fungi

Following the methodology described in the previous section, kale plants were inoculated with the four endophytic

fungi and two pathogenic fungi, to analyze colonization differences related to the profile of root GSLs for different modes of interaction with *Brassica* plants. The plants were grown in 3 l pots with a substrate consisting of peat moss (Profi-Substract, Gramoflor, Valencia, Spain) previously treated at 80°C for 24 h, and their roots were inoculated with each fungus. Thirty 3-week-old plants were inoculated per fungus with 1 ml of a conidial suspension at 2×10^7 spore ml^{-1} (determined using a hemocytometer), keeping a further 30 plants free of inoculation as controls. For *S. sclerotiorum,* all the mycelium formed in three PDA Petri dishes was collected and mixed with 30 ml of sterile distilled water in a Falcon tube. Subsequently, 1 g of Ballotini glass balls (0.15–0.25 mm and 1 mm diameter; 0.5 + 0.5 g, respectively) (Potters, Saint-Pourçain-sur-Sioule, France) was added, vigorously shaking for 20 min. A mycelium suspension was obtained, which was adjusted to the absorbance of 0.17 per mL at 520 nm, for inoculation.

Subsequently, the roots of nine plants per fungal inoculation were collected and washed with water (freezing them directly in liquid nitrogen; three pools, each representing all the roots of three different plant), at different post-fungi-inoculation times: 7, 12, and 17 days. The different root pools were used to quantify the fungal root colonization by qPCR and GSL profiles.

Quantification of fungal root colonization

Quantification of fungal DNA in kale roots was performed by qPCR as previously described by Velasco et al. (2021), with some modifications. DNA was extracted from roots of the untreated (control) and fungal (endophytes and pathogens)-inoculated plants, using the methodology previously described in this work (section 2.2.1). A mix was prepared in a 20 µl volume using 100 ng of DNA, 10 µl of Brilliant SYBR Green QPCR Master Mix (Roche, Penzberg, Germany), the forward and reverse primers at a final concentration of 600 nM, and nuclease-free PCR-grade water (to adjust the final volume). Different endogenous genes of each of the fungi and kale were used (Supplementary Table S2). Amplifications were performed in a 7,500 Real-Time PCR System (Applied Biosystem, Forster City, CA, United States) programmed for 40 cycles under the following conditions: denaturation, 95°C for 15 s; annealing, 60°C for 1 min; extension, 72°C for 1 min. DNA extracted from the root pools of each fungal inoculation and for each post-inoculation time was used, performing each PCR in triplicate. Cycle threshold values assisted us to calculate the amount of fungal DNA using standard curves. The values obtained for fungus DNA were referenced against the values obtained for kale DNA in each of the samples.

GSLs analysis

Analysis of the GSL profiles in the samples was carried out following the methodology described by Kliebenstein et al. (2001), with minor modifications. Twelve milligrams of freeze-dried kale root powder was mixed with 400 µl of 70% (v/v) methanol preheated to 70°C, 10 µl of PbAc (0.3 M) and 120 µl of ultra-pure water preheated to 70°C, and 20 µl of glucotropaeolin (added as the internal standard). After shaking in a microplate incubator (OVAN Orbital Midi; OVAN, Badalona, Spain), 400 µl of the glucosinolate extracts were pipetted into an ion-exchange column with Sephadex DEAE-A25 (Sigma-Aldrich, St. Louis, MO, United States). For desulfation, purified sulfatase (E.C. 3.1.6.1, type H-1 from *Helix pomatia*; Sigma-Aldrich, St. Louis, MO, United States) was added. Finally, the desulfated GSLs were diluted in 200 µl of ultra-pure water and 200 µl of 70% methanol and kept frozen for further analyses.

The chromatographic analyses were conducted on a UHPLC (Nexera LC-30 AD; Shimadzu, Kyoto, Japan) equipped with an injector (Nexera SIL-30 AC, Shimadzu, Kyoto, Japan) and one SPDM20A UV/VIS photodiode array detector (Shimadzu, Kyoto, Japan). UHPLC column X Select ®HSS T3 (2.5 µm, 2.1 × 100 mm i.d.) from Waters (Waters Corporation, Milford, MA, United States) was used, which was protected with a VanGuard pre-column. GSLs were separated in aqueous acetonitrile, with a flow of 0.5 ml $min^{-1:1.5}$ at 100% H_2O, an 11 min gradient from 5 to 25% (v/v) acetonitrile, 1.5 min at 25% (v / v) acetonitrile, a minute gradient from 25 to 0% (v/v) acetonitrile, and a final 3 min at 100% H_2O; then, they were quantified at 229 nm. Identification of the GSLs was carried out by comparison with commercial standards (Phytoplan, Heidelberg, Germany).

Statistical analysis

To compare the means for each fungal inoculation treatment with the control, Student's *t*-test was used at $p < 0.05$ for each assay, using the measurements of 10 plants per treatment for plant growth quantification and the measurements of three root pools with three complete roots each for GSLs analysis. To quantify the colonization, one-way ANOVA using Tukey's multiple range test was used, by analyzing the measurements of three root pools with three complete roots each.

Results

Phylogenetic analysis

To identify the four isolates, several phylogenetic trees were created. Identification of the fungal strains isolated in this study was carried out through a BLAST search against the GenBank database using ITS sequences, which gave the following results: strain H22 (formerly named: *Acrocalymma* sp.; Poveda et al., 2020a) is a representative of *Acrocalymma vagum*, H64 (formerly named: Pleosporales sp. A; Poveda et al., 2020a) of *Setophoma terrestris*, and H890 (formerly named: *Fusarium* sp.; Poveda et al., 2020a) of *Fusarium oxysporum*. The results of our maximum

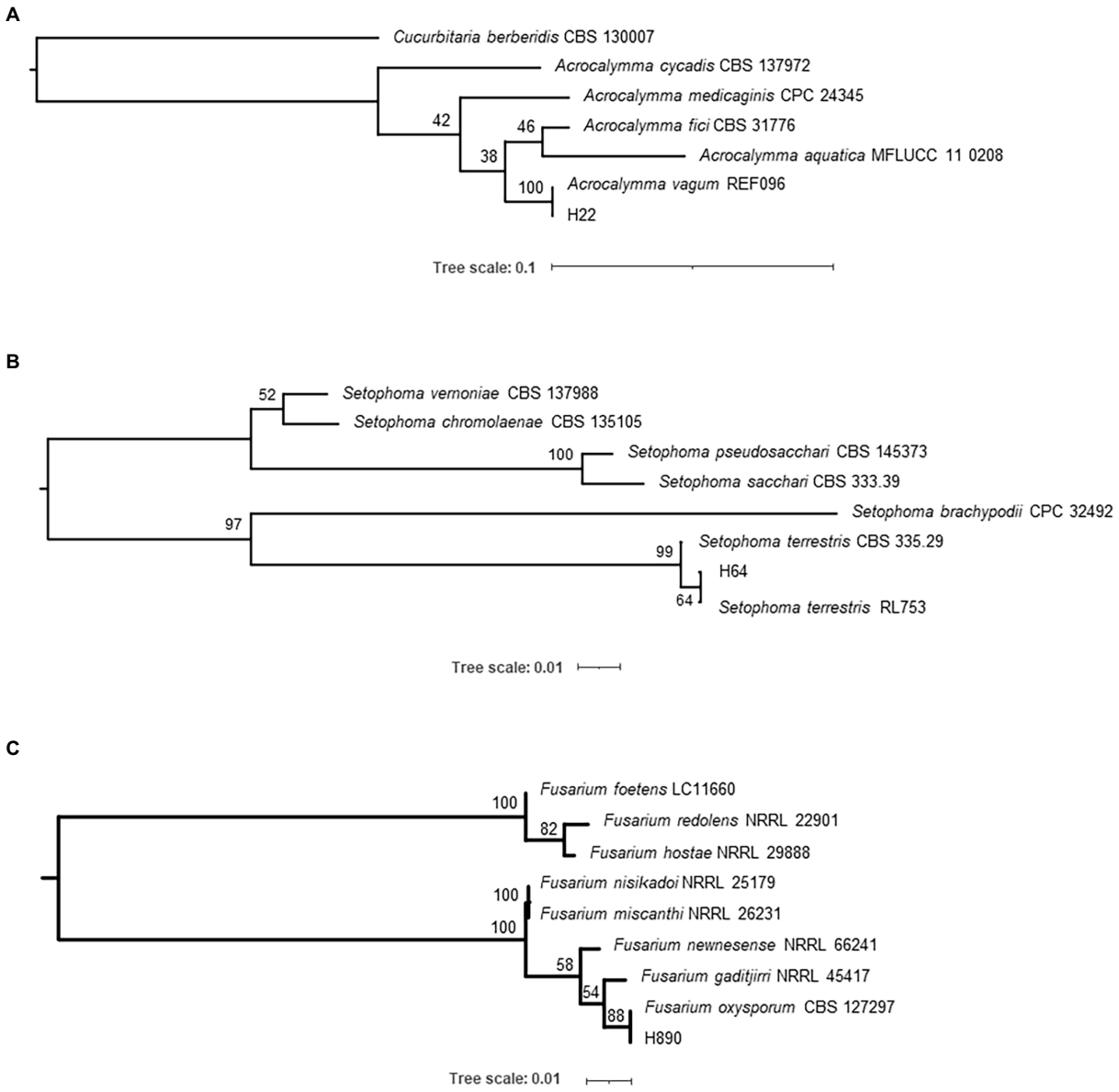

FIGURE 1
Phylogenetic trees displaying the relationships between isolates H22 **(A)**, H64 **(B)**, and H890 **(C)**. The trees were calculated in IQ-TREE 2.1.2 using ITS (rDNA) sequences with a TrNef+G substitution model and 1,000 standard bootstrap repeats.

likelihood analysis representing the phylogenetic relationships with closely related species are depicted in Figure 1 and the fungal morphology in Supplementary Figures S1–S3. On the other hand, the BLAST search for strain H441 (formerly named: Pleosporales sp. B) failed to identify the strain to the species level. Based on the results of a phylogenetic analysis using the four DNA loci depicted in Figure 2 and Supplementary Figure S4, strain H441 was described as the new species *Pyrenophora gallaeciana* sp. nov., forming a clade with *P. nobleae*, *P. fugax*, *P. novozelandica*, and *P. phaeocomes* in single-locus trees based on ITS and GAPDH, and clustering with *P. chaetomioides* and *P. lolii* in an RPB2 tree (albeit with very low support). The tree based on LSU sequences was poorly resolved because of little variation in the alignment. In the tree calculated from all four loci, *P. gallaeciana* was located in the clade with *P. nobleae*, *P. fugax*, *P. novozelandica*, and *P. phaeocomes*. This clade, as well as other deep nodes, acquired quite high bootstrap support, unlike trees based on single-locus alignment, but this is likely an artifact caused by concatenation (Kubatko and Degnan, 2007).

Pyrenophora gallaeciana* J. Poveda, V. M. Rodríguez and P. Velasco, *sp. nov. MycoBank MB- 842942. Figure 3.

Etymology: *gallaeciana* [gal·lækiana]: pertaining to Gallaecia (Galicia), the northwestern region of Spain, where the representatives of this species were isolated.

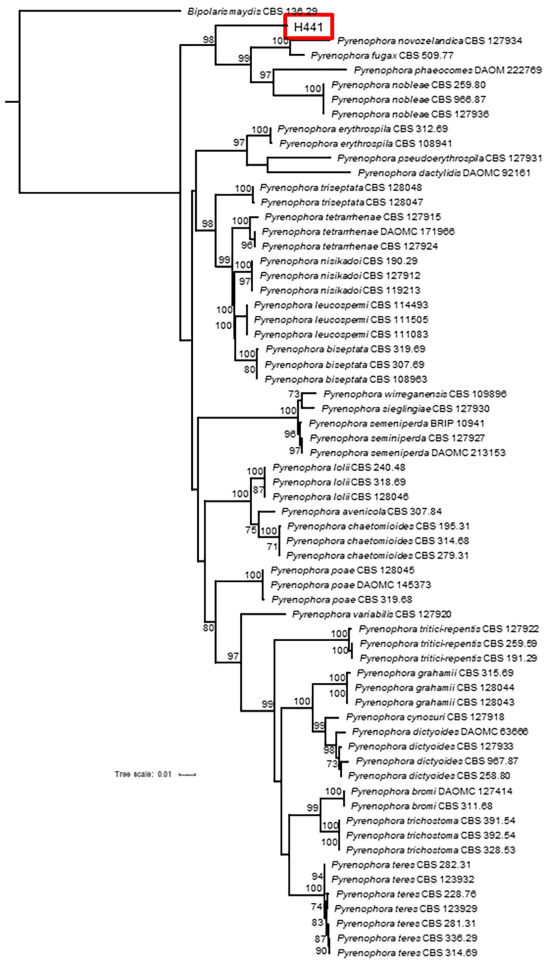

FIGURE 2
Phylogenetic tree displaying the relationship of isolate H441 with several species of genus *Pyrenophora*. The tree was calculated by partitioned analysis in IQ-TREE 2.1.2 using DNA sequences from four loci (GAPDH—HKY+I+G; ITS—TrNef+I+G; LSU—K80+I; RPB2—K80+I+G) and 1,000 standard bootstrap repeats.

Typus: Spain, Pontevedra, Misión Biológica de Galicia, from roots of *B. oleracea* var. *acephala*, May 2016, J. Poveda, V. M. Rodríguez, and P. Velasco (holotype: CECT-21208, culture ex-type CECT-21208 = CCF 6607 = MB842942).

Colony diam, 25°C, 7 d (mm): PDA: 45.3.

Culture characteristics, 25°C, 7 d: PDA: The isolate produced dim gray (6D6C72) upper and raisin black (27292B) bottom colonies. The colony morphology is characterized by irregular margins, a wrinkled form, and crateriform elevation (Figure 3A).

Micromorphology: Branched hyphae 2.5 µm thick (min.: 2 µm; max.: 3.5 µm) (Figures 3B,C). Constricted hyphae, structures (25–35 × 6–10 µm) probably involved in asexual reproduction, possibly conidia, but with different (much simpler) morphology in comparison to other *Pyrenophora* species (Figures 3C,D).

Analysis of PGP and enzymatic traits

The potential of the endophytic fungi to promote plant growth and their ability to hydrolyze plant cell compounds (first step to enter the plant tissues) were analyzed through *in vitro* tests. The results are summarized in Table 1. The four endophytic fungal isolates could produce IAA-like molecules at different levels. *A. vagum* did not demonstrate any other PGP mechanism. *S. terrestris* had the ability to solubilize phosphorus and engage in xylanase and amylase activity. *P. gallaeciana* and *F. oxysporum* could produce siderophores and, also, engaged in cellulase and xylanase activity. Furthermore, *P. gallaeciana* exhibited amylase activity.

Growth promotion In *Brassica* U's triangle crops

The four endophytic fungi under study were used to evaluate the growth of the six *Brassica* species that make up the U's triangle. Root inoculation with the endophytic fungus *A. vagum* caused an increase in the weight of the aerial part of *B. juncea* and *B. nigra* compared to uninoculated plants, and significantly reduced the fresh weight of *B. carinata*. In the case of *S. terrestris*, a significant increase in fresh weight was reported in *B. nigra* and *B. carinata* compared to uninoculated plants, and a significant reduction in *B. napus*. The presence of *P. gallaeciana* in roots of *B. rapa*, *B. juncea,* and *B. nigra* significantly increased the fresh weight of the aerial part compared to the plants without fungal inoculation. Finally, root inoculation with *F. oxysporum* produced an increase in the fresh weights of *B. rapa*, *B. juncea,* and *B. carinata* compared to uninoculated plants (Figure 4). The same biomass trend was reported by analysing dry weight (Supplementary Figure S6).

Root colonization assays with endophytic and pathogenic fungi

To study the role of GSLs in the colonization of *Brassica* roots by pathogenic and endophytic fungi, kale plants were inoculated with the four endophytic fungal isolates (*A. vagum*, *S. terrestris*, *P. gallaeciana,* and *F. oxysporum*) and two pathogens (*L. maculans* and *S. sclerotiorum*) separately.

In the roots collected 7 days post-inoculation, *F. oxysporum* fungus colonized the roots least significantly. Meanwhile, *A. vagum* and *S. terrestris* colonized kale roots significantly more (Figure 5). Both fungi continued to colonize the roots with the greatest significance 12 days post-inoculation, followed in order of significance by *L. maculans*, *P. gallaeciana,* and *S. sclerotiorum*. The fungus that colonized kale roots to a lesser extent continued to be *F. oxysporum* (Figure 5). Finally, 17 days post-inoculation, the four endophytic fungi (*A. vagum*, *S. terrestris*, *P. gallaeciana,* and *F. oxysporum*) colonized the roots without significant differences between them. The two pathogenic fungi (*L. maculans*

10.3389/fmicb.2022.981507

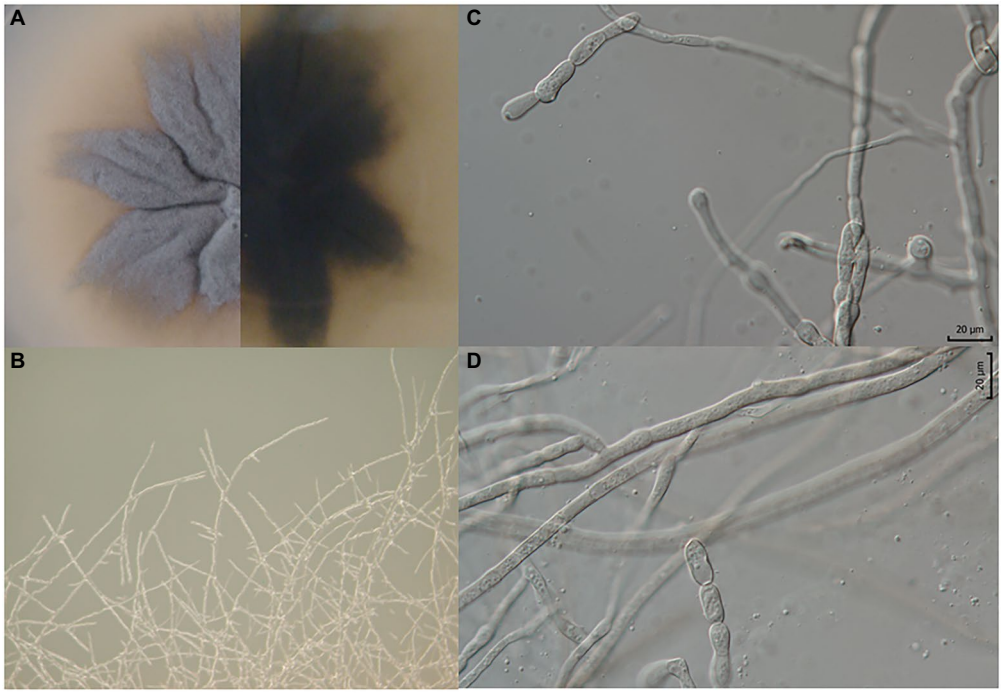

FIGURE 3
Pyrenophora gallaeciana. **(A)** Colony on PDA (front and reverse) (120h old); **(B)** mycelium on PDA (120h old); **(C, D)** structures probably involved in asexual reproduction.

TABLE 1 PGP attributes of the fungal isolates.

Isolate	IAA-like molecules ($\mu g \cdot mL^{-1}$)	Siderophores	P solubilization	K solubilization	Cellulase	Xylanase	Amylase
A. vagum	9.64	w	–	–	w	w	–
S. terrestris	5.75	w	+	–	w	+	+
P. gallaeciana	14.67	+	–	–	+	+	+
F. oxysporum	29.26	+	–	–	+	+	w

w: weak. Supplementary Figure S5 shows examples of the results of this table.

and *S. sclerotiorum*) showed significantly higher kale root colonization (Figure 5).

GSL profiles

At early stages of inoculation (7 days post-inoculation), fungus colonization significantly reduced the levels of root GSLs. This reduction affected aliphatic and indolic GSLs equally in all tested fungi (Figure 6). However, at 12 days post-inoculation, plants inoculated with endophytic fungi recovered the control amount of GSLs, mainly due to a higher quantity of indolic GSLs, since aliphatic GSLs remained at significantly lower levels that those observed with the control. Roots inoculated with pathogenic fungi accumulated higher levels of total GSLs; there was no common pattern between the two fungi since this increase in plants inoculated with *S. sclerotiorum* was due to the accumulation of aliphatic GSLs, whereas plants inoculated with *L. maculans* accumulated significantly more indolic GSLs. Surprisingly, at 17 days post-inoculation, a significant decrease in the total GSL content was observed, except for in plants inoculated with *S. sclerotiorum*. Quantified aliphatic GSLs included progoitrin, sinigrin, and glucoiberverin. In the case of progoitrin, a significant decrease in its 7 day post-inoculation content was quantified in roots inoculated with *A. vagum*, *S. terrestris*, *L. maculans,* or *S. sclerotiorum*, in comparison with uninoculated plants. The results 12 days post-inoculation continued to be significantly lower in progoitrin in inoculations with *A. vagum*, *S. terrestris*, or *L. maculans*. Meanwhile, 17 days post-inoculation, only the roots inoculated with *L. maculans* showed significant lower levels compared to uninoculated plants (Figure 6). With respect to sinigrin, root inoculation with any fungus caused a significant decrease in kale roots' sinigrin content compared to uninoculated plants 7 days post-inoculation. The same significantly lower levels

10.3389/fmicb.2022.981507

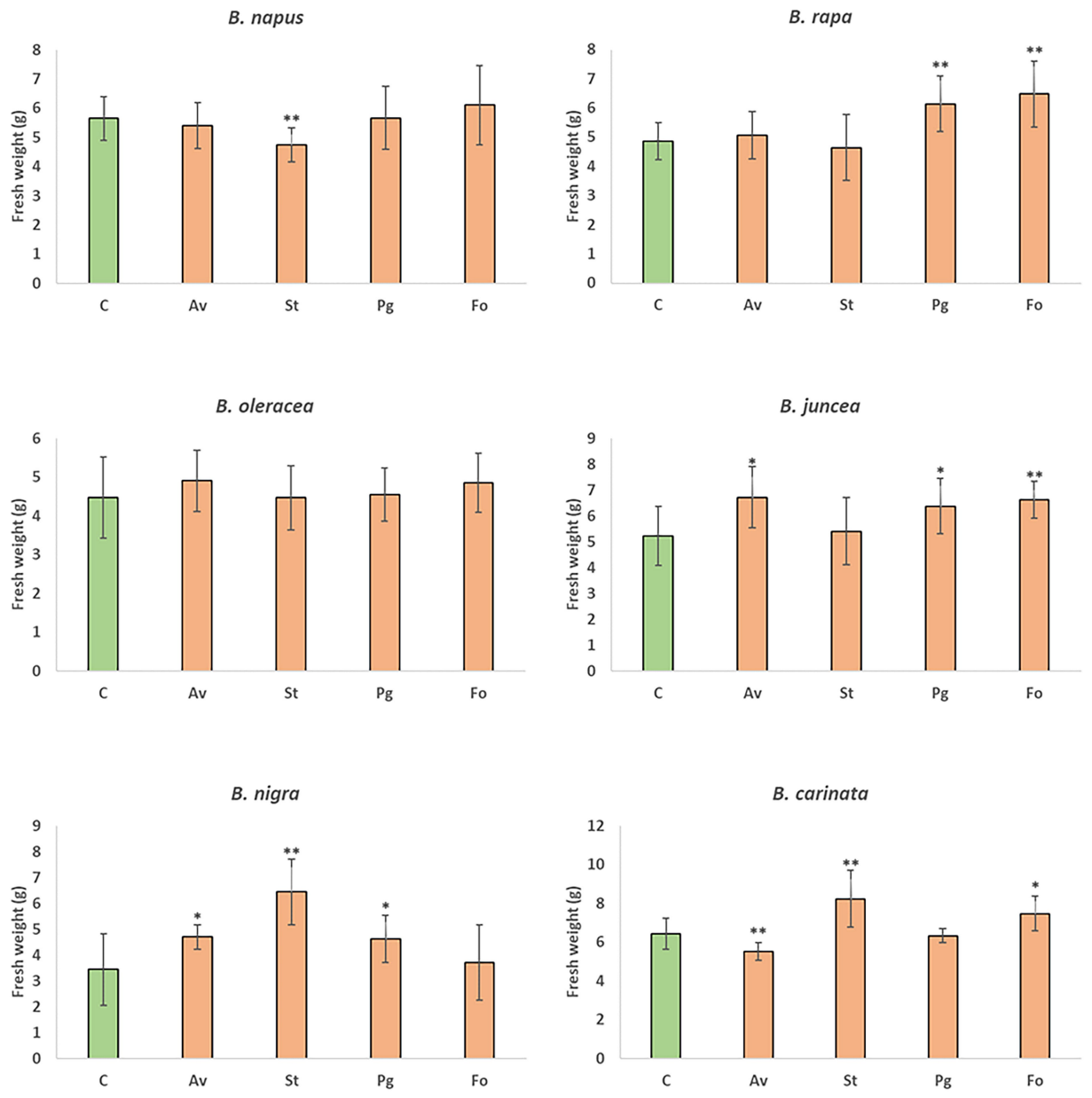

FIGURE 4
Mean of fresh weights of *B. napus*, *B. rapa*, *B. oleracea* var. *acephala*, *B. juncea*, *B. nigra*, and *B. carinata* plants grown in greenhouse. Plants without inoculation (C) and those inoculated with *A. vagum* (Av), *S. terrestris* (St), *P. gallaeciana* (Pg), and *F. oxysporum* (Fo) were gathered at 12weeks old. The fresh weights of the aerial parts of 10 plants for treatment were measured and are shown as the mean±standard deviation. Differences between treatments were calculated using Student's *t*-test. Asterisks denote significant differences at $p \leq 0.05$ (*) and $p \leq 0.01$ (**).

were quantified 12 days post-inoculation and 17 days post-inoculation with all fungi, except for *S. sclerotiorum* (at both times) and *L. maculans* (at 17 days post-inoculation) (Figure 6). Finally, in the case of glucoiberverin, in the roots inoculated with fungi *S. terrestris*, *P. gallaeciana*, *F. oxysporum*, or *L. maculans* had significantly lower content glucoiberverin contents 7 days post-inoculation compared to uninoculated plants. Then, 12 days post-inoculation, roots inoculated with *A. vagum*, *S. terrestris*, *P. gallaeciana* or *L. maculans* had significantly lower levels of glucoiberverin than uninoculated plants. However, roots inoculated with *S. sclerotiorum* had significantly higher GSL levels. These significantly higher levels were also quantified in *S. sclerotiorum* 17-days-post-inoculation. In the cases of *S. terrestris* and *L. maculans*, significantly lower levels were maintained than in the uninoculated plants (Figure 6).

As far as indolic GSLs are concerned, glucobrassicin, 4-hydroxyglucobrassicin, 4-methoxyglucobrassicin, and neoglucobrassicin were quantified. The glucobrassicin content decreased significantly in roots inoculated with *S. terrestris*, *P. gallaeciana*, or *F. oxysporum* compared to the uninoculated

10.3389/fmicb.2022.981507

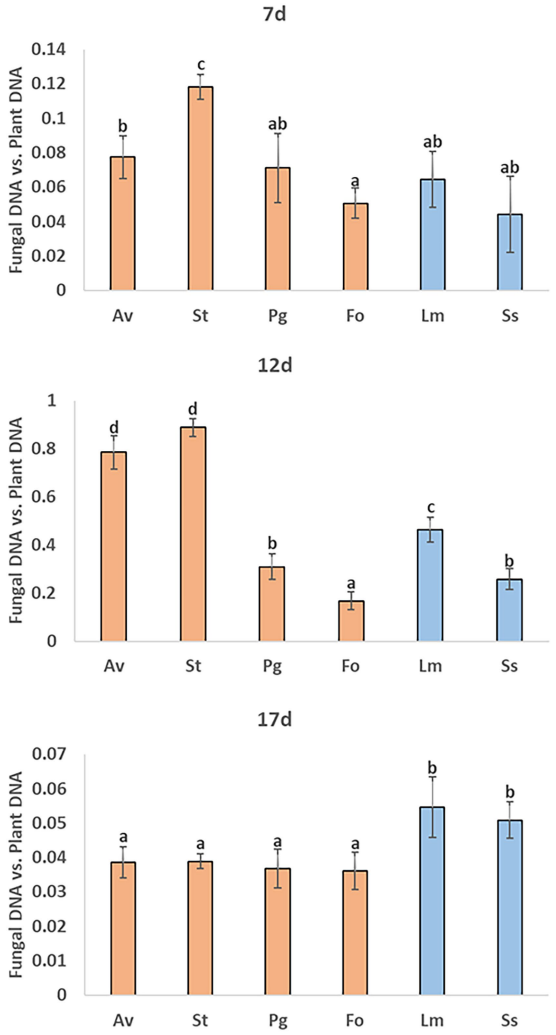

FIGURE 5
Measurements of kale root colonization by different endophytic and pathogenic fungi using qPCR. *A. vagum* (Av), *S. terrestris* (St), *P. gallaeciana* (Pg), and *F. oxysporum* (Fo) inoculated roots were collected 7-, 12-, and 17-days post-inoculation. Values are the proportion of fungal DNA to plant DNA; means of three root pools (with three plants each) are given with the corresponding standard deviations. One-way analysis of variance (ANOVA) was performed, followed by the Tukey's test. Different letters represent significant differences ($p<0.05$).

plants at 7 days post-inoculation. However, 12 days post-inoculation, a significant increase was reported in roots inoculated with *A. vagum*, *P. gallaeciana,* or *L. maculans*. Seventeen days post-inoculation, a significant reduction in the root contents of glucobrassicin was quantified with the fungi *F. oxysporum* and *L. maculans* (Figure 6). In the case of 4-hydroxyglucobrassicin, both 7 and 17 days post-inoculation, the root contents were significantly reduced with the inoculation of all fungi compared to the uninoculated plants. However, 12 days post-inoculation, only the 4-hydroxyglucobrassicin content was significantly reduced with the fungi *A. vagum*, *F. oxysporum*, and *L. maculans* (Figure 6). Seven days post-inoculation, a reduction in the root 4-methoxyglucobrassicin contents of kale plants was quantified with all fungal inoculations, except for *A. vagum*, compared to uninoculated plants. In contrast, 12 days post-inoculation, there was a significant increase in roots inoculated with *P. gallaeciana* and *L. maculans* compared to uninoculated plants. At 17 days post-inoculation, a significant reduction in root inoculation with *L. maculans* was only found (Figure 6). Finally, in the case of neoglucobrassicin, significantly lower levels were reported in roots inoculated with all fungi compared to uninoculated plants at 7 days post-inoculation. However, 12 days post-inoculation, root inoculated with *A. vagum*, *P. gallaeciana*, *F. oxysporum,* or *L. maculans* showed significantly higher neoglucobrassicin contents than uninoculated plants. Finally, the plants inoculated with *A. vagum*, *P. gallaeciana*, or *L. maculans* demonstrated significantly lower levels compared to uninoculated plants at 17 days post-inoculation (Figure 6).

Discussion

Endophytic fungi have received increasing interest in recent years. However, the numbers of isolates and newly described fungi are still low, especially within *Brassica* crops (Poveda et al., 2022). The ability of different endophytic fungi to promote plant growth in crops, thanks to various mechanisms, has been widely reviewed in recent years (Rana et al., 2019; Rigobelo and Baron, 2021). Although some microbes are adapted to an endophytic lifestyle, to reach roots' inner tissues, they must first compete and succeed in the rhizosphere, where they can benefit the plant health by providing nutrients and hormones (Jiménez-Gómez et al., 2020). It is important to note that the plant growth-promoting ability may be fungal strain- and plant genotype-specific (Rigobelo and Baron, 2021; Poveda et al., 2021a).

In this study, the specific taxonomic classification of four species of endophytic fungi from kale (*B. oleracea* var. *acephala*) was carried out, with one of them described as a new species. These fungal isolates were obtained in a previous work, although only identified to order or genus level (Poveda et al., 2020a). The four species of endophytic fungi taxonomically described in this work represent the first description, at the species level, of endophytic fungi from kale. These results highlight the importance of studying the diversity of endophytic fungi present in *Brassica* crops.

Here, the production of auxins at different levels was a common PGP trait among the isolates. Although it is known that some strains of *A. vagum* can increase auxin synthesis in plant hosts (Liu and Wei, 2019), this was the first description of the fungus as a putative producer of IAA-like compounds. This mechanism could be involved in its ability to promote the growth of the *Brassica* U triangle crops *B. juncea* and *B. nigra*, the growth promotion previously reported in kale (Poveda et al., 2021a), or *Medicago sativa* growth (Hou et al., 2019). However, in this work the root inoculation of *B. carinata* with *A. vagum* causes a reduction in plant growth, an aspect not previously mentioned for any crop.

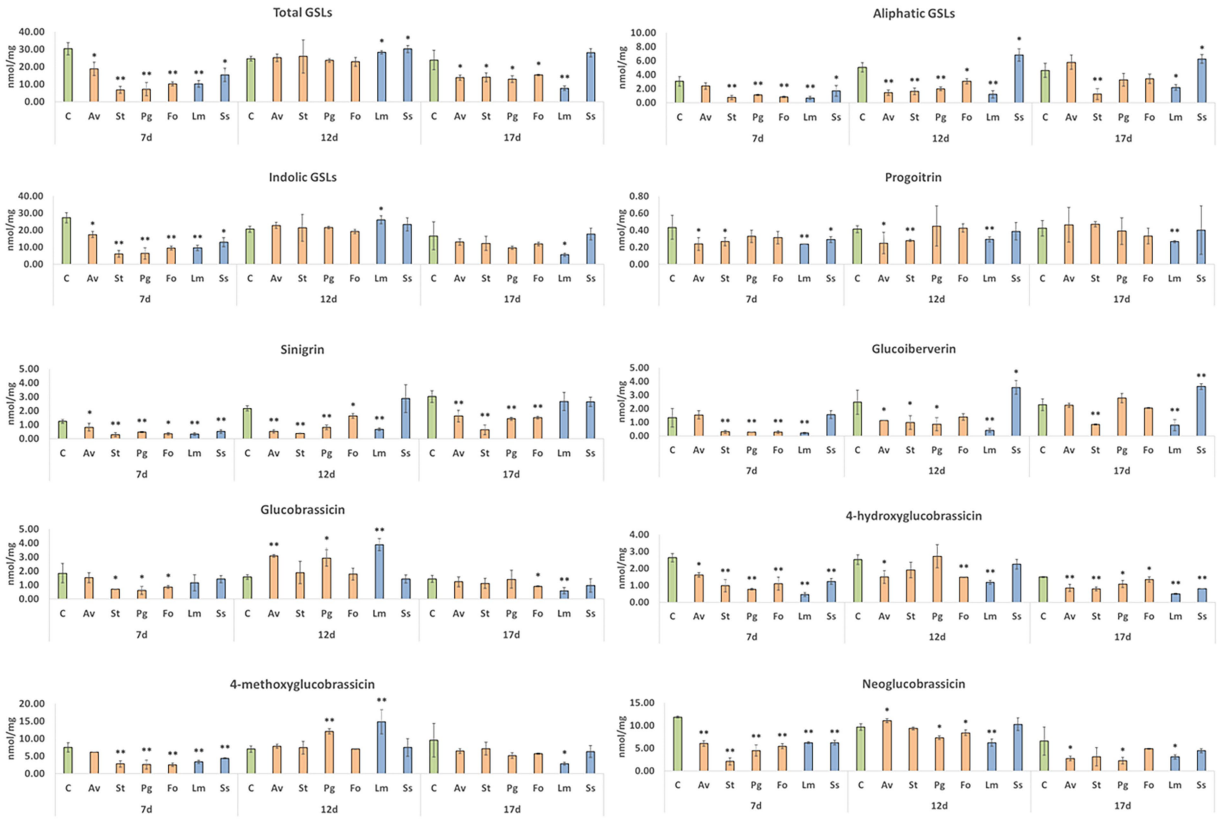

FIGURE 6
GSL content in kale roots colonized by different endophytic and pathogenic fungi. *A. vagum* (Av), *S. terrestris* (St), *P. gallaeciana* (Pg), and *F. oxysporum* (Fo) inoculated roots were collected 7-, 12-, and 17-days post-inoculation. Data are the means of three root pools (with three plants each) per inoculation with the corresponding standard deviations. Student's t-test was performed. Asterisks denote significant differences at $p \leq 0.05$ (*) and $p \leq 0.01$ (**).

The ability of *F. oxysporum* to produce auxins has been previously described, along with its role in promoting the growth of maize (Mehmood et al., 2018). However, our *F. oxysporum* isolate represents the first description of an endophytic isolate of this species as a producer of siderophores. Cellulolytic and xylanase activity have been previously reported for endophyte *F. oxysporum* (Onofre et al., 2013; Farouk et al., 2020). All of these mechanisms could be involved in the growth promotion reported in *B. juncea, B. rapa,* and *B. carinata*, as was previously verified with kale (Poveda et al., 2021a).

The *S. terrestris* isolate solubilizes phosphorus, and it carries out xylanase and amylase activity; ours is the first description of a member of the genus *Setophoma* showing these capacities. Although *Setophoma* species have been previously described as endophytes of Brassicaceae plants, such as horseradish (*Armoracia rusticana*; Szűcs et al., 2018) or kale (Poveda et al., 2021a), this study presents the first description of plant growth-promotion activity by a *Setophoma* species, particularly in *B. nigra* and *B. carinata*. However, our results showed growth reduction when *B. napus* roots were inoculated. A previous study reported the first case of pink root rot in *B. napus* produced by *S. terrestris* (Yang et al., 2017). The thin line between beneficial and pathogenic behavior of some endophytic fungi, when interacting with different hosts, needs further research.

In this work, a new species of endophytic fungi is described: *P. gallaeciana* (meaning: from Galicia, Spain). *P. gallaeciana*-type isolates could produce auxins and siderophores and carry out cellulase, xylanase, and amylase activities. Members of the genus *Pyrenophora*, such as the barley fungal pathogens *P. teres* f. sp. *teres* and *P. graminea* (Ellwood et al., 2010; Bakri et al., 2011; Ismail et al., 2014), showed similar mechanisms. Here, *P. gallaeciana* is a plant growth promoter in *B. juncea, B. rapa,* and *B. nigra*, which is consistent with previous results on the *Pyrenophora*-kale interaction (Poveda et al., 2021a).

The PGP results obtained with these fungal isolates also report important differences according to the mode of application. Poveda et al. (2020a) obtained a higher kale plants growth with inoculation with beet pulp colonized by *F. oxysporum* or *P. gallaeciana* (then identified as *Fusarium* sp. and Pleosporales sp. B, respectively). However, in our current work, inoculation with spores of both fungi did not report a PGP. It is noteworthy that the application of spores allows knowing the exact amount of inoculated endophyte fungus, while the use of mycelium colonizing beet pulp does not, making it impossible to make a real comparison between different fungi. These differences were also reported with the isolate *Trichoderma hamatum*, which did not

report PGP capacity in kale plants in its application as mycelium in beet pulp (Poveda et al., 2020c), but showed PGP when applied as spores (Velasco et al., 2021).

The Brassicaceae plants' pathogenic fungi need to tolerate or eliminate GSLs from plant tissues to colonize and infect them. *Botrytis cinerea* tolerates GSLs through the *mfsG* membrane transporter, which rapidly removes the products of GSLs' hydrolysis (Vela-Corcía et al., 2019). *S. sclerotiorum* acts directly on these toxic hydrolysis products through an isothiocyanate hydrolase (Chen et al., 2020). In the specific case of endophytic fungi, GSLs' tolerance that supports them to colonize their hosts' tissues is not fully understood (Poveda et al., 2022). In the case of *Trichoderma*, the production of myrosinase-binding proteins modifies the hydrolysis of GSLs to allow/contribute to Brassicaceae root colonization (Poveda et al, 2019), with the indole GSLs involved in controling the level of colonization (Poveda, 2021). Other endophytic fungi, including *F. oxysporum* and *S. terrestris*, directly degrade the GSLs present in their hosts and use them as nutrients (Szűcs et al., 2018).

*Brassica*s are non-mycorrhizal plants, with the presence of GSLs precisely proposed as the reason why these plants cannot be mycorrhized (Vierheilig et al., 2000; Anthony et al., 2020). These plants have been described as the main metabolites involved in the control of the endophytic fungal microbiota on this plant family (Plaszkó et al., 2022). Therefore, root colonization by endophytic fungi in *Brassica* plants must be closely related to the GSL content and profile of plant tissues.

The analyses of root colonization levels at 12 days post-inoculation revealed no differences between mock-inoculated plants and endophytic fungi-inoculated ones. Conversely, pathogenic fungi-inoculated plants showed an increased level of colonization. Specifically, with *S. sclerotiorum*, aliphatic GSLs increased. This was previously described in *A. thaliana* infection, where *S. sclerotiorum* induces the expression of synthesis genes (Stotz et al., 2011). Meanwhile, with *L. maculans,* indole GSLs increased, something previously observed in *B. rapa* (Abdel-Farid et al., 2010).

Two common aspects were found as corelated in all endophytic fungal strains vs. tested pathogenic fungal strains at 17 days post-inoculation: root colonization and the sinigrin content. The sinigrin contents were similar for root colonization with any pathogenic strain. However, the sinigrin contents decreased with endophytes' root colonization. This is possibly due to sinigrin hydrolysis by endophytic fungi and further fungicide activity of the hydrolysis residuals, such as allyl isothiocyanate (Vandicke et al., 2020). Our results suggest that low sinigrin levels detected in roots inoculated with isolates from *P. gallaeciana* and *F. oxysporum* are directly related to their lower levels of root colonization. However, *P. gallaeciana* kale roots' colonization reached its maximum at 12 days post-inoculation compared to roots inoculated with *F. oxysporum*. In both cases, the 4-hydroxyglucobrassicin content was lower than in mock-inoculated plants, except for roots inoculated with *P. gallaeciana* at 12 days post-inoculation. Thus, 4-hydroxyglucobrassicin hydrolysis products may inhibit both fungi's root colonization, at different timepoints depending on the fungal strain.

Kale root colonization by endophytes *A. vagum* and *S. terrestris* was higher than for the other fungi at 7 and 12 days post-inoculation, possibly due to a decrease in progroitrin levels, which does not occur 17 days post-inoculation. Similarly, increased root colonization by *L. maculans* at 12 days post-inoculation could also be related to a decrease in the root progoitrin content. Similar GSL profiles for roots colonized by fungal endophytes and certain fungal pathogens could be related to the hemibiotrophic lifestyle, which involves an early stage of endophytism not present in the necrotrophic lifestyle (Newton et al., 2010). Accordingly, lower levels of progoitrin may be related to greater plant colonization by fungal endophytes and pathogens.

Endophytic fungi could induce the expression of synthesis genes, the activation of plant enzymes that hydrolyze them, or act directly against them (Poveda et al., 2022). In this sense, differences in tolerance and/or degradation of GSLs by endophytic and pathogenic fungi may be explained by specific genomic comparisons. However, the sequences of these species are not yet available. Furthermore, the GSL content in the roots does not depend on localized synthesis but can be transported from other plant organs such as leaves (Witzel et al., 2015). Although our results provide some insights, the mechanisms involved in the changes in GSL levels in *Brassica* roots require further research.

In conclusion, this work presents not only the first description at the species level of endophytic fungi of a *B. oleracea* crop but also a description of a new species: *P. gallaeciana*. The strains displayed plant growth-promotion mechanisms, as well as production of hydrolytic enzymes, and could promote the growth of *B. rapa*, *B. napus*, *B. nigra, B. juncea,* and *B. carinata*. Remarkably, our results strongly suggest that progoitrin levels control fungal root colonization independently of the fungal nature, while the hydrolysis of sinigrin reduces colonization only in the case of endophytic fungi.

Data availability statement

The datasets presented in this study can be found in online repositories. The names of the repository/repositories and accession number(s) can be found in the article/Supplementary material.

Author contributions

PV and JP conceived the study. JP drafted the initial manuscript. PV, JP, and VR discussed the results and performed statistical analysis of the data. PV, JP, and FS carried out the fungi identification and phylogenetic analysis. MD-U maintained the fungal collection. ZS-S and EM performed the *in vitro* PGP assays. PV, VR, and MD-U performed the *in planta* PGP assays. JP and VR carried out the root colonization assays. PV and VR analyzed the GSLs profile. All authors contributed to the article and approved the submitted version.

Funding

This research was financially supported by projects RTI2018-096591-B-I00 34 (MCIU/AEI/FEDER, UE) and IN607A 2021/03 (Xunta de Galicia, Spain).

Acknowledgments

EM acknowledges an European Union's Horizon 2020 Marie Sklodowska-Curie Actions (Grant Agreement nº 897795). Thanks to Dra. Alba Boscá from the University of Bristol-University of Salamanca for her advice on the choice of the new scientific name (*Pyrenophora gallaeciana*) based on Latin etymology.

Publisher's note

Conflict of interest

The authors declare that the research was conducted in the absence of any commercial or financial relationships that could be construed as a potential conflict of interest.

Publisher's note

All claims expressed in this article are solely those of the authors and do not necessarily represent those of their affiliated organizations, or those of the publisher, the editors and the reviewers. Any product that may be evaluated in this article, or claim that may be made by its manufacturer, is not guaranteed or endorsed by the publisher.

Supplementary material

The Supplementary material for this article can be found online at: https://www.frontiersin.org/articles/10.3389/fmicb.2022.981507/full#supplementary-material

References

Abdel-Farid, I. B., Jahangir, M., Mustafa, N. R., Van Dam, N. M., Van den Hondel, C. A., Kim, H. K., et al. (2010). Glucosinolate profiling of *Brassica rapa* cultivars after infection by *Leptosphaeria maculans* and *fusarium oxysporum*. *Biochem. System. Ecol.* 38, 612–620. doi: 10.1016/j.bse.2010.07.008

Al-Ani, L. K. T. (2019). "Recent patents on endophytic fungi and their international market" in *Intellectual Property Issues in Microbiology*. eds. H. B. Singh, C. Keswani and S. P. Singh (Berlin, Germany: Springer). 271–284.

Amaike, S., Ozga, J. A., Basu, U., and Strelkov, S. E. (2008). Quantification of *ToxB* gene expression and formation of appressoria by isolates of *Pyrenophora tritici-repentis* differing in pathogenicity. *Plant Pathol.* 57, 623–633. doi: 10.1111/j.1365-3059.2007.01821.x

Anthony, M. A., Celenza, J. L., Armstrong, A., and Frey, S. D. (2020). Indolic glucosinolate pathway provides resistance to mycorrhizal fungal colonization in a non-host Brassicaceae. *Ecosphere* 11:e03100. doi: 10.1002/ecs2.3100

Bakri, Y., Arabi, M. I. E., and Jawhar, M. (2011). Heterogeneity in the ITS of the ribosomal DNA of *Pyrenophora graminea* isolates differing in xylanase and amylase production. *Microbiology* 80, 492–495. doi: 10.1134/S0026261711040023

Berbee, M. L., Pirseyedi, M., and Hubbard, S. (1999). *Cochliobolus* phylogenetics and the origin of known, highly virulent pathogens, inferred from ITS and glyceraldehyde-3-phosphate dehydrogenase gene sequences. *Mycologia* 91, 964–977. doi: 10.1080/00275514.1999.12061106

Card, S. D., Hume, D. E., Roodi, D., McGill, C. R., Millner, J. P., and Johnson, R. D. (2015). Beneficial endophytic microorganisms of *brassica*–a review. *Biol. Control* 90, 102–112. doi: 10.1016/j.biocontrol.2015.06.001

Chen, J., Ullah, C., Reichelt, M., Beran, F., Yang, Z. L., Gershenzon, J., et al. (2020). The phytopathogenic fungus *Sclerotinia sclerotiorum* detoxifies plant glucosinolate hydrolysis products via an isothiocyanate hydrolase. *Nat. Commun.* 11, 3090–3012. doi: 10.1038/s41467-020-16921-2

Ellwood, S. R., Liu, Z., Syme, R. A., Lai, Z., Hane, J. K., Keiper, F., et al. (2010). A first genome assembly of the barley fungal pathogen *Pyrenophora teres* f. *teres*. *Genome Biol.* 11, R109–R114. doi: 10.1186/gb-2010-11-11-r109

Eugui, D., Escobar, C., Velasco, P., and Poveda, J. (2022). Glucosinolates as an effective tool in plant-parasitic nematodes control: exploiting natural plant defenses. *Appl. Soil Ecol.* 176:104497. doi: 10.1016/j.apsoil.2022.104497

Farouk, H. M., Attia, E. Z., and El-Katatny, M. M. H. (2020). Hydrolytic enzyme production of endophytic fungi isolated from soybean (*Glycine max*). *J. Mod. Res.* 2, 1–7. doi: 10.21608/jmr.2019.15748.1008

Francisco, M., Tortosa, M., Martínez-Ballesta, M. D. C., Velasco, P., García-Viguera, C., and Moreno, D. A. (2017). Nutritional and phytochemical value of *brassica* crops from the Agri-food perspective. *Ann. Appl. Biol.* 170, 273–285. doi: 10.1111/aab.12318

Garcia-Fraile, P., Rivas, R., Willems, A., Peix, A., Martens, M., Martinez-Molina, E., et al. (2007). *Rhizobium cellulosilyticum* sp. nov., isolated from sawdust of *Populus alba*. *Int. J. Syst. Evol. Microbiol.* 57, 844–848. doi: 10.1099/ijs.0.64680-0

Hou, L., Yu, J., Zhao, L., and He, X. (2019). Dark septate endophytes improve the growth and tolerance of *Medicago sativa* and *Ammopiptanthus mongolicus* under cadmium stress. *Front. Microbiol.* 10:3061. doi: 10.3389/fmicb.2019.03061

Hu, X., Chen, J., and Guo, J. (2006). Two phosphate-and potassium-solubilizing bacteria isolated from Tianmu Mountain, Zhejiang, China. *World J. Microbiol. Biotechnol.* 22, 983–990. doi: 10.1007/s11274-006-9144-2

Hu, Z., Parekh, U., Maruta, N., Trusov, Y., and Botella, J. R. (2015). Down-regulation of *fusarium oxysporum* endogenous genes by host-delivered RNA interference enhances disease resistance. *Front. Chem.* 3:1. doi: 10.3389/fchem.2015.00001

Ismail, I. A., Godfrey, D., and Able, A. J. (2014). Proteomic analysis reveals the potential involvement of xylanase from *Pyrenophora teres* f. *teres* in net form net blotch disease of barley. *Australas. Plant Pathol.* 43, 715–726. doi: 10.1007/s13313-014-0314-7

Jiménez-Gómez, A., Saati-Santamaría, Z., Igual, J. M., Rivas, R., Mateos, P. F., and García-Fraile, P. (2019). Genome insights into the novel species *microvirga brassicacearum*, a rapeseed endophyte with biotechnological potential. *Microorganisms* 7:354. doi: 10.3390/microorganisms7090354

Jiménez-Gómez, A., Saati-Santamaría, Z., Kostovcik, M., Rivas, R., Velázquez, E., Mateos, P. F., et al. (2020). Selection of the root endophyte *pseudomonas brassicacearum* CDVBN10 as plant growth promoter for *Brassica napus* L. crops. *Agronomy* 10:1788. doi: 10.3390/agronomy10111788

Katoh, K., and Standley, D. M. (2013). MAFFT multiple sequence alignment software version 7: improvements in performance and usability. *Mol. Biol. Evol.* 30, 772–780. doi: 10.1093/molbev/mst010

Khalid, A., Arshad, M., and Zahir, Z. A. (2004). Screening plant growth-promoting rhizobacteria for improving growth and yield of wheat. *J. Appl. Microbiol.* 96, 473–480. doi: 10.1046/j.1365-2672.2003.02161.x

Khan, A. L., Hussain, J., Al-Harrasi, A., Al-Rawahi, A., and Lee, I. J. (2015). Endophytic fungi: resource for gibberellins and crop abiotic stress resistance. *Crit. Rev. Biotechnol.* 35, 62–74. doi: 10.3109/07388551.2013.800018

Kim, C. K., Seol, Y. J., Perumal, S., Lee, J., Waminal, N. E., Jayakodi, M., et al. (2018). Re-exploration of U's triangle *brassica* species based on chloroplast genomes and 45S nrDNA sequences. *Sci. Rep.* 8, 1–11. doi: 10.1038/s41598-018-25585-4

Kliebenstein, D. J., Kroymann, J., Brown, P., Figuth, A., Pedersen, D., Gershenzon, J., et al. (2001). Genetic control of natural variation in *Arabidopsis* glucosinolate accumulation. *Plant Physiol.* 126, 811–825. doi: 10.1104/pp.126.2.811

Kubatko, L. S., and Degnan, J. H. (2007). Inconsistency of phylogenetic estimates from concatenated data under coalescence. *Syst. Biol.* 56, 17–24. doi: 10.1080/10635150601146041

Larsson, A. (2014). AliView: a fast and lightweight alignment viewer and editor for large data sets. *Bioinformatics* 30, 3276–3278. doi: 10.1093/bioinformatics/btu531

Letunic, I., and Bork, P. (2021). Interactive tree of life (iTOL) v5: an online tool for phylogenetic tree display and annotation. *Nucleic Acids Res.* 49, W293–W296. doi: 10.1093/nar/gkab301

Liu, Y., and Wei, X. (2019). Dark septate endophyte improves drought tolerance of *Ormosia hosiei* Hemsley & EH Wilson by modulating root morphology, ultrastructure, and the ratio of root hormones. *Forests* 10:830. doi: 10.3390/f10100830

Liu, Y. J., Whelen, S., and Hall, B. D. (1999). Phylogenetic relationships among ascomycetes: evidence from an RNA polymerse II subunit. *Mol. Biol. Evol.* 16, 1799–1808. doi: 10.1093/oxfordjournals.molbev.a026092

Madloo, P., Lema, M., Francisco, M., and Soengas, P. (2019). Role of major glucosinolates in the defense of kale against *Sclerotinia sclerotiorum* and *Xanthomonas campestris* pv. *Campestris*. *Phytopathology* 109, 1246–1256. doi: 10.1094/PHYTO-09-18-0340-R

Mateos, P. F., Jimenez-Zurdo, J. I., Chen, J., Squartini, A. S., Haack, S. K., Martinez-Molina, E., et al. (1992). Cell-associated pectinolytic and cellulolytic enzymes in *rhizobium leguminosarum* biovar *trifolii*. *Appl. Environ. Microbiol.* 58, 1816–1822. doi: 10.1128/aem.58.6.1816-1822.1992

Maximiano, M. R., de Jesus Miranda, V., de Barros, E. G., and Dias, S. C. (2020). Validation of an *in vitro* system to trigger changes in the gene expression of effectors of *Sclerotinia sclerotiorum*. *J. Appl. Microbiol.* 131, 885–897. doi: 10.1111/jam.14973

Mehmood, A., Irshad, M., Husna, A. A., and Hussain, A. (2018). *In vitro* maize growth promotion by endophytic *fusarium oxysporum* WLW. *J. Appl. Environ. Biol. Sci.* 8, 30–35.

Minh, B. Q., Schmidt, H. A., Chernomor, O., Schrempf, D., Woodhams, M. D., von Haeseler, A., et al. (2020). IQ-TREE 2: new models and efficient methods for phylogenetic inference in the genomic era. *Mol. Biol. Evol.* 37, 1530–1534. doi: 10.1093/molbev/msaa015

Murphy, B. R., Doohan, F. M., and Hodkinson, T. R. (2018). From concept to commerce: developing a successful fungal endophyte inoculant for agricultural crops. *J. Fungi* 4:24. doi: 10.3390/jof4010024

Nagaharu, U., and Nagaharu, N. (1935). Genome analysis in *brassica* with special reference to the experimental formation of *B. napus* and peculiar mode of fertilization. *Jpn. J. Bot.* 7, 389–452.

Newton, A. C., Fitt, B. D., Atkins, S. D., Walters, D. R., and Daniell, T. J. (2010). Pathogenesis, parasitism and mutualism in the trophic space of microbe–plant interactions. *Trends Microbiol.* 18, 365–373. doi: 10.1016/j.tim.2010.06.002

Onofre, S. B., Mattiello, S. P., da Silva, G. C., Groth, D., and Malagi, I. (2013). Production of cellulases by the endophytic fungus *fusarium oxysporum*. *J. Microbiol. Res.* 3, 131–134. doi: 10.5923/j.microbiology.20130304.01

Ortega, H. E., Torres-Mendoza, D., and Cubilla-Rios, L. (2020). Patents on endophytic fungi for agriculture and bio-and phytoremediation applications. *Microorganisms* 8:1237. doi: 10.3390/microorganisms8081237

Petit-Houdenot, Y., Degrave, A., Meyer, M., Blaise, F., Ollivier, B., Marais, C. L., et al. (2019). A two genes–for–one gene interaction between *Leptosphaeria maculans* and *Brassica napus*. *New Phytol.* 223, 397–411. doi: 10.1111/nph.15762

Petzel, J. P., and Hartman, P. A. (1986). A note on starch hydrolysis and β-glucuronidase activity among flavobacteria. *J. Appl. Microbiol.* 61, 421–426. doi: 10.1111/j.1365-2672.1986.tb04306.x

Plaszkó, T., Szűcs, Z., Cziáky, Z., Ács-Szabó, L., Csoma, H., Géczi, L., et al. (2022). Correlations between the metabolome and the endophytic fungal metagenome suggests importance of various metabolite classes in community assembly in horseradish (*Armoracia rusticana*, Brassicaceae) roots. *Front. Plant Sci.* 13:921008. doi: 10.3389/fpls.2022.921008

Posada, D. (2008). jModelTest: phylogenetic model averaging. *Mol. Biol. Evol.* 25, 1253–1256. doi: 10.1093/molbev/msn083

Poveda, J. (2021). Glucosinolates profile of *Arabidopsis thaliana* modified root colonization of *Trichoderma* species. *Biol. Control* 155:104522. doi: 10.1016/j.biocontrol.2020.104522

Poveda, J. (2022). Effect of volatile and non-volatile metabolites from Leptosphaeria maculans on tomato calli under abiotic stresses. *Plant Stress* 3:100054. doi: 10.1016/j.stress.2021.100054

Poveda, J., Abril-Urias, P., and Escobar, C. (2020c). Biological control of plant-parasitic nematodes by filamentous fungi inducers of resistance: *Trichoderma*, mycorrhizal and endophytic fungi. *Front. Microbiol.* 11:992. doi: 10.3389/fmicb.2020.00992

Poveda, J., and Baptista, P. (2021). Filamentous fungi as biocontrol agents in olive (*Olea europaea* L.) diseases: mycorrhizal and endophytic fungi. *Crop Prot.* 146:105672. doi: 10.1016/j.cropro.2021.105672

Poveda, J., Díaz-González, S., Díaz-Urbano, M., Velasco, P., and Sacristán, S. (2022). Fungal endophytes of Brassicaceae: molecular interactions and crop benefits. *Front. Plant Sci.* 13:932288. doi: 10.3389/fpls.2022.932288

Poveda, J., Eugui, D., Abril-Urías, P., and Velasco, P. (2021a). Endophytic fungi as direct plant growth promoters for sustainable agricultural production. *Symbiosis* 85, 1–19. doi: 10.1007/s13199-021-00789-x

Poveda, J., Eugui, D., and Velasco, P. (2020b). Natural control of plant pathogens through glucosinolates: an effective strategy against fungi and oomycetes. *Phytochem. Rev.* 19, 1045–1059. doi: 10.1007/s11101-020-09699-0

Poveda, J., Hermosa, R., Monte, E., and Nicolás, C. (2019). The *Trichoderma harzianum* Kelch protein ThKEL1 plays a key role in root colonization and the induction of systemic defense in Brassicaceae plants. *Front. Plant Sci.* 10:1478. doi: 10.3389/fpls.2019.01478

Poveda, J., Velasco, P., de Haro, A., Johansen, T. J., McAlvay, A. C., Möllers, C., et al. (2021b). Agronomic and metabolomic side-effects of a divergent selection for indol-3-ylmethylglucosinolate content in kale (*Brassica oleracea* var. *acephala*). *Meta* 11:384. doi: 10.3390/metabo11060384

Poveda, J., Zabalgogeazcoa, I., Soengas, P., Rodríguez, V. M., Cartea, M. E., Abilleira, R., et al. (2020a). *Brassica oleracea* var. *acephala* (kale) improvement by biological activity of root endophytic fungi. *Sci. Rep.* 10, 20224–20212. doi: 10.1038/s41598-020-77215-7

Rana, K. L., Kour, D., Sheikh, I., Yadav, N., Yadav, A. N., Kumar, V., et al. (2019). "Biodiversity of endophytic fungi from diverse niches and their biotechnological applications" in *Advances in Endophytic Fungal Research*. ed. B. P. Singh (Berlin: Springer), 105–144.

Rigobelo, E. C., and Baron, N. C. (2021). Endophytic fungi: a tool for plant growth promotion and sustainable agriculture. *Mycology* 13, 39–55. doi: 10.1080/21501203.2021.1945699

Rybak, K., See, P. T., Phan, H. T., Syme, R. A., Moffat, C. S., Oliver, R. P., et al. (2017). A functionally conserved *Zn2Cys6* binuclear cluster transcription factor class regulates necrotrophic effector gene expression and host-specific virulence of two major Pleosporales fungal pathogens of wheat. *Mol. Plant Pathol.* 18, 420–434. doi: 10.1111/mpp.12511

Šamec, D., Urlić, B., and Salopek-Sondi, B. (2020). Kale (*Brassica oleracea* var. *acephala*) as a superfood: review of the scientific evidence behind the statement. *Crit. Rev. Food Sci. Nutr.* 59, 2411–2422. doi: 10.1080/10408398.2018.1454400

Sotelo, T., Velasco, P., Soengas, P., Rodríguez, V. M., and Cartea, M. E. (2016). Modification of leaf glucosinolate contents in *Brassica oleracea* by divergent selection and effect on expression of genes controlling glucosinolate pathway. *Front. Plant Sci.* 7:1012. doi: 10.3389/fpls.2016.01012

Stotz, H. U., Sawada, Y., Shimada, Y., Hirai, M. Y., Sasaki, E., Krischke, M., et al. (2011). Role of camalexin, indole glucosinolates, and side chain modification of glucosinolate-derived isothiocyanates in defense of *Arabidopsis* against *Sclerotinia sclerotiorum*. *Plant J.* 67, 81–93. doi: 10.1111/j.1365-313X.2011.04578.x

Szűcs, Z., Plaszkó, T., Cziáky, Z., Kiss-Szikszai, A., Emri, T., Bertóti, R., et al. (2018). Endophytic fungi from the roots of horseradish (*Armoracia rusticana*) and their interactions with the defensive metabolites of the glucosinolate-myrosinase-isothiocyanate system. *BMC Plant Biol.* 18, 1–15. doi: 10.1186/s12870-018-1295-4

Vandicke, J., De Visschere, K., Deconinck, S., Leenknecht, D., Vermeir, P., Audenaert, K., et al. (2020). Uncovering the biofumigant capacity of allyl isothiocyanate from several Brassicaceae crops against *fusarium* pathogens in maize. *J. Sci. Food Agric.* 100, 5476–5486. doi: 10.1002/jsfa.10599

Vela-Corcía, D., Srivastava, D. A., Dafa-Berger, A., Rotem, N., Barda, O., and Levy, M. (2019). MFS transporter from *Botrytis cinerea* provides tolerance to glucosinolate-breakdown products and is required for pathogenicity. *Nat. Commun.* 10, 2886–2811. doi: 10.1038/s41467-019-10860-3

Velasco, P., Rodríguez, V. M., Soengas, P., and Poveda, J. (2021). *Trichoderma hamatum* increases productivity, glucosinolate content and antioxidant potential of different leafy *brassica* vegetables. *Plan. Theory* 10:2449. doi: 10.3390/plants10112449

Vierheilig, H., Bennett, R., Kiddle, G., Kaldorf, M., and Ludwig-Müller, J. (2000). Differences in glucosinolate patterns and arbuscular mycorrhizal status of glucosinolate-containing plant species. *New Phytol.* 146, 343–352. doi: 10.1046/j.1469-8137.2000.00642.x

Vilgalys, R., and Hester, M. (1990). Rapid genetic identification and mapping of enzymatically amplified ribosomal DNA from several *Cryptococcus* species. *J. Bacteriol.* 172, 4238–4246. doi: 10.1128/jb.172.8.4238-4246.1990

White, T. J., Bruns, T., Lee, S. J. W. T., and Taylor, J. (1990). "Amplifcation and direct sequencing of fungal ribosomal rna genes for phylogenetics" in *PCR Protocols: A Guide to Methods and Applications*. eds. M. A. Innis, D. H. Garfield, J. J. Sninsky and T. J. White (Cambridge: Academic Press), 315–322.

Witzel, K., Hanschen, F. S., Klopsch, R., Ruppel, S., Schreiner, M., and Grosch, R. (2015). *Verticillium longisporum* infection induces organ-specific glucosinolate degradation in *Arabidopsis thaliana*. *Front. Plant Sci.* 6:508. doi: 10.3389/fpls.2015.00508

Wu, X., Huang, H., Childs, H., Wu, Y., Yu, L., and Pehrsson, P. R. (2021). Glucosinolates in *brassica* vegetables: characterization and factors that influence distribution, content, and intake. *Ann. Rev. Food Sci. Tech.* 12, 485–511. doi: 10.1146/annurev-food-070620-025744

Yang, Y., Zuzak, K., Harding, M., Neilson, E., Feindel, D., and Feng, J. (2017). First report of pink root rot caused by *Setophoma* (*Pyrenochaeta*) *terrestris* on canola. *Can. J. Plant Pathol.* 39, 354–360. doi: 10.1080/07060661.2017.1355849

frontiers | Frontiers in Microbiology

TYPE Original Research
PUBLISHED 06 October 2022
DOI 10.3389/fmicb.2022.1024987

OPEN ACCESS

EDITED BY
Naser Safaie,
Tarbiat Modares University,
Iran

REVIEWED BY
Li-Wei Zhou,
Institute of Microbiology (CAS), China
Guangyuan Wang,
Qingdao Agricultural University,
China
Riyazali Zafarali Sayyed,
P.S.G.V.P.M's Arts, Science and Commerce College, India
Mina Salehi,
Tarbiat Modares University,
Iran

*CORRESPONDENCE
Yougui Li
liyougui3@126.com
Shi Zhong
zshi2002@163.com

SPECIALTY SECTION
This article was submitted to Microbe and Virus Interactions With Plants, a section of the journal Frontiers in Microbiology

RECEIVED 01 September 2022
ACCEPTED 26 September 2022
PUBLISHED 06 October 2022

CITATION
Huo J, Sun Y, Pan M, Ma H, Lin T, Lv Z, Li Y and Zhong S (2022) Non-targeted metabonomics and transcriptomics revealed the mechanism of mulberry branch extracts promoting the growth of *Sanghuangporus vaninii* mycelium. *Front. Microbiol.* 13:1024987. doi: 10.3389/fmicb.2022.1024987

Non-targeted metabonomics and transcriptomics revealed the mechanism of mulberry branch extracts promoting the growth of *Sanghuangporus vaninii* mycelium

Jinxi Huo[1], Yuqing Sun[1], Meiliang Pan[2], Huanyan Ma[2], Tianbao Lin[1], Zhiqiang Lv[1], Yougui Li[1]* and Shi Zhong[1]*

[1]Zhejiang Academy of Agricultural Sciences, Institute of Sericultural and Tea, Hangzhou, China, [2]Department of Agriculture and Rural Affairs, Zhejiang Provincial Center for Agricultural Technology Extension, Hangzhou, China

Sanghuangprous vaninii is a wood-inhabiting fungus, and its mycelium and fruiting body show excellent medicinal values. Mulberry is one of the major hosts of *S. vaninii*, however, the mechanism of mulberry affecting the growth of *S. vaninii* has not been reported. In the present study, a mulberry-inhabiting strain of *S. vaninii* was selected to explore the effects of mulberry branch extracts (MBE) on the growth of the strain. Results showed that MBE could significantly promote the growth of *S. vaninii* mycelium at the concentration of 0.2 g/l. After 16 days of liquid culture, the dry weight of mycelium in 0.2 g/l MBE medium was higher by three times compared with that in the control. The non-targeted metabonomic analysis of the culture medium at different culture times and concentrations was conducted to find the key components in MBE that promoted the growth of *S. vaninii* mycelium. Under the different concentrations of MBE culture for 10 and 16 days, 22 shared differential metabolites were identified. Next, in accordance with the peak value trend of these metabolites, HPLC–MS and liquid culture validation, four components derived from MBE (i.e., scopoletin, kynurenic acid, 3,5-dihydroxybenzoic acid and 2,4-dihydroxybenzoic acid) could significantly increase the growth rate of mycelium at the concentration of 2 mg/l. Transcriptomic and qRT-PCR analyzes showed that MBE could upregulate hydrolase-related genes, such as *serine–glycine–asparaginate–histidine* (*SGNH*) *hydrolase*, *alpha-amylase*, *poly-beta-hydroxybutyrate* (*PHB*) *depolymerase*, *glycosyl hydrolase family 61*, *cerato-platanin protein* and *Fet3*, which might enhance the nutrient absorption ability of *S. vaninii*. Importantly, MBE could significantly increase the content of harmine, androstenedione and vesamicol, which have been reported to possess various medicinal effects. Results suggested that MBE could be an excellent additive for liquid culture of *S. vaninii* mycelium, and these hydrolase-related genes also provided candidate genes for improving the nutrient absorption capacity of *S. vaninii*.

KEYWORDS

Sanghuangprous vaninii, mulberry branch extracts, liquid culture, hydrolase-related gene, non-targeted metabonomics

Introduction

Sanghuangprous vaninii (Ljub.) L.W. Zhou and Y.C. Dai., formerly named *Phellinus gilvus* (Schwein.) Pat, is an important wood-inhabiting fungus that has been widely utilised in traditional medicine in China and adjacent countries (Shen et al., 2021). The mycelium and fruiting body of *S. vaninii* show excellent medicinal values. The fruiting body of *S. vaninii* shows significantly inhibitive effects on tumour cells (Wan et al., 2020, 2022; He et al., 2021; Yu et al., 2021; Guo et al., 2022; Qiu et al., 2022). In our previous study, the protocatechualdehyde from fruiting body can induce cell cycle arrest and apoptosis in HT-29 colorectal cancer cells and B16-F10 melanoma cells (Zhong et al., 2016, 2020). 3,4-dihydroxybenzalacetone, hydroxycinnamic acid, phellibaumin D, interfungin B, phelligridimer A and inoscavin A isolated from fruiting body show effective inhibitive effects on hepatocellular carcinoma cells HepG2 (Huo et al., 2020). In addition to the anti-carcinogenesis activity of fruiting body, the mycelium of *S. vaninii* shows excellent medicinal values. For example, the basal diet containing 5 g/kg *S. vaninii* dried mycelium can markedly improve the growth and innate immunity in weaned piglets (Sun et al., 2020). Also, the ethanol extracts of *S. vaninii* mycelium can reverse the loss of dopaminergic neurons and neurovascular reduction in 1-methyl-4-phenyl-1,2,3,6-tetrahydropyridine-induced Parkinson's disease zebrafish model (Li et al., 2022). Research suggested that the mycelium and fruiting body of *S. vaninii* have remarkable commercial values and that the liquid fermentation of mycelium is an important process for harvesting the mycelium and large-scale artificial cultivation of *S. vaninii*.

Numerous macrofungi, such as *Lentinus edodes* and *S. vaninii*, parasitise woody plants. The components of the host can significantly affect the growth and metabolites of these macrofungi. For example, Wu et al. (2019) found that hemicellulose and lignin, the major components of wood, can stimulate mycelial growth and polysaccharide biosynthesis in *L. edodes*. Lignin can promote the growth of *S. vaninii* mycelia in culture plate at the concentration of 0.06 g/l (Guo et al., 2021). *S. vaninii* is a wood-inhabiting fungus that parasitises mulberry (Huo et al., 2020) and poplar (Shen et al., 2021). The effects of host on the mycelium of *S. vaninii* are worth studying.

In the present study, a mulberry-inhabiting strain of *S. vaninii* was selected to explore the effects of MBE on mycelial growth of *S. vaninii* by PDA plate culture and liquid fermentation. Next, the non-targeted metabonomic analysis of culture media was conducted to identify key components in MBE that might affect the growth of *S. vaninii* mycelium. Finally, the transcriptomic and metabonomic analyzes of mycelia were conducted to explore the mechanism of MBE affecting mycelial growth and production of active ingredients. Results will systematically evaluate the effects of MBE on the mycelium of *S. vaninii* and deepen our understanding of the interaction between host and inhabiting macrofungi.

Materials and methods

Strain culture and preparation of MBE

The strain of *S. vaninii* S12 (Huo et al., 2020) was isolated from the fruiting body grown in a mulberry tree in Tonglu, Zhejiang province of China (29.80° N, 119.67° E). A patch of the fruiting body was inoculated into potato dextrose agar (PDA) at 28°C. Mycelium free from contamination was stored at Institute of Sericulture and Tea, Zhejiang Academy of Agricultural Sciences, and the strain was ready for use after 7 days of culture on PDA at 28°C. In liquid culture, five colonies with size of 8 mm were punched from the PDA and added into 300 ml potato dextrose broth (PDB) in 500 ml flask. The mycelium was cultured at 200 rpm and 28°C, filtered to remove the culture medium and dried in an oven at 50°C for 2 days to obtain dried mycelium. All analytically pure reagents were purchased from Aladdin Co., Ltd. (China).

The dried mulberry branches were extracted with boiling water (w/v = 1:10) for 2 h. The filtered aqueous extracts were added with absolute ethanol at a ratio of 1:3. The supernatant after centrifugation was concentrated to 1/5 volume by rotary evaporator (30 rpm, 50°C, R502, Shensheng, China) and lyophilised by vacuum freeze drier (−50°C, 15 Pa; Alpha 1–4, Christ, Germany) to obtain MBE powders. The dried powders were stored at −20°C before use.

Non-targeted metabonomic analysis

The non-targeted metabonomic analysis was conducted by Guangzhou Genedenovo Biotechnology Co., Ltd. (China). The mycelia (M) and culture media (CM) at different sampling times were collected. Mycelia (100 mg) were washed thrice by PBS buffer and ground with liquid nitrogen, and the homogenate was resuspended with prechilled 80% (v/v) methanol and 0.1% (v/v) formic acid by well vortex. CM (1 ml) were freeze-dried and resuspended with prechilled 80% (v/v) methanol and 0.1% (v/v) formic acid by well vortex. Samples were incubated on ice for 5 min and centrifuged at 15000 g and 4°C for 15 min. A certain amount of the supernatant was diluted to final concentration containing 53% (v/v) methanol by LC–MS-grade water. Samples

were centrifuged at 15000 g and 4°C for 15 min. Finally, the supernatant was injected into the HPLC-MS/MS system (Want et al., 2006, 2013; Barri and Dragsted, 2013).

HPLC-MS/MS analyzes were performed using the Vanquish UHPLC system (ThermoFisher, Germany) coupled with the Orbitrap Q ExactiveTMHF-X mass spectrometer (ThermoFisher, Germany) in Guangzhou Gene Denovo Co., Ltd. (China). Samples were injected onto the Hypesil Gold column (100 × 2.1 mm, 1.9 μm) by using a 17 min linear gradient at a flow rate of 0.2 ml/min. The eluents for the positive polarity mode were eluents A (0.1% FA in water, v/v) and B (methanol). The eluents for the negative polarity mode were eluents C (5 mm ammonium acetate, pH 9.0) and D (methanol). The solvent gradient was set as follows: 2% B, 1.5 min; 2–100% B, 12.0 min; 100% B, 14.0 min; 100–2% B, 14.1 min and 2% B, 17 min. The Q ExactiveTM HF-X mass spectrometer was operated in positive/negative polarity mode with spray voltage of 3.2 kV, capillary temperature of 320°C, sheath gas flow rate of 40 arb and aux gas flow rate of 10 arb.

The raw data files generated by UHPLC–MS/MS were processed using the Compound Discoverer 3.1 (Thermo Fisher, Germany) to perform peak alignment, peak picking and quantitation for each metabolite. The main parameters were set as follows: retention time tolerance, 0.2 min; actual mass tolerance, 5 ppm; signal intensity tolerance, 30%; signal/noise ratio, 3 and minimum intensity, 100,000. After that, peak intensities were normalised to the total spectral intensity. Normalised data were used to predict the molecular formula based on additive ions, molecular ion peaks and fragment ions. Peaks were matched with the mzCloud,[1] mzVault and Masslist database to obtain accurate qualitative and relative quantitative results. Three biological repeats were established at each sampling time. The VIP value of the orthogonal partial least squares discriminant analysis and P value of *t*-test were used to screen significantly different metabolites between different comparison groups, and the threshold of significant difference was as follows: VIP ≥ 1 and *t*-test $p < 0.05$ (Worley and Powers, 2013; Saccenti et al., 2014).

Transcriptomic analysis

Mycelia at different sampling times were collected, and each sample had three biological replicates. Total RNA was isolated and purified using the TRIzol reagent (Invitrogen, United States) following the manufacturer's instructions. RNA integrity, purity and concentration were assessed using the 2,100 Bioanalyzer (Agilent, United States), NanoPhotometer spectrophotometer (Implen, Germany) and Qubit 2.0 fluorometer (Invitrogen, United States), respectively. The construction of libraries and the RNA-Seq on the Illumina sequencing platform were performed by Guangzhou Genedenovo Biotechnology Co., Ltd. Raw reads were trimmed to remove adaptors and enhance quality by fastp (version 0.18.0, Chen et al., 2018). Parameters removed reads containing adapters, more than 10% of unknown nucleotides and low quality reads containing more than 50% of low quality (*Q*-value ≤20) bases. The HISTAT2.2.4 was used to map clean reads to the genome with default parameters (Kim et al., 2015). The StringTie v1.3.1 was used to assemble transcripts with mapped reads (Pertea et al., 2015). FPKM (Fragments Per Kilobase of transcript per Million fragments mapped) was used to measure transcript or gene expression levels (Florea et al., 2013). The predicted gene sequences were annotated functionally by COG, KEGG, swiss-prot and Nr databases (Tatusov et al., 2000; Boeckmann et al., 2003; Kanehisa et al., 2004; Deng et al., 2006). During the identification of differentially expressed genes, fold change (FC) ≥ 2 and false discovery rate (FDR) < 0.05 were used as screening criteria. Pearson correlation coefficients were calculated for metabolome and transcriptome data integration. Gene and metabolite pairs were ranked in descending order of absolute correlation coefficients. The top 250 pairs of genes and metabolites (with absolute Pearson correlation >0.5) were applied for metabolite–transcript network analysis by using igraph packages in R project (Csardi and Nepusz, 2006).

Quantitative real-time PCR (qRT-PCR) analysis

Total RNA was isolated from mycelium at different sampling times. The PrimeScript RT reagent kit with gDNA Eraser (Takara Bio, Inc., Japan) and SYBR® Fast qPCR Mix (Takara Bio, Inc., Japan) were used for the CFX96 real-time PCR system (Bio-Rad Laboratories, Inc., United States). All operations were performed in accordance with the manufacturer's instructions. The thermocycling conditions consisted of initial denaturation at 95°C for 30 s followed by 40 cycles at 95°C for 5 s and 60°C for 30 s. β-Actin was used as internal reference gene, and gene expression was quantified using the comparative $2^{-\Delta\Delta}$Cq method (Schmittgen and Livak, 2008). PCR primer sequences are listed in Supplementary Table 1.

Statistical analysis

Data were expressed as mean ± SD. Statistical analysis was performed using the SPSS 16.0 software (SPSS, Inc.). One-way ANOVA was used to analyze statistical differences between groups under different conditions followed by Tukey's *post-hoc* test. $p < 0.05$ indicated a significant difference.

Results

MBE could promote the growth of *Sanghuangporus vaninii* mycelium

The effects of different concentrations of MBE on the growth of *S. vaninii* mycelium were observed. As shown in Figures 1A,B,

1 https://www.mzcloud.org/

high concentrations (1 and 0.5 g/l) of MBE inhibited the expansion of *S. vaninii* mycelium, and the mycelium became dense. At the concentration of 0.2 g/l, MBE did not inhibit the expansion of mycelium and could significantly increase the fresh weight of mycelium on PDA plate (Figure 1B). Next, whether MBE could promote the growth of *S. vaninii* mycelium in liquid culture were observed in CM containing different MBE concentrations (0.5, 0.2 and 0.1 g/l). As shown in Figures 1C,D, 0.1 and 0.2 g/l of MBE in PDB could markedly promote the mycelium growth rate. After 16 days of liquid culture, the dry weight of mycelium in MBE (0.2 g/l) medium reached 1.82 g per 300 ml, which was three times higher than that of the control group (PDB without MBE). Results suggested that at the concentration of 0.2 g/l, MBE could significantly promote the growth of *S. vaninii* mycelium.

Metabonomic analysis identified key active compounds in MBE

The metabolomic analysis of the CM at different culture times (10 and 16 days) and concentrations (0.5, 0.2, 0.1 and 0 g/l) was conducted to find the key components in MBE that promoted the growth of *S. vaninii* mycelium. A total of 2,229 differential metabolites, including 1,509 in positive ion mode and 720 in negative ion mode, were identified. Under the different concentrations of MBE culture for 10 days (CM10d_1, CM10d_2 and CM10d_5) vs. control group culture for 10 days (CM10d_0), respectively, and CM16d_1, CM16d_2 and CM16d_5 vs. control group CM160, respectively. A total of 22 shared differential metabolites in the six groups above, including 17 in positive ion mode and 5 in negative ion mode (Figure 2A). Next, according to the peak value trend of different metabolites (Supplementary Figure 1), the peak values of groups with MBE should be higher than those of control groups (CM10d_0 and CM16d_0). Nine potential components, which might promote the growth of *S. vaninii* mycelium were screened (Table 1; Figure 2B). To confirm that these ingredients were derived from MBE and not mycelial secretion, the HPLC-MS analysis of aqueous MBE solution and standards of these reagents (N6-Succinyl Adenosine, polymer Trp-Met-His [WMH] and LDGTS 8:0 were unavailable) was conducted. As shown in Supplementary Table 2, all components except 4-hydroxycoumarin could be detected in aqueous MBE solution.

Next, the effects of the five components on promoting the growth of *S. vaninii* mycelium were verified. Three concentrations (20, 2 and 0.2 mg/l) were set to check the effects on growth rate and fresh weight of *S. vaninii* mycelium on PDA. At concentrations of 2 mg/l, scopoletin, kynurenic acid, 3,5-dihydroxybenzoic acid, 2,4-dihydroxybenzoic acid and salicylic acid showed better growth potential than other concentration gradients. However, the growth rate of mycelium showed no difference from that of PDA, but the fresh weight was significantly higher than PDA except salicylic acid (Figure 3A). Next, liquid culture was conducted to confirm whether scopoletin, kynurenic acid, 3,5-dihydroxybenzoic acid

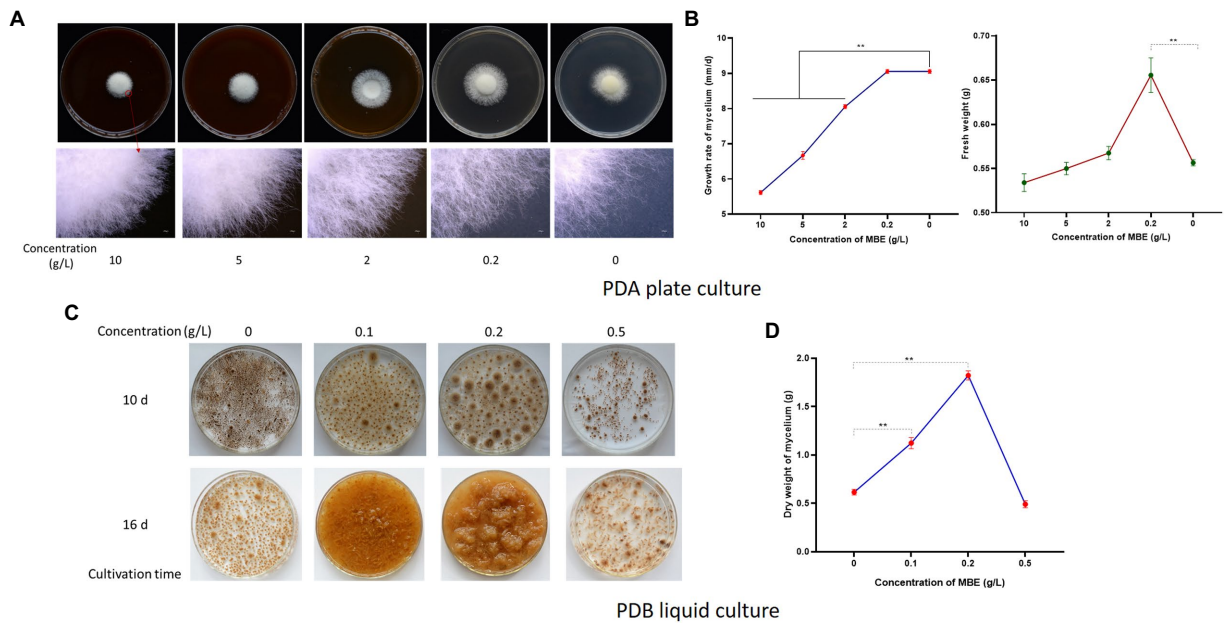

FIGURE 1
Effects of mulberry branch extracts (MBE) on *Sanghuangprous vaninii* mycelium. **(A)** Effects of different concentrations of MBE on the growth of *S. vaninii* mycelium on plate after 7days of cultivation. The upper figures are the outline of the colony, and the lower figures are the 20× edge of colony. **(B)** Statistics of growth rate and fresh weight of *S. vaninii* mycelium on plate. **(C)** Effect of different concentrations of MBE on the growth of *S. vaninii* mycelium in liquid culture. **(D)** Statistics of dry weight of *S. vaninii* mycelium after 16days of liquid cultivation. Three biological replicates were analyzed. Data are shown as means ± SEM. $^{**}p<0.01$.

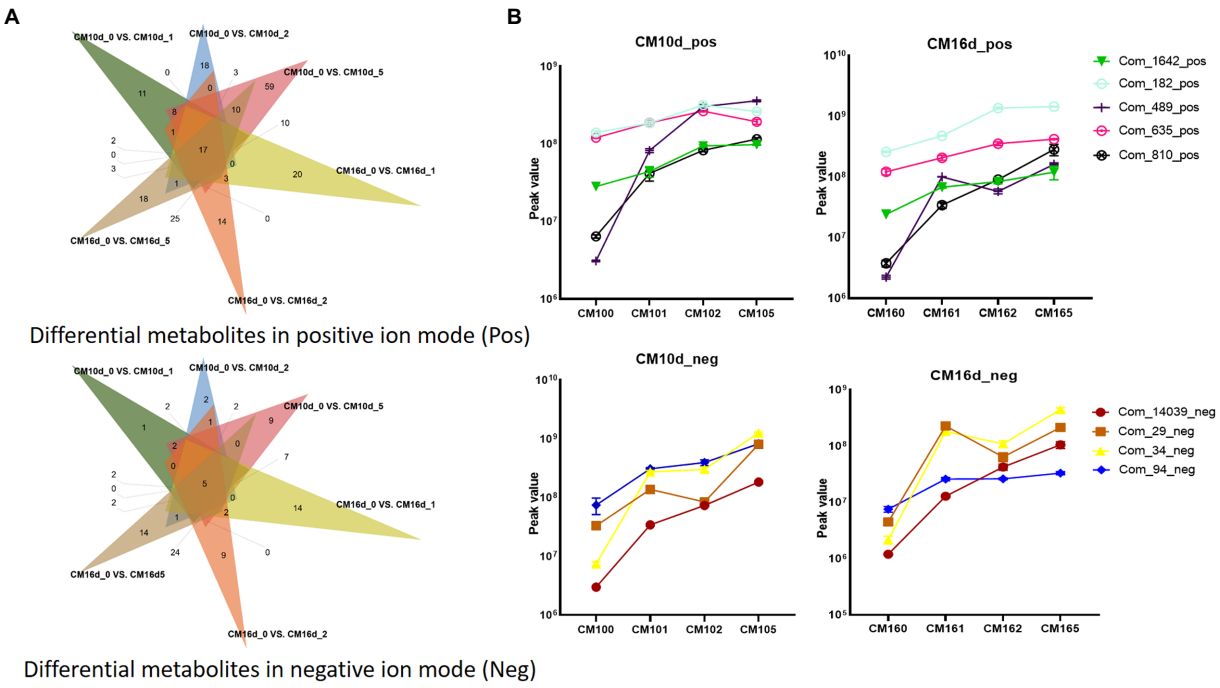

FIGURE 2
Metabolomic analysis of culture medium of *S. vaninii* mycelium. **(A)** Venn diagram of differential metabolites screening. **(B)** Peak value trend of screened metabolites.

TABLE 1 Candidate components in MBE for promoting the growth of *Sanghuangprous vaninii* mycelium.

	Name	Formula	Molecular weight
Positive ion mode (Pos)			
Com_1642_pos	Trp-Met-His [WMH]	$C_{22}H_{28}N_6O_4S$	472.1919
Com_182_pos	N6-Succinyl Adenosine	$C_{14}H_{17}N_5O_8$	383.1076
Com_489_pos	Scopoletin	$C_{10}H_8O_4$	192.0423
Com_635_pos	Kynurenic acid	$C_{10}H_7NO_3$	189.0426
Com_810_pos	LDGTS 8:0	$C_{18}H_{35}NO_6$	361.2464
Negative ion mode (Neg)			
Com_14039_neg	4-Hydroxycoumarin	$C_9H_6O_3$	162.0317
Com_29_neg	3,5-Dihydroxybenzoic acid	$C_7H_6O_4$	154.0266
Com_34_neg	2,4-Dihydroxybenzoic acid	$C_7H_6O_4$	154.0265
Com_94_neg	Salicylic acid	$C_7H_6O_3$	138.0316

and 2,4-dihydroxybenzoic acid could increase the growth rate of mycelium. As shown in Figure 3B, after 20 days of liquid culture, these four components could significantly increase the dry weight of mycelium at concentrations of 2 mg/l. The medium containing kynurenic acid could harvest 2.54 g per 300 ml dried mycelium, which was 1.8-fold higher than that of the control.

MBE primarily promoted the mycelial growth by upregulating hydrolase-related genes

To uncover the mechanism of promoted growth of *S. vaninii* mycelium by MBE, the transcriptomic analysis of mycelium, which was harvested at concentrations of 0, 0.1 and 0.2 g/l MBE for 10 and 16 days of liquid culture (M10d_0, M10d_1, M10d_2, M16d_0, M16d_1 and M16d_2) was conducted. According to the growth trend of mycelium, the parameters of screening differential expression genes (DEGs) were as follows: all upregulated DEGs in M10d_1 vs. M10d_0, M10d_2 vs. M10d_0, M16d_1 vs. M16d_0, M16 d_2 vs. M16 d_0 and M16 d_0 vs. M10 d_0 (Figure 4A). As shown in the Venn diagram (Figure 4A), the four groups involved in MBE could co-upregulate 16 genes, including 9 shared genes in M16 d_0 vs. M10 d_0 group (Figure 4A). Out of 16 genes, eight could be annotated, and two copies of *Fet3 protein* gene were annotated (Supplementary Table 3). Next, the relative expression levels of these seven genes by qRT-PCR at M10d_0, M10d_2, M16d_0 and M16d_2 were verified. All genes exerted higher expression levels at the concentration of 0.2 g/l than at the control at the same sampling time. The *Cerato-platanin protein*, *serine–glycine–asparaginate–histidine* (*SGNH*) *hydrolase*, *alpha-amylase*, *poly-beta-hydroxybutyrate* (*PHB*) *depolymerase* and *glycosyl hydrolase family 61* genes showed high expression levels at M16d_0 than M10d_0, whereas *Fet3* and *Cytochrome oxidase complex assembly protein 1* (*COA1*) were downregulated at

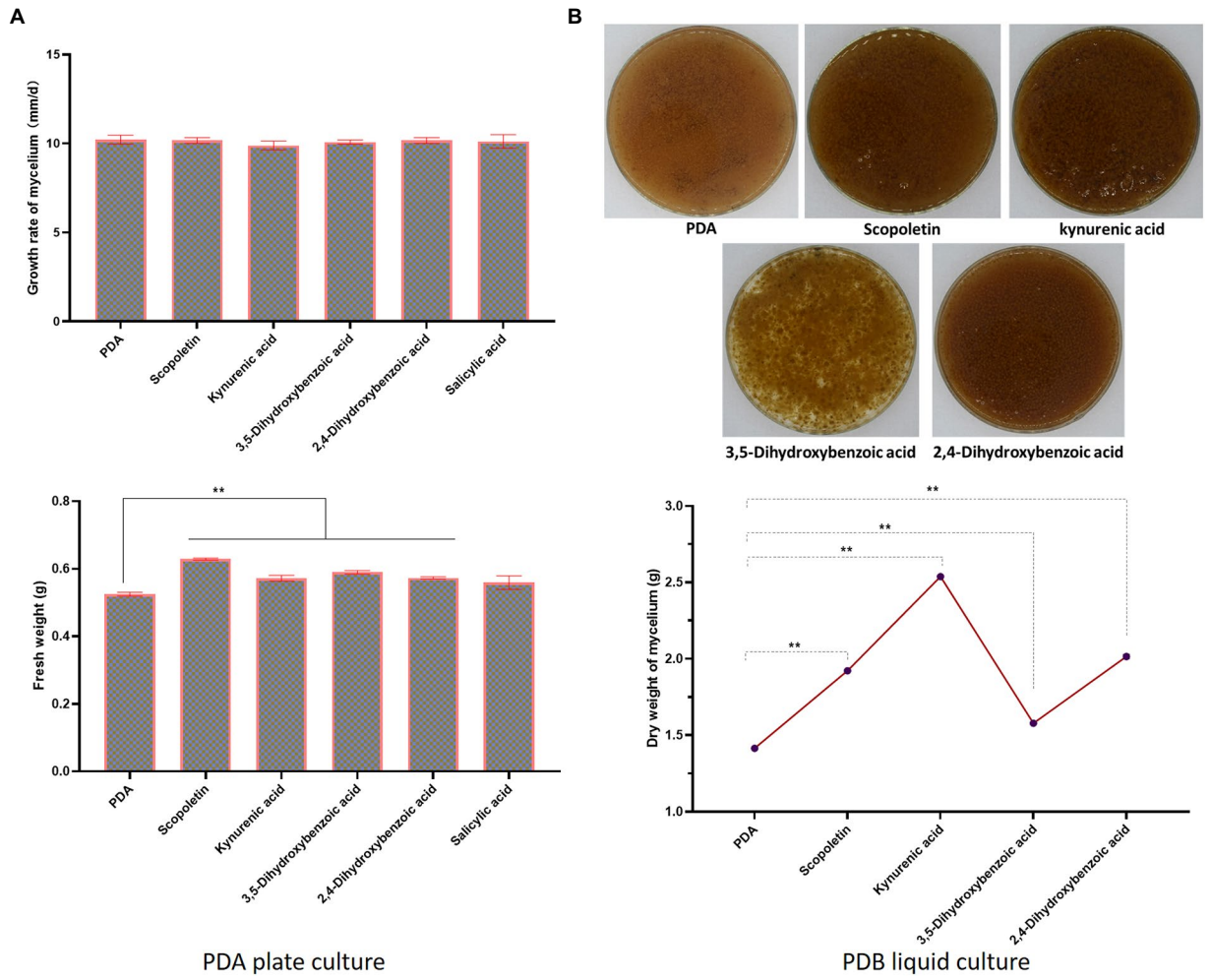

FIGURE 3
Effects of candidate metabolites in MBE on *S. vaninii* mycelium. **(A)** Statistics of growth rate and fresh weight of *S. vaninii* mycelium on plate. **(B)** Effects of four compounds on *S. vaninii* mycelium after 20days of liquid cultivation. The upper figures are harvested mycelium, and the lower figures are the statistics of dry weight of *S. vaninii* mycelium after 20days of liquid cultivation. Three biological replicates were analyzed. Data are shown as means ± SEM. $^{**}p<0.01$.

M16d_0 compared with M10d_0 (Figure 4B). The *SGNH hydrolase*, *alpha-amylase*, *PHB depolymerase*, *glycosyl hydrolase family 61*, *cerato-platanin protein* and *Fet3* are all hydrolase-related genes. The proteins encoded by these genes could hydrolyse a variety of substrates. Thus, *S. vaninii* could absorb increased nutrients for mycelial growth.

MBE significantly increased the content of active ingredients in the mycelium

The major application of liquid fermentation is the harvesting of mycelium. Therefore, the effects of MBE on mycelial components were analysed by metabolomics. The metabolomics analysis of M16d_2 vs. M16d_0 showed that 70 differential metabolites, including 53 in positive ion mode and 17 in negative ion mode, were identified. At M16d_2, 44 and 6 metabolites were significantly increased in the positive and negative ion modes, respectively, than at M16d_0 (Supplementary Table 4). Except those of some primary metabolites, the contents of active ingredients, such as harmine, androstenedione and vesamicol were significantly increased by more than 10-fold by MBE (0.2 g/l), whereas acetylcholine, N-acetylputrescine and caprolactam decreased significantly under MBE (0.2 g/l) treatment (Supplementary Table 4). Harmine has various pharmacological activities, such as anti-inflammatory and antitumor properties (Zhang et al., 2020). Androstenedione, a steroidal hormone, is thought to be an enhancer for athletic performance and build body muscles (Badawy et al., 2021). Vesamicol, a selective vesicular acetylcholine transporter inhibitor, and acetylcholine can antagonistically regulate cholinergic transmission to treat cholinergic dysfunction-associated disorders (Muramatsu et al., 2022). Results implied that the mycelium harvested from 0.02% MBE liquid culture might possess improved medicinal effects.

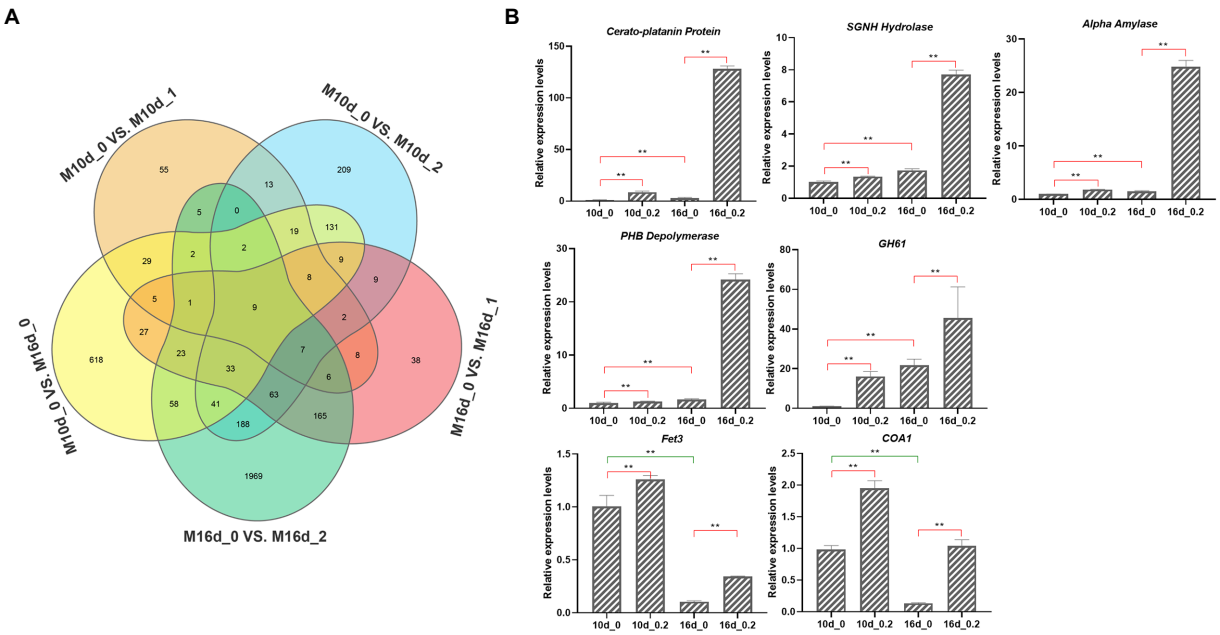

FIGURE 4
Transcriptomic analysis of *S. vaninii* mycelium. **(A)** Venn diagram of differential expression genes (DEGs). **(B)** qRT-PCR analysis of seven candidate genes. Four biological replicates were analyzed. Data are shown as means ± SEM. $^{**}p<0.01$.

To further explore the synthesis mechanism of these active ingredients, correlation analysis between mycelial metabolites and transcriptomics (M16d_2 vs. M16d_0) was carried out. KEGG analysis showed that DEGs were enriched in the 2-oxocarboxylic acid metabolism pathway and biosynthesis of amino acids pathway (Figure 5A), and differential metabolites were primarily enriched in ABC transporter pathway (Figure 5B). These enriched pathways were mostly related to the growth difference of the mycelium rather than the biosynthesis of these active ingredients. Therefore, the Pearson correlation coefficient model was used to determine the relationship between DEGs and differential metabolites. As shown in Figure 5C, harmine showed strong positive correlation (>0.99) with 58 genes, and androstenedione and vesamicol correlated positively with 2 and 3 genes, respectively. In accordance with the description of these correlated genes (Supplementary Table 5), several hydrolase family genes were annotated. In addition, cytochrome p450 genes and genes of unknown function might be involved in regulating the biosynthesis of these active ingredients. The characteristics of these genes need further research.

Discussion

As a valuable medicinal fungus, *S. vaninii* has the characteristics of slow growth and weak competitiveness, and the improvement of growth rate of mycelium can largely overcome these shortcomings. In the present study, the extracts from host of *S. vaninii* can significantly promote the growth of *S. vaninii* mycelium in liquid culture. Guo et al. (2021) found that the polymer lignin, as a component of branches, can promote the growth of *S. vaninii* mycelium at the concentration of 0.06 g/l. Findings imply that MBE may have similar effects. In the present study, after 16 days of liquid culture, the dry weight of mycelium in 0.2 g/l MBE medium reaches 1.82 g per 300 ml, which is thrice that of the control. Metabonomic analysis is conducted to identify key active compounds in MBE. Components derived from PDA are excluded by screening the differential shared metabolites of CM10d_0 vs. CM10d_1, CM10d_0 vs. CM10d_2, CM10d_0 vs. CM10d_5, CM16d_0 vs. CM16d_1, CM16d_0 vs. CM16d_2 and CM16d_0 vs. CM16d_5 (Figure 2A). Next, if the peak values of the groups with MBE are lower than the control groups (CM10d_0 and CM16d_0), these metabolites are thought be the reduced mycelial secretion under MBE treatment rather than components in MBE. And nine potential components are screened (Table 1). Further, five ingredients derived from MBE rather than mycelial secretion (Supplementary Table 2) are confirmed by HPLC-MS. And 4-hydroxycoumarin is derived from mycelial secretion. About 2 mg/l scopoletin, kynurenic acid, 3,5-dihydroxybenzoic acid and 2,4-dihydroxybenzoic acid can significantly increase the dry weight of mycelium in liquid culture, and the medium containing 2 mg/l kynurenic acid can harvest 2.54 g dried mycelium, which is 1.8-fold than that of the control group (Figure 3B). All four compounds are not reported to promote the growth of fungal mycelium. Unfortunately, none of these four compounds can achieve the same growth-promoting effects as MBE. Several components in MBE may work together

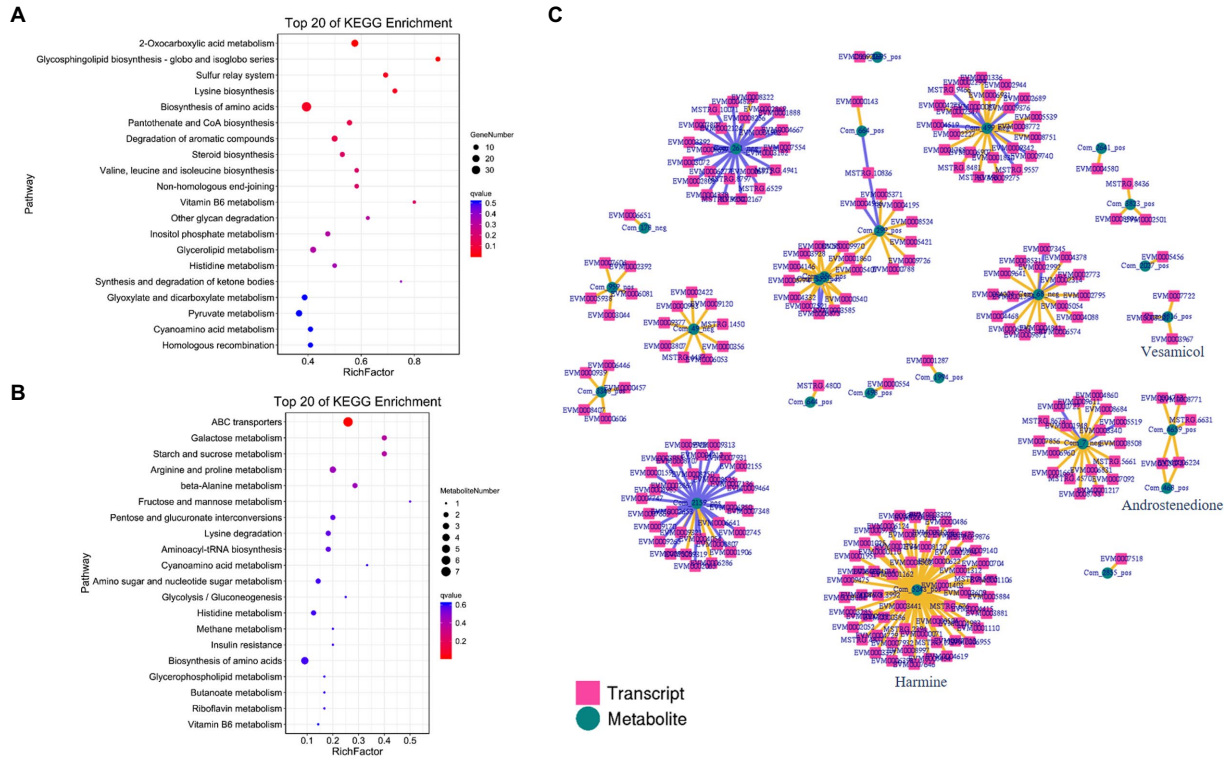

FIGURE 5
Correlation analysis between mycelial metabolites and transcriptomics (M16d_2 vs. M16d_0). **(A)** KEGG DEGs in M16d_2 vs. M16d_0. **(B)** KEGG differential metabolites in M16d_2 vs. M16d_0. **(C)** Pearson correlation coefficient calculation of DEGs and differential metabolites.

to promote the growth of *S. vaninii* mycelium, and some minor effects of compounds have not been identified.

The enhancement of the vitality of *S. vaninii*, as a wood-inhabiting fungus, primarily depends on the improved activity of the degrading complex and recalcitrant plant polymers, secreting different enzymes that hydrolyse plant cell wall polysaccharides (Guerriero et al., 2015). Polysaccharides are embedded in plant cell walls and form a network of chains bound to cellulose and pectin. Matrix polysaccharides are structurally complex and are substituted by various carbohydrates and acids (Urbániková, 2021). Upregulated genes among M10d_1 vs. M10d_0, M10d_2 vs. M10d_0, M16d_1 vs. M16d_0, M16 d_2 vs. M16 d_0 and M16 d_0 vs. M10 d_0 were screened by transcriptomics and qTR-PCR analysis (Figure 4). A total of 6 of 7 annotated genes possessed hydrolase activity. *Cerato-platanin protein*, *SGNH hydrolase*, *Alpha amylase*, *PHB depolymerase*, and *Glycosyl hydrolase family 61* genes showed higher expression levels at M16d_0 than at M10d_0, whereas *Fet3* and *COA1* were downregulated at M16d_0 than at M10d_0 (Figure 4B). Majority of the upregulated genes belongs to hydrolase-related genes. SGNH hydrolase and PHB depolymerase belong to the carbohydrate esterase family, which can remove the *o*-acetylation modification of polysaccharides for the complete degradation of the plant cell walls. The glycosyl hydrolase family 61 can hydrolase carboxymethyl cellulose and β-glucan (Karlsson et al., 2001). Alpha-amylase, also called GH13, is responsible for the endohydrolysis of (1→4)-α-D-glucosidic linkages in polysaccharides (Janíčková and Janeček, 2021). Fet3, a kind of laccase, can degrade lignin and humus (Janusz et al., 2020). Some of cerato-platanin coding proteins are produced during infection by pathogenic fungi (Yu and Li, 2014). Li et al. (2019) characterised a cerato-platanin-like protein from *Fusarium oxysporum* named FocCP1. In tobacco, the FocCP1 protein can cause the accumulation of reactive oxygen species, formation of necrotic reaction, deposition of callose, expression of defence-related genes and accumulation of salicylic and jasmonic acids in tobacco. These hydrolase-related proteins can hydrolyse complex polysaccharides, including lignin, cellulose and callose. As a result, *S. vaninii* can absorb plenty of nutrients for mycelial growth. COA1 participates in the synthesis of phosphatidylinositol (PI). PI is an important secondary messenger that can affect diverse cellular processes, including protein transport, cell polarity, cytoskeletal organisation, ion-channel function and gene expression (Finkelstein et al., 2020). *Fet3* and *COA1* are downregulated at M16d_0 than at M10d_0 (Figure 4B), suggesting that *Fet3* and *COA1* can respond to MBE treatment at an early stage. The expression levels of five other genes are high at 16 days under MBE treatment, which may be responsible for further promoting the growth of *S. vaninii* mycelium.

Liquid fermentation can provide strains for large-scale artificial substitute cultivation and directly harvest mycelium for the extraction of bioactive compounds. MBE (0.2 g/l) can remarkably increase the contents of harmine, androstenedione and vesamicol by more than 10-fold (Supplementary Table 4). Harmine has various pharmacological activities, such as anti-inflammatory, antitumor, antidiabetic and neuroprotective activities. Moreover, harmine exhibits insecticidal, antiviral and antibacterial effects (Zhang et al., 2020). Previous study (Sun et al., 2020) found that *S. vaninii* mycelium can markedly improve growth and innate immunity in weaned piglets and that the mycelium harvested from MBE (0.2 g/l) liquid culture may possess improved effects. Androstenedione, a steroidal hormone, is thought to be an enhancer for athletic performance, build body muscles, reduce fats, increase energy, maintain healthy red blood cells and increase sexual performance (Badawy et al., 2021). No relevant medicinal effect of *S. vaninii* mycelium has been reported. In the MBE (0.2 g/l) group, vesamicol, a selective vesicular acetylcholine transporter inhibitor, increases, whereas acetylcholine decreases, implying that the mycelium in MBE (0.2 g/l) group can also treat cholinergic dysfunction-associated disorders. Pearson correlation analysis showed that harmine has strong positive correlation (>0.99) with 58 genes. Except several hydrolase family genes, majority of genes are cytochrome p450s and genes of unknown function (Supplementary Table 5), which may be involved in regulating the biosynthesis of these active ingredients. The medicinal efficacy and gene function of *S. vaninii* need further exploration.

Conclusion

In the present study, MBE could promote the growth of *S. vaninii* mycelium at the concentration of 0.2 g/l and identified four key active compounds in MBE, which were primarily responsible for the growth-promoting effects. In addition, MBE promoted the mycelial growth by upregulating hydrolase-related genes. Finally, MBE could significantly increase several bioactive ingredients in mycelium. Results suggested that MBE is an excellent additive for the liquid culture of *S. vaninii* mycelium.

Data availability statement

The raw RNA-seq data for this study can be found in the NCBI database – BioProject ID: PRJNA871986. The non-targeted metabonomic datasets can be found in Figshare – https://doi.org/10.6084/m9.figshare.20524158.v1.

Author contributions

YL and SZ conceived and designed the study. JH performed the experiments with the help of YS, MP, HM, TL, and ZL. YL, SZ, and JH analyzed the data and prepared the manuscript. All authors contributed to the article and approved the submitted version.

Funding

This work was supported financially by Science and Technology Department of Zhejiang Province (LQ21C150002 and 2018C02003).

Conflict of interest

The authors declare that the research was conducted in the absence of any commercial or financial relationships that could be construed as a potential conflict of interest.

Publisher's note

Supplementary material

The Supplementary material for this article can be found online at: https://www.frontiersin.org/articles/10.3389/fmicb.2022.1024987/full#supplementary-material

References

Badawy, M. T., Sobeh, M., Xiao, J., and Farag, M. A. (2021). Androstenedione (a natural steroid and a drug supplement): a comprehensive review of its consumption, metabolism, health effects, and toxicity with sex differences. *Molecules* 26:6210. doi: 10.3390/molecules26206210

Barri, T., and Dragsted, L. O. (2013). UPLC-ESI-QTOF/MS and multivariate data analysis for blood plasma and serum metabolomics: effect of experimental artefacts and anticoagulant. *Anal. Chim. Acta* 768, 118–128. doi: 10.1016/j.aca.2013.01.015

Boeckmann, B., Bairoch, A., Apweiler, R., Blatter, M. C., Estreicher, A., Gasteiger, E., et al. (2003). The SWISS-PROT protein knowledgebase and its supplement TrEMBL in 2003. *Nucleic Acids Res.* 31, 365–370. doi: 10.1093/nar/gkg095

Chen, S., Zhou, Y., Chen, Y., and Gu, J. (2018). fastp: an ultra-fast all-in-one FASTQ preprocessor. *Bioinformatics* 34, i884–i890. doi: 10.1093/bioinformatics/bty560

Csardi, G., and Nepusz, T. (2006). The igraph software package for complex network research. *InterJournal Complex Syst.* 1695, 1–9.

Deng, Y., Li, J., Wu, S., Zhu, Y., Chen, Y., and He, F. (2006). Integrated nr database in protein annotation system and its localization. *Comput. Eng.* 32, 71–74. doi: 10.1109/INFOCOM.2006.241

Finkelstein, S., Gospe, S. M. 3rd, Schuhmann, K., Shevchenko, A., Arshavsky, V. Y., and Lobanova, E. S. (2020). Phosphoinositide profile of the mouse retina. *Cells* 9:1417. doi: 10.3390/cells9061417

Florea, L., Song, L., and Salzberg, S. L. (2013). Thousands of exon skipping events differentiate among splicing patterns in sixteen human tissues. *F1000Resarch* 2:188. doi: 10.12688/f1000research.2-188.v2

Guerriero, G., Hausman, J. F., Strauss, J., Ertan, H., and Siddiqui, K. S. (2015). Destructuring plant biomass: focus on fungal and extremophilic cell wall hydrolases. *Plant Sci.* 234, 180–193. doi: 10.1016/j.plantsci.2015.02.010

Guo, S., Duan, W., Wang, Y., Chen, L., Yang, C., Gu, X., et al. (2022). Component analysis and anti-colorectal cancer mechanism via AKT/mTOR signalling pathway of *Sanghuangporus vaninii* extracts. *Molecules* 27:1153. doi: 10.3390/molecules27041153

Guo, Q., Zhao, L., Zhu, Y., Wu, J., Hao, C., Song, S., et al. (2021). Optimization of culture medium for *Sanghuangporus vaninii* and a study on its therapeutic effects on gout. *Biomed. Pharmacother.* 135:111194. doi: 10.1016/j.biopha.2020.111194

He, P. Y., Hou, Y. H., Yang, Y., and Li, N. (2021). The anticancer effect of extract of medicinal mushroom *Sanghuangprous vaninii* against human cervical cancer cell via endoplasmic reticulum stress-mitochondrial apoptotic pathway. *J. Ethnopharmacol.* 279:114345. doi: 10.1016/j.jep.2021.114345

Huo, J., Zhong, S., Du, X., Cao, Y., Wang, W., Sun, Y., et al. (2020). Whole-genome sequence of *Phellinus gilvus* (mulberry Sanghuang) reveals its unique medicinal values. *J. Adv. Res.* 24, 325–335. doi: 10.1016/j.jare.2020.04.011

Janíčková, Z., and Janeček, Š. (2021). In silico analysis of fungal and chloride-dependent α-amylases within the family GH13 with identification of possible secondary surface-binding sites. *Molecules* 26:5704. doi: 10.3390/molecules26185704

Janusz, G., Pawlik, A., Świderska-Burek, U., Polak, J., Sulej, J., Jarosz-Wilkołazka, A., et al. (2020). Laccase properties, physiological functions, and evolution. *Int. J. Mol. Sci.* 21:966. doi: 10.3390/ijms21030966

Kanehisa, M., Goto, S., Kawashima, S., Okuno, Y., and Hattori, M. (2004). The KEGG resource for deciphering the genome. *Nucleic Acids Res.* 32, 277D–2280D. doi: 10.1093/nar/gkh063

Karlsson, J., Saloheimo, M., Siika-Aho, M., Tenkanen, M., Penttilä, M., and Tjerneld, F. (2001). Homologous expression and characterization of Cel61A (EG IV) of *Trichoderma reesei*. *Eur. J. Biochem.* 268, 6498–6507. doi: 10.1046/j.0014-2956.2001.02605.x

Kim, D., Langmead, B., and Salzberg, S. L. (2015). HISAT: a fast spliced aligner with low memory requirements. *Nat. Methods* 12, 357–360. doi: 10.1038/nmeth.3317

Li, S., Dong, Y., Li, L., Zhang, Y., Yang, X., Zeng, H., et al. (2019). The novel cerato-platanin-like protein FocCP1 from *Fusarium oxysporum* triggers an immune response in plants. *Int. J. Mol. Sci.* 20:2849. doi: 10.3390/ijms20112849

Li, X., Gao, D., Paudel, Y. N., Li, X., Zheng, M., Liu, G., et al. (2022). Anti-parkinson's disease activity of *Sanghuangprous vaninii* extracts in the MPTP-induced zebrafish model. *ACS Chem. Neurosci.* 13, 330–339. doi: 10.1021/acschemneuro.1c00656

Muramatsu, I., Uwada, J., Chihara, K., Sada, K., Wang, M. H., Yazawa, T., et al. (2022). Evaluation of radiolabeled acetylcholine synthesis and release in rat striatum. *J. Neurochem.* 160, 342–355. doi: 10.1111/jnc.15556

Pertea, M., Pertea, G. M., Antonescu, C. M., Chang, T., Mendell, J. T., and Salzberg, S. L. (2015). StringTie enables improved reconstruction of a transcriptome from RNA-seq reads. *Nat. Biotechnol.* 33, 290–295. doi: 10.1038/nbt.3122

Qiu, P., Liu, J., Zhao, L., Zhang, P., Wang, W., Shou, D., et al. (2022). Inoscavin a, a pyrone compound isolated from a *Sanghuangporus vaninii* extract, inhibits colon cancer cell growth and induces cell apoptosis via the hedgehog signaling pathway. *Phytomedicine* 96:153852. doi: 10.1016/j.phymed.2021.153852

Saccenti, E., Hoefsloot, H. C. J., Smilde, A. K., Westerhuis, J. A., and Hendriks, M. M. W. B. (2014). Reflections on univariate and multivariate analysis of metabolomics data. *Metabolomics* 10, 361–374. doi: 10.1007/s11306-013-0598-6

Schmittgen, T. D., and Livak, K. J. (2008). Analyzing real-time PCR data by the comparative C_T method. *Nat. Protoc.* 3, 1101–1108. doi: 10.1038/nprot.2008.73

Shen, S., Liu, S. L., Jiang, J. H., and Zhou, L. W. (2021). Addressing widespread misidentifications of traditional medicinal mushrooms in *Sanghuangporus* (Basidiomycota) through ITS barcoding and designation of reference sequences. *IMA Fungus* 12:10. doi: 10.1186/s43008-021-00059-x

Sun, Y., Zhong, S., Deng, B., Jin, Q., Wu, J., Huo, J., et al. (2020). Impact of *Phellinus gilvus* mycelia on growth, immunity and fecal microbiota in weaned piglets. *PeerJ* 8:e9067. doi: 10.7717/peerj.9067

Tatusov, R. L., Galperin, M. Y., Natale, D. A., and Koonin, E. V. (2000). The COG database: a tool for genome-scale analysis of protein functions and evolution. *Nucleic Acids Res.* 28, 33–36. doi: 10.1093/nar/28.1.33

Urbániková, Ľ. (2021). CE16 acetylesterases: in silico analysis, catalytic machinery prediction and comparison with related SGNH hydrolases. 3. *Biotech* 11:84. doi: 10.1007/s13205-020-02575-w

Wan, X., Jin, X., Wu, X., Yang, X., Lin, D., Li, C., et al. (2022). Structural characterisation and antitumor activity against non-small cell lung cancer of polysaccharides from *Sanghuangporus vaninii*. *Carbohydr. Polym.* 276:118798. doi: 10.1016/j.carbpol.2021.118798

Wan, X., Jin, X., Xie, M., Liu, J., Gontcharov, A. A., Wang, H., et al. (2020). Characterization of a polysaccharide from *Sanghuangporus vaninii* and its antitumor regulation via activation of the p 53 signaling pathway in breast cancer MCF-7 cells. *Int. J. Biol. Macromol.* 163, 865–877. doi: 10.1016/j.ijbiomac.2020.06.279

Want, E. J., Masson, P., Michopoulos, F., Wilson, I. D., Theodoridis, G., Plumb, R. S., et al. (2013). Global metabolic profiling of animal and human tissues via UPLC-MS. *Nat. Protoc.* 8, 17–32. doi: 10.1038/nprot.2012.135

Want, E. J., O'Maille, G., Smith, C. A., Brandon, T. R., Uritboonthai, W., Qin, C., et al. (2006). Solvent-dependent metabolite distribution, clustering, and protein extraction for serum profiling with mass spectrometry. *Anal. Chem.* 78, 743–752. doi: 10.1021/ac051312t

Worley, B., and Powers, R. (2013). Multivariate analysis in metabolomics. *Curr. Metabolom.* 1, 92–107. doi: 10.2174/2213235x130108

Wu, F., Jia, X., Yin, L., Cheng, Y., Miao, Y., and Zhang, X. (2019). The effect of hemicellulose and lignin on properties of polysaccharides in *Lentinus edodes* and their antioxidant evaluation. *Molecules* 24:1834. doi: 10.3390/molecules24091834

Yu, H., and Li, L. (2014). Phylogeny and molecular dating of the cerato-platanin-encoding genes. *Genet. Mol. Bol.* 37, 423–427. doi: 10.1590/s1415-47572014005000003

Yu, T., Zhong, S., Sun, Y., Sun, H., Chen, W., Li, Y., et al. (2021). Aqueous extracts of *Sanghuangporus vaninii* induce S-phase arrest and apoptosis in human melanoma A375 cells. *Oncol. Lett.* 22:628. doi: 10.3892/ol.2021.12889

Zhang, L., Li, D., and Yu, S. (2020). Pharmacological effects of harmine and its derivatives: a review. *Arch. Pharm. Res.* 43, 1259–1275. doi: 10.1007/s12272-020-01283-6

Zhong, S., Jin, Q., Yu, T., Zhu, J., and Li, Y. (2020). *Phellinus gilvus*-derived protocatechualdehyde induces G0/G1 phase arrest and apoptosis in murine B16-F10 cells. *Mol. Med. Rep.* 21, 1107–1114. doi: 10.3892/mmr.2019.10896

Zhong, S., Li, Y. G., Ji, D. F., Lin, T. B., and Lv, Z. Q. (2016). Protocatechualdehyde induces S-phase arrest and apoptosis by stimulating the $p27^{KIP1}$-Cyclin A/D1-CDK2 and mitochondrial apoptotic pathways in HT-29 cells. *Molecules* 21:934. doi: 10.3390/molecules21070934

frontiers | Frontiers in Microbiology

TYPE Review
PUBLISHED 11 October 2022
DOI 10.3389/fmicb.2022.1010332

OPEN ACCESS

EDITED BY
Naser Safaie,
Tarbiat Modares University, Iran

REVIEWED BY
Sanjai Saxena,
Thapar Institute of Engineering & Technology, India
Vagish Dwibedi,
Chandigarh University, India
Luigi Bavaresco,
Catholic University of the Sacred Heart, Italy

*CORRESPONDENCE
Abdallah M. A. Hassane
abdallahhassane@azhar.edu.eg
Mohamed E. Abouelela
m_abouelela@azhar.edu.eg

SPECIALTY SECTION
This article was submitted to Microbe and Virus Interactions with Plants, a section of the journal Frontiers in Microbiology

RECEIVED 03 August 2022
ACCEPTED 23 August 2022
PUBLISHED 11 October 2022

CITATION
Abo-Kadoum MA, Abouelela ME, Al Mousa AA, Abo-Dahab NF, Mosa MA, Helmy YA and Hassane AMA (2022) Resveratrol biosynthesis, optimization, induction, bio-transformation and bio-degradation in mycoendophytes. *Front. Microbiol.* 13:1010332. doi: 10.3389/fmicb.2022.1010332

Resveratrol biosynthesis, optimization, induction, bio-transformation and bio-degradation in mycoendophytes

M. A. Abo-Kadoum[1], Mohamed E. Abouelela[2,3]*, Amal A. Al Mousa[4], Nageh F. Abo-Dahab[1], Mohamed A. Mosa[5], Yosra A. Helmy[6,7] and Abdallah M. A. Hassane[1]*

[1]Department of Botany and Microbiology, Faculty of Science, Al-Azhar University, Assiut, Egypt, [2]Department of Pharmacognosy, Faculty of Pharmacy, Al-Azhar University, Assiut, Egypt, [3]Department of Pharmaceutical Sciences, College of Pharmacy, University of Kentucky, Lexington, KY, United States, [4]Department of Botany and Microbiology, College of Science, King Saud University, Riyadh, Saudi Arabia, [5]Nanotechnology and Advanced Nano-Materials Laboratory (NANML), Plant Pathology Research Institute, Agricultural Research Center, Giza, Egypt, [6]Department of Veterinary Science, College of Agriculture, Food and Environment, University of Kentucky, Lexington, KY, United States, [7]Department of Animal Hygiene, Zoonoses and Animal Ethology, Faculty of Veterinary Medicine, Suez Canal University, Ismailia, Egypt

Resveratrol (3,4,5-trihydroxystilbene) is a naturally occurring polyphenolic stilbene compound produced by certain plant species in response to biotic and abiotic factors. Resveratrol has sparked a lot of interest due to its unique structure and approved therapeutic properties for the prevention and treatment of many diseases such as neurological disease, cardiovascular disease, diabetes, inflammation, cancer, and Alzheimer's disease. Over the last few decades, many studies have focused on the production of resveratrol from various natural sources and the optimization of large-scale production. Endophytic fungi isolated from various types of grapevines and *Polygonum cuspidatum*, the primary plant sources of resveratrol, demonstrated intriguing resveratrol-producing ability. Due to the increasing demand for resveratrol, one active area of research is the use of endophytic fungi and metabolic engineering techniques for resveratrol's large-scale production. The current review addresses an overview of endophytic fungi as a source for production, as well as biosynthesis pathways and relevant genes incorporated in resveratrol biosynthesis. Various approaches for optimizing resveratrol production from endophytic fungi, as well as their bio-transformation and bio-degradation, are explained in detail.

KEYWORDS

resveratrol, endophytic fungi, biosynthesis, key genes, induction, optimization, bio-transformation, bio-degradation

Introduction

Endophytes are a group of microorganisms including fungi, bacteria, algae, and actinomycetes that preferentially coexist inside the living plant tissues without causing harmful effects during the life cycle of their host plant (de Bary, 1866; Nair and Padmavathy, 2014). They represent an important partner for the host-plant ecosystem (Aly et al., 2011). It has been reported that they can manipulate host metabolic pathways and participate in the biosynthesis and bioconversion of secondary metabolites that possess biologically active roles in medicine and agriculture (Nisa et al., 2015). Endophytes are the most abundant pool for novel bioactive natural products (Liu et al., 2016a). Fungal endophytes are a specific class of fungi that colonize the intercellular space of host-plant tissues and prompt host growth *via* facilitating nutrient uptake and increasing host resistance against environmental stress (Dwibedi and Saxena, 2018). Endophytic fungi have the metabolic capability to produce secondary metabolites with similar structure and function to their plant host. This is due to co-evolution with their plant host and horizontal gene transfer (HGT) (Aly et al., 2013). Some endophyte biosynthetic enzymes are homologous to those found in plants, corroborating the HGT phenomenon (Aly et al., 2013). Currently, fungal endophytes attracted a lot of attention for their bio-prospecting due to their capacity for the production of novel natural bioactive molecules. These compounds can be used in medicine, agriculture, and industry such as taxol, podophyllotoxin, vincristine, camptothecin, and harzianic acid (Aly et al., 2011; Adeniji, 2019; Dwibedi et al., 2019).

Resveratrol (3, 4, 5-trihydroxystilbene) is a natural polyphenolic compound that belongs to the stilbene family and consists of two benzene rings linked together by isopropyl moiety (Kasiotis et al., 2013). Resveratrol was first isolated from the roots of the poisonous plant *Veratrum grandiflorum* (white hellebore) by Takaoka in 1939 (Dwibedi and Saxena, 2018). Chinese medicine uses resveratrol, which was extracted from *P. cuspidatum* after 20 years, for therapeutic purposes (Nonomura et al., 1963). Resveratrol is widely distributed in numerous plant types such as grapes (*Vitis vinifera*), berries, peanuts (*Arachis hypogaea*), chocolate, tea, and cassia seeds (Burns et al., 2002; Baur and Sinclair, 2006; Wang et al., 2013; Mei et al., 2015). Grapes are considered the most abundant source of resveratrol content compared to other plants (Langcake and Pryce, 1977; Creasy and Coffee, 1988; Aleynova et al., 2021). Resveratrol is produced as phytoalexin to protect plants upon exposure to biotic stress such as fungal and bacterial attacks or abiotic stress such as UV radiation (Adrian et al., 2000; Cichewicz et al., 2000; Bavaresco et al., 2012; Dwibedi and Saxena, 2022). Due to the unique structure and therapeutic properties of resveratrol, it was used for protection against foodborne pathogens, neurological and cardiovascular diseases, diabetes, inflammation, cancer, longevity, free radicals, obesity, and Alzheimer's diseases (Parker et al., 2005; Aggarwal and Shishodia, 2006; Petrovski et al., 2011; Chen et al., 2013a; Ma et al., 2018). The marvelous role of resveratrol attracted researcher's attention to maximize their production rate and to find alternative sources for biosynthesis.

Extraction of resveratrol from producing plants is a confined process owing to low yields and specific seasons of plant growth (Kiselev, 2011). Mimicking the resveratrol biosynthetic pathway in microorganisms is a promising approach mediated with the aid of using both moving the whole pathway or specific genes to broaden metabolically changed strains, but this approach is steeply priced and time-consuming (Jeandet et al., 2012; Lu et al., 2016). Due to the co-evolution with the host plant, endophytic fungi possess the biosynthetic capacity to produce resveratrol. Bio-prospecting of resveratrol-producing endophytic fungi is a relatively new aspect initiated in the last decade (Dwibedi and Saxena, 2018). In this review, we will emphasize endophytic fungi as a promising alternative source for resveratrol production and underline its biosynthetic mechanism. In addition, we will give highlight on optimization and induction of resveratrol bio-production, bio-transformation, and bio-degradation (**Figure 1**).

Resveratrol-producing entophytic fungi

Fungal endophytes with resveratrol production capacity were initially isolated from various parts of their host plant tissues including leaves, stems, roots, and fruits. Powell et al. (1994) isolated resveratrol in high quantity from the grasses, *Festuca versuta* and *F. arundinacea* infected naturally with the endophytic fungus *Acremonium*. The authors found that the obtained resveratrol from endophyte-free plants was reduced and they suggested that this was attributed to the effect of

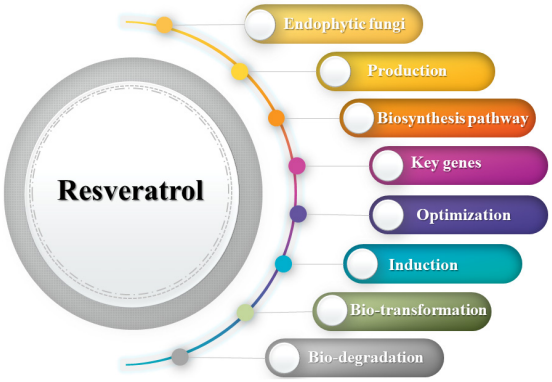

FIGURE 1
Summary of the review key points.

unknown environmental factors, and the reduction of the endophytic fungus *Acremonium* (Powell et al., 1994). Recently, the modulatory effect of endophytic fungi on their host-plant metabolites has been delineated (Nisa et al., 2015).

Several studies have addressed the production of resveratrol from endophytic fungi. Grape plants are the most frequently colonized hosts including *V. vinifera*, *Vitis quinquangularis*, and *Cayratia trifolia* (Roat and Saraf, 2017), together with the Japanese knotweed *P. cuspidatum*. Grapevine is one of the most economically important plants worldwide and a large proportion are directed to wine making (Reynolds, 2017). When the endophytic fungi colonize the grapevine, it increases the nutritional value in berries and prevents the pathogen attack associated with conferring resistance in response to abiotic environmental stress (Aleynova et al., 2021). *P. cuspidatum* is a medicinal plant that contains a high quantity of bioactive secondary metabolites, therefore it was used as traditional Chinese therapy for the treatment of immune diseases, diarrhea, hepatitis, and cancer (Chu et al., 2005). Resveratrol is the main active molecule produced by *P. cuspidatum* (Wang et al., 2013). The incidence of endophytic fungi within *P. cuspidatum* promotes plant growth and enhances the content of bioactive metabolites (Sun et al., 2022).

Resveratrol-producing endophytic fungi are belonging to diverse genera including *Alternaria*, *Botryosphaeria*, *Penicillium*, *Cephalosporium*, *Aspergillus*, *Geotrichum*, *Mucor, Arcopilus, Fusarium, Xylaria*, and *Nigrospora. Alternaria* is the most frequently occurring genus which is isolated from different types of grapevines and *P. cuspidatum* (Shi et al., 2012). Few strains exhibit the ability to produce high and constant levels of resveratrol such as *Alternaria* sp. MG1 (Shi et al., 2012), *Arcopilus aureus* (Dwibedi and Saxena, 2018), *Fusarium equiseti* (Dwibedi and Saxena, 2019a), and *Aspergillus stellifer* (Roat and Saraf, 2020). The rest of the isolated strains showed fluctuated production rates and most of them lost their ability for producing resveratrol, especially during the third sub-culture such as *Cephalosporium, Mucor, Geotrichum*, and *Penicillium* (Shi et al., 2012; Roat and Saraf, 2020). This phenomenon is in accordance with the fact that the fungal capacity to produce active components was reduced over the continuous cultivation for a long time *in vitro* with difficulty to be recovered. The instability of resveratrol production *via* endophytic fungi during *in vitro* culturing discloses the crucial role of the plant host as a partner and reveals that, resveratrol production is a concerted mechanism fine-tuned by host-fungus cross talk. Absence of the plant host results in fluctuated expression of resveratrol-related genes and its metabolic flux in endophytic fungi (Shi et al., 2012; Dwibedi and Saxena, 2019a).

Alternaria is a phytopathogenic fungus for many plants such as tomatoes, apples, carrots, and sweet potatoes (Akamatsu et al., 1999; Akamatsu, 2004). *Alternaria* spp. is ubiquities in grapevine, living in a mutual relationship or as a pathogen causing disease through the production of extracellular toxins (González and Tello, 2010). *Alternaria* sp. MG1 strain was isolated from the rachis part of the *V. vinifera* cultivar (Merlot) and showed the highest and most stable resveratrol production rate (104 μg/L) among all isolated strains (**Table 1**; Shi et al., 2012). Interestingly, the accumulation of resveratrol inside the MG1 strain was initiated at the early stage of the exponential phase contradicting the previous reports in which most of the secondary metabolites are accumulated at the late stage (Chomcheon et al., 2009; Kornsakulkarn et al., 2011). Among thirteen endophytic fungal isolates belonging to *Penicillium*, *Alternaria*, and *Aspergillus* obtained from different parts of the Brinjal plant (*Solanum melongena*), *Alternaria alternata* was the highest resveratrol producer (206 μg/L) (Abdel-Hadi et al., 2022). Whereas, resveratrol is not detected in the Brinjal plant (Singh et al., 2016).

Dwibedi and Saxena (2019a) reported 11 endophytic fungi isolated from different cultivars of *V. vinifera* and identified as resveratrol producers (**Table 1**). *A. aureus* #12VVLPM was the most potent producer (89.1 μg/ml) when it is growing on the Czapek Dox broth medium. The production of resveratrol by *A. aureus* was stable during subculturing compared to other isolates (Dwibedi and Saxena, 2018). Interestingly, the #12VVLPM strain was reported to produce the same resveratrol concentration when it is cultivated on potato dextrose broth (PDB) (Dwibedi and Saxena, 2019b), indicating that resveratrol production by *A. aureus* is medium-independent. Genus *Xylaria* is typically found on leaves and seeds of many woody plants (González and Tello, 2010). The strain *Xylaria psidii* #22(P) VVLPM which was isolated from the leaves of *V. vinifera* (Shiraz) was reported to produce less amount of resveratrol (35.43 μg/ml) compared to *A. aureus* when growing on the same PDB medium (Dwibedi et al., 2019).

The endophytic fungi belonging to the genus *Fusarium* are active producers of diverse secondary metabolites such as naphthoquinones that possess antibacterial and antifungal properties (Kornsakulkarn et al., 2011). *Fusarium* has been frequently reported to be associated with *V. vinifera* (González and Tello, 2010; Dwibedi and Saxena, 2019a). Dwibedi and Saxena identified thirteen strains as resveratrol-producing entophytic fungi isolated from *V. vinifera* (Dwibedi and Saxena, 2019a). *Fusarium* includes two strains, *F. equiseti* from the Pinot noir cultivar and *Fusarium solani* from Shiraz. *F. equiseti* is the most potent producer (52.3 μg/ml) owing to the presence of stilbene synthase (*STS*) as a key gene in the resveratrol production pathway (**Table 1**; Dwibedi and Saxena, 2019a). Furthermore, *Aspergillus* has been frequently isolated from *V. vinifera* and *V. quinquangularis* (Shi et al., 2012; Roat and Saraf, 2020). *A. stellifer* was isolated from the leaf of *V. vinifera* cultivar Merlot and showed stable resveratrol production capacity (288 μg/L) (Roat and Saraf, 2020). Cabernet Sauvignon is the main cultivar of wine grapes in the Shihezi region, China, where *Aspergillus niger* has been isolated and produced 1.48 mg/L of resveratrol (**Table 1**; Liu et al., 2016a).

10.3389/fmicb.2022.1010332

TABLE 1 Endophytic fungi produce resveratrol, their host plant, isolation part, used media, incubation time, and the quantity of produced resveratrol according to previous literature.

Endophytic fungi	Host plant	Part	Production media	Incubation time	Resveratrol quantity	References
Aspergillus stellifer AB4	*Vitis vinifera* (Merlot)	Leaf	PDA	6–7 days	288 μg/L	Roat and Saraf, 2020
Alternaria sp. AB5		Stem			143 μg/L	
Cephalosporium sp. AB6		Fruit skin	GA		134 μg/L	
Penicillium sp. AB7		Tendril	PDA		123 μg/L	
Alternaria sp. AB8		Fruit			14 μg/L	
Aspergillus sp. AB9		Rachis			131 μg/L	
Penicillium sp. AB10		Root			16 μg/L	
Alternaria sp. CD2	*Cayratia trifolia* (wild *Vitis*)	Stem	NA		126 μg/L	
Cephalosporium sp. CD3		Rachis	GA		10 μg/L	
Penicillium sp. CD4		Fruit			154 μg/L	
Penicillium sp. CD5		Root	PDA		152 μg/L	
Alternaria sp. EF3	*Vitis quinquangularis* (Rehd)	Rachis	GA1		143 μg/L	
Aspergillus sp. EF4		Root	PDA		145 μg/L	
Arcopilus aureus	*Vitis vinifera*	Not recorded	PDB	10 days	89.1 mg/L	Dwibedi and Saxena, 2019b
Fusarium equiseti					52.3 mg/L	
Xylaria psidii					35.4 mg/L	
Fusarium solani					31.3 mg/L	
Alternaria sp. MG1	*Vitis vinifera* (Merlot)	Rachis	GA1	7 days	104 μg/L	Shi et al., 2012
Alternaria sp. MG2					34 μg/L	
Alternaria sp. MG3					23 μg/L	
Alternaria sp. MG6		Skin			11 μg/L	
Alternaria sp. MG7					12 μg/L	
Alternaria sp. MP11			PDA		6 μg/L	
Alternaria sp. MP15					95 μg/L	
Botryosphaeria sp. YG3	*Vitis quinquangularis* (wild *Vitis*)	Stem	GA1		94 μg/L	
Penicillium sp. YP30			PDA		17 μg/L	
Cephalosporium sp. YG6		Rachis	GA1		35 μg/L	
Aspergillus sp. YG8					38 μg/L	
Cephalosporium sp. YP7			PDA		21 μg/L	
Penicillium sp. YP2		Skin			24 μg/L	
Geotrichum sp. HP7	*Polygonum cuspidatum*	Root			43 μg/L	
Mucor sp. HP9					21 μg/L	
Cephalosporium sp. HG16			GA1		67 μg/L	
Cephalosporium sp. HG5		Stem			11 μg/L	
Alternaria sp. HG6					123 μg/L	
Cephalosporium sp. HG7					56 μg/L	
Aspergillus niger	Wine grape (Cabernet Sauvignon)		PDB	3 days	1.48 mg/L	Liu et al., 2016a
Penicillium sp.	*Vitis vinifera* (Merlot)	Stem	CDB	7 days	21.9 μg/ml	Dwibedi and Saxena, 2018
Nigrospora sp.		Leaf			25.2 μg/ml	
Aspergillus sp.					4.4 μg/ml	
Alternaria sp.					24.1 μg/ml	
Aspergillus sp.					22.4 μg/ml	
Unidentified					11.9 μg/ml	

(Continued)

TABLE 1 (Continued)

Endophytic fungi	Host plant	Part	Production media	Incubation time	Resveratrol quantity	References
Aspergillus sp.	*Vitis vinifera* (Wild)	Stem			23.9 μg/ml	
Unidentified					13.2 μg/ml	
Arcopilus aureus	*Vitis vinifera* (Muscat)	Leaf			89.1 μg/ml	
Botryosphaeria sp.	*Vitis vinifera* (Pinot noir)				37.3 μg/ml	
Penicillium sp.					15.3 μg/ml	
Botryosphaeria sp.	*Vitis vinifera* (Pinot noir)	Leaf and stem	PDB	10 days	15.3 μg/ml	Dwibedi and Saxena, 2019a
Botryosphaeria sp.					37.3 μg/ml	
Fusarium equiseti					52.3 μg/ml	
Aspergillus sp.	*Vitis vinifera* (Merlot)				22.4 μg/ml	
Nigrospora sp.					25.2 μg/ml	
Penicillium sp.					21.9 μg/ml	
Aspergillus sp.					4.4 μg/ml	
Alternaria sp.					24.1 μg/ml	
Unidentified					11.9 μg/ml	
Aspergillus sp.	*Vitis vinifera* (Wild)				23.9 μg/ml	
Unidentified					13.2 μg/ml	
Xylaria sp.	*Vitis vinifera* (Shiraz)				35.4 μg/ml	
Fusarium sp.					31.3 μg/ml	
Xylaria psidii	*Vitis vinifera* (Shiraz)	Leaf	PDB	10 days	35.43 μg/ml	Dwibedi et al., 2019
Alternaria alternata SK.	Brinjal	Leaf	PDB	8–10 days	206 μg/L	Abdel-Hadi et al., 2022
Quambalaria cyanescens	*Vitis vinifera*	Stem	CDB	15 days	40 mg/L	Meshram et al., 2022

Quambalaria cyanescens is an endophytic fungus that colonizes corymbia and eucalyptus. *Q. cyanescens* is an active producer of bioactive metabolites that possess a broad spectrum of antimicrobial and anticancer potential such as quambalarine and quambalarine B, respectively (Meshram et al., 2022). *Q. cyanescens* obtained from the stems of *V. vinifera* was the active producer of resveratrol at 40 mg/L and the produced resveratrol is stable over three passages (**Table 1**; Meshram et al., 2022).

Host–fungal interaction

Endophytes are crucial for their host plant life in which they promote their growth *via* increasing nutrient availability and acquisition (Yang et al., 2016). They can equip the host plant against biotic and abiotic stress (Yang et al., 2016). Alteration in the phytochemical response of the host upon exposure to endophytes was recorded in a few previous reports, therefore, evaluating plant secondary metabolites should consider the presence of endophytes (Yang et al., 2016). The potential effect of endophytes on the host metabolites has been supported by various evidences. For instance, the production of Chinese medicine "dragon's blood" by *Dracaena cochinchinensis* is significantly elicited due to the coexistence of the endophytic fungus *Fusarium proliferatum* (Wang et al., 2011). Additionally, co-cultivation of endophytic fungi *A. alternata* and *Epicoccum nigrum* with the grape cells modulate the anthocyanin content and the activity of phenylalanine ammonia-lyase (PAL) indicating the metabolic alteration in the grape cells upon exposure to endophytic fungi (Yu et al., 2020). Endophytes modulate the chemical profile of their host plant through various mechanisms such as biosynthesis and they also export the metabolites directly to the host *via* eliciting signaling cascades and producing enzymes to dictate the host metabolic pathways (Yang et al., 2016).

Endophytic fungi can be utilized as a metabolic regulator to pinpoint the character and quality of the hosting plant, especially for those who produce organoleptic products, like wine and coffee (Yang et al., 2016). Several studies revealed that fungal endophytes can enhance resveratrol production in grape plants. Yang et al. (2016) reported eight endophytic fungi including *Alternaria* spp., *Chaetomium* sp., *Colletotrichum* sp., *Fusarium* sp., *Gibberella* sp., *Nigrospora* sp., and *Xylaria* sp., that were isolated from grapevines and co-cultivated with grapevines in the field. The amount of resveratrol was greatly improved in grapevines upon co-cultivation in leaves and fruits specifically during the maturity stage. Interestingly, *Chaetomium* sp., *Nigrospora* sp., and *Xylaria* sp. were significantly induced resveratrol production than the rest of the isolated fungi

(Yang et al., 2016), suggesting the potential effect of applying endophytic consortium to create different patterns of wine grape chemical profile and the resultant wine. Co-cultivation of tissue culture seedlings with endophytic fungi is similar to their daily growth and it was a potential system to enhance the content of bioactive metabolites (Aleynova et al., 2021). The amount of stilbene and trans-resveratrol was increased in *Vitis amurensis* cells co-cultured with endophytic fungi *Biscogniauxia* sp., *Cladosporium* sp., and *Didymella* spp. The highest concentration of trans-resveratrol (2.9 mg/g) dry weight was detected upon induction of endophytic fungus *Biscogniauxia* sp. The induction of trans-resveratrol by endophytic fungi was accompanied by significant up-regulation of resveratrol biosynthesis relevant genes PAL and STS (Aleynova et al., 2021).

Endophytic fungi of medicinal plants promote the accumulation of bioactive secondary metabolites inside their host (Teimoori-Boghsani et al., 2019). The medicinal plant *Rumex gmelini* Turcz (RGT) is a rich source of resveratrol and other bioactive secondary metabolites. RGT possesses diverse pharmacological activities as anticancer, antioxidant, antifungal, antihypertensive, antitussive, antiasthmatic, and antiviral (Zhang et al., 2008). Endophytic fungus *Aspergillus oryzae* promotes the accumulation of resveratrol in tissue culture seedling of RGT by 3.70-folds compared to the non-treated group. However, the level of polydatin (stilbene constituent in *R. gmelini*) was decreased; this may due to the ability of *A. oryzae* to convert polydatin into resveratrol under optimum conditions (Wang et al., 2007). Correspondingly, co-cultivation of *Ramularia* sp. with RGT tissue culture significantly dampens the resveratrol yield (Ding et al., 2018), suggesting the contradicted effect of RGT endophytic fungi.

Phytopathogenic fungi can promote the resveratrol yield in their host plant. *Botryodiplodia theobromae* LBBT HC6-1 and *Botrytis cinerea* FCBC TN1 have significantly induced the level of trans-resveratrol in peanut callus by 8.92 and 16.35 μg/g, respectively (Yang et al., 2010). A similar effect was found in grapevine upon *B. cinerea* FCBC TN1 infection (Paul et al., 1998). Viniferin diglucosides is a resveratrol dimer that was reported to be accumulated in the early stage of the grape fruits' development in response to *Botrytis* during the Noble Rot infection (Blanco-Ulate et al., 2015). Furthermore, resveratrol derivative, 2,4,6-Trihydroxyphenanthrene-2-*O*-glucoside, was detected in vine leaves upon *Plasmopara viticola* infection (Triska et al., 2012). The chitin layer of the fungal cell wall is a crucial component that is believed to induce resveratrol upon the fungal infection. The amount of trans-resveratrol induction by chitin was two-thirds compared to that elicited by sterilized fungi in peanut callus (Yang et al., 2010). Chitin and its fragments can elicit cascades of defense signaling and promote the activation of the phytoalexin system in the host plant. Melchior et al. (1991) studied the up-regulation of resveratrol biosynthesis-related proteins STS and PAL in the grapevine cell culture treated with fragments of *B. cinerea* cell wall. Those proteins have chitinase and glucanase activities and participate in the defense system *via* destroying the fungal mass (Yang et al., 2010).

Biosynthesis pathways and relevant genes

Deciphering the resveratrol biosynthesis pathway and its relevant key genes in endophytic fungi is substantial for delicate control of the production condition and overcoming the problems of low and unstable yield (Che et al., 2016b). The complete biosynthetic pathway of resveratrol is only identified in plants as the phenylpropanoid pathway (**Figure 2**). The key enzymes involved in this pathway are phenylalanine/tyrosine ammonia lyase (PAL/TAL), trans-cinnamate 4-hydroxylase (C4H), 4 coumarate-CoA ligase (4CL), STS, and resveratrol synthase (ST) or chalcone synthase (CHS) (Mei et al., 2015). PAL, C4H, and 4CL are responsible for the biosynthesis of natural phenolic-related metabolites including lignin and flavonols (Mei et al., 2015). PAL and TAL belong to the same protein family with a lyase domain in which they catalyze the breaking of amino acids into α and β-unsaturated acids which are accompanied by removing ammonia (Jendresen et al., 2015). The activity of PAL and TAL is substrate-dependent, in which phenylalanine is specific for PAL and tyrosine for TAL. However, when a point mutation occurred at position 89 (His–Phe), the substrate specificity of TAL switched to phenylalanine (Pinto et al., 2015). The resveratrol biosynthesis pathway is initiated by the deamination of phenylalanine mediated by PAL, and then C4H catalyzes the hydroxylation of trans-cinnamic acid to p-coumaric acid using ATP and coenzyme A. Finally, one 4-coumaroyl-CoA combined with three malonyl-CoA units to form resveratrol is catalyzed by the CHS/ST (Jeandet et al., 2002; Tavares et al., 2013).

Interestingly, the key enzymes for the resveratrol biosynthesis pathway have been reported separately in some yeast strains. For example, PAL in *Rhodotorula glutinis* and *Rhodosporidium toruloides* (Vannelli et al., 2007a; Wu et al., 2009), TAL in *R. glutinis*, *Trichosporon cutaneum*, and *Saccharothrix espanaensis* (Berner et al., 2006; Vannelli et al., 2007b), 4CL in *Streptomyces coelicolor* (Park et al., 2009), and CHS/ST in *Saccharopolyspora erythraea* (Magdevska et al., 2010). Genetically modified yeast, bacteria, and algae (**Figure 3**) with resveratrol-producing capacity are successfully constructed either *via* transforming the entire pathway or specific key genes (Liu et al., 2011; Dai et al., 2012; Xiang et al., 2020). However, constructions of key genes originating from plant sources complicated the resveratrol metabolic flux in microorganisms, resulting in low and unstable yield (Che et al., 2016c).

The phenylpropanoid pathway has not yet been identified in microorganisms. However, their key enzymes have been addressed in the endophytic fungus *Alternaria* sp. MG1. The

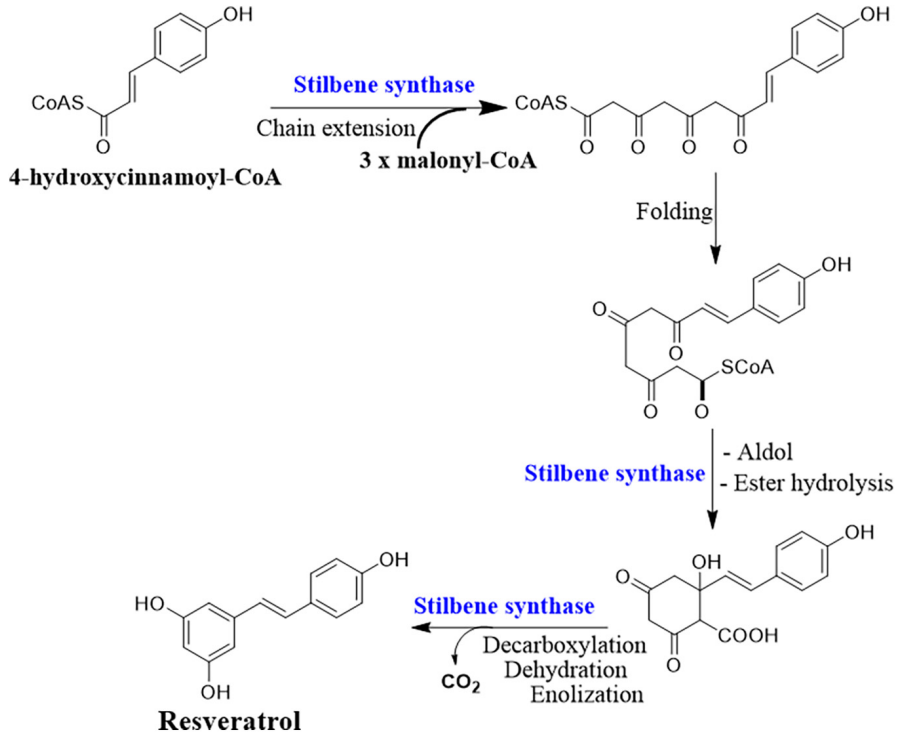

FIGURE 2
Resveratrol biosynthesis pathway.

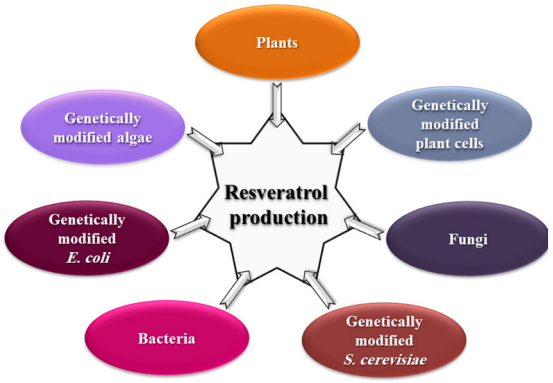

FIGURE 3
Different natural sources for resveratrol production.

accumulation of intermediate metabolites in *Alternaria* sp. MG1 such as cinnamic acid and p-coumaric acid were detected in association with the activity of upstream enzymes PAL, TAL, C4H, and 4CL in the presence of phenylalanine as a sole substrate, and consistent with the metabolic flux of phenylpropanoid pathway in the plant (Zhang et al., 2013). However, this study failed to detect the downstream enzymes, such as STS, ST, and CHS. Development of molecular techniques such as whole genome sequencing (WGS) and RNA-Seq analysis have helped to understand the complete picture of the resveratrol biosynthesis pathway and related genes in endophytic fungi (Lu et al., 2019). *De novo* transcriptome sequencing of *Alternaria* sp. MG1 was conducted during resveratrol production and a total of 84 genes were annotated encompassing four major resveratrol metabolic pathways that represent 38 coding enzymes (20 for glycolysis, 10 for phenylalanine biosynthesis, 4 for phenylpropanoid biosynthesis, and 4 for stilbenoid biosynthesis). The expression of PAL, 4CL, and CYP73A-related genes was observed (Che et al., 2016b). Additionally, Lu et al. (2019) used the WGS and obtained the same results and found that 4CL and CHS were up-regulated, resulting in a twofold increase in resveratrol production. Resveratrol synthase (ST) was not annotated in the previous studies (Che et al., 2016b; Lu et al., 2019), however, CHS was successfully annotated instead (Jeandet et al., 2010). CHS is an isoenzyme of ST that is responsible for the biosynthesis of naringenin and possesses catalytic activity to form resveratrol, whereas naringenin and resveratrol are produced from the same substrate, p-coumaric acid (Lu et al., 2019). Notably, the amino acid sequences of STSs and CHSs are similar which often hamper their distinction in gene annotation (Yu et al., 2005). Che et al. (2016a) detected the activity of PAL, TAL, C4H, and 4CL in the enzymatic extract of *Alternaria* sp. MG1, confirming the presence of phenylpropanoid biosynthesis pathway. Recently, the functional analysis of CHS and 4CL

from *Alternaria* sp. MG1 has been verified. The two genes were heterologously expressed in *Saccharomyces cerevisiae*, and the recombinant strain revealed resveratrol-producing capability reached 113.2 μg/L in the co-culture system (Lu et al., 2021b).

Some key genes are involved indirectly to enhance resveratrol production in *Alternaria* sp. MG1, including uridine-cytidine kinase (UCK) which is responsible for generating uridine monophosphate (UMP) and adenosine diphosphate (ADP) as cofactors participating in resveratrol synthesis, and phosphofructokinase (PFK) which channelizes the metabolic flux to pentose phosphate pathway (Lu et al., 2019). Several cofactors play an important role in resveratrol biosynthesis at different stages. For example, acetyl-CoA is a precursor for the formation of malonyl-CoA, the direct precursor in the last step of resveratrol biosynthesis. The resveratrol flux increased in association with elevated levels of acetyl-CoA (Lu et al., 2019). ATP is a crucial component in the CoA formation by which low ATP yield led to low CoA and subsequently low resveratrol production. Correspondingly, the simultaneous addition of CoA and ATP prompts resveratrol production (Zhang et al., 2013).

Optimization of resveratrol production

Resveratrol is a natural antioxidant (naturally stilbene occurring phytoalexin) produced by plants in response to resisting the pathogen's infection and is considered the principal component produced by phytotoxin reaction (Gambini et al., 2015). Resveratrol is a low molecular weight polyphenol compound with high content in grapes, mainly accumulated in high content grape leaves and peels to resist different biotic and abiotic stresses including fungal invasions and exposure to chemicals and UV radiation (Weiskirchen and Weiskirchen, 2016; Hasan and Bae, 2017). Extraction of resveratrol from plants is a classical technique that exhibited remarkable disadvantages, such as prolonged growth time, high cost, reduced yield, and the demand for induction through abiotic and biotic factors (Berman et al., 2017; Wang et al., 2018; Lu et al., 2021a). Chemical synthesis of resveratrol needs ordains complicated steps, utilize hazardous solvents, and produces toxic byproducts (Lu et al., 2019). Therefore, the exploitation of microorganisms to imitate resveratrol production by fermentation is a hopeful strategy (Dwibedi and Saxena, 2018). Endophytic fungi can mimic the productivity of their host phytochemicals due to their association with the host plant (Strobel and Daisy, 2003; Suryanarayanan et al., 2009).

Many researchers have reported the isolation and screening of endophytic fungi from *V. vinifera* for resveratrol production (Dwibedi and Saxena, 2018). Moreover, the isolation of fungal endophytes with the ability to produce resveratrol was affected by the type of isolation media and the plant part from where they were isolated (Shi et al., 2012). In addition, the diversity in endophytic fungal taxa from the same host is due to the incidence of infrequent species in different parts of the plant (Bills and Polishook, 1994). The variation in resveratrol-producing capacity in fungal isolates could be attributed to gene expression fluctuation (Dwibedi and Saxena, 2018). Engineered microorganisms including *S. cerevisiae*, *Escherichia coli*, and *Yarrowia lipolytica* are considered promising candidates for maximizing resveratrol production through diverse fermentation processes (Lu et al., 2016). Due to its scale-up productivity, elevated efficacy, and its cheap price, microbial fermentation including solid state (SSF) and submerged (SmF) has been utilized to produce different valuable economical products (Chemler and Koffas, 2008; Al Mousa et al., 2021; Mohamed et al., 2021a; Hassane et al., 2022a,b).

Extraction and purification of resveratrol produced by SSF or SmF were carried out using various organic solvents. Ethyl acetate is considered the most commonly used solvent which has distinct chemical and biological properties, including extraction of a wide range of bioactive polar and non-polar compounds as well as low toxicity on test strains (Mohamed et al., 2021b). Many novel analytical technologies methods including LC-MS, LC-UVD, and GC–MS was developed to detect resveratrol and its glucoside (Flamini et al., 2013; Fabjanowicz et al., 2018; Grace et al., 2019; Li et al., 2019; Guo et al., 2022). Compared with GC–MS, LC-MS is simpler and more efficient without derivatization (Careri et al., 2004; Grace et al., 2019).

It is well known that the production of secondary metabolites depends on physiological and nutritional parameters (Shi et al., 2012; Liu et al., 2016a; Dwibedi and Saxena, 2019b). The optimization of culture media and fermentation conditions has been critical in the production of metabolites, which is frequently required to improve extraction yield and reaction rate (Chen et al., 2013b). Various physiological and nutritional parameters are important in the fermentative production of bioactive compounds, as well as in developing a process for maximum secondary metabolite production (Shi et al., 2012; Saran et al., 2015). The traditional optimization studies include the variation of one independent factor and maintaining other variables constant, therefore, this design is not competent to indicate the ideal conditions due to its inability to involve interaction among the variables (Tanyildizi et al., 2005; Lau et al., 2020).

The classical approach for process optimization of bioactive compounds is performed by using one variable at a time (OVAT) which is oppressive, monotonous, and time-consuming especially when the number of variables is large; hence, there was a need for an alternative method that is more efficient and less time consuming (Tassoni et al., 2005; Fan et al., 2010). To overcome this problem, another method based on the statistical approach named response surface methodology (RSM) can be used to carry out optimization studies (Saran

et al., 2015; Yun et al., 2018). The RSM has been widely used to evaluate and understand the interaction between different critical factors (independent and dependent) affecting the secondary metabolite production by different microorganisms (Bezerra et al., 2008; Silroy et al., 2014), and to investigate the influence of different variables and their interactions at different levels (Priya and Kanmani, 2011) for the development, improvement, and optimization processes through minimizing the number of needed experiments to assess the influence of several variables and their interaction among the independent variables (Yin et al., 2011; Myers et al., 2016). RSM is an integrated statistical and mathematical tool based on the polynomial equation, significance analysis, and stationary point location which can determine the optimum level of variables for the desired response and estimates the interaction between physiological and nutritional parameters (Shi et al., 2012).

Compared with the OVAT method, statistically designed experiments can predict the interaction between the factors in linear and quadratic terms (Lu et al., 2016). Positive diagnostic plots and coefficient of determination (R^2) values show that RSM is very effective at optimizing the parameters (Rajput et al., 2018). Furthermore, the model's significance was demonstrated using analysis of variance (ANOVA) through Fisher test (F) and low probability (p) values, as well as three-dimensional diagrams and contour plots of these parameters using Design Expert® or Minitab® software (Al Mousa et al., 2022a,b; Guo et al., 2022).

Shi et al. (2012) reported that during the cultivation of *Alternaria* sp. MG1 in PDB, biosynthesis of resveratrol started on the first day, reached its maximum production on the seventh day, and then reduced. Consequently, fungal biomass raised to a peak level after 5 days of cultivation. The results revealed that the fluctuation of resveratrol biosynthesis may be attributed to the non-attendance of the host plant during fungal cultivation, which could result in unsteady resveratrol gene expression. Therefore, investigating the key genes encoding the resveratrol pathways would supply basic information about the mechanism of transformation and decreased productivity (Shi et al., 2012). Resveratrol accumulation in *Alternaria* sp. MG1 was found to be directly proportional with increased biomass which suggests that resveratrol could be a constitutive product.

However, the biosynthesis of secondary metabolites by most microorganisms began at the end of the log phase of cell development (Chomcheon et al., 2009; Kornsakulkarn et al., 2011). *Alternaria* sp. MG1 showed preferable resveratrol-producing parameters (422 μg/L) through fermentation in PDB, using Box–Behnken design (BBD) of RSM tactic, where an inoculum size of 6% (spore suspension 1×10^4 spore/ml), a 250-ml flask holding 125 ml medium, 27°C incubation temperature, and shaking at 101 rpm. The influence of the tested optimization parameters on resveratrol accumulation is correlated to MG1 strain growth where decreased inoculum size produced a relatively slow increase in fungal cell development, while excessive inoculum size could cause cell degeneration thus resulting in decreased biomass. Sequentially, a low medium content results in raised inoculum size and vice versa. Therefore, corresponding cell growth results were derived due to the impact of the medium volume and inoculum size. Also, resveratrol production by *Alternaria* sp. MG1 is prospected to be related to its adaptation to the incubation temperature (Shi et al., 2012). The impact of high shaking speed on low resveratrol production could be attributed to the elevated content of oxygen where speed of rotation and oxygen amounts are directly proportional (King et al., 2006; Santos et al., 2011). ANOVA indicated the height significance of the model with $F = 36.2789$ and low $p = 0.0001$, as well as high $R^2 = 0.9591$ and adjusted $R^2 = 0.9327$ values (Shi et al., 2012).

Furthermore, Zhang et al. (2013) determined the optimal conditions for resveratrol production in bioconversion using a non-genetically modified *Alternaria* sp. MG1 strain resting cells. The calculated optimal conditions for the BBD and RSM analysis, based on the levels corresponding to the peak of resveratrol production in the single-factor design, were phenylalanine concentration, 4.66 mM; inoculum size, 12.16%; resting time, 21.3 h. The resveratrol production was predicted to be 1.26 μg/L and was 1.38 μg/L in experimental, nearly twofold obtained from basal concentration (0.70 μg/L). ANOVA cleared that the model was significant and well fitted with the data, as explicit from $F = 8.36$, low $p < 0.01$, high $R^2 = 0.9149$, and adjusted $R^2 = 0.8055$ values (Zhang et al., 2013).

One variable at a time approach is a conventional method for any optimization study to enhance the production of any biological product. In the present study, this approach was adopted, wherein the different physiological parameters such as temperature, pH, agitation rate, inoculum age, incubation period, and nutritional parameters such as carbon source, and nitrogen source were evaluated and optimized. All experiments were carried out in triplicates and the standard deviation was calculated (Shi et al., 2012; Saran et al., 2015). The optimization of resveratrol production by *A. aureus* #12VVLPM, a strain previously isolated from the Merlot grape (Dwibedi and Saxena, 2018), was performed with help of RSM. Among the variables tested for OVAT, six variables RPM, temp, incubation days, pH, glucose concentration, and peptone concentration were taken for BBD of RSM to assess their impact on resveratrol production by *A. aureus* (Dwibedi et al., 2021).

Optimization results of physicochemical and nutritional parameters using the OVAT approach (in 8 days of incubation, agitation/aeration 120 rpm, temperature 30°C, pH 7.0 at a glucose concentration of 1% and peptone 0.5%) exhibited a 1.23-fold enhancement in production of resveratrol when compared to the initial yield of 89.1 ± 0.08 μg/ml. RSM using BBD resulted in a 1.49-fold enhancement in resveratrol production (133.53 μg/ml) in 8.5 days of incubation, 115 rpm, temperature 30°C, pH 7.0 at a glucose concentration of 1.25%, and peptone 0.625% (Dwibedi et al., 2021). Evaluated ANOVA showed the significance of the model with an F-value equal to 21.76

and a probability value less than 0.05. The R^2 value (0.9576) demonstrates that 95.76% variation in the model is caused by three variables and only 4.24% variation could not be explained by the model. The predicted *R*-squared (pred. R^2) of 0.7786 is in reasonable agreement with the adjusted *R*-Squared (adj. R^2) of 0.9136. The adequate precision value measures the signal-to-noise ratio where a ratio of 14.732 greater than 4 is desirable and indicates an adequate signal (Dwibedi et al., 2021).

An enzymatic reaction system, prepared from *Alternaria* sp. MG1 grape endophyte was developed and optimized for bioconversion of resveratrol from glucose. Using the RSM with the enzyme solution, the highest value of resveratrol production (224.40 μg/L) was found under the conditions of pH 6.84, 0.35 g/L glucose, 0.02 mg/L coenzyme A, and 0.02 mg/L ATP within 120 min. The ANOVA for the model elucidated its significance and convenience, as apparent from the $F = 46.67$, low $p < 0.01$, high $R^2 = 0.9776$, and high adjusted $R^2 = 0.9566$ values. The lack-of-fit $F = 1.76$ and the accomplice *p*-value of 0.2763 articulated its insignificance (Che et al., 2016a). Enzymatic biosynthesis of resveratrol could be a promising process due to its independence from cell growth, conservative process conditions, and qualification, thus minimizing the inverse impacts facing resveratrol biosynthesis (Park et al., 2010; Yeo et al., 2012).

Induction of resveratrol production

Resveratrol is a phytoalexin in plants synthesized through the phenylpropanoid pathway in response to a wide range of biotic and abiotic stress factors including fungal infection, UV radiation exposure, anoxic treatment, ozone stress, heavy metals, chemicals, and wounding (Belhadj et al., 2008; Wang et al., 2010; Lu et al., 2016). However, without these stresses, the resveratrol is produced in a low concentration ranging from 0.2 to 16.5 mg/kg fresh weights of existence in leaves, stems, and roots (Wang et al., 2010). The role of resveratrol in fungi is completely ignored; however, it is known that plants produce it as a defense mechanism against fungal attacks. This fact may suggest that resveratrol could exert allelopathic activity against fungal competitors. Volatiles and lysing enzymes are visualized as chemical defenses, which generate several types of stress in such competitors (Chang et al., 2011).

Biosynthesis and extraction of resveratrol from plants ordinarily require months or years for plant development in addition to 2 days or more for the extraction process (Ballard et al., 2010; Chainukool et al., 2014). To shorten the growth period, techniques of plant cell culture (consuming 120 h), genetically modified *S. cerevisiae* (80 h), and genetically modified *E. coli* (20 h) were applied (Watts et al., 2006; Katsuyama et al., 2007; Donnez et al., 2009). Production of resveratrol using genetically modified microorganisms needs 36–96 h and expensive precursors, such as p-coumaric acid, to induce the synthesis of resveratrol in the system (Wang and Yu, 2012). Overexpression of the genes encoding coumarate–CoA ligase and resveratrol synthase, the enzymes involved in the resveratrol synthesis pathway, has also been found to improve resveratrol production by genetically modified yeast and *E. coli* (Beekwilder et al., 2006; Shin et al., 2011; Wang and Yu, 2012). The production of resveratrol by extraction from plants was 3.5–170 mg/L (Ballard et al., 2010; Mantegna et al., 2012), 11–35 mg/L using grape cells cultures (Medina-Bolivar et al., 2007; Kim et al., 2008), 200–315 mg/L by genetically modified plant cells (Kiselev et al., 2007; Dubrovina et al., 2010), 171 and 8.2 mg/L using genetically modified *E. coli* and *S. cerevisiae*, respectively (Watts et al., 2006; Katsuyama et al., 2007; Sun et al., 2015).

In ripe grape fruits, resveratrol biosynthesis is regularly reduced with disruption in the expression of inducible STS, thus revealing increased susceptibility of ripe *Vitis* berries to *B. cinerea* infection (Bais et al., 2000). The activation mechanism of stilbene phytoalexin biosynthesis in grape cells was reported through triggering by *B. cinerea* endopolygalacturonase 1 which can elicit nitric oxide (NO) production *via* NO synthase. NO is involved in the expression of PAL and STS defense genes (Jeandet et al., 2002; Vandelle et al., 2006).

Microbial fermentation using transgenic *Y. lipolytica*, *E. coli*, and *S. cerevisiae*, has advantages including an eco-friendly approach, fast growth rate, simple and inexpensive culture medium, ease of genetic manipulation, environmentally safe and auspicious maximization of resveratrol production (Lu et al., 2016; Wang et al., 2016). However, metabolic engineering *via* inserting of particular genes is a high cost and depletes time. Alternatively, mycondophytes offer considerable potency for biosynthesizing plant-patent secondary metabolites (Venugopalan and Srivastava, 2015). Mycondophytes secured the capacity to produce functional metabolites corresponding to their host plants' symbionts. Moreover, endophytic fungi exhibited peculiarities of producing high amounts of metabolites that could be toxic, while they own high resistance to their self-produced byproducts (Kusari et al., 2011).

Resveratrol production by fungi could be perspectively improved by stimulation through induction of chemical, physical, and biological elicitors (**Figure 4**). Epigenetic modulations in the endophytic fungi ameliorate the spectrum of secondary metabolite production and also conquer a new prospect for regulation of secondary product biosynthesis. Advancements in fungal molecular genetics have revealed that under laboratory culture conditions, many genes of the microbes are unexpressed or phenotypically silent (Dwibedi and Saxena, 2022). Induction of functionality in these genes could be possibly achieved through the *in vitro* use of epigenetic modifiers as well as other interventions such as co-culturing, chemical elicitors, precursors resulting in enhancement of a known host metabolite or novel secondary metabolites

that would find applications in pharmaceutical as well as agrochemical industry (Ul-Hassan et al., 2012; Abdulla et al., 2013; Kumar et al., 2016).

For physical induction, UV radiation (350 nm, 20 min) significantly promoted the biosynthesis of resveratrol in *Alternaria* sp. MG1 with highest production (240.57 μg/L) which increased by 45.8% compared with the control at 28°C on the seventh day of incubation. Also, UV irradiation for 20 min significantly upregulated the expression of key genes of the resveratrol biosynthesis pathway by about 3–4 times compared to the control. UV radiation is ordinarily utilized to boost the biosynthesis rate and the catalytic efficiency of fungal enzymes. The increase in the UV treatment time boosts resveratrol production by *Alternaria* sp. MG1, which could be a self-adaptive preservation counter inconvenient environment. Increasing the UV exposure to 30 min, may harm the enzymatic activities and cellular structures, leading to the regression of resveratrol production (Lu et al., 2021a).

On the other hand, ultrasound (40 kHz, 10 min) did not affect *Alternaria* sp. MG1 ability to biosynthesize resveratrol could be ascribed to the insusceptibility of MG1 strain to ultrasound disruption (Lu et al., 2021a). Ultrasound is commonly accounted to affect the growth rates, enzymatic activities, and biosynthesis efficacy of metabolites through enhancing cell permeability across cell membranes (Behzadnia et al., 2020). However, ultrasonic-assisted extraction has the advantages of increasing the extraction rate and reducing the use of organic solvents (Zwingelstein et al., 2020). Ultrasonic cavitation in plants can improve mass transfer in a solid–liquid system, enhance the penetration of medium molecules, accelerate the speed of molecular movement, and quickly penetrate the biomass cells, allowing the extraction solvent to fully contact the biomass, thereby improving the extraction efficiency of target substances and reduce the extraction time (Rodríguez De Luna et al., 2020). In addition, polyphenols are stable and will not be degraded after ultrasonic treatment (Jin et al., 2020). However, the excessive ultrasonic power will degrade or decompose the antioxidant components during the extracted process (O'Brien, 2007).

For chemical induction, *Alternaria* sp. MG1 resveratrol biosynthetic ability was positively influenced by ethanol which acts as a carbon source and increased resveratrol accumulation by 26.31% in a concentration-dependent (Lu et al., 2019). Lu et al. (2021a) found that sodium butyrate at a concentration of 100 μm exerted a negative impact against *Alternaria* sp. MG1 resveratrol production capability and attributed that to the fungal growth reduction which causes deficiency in supplements representing essential precursors for resveratrol biosynthesis. Moreover, Mohammadipanah et al. (2020) speculated that the induction ability of sodium butyrate could be concentration-dependent. On the other hand, El-Hawary et al. (2018) and Mohammadipanah et al. (2020) reported a histone deacetylases inhibition ability of sodium butyrate, which permits the expression of many silent genes. Consequentially, several enzymes are activated, and new secondary products are biosynthesized due to the enhancement role of sodium butyrate. Oligomeric proanthocyanidin (OPC), an important nutrient component in grape fruit, at 100 μm had a positive influence on resveratrol production (255.01 μg/L) in *Alternaria* sp. MG1, which represents an enhancement of 60.63% over the control.

Meanwhile, resveratrol biosynthesis was prohibited at 200 μm OPC which exhibited the impact of OPC on resveratrol cumulation was concentration-dependent. Lu et al. (2021b) revealed the harmony of the expression of the key genes in the resveratrol pathway and resveratrol production after OPC treatment. OPC activates Ca^{2+} channels *via* interacting with Ca^{2+} signal-related proteins, and calcium-dependent protein kinases (CDPKs), thereby activating the upregulation of downstream resveratrol and related genes to resist the stress environment caused by OPC.

Villa-Ruano et al. (2021) found that variable concentrations of amino acid precursors phenylalanine and tyrosine (50–500 mg/L) stimulated resveratrol production by *A. aureus* MaC7A from 127.9 to 221.8 mg/L in basic cultures developed in PDB (pH 7) added with 10 g/L peptones at 30°C. While, among the tested volatiles monoterpenes (limonene, camphor, citral, thymol, and menthol), citral (50 mg/L) enhanced resveratrol production until 187.8 mg/L in basic cultures. Moreover, mixtures of hydrolytic enzymes (Glucanex 100 mg/L), as elicitors, boosted fungal resveratrol productivity (198.3 mg/L). Optimized batch cultures containing tyrosine, citral, thymol, and Glucanex (200, 50, 50, and 100 mg/L, respectively) produced resveratrol up to 237.6 mg/L. Thus, suggests an increase in the production of resveratrol by *A. aureus* MaC7A at mixtures of isoenzymes and low concentrations of volatiles. Endophytic fungus *A. aureus* #12VVLMP, isolated from leaves of *V. vinifera* – Merlot variety and produced 89.13 μg/ml resveratrol extracellularly as a basal concentration (Dwibedi and Saxena, 2018), was inoculated into 50 ml of pre-sterilized PDB was amended with 500 μl of crude methanolic extracts of grape seed and grape skin, as natural supplements, with estimated resveratrol concentrations of 17.3 and 3.3 μg/ml in these extracts, respectively, and incubated at 26 ± 2°C, 120 rpm for 7 days.

Salicylic acid and cyclodextrin (1% v/v), chemical elicitors, were used as chemical elicitors used in the liquid culture of *A. aureus* for enhancing resveratrol production. p-Coumaric acid and cinnamic acid, as precursor feeding, were evaluated as precursors for resveratrol biosynthesis at 1% v/v in 50 ml PDB. An increase of 27.7% was recorded over the basal concentration of 89.13 μg/ml in the case of grape seed extract, while only 13.7% enhancement was observed in the case of grape skin extract. A significant reduction in the total resveratrol content was observed with salicylic acid and cyclodextrin treatment. The production of resveratrol by the use of p-coumaric acid was 1.35% (90.33 μg/ml) higher than the basal concentration

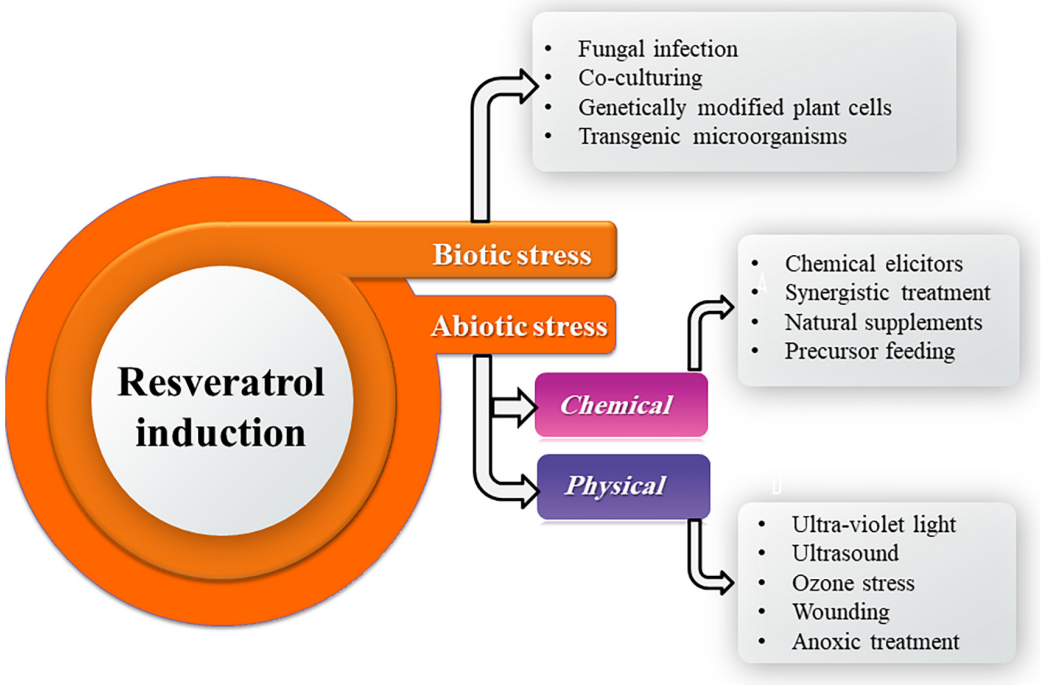

FIGURE 4
Different elicitors for resveratrol induction.

produced by *A. aureus*, while a 0.27% increase was observed in the case of cinnamic acid (Dwibedi and Saxena, 2022). The synergistic impact of several elicitors is an efficient trend to raise the biosynthesis of secondary products obtained from microbial or plant origins. Synergistic treatment of UV irradiation (350 nm, 20 min) and OPC (100 μm) increased the production of resveratrol in *Alternaria* sp. MG1by 70.37% (276.31 μg/L) compared to control (Lu et al., 2021b).

Epigenetics permits targeting a wide variety of fungi without any prior information about their genome. Epigenetic modifiers can therefore be used as a strategy to regulate gene transcription in endophytic fungi for modulating gene expression and inducing the biosynthesis of desired secondary metabolites (Dwibedi et al., 2019). The endophytic *X. psidii* #22(P) VVLPM derived from the leaf of *V. vinifera* leaves showed enhanced resveratrol concentrations, in comparison with control (35.43 μg/ml), treatment with 5 μm suberoylanilide hydroxamic acid (SAHA) produced 52.32 μg/ml resveratrol and with 10 μm 5-azacytidine (AZA) (48.94 μg/ml) pursued by 10 μm SAHA (41.10 μg/ml), and 5 μm AZA (37.72 μg/ml) that acting as chemical elicitors and epigenetic modulators (Dwibedi et al., 2019). Chemical enhancers have been used to target biosynthetic pathways, where AZA induces hypomethylation of the stocktickerDNA (Cherblanc et al., 2012, 2013), while SAHA acts as a histone deacetylase inhibitor (Williams et al., 2008; Sharma et al., 2017). Thus, they exemplify a spectacular chemical implementation for the expression of cryptic genes which are not expressed under standard laboratory conditions (Dwibedi and Saxena, 2019a).

For biological induction, co-culturing of endophytes *Alternaria* sp. MG1 (CCTCC M 2011348) and *Phomopsis* sp. XP-8 (CCTCC M 209291) showed an evident influence on resveratrol biosynthesis, which raised its accumulation by 40%, and altered the patterns of secondary metabolites in MG1 by enhancing stilbenes biosynthesis and inhibiting the synthesis of lignin compounds and originating new flavonoids [(+)-catechin, naringin, and (±)-taxifolin]. Accordingly, the microbial interaction may induce the expression of related cryptic gene clusters (Lu et al., 2021b). Whereas co-cultivation of *A. aureus* #12VVLMP with *Fusarium* sp. #19 VVLPM enhanced the resveratrol production by 9.4% (97.47 μg/ml) over 89.13 μg/ml resveratrol extracellular production by *A. aureus* as a basal concentration (Dwibedi and Saxena, 2022).

Several genes involved in the biosynthesis of secondary metabolites remain silent under optimal laboratory conditions and are known to be induced by epigenetic regulation of microbial endophytes (Rutledge and Challis, 2015; Fischer et al., 2016). Bioactive natural compounds can modify histones and DNA methylation and histone epigenetically which results in cryptic gene activation (Meeran et al., 2010). Resveratrol is well known to be potent to introduce epigenetic modification requested to induce silent gene expression. The treatment of *Colletotrichum gloeosporioides* by 10 mg/ml of crude methanolic extract of grape skin (resveratrol enriched natural supplements),

for 21 days at 26°C, promoted the production of several cryptic components that were not detected in the control samples. The analytical profile of the secondary metabolites in the treated culture showed the existence of 37 compounds, while the untreated control culture displayed 34 compounds. Twenty cryptic compounds were detected within *C. gloeosporioides* cultures supplemented with grape skin extract. Seventeen compounds were detected in both the treated and control cultures, while certain metabolites were missed in the treated culture (Sharma et al., 2017).

Resveratrol bio-transformation and bio-degradation

Because of their biological importance, the production of resveratrol as well as its derivatives through bioconversion and biotransformation has been the subject of intensive research studies. Resveratrol is a biodegradable compound that can be metabolized into various bioactive analogues *via* microorganisms. Incubating resveratrol with the cell filtrate of *Bacillus cereus* results in the production of resveratrol 3-O-β-D-glucoside (piceid) as an active analog (Cichewicz and Kouzi, 1998). Similarly, *Streptomyces* sp. isolated from *P. cuspidatum* showed the ability to transform resveratrol into its methylated form 3, 5, 4′-trimethoxy-trans-stilbenes. Interestingly, the transformed derivative exerted stronger anticancer activity in a concentration-independent manner compared with the parent compound (Jiewei et al., 2018).

A number of endophytic fungi isolated from selected plants were analyzed for their resveratrol-producing ability. Few studies have addressed the biotransformation of resveratrol by mycoendophytes. The endophytic fungus *Penicillium* sp. derived from *P. cuspidatum* can transform resveratrol when cultured in a PDB medium into trans-3,5-dimethoxy-4′ hydroxystilbene which is known as pterostilbene. The latter is a dimethylated derivative of resveratrol; this modification improves the biological efficacy, membrane permeability, and metabolic stability of pterostilbene over resveratrol. Hence, pterostilbene is considered the next generation of resveratrol and is expected to play a crucial pharmacological role in several human diseases (Xu et al., 2020). Resveratrol is produced by peanuts and accumulated in the surrounding soil conferring allelopathic impact in the peanut mono-cropping systems. This phenomenon undermines the peanut output through different strategies such as inhibiting nodule formation, decreasing the microbial abundance in the soil, and reducing the level of soil carbon. Endophytic fungus *Phomopsis liquidambari* transform approximately 97% of resveratrol *in vitro* and under soil conditions into 3,5-dihydroxybenzaldehyde and 4-hydroxybenzaldehyde, and further oxidize them to 3,5-dihydroxybenzoic acid and 4-hydroxybenzoic acid. The activity of *P. liquidambari* toward resveratrol is attributed to the enhanced expression of resveratrol cleavage oxygenase (*resB3)* and other related genes upon resveratrol induction (Wang et al., 2019). Incubation of resveratrol with resveratrol cleavage oxygenase (Rco1) derived from *Ustilago maydis* results in cleaves of Ca–Cb interphenyl double bond, Rco1 is the first eukaryotic enzyme for resveratrol biodegradation (Brefort et al., 2011).

Various strains of the plant pathogen *B. cinerea* demonstrated the ability to degrade resveratrol accompanied by pathogenicity to grapevines *Vitis rupestris*. The degradation was related to the presence of laccase activity in the culture filtrates contradicted the above study. Interestingly, laccase can be produced in high amounts in a culture medium lacking resveratrol as an inducer (Sbaghi et al., 1996). Resveratrol accumulates in grape plants in response to grapevine trunk diseases (GTD). *Neofusicoccum parvum* and *Diplodia seriata* are two major fungi associated with GTD, these fungi are able efficiently to metabolize resveratrol. Higher diversity of resveratrol metabolization products was found with enzymes of *N. parvum* compared to *D. seriata* (Labois et al., 2021).

The investigation of *Alternaria* sp. MG1 cultured on liquid potato dextrose culture resulted in the production of resveratrol on the first day and reached its peak levels on day 7 (Shi et al., 2012). Moreover, the filamentous fungi *A. aureus* MaC7A was able to produce resveratrol under controlled conditions of amino acid precursors (PHE and TYR), and low monoterpenes (limonene, camphor, citral, thymol, and menthol) percentile, and mixtures of hydrolytic enzymes (Glucanex) as elicitors for boosting fungal resveratrol. The peak levels of resveratrol and biomass were maintained during days 6–8 and decreased from days 10–12 without any loss of biomass (Villa-Ruano et al., 2021). In addition, *A. niger* showed stable genetic properties producing a high percentage of resveratrol (Liu et al., 2016b). *Q. cyanescens*, a fungal endophyte of *V. vinifera*, has shown a high amount of resveratrol production (Meshram et al., 2022). *A. stellifer* AB4 isolated from the leaves of *V. vinifera* has shown stable production capability of resveratrol with peak production on day 9 of fermentation (Roat and Saraf, 2020).

Further, the transformation of resveratrol into pterostilbene (**Figure 5**) to increase the stability and bioefficiency was achieved by endophytic *Penicillium* sp. JQ228238 and *Penicillium* sp. F5 from *Polygonum cuspidatum* (Xu et al., 2020; Liu et al., 2021). Moreover, arahypin-16, a biotransformed resveratrol derivative, has been isolated from whole-cell fermentation of *Aspergillus* sp. SCSIOW2 (Wang et al., 2016). The fungus *Beauveria bassiana*, one of the most frequently used microorganisms for the biotransformation of polyphenols, showed the ability of resveratrol conversion to resvebassianol A, a glycosylated metabolite of resveratrol (Darlami and Shin, 2021).

Many investigations into optimizing the bioconversion of polydatin to resveratrol have been conducted. *A. niger* and yeast were able to biotransform polydatin to resveratrol in

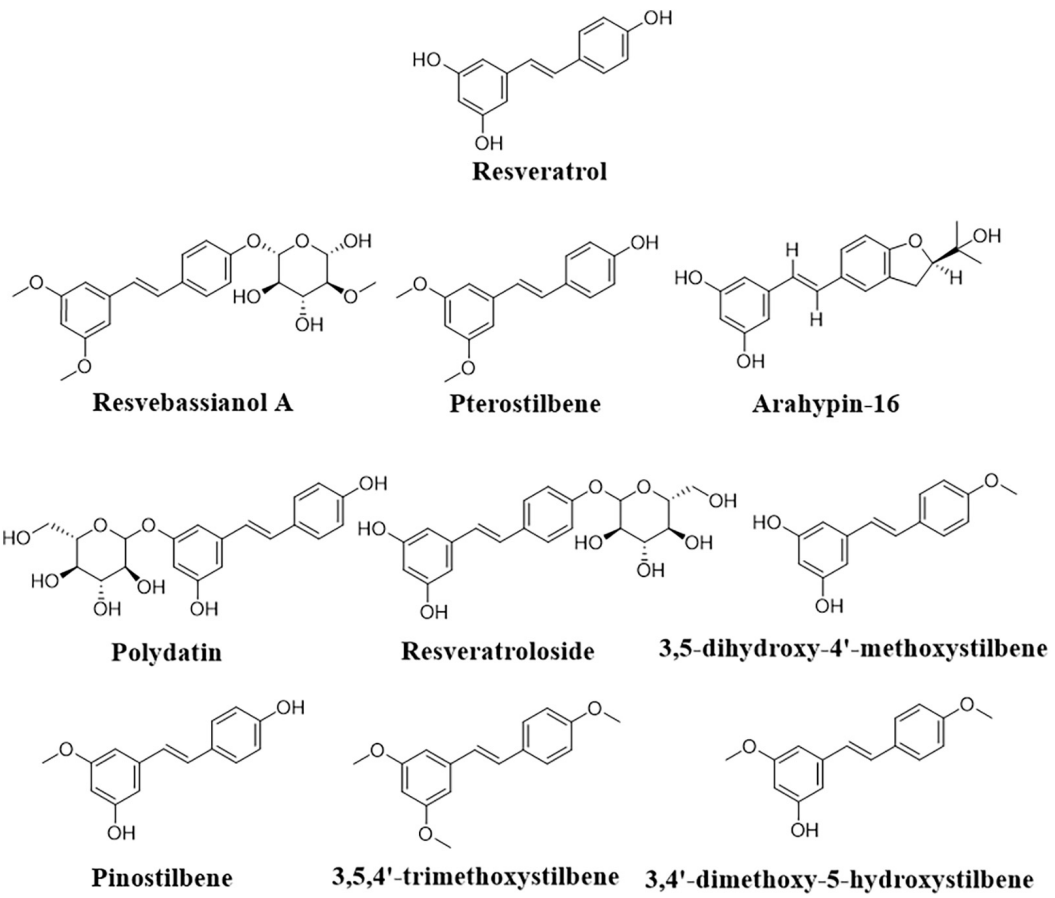

FIGURE 5
Representative structure of resveratrol biotransformed derivatives.

P. cuspidatum roots (Wang et al., 2016). *Dekkera bruxellensis* demonstrated promising activity in hydrolyzing glycosidic-linked resveratrol from *P. cuspidatum*, which could significantly increase resveratrol production (Kuo et al., 2017).

On the other hand, the enzymes obtained from different organisms showed a potential ability for resveratrol biotransformation. The unspecific peroxygenases obtained from the basidiomycetes *Agrocybe aegerita*, *Coprinopsis cinerea,* and *Marasmius rotula* were able to catalyze the hydroxylation of the pin to resveratrol (Aranda et al., 2018). Furthermore, an immobilized enzyme derived from the endophytic fungus *Alternaria* sp. MG1 was successful in the bioconversion of glucose to resveratrol, maintaining high resveratrol production during recycling use two to five times within 2 h for each cycle (Zhang et al., 2013; Che et al., 2016a). The cyclodextrin glycosyltransferase (CGTase) produced by *Paenibacillus* sp. RB01 was used to catalyze the transglycosylation reaction from glycosyl donors (starch, β-cyclodextrin, or maltoheptaose) to resveratrol, resulting in resveratrol glycoside formation (Anurutphan and Prousoontorn, 2014).

According to Schouten et al. (2002), resveratrol is converted to a mycotoxic compound by a specific laccase of *B. cinerea*, which causes autotoxicity by catalyzing the oxidation of phenolic compounds and the reduction of molecular oxygen into water and may be involved in *V. vinifera* grape resistance to *B. cinerea* infection. Recently, genetic bioengineering has played an important role in resveratrol bioproduction. The ability of *E. coli* and *S. cerevisiae* engineered to express the resveratrol *O*-methyltransferase gene from *V. vinifera* to produce pterostilbene from resveratrol was confirmed (Wang et al., 2015). On the other hand, Camacho-Zaragoza et al. (2016) adapted a co-culture system comprised of two populations of engineered *E. coli* strains with genes to produce malonyl-CoA and provide it to the STS for yielding resveratrol. The co-culture of these strains produced 22.58 mg/L resveratrol from 10 g/L glycerol after 30 h while keeping the growth rates of both strains during co-culture cultivation (Camacho-Zaragoza et al., 2016). A similar co-culture design was used for the biosynthesis of polydatin and resveratrol side glycosylated resveratrol products (**Figure 5**), as well as the conversion of exogenous *p*-coumaric

acid *via* over-expression of 4-coumarate-coenzyme A ligase and STS, and to boost UPD-glucose formation (Chen et al., 2019).

In an *E. coli* system containing codon-optimized *O*-methyltransferase genes from sorghum in addition to the resveratrol biosynthetic genes, an artificial biosynthetic pathway was able to produce methylated resveratrol derivatives, such as 3,5-dihydroxy-4′-methoxystilbene, pinostilbene, 3,4′-dimethoxy-5-hydroxystilbene, and 3,5,4′-trimethoxystilbene (**Figure 5**; Kang et al., 2014). The *Bacillus aryabhattai* endophytic bacteria isolated from the rhizome tissue of *Reynoutria japonica* as well as *Bacillus safensis* has also shown potential transformation of polydatin to resveratrol (Hu et al., 2019; Liu et al., 2020).

Conclusion

It has been reported that several plant species can produce pharmacologically significant natural products that could be used as a scaffold for the development of new therapeutic candidates. Despite their importance, some of these compounds are obtained in small quantities from plants and cannot be synthesized on a large scale. Fungal endophytes have recently emerged as valuable sources of bio-effective metabolites, either through the production of the same product as host sources or through biotransformation to achieve large-scale production of targeted compounds. Since the stilbene compounds resveratrol and its derivatives have been shown to have important bioactive roles in medicine, we reported here that advancements in fermentation process optimization and genetic manipulation technologies play a critical role in supplying a maximum fungal production of these bioactive metabolites with the least amount of effort and cost. Furthermore, tracking the biosynthesis pathway and key genes involved in biotransformation paves the way for it to be enhanced and improved have been reported. As a result, studying mycoendophytes in various plant species can provide an amazing avenue for maximizing resveratrol production and supplying a consistent yield, as it is an important candidate against various human diseases.

Author contributions

All authors listed have made a substantial, direct, and intellectual contribution to the work, and approved it for publication.

Conflict of interest

The authors declare that the research was conducted in the absence of any commercial or financial relationships that could be construed as a potential conflict of interest.

Publisher's note

All claims expressed in this article are solely those of the authors and do not necessarily represent those of their affiliated organizations, or those of the publisher, the editors and the reviewers. Any product that may be evaluated in this article, or claim that may be made by its manufacturer, is not guaranteed or endorsed by the publisher.

References

Abdel-Hadi, A., Aloyuni, S., Alharbi, R., Jahan, S., Darwish, O., Senthilkumar, S., et al. (2022). Stroke preventing effect of resveratrol isolated from fungi and *in vivo* activity in male albino rats. *J. King Saud Univ. Sci.* 34:102074. doi: 10.1016/j.jksus.2022.102074

Abdulla, A., Zhao, X., and Yang, F. (2013). Natural polyphenols inhibit lysine-specific demethylase-1 *in vitro*. *J. Biochem. Pharmacol. Res.* 1, 56–63.

Adeniji, A. (2019). The methods of controlling yam tuber rot in storage: a review. *Int. J. Innov. Biol. Chem. Sci.* 12, 11–17.

Adrian, M., Jeandet, P., Douillot-Breuil, A. C., Tesson, L., and Bessis, R. (2000). Stilbene content of mature *Vitis vinifera* berries in response to UV-elicitation. *J. Agric. Food Chem.* 48, 6103–6105. doi: 10.1021/jf0009910

Aggarwal, G., and Shishodia, S. (2006). *Resveratrol in health and disease*. Boca Raton, FL: CRC Taylor and Francis.

Akamatsu, H. (2004). Molecular biological studies on the pathogenicity of *Alternaria alternata* tomato pathotype. *J. Gen. Plant Pathol.* 70, 389–389. doi: 10.1007/s10327-004-0148-1

Akamatsu, H., Taga, M., Kodama, M., Johnson, R., Otani, H., and Kohmoto, K. (1999). Molecular karyotypes for *Alternaria* plant pathogens known to produce host-specific toxins. *Curr. Genet.* 35, 647–656. doi: 10.1007/s002940050464

Al Mousa, A. A., Abo-Dahab, N. F., Hassane, A. M. A., Gomaa, A. E.-R. F., Aljuriss, J. A., and Dahmash, N. D. (2022a). Harnessing *Mucor* spp. for xylanase production: statistical optimization in submerged fermentation using agro-industrial wastes. *Biomed Res. Int.* 2022:3816010. doi: 10.1155/2022/3816010

Al Mousa, A. A., Hassane, A. M. A., Gomaa, A. F., Aljuriss, J. A., Dahmash, N. D., and Abo-Dahab, N. F. (2022b). Response-surface statistical optimization of submerged fermentation for pectinase and cellulase production by *Mucor circinelloides* and *M. hiemalis*. *Fermentation* 8:205. doi: 10.3390/fermentation8050205

Al Mousa, A. A., Mohamed, H., Hassane, A. M. A., and Abo-Dahab, N. F. (2021). Antimicrobial and cytotoxic potential of an endophytic fungus *Alternaria tenuissima* AUMC14342 isolated from *Artemisia judaica* L. growing in Saudi Arabia. *J. King Saud. Univ. Sci.* 33:101462. doi: 10.1016/j.jksus.2021.101462

Aleynova, O. A., Suprun, A. R., Nityagovsky, N. N., Dubrovina, A. S., and Kiselev, K. V. (2021). The influence of the grapevine bacterial and fungal endophytes on biomass accumulation and stilbene production by the *in vitro* cultivated cells of *Vitis amurensis* Rupr. *Plants* 10:1276. doi: 10.3390/plants10071276

Aly, A. H., Debbab, A., and Proksch, P. (2011). Fungal endophytes: unique plant inhabitants with great promises. *Appl. Microbiol. Biotechnol.* 90, 1829–1845. doi: 10.1007/s00253-011-3270-y

Aly, A. H., Debbab, A., and Proksch, P. (2013). Fungal endophytes - secret producers of bioactive plant metabolites. *Pharmazie* 68, 499–505.

Anurutphan, N., and Prousoontorn, M. H. (2014). "Enzymatic synthesis of resveratrol glycosides by cyclodextrin glycosyltransferase from *Paenibacillus* sp. RB01," in *Proceedings of the 26th Annual Meeting of the Thai Society for Biotechnology and International Conference*, Bangkok.

Aranda, C., Ullrich, R., Kiebist, J., Scheibner, K., Jose, C., Hofrichter, M., et al. (2018). Selective synthesis of the resveratrol analogue 4, 4'-dihydroxy-trans-stilbene and stilbenoids modification by fungal peroxygenases. *Catal. Sci. Technol.* 8, 2394–2401. doi: 10.1039/C8CY00272J

Bais, A. J., Murphy, P. J., and Dry, I. B. (2000). The molecular regulation of stilbene phytoalexin biosynthesis in *Vitis vinifera* during grape berry development. *Aust. J. Plant Physiol.* 27, 425–4333. doi: 10.1071/PP00007

Ballard, T. S., Mallikarjunan, P., Zhou, K., and O'Keefe, S. (2010). Microwave-assisted extraction of phenolic antioxidant compounds from peanut skins. *Food Chem.* 120, 1185–1192. doi: 10.1016/j.foodchem.2009.11.063

Baur, J. A., and Sinclair, D. A. (2006). Therapeutic potential of resveratrol: the *in vivo* evidence. *Nat. Rev. Drug. Discov.* 5, 493–506. doi: 10.1038/nrd2060

Bavaresco, L., Mattivi, F., De Rosso, M., and Flamini, R. (2012). Effects of elicitors, viticultural factors, and enological practices on resveratrol and stilbenes in grapevine and wine. *Mini Rev. Med. Chem.* 12, 1366–1381. doi: 10.2174/13895575112091366

Beekwilder, J., Wolswinkel, R., Jonker, H., Hall, R., de Vos, C. R., and Bovy, A. (2006). Production of resveratrol in recombinant microorganisms. *Appl. Environ. Microbiol.* 72, 5670–5672. doi: 10.1128/AEM.00609-06

Behzadnia, A., Moosavi-Nasab, M., Ojha, S., and Tiwari, B. K. (2020). Exploitation of ultrasound technique for enhancement of microbial metabolites production. *Molecules* 25:5473. doi: 10.3390/molecules25225473

Belhadj, A., Telef, N., Saigne, C., Cluzet, S., Barrieu, F., Hamdi, S., et al. (2008). Effect of methyl jasmonate in combination with carbohydrates on gene expression of PR proteins, stilbene and anthocyanin accumulation in grapevine cell cultures. *Plant Physiol. Biochem.* 46, 493–499. doi: 10.1016/j.plaphy.2007.12.001

Berman, A. Y., Motechin, R. A., Wiesenfeld, M. Y., and Holz, M. K. (2017). The therapeutic potential of resveratrol: a review of clinical trials. *NPJ Precis. Oncol.* 1, 1–9. doi: 10.1038/s41698-017-0038-6

Berner, M., Krug, D., Bihlmaier, C., Vente, A., Muller, R., and Bechthold, A. (2006). Genes and enzymes involved in caffeic acid biosynthesis in the actinomycete *Saccharothrix espanaensis*. *J. Bacteriol.* 188, 2666–2673. doi: 10.1128/JB.188.7.2666-2673.2006

Bezerra, M. A., Santelli, R. E., Oliveira, E. P., Villar, L. S., and Escaleira, L. A. (2008). Response surface methodology (RSM) as a tool for optimization in analytical chemistry. *Talanta* 76, 965–977. doi: 10.1016/j.talanta.2008.05.019

Bills, G. F., and Polishook, J. D. (1994). Abundance and diversity of microfungi in leaf litter of a lowland rain forest in Costa Rica. *Mycologia* 86, 187–198. doi: 10.1080/00275514.1994.12026393

Blanco-Ulate, B., Amrine, K. C., Collins, T. S., Rivero, R. M., Vicente, A. R., Morales-Cruz, A., et al. (2015). Developmental and metabolic plasticity of white-skinned grape berries in response to *Botrytis cinerea* during Noble Rot. *Plant Physiol.* 169, 2422–2443. doi: 10.1104/pp.15.00852

Brefort, T., Scherzinger, D., Limon, M. C., Estrada, A. F., Trautmann, D., Mengel, C., et al. (2011). Cleavage of resveratrol in fungi: characterization of the enzyme Rco1 from *Ustilago maydis*. *Fungal Genet. Biol.* 48, 132–143. doi: 10.1016/j.fgb.2010.10.009

Burns, J., Yokota, T., Ashihara, H., Lean, M. E., and Crozier, A. (2002). Plant foods and herbal sources of resveratrol. *J. Agric. Food. Chem.* 50, 3337–3340. doi: 10.1021/jf0112973

Camacho-Zaragoza, J. M., Hernandez-Chavez, G., Moreno-Avitia, F., Ramirez-Iniguez, R., Martinez, A., Bolivar, F., et al. (2016). Engineering of a microbial coculture of *Escherichia coli* strains for the biosynthesis of resveratrol. *Microb. Cell Fact.* 15, 1–11. doi: 10.1186/s12934-016-0562-z

Careri, M., Corradini, C., Elviri, L., Nicoletti, I., and Zagnoni, I. (2004). Liquid chromatography-electrospray tandem mass spectrometry of cis-resveratrol and trans-resveratrol: development, validation, and application of the method to red wine, grape, and winemaking byproducts. *J. Agric. Food Chem.* 52, 6868–6874. doi: 10.1021/jf049219d

Chainukool, S., Goto, M., Hannongbua, S., and Shotipruk, A. (2014). Subcritical water extraction of resveratrol from barks of *Shorea roxburghii* G. Don. *Sep. Sci. Technol.* 49, 2073–2078. doi: 10.1080/01496395.2014.905595

Chang, X., Heene, E., Qiao, F., and Nick, P. (2011). The phytoalexin resveratrol regulates the initiation of hypersensitive cell death in *Vitis* cell. *PLoS One* 6:e26405. doi: 10.1371/journal.pone.0026405

Che, J., Shi, J., Gao, Z., and Zhang, Y. (2016b). Transcriptome analysis reveals the genetic basis of the resveratrol biosynthesis pathway in an endophytic fungus (Alternaria sp. MG1) isolated from Vitis vinifera. *Front. Microbiol.* 7:1257. doi: 10.3389/fmicb.2016.01257

Che, J. X., Shi, J. L., Lu, Y., and Liu, Y. L. (2016c). Validation of reference genes for normalization of gene expression by qRT-PCR in a resveratrol-producing entophytic fungus (*Alternaria* sp. MG1). *AMB Express* 6, 106–116. doi: 10.1186/s13568-016-0283-z

Che, J., Shi, J., Gao, Z., and Zhang, Y. (2016a). A new approach to produce resveratrol by enzymatic bioconversion. *J. Microbiol. Biotechnol.* 26, 1348–1357. doi: 10.4014/jmb.1512.12084

Chemler, J. A., and Koffas, M. A. (2008). Metabolic engineering for plant natural product biosynthesis in microbes. *Curr. Opin. Biotechnol.* 19, 597–605. doi: 10.1016/j.copbio.2008.10.011

Chen, J., Chen, Y., Lin, F., Hu, Y., and Liao, F. (2013a). Resveratrol inhibits alpha-melanocyte-stimulating hormone signaling, viability, and invasiveness in melanoma cells. *Evid. Based. Complement. Alternat. Med.* 2013:632121. doi: 10.1155/2013/632121

Chen, J., Liu, D., Shi, B., Wang, H., Cheng, Y., and Zhang, W. (2013b). Optimization of hydrolysis conditions for the production of glucomanno-oligosaccharides from konjac using β-mannanase by response surface methodology. *Carbohydr. Polym.* 93, 81–88. doi: 10.1016/j.carbpol.2012.05.037

Chen, T., Zhou, Y., Lu, Y., and Zhang, H. (2019). Advances in heterologous biosynthesis of plant and fungal natural products by modular co-culture engineering. *Biotechnol. Lett.* 41, 27–34. doi: 10.1007/s10529-018-2619-z

Cherblanc, F., Chapman-Rothe, N., Brown, R., and Fuchter, M. (2012). Current limitations and future opportunities for epigenetic therapies. *Future Med. Chem.* 4, 425–446. doi: 10.4155/fmc.12.7

Cherblanc, F. L., Davidson, R. W., Di Fruscia, P., Srimongkolpithak, N., and Fuchter, M. J. (2013). Perspectives on natural product epigenetic modulators in chemical biology and medicine. *Nat. Prod. Rep.* 30, 605–624. doi: 10.1039/c3np20097c

Chomcheon, P., Wiyakrutta, S., Sriubolmas, N., Ngamrojanavanich, N., Mahidol, C., Ruchirawat, S., et al. (2009). Metabolites from the endophytic mitosporic Dothideomycete sp. LRUB20. *Phytochemistry* 70, 121–127. doi: 10.1016/j.phytochem.2008.10.007

Chu, X., Sun, A., and Liu, R. (2005). Preparative isolation and purification of five compounds from the Chinese medicinal herb *Polygonum cuspidatum* Sieb. et Zucc by high-speed counter-current chromatography. *J. Chromatogr. A* 1097, 33–39. doi: 10.1016/j.chroma.2005.08.008

Cichewicz, R. H., and Kouzi, S. A. (1998). Biotransformation of resveratrol to piceid by *Bacillus cereus*. *J. Nat. Prod.* 61, 1313–1314. doi: 10.1021/np980139b

Cichewicz, R. H., Kouzi, S. A., and Hamann, M. T. (2000). Dimerization of resveratrol by the grapevine pathogen *Botrytis cinerea*. *J. Nat. Prod.* 63, 29–33. doi: 10.1021/np990266n

Creasy, L. L., and Coffee, M. (1988). Phytoalexin production potential of grape berries. *J. Amer. Soc. Hortic. Sci.* 113, 230–234. doi: 10.21273/JASHS.113.2.230

Dai, R., Ge, H., Howard, S., and Qiu, W. (2012). Transcriptional expression of stilbene synthase genes are regulated developmentally and differentially in response to powdery mildew in Norton and Cabernet Sauvignon grapevine. *Plant Sci.* 197, 70–76. doi: 10.1016/j.plantsci.2012.09.004

Darlami, O., and Shin, D. (2021). Total synthesis of resvebassianol A, a metabolite of resveratrol by *Beauveria bassiana*. *Antioxidants* 10, 1509–1524. doi: 10.3390/antiox10101509

de Bary, A. (1866). *Morphologie und Physiologie der Pilze, Flechten, und Myxomyceten. Hofmeister's Handbook of Physiological Botany*. Leipzig: Verlag Von Wilhelm Engelmann.

Ding, C. H., Wang, Q. B., Guo, S., and Wang, Z. Y. (2018). The improvement of bioactive secondary metabolites accumulation in *Rumex gmelini* Turcz through co-culture with endophytic fungi. *Braz. J. Microbiol.* 49, 362–369. doi: 10.1016/j.bjm.2017.04.013

Donnez, D., Jeandet, P., Clement, C., and Courot, E. (2009). Bioproduction of resveratrol and stilbene derivatives by plant cells and microorganisms. *Trends Biotechnol.* 27, 706–713. doi: 10.1016/j.tibtech.2009.09.005

Dubrovina, A. S., Manyakhin, A. Y., Zhuravlev, Y. N., and Kiselev, K. V. (2010). Resveratrol content and expression of phenylalanine ammonia-lyase and stilbene synthase genes in *rolC* transgenic cell cultures of *Vitis amurensis*. *Appl. Microbiol. Biotechnol.* 88, 727–736. doi: 10.1007/s00253-010-2792-z

Dwibedi, V., Kalia, S., and Saxena, S. (2019). Isolation and enhancement of resveratrol production in *Xylaria psidii* by exploring the phenomenon of epigenetics: using DNA methyltransferases and histone deacetylase as epigenetic modifiers. *Mol. Biol. Rep.* 46, 4123–4137. doi: 10.1007/s11033-019-04862-z

Dwibedi, V., Rath, S. K., Prakash, R., and Saxena, S. (2021). Response surface statistical optimization of fermentation parameters for resveratrol production by

the endophytic fungus *Arcopilus aureus* and its tyrosinase inhibitory activity. *Biotechnol. Lett.* 43, 627–644. doi: 10.1007/s10529-020-03032-7

Dwibedi, V., and Saxena, S. (2018). Arcopilus aureus, a resveratrol-producing endophyte from *Vitis vinifera*. *Appl. Biochem. Biotechnol.* 186, 476–495. doi: 10.1007/s12010-018-2755-x

Dwibedi, V., and Saxena, S. (2019a). Diversity and phylogeny of resveratrol-producing culturable endophytic fungi from *Vitis* species in India. *3 Biotech* 9:182. doi: 10.1007/s13205-019-1712-x

Dwibedi, V., and Saxena, S. (2019b). *In vitro* anti-oxidant, anti-fungal and anti-staphylococcal activity of resveratrol-producing endophytic fungi. *Proc. Natl. Acad. Sci. India Sect. B Biol. Sci.* 90, 207–219. doi: 10.1007/s40011-019-01098-6

Dwibedi, V., and Saxena, S. (2022). Effect of precursor feeding, dietary supplementation, chemical elicitors and co-culturing on resveratrol production by *Arcopilus aureus*. *Prep. Biochem. Biotechnol.* 52, 404–412. doi: 10.1080/10826068.2021.1955709

El-Hawary, S. S., Sayed, A. M., Mohammed, R., Hassan, H. M., Zaki, M. A., Rateb, M. E., et al. (2018). Epigenetic modifiers induce bioactive phenolic metabolites in the marine-derived fungus *Penicillium brevicompactum*. *Mar. Drugs* 16:253. doi: 10.3390/md16080253

Fabjanowicz, M., Płotka-Wasylka, J., and Namiesnik, J. (2018). Detection, identification and determination of resveratrol in wine. Problems and challenges. *Trends Analyt. Chem.* 103, 21–33. doi: 10.1016/j.trac.2018.03.006

Fan, E., Zhang, K., Zhu, M., and Wang, Q. (2010). Obtaining resveratrol: from chemical synthesis to biotechnological production. *Mini Rev. Org. Chem.* 7, 272–281. doi: 10.2174/157019310792246454

Fischer, J., Schroeckh, V., and Brakhage, A. A. (2016). "Awakening of fungal secondary metabolite gene clusters," in *Gene expression systems in fungi: Advancements and applications*, eds M. Schmoll and C. Dattenböck (Berlin: Springer), 253–273. doi: 10.1007/978-3-319-27951-0_11

Flamini, R., De Rosso, M., De Marchi, F., Vedova, A. D., Panighel, A., Gardiman, M., et al. (2013). An innovative approach to grape metabolomics: stilbene profiling by suspect screening analysis. *Metabolomics* 9, 1243–1253. doi: 10.1007/s11306-013-0530-0

Gambini, J., Ingles, M., Olaso, G., Lopez-Grueso, R., Bonet-Costa, V., Gimeno-Mallench, L., et al. (2015). Properties of resveratrol: *in vitro* and *in vivo* studies about metabolism, bioavailability, and biological effects in animal models and humans. *Oxid. Med. Cell. Longev.* 2015:837042. doi: 10.1155/2015/837042

González, V., and Tello, M. L. (2010). The endophytic mycota associated with *Vitis vinifera* in central Spain. *Fungal Divers.* 47, 29–42. doi: 10.1007/s13225-010-0073-x

Grace, M. H., Xiong, J., Esposito, D., Ehlenfeldt, M., and Lila, M. A. (2019). Simultaneous LC-MS quantification of anthocyanins and non-anthocyanin phenolics from blueberries with widely divergent profiles and biological activities. *Food Chem.* 277, 336–346. doi: 10.1016/j.foodchem.2018.10.101

Guo, J., Zhao, J., Zhang, M., Sun, Z., and Liu, L. (2022). Optimization of the ultrasonic-assisted extraction of trans-resveratrol and its glucoside from grapes followed by UPLC-MS/MS using the response surface methodology. *J. Food Meas. Charact.* 16, 1124–1136. doi: 10.1007/s11694-021-01236-7

Hasan, M. M., and Bae, H. (2017). An overview of stress-induced resveratrol synthesis in grapes: Perspectives for resveratrol-enriched grape products. *Molecules* 22:294. doi: 10.3390/molecules22020294

Hassane, A. M. A., Taha, T. M., Awad, M. F., Mohamed, H., and Melebari, M. (2022a). Radical scavenging potency, HPLC profiling and phylogenetic analysis of endophytic fungi isolated from selected medicinal plants of Saudi Arabia. *Electron. J. Biotechnol.* 58, 37–45. doi: 10.1016/j.ejbt.2022.05.001

Hassane, A. M. A., Hussien, S. M., Abouelela, M. E., Taha, T. M., Awad, M. F., Mohamed, H., et al. (2022b). *In vitro* and *in silico* antioxidant efficiency of bio-potent secondary metabolites from different taxa of black seed-producing plants and their derived mycoendophytes. *Front. Bioeng. Biotechnol.* 10:930161. doi: 10.3389/fbioe.2022.930161

Hu, X., Liu, Y., Li, D., Feng, W., Ni, H., Cao, S., et al. (2019). An innovative biotransformation to produce resveratrol by *Bacillus safensis*. *RSC Adv.* 9, 15448–15456. doi: 10.1039/C9RA01338E

Jeandet, P., Delaunois, B., Aziz, A., Donnez, D., Vasserot, Y., Cordelier, S., et al. (2012). Metabolic engineering of yeast and plants for the production of the biologically active hydroxystilbene, resveratrol. *J. Biomed. Biotechnol.* 2012:579089. doi: 10.1155/2012/579089

Jeandet, P., Delaunois, B., Conreux, A., Donnez, D., Nuzzo, V., Cordelier, S., et al. (2010). Biosynthesis, metabolism, molecular engineering, and biological functions of stilbene phytoalexins in plants. *Biofactors* 36, 331–341. doi: 10.1002/biof.108

Jeandet, P., Douillet-Breuil, A.-C., Bessis, R., Debord, S., Sbaghi, M., and Adrian, M. (2002). Phytoalexins from the Vitaceae: biosynthesis, phytoalexin gene expression in transgenic plants, antifungal activity, and metabolism. *J. Agric. Food Chem.* 50, 2731–2741. doi: 10.1021/jf011429s

Jendresen, C. B., Stahlhut, S. G., Li, M., Gaspar, P., Siedler, S., Forster, J., et al. (2015). Highly active and specific tyrosine ammonia-lyases from diverse origins enable enhanced production of aromatic compounds in bacteria and *Saccharomyces cerevisiae*. *Appl. Environ. Microbiol.* 81, 4458–4476. doi: 10.1128/AEM.00405-15

Jiewei, T., Lei, W., Xiufeng, L., Heming, Z., Xiaoguang, L., Haiyan, F., et al. (2018). Microbial transformation of resveratrol by endophyte *Streptomyces* sp. A12 isolated from *Polygonum cuspidatum*. *Nat. Prod. Res.* 32, 2343–2346. doi: 10.1080/14786419.2017.1405411

Jin, S., Gao, M., Kong, W., Yang, B., Kuang, H., Yang, B., et al. (2020). Enhanced and sustainable pretreatment for bioconversion and extraction of resveratrol from peanut skin using ultrasound-assisted surfactant aqueous system with microbial consortia immobilized on cellulose. *3 Biotech* 10:293. doi: 10.1007/s13205-020-02287-1

Kang, S.-Y., Lee, J. K., Choi, O., Kim, C. Y., Jang, J.-H., Hwang, B. Y., et al. (2014). Biosynthesis of methylated resveratrol analogs through the construction of an artificial biosynthetic pathway in *E. coli*. *BMC Biotechnol.* 14:67. doi: 10.1186/1472-6750-14-67

Kasiotis, K. M., Pratsinis, H., Kletsas, D., and Haroutounian, S. A. (2013). Resveratrol and related stilbenes: their anti-aging and anti-angiogenic properties. *Food Chem. Toxicol.* 61, 112–120. doi: 10.1016/j.fct.2013.03.038

Katsuyama, Y., Funa, N., Miyahisa, I., and Horinouchi, S. (2007). Synthesis of unnatural flavonoids and stilbenes by exploiting the plant biosynthetic pathway in *Escherichia coli*. *Chem. Biol.* 14, 613–621. doi: 10.1016/j.chembiol.2007.05.004

Kim, J. S., Lee, S. Y., and Park, S. U. (2008). Resveratrol production in hairy root culture of peanut, *Arachis hypogaea* L. transformed with different *Agrobacterium rhizogenes* strains. *Afr. J. Biotechnol.* 7, 3788–3790.

King, R. E., Bomser, J. A., and Min, D. B. (2006). Bioactivity of resveratrol. *Compr. Rev. Food Sci.* 5, 65–70. doi: 10.1111/j.1541-4337.2006.00001.x

Kiselev, K., Dubrovina, A., Veselova, M., Bulgakov, V., Fedoreyev, S., and Zhuravlev, Y. N. (2007). The *rolB* gene-induced overproduction of resveratrol in *Vitis amurensis* transformed cells. *J. Biotechnol.* 128, 681–692. doi: 10.1016/j.jbiotec.2006.11.008

Kiselev, K. V. (2011). Perspectives for production and application of resveratrol. *Appl. Microbiol. Biotechnol.* 90, 417–425. doi: 10.1007/s00253-011-3184-8

Kornsakulkarn, J., Dolsophon, K., Boonyuen, N., Boonruangprapa, T., Rachtawee, P., Prabpai, S., et al. (2011). Dihydronaphthalenones from endophytic fungus *Fusarium* sp. BCC14842. *Tetrahedron* 67, 7540–7547. doi: 10.1016/j.tet.2011.07.078

Kumar, J., Sharma, V. K., Singh, D. K., Mishra, A., Gond, S. K., Verma, S. K., et al. (2016). Epigenetic activation of antibacterial property of an endophytic *Streptomyces coelicolor* strain AZRA 37 and identification of the induced protein using MALDI TOF MS/MS. *PLoS One* 11:e0147876. doi: 10.1371/journal.pone.0147876

Kuo, H.-P., Wang, R., Lin, Y.-S., Lai, J.-T., Lo, Y.-C., and Huang, S.-T. (2017). Pilot scale repeated fed-batch fermentation processes of the wine yeast *Dekkera bruxellensis* for mass production of resveratrol from *Polygonum cuspidatum*. *Bioresour. Technol.* 243, 986–993. doi: 10.1016/j.biortech.2017.07.053

Kusari, S., Kosuth, J., Cellarova, E., and Spiteller, M. (2011). Survival-strategies of endophytic *Fusarium solani* against indigenous camptothecin biosynthesis. *Fungal Ecol.* 4, 219–223. doi: 10.1016/j.funeco.2010.11.002

Labois, C., Stempien, E., Schneider, J., Schaeffer-Reiss, C., Bertsch, C., Goddard, M. L., et al. (2021). Comparative study of secreted proteins, enzymatic activities of wood degradation and stilbene metabolization in grapevine *Botryosphaeria* Dieback Fungi. *J. Fungi* 7:568. doi: 10.3390/jof7070568

Langcake, P., and Pryce, R. J. (1977). A new class of phytoalexins from grapevines. *Experientia* 33, 151–152. doi: 10.1007/BF02124034

Lau, T., Harbourne, N., and Oruna-Concha, M. J. (2020). Optimization of enzyme-assisted extraction of ferulic acid from sweet corn cob by response surface methodology. *J. Sci. Food Agric.* 100, 1479–1485. doi: 10.1002/jsfa.10155

Li, C.-P., Tan, S., Ye, H., Cao, J., and Zhao, H. (2019). A novel fluorescence assay for resveratrol determination in red wine based on competitive host-guest recognition. *Food Chem.* 283, 191–198. doi: 10.1016/j.foodchem.2018.12.133

Liu, J., Zhang, X., Yan, T., Wang, F., Li, J., Jia, L., et al. (2020). Screening of an endophyte transforming polydatin to resveratrol from *Reynoutria japonica* Houtt and the optimization of its transformation parameters. *Molecules* 25:4830. doi: 10.3390/molecules25204830

Liu, X., Zhou, Z.-Y., Cui, J.-L., Wang, M.-L., and Wang, J.-H. (2021). Biotransformation ability of endophytic fungi: from species evolution to industrial applications. *Appl. Microbiol. Biotechnol.* 105, 7095–7113. doi: 10.1007/s00253-021-11554-x

Liu, Y., Nan, L., Liu, J., Yan, H., Zhang, D., and Han, X. (2016a). Isolation and identification of resveratrol-producing endophytes from wine grape Cabernet Sauvignon. *Springerplus* 5:1029. doi: 10.1186/s40064-016-2571-0

Liu, Y., Zhou, J., Qu, Y., Yang, X., Shi, G., Wang, X., et al. (2016b). Resveratrol antagonizes antimicrobial lethality and stimulates recovery of bacterial mutants. *PLoS One* 11:e0153023. doi: 10.1371/journal.pone.0153023

Liu, Z., Zhuang, C., Sheng, S., Shao, L., Zhao, W., and Zhao, S. (2011). Overexpression of a resveratrol synthase gene (PcRS) from *Polygonum cuspidatum* in transgenic *Arabidopsis* causes the accumulation of trans-piceid with antifungal activity. *Plant Cell Rep.* 30, 2027–2036. doi: 10.1007/s00299-011-1110-2

Lu, Y., Shao, D., Shi, J., Huang, Q., Yang, H., and Jin, M. (2016). Strategies for enhancing resveratrol production and the expression of pathway enzymes. *Appl. Microbiol. Biotechnol.* 100, 7407–7421. doi: 10.1007/s00253-016-7723-1

Lu, Y., Song, Y., Zhu, J., Xu, X., Pang, B., Jin, H., et al. (2021b). Potential application of CHS and 4CL genes from grape endophytic fungus in production of naringenin and resveratrol and the improvement of polyphenol profiles and flavour of wine. *Food Chem.* 347:128972. doi: 10.1016/j.foodchem.2020.128972

Lu, Y., Shi, J., Zhao, X., Song, Y., Qin, Y., and Liu, Y. (2021a). Improvement of the biosynthesis of resveratrol in endophytic fungus (*Alternaria* sp. MG1) by the synergistic effect of UV light and oligomeric proanthocyanidins. *Front. Microbiol.* 12:770734. doi: 10.3389/fmicb.2021.770734

Lu, Y., Ye, C., Che, J., Xu, X., Shao, D., Jiang, C., et al. (2019). Genomic sequencing, genome-scale metabolic network reconstruction, and *in silico* flux analysis of the grape endophytic fungus *Alternaria* sp. MG1. *Microb. Cell Fact.* 18:13. doi: 10.1186/s12934-019-1063-7

Ma, D. S., Tan, L. T.-H., Chan, K.-G., Yap, W. H., Pusparajah, P., Chuah, L.-H., et al. (2018). Resveratrol-potential antibacterial agent against foodborne pathogens. *Front. Pharmacol.* 9:102. doi: 10.3389/fphar.2018.00102

Magdevska, V., Gaber, R., Goranovic, D., Kuscer, E., Boakes, S., Alonso, M. B. D., et al. (2010). Robust reporter system based on chalcone synthase rppA gene from *Saccharopolyspora erythraea*. *J. Microbiol. Methods* 83, 111–119. doi: 10.1016/j.mimet.2010.08.001

Mantegna, S., Binello, A., Boffa, L., Giorgis, M., Cena, C., and Cravotto, G. (2012). A one-pot ultrasound-assisted water extraction/cyclodextrin encapsulation of resveratrol from *Polygonum cuspidatum*. *Food Chem.* 130, 746–750. doi: 10.1016/j.foodchem.2011.07.038

Medina-Bolivar, F., Condori, J., Rimando, A. M., Hubstenberger, J., Shelton, K., O'Keefe, S. F., et al. (2007). Production and secretion of resveratrol in hairy root cultures of peanut. *Phytochemistry* 68, 1992–2003. doi: 10.1016/j.phytochem.2007.04.039

Meeran, S. M., Ahmed, A., and Tollefsbol, T. O. (2010). Epigenetic targets of bioactive dietary components for cancer prevention and therapy. *Clin. Epigenetics* 1, 101–116. doi: 10.1007/s13148-010-0011-5

Mei, Y. Z., Liu, R. X., Wang, D. P., Wang, X., and Dai, C. C. (2015). Biocatalysis and biotransformation of resveratrol in microorganisms. *Biotechnol. Lett.* 37, 9–18. doi: 10.1007/s10529-014-1651-x

Melchior, F., Hohmann, F., Schwer, B., and Kindl, H. (1991). Induction of stilbene synthase by *Botrytis cinerea* in cultured grapevine cells. *Planta* 183, 307–314. doi: 10.1007/BF00197803

Meshram, V., Kapoor, N., Dwibedi, V., Srivastava, A., and Saxena, S. (2022). Extracellular resveratrol producing endophytic fungus, *Quambalaria cyanescens*. *S. Afr. J. Bot.* 146, 409–416. doi: 10.1016/j.sajb.2021.11.026

Mohamed, H., Hassane, A., Atta, O., and Song, Y. (2021a). Deep learning strategies for active secondary metabolites biosynthesis from fungi: harnessing artificial manipulation and application. *Biocatal. Agric. Biotechnol.* 38:102195. doi: 10.1016/j.bcab.2021.102195

Mohamed, H., Hassane, A., Rawway, M., El-Sayed, M., Gomaa, A. E.-R., Abdul-Raouf, U., et al. (2021b). Antibacterial and cytotoxic potency of thermophilic *Streptomyces werraensis* MI-S. 24-3 isolated from an Egyptian extreme environment. *Arch. Microbiol.* 203, 4961–4972. doi: 10.1007/s00203-021-02487-0

Mohammadipanah, F., Kermani, F., and Salimi, F. (2020). Awakening the secondary metabolite pathways of *Promicromonospora kermanensis* using physicochemical and biological elicitors. *Appl. Biochem. Biotechnol.* 192, 1224–1237. doi: 10.1007/s12010-020-03361-3

Myers, R. H., Montgomery, D. C., and Anderson-Cook, C. M. (2016). *Response surface methodology: Process and product optimization using designed experiments*, 2nd Edn. New York, NY: Wiley, 856.

Nair, D. N., and Padmavathy, S. (2014). Impact of endophytic microorganisms on plants, environment and humans. *Sci. World J.* 2014:250693. doi: 10.1155/2014/250693

Nisa, H., Kamili, A. N., Nawchoo, I. A., Shafi, S., Shameem, N., and Bandh, S. A. (2015). Fungal endophytes as prolific source of phytochemicals and other bioactive natural products. A review. *Microb. Pathog.* 82, 50–59. doi: 10.1016/j.micpath.2015.04.001

Nonomura, S., Kanagawa, H., and Makimoto, A. (1963). Chemical constituents of Polygonaceous plants. I. Studies on the components of Ko-J O-Kon. (*Polygonum cuspidatum* Sieb. Et Zucc.). *Yakugaku Zasshi* 83, 988–990. doi: 10.1248/yakushi1947.83.10_988

O'Brien, W. D. Jr. (2007). Ultrasound–biophysics mechanisms. *Prog. Biophys. Mol. Biol.* 93, 212–255. doi: 10.1016/j.pbiomolbio.2006.07.010

Park, H.-J., Uhm, K.-N., and Kim, H.-K. (2010). Biotransformation of amides to acids using a co-cross-linked enzyme aggregate of *Rhodococcus erythropolis* amidase. *J. Microbiol. Biotechnol.* 20, 325–331. doi: 10.4014/jmb.1009.09009

Park, S. R., Yoon, J. A., Paik, J. H., Park, J. W., Jung, W. S., Ban, Y. H., et al. (2009). Engineering of plant-specific phenylpropanoids biosynthesis in *Streptomyces venezuelae*. *J. Biotechnol.* 141, 181–188. doi: 10.1016/j.jbiotec.2009.03.013

Parker, J. A., Arango, M., Abderrahmane, S., Lambert, E., Tourette, C., Catoire, H., et al. (2005). Resveratrol rescues mutant polyglutamine cytotoxicity in nematode and mammalian neurons. *Nat. Genet.* 37, 349–350. doi: 10.1038/ng1534

Paul, B., Chereyathmanjiyil, A., Masih, I., Chapuis, L., and Benoit, A. (1998). Biological control of *Botrytis cinerea* causing grey mould disease of grapevine and elicitation of stilbene phytoalexin (resveratrol) by a soil bacterium. *FEMS Microbiol. Lett.* 165, 65–70. doi: 10.1111/j.1574-6968.1998.tb13128.x

Petrovski, G., Gurusamy, N., and Das, D. K. (2011). Resveratrol in cardiovascular health and disease. *Ann. N. Y. Acad. Sci.* 1215, 22–33. doi: 10.1111/j.1749-6632.2010.05843.x

Pinto, G. P., Ribeiro, A. J., Ramos, M. J., Fernandes, P. A., Toscano, M., and Russo, N. (2015). New insights in the catalytic mechanism of tyrosine ammonia-lyase given by QM/MM and QM cluster models. *Arch. Biochem. Biophys.* 582, 107–115. doi: 10.1016/j.abb.2015.03.002

Powell, R. G., TePaske, M. R., Plattner, R. D., White, J. F., and Clement, S. L. (1994). Isolation of resveratrol from *Festuca versuta* and evidence for the widespread occurrence of this stilbene in the Poaceae. *Phytochemistry* 35, 335–338. doi: 10.1016/S0031-9422(00)94759-9

Priya, R., and Kanmani, S. (2011). Optimization of photocatalytic production of hydrogen from hydrogen sulfide in alkaline solution using response surface methodology. *Desalination* 276, 222–227. doi: 10.1016/j.desal.2011.03.053

Rajput, H., Dhir, A., and Sangal, V. K. (2018). GO mediated TiO_2 nanotube electrode for the photoelectrocatalytic degradation of pentachlorophenol. *J. Electrochem. Soc.* 165, 16–26. doi: 10.1149/2.0871802jes

Reynolds, A. G. (2017). "The grapevine, viticulture, and winemaking: a brief introduction," in *Grapevine viruses: Molecular biology, diagnostics and management*, eds B. Meng, G. Martelli, D. Golino, and M. Fuchs (Berlin: Springer), 3–29. doi: 10.1007/978-3-319-57706-7_1

Roat, C., and Saraf, M. (2017). Isolation and screening of resveratrol producing endophytes from wild grape *Cayratia trifolia*. *Int. J. Adv. Agric. Sci. Technol.* 4, 27–33.

Roat, C., and Saraf, M. (2020). Isolation and characterization of t-resveratrol and α-viniferin, a bioactive secondary metabolite of an endophytic fungus *Aspergillus stellifer* AB4, from *Vitis vinifera*. *J. Microbiol. Biotechnol. Food Sci.* 9, 708–713. doi: 10.15414/jmbfs.2020.9.4.708-713

Rodríguez De Luna, S. L., Ramirez-Garza, R., and Serna Saldívar, S. O. (2020). Environmentally friendly methods for flavonoid extraction from plant material: impact of their operating conditions on yield and antioxidant properties. *Sci. World J.* 2020:6792069. doi: 10.1155/2020/6792069

Rutledge, P. J., and Challis, G. L. (2015). Discovery of microbial natural products by activation of silent biosynthetic gene clusters. *Nat. Rev. Microbiol.* 13, 509–523. doi: 10.1038/nrmicro3496

Santos, A. C., Veiga, F., and Ribeiro, A. J. (2011). New delivery systems to improve the bioavailability of resveratrol. *Expert Opin. Drug Deliv.* 8, 973–990. doi: 10.1517/17425247.2011.581655

Saran, S., Mukherjee, S., Dalal, J., and Saxena, R. K. (2015). High production of erythritol from *Candida sorbosivorans* SSE-24 and its inhibitory effect on biofilm formation of *Streptococcus mutans*. *Bioresour. Technol.* 198, 31–38. doi: 10.1016/j.biortech.2015.08.146

Sbaghi, M., Jeandet, P., Bessis, R., and Leroux, P. (1996). Degradation of stilbene-type phytoalexins in relation to the pathogenicity of *Botrytis cinerea* to grapevines. *Plant Pathol.* 45, 139–144. doi: 10.1046/j.1365-3059.1996.d01-101.x

Schouten, A., Wagemakers, L., Stefanato, F. L., Kaaij, R. M., and Kan, J. A. (2002). Resveratrol acts as a natural profungicide and induces self-intoxication by a specific laccase. *Mol. Microbiol.* 43, 883–894. doi: 10.1046/j.1365-2958.2002.02801.x

Sharma, V. K., Kumar, J., Singh, D. K., Mishra, A., Verma, S. K., Gond, S. K., et al. (2017). Induction of cryptic and bioactive metabolites through natural dietary components in an endophytic fungus *Colletotrichum gloeosporioides* (Penz.) Sacc. *Front. Microbiol.* 8:1126. doi: 10.3389/fmicb.2017.01126

Shi, J., Zeng, Q., Liu, Y., and Pan, Z. (2012). *Alternaria* sp. MG1, a resveratrol-producing fungus: isolation, identification, and optimal cultivation conditions for resveratrol production. *Appl. Microbiol. Biotechnol.* 95, 369–379. doi: 10.1007/s00253-012-4045-9

Shin, S.-Y., Han, N. S., Park, Y.-C., Kim, M.-D., and Seo, J.-H. (2011). Production of resveratrol from p-coumaric acid in recombinant Saccharomyces cerevisiae expressing 4-coumarate: coenzyme A ligase and stilbene synthase genes. *Enzyme Microb. Technol.* 48, 48–53. doi: 10.1016/j.enzmictec.2010.09.004

Silroy, S., Sengupta, A., Bhattacharyya, D., and Ghosh, M. (2014). Optimization of reaction parameters of acidolysis reaction between mustard oil and capric acid by using *Thermomyces lanuginosus* lipase. *J. Food Sci. Technol.* 51, 715–721. doi: 10.1007/s13197-011-0543-5

Singh, J. P., Kaur, A., Shevkani, K., and Singh, N. (2016). Composition, bioactive compounds and antioxidant activity of common Indian fruits and vegetables. *J. Food Sci. Technol.* 53, 4056–4066. doi: 10.1007/s13197-016-2412-8

Strobel, G., and Daisy, B. (2003). Bioprospecting for microbial endophytes and their natural products. *Microbiol. Mol. Biol. Rev.* 67, 491–502. doi: 10.1128/MMBR.67.4.491-502.2003

Sun, P., Liang, J. L., Kang, L. Z., Huang, X. Y., Huang, J. J., Ye, Z. W., et al. (2015). Increased resveratrol production in wines using engineered wine strains *Saccharomyces cerevisiae* EC1118 and relaxed antibiotic or auxotrophic selection. *Biotechnol. Prog.* 31, 650–655. doi: 10.1002/btpr.2057

Sun, R. T., Feng, X. C., Zhang, Z. Z., Zhou, N., Feng, H. D., Liu, Y. M., et al. (2022). Root endophytic fungi regulate changes in sugar and medicinal compositions of *Polygonum cuspidatum*. *Front. Plant Sci.* 13:818909. doi: 10.3389/fpls.2022.818909

Suryanarayanan, T., Thirunavukkarasu, N., Govindarajulu, M., Sasse, F., Jansen, R., and Murali, T. (2009). Fungal endophytes and bioprospecting. *Fungal Biol. Rev.* 23, 9–19. doi: 10.1016/j.fbr.2009.07.001

Tanyildizi, M. S., Ozer, D., and Elibol, M. (2005). Optimization of α-amylase production by *Bacillus* sp. using response surface methodology. *Process Biochem.* 40, 2291–2296. doi: 10.1016/j.procbio.2004.06.018

Tassoni, A., Fornale, S., Franceschetti, M., Musiani, F., Michael, A. J., Perry, B., et al. (2005). Jasmonates and Na-orthovanadate promote resveratrol production in *Vitis vinifera* cv. Barbera cell cultures. *New Phytol.* 166, 895–906. doi: 10.1111/j.1469-8137.2005.01383.x

Tavares, S., Vesentini, D., Fernandes, J. C., Ferreira, R. B., Laureano, O., Ricardo-Da-Silva, J. M., et al. (2013). *Vitis vinifera* secondary metabolism as affected by sulfate depletion: diagnosis through phenylpropanoid pathway genes and metabolites. *Plant Physiol. Biochem.* 66, 118–126. doi: 10.1016/j.plaphy.2013.01.022

Teimoori-Boghsani, Y., Ganjeali, A., Cernava, T., Muller, H., Asili, A., and Berg, G. (2019). Endophytic fungi of native *Salvia abrotanoides* plants reveal high taxonomic diversity and unique profiles of secondary metabolites. *Front. Microbiol.* 10:3013. doi: 10.3389/fmicb.2019.03013

Triska, J., Vrchotova, N., Olejnickova, J., Jilek, R., and Sotolar, R. (2012). Separation and identification of highly fluorescent compounds derived from trans-resveratrol in the leaves of *Vitis vinifera* infected by *Plasmopara viticola*. *Molecules* 17, 2773–2783. doi: 10.3390/molecules17032773

Ul-Hassan, S. R., Strobel, G. A., Booth, E., Knighton, W. B., Floerchinger, C., and Sears, J. (2012). Modulation of volatile organic compound formation in the mycodiesel-producing endophyte *Hypoxylon* sp. CI-4. *Microbiology* 158, 465–473. doi: 10.1099/mic.0.054643-0

Vandelle, E., Poinssot, B., Wendehenne, D., Bentejac, M., and Pugin, A. (2006). Integrated signaling network involving calcium, nitric oxide, and active oxygen species but not mitogen-activated protein kinases in BcPG1-elicited grapevine defenses. *Mol. Plant Microbe Interact.* 19, 429–440. doi: 10.1094/MPMI-19-0429

Vannelli, T., Wei Qi, W., Sweigard, J., Gatenby, A. A., and Sariaslani, F. S. (2007a). Production of p-hydroxycinnamic acid from glucose in *Saccharomyces cerevisiae* and *Escherichia coli* by expression of heterologous genes from plants and fungi. *Metab. Eng.* 9, 142–151. doi: 10.1016/j.ymben.2006.11.001

Vannelli, T., Xue, Z., Breinig, S., Qi, W. W., and Sariaslani, F. S. (2007b). Functional expression in *Escherichia coli* of the tyrosine-inducible tyrosine ammonia-lyase enzyme from yeast *Trichosporon cutaneum* for production of p-hydroxycinnamic acid. *Enzyme Microb. Technol.* 41, 413–422. doi: 10.1016/j.enzmictec.2007.03.013

Venugopalan, A., and Srivastava, S. (2015). Endophytes as *in vitro* production platforms of high value plant secondary metabolites. *Biotechnol. Adv.* 33, 873–887. doi: 10.1016/j.biotechadv.2015.07.004

Villa-Ruano, N., Morales-Mora, L. Á, Varela-Caselis, J. L., Rivera, A., Valencia de Ita, M. D. L. Á, and Romero-Arenas, O. (2021). *Arcopilus aureus* MaC7A as a new source of resveratrol: assessment of amino acid precursors, volatiles, and fungal enzymes for boosting resveratrol production in batch cultures. *Appl. Sci.* 11, 4583–4596. doi: 10.3390/app11104583

Wang, D. G., Liu, W. Y., and Chen, G. T. (2013). A simple method for the isolation and purification of resveratrol from *Polygonum cuspidatum*. *J. Pharm. Anal.* 3, 241–247. doi: 10.1016/j.jpha.2012.12.001

Wang, H., Liu, L., Guo, Y. X., Dong, Y. S., Zhang, D. J., and Xiu, Z. L. (2007). Biotransformation of piceid in *Polygonum cuspidatum* to resveratrol by *Aspergillus oryzae*. *Appl. Microbiol. Biotechnol.* 75, 763–768. doi: 10.1007/s00253-007-0874-3

Wang, H. W., Sun, K., Guan, Y. X., Qiu, M. H., Zhang, L., and Dai, C. C. (2019). Fungal endophyte *Phomopsis liquidambari* biodegrades soil resveratrol: a potential allelochemical in peanut monocropping systems. *J. Sci. Food Agric.* 99, 5899–5909. doi: 10.1002/jsfa.9865

Wang, J., Yang, Y., and Yan, Y. (2018). "Bioproduction of resveratrol," in *Biotechnology of natural products*, eds W. Schwab, B. M. Lange, and M. Wüst (Berlin: Springer), 61–79. doi: 10.1007/978-3-319-67903-7_3

Wang, L., Wu, Y., Chen, Y., Zou, J., and Li, X. (2016). Biotransformation of resveratrol: new prenylated trans-resveratrol synthesized by *Aspergillus* sp. SCSIOW2. *Molecules* 21:883. doi: 10.3390/molecules21070883

Wang, W., Tang, K., Yang, H.-R., Wen, P.-F., Zhang, P., Wang, H.-L., et al. (2010). Distribution of resveratrol and stilbene synthase in young grape plants (*Vitis vinifera* L. cv. Cabernet Sauvignon) and the effect of UV-C on its accumulation. *Plant Physiol. Biochem.* 48, 142–152. doi: 10.1016/j.plaphy.2009.12.002

Wang, X. H., Zhang, C., Yang, L. L., and Gomes-Laranjo, J. (2011). Production of dragon's blood in *Dracaena cochinchinensis* plants by inoculation of *Fusarium proliferatum*. *Plant Sci.* 180, 292–299. doi: 10.1016/j.plantsci.2010.09.007

Wang, Y., Bhuiya, M. W., Zhou, R., and Yu, O. (2015). Pterostilbene production by microorganisms expressing resveratrol O-methyltransferase. *Ann. Microbiol.* 65, 817–826. doi: 10.1007/s13213-014-0922-z

Wang, Y., and Yu, O. (2012). Synthetic scaffolds increased resveratrol biosynthesis in engineered yeast cells. *J. Biotechnol.* 157, 258–260. doi: 10.1016/j.jbiotec.2011.11.003

Watts, K. T., Lee, P. C., and Schmidt-Dannert, C. (2006). Biosynthesis of plant-specific stilbene polyketides in metabolically engineered *Escherichia coli*. *BMC Biotechnol.* 6:22. doi: 10.1186/1472-6750-6-22

Weiskirchen, S., and Weiskirchen, R. (2016). Resveratrol: How much wine do you have to drink to stay healthy? *Adv. Nutr.* 7, 706–718. doi: 10.3945/an.115.011627

Williams, R. B., Henrikson, J. C., Hoover, A. R., Lee, A. E., and Cichewicz, R. H. (2008). Epigenetic remodeling of the fungal secondary metabolome. *Org. Biomol. Chem.* 6, 1895–1897. doi: 10.1039/b804701d

Wu, L., Wang, X., Xu, W., Farzaneh, F., and Xu, R. (2009). The structure and pharmacological functions of coumarins and their derivatives. *Curr. Med. Chem.* 16, 4236–4260. doi: 10.2174/092986709789578187

Xiang, C., Liu, J., Ma, L., and Yang, M. (2020). Overexpressing codon-adapted fusion proteins of 4-coumaroyl-CoA ligase (4CL) and stilbene synthase (STS) for resveratrol production in *Chlamydomonas reinhardtii*. *J. Appl. Phycol.* 32, 1669–1676. doi: 10.1007/s10811-020-02123-2

Xu, Z., Tian, J., Gan, L., and Tian, Y. (2020). Discovery of the endophytic fungi from *Polygonum cuspidatum* and biotransformation of resveratrol to pterostillbene by the endophyte *Penicillium* sp. F5. *Appl. Biochem. Microbiol.* 56, 313–320. doi: 10.1134/s0003683820030163

Yang, M. H., Kuo, C. H., Hsieh, W. C., and Ku, K. L. (2010). Investigation of microbial elicitation of trans-resveratrol and trans-piceatannol in peanut callus led to the application of chitin as a potential elicitor. *J. Agric. Food. Chem.* 58, 9537–9541. doi: 10.1021/jf1022725

Yang, M. Z., Ma, M. D., Yuan, M. Q., Huang, Z. Y., Yang, W. X., Zhang, H. B., et al. (2016). Fungal endophytes as a metabolic fine-tuning regulator for wine grape. *PLoS One* 11:e0163186. doi: 10.1371/journal.pone.0163186

Yeo, H.-K., Hyun, Y.-J., Jang, S.-E., Han, M.-J., Lee, Y.-S., and Kim, D.-H. (2012). Development of fecal microbial enzyme mix for mutagenicity assay of natural products. *J. Microbiol. Biotechnol.* 22, 838–848. doi: 10.4014/jmb.1112.12028

Yin, X., You, Q., and Jiang, Z. (2011). Optimization of enzyme assisted extraction of polysaccharides from *Tricholoma matsutake* by response surface

methodology. *Carbohydr. Polym.* 86, 1358–1364. doi: 10.1016/j.carbpol.2011.06.053

Yu, C. K., Springob, K., Schmidt, J., Nicholson, R. L., Chu, I. K., Yip, W. K., et al. (2005). A stilbene synthase gene (SbSTS1) is involved in host and nonhost defense responses in sorghum. *Plant Physiol.* 138, 393–401. doi: 10.1104/pp.105.059337

Yu, M., Chen, J. C., Qu, J. Z., Liu, F., Zhou, M., Ma, Y. M., et al. (2020). Exposure to endophytic fungi quantitatively and compositionally alters anthocyanins in grape cells. *Plant Physiol. Biochem.* 149, 144–152. doi: 10.1016/j.plaphy.2020.02.006

Yun, T. Y., Feng, R. J., Zhou, D. B., Pan, Y. Y., Chen, Y. F., Wang, F., et al. (2018). Optimization of fermentation conditions through response surface methodology for enhanced antibacterial metabolite production by *Streptomyces* sp. 1-14 from cassava rhizosphere. *PLoS One* 13:e0206497. doi: 10.1371/journal.pone.0206497

Zhang, G., Zhao, H., Wang, Z., Cheng, J., and Tang, X. (2008). Recent advances in the study of chemical constituents and bioactivity of *Rumex* L. *World Sci. Technol.* 10, 86–93. doi: 10.11842/wst.2008.5

Zhang, J., Shi, J., and Liu, Y. (2013). Substrates and enzyme activities related to biotransformation of resveratrol from phenylalanine by *Alternaria* sp. MG1. *Appl. Microbiol. Biotechnol.* 97, 9941–9954. doi: 10.1007/s00253-013-5212-3

Zwingelstein, M., Draye, M., Besombes, J.-L., Piot, C., and Chatel, G. (2020). Viticultural wood waste as a source of polyphenols of interest: opportunities and perspectives through conventional and emerging extraction methods. *J. Waste Manag.* 102, 782–794. doi: 10.1016/j.wasman.2019.11.034

frontiers | Frontiers in Microbiology

TYPE Original Research
PUBLISHED 04 November 2022
DOI 10.3389/fmicb.2022.974526

OPEN ACCESS

EDITED BY
Naser Safaie,
Tarbiat Modares University, Iran

REVIEWED BY
Debdulal Banerjee,
Vidyasagar University, India
Pavan Kumar,
Guru Angad Dev Veterinary and Animal Sciences University, India

*CORRESPONDENCE
Deni Elfiati
deni1@usu.ac.id
Asep Hidayat
ashephidayat12@gmail.com

†These authors have contributed equally to this work

SPECIALTY SECTION
This article was submitted to Microbe and Virus Interactions with Plants, a section of the journal Frontiers in Microbiology

RECEIVED 21 June 2022
ACCEPTED 03 October 2022
PUBLISHED 04 November 2022

CITATION
Elfiati D, Faulina SA, Rahayu LM, Aryanto A, Dewi RT, Rachmat HH, Turjaman M, Royyani MF, Susilowati A and Hidayat A (2022) Culturable endophytic fungal assemblages from *Styrax sumatrana* and *Stryax benzoin* and their potential as antifungal, antioxidant, and alpha-glucosidase inhibitory resources. *Front. Microbiol.* 13:974526. doi: 10.3389/fmicb.2022.974526

Culturable endophytic fungal assemblages from *Styrax sumatrana* and *Stryax benzoin* and their potential as antifungal, antioxidant, and alpha-glucosidase inhibitory resources

Deni Elfiati[1*†], Sarah Asih Faulina[2†], Laras Murni Rahayu[2†], Aryanto Aryanto[2†], Rizna Triana Dewi[3†], Henti Hendalastuti Rachmat[4†], Maman Turjaman[2†], Mohammad Fathi Royyani[4†], Arida Susilowati[1†] and Asep Hidayat[2*†]

[1]Faculty of Forestry, Universitas Sumatera Utara, Medan, Indonesia, [2]Research Center for Applied Microbiology, National Research and Innovation Agency, Bogor, Indonesia, [3]Research Center for Pharmaceutical Ingredients and Traditional Medicine, National Research and Innovation Agency, Serpong, Indonesia, [4]Research Center for Ecology and Ethnobiology, National Research and Innovation Agency, Bogor, Indonesia

Benzoin resin, produced by the native Indonesian trees *Styrax sumatrana* and *Styrax benzoin*, has been incorporated into medical practices to treat wounds, erythema, and many other conditions for centuries. Endophytic fungi that reside within medicinal plants have antimicrobial, antioxidant, and α-glucosidase inhibitory capacities, contributing to plant health and derivative products. In this study, we determined the antifungal, antioxidant, and α-glucosidase inhibitory capacities of endophytic fungal isolates from three different tissues (leaves, bark, and stems) of *S. sumatrana* and *S. benzoin* trees. The genera of fungal isolates were determined by phylogenetic analysis of internal transcribed spacer sequences. A total of 58 fungal isolates were classified into 15 different fungal genera from eight taxonomic orders—Hypocreales, Botryosphaeriales, Glomerellales, Diaphortales, Pleosporales, Eurotiales, Xylariales, and Mucorales—with a pattern of host species specificity. Among these isolates, *Trichoderma* sp. 6407 consistently exhibited high inhibition of the growth of plant pathogens *Fusarium* sp., *Trichoderma viride*, and *Aspergillus niger*. With respect to antioxidant activity, *Phyllosticta* sp. 6454 consistently showed 2,2-diphenyl-1-picrylhydrazyl inhibition (37.59 ± 0.05%), 2,2′-azino-bis (3-ethylbenzothiazoline-6-sulphonic acid)-based antioxidant activity (25.04 ± 0.27 mgTE/g), and α-glucosidase inhibitory activity (52.15 ± 10.08%). *Neopestalotiopsis* sp. 6431 was notably potent in 2,2-diphenyl-1-picrylhydrazyl inhibition (49.65 ± 0.80%), ferric reducing

antioxidant power-based antioxidant activity (197.49 ± 8.65 mgTE/g), and α-glucosidase inhibitory activity (52.88 ± 4.93%). This study revealed that *Trichoderma* sp. 6407, *Phyllosticta* sp. 6454, and *Neopestalotiopsis* sp. 6431 exhibited antifungal, antioxidant, and α-glucosidase inhibitory activities.

KEYWORDS

medicinal plant, benzoin resin, antifungal, antioxidant, *Trichoderma*, *Phyllosticta*, *Neopestalotiopsis*

Introduction

Humankind has long used fragrances for health, beauty, and ceremonial purposes. The burning of fragrant incense has been observed in numerous cultures and religious ceremonies (Nir, 2004; Smit, 2004; Baum, 2013; Ergin, 2014; le Maguer, 2015; Milburn, 2016; Gershon, 2019). Ancient Greek, early Christian, Jewish, and Islamic societies used or use various fragrances, including balsamic resin, in their ritual practices (Haran, 1960; Nir, 2004; Smit, 2004; Ergin, 2014; le Maguer, 2015; Gershon, 2019). Balsamic resin has been traditionally used in Chinese culture for ceremonial and medicinal purposes, and the tradition has spread to other Asian countries (Milburn, 2016). Such practices have made the substance a valuable trading commodity (Kashio and Johnson, 2001; Ergin, 2014; le Maguer, 2015).

Styrax trees produce a balsamic resin known as benzoin resin (Kashio and Johnson, 2001). *Styrax sumatrana* and *Styrax benzoin* are native Indonesian trees that are widely cultivated in North Sumatra, Indonesia, where their resin has been traditionally used for herbal remedies and cultural ceremonies. For such applications, benzoin resin is valuable as a nontimber forest product (Nurwahyuni et al., 2021). Benzoin resin and its derivatives are incorporated into incense, cosmetics, and pharmaceutical products for their anti-inflammatory, antioxidant, and antimicrobial properties (Sharif et al., 2016; Hidayat et al., 2018, 2019b). The radical scavenging activity of resin from *S. sumatrana* has been reported to have high potency as an antioxidant; hence, it is a good candidate as a natural antioxidant resource (Nurwahyuni et al., 2021). Despite supporting the livelihood of 70% of local people in North Sumatra, Indonesia (Iswanto et al., 2016), and their value as a natural antioxidant resource, *Styrax* plantations for benzoin resin have gradually decreased because of land conversion (Saputra and Lee, 2021). Such limitations in plantation areas necessitate innovations in the sustainable production of benzoin resins and their derivatives.

In most plants, endophytic fungi that colonize the inner tissue play significant ecological roles, such as strengthening plant defenses against pathogens and abiotic stressors (Arnold et al., 2003; Schardl et al., 2004; Mejía et al., 2008). Particularly, in medicinal plants, these fungi have been reported to have distinctive relationships with their hosts; they influence the plant's secondary metabolite production and antioxidant enzyme functioning and even incorporate their own metabolites into the host plant's tissues, which consequently enhances the plant's ability to withstand stress (Zhao et al., 2010; Ogbe et al., 2020). However, whether benzoin resin is synthesized and accumulated by endophytic fungi that reside within these plants remains an intriguing question.

Naturally sourced antioxidants have desirable properties that may reduce the use of chemically synthesized additives in food products (Brewer, 2011). The carcinogenic potential and other health risks of synthetic additives have limited their use and instigated the search for natural antioxidants (Capitani et al., 2013). A similar trend has been observed for cosmetics and pharmaceutical products. If the capacity of such functional substances from endophytic fungi is better than that of the host plant, endophytic fungi could be a more manageable and sustainable source option. Endophytic fungi isolated from medicinal plants, such as *Pinus roxburghii, Ginko biloba, Rauwolfia tetraphylla,* and agarwood-producing trees *Aquilaria* and *Gyrinops* have been reported to have antimicrobial and antioxidant capacities (Xiao et al., 2013; Bhardwaj et al., 2015; Alurappa and Chowdappa, 2018). However, information on endophytic fungi from *S. sumatrana* and *S. benzoin* remains scarce (Elfiati et al., 2021; Slamet et al., 2021). Considering the well-known role of endophytic fungi in enhancing plant defense against pathogens and the antioxidant function of benzoin resin (Hidayat et al., 2018), this study aimed to determine the antifungal, antioxidant, and alpha-glucosidase inhibitory activities of endophytic fungi isolated from the leaves, stems, and bark of *S. sumatrana* and *S. benzoin* trees.

Materials and methods

Sample collection and endophytic fungal isolation

Asymptomatic (healthy) 25- to 30-year-old *S. benzoin* and *S. sumatrana* trees with heights between 15 and 20 m and

breast-high diameters between 15 and 25 cm were selected for this study (Slamet et al., 2021). Fragments were collected from plantations in North Sumatra Province, Indonesia, at elevations of 800–1,000 m asl and temperatures between 15 and 24°C. Tree fragments or plant organs (leaves, stems, or bark) were surface sterilized, and their inner parts were cut and planted aseptically on four chloramphenicol-supplemented isolation media: potato dextrose agar, Pachlewski, yeast dextrose agar, and yeast malt extract (Atlas, 2004; Hidayat et al., 2019a, 2021a); thereafter, successful endophytic fungal isolation was validated (Hidayat et al., 2019a, 2021a). The obtained fungal isolates were deposited in the Indonesian Tropical Forest Culture Collection.

Molecular identification, phylogenetic, and clustering analyses

Genomic DNA was extracted from a 7-day-old mycelial culture grown in potato dextrose broth with a DNA Wizard Kit (Promega, Madison, WI, USA) using the manufacturer's method. Polymerase chain reaction (PCR) with Go Taq Green Master Mix (Promega) and ITS1 and ITS4 primers (White et al., 1990) was used to amplify the internal transcribed spacer (ITS) region of fungal DNA. PCR products were subjected to Sanger sequencing (1st BASE Sequencing Service, Singapore) and sequences were aligned using the Basic Local Alignment Search Tool from the National Center for Biotechnology Information database to identify closely related genera. The closest genera and number of isolates are referred to sequentially hereinafter as the isolate identities. A phylogenetic tree was constructed using Mega 11 (Tamura et al., 2021) and the neighbor-joining method (Saitou and Nei, 1987; Tamura et al., 2004). All sequences were deposited in the NCBI database with accession numbers ON796950 to ON97007 (**Supplementary Table 1**).

Single linkage with combined rescaled distance was calculated to observe the clustering of endophytic fungal genera based on the combination of host tree species and plant organs. Binary values were standardized before analysis. A dendrogram was constructed using hierarchical cluster analysis in IBM SPSS Statistics 25 (IBM Corp., Armonk, NY, USA) to determine relationships among endophytic fungi based on their origins. Squared Euclidean distance was used to express the cluster distance (Mufarhatun et al., 2021).

Antifungal assay

A dual culture assay was used to screen fungal isolates for their ability to suppress mycelial growth of the plant pathogenic fungi *Fusarium* sp. (INTROF CC 0509) and *Trichoderma viride*, and *Aspergillus niger*. *T. viride*, and *A. niger* cultures were obtained from IPB University Culture Collection. Five-millimeter-diameter agar discs of endophytic and pathogenic fungal cultures were co-inoculated 3 cm apart on potato dextrose agar plates (90 mm diameter) and incubated at 25°C for 7 days. The percentage of inhibition (*%I*) was calculated using the following formula:

$$\%I = [(\mathbf{Jc} - \mathbf{Jt})/\mathbf{Jc}] \times 100\% \quad (1)$$

where *Jc* is the pathogen's radial outward growth (control) and *Jt* is its radial growth in the direction of the endophytic fungi (Hajieghrari et al., 2010). Each treatment was repeated five times.

Antioxidant and antidiabetic assays

Prior to phytochemical assays for bioactive compounds, fungal extracts were prepared according to the method described by Hidayat et al. (2019a), with three replicates for each assay. Antioxidant activities were determined using three approaches: 2,2-diphenyl-1-picrylhydrazyl (DPPH), 2,2′-azino-bis (3-ethylbenzothiazoline-6-sulphonic acid) (ABTS), and ferric reducing antioxidant power (FRAP).

Determination of antioxidant activity *via* DPPH depletion followed the protocol described by Hidayat et al. (2021b). The effective concentration at which 50% of the radicals were scavenged (IC_{50} value) was obtained by interpolation from the linear regression analysis (Dewi et al., 2013). Concentrations of DPPH in ppm (based on IC_{50} estimation, *E*) were ranked as follows: $E < 50$, very strong; $50 \leq E < 100$, strong; $100 \leq E < 150$, moderate; $150 \leq E < 200$, weak; and ≥ 200, undetected.

Measurement of antioxidant activity using the ABTS approach was based on Trolox equivalent antioxidant capacity. The activity was expressed as Trolox equivalent in fungal extracts (mg TE/g), where the capacity of the sample to neutralize ABTS radicals is equivalent to that of Trolox (Wang et al., 2013). ABTS radical solution was prepared as follows: ABTS solution (7 mM) was mixed with potassium persulfate (140 mM) at a 62.5:1 ratio for the stock solution. The mixture was then kept in a dark room at 25°C for 16 h. For measurement, an ABTS radical solution with a 0.7 absorbance value at 734 nm was prepared. The assay was performed by mixing sample solution (5 μL, 1 mg/mL) with 200 μL of ABTS radical solution. The mixture was kept in a dark room for 6 min before absorbance reading at 734 nm. A Trolox solution with a range of concentrations was used to construct the standard curve.

Antioxidant capacity was determined using the FRAP approach according to the methods described by Dudonné et al. (2009) with slight modifications. FRAP reagent was prepared with 300 mM acetate buffer (pH 3.6), 10 mM 2,4,6-tri(2-pyridyl)-s-triazine, and 20 mM $FeCl_3$ in a 10:1:1 ratio. Fungal

extracts (40 μL) were then mixed with 1,200 μL FRAP reagent and incubated at 37°C for 30 min. FRAP values were based on the standard Trolox calibration curve and expressed in mg TE/g.

Measurement of total flavonoid content was performed according to the protocol described by Tambe and Bhambar (2014) with some modifications. A volume of 0.1 mL of the sample (1,000 μg/mL) was added to 2.6 mL distilled water and 0.15 mL 5% $NaNO_2$, mixed, and incubated for 5 min. The mixture was combined with 0.15 mL 10% $AlCl_3$ 10%, stirred, and incubated for 6 min before being combined with 2 mL NaOH 1 N, mixed, and incubated at 25°C for 30 min. Absorbance was measured at 510 nm. Quercetin at concentrations of 50, 100, 250, 500, and 1,000 μg/mL was used to construct the standard curve. Flavonoid content was expressed as quercetin equivalents (mg QE/g).

Total phenolic content was measured as previously described (Tambe and Bhambar, 2014) with some modifications. A volume of 0.1 mL of the sample (1,000 μg/mL) was combined with 1.4 mL distilled water and 0.25 mL Folin–Ciocalteau reagent. The mixture was incubated for 8 min, combined with 0.75 mL 20% Na_2CO_3, stirred, and incubated for 2 h at 27°C. Absorbance was measured at 750 nm wavelength. Three replicates of gallic acid at concentrations of 20, 40, 60, 80, and 100 μg/mL were used to construct the standard curve. Phenolic content was expressed as gallic acid equivalents (mg GAE/g).

Fungal extracts were evaluated for α-glucosidase inhibitory activity as described in our previous report (Dewi et al., 2013). Inhibition of α-glucosidase activity was determined by the reaction of α-glucosidase with the p-nitrophenyl-α-D-glucopyranoside substrate, resulting in the formation of p-nitrophenol (405 nm). Each assay was performed in triplicate, and the results are expressed as percentages of inhibition [% inhibition = (AB–AS)/AB × 100%], where AB is the absorbance of the blank solution and AS is the absorbance of the sample. Values are presented as the mean ± standard deviation.

Liquid chromatography–high resolution mass spectrometer analysis

Secondary metabolites from the fungal extracts were determined using a Xevo G2-XS Quadrupole Time of Flight Mass Spectrometer (Waters Corp., Milford, MA, USA) equipped with an electrospray ionization source coupled to a Waters Acquity Ultra Performance LC system. Approximately, 1.5 mg of fungal extract was added to MeOH (LiChrosolv, hypergrade for LC–MS, Merck KGaA, Darmstadt, Germany) and sonicated for 10 min until completely dissolved. Samples were then filtered through a 0.22-μm polytetrafluoroethylene syringe filter (Waters Corp.) to obtain a final concentration of 1 mg/mL. LC–HRMS analysis was performed as described previously (Dewi et al., 2022). Bioactive compounds were identified and analyzed using the LC-HRMS and UNIFI software version 1.5. Peaks were tentatively assigned with the comparison to water built-in library.

Statistical analysis

All results are presented as the mean of triplicate measurements and the standard deviation.

Results

Fungi isolated from *Styrax sumatrana* and *Styrax benzoin*, their molecular phylogeny, and origin-based clustering

Fifty-eight fungal isolates were obtained from the bark, stems, and leaves of *S. sumatrana* and *S. benzoin* trees. Thirty-eight isolates were obtained from 14 bark, eight stem, and nine leaf samples of *S. sumatrana* grown in four types of isolating media. Twenty isolates from four bark, nine stem, and seven leaf samples of *S. benzoin* were obtained using the same set of agar media.

The genera of all 58 isolates were determined based on ITS sequences. The closest matching genera based on sequence similarity are shown in **Figure 1**. Almost all isolates belonged to the phylum Ascomycota, except *Lichtheimia* sp. 6410, which belonged to the phylum Mucoromycota. The 58 fungi identified in this study were classified into 15 genera belonging to 12 families that belong to eight orders: Hypocreales, Botryosphaeriales, Glomerellales, Diaphortales, Pleosporales, Eurotiales, Xylariales, and Mucorales (**Figure 1**). *Fusarium, Pestalotiopsis,* and *Neopestalotiopsis* were the most common genera, with 20, 9, and 8 isolates, respectively.

Six possible combinations of two variables (host species and host organ) from which endophytic fungal genera originated are presented in **Figure 2**. A shorter Euclidean distance indicates a closer relationship; that is, the two variables share more similarities. Conversely, a longer Euclidean distance indicates greater heterogeneity and fewer similarities. Clustering analysis of endophytic fungal species based on the combination of plant organs and host plant species revealed two large groups. Host plant species seemed to be more important than plant organs in determining the grouping. Fungal communities residing in the leaves, bark, and stem of *S. sumatrana* tended to have more similarities and were thus grouped into one distinct cluster. The other cluster consisted of fungal communities residing in the leaves, bark, and stem of *S. benzoin*. A slightly different pattern was observed in each host plant species: in *S. benzoin*, fungal diversities in bark and stem organs showed more similarities to those residing in leaves, whereas in *S. sumatrana*, fungal diversities in bark

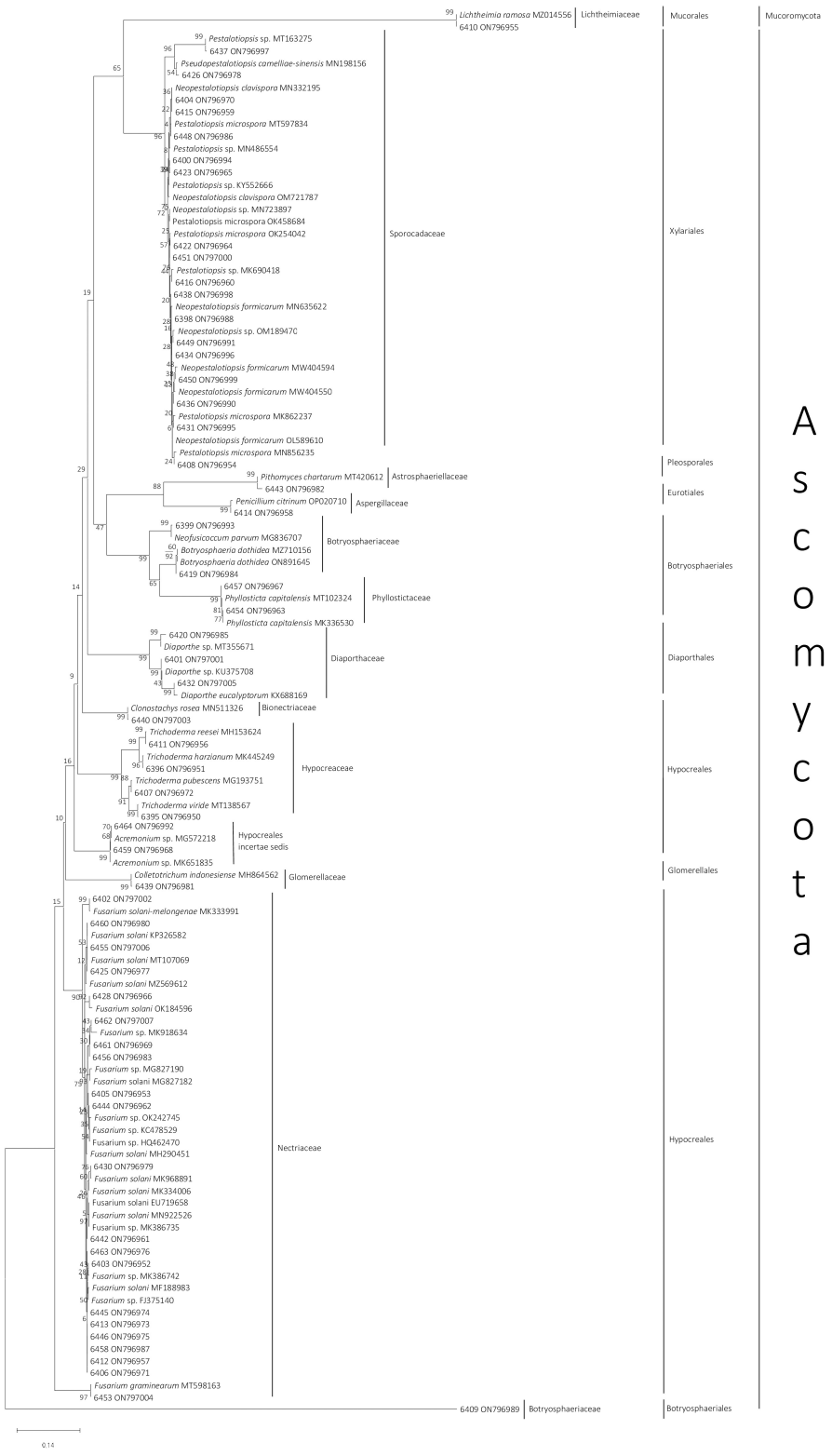

FIGURE 1

Neighbor-joining phylogenetic tree of 58 endophytic fungi isolated from *Styrax sumatrana* and *Styrax benzoin* and their respective reference based on fungal internal transcribed spacer sequence. Fungi from this study are presented as their isolate number followed by their National Center for Biotechnology Information accession number, whereas for reference sequences, species name, and accession number are given (**Supplementary Table 1**).

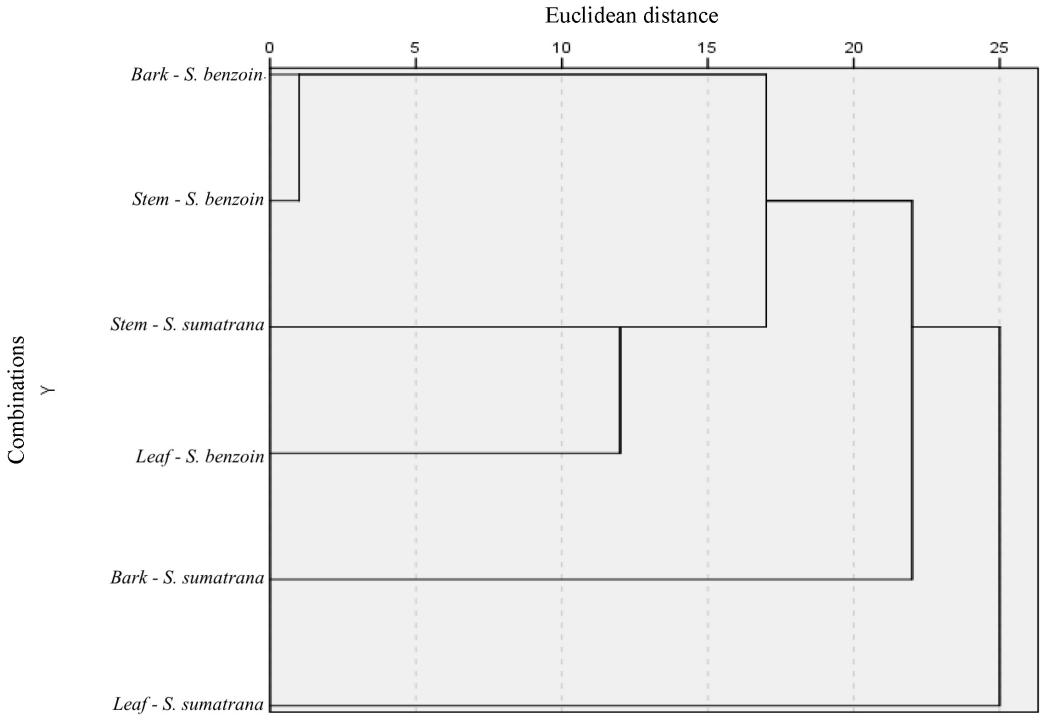

FIGURE 2
Single-linkage dendrogram with combined rescaled distance clusters. Endophytic fungi species were clustered based on their origins, plant organ (bark, stem, and leaf), and host plant species (*Styrax sumatrana* and *Styrax benzoin*).

and leaves showed more similarities to each other than to those in the stem.

Antagonistic activity of endophytic fungal isolates against plant pathogenic fungi

All 58 endophytic fungal isolates exhibited *in vitro* growth inhibition of three plant-pathogenic fungi. The percentage inhibition ranged from 10.27 to 78.59%, 18.33 to 82.67%, and 6.31 to 73.57% for *Fusarium* sp., *T. viride,* and *A. niger*, respectively (**Supplementary Table 2**). Three most inhibiting isolates against *Fusarium* sp. were *Trichoderma* sp. 6395, *Trichoderma* sp. 6411, and *Trichoderma* sp. 6407, with averages of 78.59 ± 1.03%, 74.41 ± 3.61%, and 73.57 ± 7.56% inhibition, respectively. *Trichoderma* sp. 6407, *Fusarium* sp. 6413, and *Fusarium* sp. 6445 were the most inhibiting against *T. viride*, with 82.67 ± 4.94%, 76.00 ± 2.79%, and 69.00 ± 5.35% inhibition, respectively. *A. niger*, *Trichoderma* sp. 6407, *Neofusicoccum* sp. 6399, and *Trichoderma* sp. 6396 were the most inhibiting (73.57 ± 7.56%, 62.66 ± 3.25%, and 59.77 ± 10.50%, respectively) (**Table 1**).

Corroborating Wheeler and Hocking (1993), *Trichoderma* sp. 6407, which inhibited all three pathogenic fungi, displayed interaction type B against *T. viride,* where both fungi inhibited each other's growth and created less than 2 mm space between their colonies (**Figure 3A**, left). Both *Fusarium* spp. 6413 and 6445 exhibited interaction type C against *T. viride,* where the growth of each endophytic fungus was lower than that of the pathogen, followed by slower fungal growth when a barrier between colonies was apparent (**Figure 3A**, center and right). *Neofusicoccum* sp. 6399 and *A. niger* pathogen appeared to have type D interaction, where both cultures inhibited each other and created a space of 2 mm or more between colonies (**Figure 3B**, center). Interaction type E was observed in *Trichoderma* sp. 6395 and pathogenic *Fusarium* sp. dual cultures, where the pathogen's growth was smaller and covered by endophytic fungi; however, the growth of both fungi decreased, and a barrier between colonies was apparent (**Figure 3C**, left). Interaction type F was observed in the remaining dual cultures, where pathogen growth was smaller than that in the endophytic fungal cultures, which later covered the pathogen's colony (**Figure 3C**, center and right, and **Figure 3B**, left and right).

Antioxidant activity of endophytic fungal extracts

Antioxidant activities of the endophytic fungal extracts were measured using DPPH, ABTS, and FRAP assays

TABLE 1 The high antagonistic activity of endophytic fungal isolates against plant pathogenic fungi, *Fusarium sp, Trichoderma viride, and Aspergillus niger* using dual culture assay*.

Host plant	Plant organ	Isolate number	Closest genus	Pathogenic fungal growth inhibition(%)**		
				Fusarium sp.	*Trichoderma viride*	*Aspergillus niger*
Styrax sumatrana	Bark	6395	*Trichoderma*	**78.59 ± 1.03**	38.67 ± 3.80	48.00 ± 13.83
		6396	*Trichoderma*	35.27 ± 19.14	58.67 ± 4.47	**59.77 ± 10.50**
		6411	*Trichoderma*	**74.41 ± 3.61**	63.33 ± 1.18	53.63 ± 14.39
	Stem	6407	*Trichoderma*	**73.57 ± 7.56**	**82.67 ± 4.94**	**73.57 ± 7.56**
		6413	*Fusarium*	65.00 ± 1.60	**76.00 ± 2.79**	55.10 ± 4.98
		6445	*Fusarium*	63.43 ± 2.10	**69.00 ± 5.35**	44.49 ± 14.38
Styrax benzoin	Stem	6399	*Neofusicoccum*	56.99 ± 18.96	59.00 ± 4.01	**62.66 ± 3.25**

*A complete list of 58 endophytic fungal isolates against plant pathogenic fungi is presented in Supplementary Table 2; **values are presented as mean ± standard deviation, which were performed in triplicate. The three isolates that showed the highest values of pathogenic fungal growth inhibition are presented in bold font.

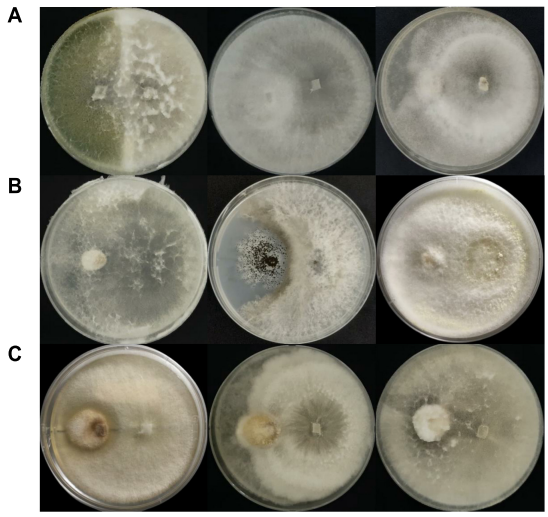

FIGURE 3
Inhibition of pathogenic fungi (placed on the left side of the plate); inhibition of **(A)** *Trichoderma viride*, **(B)** *Aspergillus niger*, and **(C)** *Fusarium* sp. by endophytic fungi (placed on the right side of the plate) in dual culture plates. The three highest inhibition percentages for each pathogen were obtained from isolates (left to right): **(A)** 6407, 6413, and 6445; **(B)** 6407, 6399, and 6396; **(C)** 6395, 6411, and 6407.

(Supplementary Table 2). Seven isolates with the highest values were exclusive for each method. The remaining three isolates were able to perform among the highest levels for the two methods. *Neopestalotiopsis* sp. 6431 extract performed the best in DPPH inhibition, with an average of 49.65 ± 0.80% or IC_{50} estimated concentration of 100.71 ppm, followed by *Trichoderma* sp. 6395, *Phyllosticta* sp. 6454, and *Fusarium* sp. 6430 extracts, tied at 37.59% or IC_{50} estimated concentration of 133.02 ppm. As previously mentioned, *Trichoderma* sp. 6395 was the most inhibiting in the dual culture assay against pathogenic *Fusarium* sp.

Estimated IC_{50} concentrations were all categorized as medium. For ABTS-based antioxidant activity, isolate 6412 extract led to an average of 28.41 ± 0.04 mg TE/g, closely followed by *Fusarium* sp. 6430 and *Phyllosticta* sp. 6454 extracts, with averages of 27.74 ± 0.34 and 25.04 ± 0.27 mg TE/g, respectively. The last two isolates were among the highest achievers of DPPH inhibition. *Neopestalotiopsis* sp. 6431, *Neopestalotiopsis* sp. 6450, and *Neofusicoccum* sp. 6399 were the three isolates with the highest antioxidant activities for the FRAP method: 197.49 ± 8.65, 167.39 ± 8.57, and 152.05 ± 32.40 mg TE/g, respectively. Moreover, the *Neopestalotiopsis* sp. 6431 extract exhibited the highest activity for both the DPPH and FRAP methods (Table 2).

An entirely different set of isolates, *Colletotrichum* sp. 6439, *Fusarium* sp. 6456, and *Fusarium* sp. 6444, produced extracts that contained the three highest concentrations of flavonoid compounds (155,79 ± 7.47, 108.86 ± 94.86, and 88.86 ± 14.49 mg QE/g, respectively) (Table 3). As for the total phenolic compounds, the three highest producers were fungal extracts from *Phyllosticta* sp. 6454, *Neopestalotiopsis* sp. 6431, and *Fusarium* sp. 6430 (110.87 ± 18.52, 43.02 ± 1.25, and 41.33 ± 1.50 mg GAE/g, respectively). These isolates were also the most inhibiting in the DPPH-based antioxidant capacity assay (Table 2).

α-glucosidase inhibitory activity

α-glucosidase inhibitory activity of the 58 endophytic fungal isolates ranged from 0.00 to 65.00% (Supplementary Table 2). Fungal extracts of *Pestalotiopsis* sp. 6416, *Neopestalotiopsis* sp. 6431, and *Phyllosticta* sp. 6454 were the most inhibiting at 65.00 ± 0.28%, 52.88 ± 4.93%, and 52.15 ± 10.08%, respectively (Table 4). *Phyllosticta* sp. 6454 repeatedly resurfaced among the top three isolates for DPPH inhibition, ABTS-based antioxidant capacity, phenolic content, and α-glucosidase inhibitory activity. Similarly, *Neopestalotiopsis* sp. 6431 was the top performer in four assays: DPPH inhibition, FRAP-based antioxidant

TABLE 2 Fungal isolates with high antioxidant activity determined by 2,2-diphenyl-1-picrylhydrazyl (DPPH), 2,2′ -azino-bis (3-ethylbenzothiazoline-6-sulphonic acid) (ABTS), and ferric reducing antioxidant power (FRAP) assay*.

Host plant	Plant organ	Isolate number	Closest genus	Antioxidant activity**			
				DPPH			
				Inhibition (%)***	IC_{50} (ppm)	ABTS (mg TE/g)	FRAP (mgTE/g)
Styrax sumatrana	Bark	6395	*Trichoderma*	**37.59 ± 0.24**	**133,02**	2.72 ± 0.06	15.27 ± 0.16
		6412	*Fusarium*	26.24 ± 11.89	190,54	**28.41 ± 0.04**	93.99 ± 3.86
		6454	*Phyllosticta*	**37.59 ± 0.05**	**133,02**	**25.04 ± 0.27**	36.37 ± 2.22
	Stem	6430	*Fusarium*	**37.59 ± 0.56**	**133,02**	**27.74 ± 0.34**	40.20 ± 7.69
Styrax benzoin	Stem	6399	*Neofusicoccum*	ND	ND	22.21 ± 0.89	**152.05 ± 32.40**
		6431	*Neopestalotiopsis*	**49.65 ± 0.80**	**100,71**	3.35 ± 0.14	**197.49 ± 8.65**
		6450	*Neopestalotiopsis*	7.27 ± 6.98	687,41	18.71 ± 1.36	**167.39 ± 8.57**

*A complete list of 58 endophytic fungal isolates against plant pathogenic fungi is presented in Supplementary Table 2; **values are presented as mean ± standard deviation, which were performed in triplicate. Three isolates that achieved the highest values of antioxidant activity are presented in bold font are presented in bold font; ***the final concentration of each fungal extracted was applied at 100 μg/mL; ND: not detected; TE: Trolox equivalent.

TABLE 3 Fungal isolates with high content of flavonoid by using aluminum chloride assay, and phenol by using Folin–Ciocalteau reagent assay*.

Host plant	Plant organ	Isolate number	Closest genus	Phytochemical assay **	
				Flavonoid (mg QE/g)	Phenol (mg GAE/g)
Styrax sumatrana	Bark	6444	*Fusarium*	**88.86 ± 14.49**	27.10 ± 1.33
		6454	*Phyllosticta*	47.88 ± 8.52	**110.87 ± 18.52**
	Stem	6430	*Fusarium*	30.72 ± 7.00	**41.33 ± 1.50**
	Leaf	6439	*Colletotrichum*	**155.79 ± 7.47**	3.88 ± 0.20
		6456	*Fusarium*	**108.86 ± 94.86**	6.21 ± 0.32
Styrax benzoin	Stem	6431	*Neopestalotiopsis*	33.52 ± 0.28	**43.02 ± 1.25**

*A complete list of 58 endophytic fungal isolates against plant pathogenic fungi is presented in Supplementary Table 2; **values are presented as mean ± standard deviation, which were performed in triplicate; QE: quercetin equivalent; GAE: gallic acid equivalent. The three isolates that achieved the highest values in the phytochemical assay are presented in bold font.

TABLE 4 Fungal isolates with high α-glucosidase inhibition determined by p-nitrophenyl-α-D-glucopyranoside as substrate*.

Host plant	Plant organ	Isolate number	Closest genus	α-glucosidase inhibition (%)**
Styrax sumatrana	Bark	6416	*Pestalotiopsis*	65.00 ± 0.28
		6454	*Phyllosticta*	52.15 ± 10.08
Styrax benzoin	Stem	6431	*Neopestalotiopsis*	52.88 ± 4.93

*A complete list of 58 endophytic fungal isolates active against plant pathogenic fungi are presented in Supplementary Table 2; ** values are presented as mean ± standard deviation and were performed in triplicate for each fungal extract at a final concentration of 100 μg/mL.

capacity, phenolic content, and α-glucosidase inhibitory activity (Tables 2–4).

Detection of bioactive compounds

Based on the LC-HRMS results from base line (Figure 4A) and fungal crude extracts (Figures 4B–D), the crude extract of *Trichoderma* sp. 6407, which showed prominent antifungal activities, had eight peaks in total, with four main peaks indicating the active compounds (Figure 4B). The first four major peaks occurred at a retention time (t_R) of 7.87 min, with a molecular ion (*m/z*) value of 279.2321 $[M+H]^+$, and molecular formula $C_{18}H_{30}O_2$. Bioactive compounds with such properties were predicted to be methyl hydroxysterpurate ethylidene acetal or xylarinorditerpene Q (Figures 4B, 5A1). The second four major peaks occurred at t_R = 8.67 min, with a *m/z* value of 319.2251 $[M+H]^+$, and molecular formula $C_{18}H_{32}O_3$, which could be (1S,2S)-3-oxo-2-pentylcyclopentane-1-octanoic acid or 3,7-dimethyl-9-(-2,2,5,5-tetramethyl-1,3-dioxolan-4-yl)nona-1,6-dien-3-ol (Figures 4B, 5A2). The third four major peaks occurred at t_R = 9.98 min, with an *m/z* value of 395.3310 $[M+H]^+$, and molecular formula $C_{28}H_{42}O$, which were predicted to be ergosta-4,6,8,22E-tetraen-11β-OL (Figures 4B, 5A3). The last detected major peak

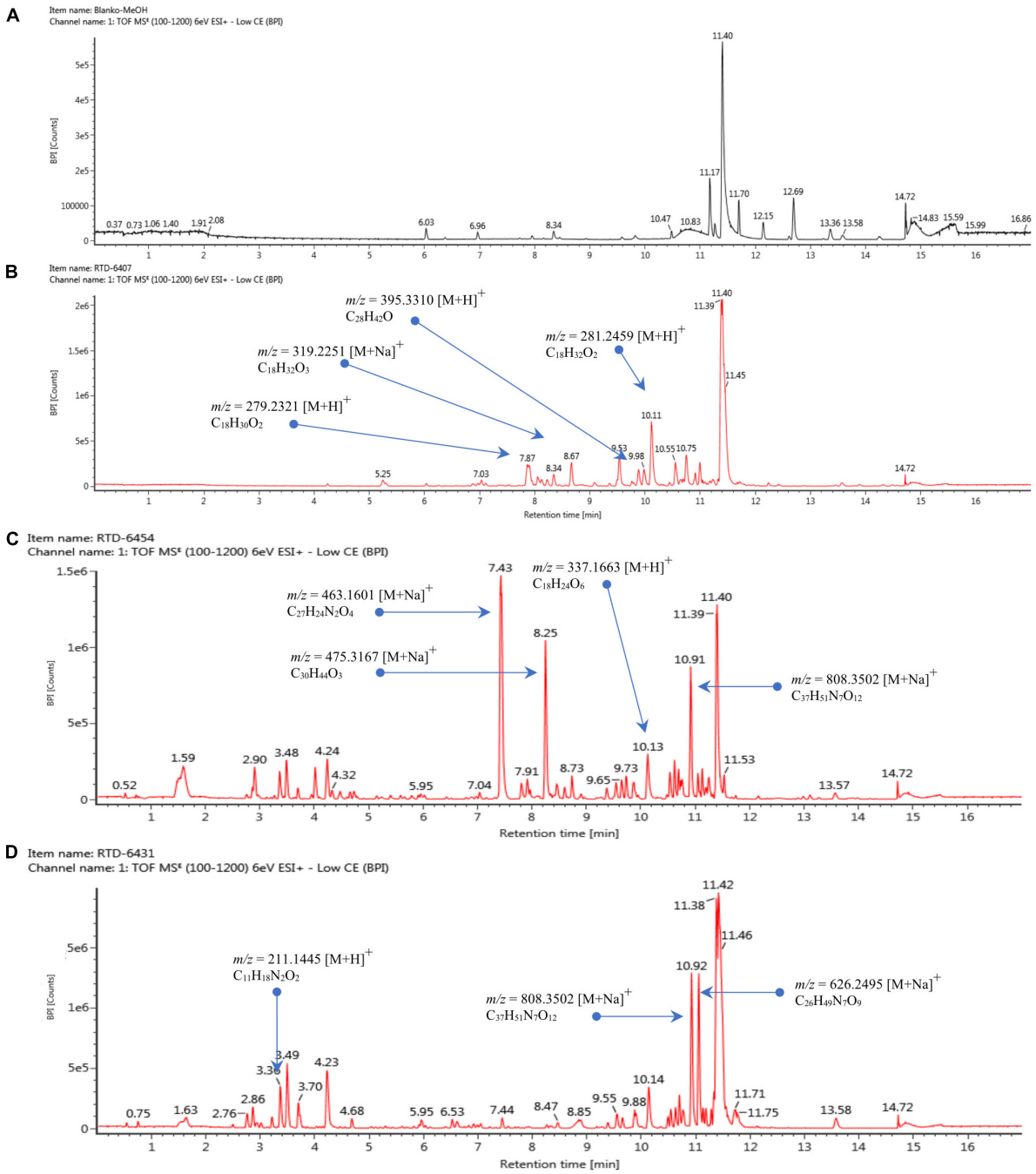

FIGURE 4
Liquid chromatography–mass spectrometry chromatogram of baseline **(A)**, extracted isolates *Trichoderma* sp. 6407 **(B)**, *Phyllosticta* sp. 6454 **(C)**, and *Neopestalotiopsis* sp. 6431 **(D)**.

occurred at t_R = 10.91 min, with a predicted *m/z* value of 281.2459 $[M+H]^+$, and molecular formula $C_{18}H_{32}O_2$, which were approximated to be 4-Me-6E,8E-16:2 methyl ester or 4-methyl-7,11-heptadecadienoic acid (Figures 4B, 5A4).

Several ionic predictions and molecular formulas for *Phyllosticta* sp. 6454 extracts, which showed antioxidant and α-glucosidase activity, were identified (Figures 4C, 5B). The LC–HRMS results showed at least 10 peaks for active compounds. The four largest peaks had a t_R of 7.43, 8.25, 10.13, and 10.19 min (Figure 4C), with the following respective *m/z* values and molecular formulas: *m/z* = 463.1601 $[M+Na]^+$ and molecular formula $C_{27}H_{24}N_2O_4$ (predicted to be

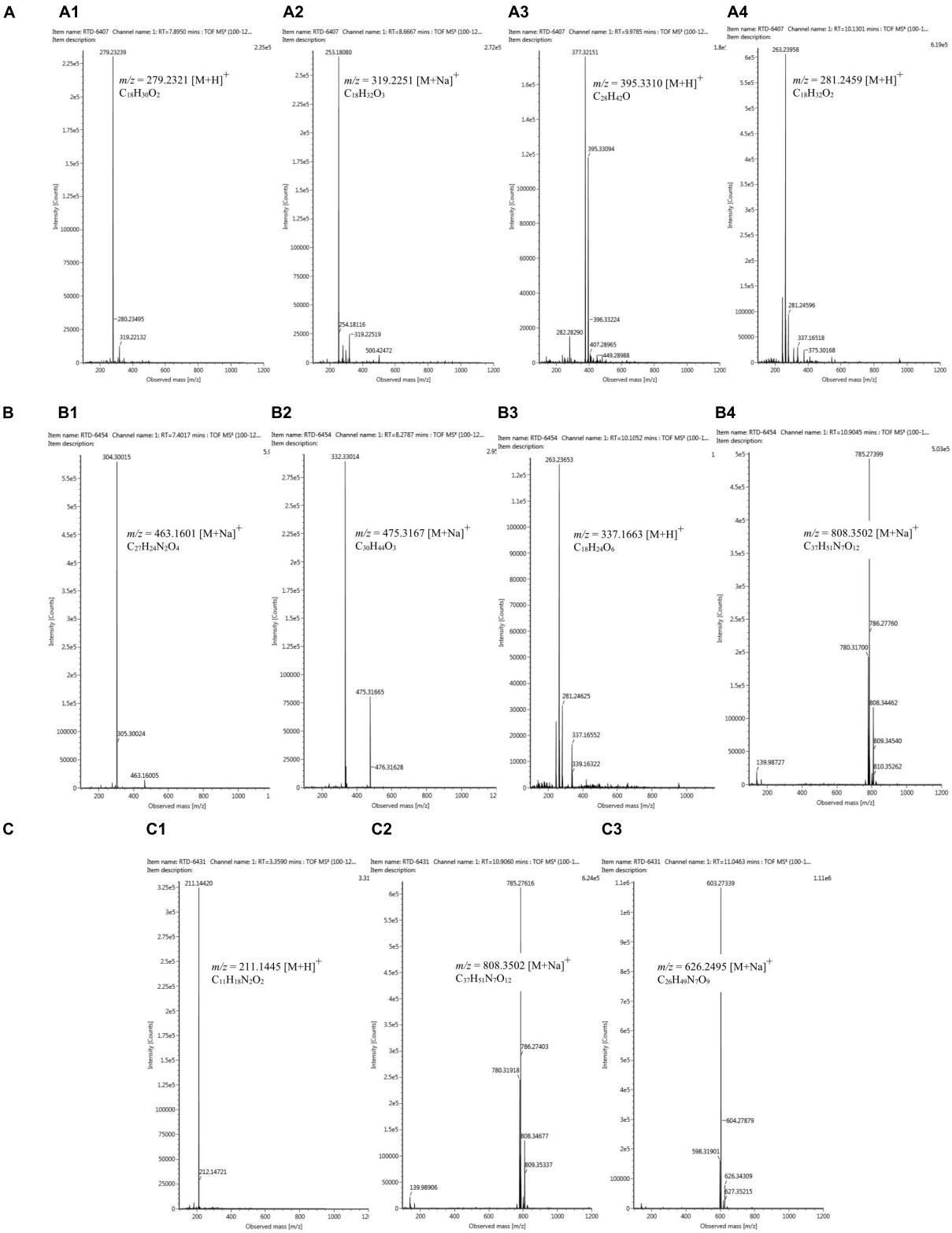

FIGURE 5
Mass chromatogram of metabolite compounds from extracted isolates *Trichoderma* sp. 6407 **(A1–4)**, *Phyllosticta* sp. 6454 **(B1–4)**, and *Neopestalotiopsis* sp. **(C1–3)**.

SF2809-IV (4-hydroxy-3-[[3-(2-hydroxyethyl)-1H-indol-2-yl]-(4-hydroxyphenyl)methyl]-1-methylquinolin-2-one) compound); *m/z* = 475.3167 $[M+Na]^+$ and molecular formula $C_{30}H_{44}O_3$ (predicted to be igniarine); *m/z* = 337.1663 $[M+H]^+$ and molecular formula $C_{18}H_{24}O_6$ (predicted to be corynechromone or cytosprone); and *m/z* = 808.3502 $[M+Na]^+$ and molecular formula $C_{37}H_{51}N_7O_{12}$ (**Figures 5B1–4**).

For the active compounds in *Neopestalotiopsis* sp. 6431 extracts, which may be responsible for the exhibited antioxidant activities, at least nine peaks were predicted (**Figure 4D**). The three largest peaks were detected at a t_R of 3.36, 10.92, and 11.05 min (**Figure 4D**), with the following respective *m/z* values and molecular formulas: *m/z* = 211.1445 $[M+H]^+$ and molecular formula $C_{11}H_{18}N_2O_2$; *m/z* = 808.3502 $[M+Na]^+$ and molecular formula $C_{37}H_{51}N_7O_{12}$; and *m/z* = 626.3495 $[M+Na]^+$ and molecular formula $C_{26}H_{49}N_7O_9$ (**Figures 5C1–3**).

Discussion

All the closest matches of the isolates belong to the phylum Ascomycota, except for *Lichtheimia*, which belongs to Mucoromycota. The dominance of Ascomycota in endophytic fungal assemblages has also been observed elsewhere (Hamzah et al., 2018; Zhou et al., 2018; Nguyen et al., 2021). This study complements previous reports on endophytic fungi isolated from *S. sumatrana* and *S. benzoin* and adds the newly reported genera *Lichtheimia, Penicillium, Pseudopestalotiopsis,* and *Colletotrichum* from *S. sumatrana* and *Botryosphaeria* from *S. benzoin* (Hidayat et al., 2021a; Slamet et al., 2021). All of the closest-matched genera have been previously reported as endophytes (Shetty et al., 2016; Huang et al., 2020). Various factors are involved in the dynamics of endophytic fungal communities, including macroenvironmental factors such as season, geographic location (Mishra et al., 2012; Slamet et al., 2021), and water availability (Costa et al., 2018). Each microenvironmental biotic factor, including host species, host tissue/organ (Moricca et al., 2012; Slamet et al., 2021), and other coexisting endophytes or pathogens (Sicard et al., 2007), adds to the community dynamics. These complex mechanisms may act as selection pressures for endophytic fungi, leading to host species and/or host organ specificities (Slamet et al., 2021).

Clustering the endophytic fungal genera based on the plant host species and plant organs demonstrated a specific pattern only for the plant host species. Endophytic fungal communities in the bark and stems of *S. benzoin* clustered within the shortest Euclidean distance, indicating higher genus similarity and homogeneity between them. The fungal community in the leaves of the same host species was clustered at a longer distance but was still within the same cluster. Although these organs have different structures (Romero, 2014), the closer proximity of the bark and stem may accommodate fungal mycelia extending between these two organs and consequently having more shared species. In the other cluster, the fungal community residing in the bark and leaf organs of *S. sumatrana* shared more similarities than those residing in the stems of the same host plant species. This pattern of similarities indicates the tendency of fungal genus specificity to be based on host plant species. These observations are based on the genus taxonomic rank, which is limited to a less restrictive interpretation. Multi-locus taxonomy identification and/or an inclusive metagenomic approach is recommended for further studies to scrutinize these mechanisms.

Trichoderma sp. 6407, isolated from the stems of *S. sumatrana*, consistently showed the highest antifungal activity against all tested pathogenic fungi. Plant-protective members of the *Trichoderma* genus, including *T. pubescens*, produce a group of polypeptide antibiotics that may contribute to their antagonistic potential against fungal diseases in grapevine trunks (Degenkolb et al., 2006). Other species of *Trichoderma* have been shown to reduce disease severity by inhibiting the growth of the pathogenic fungus *Rhizoctonia solani* (Molan et al., 2008). The predicted methyl hydroxysterpurate ethylidene acetal or xylarinorditerpene Q compounds from *Trichoderma* sp. 6407 extracts were previously reported to be isolated from endophytic fungi and also have antifungal properties (Xie and Li, 1992; Wu et al., 2014; Chen et al., 2020). The predicted (1S,2S)-3-oxo-2-pentylcyclopentane-1-octanoic acid or 3,7-dimethyl-9-(-2,2,5,5-tetramethyl-1,3-dioxolan-4-yl)nona-1,6-dien-3-ol compounds have also been reported to be produced by endophytic fungi (Miersch et al., 1999; Lin et al., 2016). The prediction ergosta-4,6,8,22E-tetraen-11β-OL compound has previously been reported to be isolated from the fruiting body of *Coprinus setulosus* (Ma et al., 2018), whereas, the postulated 4-Me-6E,8E-16:2 methyl ester or 4-methyl-7,11-heptadecadienoic acid compounds were reported to be isolated from liquid cultures of *Clonostachys rosea* and *Sporothrix* sp. and have the potential to inhibit the growth of MFC-7 cancer cells, *F. oxysporum* f. sp. *lycospersici, T. viride*, and *Bacillus subtilis* (Choudhury et al., 1994; Dias et al., 2015). In this study, the metabolites produced by *Trichoderma* sp. 6407 displayed four major peaks; however, other minor peaks still have the potential to represent other active compounds. Considering the vital role of endophytic fungi in strengthening plant defense against pathogens and promoting overall health (Mejía et al., 2008), purification and elucidation of the active compounds produced by *Trichoderma* sp. 6407 and further investigation of antifungal mechanisms are required to optimize their biocontrol potential.

Phyllosticta sp. 6454, which was isolated from the bark of *S. sumatrana*, is characterized by its high antioxidant and α-glucosidase activity. This genus is a widely distributed fungal endophyte and is found in 70 plant families

(Wikee et al., 2013). Despite its widespread distribution, information regarding its antioxidant capacity is limited. Endophytic *Phyllosticta* sp. isolated from the medicinal plant *Guazuma tomentosa* has been reported to have antioxidant properties, with phenol and flavonoid contents that are one-sixth and one-fourteenth, respectively, of those observed in *Phyllosticta* sp. 6454 (Srinivasan et al., 2010). The presumed SF2809-IV (4-hydroxy-3-[[3-(2-hydroxyethyl)-1H-indol-2-yl]-(4-hydroxyphenyl)methyl]-1-methylquinolin-2-one) compound from *Phyllosticta* sp. 6454 extracts were previously isolated from *Dactylosporangium* sp., and some of its derivatives have been shown to inhibit recombinant human chymase activity (Tani et al., 2004). Secondary metabolites from *Phyllosticta* with antimicrobial activities have been previously reported (Taher et al., 2022) and may be related to the phenol and flavonoid contents of *Phyllosticta* sp. 6454 extracts.

Neopestalotiopsis sp. 6431, isolated from the stems of *S. benzoin*, also exhibited high antioxidant activity. *Neopestalotiopsis* is a common endophytic fungal genus (Hamzah et al., 2018; Azuddin et al., 2021) and was among the most commonly isolated genera in this study. This genus was also previously discovered in the bark of *S. benzoin* (Ilyas et al., 2019). A member of the genus *Neopestalotiopsis* has been reported to produce antimicrobial and antioxidant agents, such as eugenol, myristaldehyde, lauric acid, and caprylic acid (Tanapichatsakul et al., 2019). However, based on the LC–HRMS results of the present study, *Neopestalotiopsis* sp. 6431 may have produced different secondary metabolites.

Fusarium sp. 6430 isolated from the stems of *S. sumatrana* was the most frequently isolated genus in this study and displayed high antioxidant activity. This genus has been reported to exude diverse bioactive compounds and exert biocontrol functions to enhance plant health. Secondary metabolites, aza-anthraquinones, isolated from an endophytic *F. solani* strain, the crude extract of which shows antimicrobial and antioxidant activities, have been reported to be potent bioactive compounds for anticancer and antimicrobial agents (Khan et al., 2018). *Fusarium* sp. evinced the production of a new antifungal and antimalarial cyclodepsipeptide, known as fusaripeptide (Ibrahim et al., 2018). The observed antioxidant activity and phenol content of *Phyllosticta* sp. 6454, *Neopestalotiopsis* sp. 6431, and *Fusarium* sp. 6430 suggests that these isolates are strong candidates for natural antioxidant sources. Future studies, including methods of purifying bioactive compounds, are required to further optimize their potential as bioresources.

Antioxidants are compounds that inhibit the initiation or propagation of chain oxidation reactions. The chemical structure of antioxidants, source of free radicals, and physicochemical properties of different sample preparations can provide different test results for antioxidant activity (Karamać et al., 2005). Therefore, it is necessary to analyze the antioxidant activity of a specific sample type. In this study, antioxidant testing using DPPH, ABTS, and FRAP assays was conducted. The DPPH assay measures the ability of compounds to donate hydrogen to a stable DPPH• molecule, resulting in the formation of a purple color (520 nm). In contrast, the ABTS cation radical ($ABTS^{\bullet+}$), which absorbs light at 743 nm, changes to stable ABTS by accepting hydrogen from antioxidant compounds, resulting in solution decolorization (Chu et al., 2000). This method is based on a reduction reaction in an acidic atmosphere to a yellow Fe^{3+} (potassium hexacyanoferrate) complex compound to a bluish-green Fe^{2+} complex compound owing to electrons donated by antioxidant compounds (Craft et al., 2012).

Furthermore, we investigated the α-glucosidase inhibitory activity of the fungal extracts in this study. Phenolic compounds are antioxidants and can also inhibit natural α-glucosidase enzymes because they inhibit carbide enzymes owing to their ability to bind proteins (Zhang et al., 2015). This assay is based on the formation of p-nitrophenol, which results from the cleavage of p-nitrophenyl-α-D-glucopyranose at 410 nm.

These findings lay the groundwork for further studies that will identify the compounds responsible for the observed antioxidant and α-glucosidase inhibitory activities and their underlying mechanisms, which will potentially guide the optimization of their production.

Data availability statement

The datasets presented in this study can be found in online repositories. The names of the repository/repositories and accession number(s) can be found in the article/**Supplementary material**.

Author contributions

DE, SF, LR, AA, RD, HR, MT, MR, AS, and AH contributed to the conceptualization, methodology, experiment, validation, analysis, resources, writing, review, and editing of the manuscript. All authors have read and agreed to the published version of the manuscript.

Funding

This research was funded by the Directorate of Research and Community Service of the Ministry of Research and Technology/National Research and Innovation Agency, Indonesia, Number: 61/UN5.2.3.1/PPM/KP-DRPM/2021 dated March 17, 2021.

Acknowledgments

We acknowledge the Indonesian Ministry of Environment and Forestry for facilitating and supporting this research. We are grateful to the reviewers for their helpful comments on an earlier draft of the manuscript.

Conflict of interest

The authors declare that the research was conducted in the absence of any commercial or financial relationships that could be construed as a potential conflict of interest.

Publisher's note

All claims expressed in this article are solely those of the authors and do not necessarily represent those of their affiliated organizations, or those of the publisher, the editors and the reviewers. Any product that may be evaluated in this article, or claim that may be made by its manufacturer, is not guaranteed or endorsed by the publisher.

Supplementary material

The Supplementary Material for this article can be found online at: https://www.frontiersin.org/articles/10.3389/fmicb.2022.974526/full#supplementary-material

References

Alurappa, R., and Chowdappa, S. (2018). Antimicrobial activity and phytochemical analysis of endophytic fungal extracts isolated from ethno-pharmaceutical plant *Rauwolfia tetraphylla* L. *J. Pure Appl. Microbiol.* 12, 317–332. doi: 10.22207/JPAM.12.1.38

Arnold, A. E., Mejía, L. C., Kyllo, D., Rojas, E. I., Maynard, Z., Robbins, N., et al. (2003). Fungal endophytes limit pathogen damage in a tropical tree. *Proc. Natl Acad. Sci. U.S.A.* 100, 15649–15654. doi: 10.1073/PNAS.2533483100

Atlas, R. M. (2004). *Handbook of microbiological media*. Great Britain: Taylor & Francis. doi: 10.1201/9781420039726

Azuddin, N. F., Mohd, M. H., Rosely, N. F. N., Mansor, A., and Zakaria, L. (2021). Molecular phylogeny of endophytic fungi from rattan (*Calamus castaneus* griff.) spines and their antagonistic activities against plant pathogenic fungi. *J. Fungi* 7:301. doi: 10.3390/JOF7040301

Baum, J. M. (2013). From incense to idolatry: The reformation of olfaction in late medieval german ritual. *Sixteenth Century J.* 44, 323–344.

Bhardwaj, A., Sharma, D., Jadon, N., and Agrawal, P. K. (2015). Antimicrobial and phytochemical screening of endophytic fungi isolated from spikes of Pinus roxburghii. *Arch. Clin. Microbiol.* 6, 1–9.

Brewer, M. S. (2011). Natural antioxidants: Sources, compounds, mechanisms of action, and potential applications. *Comput. Rev. Food Sci. Food Saf.* 10, 221–247. doi: 10.1111/J.1541-4337.2011.00156.X

Capitani, C. D., Hatano, M. K., Marques, M. F., and Castro, I. A. (2013). Effects of optimized mixtures containing phenolic compounds on the oxidative stability of sausages. *Food Sci. Technol. Int.* 19, 69–77. doi: 10.1177/1082013212442184

Chen, H. P., Zhao, Z. Z., Cheng, G. G., Zhao, K., Han, K. Y., Zhou, L., et al. (2020). Immunosuppressive nor-isopimarane diterpenes from cultures of the fungicolous fungus *Xylaria longipes* HFG1018. *J. Nat. Prod.* 83, 401–412. doi: 10.1021/acs.jnatprod.9b00889

Choudhury, S. R., Traquair, J. A., and Jarvis, W. R. (1994). 4-methyl-7,11-heptadecadienal and 4-methyl-7,11-heptadecadienoic acid: New antibiotics from *Sporothrix flocculosa* and *Sporothrix rugulosa*. *J. Nat. Prod.* 57, 700–704. doi: 10.1021/np50108a003

Chu, Y. H., Chang, C. L., and Hsu, H. F. (2000). Flavonoid content of several vegetables and their antioxidant activity. *J. Sci. Food Agric.* 80, 561–566. doi: 10.1002/(SICI)1097-0010(200004)80:5<561::AID-JSFA574<3.0.CO;2-\#

Costa, D., Tavares, R. M., Baptista, P., and Lino-Neto, T. (2018). Diversity of fungal endophytic community in *Quercus suber* L. under different climate scenarios. *Revista de Ciências Agrárias* 41, 22–30. doi: 10.19084/RCA.17063

Craft, B. D., Kerrihard, A. L., Amarowicz, R., and Pegg, R. B. (2012). Phenol-based antioxidants and the in vitro methods used for their assessment. *Comput. Rev. Food Sci. Food Saf.* 11, 148–173. doi: 10.1111/J.1541-4337.2011.00173.X

Degenkolb, T., Gräfenham, T., Berg, A., Nirenberg, H. I., Gams, W., and Brückner, H. (2006). Peptaibiomics: Screening for polypeptide antibiotics (peptaibiotics) from plant-protective *Trichoderma* species. *Chem. Biodivers.* 3, 593–610. doi: 10.1002/CBDV.200690063

Dewi, R. T., Tachibana, S., and Darmawan, A. (2013). Effect on α-glucosidase inhibition and antioxidant activities of butyrolactone derivatives from *Aspergillus terreus* MC751. *Med. Chem. Res.* 23, 454–460. doi: 10.1007/S00044-013-0659-4

Dewi, R. T., Primahana, G., Septama, A. W., Angelina, M., Meilawati, L., Fajriah, S., et al. (2022). Quality control standardization of indonesian noni fruit (*Morinda citrifolia*) extract and evaluation of their angiotensin-converting enzyme inhibitory activity. *Pharmacia* 69, 709–717. doi: 10.3897/pharmacia.69.e86854

Dias, A. C. D. S., Ruiz, N., Couzinet-Mossion, A., Bertrand, S., Duflos, M., Pouchus, Y. F., et al. (2015). The marine-derived fungus *Clonostachys rosea*, source of a rare conjugated 4-me-6E,8E-hexadecadienoic acid reducing viability of MCF-7 breast cancer cells and gene expression of lipogenic enzymes. *Mar. Drugs* 13, 4934–4948. doi: 10.3390/md13084934

Dudonné, S., Vitrac, X., Coutiére, P., Woillez, M., and Mérillon, J. M. (2009). Comparative study of antioxidant properties and total phenolic content of 30 plant extracts of industrial interest using DPPH, ABTS, FRAP, SOD, and ORAC assays. *J. Agric. Food Chem.* 57, 1768–1774. doi: 10.1021/JF803011R

Elfiati, D., Susilowati, A., and Hidayat, A. (2021). Isolation of endophytic fungi from styrax sumatrana tree from humbang hasundutan, north sumatra. *Earth Environ. Sci.* 782:2045. doi: 10.1088/1755-1315/782/4/042045

Ergin, N. (2014). The fragrance of the divine: Ottoman incense burners and their context. *Art Bull.* 96, 70–97. doi: 10.1080/00043079.2014.877306

Gershon, L. (2019). *Smells like divine spirit*. Available online at: https://daily.jstor.org/smells-like-divine-spirit/ (accessed March 27, 2022).

Hajieghrari, B., Torabi-Giglou, M., Mohammadi, M. R., and Davari, M. (2010). Biological potantial of some Iranian trichoderma isolates in the control of soil borne plant pathogenic fungi. *Afr. J. Biotechnol.* 7, 967–972. doi: 10.4314/ajb.v7i8.58586

Hamzah, T. N. T., Lee, S. Y., Hidayat, A., Terhem, R., Faridah-Hanum, I., and Mohamed, R. (2018). Diversity and characterization of endophytic fungi isolated from the tropical mangrove species, rhizophora mucronata, and identification of potential antagonists against the soil-borne fungus, *Fusarium solani*. *Front. Microbiol.* 9:1707. doi: 10.3389/FMICB.2018.01707

Haran, M. (1960). The uses of incense in the ancient israelite ritual. *Vetus Testamentum* 10, 129. doi: 10.2307/1516131

Hidayat, A., Iswanto, A. H., Susilowati, A., and Rachmat, H. H. (2018). Radical scavenging activity of kemenyan resin produced by an Indonesian native plant, *Styrax sumatrana*. *J. Korean Wood Sci. Technol.* 46, 346–354. doi: 10.5658/WOOD.2018.46.4.346

Hidayat, A., Susilowati, A., Faulina, S. A., Elfiati, D., Imanuddin, R., and Turjaman, M. (2021a). Diversity of endophytic fungi isolated from benzoin-producing tree styrax sumatrana. *Earth Environ. Sci.* 762, 12002. doi: 10.1088/1755-1315/762/1/012002

Hidayat, A., Turjaman, M., Qamyari, R., Imanuddin, R., Tohir, D., Rahmanto, R. G. H., et al. (2021b). Bioactive composition, antifungal, antioxidant, and anticancer potential of agarwood essential oil from decaying logs (*Gyrinops* spp.) of papua Island (indonesia). *J. Appl. Pharm. Sci.* 11, 070–078. doi: 10.7324/JAPS.2021.1101010

Hidayat, A., Turjaman, M., Faulina, S. A., Ridwan, F., Aryanto, Najmulah, et al. (2019a). Antioxidant and antifungal activity of endophytic fungi associated with agarwood trees. *J. Korean Wood Sci. Technol.* 47, 459–471. doi: 10.5658/WOOD.2019.47.4.459

Hidayat, N., Yati, K., Krisanti, E. A., and Gozan, M. (2019b). Extraction and antioxidant activity test of black sumatran incense. *AIP Conference Proc.* 2193, 30017. doi: 10.1063/1.5139354

Huang, L. Q., Niu, Y. C., Su, L., Deng, H., and Lyu, H. (2020). The potential of endophytic fungi isolated from cucurbit plants for biocontrol of soilborne fungal diseases of cucumber. *Microbiol. Res.* 231, 126369. doi: 10.1016/J.MICRES.2019.126369

Ibrahim, S. R. M., Abdallah, H. M., Elkhayat, E. S., Musayeib, N. M., Asfour, H. Z., Zayed, M. F., et al. (2018). Fusaripeptide a: New antifungal and anti-malarial cyclodepsipeptide from the endophytic fungus *Fusarium* sp. *J. Asian Nat. Prod. Res.* 20, 75–85. doi: 10.1080/10286020.2017.1320989

Ilyas, M., Praptiwi, Wulansari, D., Fathoni, A., and Agusta, A. (2019). An assemblages of fungal endophytes isolated from medicinal plants collected from toba and samosir, north sumatra. *Earth Environ. Sci.* 308:012070. doi: 10.1088/1755-1315/308/1/012070

Iswanto, A. H., Susilowati, A., Azhar, I., Riswan, S., Tarigan, J. E., et al. (2016). Physical and mechanical properties of local styrax woods from north tapanuli in indonesia. *J. Korean Wood Sci. Technol.* 44, 539–550. doi: 10.5658/WOOD.2016.44.4.539

Karamać„ M., Kosińska, A., and Pegg, R. B. (2005). Comparison of radical-scavenging activities for selected phenolic acids. *Polish J. Food Nutr. Sci.* 55, 165–170.

Kashio, M., and Johnson, D. V. (2001). *Monograph on benzoin (balsamic resin from styrax species. food and agriculture organization of the united nations. regional office for asia and the pacific*. Bangkok: RAP. Publication, 21.

Khan, N., Afroz, F., Begum, M. N., Roy Rony, S., Sharmin, S., Moni, F., et al. (2018). Endophytic *Fusarium solani*: A rich source of cytotoxic and antimicrobial napthaquinone and aza-anthraquinone derivatives. *Toxicol. Rep.* 5, 970–976. doi: 10.1016/J.TOXREP.2018.08.016

le Maguer, S. (2015). "The incense trade during the islamic period," in *Proceedings of the seminar for arabian studies*, Vol. 45, (Oxford: Archaeopress Publishing Ltd.), 175–183.

Lin, X., Yu, M., Lin, T., and Zhang, L. (2016). Secondary metabolites of *Xylaria* sp., an endophytic fungus from *Taxus mairei*. *Nat. Prod. Res.* 30, 2442–2447. doi: 10.1080/14786419.2016.1198350

Ma, Q. Y., Yang, S., Huang, S. Z., Kong, F. D., Xie, Q. Y., Dai, H. F., et al. (2018). Ergostane steroids from coprinus setulosus. *Chem. Nat. Compd.* 54, 710–713. doi: 10.1007/s10600-018-2451-7

Mejía, L. C., Rojas, E. I., Maynard, Z., van Bael, S., Arnold, A. E., Hebbar, P., et al. (2008). Endophytic fungi as biocontrol agents of *Theobroma cacao* pathogens. *Biol. Control* 46, 4–14. doi: 10.1016/J.BIOCONTROL.2008.01.012

Miersch, O., Bohlmann, H., and Wasternack, C. (1999). Jasmonates and related compounds from Fusarium oxysporum. *Phytochemistry* 50, 517–523. doi: 10.1016/S0031-9422(98)00596-2

Milburn, O. (2016). Aromas, scents, and spices: Olfactory culture in China before the arrival of buddhism. *J. Am. Orient. Soc.* 136, 441–464. doi: 10.7817/JAMERORIESOCI.136.3.0441/0

Mishra, A., Gond, S. K., Kumar, A., Sharma, V. K., Verma, S. K., Kharwar, R. N., et al. (2012). Season and tissue type affect fungal endophyte communities of the Indian medicinal plant *Tinospora cordifolia* more strongly than geographic location. *Microb. Ecol.* 64, 388–398. doi: 10.1007/S00248-012-0029-7

Molan, Y. Y., Kamel, A., and El-Hussieni, S. (2008). Bicontrol of R. solani AG – 4 with piperitone product from *Cymbopogon proximus* and comparison with bicontrol agents (*Trichoderma* Spp). *Alex. Sci. Exch. J.* 29, 16–25. doi: 10.21608/ASEJAIQJSAE.2008.3178

Moricca, S., Ginetti, B., and Ragazzi, A. (2012). Species- and organ-specificity in endophytes colonizing healthy and declining *Mediterranean* oaks. *Phytopathol. Mediterr.* 51, 587–598.

Mufarhatun, N., Hilwan, I., and Rachmat, H. H. (2021). Identification of red meranti group (*Shorea* spp., dipterocarpaceae) saplings based on variations in the morphological features of quantitative leaves. *J Penelitian Hutan Konservasi Alam* 18, 137–149. doi: 10.20886/JPHKA.2021.18.2.137-149

Nguyen, M. H., Shin, K. C., and Lee, J. K. (2021). Fungal community analyses of endophytic fungi from two oak species, quercus mongolica and quercus serrata, in Korea. *Mycobiology* 49, 385–395. doi: 10.1080/12298093.2021.1948175/SUPPL_FILE/TMYB_A_1948175_SM3053.XLSX

Nir, R. (2004). The aromatic fragrances of paradise in the greek life of adam and eve and the christian origin of the composition. *Novum Testamentum* 46, 20–45. doi: 10.1163/156853604772719739

Nurwahyuni, I., Situmorang, M., and Sinaga, R. (2021). Identification of mother plant for in vitro propagation of sumatra benzoin as a strategy to improve non-timber forest product. *J. Physics Conf. Ser.* 1811, 12018. doi: 10.1088/1742-6596/1811/1/012018

Ogbe, A. A., Finnie, J. F., and van Staden, J. (2020). The role of endophytes in secondary metabolites accumulation in medicinal plants under abiotic stress. *Soc. Afr. J. Bot.* 134, 126–134. doi: 10.1016/J.SAJB.2020.06.023

Romero, C. (2014). Bark: Structure and functional ecology. *Adv. In Econ. Bot.* 17, 5–25.

Saitou, N., and Nei, M. (1987). The neighbor-joining method: A new method for reconstructing phylogenetic trees. *Mol. Biol. Evol.* 4, 406–425. doi: 10.1093/OXFORDJOURNALS.MOLBEV.A040454

Saputra, M. H., and Lee, H. S. (2021). Evaluation of climate change impacts on the potential distribution of Styrax sumatrana in north sumatra, indonesia. *Sustainability* 13:462. doi: 10.3390/SU13020462

Schardl, C. L., Leuchtmann, A., and Spiering, M. J. (2004). Symbioses of grasses with seedborne fungal endophytes. *Annu. Rev. Plant Biol.* 55, 315–340. doi: 10.1146/ANNUREV.ARPLANT.55.031903.141735

Sharif, A., Nawaz, H., Rehman, R., Mushtaq, A., and Rashid, U. (2016). A review on bioactive potential of benzoin resin. *IJCBS* 10, 106–110.

Shetty, K. G., Rivadeneira, D., Jayachandran, K., and Walker, D. (2016). Isolation and molecular characterization of the fungal endophytic microbiome from conventionally and organically grown avocado trees in south florida. *Mycol. Prog.*15, 977–986. doi: 10.1007/s11557-016-1219-3

Sicard, D., Pennings, P. S., Grandclément, C., Acosta, J., Kaltz, O., and Shykoff, J. A. (2007). Specialization and local adaptation of a fungal parasite on two host plant species as revealed by two fitness traits. *Evolution* 61, 27–41. doi: 10.1111/J.1558-5646.2007.00003.X

Slamet, W. Y., Faulina, S. A., Hidayat, A., Susilowati, A., Elfiati, D., Rahayu, L. M., et al. (2021). Diversity of endophytic fungal species from styrax benzoin found in benzoin-producing locations in north sumatra. *Earth Environ. Sci.* 914:12041. doi: 10.1088/1755-1315/914/1/012041

Smit, P. B. (2004). Incense revisited: Reviewing the evidence for incense as a clue to the christian provenance of the greek life of adam and eve. *Novum Testamentum* 46, 369–375. doi: 10.1163/1568536042650595

Srinivasan, K., Jagadish, L. K., Shenbhagaraman, R., and Muthumary, J. (2010). Antioxidant activity of endophytic fungus *Phyllosticta* sp. isolated from *Guazuma tomentosa*. *J. Phytol.* 2, 37–41.

Taher, M. A., Tan, W. N., Chear, N. J. Y., Leong, C. R., Rashid, S. A., and Tong, W. Y. (2022). Metabolites characterisation of endophytic *Phyllosticta fallopiae* L67 isolated from aloe vera with antimicrobial activity on diabetic wound microorganisms. *Nat. Prod. Res.* 2022, 1–6. doi: 10.1080/14786419.2022.2103127

Tambe, V. D., and Bhambar, R. S. (2014). Estimation of total phenol, tannin, alkaloid and flavonoid in *Hibiscus tiliaceus* Linn. wood extracts. *RRJPP* 2, 41–47.

Tamura, K., Nei, M., and Kumar, S. (2004). Prospects for inferring very large phylogenies by using the neighbor-joining method. *Proc. Natl. Acad. Sci. U.S.A.* 101, 11030–11035. doi: 10.1073/PNAS.0404206101

Tamura, K., Stecher, G., and Kumar, S. (2021). MEGA11: Molecular evolutionary genetics analysis version 11. *Mol. Biol. Evol.* 38, 3022–3027. doi: 10.1093/MOLBEV/MSAB120

Tanapichatsakul, C., Khruengsai, S., Monggoot, S., and Pripdeevech, P. (2019). Production of eugenol from fungal endophytes *Neopestalotiopsis* sp. and *Diaporthe* sp. isolated from *Cinnamomum loureiroi* leaves. *PeerJ* 7:e6427. doi: 10.7717/PEERJ.6427/SUPP-3

Tani, M., Harimaya, K., Gyobu, Y., Sasaki, T., Takenouchi, O., Kawamura, T., et al. (2004). SF2809 compounds, novel chymase inhibitors from *Dactylosporangium* sp. 2. *Struct. Eluc. J Antibiot.* 57, 89–96. doi: 10.7164/antibiotics.57.89

Wang, S. S., Wang, D. M., Pu, W. J., and Li, D. W. (2013). Phytochemical profiles, antioxidant and antimicrobial activities of three *Potentilla* species. *BMC Complement. Altern. Med.* 13:1–11. doi: 10.1186/1472-6882-13-321

Wheeler, K. A., and Hocking, A. D. (1993). Interactions among xerophilic fungi associated with dried salted fish. *J. Appl. Bacteriol.* 74, 164–169. doi: 10.1111/J.1365-2672.1993.TB03010.X

White, T. J., Bruns, T., Lee, S., and Taylor, J. (1990). "Amplification and direct sequencing of fungal ribosomal RNA genes for phylogenetics," in *PCR protocols,*

a guide to methods and applications, (Academic Press), 315–322. *editor. doi: 10.1016/B978-0-12-372180-8.50042-1

Wikee, S., Lombard, L., Crous, P. W., Nakashima, C., Motohashi, K., Chukeatirote, E., et al. (2013). Phyllosticta capitalensis, a widespread endophyte of plants. *Fungal Divers.* 60, 91–105. doi: 10.1007/S13225-013-0235-8

Wu, S. H., He, J., Li, X. N., Huang, R., Song, F., Chen, Y. W., et al. (2014). Guaiane sesquiterpenes and isopimarane diterpenes from an endophytic fungus *Xylaria* sp. *Phytochemistry* 105, 197–204. doi: 10.1016/j.phytochem.2014.04.016

Xiao, Y., Li, H. X., Li, C., Wang, J. X., Li, J., Wang, M. H., et al. (2013). Antifungal screening of endophytic fungi from ginkgo biloba for discovery of potent anti-phytopathogenic fungicides. *FEMS Microbiol. Lett.* 339, 130–136. doi: 10.1111/1574-6968.12065

Xie, J. L., and Li, L. P. (1992). New metabolites from the fungus *Stereum purpureum*. *Chin. J. Chem.* 10, 537–543. doi: 10.1002/cjoc.19920100610

Zhang, H., Wang, G., Beta, T., and Dong, J. (2015). Inhibitory properties of aqueous ethanol extracts of propolis on alpha-glucosidase. *Evid. Based Complement. Alternat. Med.* 2015:383. doi: 10.1155/2015/587383

Zhao, J., Zhou, L., Wang, J., Shan, T., Zhao, J., Zhou, L., et al. (2010). Endophytic fungi for producing bioactive compounds originally from their host plants. *Curr. Res. Technol. Educ. Trop. Appl. Microbiol. Microbial. Biotechnol.* 1, 567–576.

Zhou, J., Diao, X., Wang, T., Chen, G., Lin, Q., Yang, X., et al. (2018). Phylogenetic diversity and antioxidant activities of culturable fungal endophytes associated with the mangrove species *Rhizophora stylosa* and R. mucronata in the South China sea. *PLoS One.* 13:e0197359. doi: 10.1371/JOURNAL.PONE.0197359

frontiers | Frontiers in Microbiology

TYPE Original Research
PUBLISHED 07 November 2022
DOI 10.3389/fmicb.2022.1024001

OPEN ACCESS

EDITED BY
Naser Safaie,
Tarbiat Modares University,
Iran

REVIEWED BY
Jadson Diogo Pereira Bezerra,
Universidade Federal de Goiás, Brazil
Wei Yan,
Nanjing Agricultural University,
China

*CORRESPONDENCE
Leila Ebrahimi
Le_ebrahimi@ut.ac.ir

SPECIALTY SECTION
This article was submitted to Microbe and Virus Interactions with Plants, a section of the journal Frontiers in Microbiology

RECEIVED 20 August 2022
ACCEPTED 14 October 2022
PUBLISHED 07 November 2022

CITATION
Ebrahimi L, Hatami Rad S and Etebarian HR (2022) Apple Endophytic fungi and their antagonism against apple scab disease.
Front. Microbiol. 13:1024001.
doi: 10.3389/fmicb.2022.1024001

Apple Endophytic fungi and their antagonism against apple scab disease

Leila Ebrahimi*, Sepideh Hatami Rad and Hassan Reza Etebarian

Department of Entomology and Plant Pathology, College of Aburaihan, University of Tehran, Tehran, Iran

Endophytic fungi are microorganisms with the ability to colonize plants for the entire or at least a significant part of their life cycle asymptomatically, establishing a plant-fungus association. They play an important role in balancing ecosystems, as well as benefiting host through increasing plant growth, and protecting the host plants from abiotic and biotic stresses using various strategies. In the present study, endophytic fungi were isolated from wild and endemic apple cultivars, followed by characterizing their antifungal effect against *Venturia inaequalis*. To characterize the endophytic fungi, 417 fungal strains were separated from 210 healthy fruit, leaf, and branch samples collected from the north of Iran. Among the purified fungal isolates, 33 fungal genera were identified based on the morphological characteristics, of which 38 species were detected according to the morphological features and molecular data of ITS, *tef-1α*, and *gapdh* genomic regions (related to the genus). The results represented that most of the endophytic fungi belonged to Ascomycota (67.8%), 31.4% of isolates were mycelia sterilia, while the others were Basidiomycota (0.48%) and Mucoromycota (0.24%). Additionally, *Alternaria*, *Cladosporium*, and *Nigrospora* were determined as the dominant genera. The antifungal properties of the identified isolates were evaluated against *V. inaequalis in vitro* to determine the release of media-permeable metabolites, Volatile Organic Compounds (VOCs), chitinase, and cellulase as antifungal mechanisms, as well as producing phosphate solubilisation as growth-promoting effect. Based on the results of metabolite and VOC tests, the six isolates of *Acremonium sclerotigenum* GO13S1, *Coniochaeta endophytica* 55S2, *Fusarium lateritium* 61S2, *Aureobasidium microstictum* 7F2, *Chaetomium globosum* 2S1 and *Ch. globosum* 3L2 were selected for greenhouse tests. Further, *Co. endophytica* 55S2 and *F. lateritium* 61S2 could solubilize inorganic phosphate. All isolates except *Ch. globosum* 3L2 exhibited cellulase activity, while chitinase activity was observed in *Ch. globosum* 2S1, *Ch. globosum* 3L2, and *F. lateritium* 61S2. Finally, *Co. endophytica* 55S2 and *Ch. globosum* 2S1 completely controlled the disease on the apple seedling leaves under greenhouse conditions.

KEYWORDS

biocontrol, chitinase activity, cellulase activity, endophyte, metabolites, volatile organic compounds

Introduction

Apple (*Malus* sp.), which belongs to the Rosaceae family, is considered as the most common and culturally important fruit crop worldwide, as well as one of the superior crops in Iran due to its nutritional and export value (Ebrahimi et al., 2016). The apple scab caused by *Venturia inaequalis* (Cooke) G. Winter is among the most main diseases in the apple-growing regions across the globe (Tenzer and Gessler, 1997), especially the areas with cool and wet spring, as well as early summer (MacHardy, 1996). The management of this disease is often based on the repeated fungicide application which is expensive and time-consuming. However, some fungicides may lose their efficacy following the development of resistance in the fungus causing apple scab. Nevertheless, the need for nonchemical control methods to reduce the crop losses is becoming increasingly important for protecting the environment and human health (Wenneker and Thomma, 2020). In this regard, a global trend tries to explore the new alternatives to synthetic fungicides, which minimize the risks associated with the development of the populations insensitive to the chemical compounds and are consistent with the food safety standards (Chen et al., 2019). Biological control is an excellent and effective alternative way to control plant diseases (Zhang et al., 2018). In addition, endophytes are a potential source of biological control agents, which are already adapted to live and persist in the plant with minimal adverse effects.

The endophytes are the microorganisms living inside plant tissues for the entire or at least a large part of their life cycle without causing any symptom or adverse harm to the host (Petrini, 1991; Saikkonen et al., 1998). The endophytic fungi can be considered as potential biological competitors since they have evolved to exploit the same resources as plant pathogens (Silva et al., 2018). They contribute to plant health by producing protective metabolites, inducing biotic and abiotic stress resistance in host plants, and improving their growth with phytohormones (Rai et al., 2014; Terhonen et al., 2019). The microorganisms can potentially protect plants from pathogenic fungi through a diverse array of modes of action such as direct inhibition *via* competition, antibiosis or mycoparasitism, and indirect inhibition by induced resistance (Latz et al., 2018). Recently, endophytic fungi stood out as the most common group of microorganisms elaborated in the laboratory to produce a variety of secondary metabolites such as alkaloids, flavonoids, terpenoids, volatile organic compounds (VOC), phenols and its derivatives, and different enzymes (Zhang et al., 2006; Strobel, 2018) with potential use in industrial application or as fungicides to control the growth of phytopathogenic fungi (Meenavalli et al., 2011; Toghueo et al., 2017). These microorganisms inside the plant are able to degrade a portion of plant lignin and cellulose (Li et al., 2021) which helps host plants to protect themselves against invasive pathogens (Marques et al., 2018). Also, endophytes with the ability to secrete extracellular chitinase would decompose chitin, a β-(1,4)-linked polymer of N-acetyl-D-glucosamine, and the cell wall structure of most phytopathogenic fungi along with other versatile bioactive compounds (Hartl et al., 2012). Endophytes contribute to several processes related to plant growth and development similar to the rhizospheric microbes, such as, nitrogen fixation, phosphate solubilization, etc. (Santoyo et al., 2016). Inorganic phosphate solubilization, through microorganisms, is one of the major mechanisms involved in plant growth (Adhikari and Pandey, 2019). Solubilization of inorganic insoluble phosphate salts by different microorganisms depends on their ability to produce organic acids in the respective environment. These organic acids decrease the pH of the soil or any medium, providing the facility to exchange the metal part of insoluble phosphates to potassium or sodium, resulting in the formation of soluble phosphate salts (Singh and Satyanarayana, 2011; Rinu et al., 2012) which is absorbable for plants.

Several studies have assessed the endophytic fungal communities of apple (e.g., Camatti-Sartori et al., 2005; Alijani et al., 2016a; Liu et al., 2017; Muresan, 2017; Afandhi et al., 2018; Liu et al., 2018; Arrigoni et al., 2020; Olivieri et al., 2021), some of which have focused on the biological control potential of the endophytes against apple fungal diseases. Based on the results, apple tissues are colonized by a diverse array of fungal taxa (e.g., *Alternaria* Nees, *Arthrinium* Kunze, *Aspergillus* P. Micheli ex Haller, *Biscogniauxia* Kuntze, *Botryosphaeria* Ces. & De Not., *Chaetomium* Kunze, *Colletotrichum* Corda, *Dicyma* Boulanger, *Doratomyces* Corda, *Epicoccum* Link, *Neosetophoma* Gruyter, Aveskamp & Verkley, *Paraconiothyrium* Verkley, *Penicillium* Link, *Stemphylium* Wallr., *Trichoderma* Pers., *Trichothecium* Link, *Xylaria* Hill ex Schrank, *Sporobolomyces* Kluyver & C.B. Niel, *Rhodotorula* F.C. Harrison, *Debaryomyces* Klöcker and *Cryptococcus* Kütz and etc). Alijani et al. (2016a) purified about 350 isolates from the shoots, leaves, and barks of endemic and commercial apple trees in West Azerbaijan province, Iran and identified 24 species belonging to 10 genera of Ascomycota. They examined the antagonistic properties of the isolates against *Diplodia bulgarica* A.J.L. Phillips, J. Lopes & Bobev, the causal agent of apple canker disease, *in vitro* and found various interactions in the paired combinations of endophytic fungi and *D. bulgarica* (Alijani et al., 2016b). Liu et al. (2017) highlighted the biological control potential of 81 endophytic fungi from apple shoots to preserve apple trees against *Neonectria ditissima* (Tul. & C. Tul.) Samuels & Rossman infection *in vitro*. They mentioned that 18 fungal isolates inhibited the radial growth of three *N. ditissima* isolates, among which 15 selected ones were identified as *Epicoccum*, *Chaetomium*, *Biscogniauxia*, *Neosetophoma*, and *Penicillium* species. In another study, a collection of 60 endophytic fungal isolates was obtained from apple trees in Canada, 60% of which were *Penicillium* or *Trichoderma* species (Muresan, 2017). Furthermore, 55 isolates significantly inhibited *V. inaequalis* growth *in vitro*, the most effective one of which was *Fusarium oxysporum* Schltdl. isolate FRS09 with 83% inhibition.

The endophytic fungi play roles in protecting the plant from herbivorous insects and diseases, as well as supporting the absorption process of the nutrients required for photosynthesis (Gimenez et al., 2007; Rozpądek et al., 2015; Vergara et al., 2017;

Li et al., 2018). Given the crucial role of endophytic fungi, the present study focused on the endophytic fungi from wild and endemic apple cultivars in the north of Iran. In the study, the endophytic fungi were isolated from the healthy leaves, fruits, and branches of the cultivars, and tested for their efficacy against *V. inaequalis* and ability to prevent apple scab infection and its symptoms. The fungi were identified with consistent biological control capacity against apple scab *in vitro* and greenhouse tests. The results provide evidence that the naturally-occurring endophytic fungi can be a novel source for biological control agents.

Materials and methods

Sampling and endophytic fungi isolation

The healthy leaf, fruit, and branch samples of wild and endemic apple cultivars were collected from 70 trees in the north of Iran (Guilan, Mazandaran and Golestan provinces) during July–September 2019. They were placed in paper bags and stored at 4°C. Additionally, plant materials were disinfected based on the method modified by Strobel and Daisy (2003) (Ebrahimi et al., 2021). The fungi were separated on the three media of Water Agar (WA), Corn Meal Agar (CMA), and Potato Dextrose Agar (PDA), and hyphal tip method was applied for purification. All of the identified isolates were deposited in the Fungal Culture Collection (IRAN) of the Iranian Research Institute of Plant Protection (Tehran, Iran).

Endophytic fungi identification

The appearance of colony, structure and color of mycelium, type of teleomorph and/or anamorph, and morphology of ascoma, conidiomata, conidia, and conidiophores (e.g., size, color, shape, and ornamentation), as well as conidiogenous cells, and spore production mechanism were studied for examining fungi morphologically (Ellis, 1971, 1976; Sutton, 1980; Sivanesan, 1987; Klich and Pitt, 1988; Klich, 2002; Leslie and Summerell, 2006; Simmons, 2007). Each of the fungal isolates was separately sub-cultured on the PDA; Czapek Yeast Extract Agar (CYA; sucrose 30 g, yeast extract 5 g, K_2HPO_4 1 g, $NaNO_3$ 3 g, KCl 0.05 g, $MgSO_4.7H_2O$ 0.05 g, $FeSO_4.7H_2O$ 1 mg, agar 20 g/l, final pH 6.0–6.5); Carnation Leaf Agar (CLA; autoclaved Carnation leaves pieces on nearly solid 2% WA; agar 20 g/l water); Corn Meal Agar (CMA; corn meal infusion from 50 g solids, agar 20 g/l); Oatmeal Agar (OA; oat meal infusion from 30 g solids, agar 20 g/l); Potato Carrot Agar (PCA; potato infusion from 20 g solids, carrot infusion from 20 g solids, agar 20 g/l); Malt Extract Agar (MEA; malt extract 30 g, peptone 5 g, agar 20 g/l); Synthetic Nutrient Agar (SNA; KH_2PO_4 1 g, KNO_3 1 g, $MgSO_4.7H_2O$ 0.5 g, KCl 0.5 g, Glucose 0.2 g, Sucrose 0.2 g, agar 20 g/l); and Tap Water Agar plus wheat straw (TWA; agar 20 g/l tap water plus autoclaved wheat straw) for inducing sporulation. Further, microscopic slides were prepared in lacto-phenol or lacto-phenol cotton blue solutions after 7, 14, and/or 30 days (due to the fungal species), followed by assessment under a BH2 light microscope (Olympus, Japan). The isolates were classified into morphotypes according to their morphological appearance, and at least one isolate of each morphotype was kept for molecular identification.

Furthermore, the rapid simplified DNA extraction protocol provided by Cenis (1992) was employed for the DNA extraction from seven-day-old fresh mycelia. The fungal isolates were molecularly identified based on the Internal Transcribed Spacer (ITS)-rDNA, glyceraldehyde-3-phosphate dehydrogenase (*gapdh*), and translation elongation factor 1-alpha (*tef-1α*) sequences which were, respectively, amplified by using the ITS1/ITS4 (White et al., 1990), EF1/EF2 (O'Donnell et al., 1998) and gpd1/gpd2 (Berbee et al., 1999) primer pairs related to the fungal genus. In the present study, the reaction mixture and PCR conditions for ITS, *tef-1α*, and *gapdh* were the same as those presented by Ebrahimi and Fotouhifar (2016), O'Donnell et al. (1998), and Song et al. (2019), respectively. PCR products were purified and directly sequenced in one direction with ITS1, EF1, and gpd1 primers by BGI Company (Denmark), respectively.

The ITS, *tef-1α*, and *gapdh* sequences were compared with those of the most closely-related fungal species according to the NCBI BLAST program, relevant websites, observed colony, and spore morphology to confirm the taxonomic status of the intended fungal isolates. Finally, the sequence data were deposited in the GenBank database.

For phylogenetic analyses, sequences of genomic regions of *gapdh*, *tef-1α*, and ITS from different species were aligned with the homologous reference sequences of the respective genomic regions of related species obtained from GenBank (Supplementary Table S1) using ClustalW (Thompson et al., 1994). Maximum likelihood (ML) (Felsenstein, 1981) analysis was done by heuristic search with MEGA software ver. 7 (Kumar et al., 2016). Models TN93 + G, K2 + G and K2 + I were recommended by MEGA as the optimal nucleotide substitution models for *gapdh*, *tef-1α*, and ITS data, respectively. Characters were treated as un-weighted and unordered with gaps treated as missing data. Confidence of individual clades was assessed by ML bootstrap analysis (Felsenstein, 1985) with 1,000 replicates.

Biocontrol experiments *in vitro*

Cellophane membrane-based method

The cellophane membrane-based method (Dennis and Webster, 1971) was performed in duplicate to screen the endophytic isolates based on their antagonism against *V. inaequalis* (IRAN 16870 F). Then, the isolates expressing the visually-detected antifungal activity (Table 1) were subjected to a secondary screening (the cellophane membrane-based method in triplicate). In this technique, a sterile cellophane membrane of the same diameter as a Petri

TABLE 1 Identified endophytic fungi of Iranian endemic and wild apple based on morphology and by ITS, translation elongation factor 1-alpha (*tef-1α*) and glyceraldehyde-3-phosphate dehydrogenase (*gapdh*) sequences.

Isolate	Species	Host	Geographical region	Collection accession number	Genbank accession number
					ITS
2S1	*Chaetomium globosum*	Endemic apple branch	Golestan, Gonbad Kavous	IRAN 4355C	MZ151358
3 L2	*Chaetomium globosum*	Endemic apple leaf	Golesta, Minoudasht	IRAN 4356C	MZ151359
7F2	*Aureobasidium microstictum*	Wild apple fruit	Golesta, Minoudasht	IRAN 4378C	MZ151360
11S1	*Venturia inaequalis*	Wild apple branch	Golestan, Ramian	IRAN 4379C	MZ151361
12S2	*Penicillium chrysogenum*	Wild apple branch	Golestan, Ramian	IRAN 4357C	MZ151362
16 L1	*Alternaria infectoria*	Wild apple leaf	Golestan, Ramian	IRAN 4380C	MZ151363
17S2	*Aposphaeria corallinolutea*	Endemic apple branch	Golestan, Khanbebin	IRAN 4381C	MZ151364
GO2L3	*Hypoxylon fragiforme*	Endemic apple leaf	Golesta, Minoudasht	IRAN 4382C	MZ151387
GO2S2	*Neosetophoma salicis*	Endemic apple branch	Golesta, Minoudasht	IRAN 4383C	MZ151388
GO3S1	*Neosetophoma salicis*	Endemic apple branch	Golesta, Minoudasht	IRAN 4384C	MZ151389
GO5L3	*Nigrospora oryzae*	Endemic apple leaf	Golestan, Gonbad Kavous	IRAN 4358C	MZ151390
GO5S1	*Talaromyces verruculosus*	Endemic apple branch	Golestan, Gonbad Kavous	IRAN 4359C	MZ151391
GO7L1	*Nemania serpens*	Endemic apple leaf	Golesta, Minoudasht	IRAN 4385C	MZ151392
GO8S2	*Hydeomyces desertipleosporoides*	Endemic apple branch	Golesta, Minoudasht	IRAN 4386C	MZ151393
GO13S1	*Acremonium sclerotigenum*	Endemic apple branch	Golestan, Ramian	IRAN 4360C	MZ151394
22S4	*Discostroma corticola*	Endemic apple branch	Mazandarn, Kiasar	IRAN 4387C	MZ151365
23 L3	*Aspergillus terreus*	Endemic apple leaf	Mazandarn, Kiasar	IRAN 4361C	MZ151366
32 L2	*Ramularia* sp.	Wild apple leaf	Mazandarn, Neka	IRAN 4388C	MZ151367
33 L1	*Alternaria tenuissima*	Endemic apple leaf	Mazandarn, Neka	IRAN 4362C	MZ151368
33 L6	*Stachybotrys chartarum*	Endemic apple leaf	Mazandarn, Neka	IRAN 4397C	OM674386
36F4	*Neoscytalidium dimidiatum*	Endemic apple fruit	Mazandarn, Polsefid	IRAN 4363C	MZ151369
39S5	*Gibellulopsis nigrescens*	Endemic apple branch	Mazandarn, Savadkouh	IRAN 4389C	MZ151370
39S6	*Chaetomium globosum*	Endemic apple branch	Mazandarn, Savadkouh	IRAN 4364C	MZ151371
43 L3	*Pseudoanthostomella sepelibilis*	Endemic apple leaf	Guilan, Siahkal	IRAN 4390C	MZ151372
44 L1	*Nigrospora oryzae*	Endemic apple leaf	Guilan, Paresar	IRAN 4398C	MZ151373
47 L1	*Colletotrichum godetiae*	Wild apple leaf	Guilan, Paresar	IRAN 4391C	MZ151375
47F1	*Aspergillus versicolor*	Wild apple fruit	Guilan, Paresar	IRAN 4365C	MZ151374
51 L3	*Nigrospora oryzae*	Endemic apple leaf	Guilan, Rezvanshahr	IRAN 4399C	MZ151376
52 L2	*Coprinopsis atramentaria*	Endemic apple leaf	Guilan, Fouman	IRAN 4392C	MZ151377
53 L1	*Colletotrichum gloeosporioides*	Endemic apple leaf	Guilan, Fouman	UT53 L1	MZ151386
54 L1	*Annulohypoxylon stygium*	Endemic apple leaf	Guilan, Siahkal	IRAN 4393C	MZ151378
55S2	*Coniochaeta endophytica*	Endemic apple branch	Guilan, Paresar	IRAN 4366C	MZ151379
56F3	*Gleoephyllum trabeum*	Endemic apple fruit	Guilan, Bazarjomee	IRAN 4367C	MZ151380
59 L6	*Pestalotiopsis lespedezae*	Wild apple leaf	Guilan, Paresar	IRAN 4396C	MZ151381
60S1	*Paecillomyces maximus*	Wild apple branch	Guilan, Fouman	IRAN 4368C	MZ151383
62 L1	*Nigrospora oryzae*	Endemic apple leaf	Guilan, Rezvanshahr	IRAN 4394C	MZ151384
62 L3	*Neopestalotiopsis clavispora*	Endemic apple leaf	Guilan, Rezvanshahr	IRAN 4369C	MZ151385
60 L4	*Colletotrichum fructicola*	Wild apple leaf	Guilan, Fouman	IRAN 4395C	MZ151382
					gapdh
58 L2	*Curvularia hominis*	Wild apple leaf	Guilan, Siahkal	IRAN 4400C	MZ339272
26S2	*Curvularia spicifera*	Endemic apple branch	Mazandarn, Kiasar	IRAN 4370C	MZ339270
33S2	*Curvularia spicifera*	Endemic apple branch	Mazandarn, Neka	IRAN 4371C	MZ339271
					tef-1α
61S2	*Fusarium lateritium*	Endemic apple branch	Guilan, Siahkal	IRAN 4470C	MZ339268
25S3	*Fusarium incarnatum*	Endemic apple branch	Mazandarn, Kiasar	IRAN 4372C	MZ339266
37F6	*Fusarium fujikuroi*	Endemic apple fruit	Mazandarn, Polsefid	IRAN 4373C	MZ339267
GO2L1	*Fusarium acuminatum*	Endemic apple leaf	Golesta, Minoudasht	IRAN 4374C	MZ339269

plate was overlaid on the PDA medium by using sterile forceps. A disc of endophytic isolate was inoculated at the membrane center and maintained at 20°C for 3–5 days related to isolate growth speed. Following incubation, the isolate culture along with the membrane was carefully removed from the plate, and a plug of *V. inaequalis* was positioned on the plate and kept at 20°C for 1 month. The colony diameter of *V. inaequalis* was measured and compared to the value obtained by culturing *V. inaequalis* on fresh PDA plates (control treatment). The percentage of growth inhibition was calculated by using the formula $n = (a - b)/a \times 100$, where n is considered as the growth inhibition percentage, a indicates the colony diameter of uninhibited *V. inaequalis*, and b shows the colony diameter of antagonist-treated *V. inaequalis* (Etebarian et al., 2005).

Volatile organic compound-mediated interactions

In addition, the effect of endophyte Volatile Organic Compounds (VOCs) on *V. inaequalis* was examined by using sandwiched Petri plates explained by Lillbro (2005). After inoculating the endophytic isolates and *V. inaequalis* on the PDA plates, *V. inaequalis* plates were placed on top of an isolate plate, sealed with Parafilm, and incubated at 20°C. Further, plates with *V. inaequalis* were sandwiched with uninoculated PDA plates as a control treatment. Each treatment was repeated three times. The colony diameter of *V. inaequalis* was obtained after 1 month and the above-mentioned formula was used to compute the growth inhibition percentage.

Chitinase activity

The method of Hsu and Lockwood (1975) was applied to determine chitinase production. Briefly, the endophytic isolates were grown on the chitin agar containing 0.4% colloidal chitin and 1.5% agar adjusted to pH 7.2. Furthermore, the colloidal chitin was prepared according to Berger and Reynolds (1958). The plates were incubated for 5 days at 25°C. The ability of chitinase production was revealed by a clear halo around the colonies. Ultimately, the ratio of the clear zone diameter to colony diameter was calculated as chitinase activity.

Cellulase activity

Regarding congo red cellulase activity, all fungal isolates were developed on the carboxymethyl cellulose (CMC) agar medium consisting of 0.4 g/l KH_2PO_4, 0.02 g/l $CaCl_2$, 0.02 g/l NaCl, 0.02 g/l $FeSO_4$ $7H_2O$, 2.5 g/l CMC, and 15.0 g/l agar at 25°C for 7 days. The pH was set to 7.2 by using 1 M NaOH. To visualize the hydrolysis zone, agar medium was flooded with an aqueous congo red solution (1 mg/ml) for 20 min. Then, congo red solution was poured off, and the plates were further treated by flooding with 1 M NaCl for 15 min. The cellulase activity was obtained by measuring the diameter of the clear zone around each colony. In fact, it was computed as the ratio of the clear zone diameter to colony diameter (Majidi et al., 2011).

Phosphate solubilization

To assess phosphate solubilization ability, a five-mm agar plug of the endophytic isolate was placed in the center of a plate containing the Sperber medium (Sperber, 1958) prepared with insoluble phosphate. Before autoclaving, the medium pH was adjusted to 7.2. The cultures were incubated at 25°C for 7 days. Then, solubilization index was evaluated based on the ratio of the clear zone diameter to colony diameter.

Greenhouse experiments

Additionally, the two-year-old seedlings of Golab apple cultivar., which is sensitive to apple scab disease, were utilized in this study. The pathogenicity test was first conducted to ensure the pathogenicity of *V. inaequalis* isolate and optimize the greenhouse conditions for further tests. The conidia suspension (10^5 conidia/ml) of *V. inaequalis* was sprayed on the apple leaves. Further, all of the inoculated branches were individually covered with plastic bags for maintaining a relative humidity of 100% for 48 h. Then, the pots were kept in a greenhouse with the humidity of >80% at 18–20°C, followed by the daily monitoring of the symptom appearance.

The selected endophytic isolates were tested for biological control potential. For this purpose, the apple seedlings were inoculated with endophytic isolates at a final concentration of 10^8 conidia/ml. At 48 h after antagonist inoculation, *V. inaequalis* suspension was inoculated. To do this, as we needed much amount of pathogen suspension, hyphal suspension of the pathogen was prepared from 3-week-old colony grown on PDA (in 6 cm plates) at 25°C and homogenized in distilled water. The culture of the isolate was put into a mortar and ground with a small amount of sterile water to make a syrupy suspension, and it was sprayed on the apple leaves. Each branch was covered with a plastic bag for 48 h and then kept in a greenhouse with the humidity of >80% at 18–20°C. Three seedlings were sprayed with *V. inaequalis* and sterile distilled water as the positive and negative controls, respectively. Each treatment was performed on three seedlings, the tests were repeated twice, and the symptom appearance was examined daily. The infection percentage was determined by measuring individual leaf area and disease symptoms after 1 month of pathogen inoculation. Finally, the disease inhibition rate of each antagonist was calculated compared to the control. To meet Koch's postulates, the pathogen isolate was reidentified morphologically based on structures produced on leaf spots.

Statistical analysis

The experiments were conducted in a completely randomized design and complete randomized block design for *in vitro* and *in vivo* tests, respectively. Data were analyzed by using SAS software version 9.0. All the data were subjected to the analysis of variance (ANOVA) followed by Duncan's multiple range test for determining mean differences (Steel and Torrie, 1980).

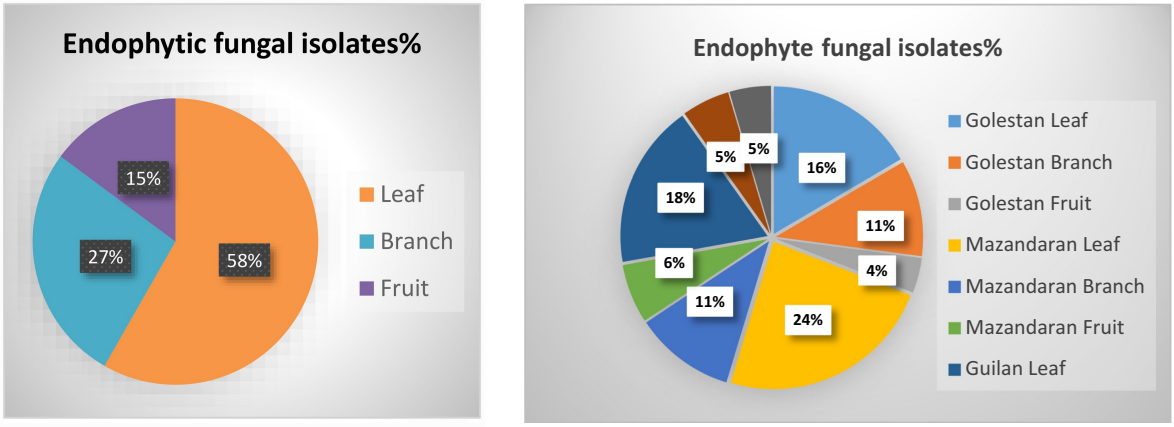

FIGURE 1
Endophytic fungal isolates were obtained from leaf, branch and fruit samples of wild and endemic apple cultivars collected from Golestan, Mazandaran and Guilan provinces of Iran.

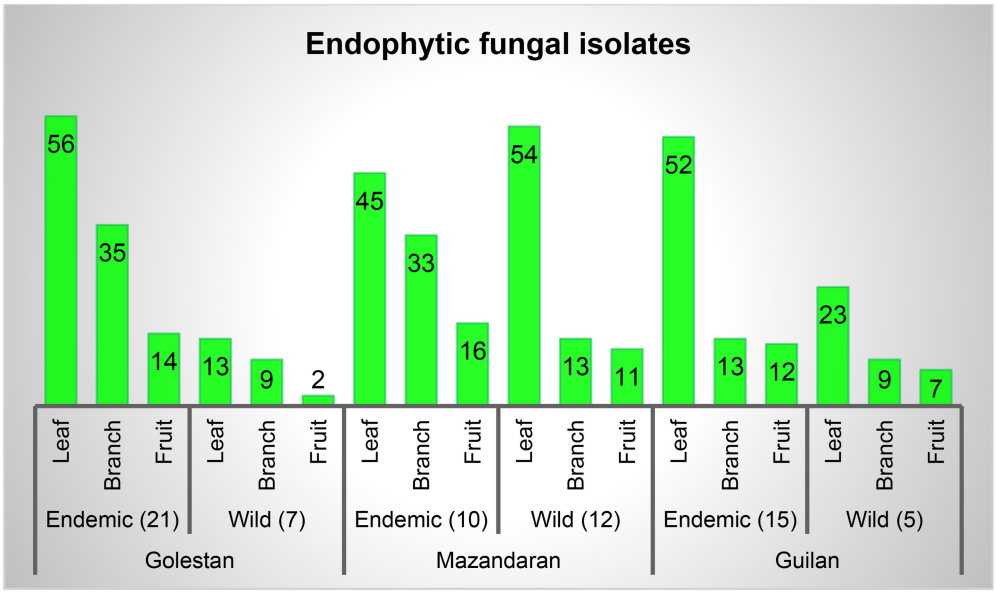

FIGURE 2
Endophytic fungal isolates percentage in leaf, branch and fruit samples, and separately in each province.

Results

Endophytic fungal isolates

A total of 70 apple samples (each consisted of branch, leaf, and fruit) were collected, of which 28 (21 endemic and 7 wild apple), 22 (10 endemic and 12 wild apple), and 20 (15 endemic and 5 wild apple) were gathered from Golestan, Mazandaran, and Guilan provinces, respectively (Figure 1). In addition, 417 endophytic fungal isolates were obtained, among which 129 (16% leaf, 11% branch, 4% fruit), 172 (24% leaf, 11% branch, 6% fruit), and 116 (18% leaf, 5% branch, 5% fruit) were, respectively, related to Golestan, Mazandaran, and Guilan provinces (Figures 1, 2).

Based on the morphological characteristics, 33 fungal genera were detected in the purified fungal isolates (Figure 3). Among these genera, 38 species were identified by considering the morphological properties and molecular data of *gapdh* (Figure 4), *tef-1α* (Figure 5), and ITS (Figure 6) genomic regions (Table 1). The results indicated the assignment of the detected isolates to Ascomycota (67.8%), mycelia sterilia (31.4%), Basidiomycota (0.48%), and Mucoromycota (0.24%). The species of *Coprinopsis atramentaria* (Bull.) Redhead, Vilgalys & Moncalvo, and *Gloeophyllum trabeum* (Pers.) Murrill, N. Amer. Fl. belonged to

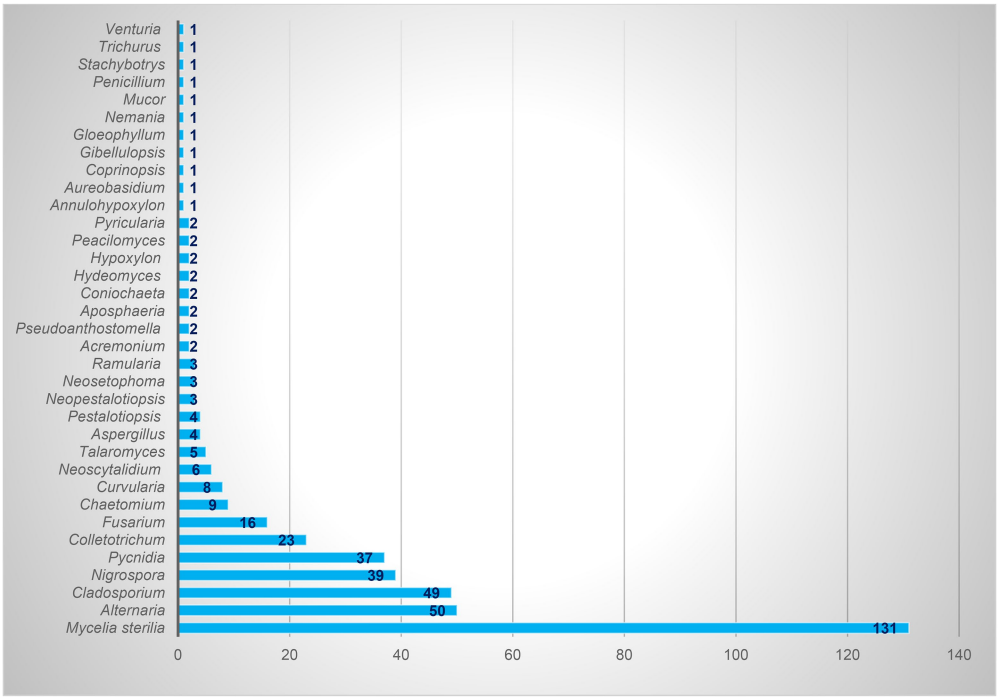

FIGURE 3
Total isolates of each identified endophytic genus.

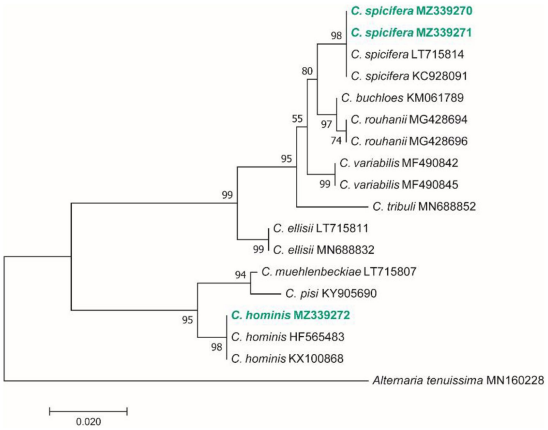

FIGURE 4
Maximum Likelihood (ML) tree based on aligned sequences of *gapdh* gene of 18 isolates generated in MEGA 7 under TN93+G model. The tree was rooted to *Alternaria tenuissima* (IRAN 2428C). Bootstrap values (1,000 replicates) indicated at the nodes. The scale bar indicates nucleotide substitution in ML analysis, values ≥50% are shown above/below the branches. The surveyed isolates in the current study are highlighted in bold.

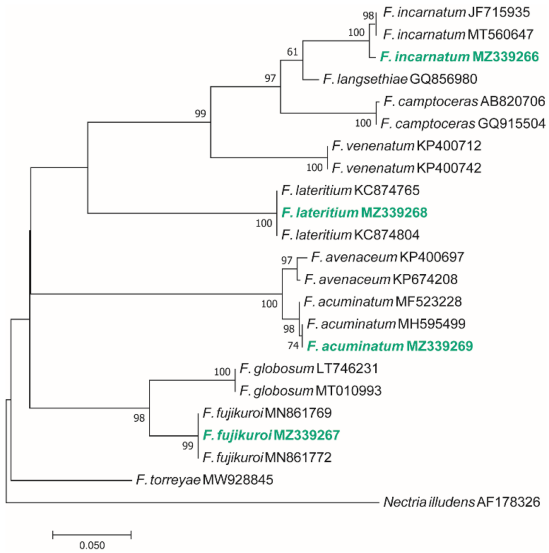

FIGURE 5
Maximum Likelihood (ML) tree based on aligned sequences of *tef-1α* gene of 23 isolates generated in MEGA 7 under K2+I model. The tree was rooted to *Nectria illudens* (NRRL 22090). Bootstrap values (1,000 replicates) indicated at the nodes. The scale bar indicates nucleotide substitution in ML analysis, values ≥50% are shown above/below the branches. The surveyed isolates in the current study are highlighted in bold.

orders Agaricales and Gloeophyllales from the class Agaricomycetes of Basidiomycota, respectively. The identified species of Ascomycota were categorized into the three classes of Sordariomycetes, Dothideomycetes, and Eurotiomyetes (Figure 6). Further, the Sordariomycetes included seven separate groups related to orders Amphisphaeriales, Xylariales, Hypocreales, Glomerellales, Coniochaetales, Sordariales, as well as another group concerning *Nigrospora* Zimm. genus which is placed in Apiosporaceae, Sordariomycetidae families incertae sedis. The

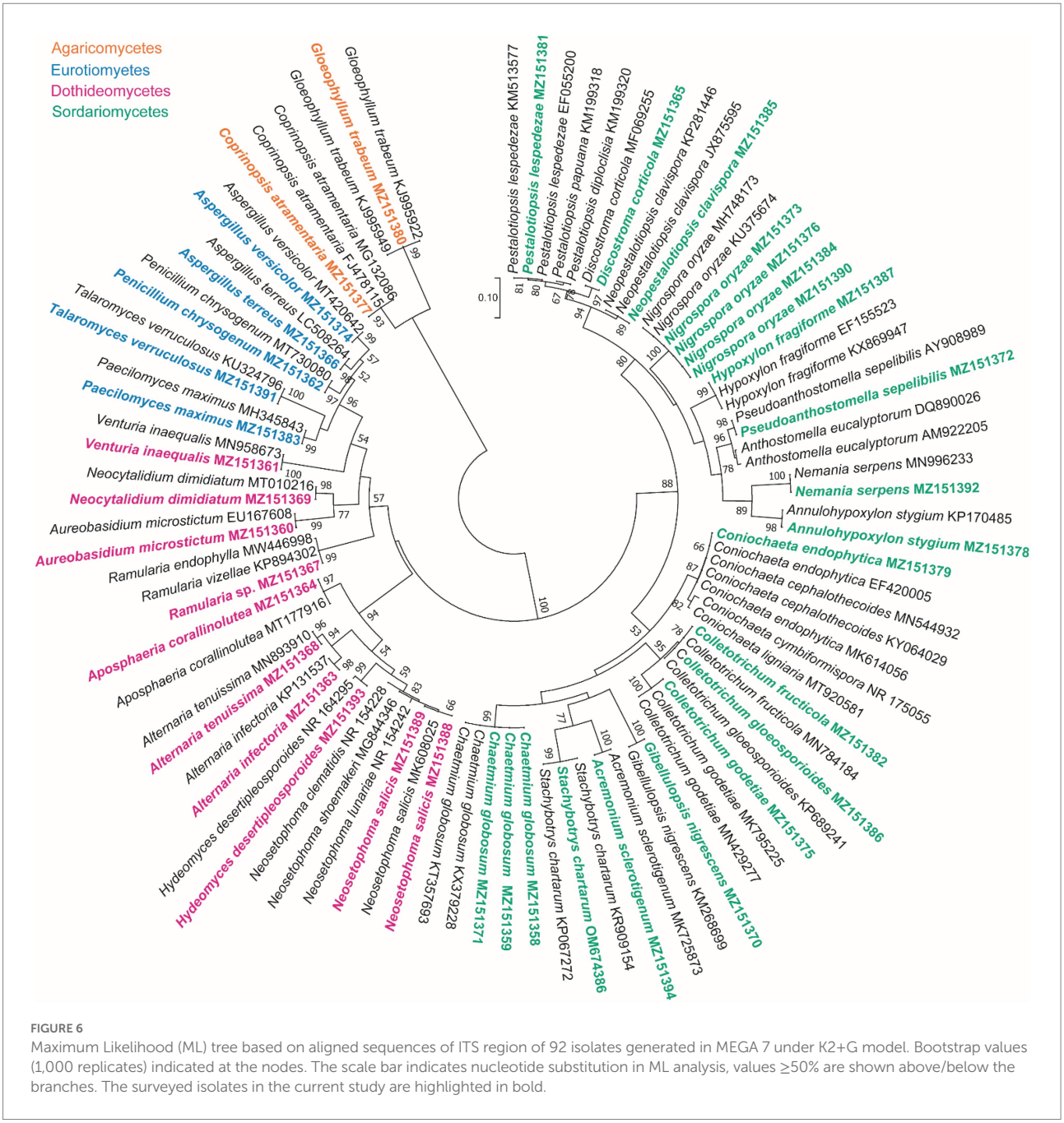

FIGURE 6
Maximum Likelihood (ML) tree based on aligned sequences of ITS region of 92 isolates generated in MEGA 7 under K2+G model. Bootstrap values (1,000 replicates) indicated at the nodes. The scale bar indicates nucleotide substitution in ML analysis, values ≥50% are shown above/below the branches. The surveyed isolates in the current study are highlighted in bold.

members of Dothideomycetes were grouped into the five orders of Venturiales, Pleosporales, Capnodiales, Dothideales, and Botryosphaeriales. The third class, Eurotiomyetes, involved the members of order Eurotiales.

Screening of endophytic fungi for antifungal activity

In this study, the endophytic fungal isolates were evaluated for antifungal activity through employing the cellophane membrane-based method. They were tested in terms of the ability to produce antifungal media-permeable metabolites against *V. inaequalis*. The other approaches such as dual culture assay are not applicable since *V. inaequalis* is a slow-growing fungus. Furthermore, the isolates belonged to the geneus *Alternaria*, *Aspergillus*, *Colletotrichum*, *Neoscytalidium* Crous & Slippers, *Nigrospora*, *Paecilomyces* Bainier, *Pestalotiopsis* Steyaert, *Penicillium* and *Talaromyces* Visagie, N. Yilmaz & K. Jacobs did not exhibit antagonistic effect. The antifungal properties against apple scab agent were observed in 29 isolates (Table 2).

Figures 7, 8 display the results related to the media-permeable metabolites of 29 endophytic isolates on the mycelial growth of *V. inaequalis*. As shown, the metabolites of *Acremonium*

TABLE 2 Antifungal activity of endophytic fungi isolated from apple based on the cellophane membrane-based method.

Endophytic fungi	Antifungal activity
Acremonium sclerotigenum	+*
Alternaria infectoria	–
Alternaria tenuissima	–
Alternaria spp.	–
Annulohypoxylon stygium	±
Aposphaeria corallinolutea	±
Aspergillus terreus	–
Aspergillus versicolor	–
Aureobasidium microstictum	±
Chaetomium globosum	+
Colletotrichum fructicola	–
Colletotrichum gloeosporioides	–
Colletotrichum godetiae	–
Colletotrichum spp.	–
Coniochaeta endophytica	+
Coprinopsis atramentaria	±
Curvularia hominis	+
Curvularia spicifera	+
Discostroma corticola	+
Fusarium acuminatum	+
Fusarium fujikuroi	±
Fusarium incarnatum	±
Fusarium lateritium	+
Gibellulopsis nigrescens	+
Gloeophyllum trabeum	+
Hydeomyces desertipleosporoides	+
Hypoxylon fragiforme	+
Nemania serpens	+
Neopestalotiopsis clavispora	±
Neoscytalidium dimidiatum	–
Neosetophoma salicis	+
Nigrospora oryzae	–
Paecilomyces maximus	–
Penicillium chrysogenum	–
Pestalotiopsis lespedezae	±
Pseudoanthostomella sepelibilis	±
Ramularia sp.	+
Stachybotrys chartarum	+
Talaromyces verruculosus	–

*– Not active; ± slightly active; + active.

sclerotigenum (Moreau & R. Moreau ex Valenta) W. Gams GO13S1, *Coniochaeta endophytica* A.H. Harrington & A.E. Arnold 55S2, and *Fusarium lateritium* Nees 61S2 lead to the maximum growth inhibition (100%) of *V. inaequalis*, followed by *Hydeomyces desertipleosporoides* Maharachch., H.A. Ariyaw., Wanas. & Al-Sadi GO8S2 (87.7%) and *Chaetomium globosum* Kunze 2S1 (78.7%).

Additionally, the VOC production was assessed in the isolates. The VOCs produced by the isolates of *Aureobasidium microstictum* (Bubák) W.B. Cooke 7F2, *Ch. globosum* 2S1, *Ch. globosum* 3 L2, *Coprinopsis atramentaria* 52 L2, *Fusarium fujikuroi* Nirenberg 37F6, *Fusarium acuminatum* Ellis & Everh. GO2L1, and *Fusarium incarnatum* (Desm.) Sacc. 25S3 completely prevented the mycelia growth of *V. inaequalis*. However, the minimum pathogen growth inhibition was detected in the VOCs of *Annulohypoxylon stygium* (Lév.) Y.M. Ju, J.D. Rogers & H.M. Hsieh 54 L1 (12.4%) and *Hypoxylon fragiforme* (Pers.) J. Kickx f. GO2L3 (9.6%). The VOCs of other isolates except *Aposphaeria corallinolutea* Gruyter, Aveskamp & Verkley 17S2 and *Discostroma corticola* (Fuckel) Brockmann 22S4 inhibited pathogen mycelia growth by more than 70% (Figures 9, 10).

Phosphate solubilization and enzyme activity

Based on the results of the biological control tests, six isolates were selected for further evaluation, of which *Co. endophytica* 55S2 and *F. lateritium* 61S2 could solubilize inorganic phosphate with the ratio of 1.2 and 1.07, respectively (Table 3). All isolates except *Ch. globosum* 3 L2 represented cellulase activity, which the highest halo zone/colony diameter ratio (2.62) was recorded for *Au. microstictum* 7F2 (Table 3). Further, chitinase activity was observed in the isolates of *Ch. globosum* 2S1, *Ch. globosum* 3L2, and *F. lateritium* 61S2 with the halo zone/colony diameter ratio of 1.2, 1.2, and 1.1, respectively (Table 3).

Biocontrol assays under greenhouse conditions

As already mentioned, six isolates were further tested in whole-plant tests under greenhouse conditions. The results demonstrated a significant reduction in the apple scab severity after 1 month when endophytes were inoculated on the leaves 48 h before pathogen (Figures 11, 12). The *in vivo* tests revealed the complete control of apple scab disease by *Co. endophytica* 55S2 and *Ch. globosum* 2S1. Furthermore, the decrease in the apple scab severity was similar for *F. lateritium* 61S2 and *Ch. globosum* 3 L2, which ranged between 50 (*F. lateritium* 61S2) and 62% (*Ch. globosum* 3L2). Finally, *Au. microstictum* 7F2 and *Ac. sclerotigenum* GO13S1 declined the disease severity by 37.5% (Figures 11, 12).

Discussion

The plant-associated habitat is considered as a dynamic environment, in which many factors affect the structure and composition of the species colonizing various tissues. The endophytic communities may spatially vary in many kinds of plants (Rivera-Orduña et al., 2011). In addition, microorganism population can be different in natural forest and agroecosystem due to the use of synthetic chemicals by

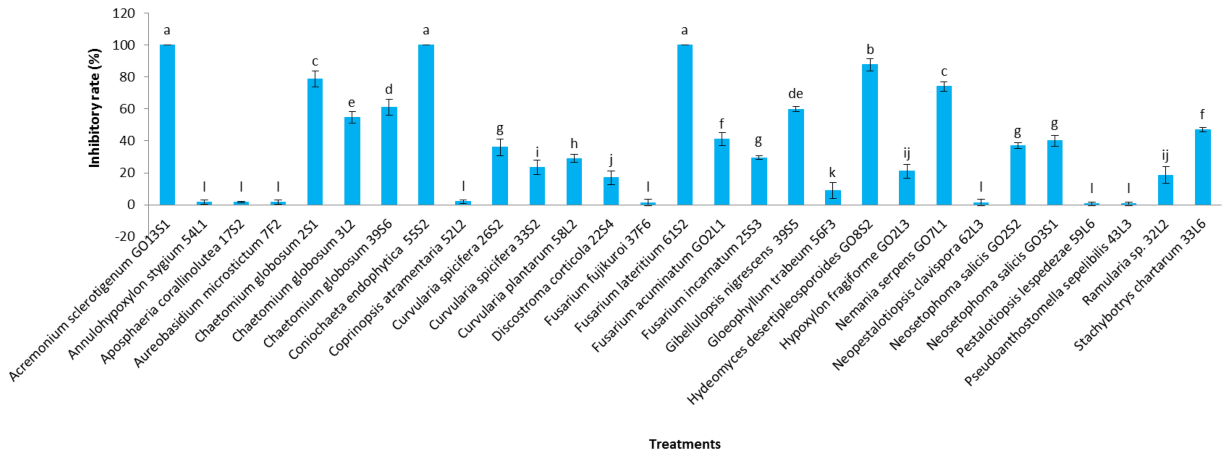

FIGURE 7
Effect of media-permeable metabolites of endophytic fungi isolated from apple on *Venturia inaequalis* mycelia growth after 1 month *in vitro*. Data are the means ± SE of three replicates. Values of histograms with common letters are not significantly different at $p \leq 0.01$ according to Duncan's multiple range test.

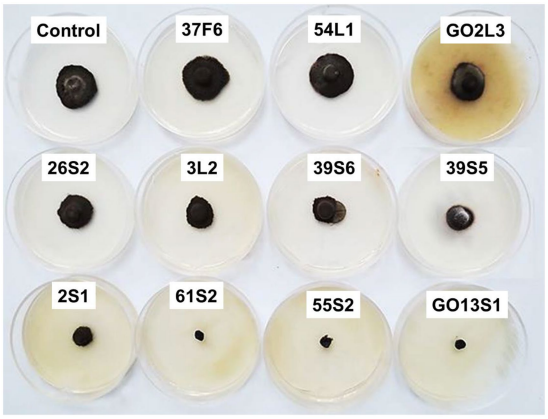

FIGURE 8
Effect of media-permeable metabolites of endophytic fungi isolated from apple on *Venturia inaequalis* mycelia growth in comparison to control after 1 month *in vitro*.

farmers. The present study highlighted the endophytic fungi associated with the wild and Iranian endemic apple cultivars which are mostly spread along the Caspian Sea coast in the north of Iran. The results revealed the differences in the apple branch, fruit, and leaf tissues in terms of the richness and abundance of endophytic fungi. Among the 417 endophytic isolates under study, 243, 112, and 62 were obtained from leaves, branches, and fruits, respectively. Generally, leaves carry more endophytic fungi than the stem due to the exposure of larger surface area to the outer environment and presence of numerous stomata which facilitate the entry of fungal hyphae (Gond et al., 2012). Camatti-Sartori et al. (2005) reported the greatest total number of endophytic isolates from the orchards under organic cultivation compared to the integrated and conventional cultivation systems. Alijani et al. (2016a) separated 14.37, 28.34, and 57.28% of endophytic fungal isolates from the apple leaf, annual and biennial branches, and bark in the commercial orchards of West Azerbaijan province, Iran (n: 350). These results are inconsistent with those of the present study regarding endophytic fungal diversity on the wild and endemic apple cultivars from the forests and natural regions. Alijani et al. (2016a) suggested the possible effect of fungicide application in commercial orchard on the endophytic fungal abundance of apple leaves. However, many other factors such as climate, orchard location, and host cultivar may influence the abundance and diversity of endophytic fungi. Afandhi et al. (2018) found that the abundance and diversity of endophytic fungi were maximized in mature apple leaves compared to the young and old ones. According to Arrigoni et al. (2020), bark age and orchard location strongly affected fungal and bacterial diversity. Further, scab disease management had an effect on the abundance of some taxa depending on bark age, orchard location, and sampling time (Arrigoni et al., 2020). Interestingly, Olivieri et al. (2021) mentioned the presence of significant differences between canker-resistant and susceptible apple cultivars with respect to the endophyte community.

In the present study, 417 endophytic fungi were separated from apple, which mostly belonged to Ascomycota (77.93%). The genera *Alternaria*, *Cladosporium*, *Nigrospora*, *Colletotrichum*, *Fusarium*, *Chaetomium*, and *Curvularia* were the most frequent fungi, the isolate number of which was 50, 49, 39, 23, 16, 9, and 8, respectively. Camatti-Sartori et al. (2005) identified genera *Colletotrichum*, *Xylaria*, and *Botryosphaeria* as the most common endophytic fungi of apple in Brazil. Based on the results of Liu

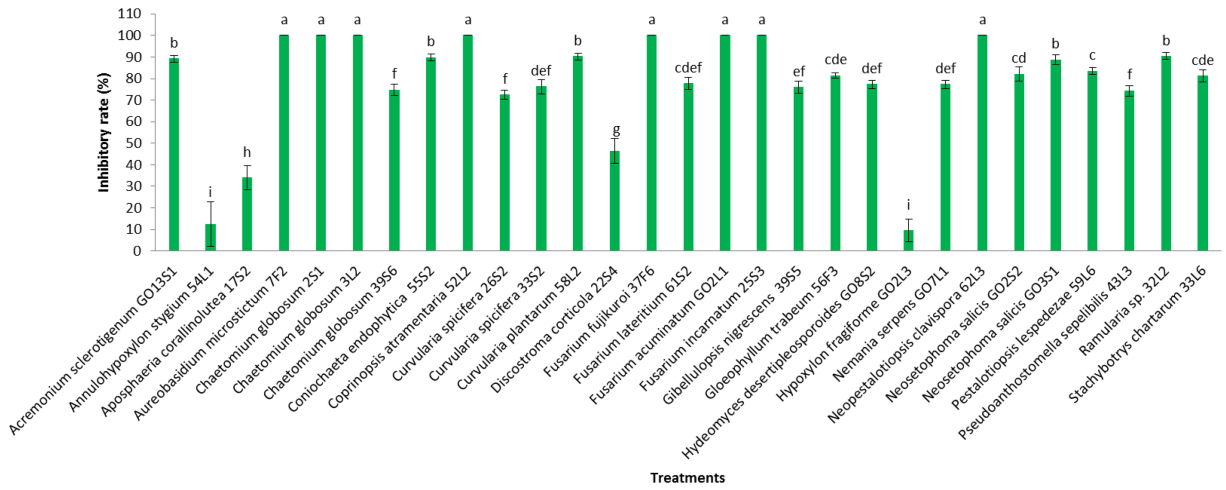

FIGURE 9
Effect of volatile organic compounds of endophytic fungi isolated from apple on *Venturia inaequalis* mycelia growth after 1 month *in vitro*. Data are the means ± SE of three replicates. Values of histograms with common letters are not significantly different at $p \leq 0.01$ according to Duncan's multiple range test.

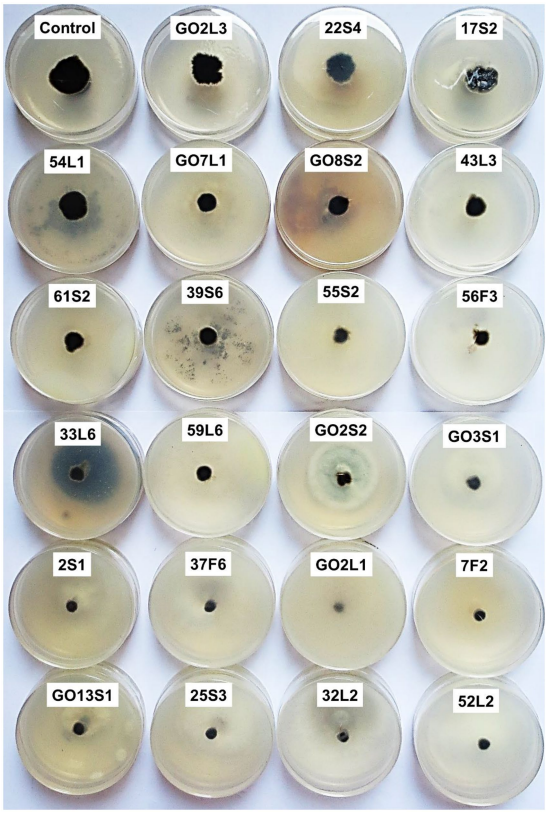

FIGURE 10
Effect of volatile organic compounds of endophytic fungi isolated from apple on *Venturia inaequalis* mycelia growth in comparison to control after 1 month *in vitro*.

TABLE 3 Phosphate solubilization and enzyme activity of selected isolates.

Endophytic fungi	Cellulase	Chitinase	Phosphate solubilization
Acremonium sclerotigenum GO13S1	1.96 ± 0.05	0.0 ± 0.00	0.0 ± 0.00
Aureobasidium microstictum 7F2	2.62 ± 0.13	0.0 ± 0.00	0.0 ± 0.00
Chaetomium globosum 2S1	1.03 ± 0.00	1.2 ± 0.05	0.0 ± 0.00
Chaetomium globosum 3 L2	0.00 ± 0.00	1.2 ± 0.00	0.0 ± 0.00
Coniochaeta endophytica 55S2	1.67 ± 0.03	0.0 ± 0.00	1.2 ± 0.05
Fusarium lateritium 61S2	1.25 ± 0.03	1.1 ± 0.04	1.07 ± 0.0

The means halo zone diameter/ colony diameter of three replications ± standard deviation is represented.

et al. (2018), Ascomycota (47.8%), Mucoromycota (31.1%), and Basidiomycota (11.6%) were the dominant endophytic fungal phyla in all apple samples studied in the USA. In general, *Zoophthora* Bałazy & Manole (31%), *Cladosporium* (17.3%), and *Aureobasidium* (11%) constituted more than 59% of the detected fungi, and the next genera were *Alternaria* (5.6%) and *Aspergillus* (1.6%), respectively (Liu et al., 2018). Alijani et al. (2016a,b) reported the presence of 12 genera of endophytic fungi, *Alternaria*, *Arthrinium*, *Aspergillus*, *Chaetomium*, *Cytospora* Ehrenb., *Dicyma*, *Doratomyces*, *Paraconiothyrium*, *Periconia* Tode, *Stemphylium*, *Trichoderma*, and *Trichothecium*, on the apple cultivated in the West Azerbaijan province, Iran. Muresan (2017) gathered a collection of 60 fungal isolates, mostly obtained from apple tree roots (78%) in Canada, 60% of which were *Penicillium* or *Trichoderma* species. Liu et al. (2017) referred to *Epicoccum*, *Chaetomium*, *Biscogniauxia*, *Neoseptophoma*, and *Penicillium* as the most species identified in the culturable endophytes from apple shoots in New Zealand. According to Afandhi et al. (2018), *Aspergillus* was dominant in the endophytic fungal isolates of apple.

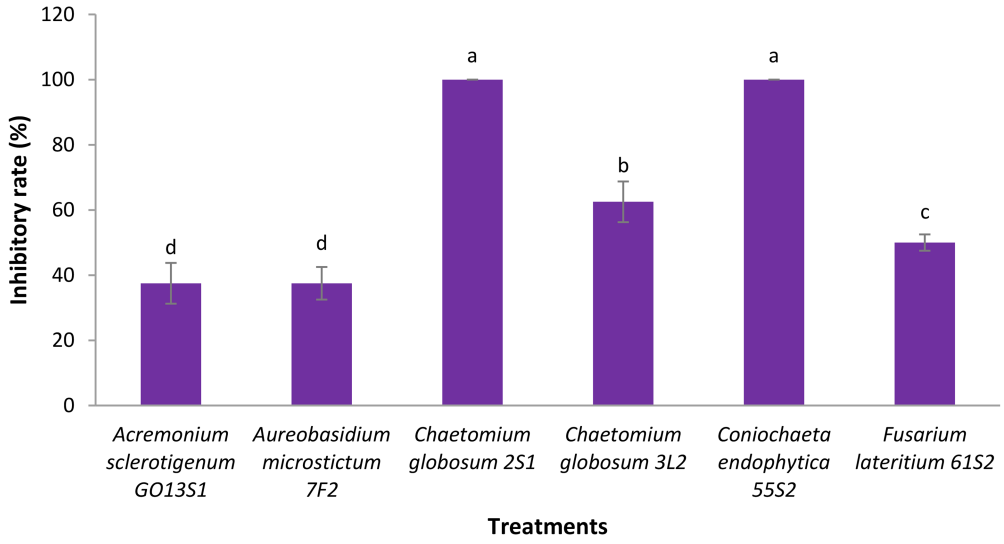

FIGURE 11
Antagonistic effect of endophytic fungi isolated from apple against apple scab disease on apple seedling after 1 month of pathogen inoculation under greenhouse conditions. Data are the means ± SE of three replicates. Values of histograms with common letters are not significantly different at $p \leq 0.01$ according to Duncan's multiple range test.

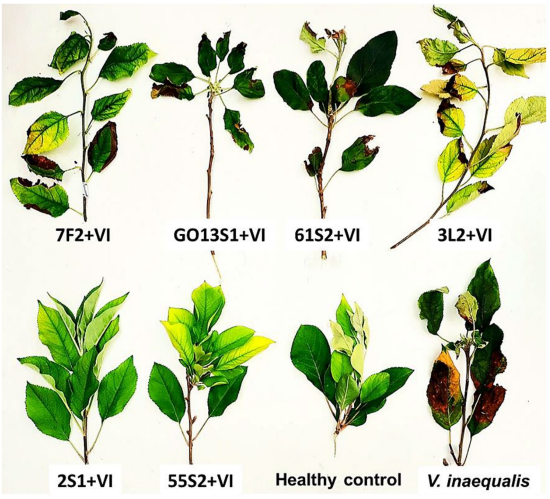

FIGURE 12
Effect of endophyte isolates on development of symptoms caused by *Venturia inaequalis* on apple leaves at 18–20°C after 1 month of pathogen inoculation in greenhouse. (Treatments: *Aureobasidium microstictum* 7F2, *Acremonium sclerotigenum* GO13S1, *Fusarium lateritium* 61S2, *Chaetomium globosum* 3L2, *Chaetomium globosum* 2S1, *Coniochaeta endophytica* 55S2, VI: *Venturia inaequalis*).

The biological control of plant pathogens instead of synthetic fungicides adequately protects plants, humans and other animals, and natural environment. The endophytic fungi play a key role in plant protection against biotic and abiotic stresses (Lugtenberg et al., 2016) through the various modes of action such as the mycoparasitism, antibiosis, competition, and plant resistance induction (Latz et al., 2018). The mechanisms may act coordinately, and their importance in the biological control process depends on the antagonist strain, pathogenic fungus, host plant, and environmental conditions (Golafrouz et al., 2020).

Many active metabolites are produced by antagonistic fungi, some of which possess significant biological activities like cytotoxicity, enzyme inhibition, and antibiosis (Yang S. X. et al., 2011; Yang S. Z. et al., 2011). Furthermore, some antagonistic fungi secrete various hydrolytic enzymes such as chitinase, glucanase, and protease to effectively digest the cell walls of their competitors, inhibit their ss growth, or surpass their capacity for metabolizing available resources leading to competitive exclusion in substrate (Wilkins et al., 2003). The endophytic fungi colonize plant tissues, as well as obtaining nutrients and highly-active cellulases produced to help the host plant defend themselves against invading pathogens (Marques et al., 2018). Therefore, some enzyme activities of endophytes such as cellulase are important in biological control. Additionally, phosphorus is known as a major plant nutrient, the insoluble calcium phosphate salts of which are mostly formed in the presence of a high concentration of calcium ions (Chen and Barak, 1982). Thus, the ability of endophytes to solubilize inorganic phosphate can help plant by improving their growth. In the present study, the six isolates of *Ac. sclerotigenum* GO13S1, *Co. endophytica* 55S2, *F. lateritium* 61S2, *Au. microstictum* 7F2, *Ch. globosum* 2S1, and *Ch. globosum* 3 L2 were selected for greenhouse tests based on the results of media-permeable metabolites and VOC tests. Among the intended isolates, *Co. endophytica* 55S2 and *F. lateritium* 61S2 had the ability to solubilize inorganic phosphate, which the ability should be investigated in soil environment to affects plant growth and disease biocontrol. The cellulase activity was observed in all

isolates except *Ch. globosum* 3 L2, while *Ch. globosum* 2S1, *Ch. globosum* 3 L2, and *F. lateritium* 61S2 exhibited chitinase activity. The results demonstrated the successful biological control of apple scab disease following the use of endophytic fungi in greenhouse so that *Co. endophytica* 55S2 and *Ch. globosum* 2S1 completely controlled the disease on apple seedling leaves.

The various studies around the world have revealed the biological control potential of different apple endophytic fungi against apple fungal pathogens. For example, Alijani et al. (2016b) evaluated the antifungal potential of 15 endophytic species of apple against *D. bulgarica in vitro*. They found that pathogen mycelia growth significantly reduced by *Trichoderma harzianum* Rifai and *Trichoderma longibrachiatum* Rifai. According to Muresan (2017), 55 endophytic isolates of apple among 60 ones significantly prevented *V. inaequalis* growth *in vitro* and *F. oxysporum* FRS09 was determined as the most effective isolate with 83% inhibition. Doolotkeldieva and Bobusheva (2017) examined the two biological control agents of *Trichoderma viride* Pers. and *Streptomyces* sp. against apple scab disease *in vitro* and field conditions. The application of *T. viride* within 35 days completely stopped the disease in seedling leaves, while *Streptomyces* sp. isolates were less effective than the *T. viride*. Further, there was a diverse range of potential biological control agents for organic apple production. Liu et al. (2017) reported the potential of the endophytes isolated from apple tissues (i.e., *Epicoccum*, *Chaetomium*, *Biscogniauxia*, *Neoseptophoma*, and *Penicillium*) for using in the sustainable control of *N. ditissima*. *Chaetomium globosum* is one of the most common species utilized in biological control against various phytopathogens such as *V. inaequalis* (Soytong and Ratanacherdchai, 2005; Zhang et al., 2010). The results of thin-layer chromatography studies reflected the production of different secondary metabolites such as chetomin, BHT, mollicelin G along with chaetoglobosin by this species (Biswas et al., 2012). Several *Chaetomium* spp. such as *Ch. cupreum* L.M. Ames and *Ch. globosum* produce resistance-inducing substances which prevent many plant diseases like *Pythium aphanidermatum* (Edson) Fitzp. in sugarcane, wilt symptoms in grain seedlings, and apple scab incited by *Venturia* spp., as well as decreasing tomato Fusarium wilt, and inhibiting the growth of pathogenic *Rhizoctonia solani* J.G. Kühn and *Botrytis* spp. (Soytong and Ratanacherdchai, 2005).

Conclusion

In this study, we have identified *Co. endophytica* 55S2, and *Ch. globosum* 2S1 as the most potent endophytic fungal isolates for controlling apple scab disease caused by *V. inaequalis* under greenhouse conditions. These isolates could therefore be considered the best candidates for development of endophytic-based biofungicide and could be integrated as a component in a sustainable integrated apple management strategy for scab. However, further studies are warranted to clearly understand the underlying mechanisms by which the presence of endophytic fungi affect *V. inaequalis* as well as validate the findings under field conditions on different cultivars of apple.

Data availability statement

The data presented in the study are deposited in the GenBank repository, accession numbers presented in Table 1.

Author contributions

LE designed and directed the research and wrote the manuscript. HE gave advice during experiments. LE and SHR carried out experiments. All authors contributed to the interpretation of the results. All authors contributed to the article and approved the submitted version.

Funding

This work was supported by the Iran National Science Foundation (INSF) (Grant No. 97021003), and University of Tehran, Iran.

Acknowledgments

We gratefully acknowledge the Iran National Science Foundation (INSF), and University of Tehran, Iran, for financial support.

Conflict of interest

The authors declare that the research was conducted in the absence of any commercial or financial relationships that could be construed as a potential conflict of interest.

Publisher's note

Supplementary material

The Supplementary material for this article can be found online at: https://www.frontiersin.org/articles/10.3389/fmicb.2022.1024001/full#supplementary-material

References

Adhikari, P., and Pandey, A. (2019). Phosphate solubilization potential of endophytic fungi isolated from *Taxus wallichiana* Zucc. *Roots Rhizosphere* 9, 2–9. doi: 10.1016/j.rhisph.2018.11.002

Afandhi, A., Choliq, F. A., Anggrilika, W. S. H., and Tarno, H. (2018). Distribution of the endophytic fungi in apple leaves. *Agri* 40, 91–100. doi: 10.17503/agrivita.v40i1.1563

Alijani, N., Ghosta, Y., and Rezaiie-Danesh, Y. (2016a). Biodiversity of endophytic fungi from apple trees in West Azerbaijan province. Proceeding of 22nd Iranian Plant Protection Congress 27–30 August. College of Agriculture and Natural Resources, University of Tehran, Karaj, Iran 155.

Alijani, N., Manafi Shabestari, M., and Ghosta, Y. (2016b). Biocontrol effects of endophytic fungi isolated from apple trees against *Diplodia bulgarica*, the causal agent of apple canker disease. Proceeding of 22nd Iranian Plant Protection Congress, August. College of Agriculture and Natural Resources, University of Tehran, Karaj, Iran.

Arrigoni, E., Antonielli, L., Longa, C. M. O., Angeli, D., Donati, C., Ioriatti, C., et al. (2020). Tissue age, orchard location and disease management influence the composition of fungal and bacterial communities present on the bark of apple trees. *Environ. Microbiol.* 22, 2080–2093. doi: 10.1111/1462-2920.14963

Berbee, M. L., Pirseyedi, M., and Hubbard, S. (1999). *Cochliobolus* phylogenetics and the origin of known, highly virulent pathogens, inferred from ITS and glyceraldehyde-3-phosphate dehydrogenase gene sequences. *Mycologia* 91, 964–977. doi: 10.1080/00275514.1999.12061106

Berger, L. R., and Reynolds, D. M. (1958). The chitinase system of a strain of *Streptomyces griseus*. *Biochim. Biophys. Acta* 29, 522–534. doi: 10.1016/0006-3002(58)90008-8

Biswas, S. K., Rashmi, A., Srivastava, K. D., Sangeeta, G., and Prem, D. (2012). Characterization of antifungal metabolites of Chaetomium globosum Kunze and their antagonism against fungal plant pathogens. *J. Biol. Control.* 26, 70–74. doi: 10.18641/jbc/26/1/45659

Camatti-Sartori, V., Da Silva-Ribeiro, R. T., Valdebenito-Sanhueza, R. M., Pagnocca, F. C., Echeverrigaray, S., and Azevedo, J. L. (2005). Endophytic yeasts and filamentous fungi associated with southern Brazilian apple (*Malus domestica*) orchards subjected to conventional, integrated or organic cultivation. *J. Basic Microbiol.* 45, 397–402. doi: 10.1002/jobm.200410547

Cenis, J. L. (1992). Rapid extraction of fungal DNA for PCR amplification. *Nucleic Acids Res.* 20:2380. doi: 10.1093/nar/20.9.2380

Chen, Y., and Barak, P. (1982). Iron nutrition of plants in calcareous soils. *Adv. Agron.* 35, 217–240. doi: 10.1016/S0065-2113(08)60326-0

Chen, X., Wang, Y., Gao, Y., Gao, T., and Zhang, D. (2019). Inhibitory abilities of *bacillus* isolates and their culture filtrates against the gray mold caused by *Botrytis cinerea* on post-harvest fruit. *Plant Pathol. J.* 35, 425–436. doi: 10.5423/PPJ.OA.03.2019.0064

Dennis, C., and Webster, J. (1971). Antagonistic propertics of specific group of *Trichoderma*: production of non-volatile antibiotics. *Trans. Br. Mycol. Soc.* 57, 25–IN3. doi: 10.1016/S0007-1536(71)80078-5

Doolotkeldieva, T., and Bobusheva, S. (2017). Scab disease caused by *Venturia inaequalis* on apple trees in Kyrgyzstan and biological agents to control this disease. *Adv. Appl. Microbiol.* 07, 450–466. doi: 10.4236/aim.2017.76035

Ebrahimi, L., and Fotouhifar, K.-B. (2016). First report of *Cyphellophora fusarioides* (Chaetothyriales) on a plant host. *Sydowia* 68, 131–137. doi: 10.12905/0380.sydowia68-2016-0131

Ebrahimi, L., Fotuhifar, K. B., Javan Nikkhah, M., Naghavi, M. R., and Baisakh, N. (2016). Population genetic structure of apple scab (*Venturia inaequalis* (coo.Ke) G. winter) in Iran. *PLoS One* 11:e0160737. doi: 10.1371/journal.pone.0160737

Ebrahimi, L., Hatami Rad, S., Ayenekar, T., Agh-Atabay, M. E., Moghimi, H., and Etebarian, H. R. (2021). New records of apple endophytic fungi for the Funga of Iran. *Mycologia Iranica* 8, 31–39. doi: 10.22043/MI.2022.358420.1214

Ellis, M. B. (1971). *Dematiaceous Hyphomycetes*. Commonwealth Mycological Institute, Kew, England

Ellis, M. B. (1976). *More dematiaceous Hyphomycetes*. Commonweath Mycological Institute, Kew, England.

Etebarian, H. R., Sholberg, P. L., Eastwell, K. C., and Sayler, R. J. (2005). Biological control of apple blue mold with *Pseudomonas fluorescens*. *Can. J. Microbiol.* 51, 591–598. doi: 10.1139/w05-039

Felsenstein, J. (1981). Evolutionary trees from DNA sequences: a maximum likelihood approach. *J. Mol. Evol.* 17, 368–376. doi: 10.1007/BF01734359

Felsenstein, J. (1985). Confidence intervals on phylogenies: an approach using bootstrap. *Evolution* 39, 783–791. doi: 10.1111/j.1558-5646.1985.tb00420.x

Gimenez, C., Cabrera, R., Reina, M., and Gonzalez-Coloma, A. (2007). Fungal endophytes and their role in plant protection. *Curr. Org. Chem.* 11, 707–720. doi: 10.2174/138527207780598765

Golafrouz, H., Safaie, N., and Khelghatibana, F. (2020). The reaction of some apple rootstocks to biocontrol of white root rot *Rosellinia necatrix* by *Trichoderma harzianum* in greenhouse. *J. Crop Prot.* 9, 577–589. doi: 20.1001.1.22519041.2020.9.4.11.4

Gond, S. K., Mishra, A., Sharma, V. K., Verma, S. K., Kumar, J., Ravindra, N., et al. (2012). Diversity and antimicrobial activity of endophytic fungi isolated from *Nyctanthes arbor-tristis*, a well-known medicinal plant of India. *Mycoscience* 53, 113–121. doi: 10.1007/S10267-011-0146-Z

Hartl, L., Zach, S., and Seidl-Seiboth, V. (2012). Fungal Chitinases: diversity, mechanistic properties, and biotechnological applications. *Appl. Microbiol. Biotechnol.* 93, 533–543. doi: 10.1007/s00253-011-3723-3

Hsu, S. C., and Lockwood, J. L. (1975). Powdered chitin agar as a selective medium for enumeration of Actinomycetes in water and soil. *Appl. Microbiol.* 29, 422–426. doi: 10.1128/am.29.3.422-426.1975

Klich, M. A. (2002). *Identification of Common Aspergillus Species*. Central voor Schimmeltures, Uterch, The Netherlands.

Klich, M. A., and Pitt, J. I. (1988). *A Laboratory Guide to the Common aspergillus Species and their Teleomorphs*. Commonwealth Scientific and Industrial Research Organization, Division of Food Processing, Australia, Canberra

Kumar, S., Stecher, G., and Tamura, K. (2016). MEGA 7: molecular evolutionary genetics analysis version 7.0 for bigger dataset. *Mol. Biol. Evol.* 33, 1870–1874. doi: 10.1093/molbev/msw054

Latz, M. A. C., Jensen, B., Collinge, D. B., and Jørgensen, H. J. L. (2018). Endophytic fungi as biocontrol agents: elucidating mechanisms in disease suppression. *Plant Ecol. Divers.* 11, 555–567. doi: 10.1080/17550874.2018.1534146

Leslie, J. F., and Summerell, B. A. (2006). *The Fusarium Laboratory Manual*. Blackwell Publishing. Hoboken

Li, H., Dou, M., Wang, X., Guo, N., Kou, P., Jiao, J., et al. (2021). Optimization of cellulase production by a novel endophytic fungus *Penicillium oxalicum* R4 isolated from *Taxus cuspidata*. *Sustainability* 13:6006. doi: 10.3390/su13116006

Li, X., Zhou, J., Xu, R. S., Meng, M., Yu, X., and Dai, C. C. (2018). Auxin, cytokinin, and ethylene involved in rice N availability improvement caused by endophyte Phomopsis liquidambari. *J. Plant Growth Regul.* 37, 128–143. doi: 10.1007/s00344-017-9712-8

Lillbro, M. (2005). Biocontrol of *Penicillium roqueforti* on grain-acomparison of mode of action of several yeast species Master thesis of the Agriculture Program, Animal Science, performed at the Department of Microbiology. Swedish University of Agricultural Sciences, Uppsala.

Liu, J., Abdelfattah, A., Norelli, J., Burchard, E., Schena, L., Droby, S., et al. (2018). Apple endophytic microbiota of different rootstock/scion combinations suggests a genotype-specific influence. *Microbiome* 6:18. doi: 10.1186/s40168-018-0403-x

Liu, J., Ridgway, H. J., and Jones, E. E. (2017). Identification of culturable endophytes isolated from apple tissues with antagonism towards *Neonectria ditissima*. Science protecting plant health. September 23–29. New Zealand.

Lugtenberg, B. J. J., Caradus, J. R., and Johnson, L. J. (2016). Fungal endophytes for sustainable crop production. *FEMS Microbiol. Ecol.* 92, 1–17. doi: 10.1093/femsec/fiw194

MacHardy, W. E. (1996). *Apple Scab: Biology, Epidemiology, and Management*. APS Press: St. Paul, Minnesota

Majidi, S., Roayaei, M., and Ghezelbash, G. (2011). Carboxymethyl-cellulase and filter-paperase activity of new strains isolated from Persian gulf. *Microbiol. J.* 1, 8–16. doi: 10.3923/mj.2011.8.16

Marques, N. P., de Cassia Pereira, J., Gomes, E., da Silva, R., Araújo, A. R., Ferreira, H., et al. (2018). Cellulases and xylanases production by endophytic fungi by solid state fermentation using lignocellulosic substrates and enzymatic saccharification of pretreated sugarcane bagasse. *Ind. Crop. Prod.* 122, 66–75. doi: 10.1016/j.indcrop.2018.05.022

Meenavalli, B., Rajulu, G., Thirunavukkarasu, N., Suryanarayanan, T. S., Ravishankar, J. P., Gueddari, N. E. E., et al. (2011). Chitinolytic enzymes from Endophytic fungi. *Fungal Divers.* 47, 43–53. doi: 10.1007/s13225-010-0071-z

Muresan, L. E. (2017). Cultivable bacterial and fungal endophytes from apple tissues and their potential for biological control of *Venturia inaequalis* Master thesis Environmental Sciences, University of Guelph. Canada

O'Donnell, K., Kistler, H. C., Cigelink, R., and Ploetz, R. C. (1998). Multiple evolutionary origins of the fungus causing Panama disease of banana: concordant evidence from nuclear and mitochondrial gene genealogies. *Proc. Nat. Acad. Sci. U. S. A.* 95, 2044–2049. doi: 10.1073/pnas.95.5.2044

Olivieri, L., Saville, R. J., Gange, A. C., and Xu, X. (2021). Apple endophyte community in relation to location, scion and rootstock genotypes and susceptibility to European canker. *FEMS Microbiol. Ecol.* 97, 1–18. doi: 10.1093/femsec/fiab131

Petrini, O. (1991). "Fungal endophyte of tree leaves" in *Microbial Ecology of Leaves*. eds. J. Andrews and S. S. Hirano (New York: Spring-Verlag)

Rai, M., Rathod, D., Agarkar, G., Dar, M., Brestic, M., Pastore, G. M., et al. (2014). Fungal growth promotor endophytes: a pragmatic approach towards sustainable food and agriculture. *Symbiosis* 62, 63–79. doi: 10.1007/s13199-014-0273-3

Rinu, K., Pandey, A., and Palni, L. M. S. (2012). "Utilization of psychrotolerant phosphate solubilizing fungi under low temperature conditions of the mountain ecosystem" in *Microorganisms in Sustainable Agriculture and Biotechnology*. eds. T. Satyanarayana and B. Johri (Dordrecht: Springer)

Rivera-Orduña, F. N., Suarez-Sanchez, R. A., Flores-Bustamante, Z. R., Gracida-Rodriguez, J. N., and Flores-Cotera, L. B. (2011). Diversity of endophytic fungi of *Taxus globosa* (Mexican yew). *Fungal Divers.* 47, 65–74. doi: 10.1007/s13225-010-0045-1

Rozpądek, P., Wężowicz, K., Nosek, M., Ważny, R., Tokarz, K., Lembicz, M., et al. (2015). The fungal endophyte *Epichloë typhina* improves photosynthesis efficiency of its host orchard grass (*Dactylis glomerata*). *Planta* 242, 1025–1035. doi: 10.1007/s00425-015-2337-x

Saikkonen, K., Faeth, S. H., Helander, M., and Sullivan, T. J. (1998). Fungal endophytes: a continuum of interactions with host plants. *Annu. Rev. Ecol. Syst.* 29, 319–343. doi: 10.1146/annurev.ecolsys.29.1.319

Santoyo, G., Moreno-Hagelsieb, G., Orozco-Mosqueda, M. C., and Glick, B. R. (2016). Plant growth-promoting bacterial endophytes. *Microbiol. Res.* 183, 92–99. doi: 10.1016/j.micres.2015.11.008

Silva, N. I. D. E., Brooks, S., Lumyong, S., and Hyde, K. D. (2018). Use of endophytes as biocontrol agents. *Rev. Fungal. Biol.* 33, 133–148. doi: 10.1016/j.fbr.2018.10.001

Simmons, E. G. (2007). *Alternaria* an identification manual. CBS biodiversity series , no. 6. The Netherlands. 775

Singh, B., and Satyanarayana, T. (2011). Microbial phytases in phosphorus acquisition and plant growth promotion. *Physiol. Mol. Biol. Plants* 17, 93–103. doi: 10.1007/s12298-011-0062-x

Sivanesan, A. (1987). Graminicolous species of *Bipolaris*, *Curvularia*, *Drechslera, Exserohilum* and their teleomorphs. *Mycol. Pap.* 81:170. doi: 10.2307/3759472

Song, J., Liang, J. F., Mehrabi-Koushki, M., Krisai Reilhuber, I., Ali, B., Kumar Bhatt, V., et al. (2019). Fungal systematics and evolution: FUSE 5. *Sydowia* 71, 141–245. doi: 10.12905/0380.sydowia71-2019-0141

Soytong, K., and Ratanacherdchai, K. (2005). Application of mycofungicide to control late blight of potato. *J. Agric. Technol.* 1, 19–32.

Sperber, J. I. (1958). The incidence of apatite-solubilizing organisms in the rhizosphere and soil. *Crop Pasture Sci.* 9, 778–781. doi: 10.1071/AR9580778

Steel, R. G. D., and Torrie, J. H. (1980). *Principles and Procedures of Statistics*. McGraw Hill book Co Inc, New York, USA.

Strobel, G. (2018). The emergence of Endophytic microbes and their biological promise. *J. Fungi* 4:57. doi: 10.3390/jof4020057

Strobel, G., and Daisy, B. (2003). Bioprospecting for microbial endophytes and their natural products. *Microbiol. Mol. Biol. Rev.* 67, 491–502. doi: 10.1128/MMBR.67.4.491-502.2003

Sutton, B. C. (1980). *The Coelomycetes. Fungi Imperfecti with Pycnidia, Acervuli and Stromata*. Common Wealth Mycologial Institute, Kew, Surrey, England

Tenzer, I., and Gessler, C. (1997). Subdivision and genetic structure of four populations of *Venturia inaequalis* in Switzerland. *Eur. J. Plant Pathol.* 103, 565–571. doi: 10.1023/A:1008636913211

Terhonen, E., Blumenstein, K., Kovalchuk, A., and Asiegbu, F. O. (2019). Forest tree microbiomes and associated fungal endophytes: functional roles and impact on forest health. *Forests* 10:42. doi: 10.3390/f10010042

Thompson, J. D., Higgins, D. G., and Gibson, T. J. (1994). CLUSTAL W: improving the sensitivity of progressive multiple sequence alignment through sequence weighting, position specific gap penalties and weight matrix choice. *Nucleic Acids Res.* 22, 4673–4680. doi: 10.1093/nar/22.22.4673

Toghueo, R. M. K., Zabalgogeazcoa, I., Vazquez de Aldana, B. R., and Boyom, F. F. (2017). Enzymatic activity of Endophytic fungi from the medicinal plants *Terminalia catappa*, *Terminalia mantaly* and *Cananga odorata*. *South Afr. J. Bot.* 109, 146–153. doi: 10.1016/j.sajb.2016.12.021

Vergara, C., Araujo, K. E. C., Urquiaga, S., Schultz, N., de Carvalho Balieiro, F., Medeiros, P. S., et al. (2017). Dark septate endophytic fungi help tomato to acquire nutrients from ground plant material. *Front. Microbiol.* 8:2437. doi: 10.3389/fmicb.2017.02437

Wenneker, M., and Thomma, B. P. (2020). Latent postharvest pathogens of pome fruit and their management: from single measures to a systems intervention approach. *Eur. J. Plant Pathol.* 156, 663–681. doi: 10.1007/s10658-020-01935-9

White, T. J., Bruns, T., Lee, S., and Taylor, J. (1990). "Amplification and direct sequencing of fungal ribosomal RNA genes for phylogenetics" in *PCR Protocols: A Guide to Methods and Applications*. eds. M. A. Innes, D. H. Gelfand, J. J. Sninsky and T. J. White (New York: Academic Press)

Wilkins, K., Nielsen, K. F., and Din, S. U. (2003). Patterns of volatile metabolites and nonvolatile Trichothecenes produced by isolates of *Stachybotrys*, *Fusarium*, *Trichoderma*, *Trichothecium*, and *Memnoniella*. *Environ. Sci. Pollut. Res.* 10, 162–166. doi: 10.1065/espr2002.05.118

Yang, S. X., Gao, J. M., Zhang, Q., and Laatsch, H. (2011). Toxic polyketides produced by *Fusarium* sp., an endophytic fungus isolated from *Melia azedarach*. *Bioorg. Med. Chem. Lett.* 21, 1887–1889. doi: 10.1016/j.bmcl.2010.12.043

Yang, S. Z., Peng, L. T., Su, X. J., Chen, F., Cheng, Y. J., Fan, G., et al. (2011). Bioassay guided isolation and identification of antifungal components from propolis against *Penicillium italicum*. *Food Chem.* 127, 210–215. doi: 10.1016/j.foodchem.2010.12.011

Zhang, J., Ge, H. M., Jiao, R. H., Li, J., Peng, H., Wang, Y. R., et al. (2010). Cytotoxic chaetoglobosins from the endophyte *Chaetomium globosum*. *Planta Med.* 76, 1910–1914. doi: 10.1055/s-0030-1249936

Zhang, H. W., Song, Y. C., and Tan, R. X. (2006). Biology and chemistry of endophytes. *Nat. Prod. Rep.* 23, 753–771. doi: 10.1039/b609472b

Zhang, S., Xu, B., Zhang, J., and Gan, Y. (2018). Identification of the antifungal activity of *Trichoderma longibrachiatum* T6 and assessment of bioactive substances in controlling phytopathgens. *Pestic. Biochem. Physiol.* 147, 59–66. doi: 10.1016/j.pestbp.2018.02.006

frontiers | Frontiers in Microbiology

TYPE Original Research
PUBLISHED 24 April 2023
DOI 10.3389/fmicb.2023.1142144

OPEN ACCESS

EDITED BY
Naser Safaie,
Tarbiat Modares University, Iran

REVIEWED BY
Somnath Holkar,
National Research Centre for Grapes (ICAR), India
Vagish Dwibedi,
Chandigarh University, India

*CORRESPONDENCE
Deeba Kamil
deebakamil@gmail.com

SPECIALTY SECTION
This article was submitted to Microbe and Virus Interactions with Plants, a section of the journal Frontiers in Microbiology

RECEIVED 11 January 2023
ACCEPTED 20 March 2023
PUBLISHED 24 April 2023

CITATION
Gangaraj R, Kundu A, Rana VS, Das A, Chawla G, Prakash G, Debbarma R, Nagaraja A, Bainsla NK, Gupta NC and Kamil D (2023) Metabolomic profiling and its association with the bio-efficacy of *Aspergillus niger* strain against *Fusarium* wilt of guava. *Front. Microbiol.* 14:1142144. doi: 10.3389/fmicb.2023.1142144

Metabolomic profiling and its association with the bio-efficacy of *Aspergillus niger* strain against *Fusarium* wilt of guava

R. Gangaraj[1], Aditi Kundu[2], Virendra Singh Rana[2], Amrita Das[1], Gautham Chawla[3], G. Prakash[1], Rubin Debbarma[1], A. Nagaraja[4], Naresh Kumar Bainsla[5], Navin Chandra Gupta[6] and Deeba Kamil[1]*

[1]Division of Plant Pathology, ICAR-Indian Agricultural Research Institute, New Delhi, India, [2]Division of Agricultural Chemicals, ICAR-Indian Agricultural Research Institute, New Delhi, India, [3]Division of Nematology, ICAR-Indian Agricultural Research Institute, New Delhi, India, [4]Division of Fruits and Horticultural Technology, ICAR-Indian Agricultural Research Institute, New Delhi, India, [5]Division of Genetics, ICAR-Indian Agricultural Research Institute, New Delhi, India, [6]ICAR-National Institute for Plant Biotechnology, New Delhi, India

Bio-control agents are the best alternative to chemicals for the successful management of plant diseases. The fungus *Aspergillus niger* is known to produce diverse metabolites with antifungal activity, attracting researchers to exploit it as a bio-control agent for plant disease control. In the present study, 11 *A. niger* strains were isolated and screened for their antagonism against the guava wilt pathogen under *in vitro* and *in planta* conditions. Strains were identified morphologically and molecularly by sequencing the internal transcribed spacer (ITS), β-tubulin, and calmodulin genes. The strains were evaluated through dual culture, volatile, and non-volatile methods under an *in vitro* study. AN-11, AN-6, and AN-2 inhibited the test pathogen *Fusarium oxysporum* f. sp. *psidii* (FOP) at 67.16%, 64.01%, and 60.48%, respectively. An *in planta* study was conducted under greenhouse conditions with 6 months old air-layered guava plants (var. Allahabad Safeda) by pre- and post-inoculation of FOP. The AN-11 strain was found to be effective under both pre- and post-inoculation trials. Furthermore, gas chromatography–mass spectrometry (GC–MS) analysis was carried out to characterize the volatile compounds of the most potential strain, *A. niger*. The hexane soluble fraction showed the appearance of characteristic peaks of hexadecenoic acid methyl ester (4.41%), 10-octadecanoic acid methyl ester (3.79%), dodecane (3.21%), undecane (3.19%), gibepyrone A (0.15%), 3-methylundecane (0.36%), and citroflex A (0.38%). The ethyl acetate fraction of the bio-control fungi revealed the occurrence of major antifungal compounds, such as acetic acid ethyl ester (17.32%), benzopyron-4-ol (12.17%), 1,2,6-hexanetriol (7.16%), 2-propenoic acid ethanediyl ester (2.95%), 1-(3-ethyloxiranyl)-ethenone (0.98%), 6-acetyl-8-methoxy dimethyl chromene (0.96%), 4-hexyl-2,5-dihydro dioxo furan acetic acid (0.19%), and octadecanoic acid (1.11%). Furthermore, bio-control abilities could be due to hyper-parasitism, the production of secondary metabolites, and competition for sites and nutrients. Indeed, the results will enrich the existing knowledge of metabolomic information and support perspectives on the bio-control mechanism of *A. niger*.

KEYWORDS

bio-control, *Aspergillus niger*, internal transcribed spacer, *Fusarium oxysporum* f. sp. *psidii*, gas chromatography-mass spectrometry, secondary metabolites

1. Introduction

Guava (*Psidium guajava* L.), an important fruit extensively grown in tropical and subtropical countries throughout the world, belongs to the family Myrtaceae. It is rich in vitamin C, phosphorus, iron, and calcium and has anti-oxidant properties (Kumari and Choudhary, 2019; Kumar et al., 2021a). In India, it is cultivated in various states (Bihar, Uttar Pradesh, Maharashtra, Andhra Pradesh, Gujarat, Karnataka, Orissa, Tamil Nadu, and Chhattisgarh), with diverse varieties of cultivars. Wilt is an important disease threatening guava production worldwide, leading to significant yield loss, and is considered a national constraint in India. The disease was first reported in Taiwan in 1926. It was initially recorded in India in Allahabad, Uttar Pradesh (Das Gupta and Rai, 1947). Disease prevalence ranges from 75% to 90%, while disease severity ranges from 30% to 55%. The disease is most prevalent in the states of Uttar Pradesh, Uttarakhand, West Bengal, Bihar, Rajasthan, Punjab, and Madhya Pradesh, causing a 30% yield loss. The infected trees initially show yellowing of the older leaves with slight curling at the terminal ends, and then, they turn reddish and start shedding leaves. The twigs become bare and do not form new leaves or flowers. The fruits remain underdeveloped, black, and hard. The presence of pathogen propagules in the xylem vessel disrupts the flow of water, resulting in the complete wilting of plants. The severity is worse in older trees than in young trees. Under severe conditions, the complete death of the plants results in 100% yield loss (Gupta et al., 2010; Suresh et al., 2019; Singh et al., 2021). Significant economic losses are also recorded in Florida (U.S.A.), Cuba, Brazil, Bangladesh, Pakistan, South Africa, Taiwan, and Australia (Junqueira et al., 2001; Lim and Manicom, 2003; Schoeman, 2011; Hussain et al., 2014; Shah et al., 2019).

The disease is reported to be associated with several pathogenic fungi. However, Fusarium spp. is considered an important pathogen characterized worldwide. Among them, *Fusarium oxysporum* f. sp. *psidii* (FOP) is predominant, and its pathogenicity is also confirmed under field conditions (Gupta et al., 2010; Gangaraj et al., 2022). Since it is a soil-borne disease, once established in the field, it is very difficult to control. Several fungicides have been used to control the guava wilt disease, but the management is not successful. The chemicals have been reported to increase the aggressiveness of the pathogen by increasing spore production (Misra and Pandey, 1999). The use of potential bio-control agents (BCAs) is an alternative, broad-spectrum, eco-friendly, and economical strategy to combat plant diseases. The BCAs remain viable for a long time in the soil, providing substantial and consistent disease control. In addition to controlling the pathogen, they also promote the growth and vigor of the plant. BCAs, such as *Trichoderma harzianum*, *T. asperellum*, *Aspergillus* spp., *Gliocladium virens*, and *Penicillium* spp., have been reported to be efficient for the management of wilt disease caused by *Fusarium* spp. *Aspergillus niger* was found to be promising in controlling the guava wilt disease caused by *F. oxysporum* f. sp. *psidii* and *F. solani* under both laboratory and field conditions (Singh et al., 2003; Gupta and Misra, 2009; Sharma et al., 2011).

Aspergillus niger is a filamentous ascomycetous soil-invading fungus that is effective against most soil-borne pathogens causing wilts (Mandol, 1998; Mukherjee and Sen, 1998; Gupta and Misra, 2009; Nayak and Vibha, 2017). The genus *Aspergillus* was initially illustrated by Micheli (1729) and later by Link (1809). It is considered generally recognized as safe (GRAS) by the Food and Drug Administration (Perrone et al., 2012). A wide range of extracellular enzymes and secondary metabolites are produced by *A. niger,* which has antimicrobial activity against *F. oxysporum*, *F. solani, Pythium* spp., *Sclerotinia sclerotiorum*, and *Pyricularia oryzae*. These include pyranones, alkaloids, cyclopentapeptides, polyketides, and sterols (Mondal et al., 2000; Patibanda and Sen, 2005; Idan et al., 2017; Yu et al., 2021). It is also reported to improve plant growth through the production of growth-promoting substances (Nielsen et al., 2009). *A. niger* produces a number of bioactive secondary metabolites with antimicrobial activity. Even though *A. niger* is found to be a promising bio-control agent, very few formulations, *viz.* Kali Sena (AN-27) and Pusa Mrida (AN-17), are available for commercial use to control phytopathogens (Mondal et al., 2000; Singh et al., 2003).

Moreover, there is a lack of availability of suitable bio-control strains of *A. niger,* and only a few commercial products are available in India. There is a lack of reports available on the secondary metabolite profiling of *A. niger* during interaction with the pathogen. The characterization of volatile organic compounds (VOCs) in GC–MS is well known because of its high sensitivity and high separation capability. In recent times, VOC-based formulations in the field have gained scope in the field of crop protection against plant pathogens (Korpi et al., 2009; Darshan et al., 2021). There is a need for a detailed understanding of the role of volatile metabolites to improve biological control efficacy and to explore and understand mechanisms and metabolites produced to improve the bio-efficacy of *A. niger* against pathogens associated with wilt disease in Indian conditions. Therefore, the present study was carried out to evaluate *A. niger* strains antagonistic activity against the guava wilt pathogen under *in vitro* and *in planta* conditions and to characterize the bioactive compounds produced during the interaction between the bio-control agent and the test pathogen. This information will facilitate extensive applications of formulation in the field of bio-control in the future for the successful management of guava wilt disease.

2. Materials and methods

2.1. Collection and isolation of the fungus

The soil and infected root samples showing symptoms of rotting at the basal region, discoloration of cortical tissues, and detachment of bark from the cortex were collected from a guava field at the ICAR—Indian Agricultural Research Institute (IARI), New Delhi. Furthermore, root samples were washed under running tap water for 2 min and cut into small pieces (<2 cm). Root pieces were surface sterilized for 1 min with sodium hypochlorite (1%) and then rinsed one more time with sterile double-distilled water (Suresh et al., 2019). The sterilized root pieces (<2 cm) were placed on potato dextrose agar (PDA) Petri plates and incubated for 7 days at 26 ± 1°C. Through the hyphal tip method, pure cultures of different isolates of the pathogens were obtained by culturing on a water agar medium, sub-culturing, and maintaining

PDA slants throughout the study. Based on morphological and molecular characteristics the isolate was confirmed as *F. oxysporum* f. sp. *psidii*. A pot experiment was conducted to confirm the pathogenicity of the guava wilt pathogen using 6 months old, air-layered guava plants (variety Allahabad Safeda) following the standard method described by Misra and Pandey (2000). The stem hole technique was performed; the wound was made with the help of a sterile blade, and a 10-day-old culture of *F. oxysporum* f. sp. *psidii* grown on PDA media with a spore concentration of 10^7 conidia/ml was inoculated at the wound, which was wrapped with paraffin to keep away from other contaminants. The symptoms of yellowing and shredding of the leaves, followed by curling of terminal branches, were observed after 15 days of inoculation. At the end of 4 months of inoculation, complete wilting was recorded and the cross-section showed brownish discoloration of the vascular system upon splitting. The pathogen was re-isolated from plants showing disease symptoms as per the methodology described (Suresh et al., 2019). *Fusarium oxysporum* f. sp. *psidii* strain (ITCC-8288) was deposited in the Indian Type Culture Collection (ITCC), New Delhi, and NCBI GenBank accession numbers (MN972593) were obtained (Gangaraj et al., 2022). In total, 11 strains of *A. niger* were collected, and isolated and pure cultures were obtained through the hyphal tip method by culturing on water agar medium, sub-cultured, and maintained on PDA slants at 26 ± 1°C (Table 1). Furthermore, all the strains were studied for their morphological characteristics (Diba et al., 2007; Javadi et al., 2012).

2.2. Genomic DNA isolation and phylogenetic analysis

Genomic DNA extraction from 11 *A. niger* strains was performed using a modified CTAB (cetyl trimethyl ammonium bromide) procedure (Cullings, 1992). PCR was performed using amplification of the ITS, β-tubulin, and calmodulin regions. The amplification of the ITS region was carried out using universal primers ITS1 5′-TCCGTAGGTGAACCTGCGG-3′ and ITS4 5′-TCCTCCGCTTATTGATATGC-3′ (White et al., 1990). Bt2a 5′-GGTAACCAAATCGGTGCTGCTTTC-3′ and Bt2b 5′-ACCCTCAGTGTAGTGACCCTTGGC-3′ primers were used for the amplification of β-tubulin region (Nasri et al., 2015). Similarly, primers CAL-228F 5′-GAGTTCAAGGAGGCCTTCTCCC-3′ and CAL-737R 5′-CATCTTTCTGGCCATCATGG-3 were used for the amplification of the calmodulin region (Carbone and Kohn, 1999). A total volume of 25 μl of PCR mixture consists of 12.5 μl of DreamTaq Green PCR Master Mix (Thermo Scientific, India) (containing 0.25 mM of each dNTP, 2 mM $MgCl_2$, and Taq DNA polymerase), 9.5 μl of nuclease-free water, 1 μl of primer (10 pmol/μl of each forward and reverse primer), and the remaining 1 μl (100 ng/μL) of DNA template was used for amplification. PCR was performed with initial denaturation for 5 min at 94°C, 35 cycles of denaturation at 94°C for 1 min, annealing temperature at 56°C for 1 min, primer extension at 72°C for 2 min, and final primer extension at 72°C for 5 min for the ITS and β-tubulin regions. The PCR for the calmodulin region was performed with an initial denaturation temperature of 94°C for 5 min, 35 cycles of denaturation at 94°C for 1 min, annealing temperature at 52°C for 1 min, primer extension at 72°C for 2 min, and a final primer extension at 72°C for 5 min. The electrophoresis was performed using 1.2% agarose gel with 0.5 mg/μl ethidium bromide in the 1 × TAE buffer (100 V, 400 mA for 35 min) to visualize the PCR product. The 1 Kb DNA Marker was used to estimate the size of the PCR product (Thermo Fisher Scientific, USA), which was further purified (Gene JET^{TM}, Thermo Fisher Scientific, USA) and sequenced (Bioengineering, India).

For the phylogenetic analysis, three gene sequences (ITS + β-tubulin + calmodulin) were used. NCBI nucleotide BLAST analysis was performed to compare the retrieved nucleotide sequences with those in the GenBank database. The sequences were constructed, modified, and aligned using Clustal W in the BioEdit sequence alignment editor. The sequences were constructed, modified, and aligned using BioEdit, which was used to perform the cluster analysis. The ambiguously aligned sites were eliminated, and gaps were treated as missing data. Furthermore, the sequences were artificially aligned, and ambiguous areas caused by insertions and deletions (indel) were removed. The sequences were concatenated after alignment, and MEGA version 7 was used largely for "Maximum Likelihood" tree construction (Tamura and Nei, 1993; Kumar et al., 2016). The ex-type strain of *A. niger* NRRL 326 (accession numbers: EF661186, EF661089, and EF661154) was employed as an outgroup, and *A. flavus* strain NRRL 1957 (accession numbers: AF027863, EF661485, and EF661508) was utilized to construct the phylogenetic tree (Samson et al., 2014). To assess the stability of branches, a bootstrap analysis with 1,000 replications was performed.

2.3. *In vitro* antagonistic assays

A dual culture assay was performed to test the *in vitro* antagonistic activity of *A. niger* strains against FOP (Chen et al., 2016). *A. niger* strains and FOP were grown on PDA plates for 7 days at 26 ± 1°C. A 5 mm disk of *A. niger* and the test pathogen (FOP) were placed exactly opposite each other at 2 cm from the periphery on the PDA plate and incubated at 26 ± 1°C for 7 days. The Petri plates containing only pathogens (FOP) were maintained separately as controls. The entire experiment was performed with three replications per treatment. The radial growth (mm) and percent inhibition were measured and calculated following the formula given by Garcia (1991): IRG (%) = 100 [(R1 – R2)/R1], where R1 denotes the farthest radial growth of the pathogen in the direction of the antagonist (control) and R2 denotes the distance on a line between the inoculation positions of the antagonist and the pathogen (Morton and Stroube, 1955).

The procedure outlined by Dennis and Webster (1971a) was used to conduct the volatile test. On the PDA plate, a 5 mm mycelial disk of *A. niger w*as placed at the center, and on another plate, a pathogen (FOP) was inoculated in the same manner. The two plates were taped together using paraffin, and they were kept at 26°C for 7 days. The control was maintained without an antagonist and PDA medium in the opposite Petri plate. The non-volatile test was assessed using the process outlined by Dennis and Webster (1971b). Strains of *A. niger* were grown in PDB for 15 days and later filtered

TABLE 1 Microscopic characteristics used for the identification of eleven strains of *A. niger* grown on potato dextrose agar (PDA) at 7 days after inoculation (DAI).

Strain	Location	Source	ITS[a]	β-tubulin[a]	Calmodulin[a]	Colony color	Conidia characteristics		
							Shape and surface morphology	Size (μm)	Color
AN-1	New Delhi	Soil	MW692855	OQ507885	OQ507894	White	Sub-globose, slightly rough, and irregular	3.87	Black
AN-2	New Delhi	Soil	MW692856	OQ507886	OQ507873	White	Globose, very rough, and irregular	4.38	Black
AN-3	New Delhi	Soil	MW692857	OQ507890	OQ507893	Milky white	Globose, rough, and irregular	3.46	Black
AN-4	New Delhi	Soil	MW692858	OQ507887	OQ507898	White	Globose, rough, and irregular	3.98	Cream
AN-5	Chandigarh	Waste of sugarcane industries	MW692859	OQ507888	OQ507877	White	Sub-globose and rough (ornamented with stripes)	4.49	Black
AN-6	Kanpur	Soil	MW692860	OQ507889	OQ507892	Creamy white	Sub-globose, rough, and irregular	4.16	Black
AN-7	Bikaner	Coconut rhizosphere	MW692861	OQ507883	OQ507896	White	Globose and slightly rough	4.02	Dark brown
AN-8	Hisar	Degrading wood	MW692862	OQ507884	OQ507874	White	Globose, rough, and irregular	4.63	Dark brown
AN-9	New Delhi	Soil, IARI	MW692863	OQ507891	OQ507895	Buff	Globose, smooth, and ornamented	3.68	Dark brown
AN-10	New Delhi	Soil, IARI	MW692864	OQ507882	OQ507875	White	Globose, slightly rough, and irregular	3.56	Black
AN-11	New Delhi	Soil, IARI	MW692865	OQ507881	OQ507876	Milky white	Sub-globose, rough, and irregular	3.94	Dark brown

[a]GenBank accession number.

10.3389/fmicb.2023.1142144

through a micropore filter. The final concentration was increased to 10% (v/v) and added to PDA media. A 5 mm disk of FOP was placed after solidification. In addition, control plates were kept without adding the culture filtrate to them. The percent mycelial growth inhibition was calculated after 7 days of inoculation as described in the dual culture assay. The entire experiment was conducted with three replications. Furthermore, based on the *in vitro* bio-efficacy assay, *A. niger* strains were characterized into three clusters, i.e., Group-1 with high potential strains showing 75–100% inhibition, Group-2 with moderate potential strains having 50–75% inhibition, and Group-3 with low potential strains having <50% inhibition of FOP growth.

2.4. *In planta* bio-control assay

The *A. niger* strains were evaluated using 6 months old air-layered guava plants (var. Allahabad Safeda) through pre- and post-inoculation treatment under greenhouse conditions against FOP. *A. niger* inoculum was cultured on sorghum grains. Several 500 ml conical flasks containing 250 g of sorghum seeds were sterilized for 2 days. Furthermore, 6-days-old *A. niger* strains growing on PDA were transferred into the sterilized sorghum seeds and incubated for 8–10 days. *A. niger* strains were further mass multiplied in 500 g of sterilized farmyard manure by adding 10 g of sorghum seeds grown in *A. niger* inoculum and incubated for 15 days (Misra and Prasad, 2004; Misra et al., 2004). Moreover, 6 months old air-layered guava plants (var. Allahabad Safeda) were grown in pots (30 cm diameter) for *in planta* evaluation at the Division of Plant Pathology, ICAR-IARI, New Delhi. The potting mixture was made up of soil and compost (1:1) that was sterilized two times. The control was maintained by inoculating only pathogens (FOP), achieving negative control with only distilled water and treating with carbendazim (0.2%). Furthermore, 7 day old FOP culture was used as a pathogen inoculum source. To establish the wilt disease, a 5 mm mycelial plug of the test pathogen was inoculated by making a wound in the stem of the guava plant, followed by covering it with cotton and adhesive tape as described by Misra and Pandey (2000). In addition, 30 ml of PDB containing FOP inoculum was also incorporated into the soil (root zone) for better establishment. In the case of pre-inoculation treatment, the test pathogen was inoculated onto the guava plants, and each *A. niger* strain was then added separately after 15 days, and vice versa in the case of the post-inoculation method. The percent reduction of wilt incidence (healthy, partially wilted, and completely wilted) was recorded as the average of data measured at 7 days intervals for up to 9 months. The percent disease incidence was calculated (Hussain et al., 2014). Using the modified scale, the wilting of guava plants in a field was scored (Misra and Pandey, 2000). The disease severity scale is as follows: 0 = healthy plants; 1 = yellowing of leaves; 2 = yellowing of leaves with 25% wilting of plants; 3 = yellow–brown discoloration with 50% wilting; 4 = pronounced wilting and entire plants started dying (75%); 5 = complete wilting and death of the plant. Each treatment consisted of three replications, and the experiment was repeated two times and was performed in a randomized complete block design (RCBD).

2.5. Microscopic study of hyphal interactions between antagonist (*A. niger*) and pathogen (*F. oxysporum* f. sp. psidii)

In order to elucidate the mechanisms of antagonism used by *A. niger* against FOP under *in vitro* conditions, a dual microculture technique was used (Chen et al., 2016). The Petri plates containing pathogens and antagonists were incubated at 26 ± 1°C for 7 days. Fungal colonies were picked from the interaction part using an inoculating needle and placed on the slide which was mounted in 50% (v/v) glycerol. The slides were covered with a cover slip (22 mm × 22 mm), observed, and photo-micrographs were taken using a Cilika BT-P Biological Digital Microscope (MedPrime Technologies Pvt. Ltd. Thane, India).

2.6. Scanning electron microscopy (SEM) analysis of dual culture plate

Microscopic image analysis was carried out following the procedure of Darshan et al. (2021). A small piece of mycelium along with some agar was taken from the inhibition zone. Specimens were fixed using chilled (4°C) 2.5% glutaraldehyde (Sigma-Aldrich) prepared in 0.1 M phosphate buffer for 2 h at room temperature. They were rinsed three more times for 15 min at a pH of 7.4 in 0.1 M phosphate buffer (Fisher Scientific). Fixed samples were dehydrated in a graded ethanol series (30%, 50%, 70%, 80%, 95%, and 100% ethanol, 15 min each) after 12 h of refrigeration. For drying the samples, hexamethyldisilazane (Sigma-Aldrich) was utilized. The dried samples were attached to the aluminum specimen mounts using a colloidal silver paste, and then 24 nm of gold palladium was sputtered on top. Samples were evaluated and documented using a scanning electron microscope (SEM) (Zeiss, EVO MA10) at an accelerating voltage of 20 kV/EHT and 10 Pa.

2.7. Secondary metabolites profiling

2.7.1. Extraction of bio-control fungi

Following a prior procedure described by Lykholat et al. (2021), with only minor adjustments, the extraction of metabolites was carried out to investigate the antagonistic ability to control *A. niger* (AN). Briefly, a small piece of fungal mycelium (FOP) was transferred to a 500 ml Erlenmeyer flask containing 100 ml of potato dextrose broth (PDB), which had been previously autoclaved at 121°C for 40 min. The medium was cultured for 15 days at 26 ± 1°C with continual 160 rpm shaking in an incubator shaker following inoculation. Mycelial biomass was then separated by filtering it through a Whatman No. 1 filter, and the filtrates were then sequentially extracted three times with an equal volume of hexane followed by ethyl acetate using a separating funnel. Using a rotary evaporator (IKA® RV 10, Germany), the extracted fractions were evaporated below 401°C to obtain concentrates of hexane and ethyl acetate. The crude extracts of FOP were then added to 100 ml PDB and inoculated with 2–3 agar disks of *A. niger* aseptically (Figure 1). Control was maintained with mycelial disks of *A. niger* and FOP crude extracts separately. Flasks were incubated for 15

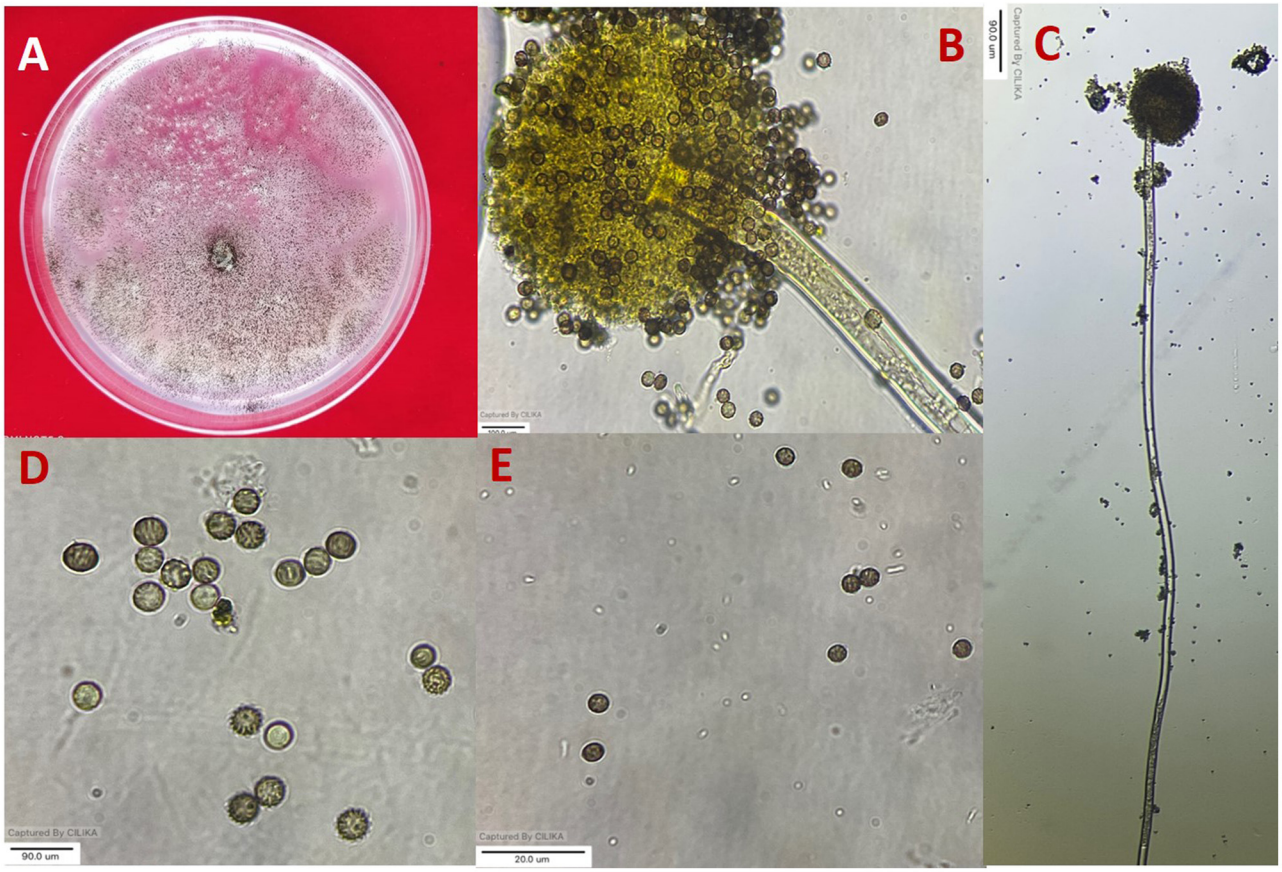

FIGURE 1
Morphological characterization of *A. niger* **(A)** colony on potato dextrose agar (PDA). **(B, C)** Conidiophore and vesicle-containing conidia. **(D, E)** Conidia.

days at 26 ± 1°C. Following liquid–liquid partitioning, cultures were re-filtered and then extracted three more times using hexane and ethyl acetate. Anhydrous sodium sulfate (10 g) was passed through several solvent layers to get rid of any remaining moisture. Concentrated extract fractions were employed for GC–MS analysis.

2.7.2. GC–MS analysis

The concentrated extract fractions were dissolved separately in GC–MS grade solvents, *viz.*, ethyl acetate (2 ml) and hexane (2 ml) and filtered with a 0.45 μm membrane (Millipore, Billerica, MA). Each sample was analyzed on a 559°C Agilent GC–MS (Agilent Technologies®, USA) to determine the volatile organic components. The mass spectrometer detected the components after they had been separated by an Agilent HP-5MS column (30 m, 0.25 mm, film thickness 0.25 m). As a carrier gas, helium gas (>99.99% purity) was used at a flow rate of 1 ml/minand a pressure of 10 psi. Each sample (1 L) was injected into the gas chromatograph (GC) using an in-built auto-injector with a 20:1 split ratio. A GC–MS temperature program was created that began at 40°C and enhanced at a rate of 3°C min^{-1} to reach 130°C, then held for 2 min. The temperature also rose at a pace of 5°C min^{-1} until it reached 210°C and was held for 2 min. The temperature was then raised to 350°C by adding 10°C min^{-1}. The samples were run for a period of 64 min. The MS acquisition parameters were set to the following values: solvent delay of 2 min, E.M. voltage of 1,214 V, ion source temperature of 200°C, electron ionization of 70 eV, transfer line temperature of 200°C, and full scan mode of 50–550 AMU. Volatile organic components were characterized by matching them with NIST (National Institute of Standards and Technology, USA) mass spectral library data, corresponding retention index (RI), and mass fragmentation pattern (Kumar et al., 2021b).

2.8. Statistical analysis

To assess differences in parameter values, the data were analyzed using ANOVA in SPSS version 20.0 statistical software (SPSS, SAS Institute, USA). The experiments were repeated two times, with three replications of each treatment. Duncan's multiple range test was used to determine differences between treatments at a 5% level of significance. VENNY 2.1.0 (http://bioinfogp.cnb.csic.es/tools/venny/index.html) and SRplot (Science and Research Online Plot) (https://bioinformatics.com.cn) were used to statistically analyze the GC–MS data and for creating Venn diagrams and heat maps (Esmail et al., 2022; Zhou et al., 2022).

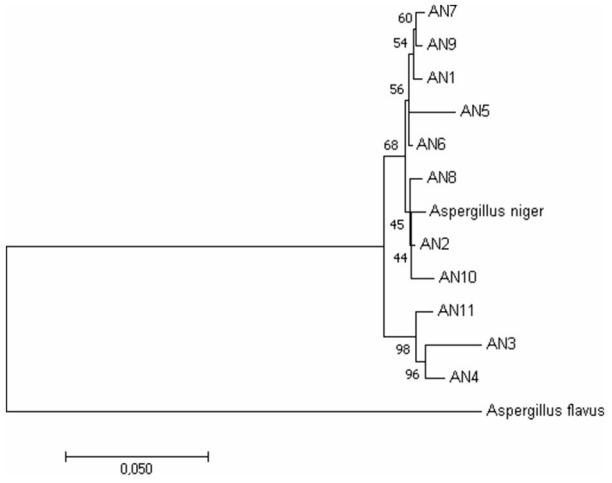

FIGURE 2
Phylogenetic relationship among *A. niger* isolates based on ITS, β-tubulin, and calmodulin genes by the Maximum Likelihood method. Bootstrap analysis was done with 1,000 replicates and values at nodes of branches refer to the number of times (%) the branching is supported.

3. Results

3.1. Morphological identification of *A. niger* strains

All 11 strains expressed rapid growth on the PDA medium, mycelial growth was uniform, and colonies were initially white but later turned dark brown to black after incubation for 7 days (Supplementary Figure 1). The AN-4 strain initially formed a cream color colony, but after a few days, it turned black. The walls of the conidiophores were smooth, hyaline, and sometimes dark toward the vesicle. A biseriate conidial head with phialides was observed, the head of the conidia was brownish-black, and the conidia were globose or sub-globose, brown to black, rough, and irregular (Figure 1). The size of the conidia was measured, which varied from 3.4 μm (AN-3) to 4.3 μm (AN-8). All these growth and microscopic characteristics signify that the strains belong to the *A. niger* group (McClenny, 2005; Diba et al., 2007) and are listed in Table 1.

3.2. Molecular identification and phylogenetic analysis

To further confirm morphological identification, the DNA was isolated, and a PCR-based molecular study was carried out using the ITS, β-tubulin, and calmodulin genes. The amplified products were separated on agarose gel through gel electrophoresis, purified, sequenced, and analyzed for their quality through Bio-Edit software. The sequences were further submitted to GenBank, and accession numbers were obtained (Table 1). These 11 *A. niger* strains' taxonomic identity was established by NCBI blast and the alignments and phylogenetic analyses (Figure 2).

TABLE 2 Inhibition of mycelial growth of *F. oxysporum* f. sp. *psidii* by *A. niger* strains under *in vitro* conditions.

Isolate	Dual culture*	Volatile*	Non-volatile*	
AN-1	90.58^{b}	14.28^{b}	67.05^{b}	57.30
AN-2	100^{a}	22.62^{a}	58.82^{d}	60.48
AN-3	100^{a}	20.24^{a}	49.41^{f}	56.55
AN-4	76.47^{c}	16.66^{b}	20.00^{h}	37.71
AN-5	83.52^{c}	19.04^{b}	38.82^{g}	47.13
AN-6	100^{a}	22.61^{a}	69.41^{a}	64.01
AN-7	78.82^{c}	16.66^{b}	62.35^{c}	52.61
AN-8	64.70^{d}	11.61^{c}	4.70^{j}	27.00
AN-9	70.00^{d}	23.80^{a}	52.9^{e}	48.90
AN-10	89.41^{b}	21.42^{a}	5.80^{i}	38.88
AN-11	100^{a}	26.19^{a}	75.29^{a}	67.16
CD @ 5%	8.012	6.043	5.036	
SE	3.88	2.92	2.43	

*Different letters after values are significantly different at $p \leq 0.05$.

3.3. *In vitro* antagonistic assays

Under a dual culture assay, the mycelial growth of FOP was significantly inhibited by 11 *A. niger* strains, with percent inhibition ranging from 64.7% to 100% ($F = 99.62$, $P < 0.05$). Among them, four *A. niger* strains, *viz.*, AN-2, AN-3, AN-6, and AN-11, showed 100% mycelial growth inhibition (Table 2, Figure 3A) after 7 days post-inoculation. The volatile compounds produced by *A. niger* strains showed 11.61–26.19% of mycelial inhibition ($F = 10.19$, $P < 0.05$) (Table 2, Figure 3B). AN-11 showed the maximum (26.19%) growth inhibition of the test pathogen, followed by AN-2 (22.62%) and AN-6 (22.61%). Under the non-volatile method, maximum inhibition was recorded in AN-11 (75.29%), and five strains (AN-1, AN-2, AN-6, AN-7, and AN-9) showed moderate growth inhibition ranging from 50 to 75%. The remaining five *A. niger* strains (AN-3, AN-4, AN-5, AN-8, and AN-10) showed low antagonism levels of 4.7–49.41% inhibition ($F = 207.71$, $P < 0.05$) (Table 2, Figure 3C) after 7 days of incubation. The collective effect of the *in vitro* bio-control assay of *A. niger* strains against FOP exhibited AN-11 as the most potential one (67.16%), followed by AN-6 (64.01%) and AN-2 (60.48%). Effective inhibition of the test pathogen was found in the dual culture method followed by the non-volatile method but very low percent mycelial inhibition was observed in the volatile method. The *A. niger* strains were divided into three groups based on their *in vitro* potentiality against *F. oxysporum* f. sp. *psidii* (Table 3).

3.4. *In planta* bio-control assay

A. niger strains, *viz.*, AN-11 (12.6%), AN-6 (20%), AN-2 (22.2%), and AN-7 (26.64%), showed lower wilting incidence when compared with control when applied as pre-inoculation

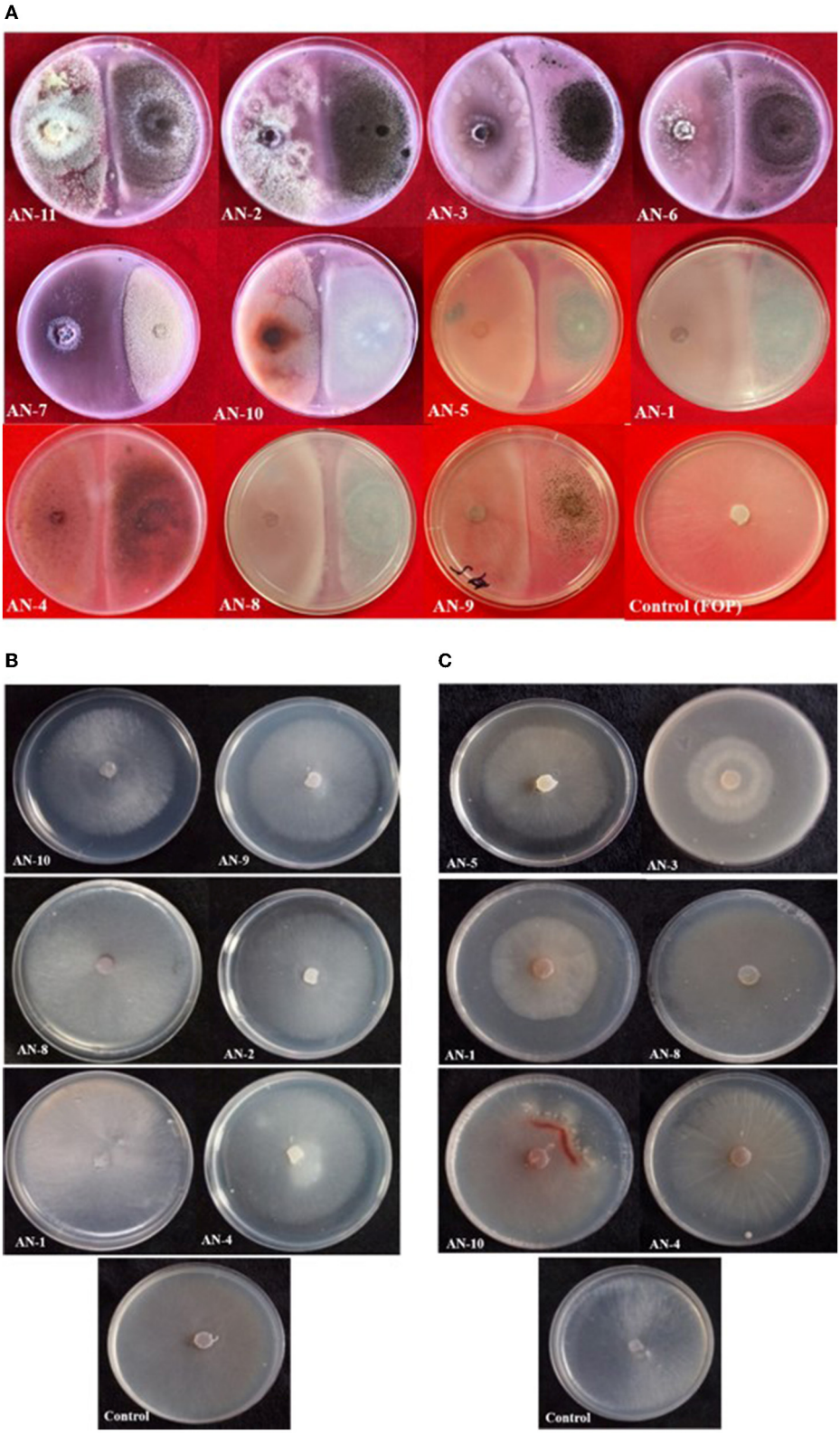

FIGURE 3
Growth inhibition of *F. oxysporum* f. sp. *psidii* by *A. niger* strains under *in vitro* conditions after 7 days of incubation on potato dextrose agar (PDA) media. **(A)** Dual culture method. **(B)** Volatile assay. **(C)** Non-volatile assay.

TABLE 3 Grouping of *A. niger* strains based on percent inhibition of *F. oxysporum* f. sp. *psidii* under *in vitro* conditions.

Inhibition	Group	% Inhibition of *F. oxysporum* f. sp. *psidii*		
		Dual culture method	Volatile assay	Non-volatile assay
High	Group 1 (75–100% inhibition)	AN1, AN2, AN3, AN4, AN5, AN6, AN7, AN9, AN10 and AN11	–	AN11
	Number of isolates	10	0	1
Moderate	Group 2 (50–75% inhibition)	AN8	–	AN1, AN2, AN6, AN7, and AN9
	Number of isolates	1	0	5
Low	Group 3 (<50 % inhibition)	–	AN1, AN2, AN3, AN4, AN5, AN6, AN7, AN8, AN9, AN10 and AN11	AN3, AN4, AN5, AN8 and AN10
	Number of isolates	0	11	5

treatment ($F = 4.44$, df = 24, $P < 0.05$) (Figures 4B, 5). Positive control plants inoculated with only FOP exhibited complete wilting and could not recover (Figure 4D). The AN-11 strain was found to be the best treatment, showing an 87.4% reduction of wilt, followed by the AN-6 strain (80%), whereas treatment with Carbendazim (2 g/l) showed a 60% reduction in disease over control (Figure 4C). The efficiency of *A. niger* strains was assessed by post-inoculation treatment with FOP. The lowest percent of wilting was observed in the treatment with AN-6 (8.78%) and AN-11 (8.78%), followed by AN-2 (17.7%) and AN-5 (20%) ($F = 4.41$, df = 24, $P < 0.05$) (Figures 4A, 5). Treatment with strain AN-7 showed the highest disease incidence (80%) (Figure 4A). Notably, AN-2, AN-5, AN-6, and AN-11 strains were found to be significantly effective, causing an 80–91% reduction in wilt incidence and maximum recovery from the disease under field conditions. The control treatment with Carbendazim resulted in a 73% disease reduction over the positive control (Figure 4C). Furthermore, the most potent strain AN-11 was used to study the antagonistic nature and to characterize the secondary metabolites during interaction with *F. oxysporum* f. sp. *psidii* (FOP).

3.5. Hyphal interactions between antagonist and pathogen

The images obtained with the compound and scanning microscopes were analyzed to identify structural changes during the interaction (Figures 6, 7). The antagonistic growth was found to be faster, and the hyphae were characterized as smaller in diameter with respect to the pathogen *F. oxysporum* f. sp. *psidii*. Initially, the antagonist grows parallel to the pathogen hyphae and later, it forms initial contact through a peg-like structure that helps in attachment. Furthermore, the perforation (hole) was formed in the pathogen hyphae. Most importantly, a hook or pincer-like structure that coils around and restricts the growth of the pathogen was observed, resulting in the death of hyphae. These results illustrate the antagonistic nature of a bio-control *A. niger* through mycoparasitism.

3.6. Chemical analysis

To confirm the potential bio-control efficacy of the VOCs from the potential *A. niger* strain, chemical analysis was performed using GC–MS. From the hexane soluble fraction of the bio-control fungal strain, identified components were grouped into different chemical classes based on their functional groups, which showed the highest content of hydrocarbons (22.88%), followed by acids (5.23%), esters (0.87%), and alcohol (0.81%) in *A. niger*. Similarly, in the interaction of *A. niger* with the hexane fraction of FOP, hydrocarbons (14.04%) secured the highest position, followed by esters (10.43%) and acids (8.96%). However, a total of 23 compounds were identified in *Fusarium* FOP, including hexadecanoic acid methyl ester (8.54%), 9-octadecanoic acid methyl ester (7.38%), dodecane (3.50%), and tridecane (3.41%). However, 23 VOCs, including octadecene (3.98%), hexadecane (3.95%), tetradecane (3.54%), and 1.3-dimethylcyclopentane (3.50%), were found in the bio-control fungi, *A. niger*. Interestingly, from the interacted plates, 30 VOCs were detected and characterized as hexadecanoic acid methyl ester (4.41%), 10-octadecanoic acid methyl ester (3.79%), dodecane (3.21%), and undecane (3.19%). In addition, minor compounds were also detected such as gibepyrone A (0.15%), 3-methylundecane (0.36%), and citroflex A (0.38%) from the interacted plate. The list of VOCs identified in the hexane fraction is listed in Table 4.

In the ethyl acetate soluble fraction of *Fusarium* FOP, predominant volatile compounds were identified and grouped into their respective chemical classes, which showed the highest content of hydrocarbons (35.52%), followed by acids (13.18%), esters (5.25%), and phenols (3.40%). Among these, *n*-hexadecanoic acid (4.37%) and 3-methoxy-2,4,5-trimethylphenol (3.40%) were most abundant in FOP. Surprisingly, alcohol (12.91%), acids (7.6%), and hydrocarbons (1.44%) were detected in the bio-control fungal strain, *A. niger*, where dodecene (13.92%), benzene ethanol (10.74%), hexadecanoic acid (7.15%), 2-2-furylethyl-N-methylaniline (3.62%), and 3-diethynyl-9,10-dimethoxyanthracene (2.29%) represented the highest components of the ethyl acetate fraction. Consequently, interaction treatment of *A. niger* and FOP exhibited an abundance of esters (24.08%) and alcohol (21.33%) including certain acids (3.05%). Here, acetic acid ethyl ester

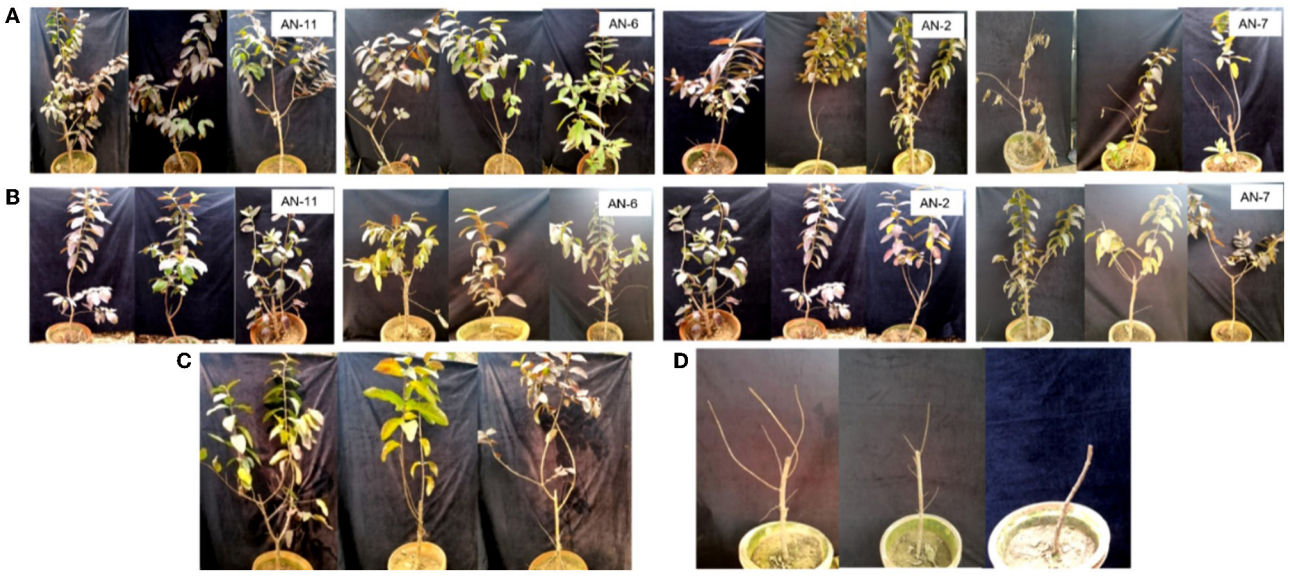

FIGURE 4
Effect of *A. niger* strains on guava wilt under greenhouse conditions (three replications per treatment). **(A)** Post-inoculation application (AN-11, AN-6, AN-2, and AN-7). **(B)** Pre-inoculation application (AN-11, AN-6, AN-2, and AN-7). **(C)** Wilted plants treated with Carbendazim @ 0.2%. **(D)** Guava plants inoculate with *F. oxysporum* f. sp. *psidii* only.

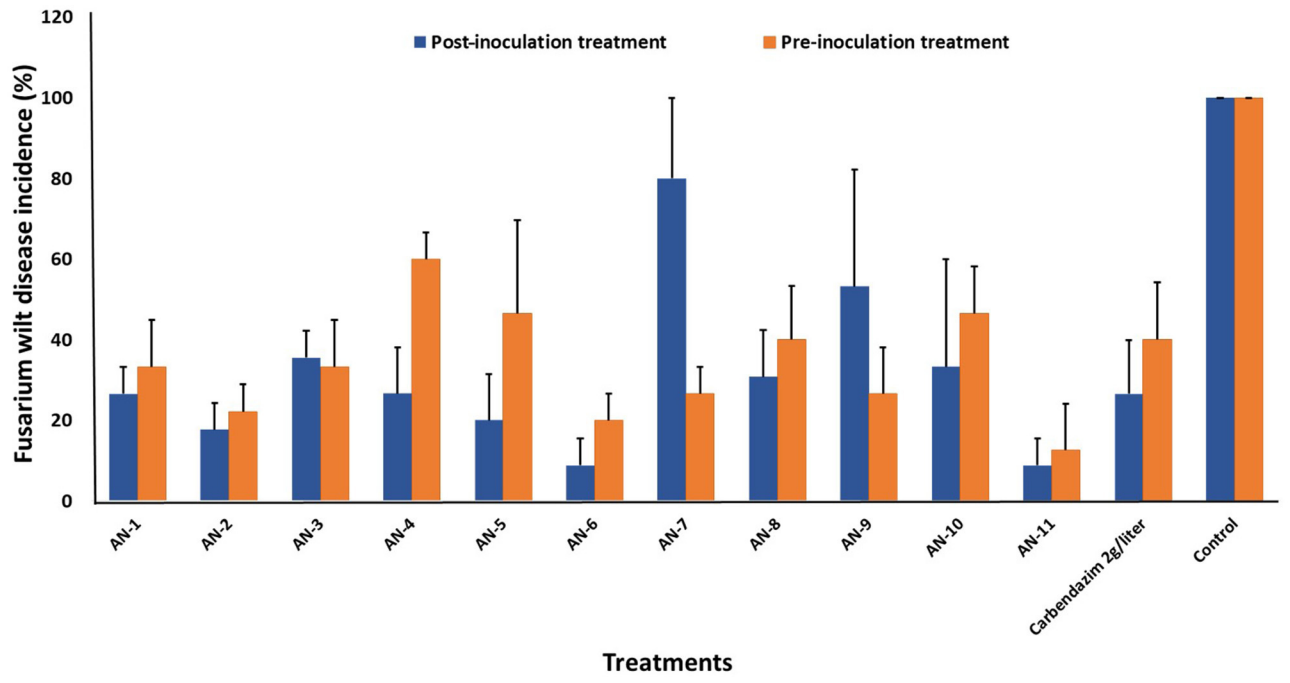

FIGURE 5
Effect of *A. niger* strains on percent wilt incidence of guava seedlings during post and pre-inoculation treatment of *F. oxysporum* f. sp. *psidii* (FOP) under greenhouse conditions. Bars represent the mean values obtained in three independent repeats and standard error is indicated by error bars. AN represents *A. niger*.

(17.32%), benzopyron-4-ol (12.17%), 1,2,6-hexanetriol (7.16%), and 2-propenoic acid ethanediyl ester (2.95%) were found as the major VOCs. In addition, minor compounds, namely, octadecanoic acid (1.11%), 1-(3-ethyloxiranyl) ethanone (0.98%), 6-acetyl-8-methoxy dimethyl chromene (0.96%), and 4-hexyl-2,5-dihydro dioxo furan acetic acid (0.19%) were also detected in the interaction treatment. The list of VOCs identified in the ethyl acetate fraction is listed in Table 5. The total ion chromatograms of the hexane and ethyl acetate fractions are shown in Supplementary Figures 2–7. Furthermore, Venn diagrams and heat maps were generated in the

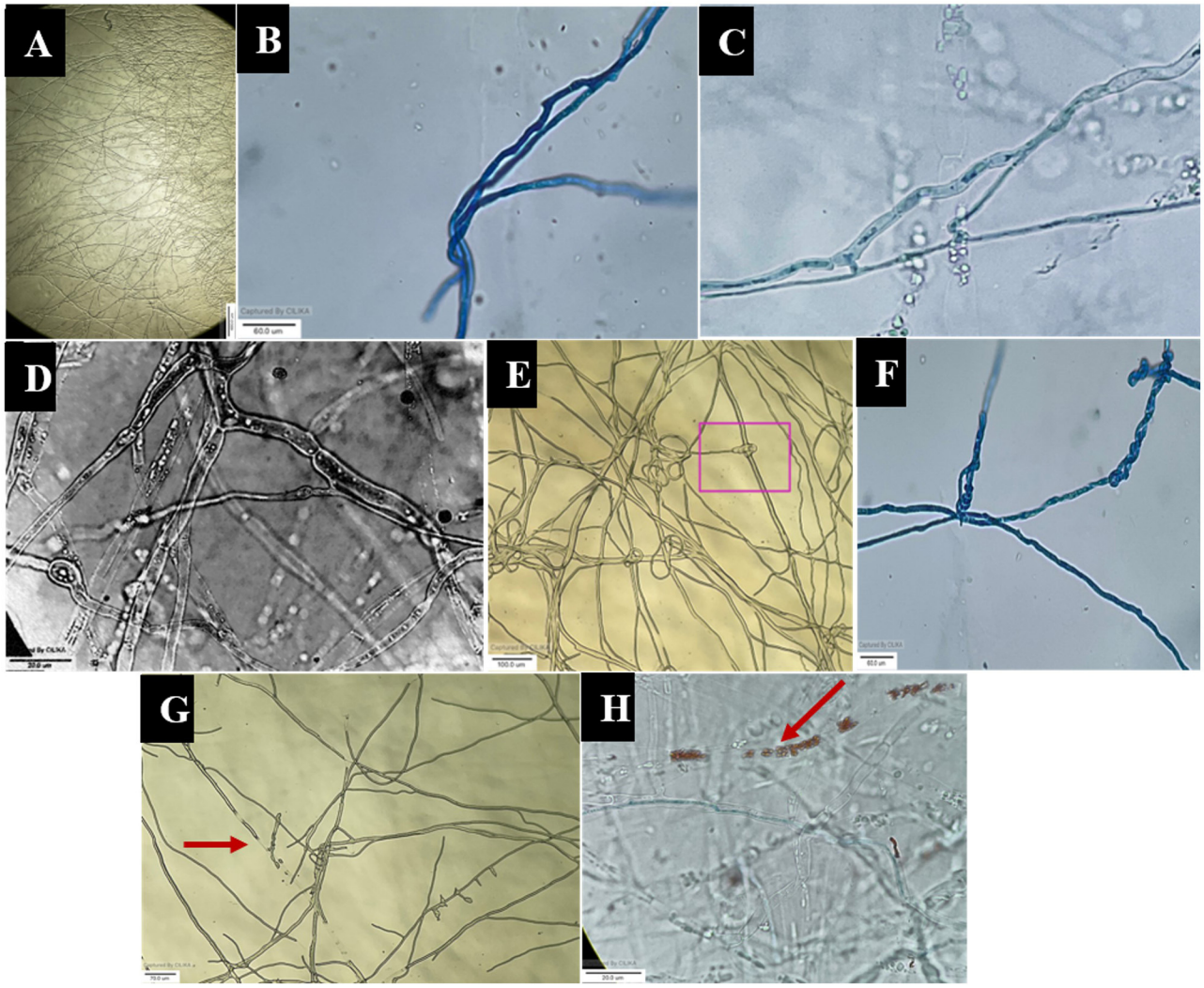

FIGURE 6
Microscopic view of mycoparasitic nature of *A. niger* (AN) on *F. oxysporum* f. sp. *psidii* (FOP). **(A)** Interaction zone; **(B)** Parallel growing of hyphae of *A. niger* (AN) to *F. oxysporum* f. sp. *psidii* (FOP) hyphae; **(C, D)** Initial contact and penetration of hyphae forming appressoria-like structure; **(E, F)** Hook or pincer-like structure (coiling) formed around *F. oxysporum* f. sp. *psidii* by *A. niger*; **(G, H)** Red arrow indicates plasmolysis leading to the death of hyphae (*F. oxysporum* f. sp. *psidii*).

current experiment to compare the visualization and interpretation of changes in the VOCs profiling during interaction (Figures 8, 9).

4. Discussion

The biotic stresses are especially caused by fungal pathogens, resulting in the huge economic loss of agricultural and horticultural crops throughout the world. The production of guava is diminishing year by year due to wilt infections caused by *Fusarium* spp. Management is not successful in the field because of the soil-borne nature of pathogens. In recent days, the use of potential BCAs for the management of pests and diseases is because of their cost-effectiveness, sustainability, and eco-friendliness. The fungus *A. niger* is proven to be a potential BCA against many plant pathogens, including guava wilt disease. Considering this, our present study is undertaken to evaluate *A. niger* strains against the guava wilt pathogen.

4.1. Morphological and molecular characterization of *A. niger* strains

The study of *Aspergillus* species has always been a confusing and challenging task due to the complex and subtle differences between them (Silva et al., 2011). In our study, 11 strains used as antagonists were confirmed as *A. niger* based on morphological and molecular characteristics. The studied morphological characteristics, such as colony morphology, conidia, vesicle, and conidiophore nature, confirmed the previous reports (McClenny, 2005; Diba et al., 2007; Varga et al., 2011; Lanka et al., 2017; Atallah et al., 2022). The conventional morphological approaches may not perform well

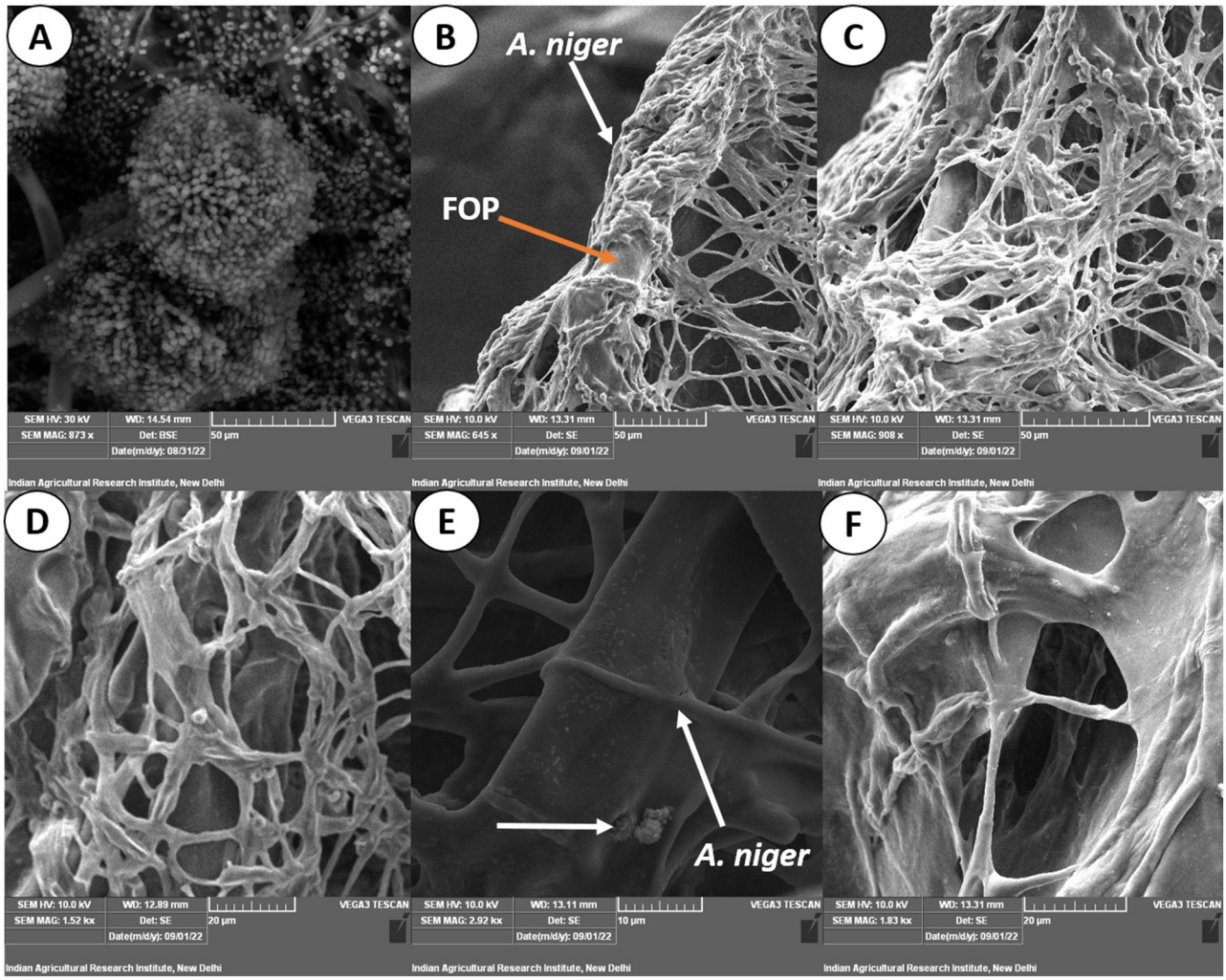

FIGURE 7
Scanning electron micrograph on mycoparasitism of *F. oxysporum* f. sp. *psidii* by *A. niger*. **(A)** Fruiting body of the bio-control *A. niger*; **(B–D)** Hyphal network of *A. niger* (white arrow) surrounding the pathogen hyphae (orange arrow); **(E)** Arrow shows coiling (pincer-like structure) and dissolution of pathogen hyphae by *A. niger*; **(F)** Plasmolysis and death of pathogen.

for the accurate identification of the genus *Aspergillus* up to the species level. The difficulties are mainly related to the identification of cryptic species, which are morphologically similar species. So, combining the morphological and molecular strategies will be an ideal tool for accurate identification. Due to its high level of sequence polymorphism, the ITS region has been considered, for a long time, the most efficient marker for the identification and detection of *Aspergillus* up to the species level (Nithiyaa et al., 2012; George and Ramteke, 2019; El-Shora et al., 2021). Housekeeping genes, particularly the β-tubulin and calmodulin genes, have proven to be highly beneficial in differentiating species belonging to section Nigri due to their species-specific traits (Samson et al., 2007; Nasri et al., 2015). The combined DNA sequence analysis of the ITS, β-tubulin, and calmodulin genes has shown a high degree of intraspecies discriminatory power for *A. niger* (Susca et al., 2013). Considering this, the combined DNA sequence and phylogenetic analysis carried out in our study confirmed that all the isolates belonged to *A. niger*. Overall, morphological and combined gene molecular analysis in the present study confirms 11 strains as *A. niger*.

4.2. Bio-efficacy test of *A. niger* strains against guava wilt pathogen

Furthermore, these 11 strains were tested against the most potent guava wilt pathogen, FOP, *A. niger,* as an effective bio-control agent. In the dual culture method, four strains exhibited 100% growth inhibition of FOP, and collectively, under *in vitro* assays, *A. niger* strain AN-11 (67.16%) was found to have the most potential, followed by AN-6 (64.01%) against the guava wilt pathogen. These results indicate that BCA *A. niger* inhibits the pathogen by various bio-control mechanisms, such as mycoparasitism, as well as by competing for space and nutrients. In addition, it produces non-volatile and volatile secondary

TABLE 4 List of volatile organic compounds (VOCs) in the hexane fraction during *F. oxysporum* f. sp. *psidii* and *A. niger* interaction, determined by GC–MS.

Sl. No	Compound	Organic Group	Chemical formula	*F. oxysporum* f. sp. *psidii* (control)		*A. niger* (control)		*F. oxysporum* f. sp. *psidii* and *A. niger* interaction	
				RT*	Area %	RT*	Area %	RT*	Area %
1	1,3-dimethylcyclopentane	Hydrocarbon	C_7H_{14}	3.71	1.31 ± 0.28	3.71	3.5 ± 1.39	–	–
2	Methyl benzol	Alcohol	$C_8H_8O_2$	5.05	0.22 ± 0.08	–	–	–	–
3	Undecane	Hydrocarbon	$C_{11}H_{24}$	21.68	1.39 ± 0.62	21.572	0.28 ± 0.12	21.91	3.19 ± 0.47
4	Tetramethyl benzene	Hydrocarbon	$C_{10}H_{14}$	24.85	0.26 ± 0.11	–	–	22.61	1.62 ± 0.32
5	Dodecane	Hydrocarbon	$C_{12}H_{26}$	28.61	3.5 ± 2.01	28.429	1.15 ± 0.71	28.741	3.21 ± 0.38
6	2,6-dimethyl undecane	Hydrocarbon	$C_{13}H_{28}$	29.39	0.74 ± 0.38	–	–	29.47	0.66 ± 0.12
7	2-methyl-dodecane	Hydrocarbon	$C_{13}H_{28}$	32.67	0.24 ± 0.09	–	–	32.71	0.18 ± 0.06
8	Tridecane	Hydrocarbon	$C_{13}H_{28}$	35.27	3.41 ± 1.15	35.055	0.4 ± 0.19	–	–
9	Tetradecane	Hydrocarbon	$C_{14}H_{30}$	41.5	0.62 ± 0.16	41.619	3.54 ± 1.46	41.538	0.47 ± 0.11
10	Tetradecanoic acid methyl ester	Ester	$C_{15}H_{30}O_2$	59.03	0.28 ± 0.73	–	–	59.032	0.16 ± 0.04
11	Hexadecanoic acid methyl ester	Ester	$C_{17}H_{34}O_2$	62.94	8.54 ± 1.64	–	–	62.929	4.41 ± 1.94
12	*cis*-9-hexadecenoic acid	Acid	$C_{16}H_{30}O_2$	63.23	0.32 ± 0.02	63.20	0.54 ± 0.22	63.282	0.49 ± 0.13
13	Hexadecanoic acid	Acid	$C_{16}H_{32}O_2$	63.58	1.51 ± 0.87	63.52	1.65 ± 1.04	63.648	1.86 ± 0.89
14	2-tetradecene	Hydrocarbon	$C_{14}H_{28}$	64.54	0.27 ± 0.06	40.95	0.26 ± 0.05	–	–
15	Cyclotetracosane	Hydrocarbon	$C_{24}H_{48}$	64.71	1.43 ± 0.11	–	–	–	–
16	Methyl-octadecadienoate	Ester	$C_{19}H_{34}O_2$	64.93	2.59 ± 0.31	–	–	–	–
17	9-octadecenoic acid methyl ester	Ester	$C_{19}H_{36}O_2$	65.06	7.38 ± 2.05	–	–	–	–
18	Octadecanoic acid methyl ester	Ester	$C_{19}H_{38}O_2$	65.25	1.35 ± 0.24	65.23	0.13 ± 0.04	65.257	0.65 ± 0.03
19	6-Octadecenoic acid	Acid	$C_{18}H_{34}O_2$	65.51	2.59 ± 0.49	65.48	1.14 ± 0.82	65.597	2.06 ± 1.38
20	9-Tricosene	Hydrocarbon	$C_{23}H_{46}$	65.65	1.29 ± 0.08	61.048	0.18 ± 0.01	–	–
21	Octadecanoic acid	Acid	$C_{18}H_{36}O_2$	65.71	0.54 ± 0.07	–	–	65.75	0.53 ± 0.07
22	1,2-dimethylcyclopentane	Hydrocarbon	C_7H_{14}	–	–	3.77	1.84 ± 0.38	–	–
23	Hexadecane	Hydrocarbon	$C_{16}H_{34}$	–	–	47.24	3.95 ± 1.93	–	–
24	2,4-dibutyl phenol	Phenol	$C_{14}H_{22}O$	–	–	53.146	0.54 ± 0.08	–	–
25	3-methylpentadecane	Hydrocarbon	$C_{16}H_{34}$	–	–	51.639	0.3 ± 0.17	–	–
26	Heptadecane	Hydrocarbon	$C_{17}H_{36}$	–	–	58.238	0.21 ± 0.02	–	–
27	4-formyl-2,6-di-tert-butylphenol	Phenol	$C_{14}H_{22}O$	–	–	59.983	0.38 ± 0.14	–	–

(Continued)

10.3389/fmicb.2023.1142144

TABLE 4 (Continued)

Sl. No	Compound	Organic Group	Chemical formula	*F. oxysporum* f. sp. *psidii* (control)		*A. niger* (control)		*F. oxysporum* f. sp. *psidii* and *A. niger* interaction	
				RT*	Area %	RT*	Area %	RT*	Area %
28	15-methyl-heptadecane	Hydrocarbon	$C_{18}H_{38}$	–	–	60.118	0.39 ± 0.18	–	–
29	Tetradecanoic acid	Acid	$C_{14}H_{28}O_2$	–	–	60.24	0.25 ± 0.04	60.274	0.1 ± 0.05
30	Octadecane	Hydrocarbon	$C_{18}H_{38}$	–	–	60.78	3.98 ± 2.07	60.72	0.19 ± 0.13
31	Eicosane	Hydrocarbon	$C_{20}H_{42}$	–	–	63.805	2.9 ± 0.83	63.77	0.19 ± 0.06
32	1-heneicosanol	Alcohol	$C_{21}H_{44}O$	–	–	64.64	0.47 ± 0.12	–	–
33	Butyl-2-ethyloctahydro epoxy indenol	Alcohol	$C_{15}H_{26}O_2$	–	–	64.897	0.34 ± 0.09	–	–
34	10-octadecenoic acid methyl ester	Ester	$C_{19}H_{36}O_2$	–	–	64.97	0.74 ± 0.32	65.06	3.79 ± 2.01
35	Nonane	Hydrocarbon	$C9H_20$	–	–	–	–	9.71	0.25 ± 0.18
36	Dimethyl octane	Hydrocarbon	$C_{10}H_{22}$	–	–	–	–	11.36	0.2 ± 0.04
37	3-ethyl-2-methyl-heptane	Hydrocarbon	$C_{10}H_{22}$	–	–	–	–	11.71	0.12 ± 0.07
38	Trimethyl-benzene	Aromatic Hydrocarbon	C_9H_{12}	–	–	–	–	13.33	1.31 ± 0.74
39	Decane	Hydrocarbon	$C10H_{22}$	–	–	–	–	15.34	1.49 ± 0.13
40	4-methyldecane	Hydrocarbon	$C_{11}H_{24}$	–	–	–	–	19.033	0.27 ± 0.09
41	2-ethylnonane	Hydrocarbon	$C_{11}H_{24}O_3$	–	–	–	–	19.69	0.33 ± 0.02
42	3-methylundecane	Hydrocarbon	$C_{12}H_{26}$	–	–	–	–	26.508	0.36 ± 0.04
43	Gibepyrone A	Ketone	$C_{10}H_{12}O_2$	–	–	–	–	48.136	0.15 ± 0.01
44	Citroflex A	Carbonyl group	$C_{20}H_{34}O_8$	–	–	–	–	60.634	0.38 ± 0.14
45	Octadecadienoic acid methyl ester	Ester	$C_{19}H_{34}O_2$	–	–	–	–	64.938	1.42 ± 0.81
46	9-octadecenoic acid	Acid	$C_{18}H_{34}O_2$	–	–	–	–	65.597	2.06 ± 0.96

Chemical groups	**Content (%)**		
Hydrocarbons	14.46	22.88	14.04
Esters	20.14	0.87	10.43
Alcohol	0.22	0.81	–
Acids	4.96	5.23	8.96
Phenols	–	0.92	–
Ketone	–	–	0.15
Carbonyl group	–	–	0.38
Total	39.78	29.90	33.96

*RT, retention time (min) of each volatile compound eluted through the HP 5MS column in GC–MS.

10.3389/fmicb.2023.1142144

TABLE 5 List of volatile organic compounds (VOCs) in the ethyl acetate fraction during *F. oxysporum* f. sp. *psidii* and *A. niger* interaction, determined by GC–MS.

Sl. No	Compound	Organic Group	Chemical formula	*F. oxysporum* f. sp. *psidii* (control)		*A. niger* (control)		*F. oxysporum* f. sp. *psidii* and *A. niger* interaction	
				RT*	Area %	RT*	Area %	RT*	Area %
1	Ethyl propanoate	Ester	$C_5H_{10}O_2$	5.13	0.18 ± 0.12	–	–	–	–
2	3-hydroxy-ethyl butyrate	Ester	$C_6H_{12}O$	12.25	1.3 ± 0.19	–	–	–	–
3	2-dodecene	Hydrocarbon	$C_{12}H_{24}$	27.90	0.98 ± 0.22	–	–	–	–
4	*n*-dodecane	Hydrocarbon	$C_{12}H_{26}$	28.39	0.15 ± 0.02	17.21	13.92 ± 3.36	–	–
5	*n*-tridecane	Hydrocarbon	$C_{13}H_{28}$	35.04	0.02 ± 0.01	–	–	–	–
6	Tetradec-1-ene	Hydrocarbon	$C_{14}H_{28}$	41.36	7.89 ± 0.95	–	–	–	–
7	*n*-tetradecane	Hydrocarbon	$C_{14}H_{30}$	41.62	0.54 ± 0.18	–	–	–	–
8	*α*-hexadecene	Hydrocarbon	$C_{16}H_{32}$	53.38	2.81 ± 0.16	–	–	–	–
9	*n*-hexadecane	Hydrocarbon	C16H34	53.60	0.62 ± 0.03	–	–	–	–
10	3-methoxy-2,4,5-trimethylphenol	Phenol	$C_{10}H_{14}O_2$	54.32	3.4 ± 0.56	–	–	–	–
11	Dodecyl acrylate	Ester	$C_{15}H_{28}O_2$	58.14	0.97 ± 0.04	–	–	–	–
12	Myristate	Ester	$C_{15}H_{30}O_2$	60.53	0.97 ± 0.11	–	–	–	–
13	1-octadecene	Hydrocarbon	$C_{18}H_{36}$	60.78	22.26 ± 2.2	–	–	–	–
14	2-tetradecene	Hydrocarbon	$C_{14}H_{28}$	60.83	0.07 ± 0.02	–	–	–	–
15	Cyclopentadecane	Hydrocarbon	$C_{15}H_{30}$	62.60	0.21 ± 0.07	–	–	–	–
16	Hexadecanoate	Ester	$C_{17}H_{34}O_2$	62.84	1.24 ± 0.92	–	–	–	–
17	3-eicosene	Hydrocarbon	$C_{20}H_4O$	63.15	0.06 ± 0.05	–	–	–	–
18	*n*-hexadecanoic acid	Acid	$C_{16}H_{32}O_2$	64.00	4.37 ± 1.84	–	–	–	–
19	1-eicosene	Hydrocarbon	$C_{20}H_4O$	64.61	0.1 ± 0.06	–	–	–	–
20	9-octadecenoic acid	Acid	$C_{18}H_{34}O_2$	64.85	8.81 ± 2.17	–	–	–	–
21	10-octadecenoic acid methyl ester	Ester	$C_{19}H_{36}O_2$	64.99	0.59 ± 0.03	–	–	–	–
22	Pentamethyl-2,3-dihydro indene	Hydrocarbon	$C_{14}H_2O$	–	–	17.82	3.3 ± 0.24	–	–
23	Tetradecane	Hydrocarbon	$C_{14}H_3O$	–	–	28.65	1.58 ± 0.87	–	–
24	Benzene ethanol	Alcohol	$C_8H_{10}O$	–	–	33.59	10.74 ± 1.48	–	–
25	Hexadecane	Hydrocarbon	$C_{16}H_{34}$	–	–	38.60	0.94 ± 0.31	–	–
26	2-2-furylethyl-*N*-methylaniline	Nitrogenous compound	C_7H_8FN	–	–	43.78	3.62 ± 1.46	–	–
27	4-ethylbenzoic acid	Acid	$C_9H_{10}O_2$	–	–	52.32	0.45 ± 0.09	–	–

(Continued)

10.3389/fmicb.2023.1142144

TABLE 5 (Continued)

Sl. No	Compound	Organic Group	Chemical formula	*F. oxysporum* f. sp. *psidii* (control)		*A. niger* (control)		*F. oxysporum* f. sp. *psidii* and *A. niger* interaction	
				RT*	Area %	RT*	Area %	RT*	Area %
28	Acetic acid ethyl ester	Ester	$C_4H_8O_2$	–	–	–	–	7.28	17.32 ± 2.19
29	3,3-dimethyl-2-hexanone	Alcohol	$C_8H_{16}O$	–	–	10.01	2.17 ± 0.94	9.62	1.02 ± 0.24
30	1,2-dimethyl benzene	Hydrocarbon	C_8H_{10}	–	–	–	–	10.1	0.56 ± 0.02
31	Methyl-2-methoxy-6-pentadecenoate	Ester	$C_{10}H_{12}O_3$	–	–	–	–	13.18	3.81 ± 1.22
32	1-(3-ethyloxiranyl) ethanone	Alcohol	$C_6H_{10}O_2$	–	–	–	–	24.75	0.98 ± 0.07
33	Benzopyran-4-ol	Alcohol	$C_9H_8O_2$	–	–	–	–	39.14	12.17 ± 3.16
34	6-acetyl-8-methoxy dimethyl chromene	Hydrocarbon	$C_{14}H_{16}O_3$	–	–	–	–	39.86	0.9 ± 0.18
35	1,2,6-hexanetriol	Alcohol	$C_6H_{14}O_3$	–	–	–	–	40.5	7.16 ± 1.92
36	Hexadecanoic acid	Acid	$C_{16}H_{32}O_2$	–	–	40.99	7.15 ± 1.45	41.96	1.75 ± 0.06
37	4-hexyl-2,5-dihydro dioxo furan acetic acid	Acid	$C_{12}H_{16}O_5$	–	–	–	–	42.03	0.19 ± 0.11
38	2-propenoic acid ethanediyl ester	Ester	$C_{10}H_{14}O_4$	–	–	–	–	42.11	2.95 ± 0.02
39	Octadecanoic acid	Acid	$C_{18}H_{36}O_2$	–	–	–	–	48.29	1.11 ± 0.04
40	3-diethynyl-9,10-dimethoxyanthracene	Hydrocarbon	$C_{16}H_{14}O_2$	–	–	55.39	2.29 ± 0.74	55.12	0.24 ±0.011
Chemical groups				**Content (%)**					
Hydrocarbons				35.52		1.44		1.76	
Esters				5.25		–		24.08	
Alcohol				–		12.91		21.33	
Acids				13.18		7.6		3.05	
Phenols				3.4		–		–	
Total				57.35		21.95		50.22	

*RT, retention time (min) of each volatile compound eluted through HP 5MS column in GC–MS.

10.3389/fmicb.2023.1142144

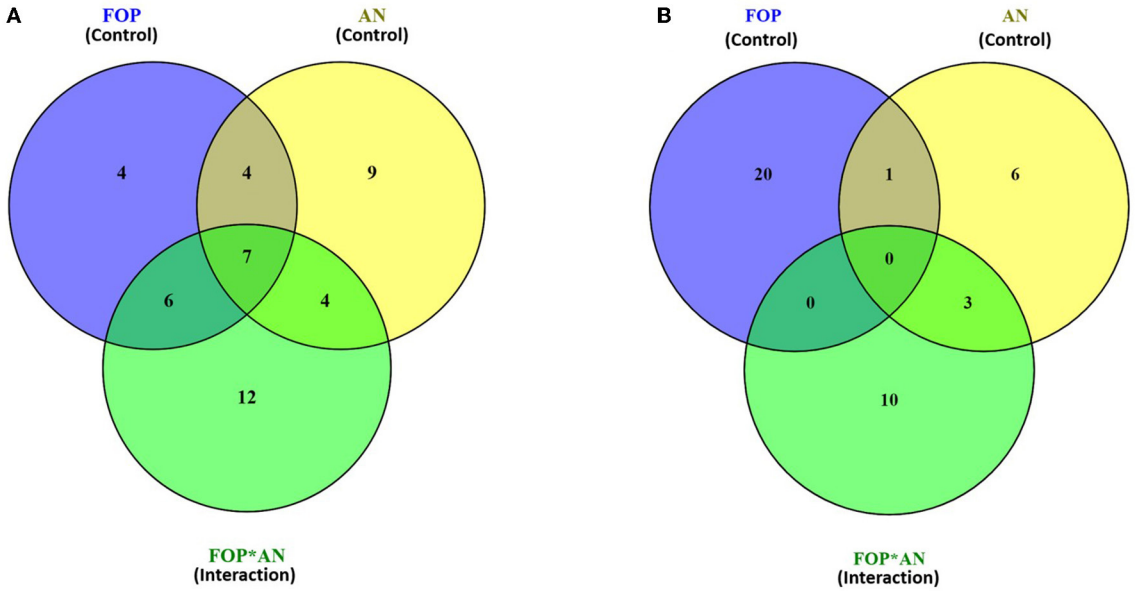

FIGURE 8
Venn diagram representing the compounds identified through GC–MS analysis of **(A)** hexane and **(B)** ethyl acetate fractions during *F. oxysporum* f. sp. *psidii* and *A. niger* interaction.

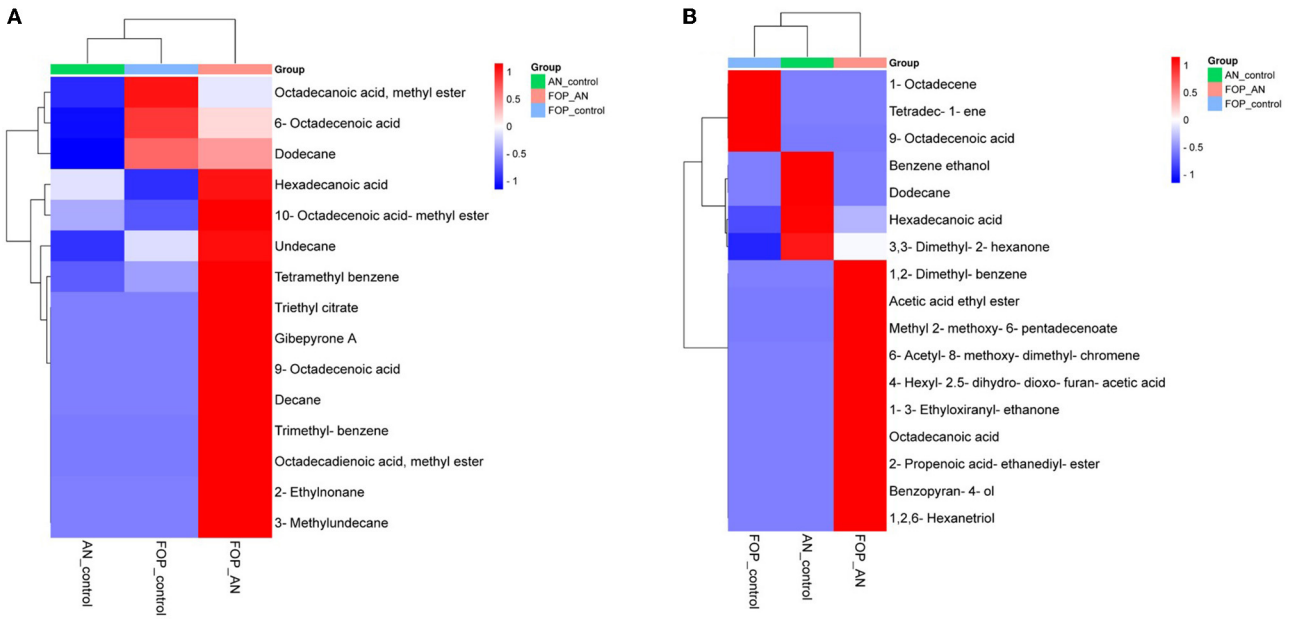

FIGURE 9
Heat map clustering of volatile organic compounds (VOCs) profiles from *A. niger* (AN) and *F. oxysporum* f. sp. *psidii* (FOP) and their interactions in **(A)** hexane and **(B)** ethyl acetate fractions.

metabolites, thereby restricting the growth of pathogens (Patibanda and Sen, 2005; Ferreira and Musumeci, 2021). *A. niger* has been found to be promising in inhibiting the guava wilt pathogen. The results are correlated with the previous studies, namely Dwivedi and Shukla (2002), Singh et al. (2003), Dwivedi and Dwivedi (2012), Naz et al. (2013), and Mandal et al. (2021). Sharma et al. (2011) tested *A. niger* against *Fusarium* wilt of tomato under *in vitro*, the highest mycelial inhibition of 74% was recorded, followed by *Trichoderma* spp., *Bacillus* spp. and, *Pencillium* spp. An *in planta* study carried out using guava pants (Allahabad Safeda) suggests that the application of *A. niger* to the soil near the root zone before the development of the disease will reduce the wilt incidence significantly, whereas, the control showed 100% wilt incidence with prominent symptoms. The wilted plants recovered

from wilting within a few days after being treated with *A. niger*. *Aspergillus versicolor* exhibited a 99.2% reduction in *F. oxysporum* f. sp. *cumini* and also has the ability to survive in hot, arid soils (Israel and Lodha, 2005). An experiment conducted by Boughalleb-M'Hamdi et al. (2018) recorded the antifungal activity of *Aspergillus* spp. against *F. oxysporum* f. sp. *niveum* and *F. solani* f. sp. *cucurbitae*. Among six bioagents evaluated against *F. oxysporum* f. sp. *melangene*, maximum mycelial growth inhibition of 65.92% and pre-emergence seedling mortality of 11.33% were recorded upon application of *A. niger* (Govardhan et al., 2020). The *in vitro* and *in planta* bio-efficacy test against peach seedling decline was conducted by Mannai and Boughalleb-M'Hamdi (2022) and resulted in the mycelial growth inhibition of *F. oxysporum* (85.82%) by *Aspergillus candidus*. Similarly, *A. flavus* and *A. niger* were found more effective against *F. solani,* with more than 60% mycelial inhibition. Attia et al. (2022) evaluated four plant growth-promoting fungi (PGPF), namely *A. flavus*, *A. niger*, *Mucor circinelloides,* and *Pencillium oxalicum,* against the tomato wilt pathogen (*F. oxysporum*). The *A. niger* significantly reduced disease severity by 16.60% and gave a high level of protection of (86.35%), thus enhancing the growth of healthy and infected tomato plants. Similarly, Atallah et al. (2022) reported that plants treated with *A. niger* and *A. japonicus* showed the highest survival rates compared to untreated plants infected with the white mold disease of beans (*S. sclerotiorum*). The results suggest that this bio-control can be used as an ideal tool to combat the disease successfully.

4.3. Microscopic study of *A. niger* and *F. oxysporum* f. sp. *psidii* interaction

From the microscopic study, it was elucidated that *A. niger* has a bio-control mechanism that involves attaching, coiling, and lysing the pathogen with hydrolytic enzymes or secondary metabolites. The majority of bio-control fungi operate similarly, which causes the pathogen to die (Mukherjee et al., 2012; Duarte-Leal et al., 2018). Our findings support earlier reports where bio-control agents produced organic acids and extracellular enzymes that inhibited hyphal growth. Cell wall degrading enzymes include chitinase, β-1,3-glucanases, β-1,6-glucanases, α-1,3-glucanases, and proteases, which act on pathogens and lead to death (Patibanda and Sen, 2005; González et al., 2012). From the aforementioned results, it is confirmed that the ability of bio-control is mainly dependent on the enzymatic activity and secondary metabolite production capacity that restrict the growth and establishment of pathogens.

4.4. Secondary metabolites profiling

It is known that *A. niger* produces a variety of bioactive secondary metabolites with antifungal, antibacterial, and toxic properties against a variety of phytopathogens, primarily soil-borne pathogens. In the present study, secondary metabolites profiling using GC–MS identified several chemical compounds that belong to organic compounds, such as fatty acids, esters, alcohols, and phenols, having antimicrobial action. The compounds found during interaction in the hexane extracts have been reported to demonstrate antimicrobial activities. Fatty acids and their esters (hexadecanoic acid, methyl ester, *cis*-9-hexadecenoic acid, hexadecanoic acid, 9 or 6-octadecenoic acid, and 10-octadecenoic acid methyl ester), undecane, dodecane, tetramethyl benzene, 2,6-dimethyl undecane, 2-methyl dodecane, dimethyl octane, and trimethyl benzene majorly found. These metabolites have already been reported to have antifungal activity (Agoramoorthy et al., 2007; Imad et al., 2015; Casuga et al., 2016; Naqvi et al., 2019). The majority of the VOCs generated were fatty acids and their esters, which inserted themselves into the lipid bilayers of fungal membranes and caused an uncontrolled release of intracellular proteins and electrolytes, which finally caused the cytoplasmatic disintegration of fungal cells (Avis and Bélanger, 2001). The same fatty acids were also examined by Liu et al. (2008) against important phytopathogenic fungi, including *Alternaria solani*, *Colletotrichum lagenarium*, *F. oxysporum* f. sp. *cucumerinum*, and *F. oxysporum* f. sp. *lycopersici*, and reduced spore germination and mycelial growth of pathogens were seen. From ethyl acetate extract, major compounds, *viz*., acetic acid ethyl ester, benzopyron-4-ol, 1,2,6-hexanetriol, 2-propenoic acid ethanediyl ester, 1-(3-ethyloxiranyl) ethenone, 6-acetyl-8-methoxy dimethyl chromene, and octadecanoic acid, were found during the interaction to have antifungal activity. Idan et al. (2017) identified around 15 major compounds of *A. niger* against *P. oryzae* (Rice blast) using GC–MS (oleic acid, *n*-hexadecanoic acid (palmitic acid), hexose, glycerol, stearic acid, tetradecanoic acid, dodecanoic acid, and 5-hydrxoymethylfurfural), most of which belong to fatty acids.

Fatty acids (oleic acid (9-octadecenoic acid), *n*-hexadecanoic acid, and stearic acids) were also found effective against *Fusarium solani* f. sp. *pisi* (Jha and Jalali, 2006), *Fusarium solani*, *Meloidogyne incognita* (Jang et al., 2016), *Candida* spp., *Micrococcus luteus, Pseudomonas aeruginosa,* and *Bacillus subtilis* (Agoramoorthy et al., 2007; Stenz et al., 2008). Furanacetic acid derivative (4-hexyl-2,5-dihydro dioxo furan acetic acid), similar to other furancarboxylic acid derivatives, has antibacterial and antifungal potential (Chang et al., 2020). Compounds having acids, esters, pyran, and furan from *A. niger* exhibited antibacterial activity against *Pseudomonas aerogenosa*, *Escherichia coli*, *Proteus mirabilis*, *Staphylococcus aureus,* and *Klebsiella pneumonia* (Imad et al., 2015). The compound 1-(3-Ethyloxiranyl) ethenone isolated from *Cordia obliqua* displayed antimicrobial properties against different microorganisms (Raj and Kumar, 2018). The compound 1,2,6-hexanetriol (a replacement of glycerin) is a sugar-derived alcohol, having antifungal activity, and chromenes (a derivative of coumarin) found in our experiment have been reported to show broad biological inhibitory antimicrobial properties (Basanagouda et al., 2010; Sahoo and Paidesetty, 2017; Ashok et al., 2018). Benzopyran-containing compounds are related to polyketide synthesis and are formed by the fusion of the benzene ring with the heterocyclic pyran ring. These are core ring structures of flavonoids, isoflavonoids, and isocoumarins, which have strong antifungal activity (Santiago et al., 2014). Most of the antifungal compounds identified from the study were produced during the interaction of bio-control and pathogens. These findings will serve as a foundation for the successful management of diseases in agriculture by using VOCs from the bio-control agent *A. niger*.

5. Conclusion

In recent years, biological control has received increasing attention as a promising alternative to chemical control of plant pathogens. In the present study, *A. niger* was found to be a promising antagonist for the management of the guava wilt pathogen FOP tested under lab and greenhouse conditions. Our study also suggested that the application of *A. niger* before the establishment of the disease reduces the wilt incidence significantly. GC–MS analysis revealed the production of antifungal secondary metabolites such as acetic acid, ethyl ester, benzopyron-4-ol, 1,2,6-hexanetriol, 2-propenoic acid ethanediyl ester, 6-acetyl-8-methoxy dimethyl chromene, 4-hexyl-2,5-dihydro dioxo furan acetic acid, octadecanoic acids, and some esters and acids, which may be involved in the mycoparasitism by acting synergistically. Our findings collectively imply that *A. niger* and its antimicrobial substances have great potential to successfully manage guava wilt and other soil-borne diseases. Since BCAs perform differently at varied climatic conditions, there is a need to evaluate their efficacy at multiple locations to confirm their robustness and potentiality.

Data availability statement

The datasets presented in this study can be found in online repositories. The names of the repository/repositories and accession number(s) can be found in the article/Supplementary material.

Author contributions

RG, DK, and AK were involved in the conceptualization of the project, study design, critical inputs, and finalization of the manuscript. RG contributed to the lab work and statistical analysis and wrote the first draft. RG, DK, AN, GP, and AD finalized the outline and prepared schematics. RG, AD, RD, GP, NB, and NG helped with statistical data analysis and editing of the manuscript. RG, AK, and VR carried out GC–MS work and analysis. GC captured SEM images. All authors contributed to the article and approved the submitted version.

Acknowledgments

We are thankful to ICAR-IARI, New Delhi for encouragement, and for providing the necessary facilities and financial support throughout the research. RG is grateful to the CSIR for providing a fellowship toward the Ph.D. program.

Conflict of interest

The authors declare that the research was conducted in the absence of any commercial or financial relationships that could be construed as a potential conflict of interest.

Publisher's note

All claims expressed in this article are solely those of the authors and do not necessarily represent those of their affiliated organizations, or those of the publisher, the editors and the reviewers. Any product that may be evaluated in this article, or claim that may be made by its manufacturer, is not guaranteed or endorsed by the publisher.

Supplementary material

The Supplementary Material for this article can be found online at: https://www.frontiersin.org/articles/10.3389/fmicb.2023.1142144/full#supplementary-material

References

Agoramoorthy, G., Chandrasekaran, M., Venkatesal., and Hsu, M. J. (2007). Antibacterial and antifungal activities of fatty acid methyl esters of the blind-your-eye mangrove from India. *Braz. J. Microbiol.* 38, 739–742. doi: 10.1590/S1517-83822007000400028

Ashok, D., Gundu, S., Aamate, V. K., Devulapally, M. G., Bathini, R., and Manga, V. (2018). Dimers of coumarin-1,2,3-triazole hybrids bearing alkyl spacer: design, microwave-assisted synthesis, molecular docking and evaluation as antimycobacterial and antimicrobial agents. *J. Mol. Struct.* 1157, 312–321. doi: 10.1016/j.molstruc.2017.12.080

Atallah, O. O., Mazrou, Y. S., Atia, M. M., Nehela, Y., Abdelrhim, A. S., and Nader, M. M. (2022). Polyphasic characterization of four *Aspergillus* species as potential bio-control agents for white mold disease of bean. *J. Fungi.* 8, 626. doi: 10.3390/jof8060626

Attia, M. S., Abdelaziz, A. M., Al-Askar, A. A., Arishi, A. A., Abdelhakim, A. M., and Hashem, A. H. (2022). Plant growth-promoting fungi as bio-control tool against *Fusarium* wilt disease of tomato plant. *J. Fungi* 8, 775. doi: 10.3390/jof8080775

Avis, T. J., and Bélanger, R. R. (2001). Specificity and mode of action of the antifungal fatty acid cis-9-heptadecenoic acid produced by *Pseudozyma flocculosa*. *Appl. Environ. Microbiol.* 67, 956–960. doi: 10.1128/AEM.67.2.956-960.2001

Basanagouda, M., Shivashankar, K., Kulkarni, M. V., Rasal, V. P., Patel, H., Mutha, S. S., et al. (2010). Synthesis and antimicrobial studies on novel sulfonamides containing 4-azidomethyl coumarin. *Eur. J. Med. Chem.* 45, 1151–1157. doi: 10.1016/j.ejmech.2009.12.022

Boughalleb-M'Hamdi, N., Salem, I. B., and M'Hamdi, M. (2018). Evaluation of the efficiency of *Trichoderma*, *Penicillium*, and *Aspergillus* species as biological control agents against four soil-borne fungi of melon and watermelon. *Egypt. J. Biol. Pest Control.* 28, 1–12. doi: 10.1186/s41938-017-0010-3

Carbone, I., and Kohn, L. M. (1999). A method for designing primer sets for speciation studies in filamentous ascomycetes. *Mycologia* 91, 553–556.

Casuga, F. P., Castillo, A. L., and Corpuz, M. J. A. T. (2016). GC-MS analysis of bioactive compounds present in different extracts of an endemic plant *Broussonetia luzonica* leaves. *Asian Pac. J. Trop. Biomed.* 6, 957–961. doi: 10.1016/j.apjtb.2016.08.015

Chang, J. L., Xu, H. Z., Zhou, J., Zhou, M., Zhang, X., Guo, Y., et al. (2020). Antimicrobial furancarboxylic acids from a *Penicillium* sp. *J. Nat. Prod.* 83, 3606–3613. doi: 10.1021/acs.jnatprod.0c00758

Chen, Y., Black, D. S., and Reilly, P. J. (2016). Carboxylic ester hydrolases: Classification and database derived from their primary, secondary, and tertiary structures. *Protein Sci.* 25, 1942–1953. doi: 10.1002/pro.3016

Cullings, K. W. (1992). Design and testing of a plant-specific PCR primer for ecological and evolutionary studies. *Mol. Ecol.* 1, 233–240. doi: 10.1111/j.1365-294X.1992.tb00182.x

Darshan, K., Aggarwal, R., Bashyal, B. M., Singh, J., Kundu, A., Yadav, S., et al. (2021). Antifungal metabolite profiling in *Chaetomium globosum* potential strain Cg2 effective against *Bipolaris sorokiniana*. *Indian J. Agric. Sci.* 91, 776–782. doi: 10.56093/ijas.v91i5.113103

Das Gupta, S. N., and Rai, J. N. (1947). Wilt disease of guava (*P. guajava* L.). *Curr. Sci.* 16, 256–258.

Dennis, C., and Webster,. J. (1971a). Antagonistic properties of species groups of *Trichoderma*. II. Production of volatile antibiotics. *Trans. Brit. Mycol. Soc.* 57, 363–369. doi: 10.1016/S0007-1536(71)80050-5

Dennis, C., and Webster,. J. (1971b). Antagonistic properties of species groups of *Trichoderma*. I. Production of non-volatile antibiotics. *Trans. Brit. Mycol. Soc.* 57, 41–48. doi: 10.1016/S0007-1536(71)80078-5

Diba, K., Kordbacheh, P., Mirhendi, S. H., Rezaie, S., and Mahmoudi, M. (2007). Identification of *Aspergillus* species using morphological characteristics. *Pak. J. Med. Sci.* 23, 867–872.

Duarte-Leal, Y., Pozo-Martínez, L., and Martínez-Coca, B. (2018). Antagonismo *in-vitro* de cepas de *Trichoderma asperellum* Samuels, Lieckfeldt and Nirenberg frente aislados de *Fusarium* spp. *Rev. Protección. Veg.* 33, 1–10.

Dwivedi, B. P., and Shukla, D. N. (2002). Bio-control of *Fusarium* wilt of guava (*P. guajava*) using *Trichoderma* and *Gliocladium* species. *Karnataka. J. Agric. Sci.* 15, 399–400.

Dwivedi, S. K., and Dwivedi, N. (2012). *In vitro* bio efficacy of some selected fungal antagonists against guava wilt pathogen. *IOSR. J. Eng.* 2, 1217–1223. doi: 10.9790/3021-020512171223

El-Shora, H. M., El-Sharkawy, R. M., Khateb, A. M., and Darwish, D. B. (2021). Production and immobilization of β-glucanase from *A. niger* with its applications in bioethanol production and bio-control of phytopathogenic fungi. *Sci. Rep.* 11, 21000. doi: 10.1038/s41598-021-00237-2

Esmail, S. M., Omar, G. E., and Mourad, A. I. (2022). In-depth understanding of the genetic control of stripe rust resistance (*Puccinia striiformis* f. sp. *tritici*) induced in wheat (*Triticum aestivum* L.) by *Trichoderma asperellum* T34. *Plant Dis.* 107, 457–472. doi: 10.1094/PDIS-07-22-1593-RE

Ferreira, F. V., and Musumeci, M. A. (2021). *Trichoderma* as biological control agent: scope and prospects to improve efficacy. *World J. Microbiol. Biotechnol.* 37, 90. doi: 10.1007/s11274-021-03058-7

Gangaraj, R., Nagaraja, A., Gaba, S., Das, A., Prameeladevi, D.ebbarma, R., Choudhary, S. P., et al. (2022). Occurrence, identification and pathogenicity of *Fusarium* species associated with guava wilt disease in India. *Arch. Phytopathol. Plant Prot.* 55, 175–197. doi: 10.1080/03235408.2021.2005368

Garcia, E. F. (1991). Screening of fungal antagonist to control *Sclerotium cepivorium*. *Jensen D F et al.* 14, 79–81.

George, M., and Ramteke, P. W. (2019). Morphology, molecular identification and phylogenetic analysis based on internal transcribed spacer (ITS) of the ribosomal nuclear DNA (rDNA) sequence of a pathogenic fungal isolate *A. niger* LKO1. *Trop. Plant. Res.* 6, 166–170. doi: 10.22271/tpr.2019.v6.i2.024

González, I., Infante, D., Martínez, B., Arias, Y., González, N., Miranda, I., et al. (2012). Induction of chitinases and glucanases in *Trichoderma* spp. strains intended for biological control. *Biotecnol. Aplicada* 29, 12–16.

Govardhan, R. V., Dhutaj, D. N., Navgire, K. D., Apet, K. T., and Ambadkar, C. V. (2020). Evaluation of different fungal and bacterial antagonists against *Fusarium* wilt of eggplant caused by *F. oxysporum* f. sp. *melongenae*. *Int. J. Curr. Microbiol. Appl. Sci.* 9, 3610–3618. doi: 10.20546/ijcmas.2020.909.446

Gupta, V. K., and Misra, A. K. (2009). Efficacy of bioagents against *Fusarium* wilt of guava. *J. Plant. Pathol.* 39, 101.

Gupta, V. K., Misra, A. K., Gaur, R. K., Jain, P. K., Gaur, D., and Saroj, S. (2010). Current status of *Fusarium* wilt disease of guava (*P. guajava L.) in India*. *Biotechnology* 9, 176–195. doi: 10.3923/biotech.2010.176.195

Hussain, M. Z., Rahman, M. A., and Bashar, M. A. (2014). Incidence of guava (*P. guajava*) wilt caused by *F. oxysporum* f. sp. *psidii* in Bangladesh. *J. Asiat. Soc. Bangladesh Sci.* 40, 97–105.

Idan, A. A., Sijam, K., Kadir, J., Rashid, T. S., Awla, H. K., and Alsultan, W. (2017). Biological control of *P. oryzae* using antifungal compounds produced by *A. niger*. *Am. J. Plant Sci.* 8, 2445. doi: 10.4236/ajps.2017.810166

Imad, H. H., Lena, F. H., and Sabreen, A. K. (2015). Analysis of bioactive chemical compounds of *A. niger* by using gas chromatography-mass spectrometry and fourier-transform infrared spectroscopy. *J. Pharmacogn. Phytother.* 7, 132–163. doi: 10.5897/JPP2015.0354

Israel, S., and Lodha, S. (2005). Biological control of *F. oxysporum* f. sp. *cumini* with *Aspergillus versicolor*. *Phytopathol. Mediterr.* 44, 3–11.

Jang, J. Y., Choi, Y. H., Shin, T. S., Kim, T. H., Shin, K. S., Park, H. W., et al. (2016). Biological control of *Meloidogyne incognita* by *A. niger* F22 producing oxalic acid. *PLoS ONE* 11, e0156230. doi: 10.1371/journal.pone.0156230

Javadi, M. A., Ghanbary, M. A. T., and Tazick, Z. (2012). Isolation and molecular identification of soil inhabitant *Penicillium*. *Ann. Biol. Res.* 3, 5758–5761.

Jha, P. K., and Jalali, B. L. (2006). Biocontrol of pea root rot incited by Fusarium solani f. sp. pisi with rhizosphere mycoflora. *Indian Phytopathol.* 59, 41–43. Available online at: https://epubs.icar.org.in/index.php/IPPJ/article/view/17249

Junqueira, N. T. V., Andrade, L. D., Pereira, M., Lima, M. M., and Chaves, R. C. (2001). Diseases of guava (*P. guajava* L.) cultivated in Brazilian Cerrdos. *Circul. Techn. Embrapa Cerrados* 15, 31–31.

Korpi, A., Järnberg, J., and Pasanen, A. L. (2009). Microbial volatile organic compounds. *Crit. Rev. Toxicol.* 39, 139–193. doi: 10.1080/10408440802291497

Kumar, M., Tomar, M., Amarowicz, R., Saurabh, V., Nair, M. S., Maheshwari, C., et al. (2021a). Guava (*P. guajava* L.) leaves: nutritional composition, phytochemical profile, and health-promoting bioactivities. *Foods* 10, 752. doi: 10.3390/foods10040752

Kumar, R., Kundu, A., Dutta, A., Saha, S., Das, A., and Bhowmik, A. (2021b). Chemo-profiling of bioactive metabolites from *Chaetomium globosum* for bio-control of *Sclerotinia* rot and plant growth promotion. *Fungal biol.* 125, 167–176. doi: 10.1016/j.funbio.2020.07.009

Kumar, S., Stecher, G., and Tamura, K. (2016). MEGA7: molecular evolutionary genetics analysis version 7.0 for bigger datasets. *Mol. Biol. Evol.* 33, 1870–1874. doi: 10.1093/molbev/msw054

Kumari, A., and Choudhary, M. (2019). Crop regulation in guava: a review. *Agric. Rev.* 40, 303–308. doi: 10.18805/ag.R-1940

Lanka, S., Anjali, C. H., and Pydipalli, M. (2017). Enhanced production of alkaline protease by *A. niger* DEF 1 isolated from dairy form effluent and determination of its fibrinolytic ability. *Afr. J. Microbiol. Res.* 11, 440–449. doi: 10.5897/AJMR2016-8379

Lim, T. K., and Manicom, B. Q. (2003). *Diseases of Guava. Diseases of Tropical Fruit Crops*. Wallingford: CABI Publications, 275–289. doi: 10.1079/9780851993904.0275

Link, H. F. (1809). Observationes in ordines plantarum naturales. *Dissertatio. Mag. Ges. Naturf. Freunde. Berlin*. 3, 3–42.

Liu, S., Ruan, W., Li, J., Xu, H., Wang, J., Gao, Y., et al. (2008). Biological control of phytopathogenic fungi by fatty acids. *Mycopathologia* 166, 93–102. doi: 10.1007/s11046-008-9124-1

Lykholat, Y. V., Khromykh, N. O., Didur, O. O., Drehval, O. A., Sklyar, T. V., and Anishchenko, A. O. (2021). Chaenomeles speciosa fruit endophytic fungi isolation and characterization of their antimicrobial activity and the secondary metabolites composition. *Beni-Suef. Univ. J. Basic Appl. Sci.* 10, 1–10. doi: 10.1186/s43088-021-00171-2

Mandal, S. K., Kumari, A. R., Mandal, R. K., and Chhetri, K. B. (2021). "Guava wilt and its management," in *Innovative Approaches in Diagnosis and Management of Crop Diseases* (Washington, DC: Apple Academic Press), 201–208. doi: 10.1201/9781003187844-10

Mandol, G. (1998). *In-vitro evaluation of A. niger AN27 against soil borne pathogens and field testing against Macrophomina phaseolina on potato, India* (Ph.D. Thesis). Indian Agriculture Research Institute, New Delhi, India.

Mannai, S., and Boughalleb-M'Hamdi, N. (2022). *In-vitro* and *in-planta* potential effect of some indigenous antagonists against *Fusarium* and pythiaceous species associated with peach seedlings decline. *Egypt. J. Biol. Pest Control.* 32, 1–10. doi: 10.1186/s41938-022-00540-8

McClenny, N. (2005). Laboratory detection and identification of *Aspergillus* species by microscopic observation and culture: the traditional approach. *J. Med. Vet. Mycol.* 43, S125–S128. doi: 10.1080/13693780500052222

Micheli, P. A. (1729). *Nova Plantarum Genera luxta Tournefortii Methodum Disposita*. Florence.

Misra, A. K., and Pandey, B. K. (1999). Pathogenicity and evaluation of fungicides against guava wilt pathogens. *J. Plant Pathol.* 29, 274–275.

Misra, A. K., and Pandey, B. K. (2000). "Pathogenicity and symptom production of wilt disease of guava by a new potent pathogen *Gliocladium roseum*," in *Proceedings, Indian Phytopathological Society-Golden Jubilee, International Conference on Integrated Disease Management for Sustainable Agriculture,* 749–750.

Misra, A. K., and Prasad, D. (2004). "*Aspergillus niger* strain AN 17 potent bioagent to control wilt disease and its easy multiplication," in *Proceedings of the Symposium on Recent Advances in Fungal Bioagents and their Social Benefits,* 10–10.

Misra, A. K., Prasad, D., Prasad, B., and Shukla, S. K. (2004). "Effective management of wilt disease of guava," in *Proceedings of the National Symposium on Crop Surveillance: Disease Forecasting and Management,* 19–21.

Mondal, G., Dureja, P., and Sen, S. (2000). Fungal metabolites from *A. niger* AN27 related to plant growth promotion. *Indian J. Exp. Biol.* 38, 84–87.

Morton, D. T., and Stroube, N. H. (1955). Antagonistic and stimulatory effect of microorganism upon *Sclerotium rolfsii*. *Phytopathology* 45, 419–420.

Mukherjee, K., and Sen, B. (1998). Biological control of *Fusarium* wilt of muskmelon by formulations of *A. niger*. *Isr. J. Plant Sci.* 46, 67–72.

Mukherjee, M., Mukherjee, P. K., Horwitz, B. A., Zachow, C., Berg, G., and Zeilinger, S. (2012). Trichoderma–plant–pathogen interactions: advances in genetics of biological control. *Indian J. Microbiol.* 52, 522–529. doi: 10.1007/s12088-012-0308-5

Naqvi, S. F., Javaid, A., and Qureshi, M. Z. (2019). Evaluation of antifungal potential of leaf extract of *Chenopodium murale* against *F. oxysporum* f. sp. *lycopersici*. *Planta Daninha* 37, 139. doi: 10.1590/s0100-83582019370100139

Nasri, T., Hedayati, M. T., Abastabar, M., Pasqualotto, A. C., Armaki, M. T., Hoseinnejad, A., et al. (2015). PCR-RFLP on β-tubulin gene for rapid identification of the most clinically important species of *Aspergillus*. *J. Microbiol. Methods*. 117, 144–147. doi: 10.1016/j.mimet.2015.08.007

Nayak, S., and Vibha, S. (2017). Evaluation of organic acid producing *A. niger* isolates for the management of *Fusarium* wilt of chickpea. *Int. J. Curr. Microbiol. Appl. Sci.* 6, 256–265. doi: 10.20546/ijcmas.2017.605.029

Naz, A., Naz, H., and Ashraf, S. (2013). Management of guava wilt by biological agent. *Int. J. Food Sci. Technol.* 14, 667–670.

Nielsen, K. F., Mogensen, J. M., Johansen, M., Larsen, T. O., and Frisvad, J. C. (2009). Review of secondary metabolites and mycotoxins from the *A. niger* group. *Anal. Bioanal. Chem*. 395, 1225–1246. doi: 10.1007/s00216-009-3081-5

Nithiyaa, P., Nur Ain Izzati, M. Z., Umi Kalsom, Y., and Salleh, B. (2012). Diversity and morphological characteristics of *Aspergillus* species and *Fusarium* species isolated from cornmeal in Malaysia. *Pertanika J. Trop. Agric. Sci.* 35, 1499.

Patibanda, A. K., and Sen, B. (2005). Mechanism of *A. niger* antagonism towards *F. oxysporum* f. sp. *melonis* Sny. and Hans., muskmelon wilt pathogen. *J. Biol. Control.* 19, 115–120.

Perrone, G., Susca, A., Cozzi, G., Ehrlich, K., Varga, J., Frisvad, J. C., et al. (2012). Biodiversity of *Aspergillus* species in some important agricultural products. *Stud. Mycol.* 59, 53–66. doi: 10.3114/sim.2007.59.07

Raj, T., and Kumar, P. (2018). Preparation of hexane extract of *Cordia obliqua* and its analysis by TLC, FTIR and GCMS. *Int. Res. J. Pharm.* 95, 230–243. doi: 10.7897/2230-8407.09568

Sahoo, J., and Paidesetty, S. K. (2017). Antimicrobial activity of novel synthesized coumarin based transitional metal complexes. *J. Taibah Univ. Med. Sci.* 12, 115–124. doi: 10.1016/j.jtumed.2016.10.004

Samson, R. A., Noonim, P., Meijer, M., Houbraken, J., Frisvad, J. C., and Varga, J. (2007). Diagnostic tools to identify black *Aspergilli*. *Stud. Mycol.* 59, 129–146. doi: 10.3114/sim.2007.59.13

Samson, R. A., Visagie, M., Houbraken, J., Hong, S. B., Hubka, V., Klaassen, C. H., et al. (2014). Phylogeny, identification and nomenclature of the genus *Aspergillus*. *Stud. Mycol.* 78, 141–173. doi: 10.1016/j.simyco.2014.07.004

Santiago, C., Sun, L., Munro, M. H. G., and Santhanam, J. (2014). Polyketide and benzopyran compounds of an endophytic fungus isolated from *Cinnamomum mollissimum*: biological activity and structure. *Asian Pac. J. Trop. Biomed.* 4, 627–632. doi: 10.12980/APJTB.4.2014APJTB-2014-0030

Schoeman, M. H. (2011). The current status of guava wilt disease in South Africa. *SA Fruit J.* 10, 46–49.

Shah, M. H., Usman, M., Fatima, B., and Nawaz-Ul-Rehman, M. S. (2019). Assessment of guava wilt disease (GWD) and varietal susceptibility in Punjab-Pakistan. *Pak. J. Agric Sci.* 56, 393–399.

Sharma, B. K., Loganathan, M., Singh, R. P., Bag, T. K., Rai, R. K., Rai, A. B., et al. (2011). *Aspergillus niger*, a potential bio-control agent for controlling *Fusarium* wilt of tomato. *J. Mycopathol. Res.* 49, 115–118.

Silva, D. M., Batista, L. R., Rezende, E. F., Fungaro, M. H. P., Sartori, D., and Alves, E. (2011). Identification of fungi of the genus *Aspergillus* section *Nigri* using polyphasic taxonomy. *Braz. J. Microbiol.* 42, 761–773. doi: 10.1590/S1517-83822011000200044

Singh, G., Singh, J., and Arya, S. K. (2021). Insights on guava wilt and its different control measures. *Arch. Phytopathol. Plant Prot.* 54, 2262–2274. doi: 10.1080/03235408.2021.1926619

Singh, S. H., Ratan, V., Gaur, G. S., and Gangwar, D. (2003). Evaluation of antagonists against guava wilt pathogen. *Farm Sci. J.* 12, 58–59.

Stenz, L., François, P., Fischer, A., Huyghe, A., Tangomo, M., Hernandez, D., et al. (2008). Impact of oleic acid (cis-9-octadecenoic acid) on bacterial viability and biofilm production in Staphylococcus aureus. *FEMS Microbiol. Lett*. 287, 149–155. doi: 10.1111/j.1574-6968.2008.01316.x

Suresh, P., Poornima, K., Nakkeeran, S., Kalaiarasan, P., and Vijayakumar, R. M. (2019). Isolation and characterization of the causal organism of wilt in guava (*P. guajava* L.). *J. Pharma. Phytochem*. 8, 1231–1235. doi: 10.20546/ijcmas.2019.809.230

Susca, A., Perrone, G., Cozzi, G., Stea, G., Logrieco, A. F., and Mulè, G. (2013). Multilocus sequence analysis of *Aspergillus* Sect. Nigri in dried vine fruits of worldwide origin. *Int. J. Food Microbiol.* 165, 163–168. doi: 10.1016/j.ijfoodmicro.2013.04.027

Tamura, K., and Nei, M. (1993). Estimation of the number of nucleotide substitutions in the control region of mitochondrial DNA in humans and chimpanzees. *Mol. Biol. Evol.* 10, 512–526.

Varga, J., Frisvad, J. C., Kocsubé, S., Brankovics, B., Tóth, B., Szigeti, G., et al. (2011). New and revisited species in *Aspergillus* section Nigri. *Stud. Mycol.* 69, 1–17. doi: 10.3114/sim.2011.69.01

White, T. J., Bruns, T., Lee, S. J. W. T., and Taylor, J. (1990). Amplification and direct sequencing of fungal ribosomal RNA genes for phylogenetics. *PCR Protocols Guide Methods Appl.* 18, 315–322.

Yu, R., Liu, J., Wang, Y., Wang, H., and Zhang, H. (2021). *Aspergillus niger* as a secondary metabolite factory. *Front. Chem.* 9. doi: 10.3389/fchem.2021.701022

Zhou, T., He, Y., Zeng, X., Cai, B., Qu, S., and Wang, S. (2022). Comparative analysis of alternative splicing in two contrasting apple cultivars defense against *Alternaria alternata* apple pathotype infection. *Int. J. Mol. Sci.* 23, 14202. doi: 10.3390/ijms232214202

frontiers | Frontiers in Microbiology

TYPE Review
PUBLISHED 03 May 2023
DOI 10.3389/fmicb.2023.1160551

OPEN ACCESS

EDITED BY
Mina Salehi,
Tarbiat Modares University, Iran

REVIEWED BY
Rosa E. Cardoza,
Universidad de León, Spain
Pranab Dutta,
Central Agricultural University, India

*CORRESPONDENCE
Jingjun Ruan
✉ jjruan@gzu.edu.cn
Jie Chen
✉ jiechen59@sjtu.edu.cn

†These authors have contributed equally to this work

RECEIVED 21 February 2023
ACCEPTED 04 April 2023
PUBLISHED 03 May 2023

CITATION
Yao X, Guo H, Zhang K, Zhao M, Ruan J and Chen J (2023) *Trichoderma* and its role in biological control of plant fungal and nematode disease.
Front. Microbiol. 14:1160551.
doi: 10.3389/fmicb.2023.1160551

Trichoderma and its role in biological control of plant fungal and nematode disease

Xin Yao[1†], Hailin Guo[2†], Kaixuan Zhang[3†], Mengyu Zhao[1], Jingjun Ruan[1*] and Jie Chen[4*]

[1]College of Agronomy, Guizhou University, Guiyang, China, [2]Science and Technology Innovation Development Center of Bijie City, Bijie, China, [3]Institute of Crop Science, Chinese Academy of Agriculture Science, Beijing, China, [4]School of Agriculture and Biology, Shanghai Jiao Tong University, Shanghai, China

Trichoderma is mainly used to control soil-borne diseases as well as some leaf and panicle diseases of various plants. *Trichoderma* can not only prevent diseases but also promotes plant growth, improves nutrient utilization efficiency, enhances plant resistance, and improves agrochemical pollution environment. *Trichoderma* spp. also behaves as a safe, low-cost, effective, eco-friendly biocontrol agent for different crop species. In this study, we introduced the biological control mechanism of *Trichoderma* in plant fungal and nematode disease, including competition, antibiosis, antagonism, and mycoparasitism, as well as the mechanism of promoting plant growth and inducing plant systemic resistance between *Trichoderma* and plants, and expounded on the application and control effects of *Trichoderma* in the control of various plant fungal and nematode diseases. From an applicative point of view, establishing a diversified application technology for *Trichoderma* is an important development direction for its role in the sustainable development of agriculture.

KEYWORDS

***Trichoderma*, plant diseases, biological control, growth promotion, action mechanism**

Introduction

In the traditional crop cultivation process, the excessive use of pesticides and chemical fertilizers, as well as the long-term large-scale planting of a single crop, has led to the destruction of the farmland ecological environment, plant diseases, insect pest problems, crop pesticide residues, and soil and water environment pollution (Bardin et al., 2015). With green agricultural development, people are urgently seeking safe, effective, and environmentally friendly plant disease control measures. Biological control is mainly used to control harmful organisms in plants through beneficial organisms and their products to control plant diseases and effectively reduce the application of chemical fertilizers and pesticides (Harman et al., 2021). *Trichoderma*, a biological fungus widely used for plant pest control, mainly exists in the soil, air, plant surface, and other ecological environments and can effectively control a variety of plant diseases (Haouhach et al., 2020; Zheng et al., 2021; Wang R. et al., 2022). *Trichoderma* is mainly used to control soil-borne diseases in various plants and some leaf and spike diseases (Samuels et al., 2006; Vicente et al., 2020; Abbas et al., 2022). *Trichoderma* can prevent disease, promote plant growth, improve nutrient utilization efficiency, enhance plant resistance, and repair agrochemical pollution (Tilocca et al., 2020; Fontana et al., 2021; Sánchez-Montesinos et al., 2021; Al-Surhanee, 2022; Tyśkiewicz et al., 2022).

Trichoderma belonging to *Eumycota*, *Deuteromycotina*, *Hyphomycetes*, *Hyphomycetales*, and *Moniliaceae* (Kubicek et al., 2019). Its sexual stage includes the *Ascomycota*, Sordariomycetes, *Hypocreales*, *Hypocreaceae,* and *Trichoderma* ssp. (Sun et al., 2012). There are more than 370 *Trichoderma* spp. including *T. harzianum*, *T. viride*, *T. asperellum*, *T. hamatum*, *T. atroviride*, *T. koningii, T. longibrachiatum*, and *T. aureoviride* (Sánchez-Montesinos et al., 2021; Sun et al., 2022). *Trichoderma* has been used in biological control research, including *T. harzianum*, *T. hamatum*, *T. longibrachiatum*, *T. koningii*, *T. viride*, *T. polysporum*, and *T. asperellum* (Di Marco et al., 2022). Many studies have shown that most *Trichoderma* spp. can produce bioactive substances and have antagonistic effects on plant-pathogenic fungi and plant-pathogenic nematodes (Druzhinina et al., 2018). These bioactive substances, including secondary metabolites and cell wall-degrading enzymes, can effectively improve crop resistance, reduce plant diseases, and promote plant growth (Kubicek et al., 2019). Professor Harman of Cornell University isolated and purified *T. harzianum* T22 strain and systematically studied its application in biological control of plant pests and commercial development of biological control technology (Harman, 2000). This study systematically and comprehensively elaborated on the research progress on *Trichoderma* spp. and its role in plant disease control, its application as a biological control and its mechanism, as well as preliminarily discussed the problems and prospects of *Trichoderma* as a biological control agent, providing a reference for future research and application.

Application and mechanism of action of *Trichoderma* in plant fungal disease control

Application of *Trichoderma* in biological control of plant fungal diseases

Trichoderma is a biocontrol fungus widely distributed worldwide. *Trichoderma* has a huge application value and potential in the field of biological control of plant diseases (Tyśkiewicz et al., 2022). Research on the use of *Trichoderma* to control plant diseases has been reported worldwide. *T. viride* and *T. harzianum* have different degrees of inhibitory effects on 29 species of plant pathogenic fungi belonging to 18 genera, including *Botrytis*, *Fusarium*, and *Rhizoctonia*. *Trichoderma* has control effects on a variety of plant pathogenic fungi, such as *Rhizoctonia solani*, *Pythium ultimum*, *Fusarium oxysporum*, *Sclerotinia sclerotiorum*, *Botrytis cinerea, Pseudocercospora* spp. and *Colletotrichum* spp. (Tian et al., 2016, 2018; Saravanakumar et al., 2017; Debbi et al., 2018; Li et al., 2018; Bubici et al., 2019; Filizola et al., 2019; Herrera-Téllez et al., 2019; Álvarez-García et al., 2020; Andrade-Hoyos et al., 2020; Carro-Huerga et al., 2020; Damodaran et al., 2020; Zhang et al., 2020, 2021; Al-Askar et al., 2021; Chen et al., 2021; Degani and Dor, 2021; Dugassa et al., 2021; Intana et al., 2021; Zhang C. et al., 2022; Zhang Y. et al., 2022). *Trichoderma* has been widely used for the biological control of cotton verticillium wilt, crop gray mold, tomato gray mold, melon wilt, potato dry rot, tobacco root rot, and other plant diseases (Rashmi et al., 2016; Andrade-Hoyos et al., 2020; Alfiky and Weisskopf, 2021; Lazazzara et al., 2021; Leal et al., 2021; Manganiello et al., 2021; Degani et al., 2021a; Pollard-Flamand et al., 2022; Rees et al., 2022; Risoli et al., 2022). *T. longibrachiatum* T6 biocontrol agent has a good control effect on pepper damping off and can effectively control the spread of pepper disease (Girma, 2022). The control effect was up to 54.8%, which is 12.5% higher than that of the chemical pesticide carbendazim (Yuan et al., 2019; Al-Askar et al., 2022). *T. harzianum* has a good control effect on pepper and potato *Phytophthora* blight. It can inhibit the growth of *Phytophthora* blight in soil, reduce the number of pathogenic fungi, and effectively reduce the rate of dead seedlings and disease index of plants (Guzmán-Guzmán et al., 2017; Kappel et al., 2020; Mahmoud et al., 2021; Liu Y. et al., 2022). The control effect of 50× *T. asperellum* fungal fluid on apple canker reached 88.24%, which was significantly higher than that of benziothiazolinone (Ruangwong et al., 2021a). *T. asperellum* has different effects on different pathogenic fungi, among which its inhibitory effect on the pathogen causing corn leaf spot is the best, at up to 77.91%, followed by *Pythium* and *Fusarium*; and the worst inhibition effect is on corn sheath blight (Guo et al., 2019; Intana et al., 2022). Therefore, using *Trichoderma* to prevent and control plant diseases can not only inhibit the growth of pathogenic fungi, which is conducive to plant growth but can also reduce the use of chemical pesticides, which is conducive to protecting the ecological environment.

Storage resistance and processing technology of *Trichoderma* products

The commercial application of biocontrol *Trichoderma* depends to a large extent on the stress resistance (such as high temperature, drying, ultraviolet radiation, etc.) and storage resistance (more than 1 year at normal temperature) of the *Trichoderma* preparation (Alfiky and Weisskopf, 2021). At present, there are two main technologies: on the one hand, reducing acidity and regulating oxygen utilization to induce *Trichoderma* to produce stress-resistant chlamydospores; on the other hand, some chemical additives (such as copper) are added to the preparation. Monfil and Casas-Flores (2014) increased the resistance of *Trichoderma* to high temperature (35 ~ 40°C) and ultraviolet radiation by adding trehalose to *Trichoderma*. Monfil and Casas-Flores (2014) added glycerin to the *Trichoderma* preparation as a humectant to prolong its shelf life. Special packaging design, vacuum drying, and low-density polyethylene packaging materials can extend the shelf-life to 15 months. In the field of *Trichoderma* preparation form processing, Chen et al. (2021) developed the *Trichoderma* conidia powder agent and obtained a patented technology for inducing *Trichoderma* to produce chlamydospores. With the increasingly mature biological control technology, the types of commercial preparations for *Trichoderma* spp. are also becoming diverse. There are four main categories: (1) Wettable powders, which are made by mixing conidia powder, powdery carriers, and humectant. (2) Granules are made by mixing and stirring conidia and carrier. (3) A mixture consisting of spore powder and chemical fungicides mixed in proportion on a suitable carrier. (4) Suspenso-emulsion is prepared by suspending conidia in a lotion composed of vegetable oil, mineral oil, emulsifier, etc. In the current market for *Trichoderma* biological agents, *T. Harzianum* is the largest, followed by *T. viride* and *T. koningii*. *Trichoderma* agents widely used in plant disease control mainly include Trichodex (Makhteshim Chemical Works Ltd., Israel), a commercial preparation of *T. harzianum* T-39; RootShield (Bioworks, USA), a commercial preparation of *T. harzianum* T-22; Binab TF (Binab Bio Innovation AB, Sweden), a mixed-agent of

T. harzianum and *T. polyspora*; Sentinel (Novozymes, Denmark), a commercial preparation of *T. atrovilide*; And Supervivit (Borregaard Bioplant, Denmark), a commercial preparation of *T. harzianum*.

Mechanism of *Trichoderma*-induced endophytic microbiome synergistically stimulating plant immune response

Competitive role of *Trichoderma*

Trichoderma are saprophytic fungi with fast mycelial growth and strong adaptability to the environment. It can seize the invasive part of the pathogenic fungi in the root of a plant, thus hindering the invasion of the pathogen fungi. It can also rapidly absorb the nutrients required for the growth of the pathogen fungi, resulting in nutrient deficiency and inhibiting the growth and reproduction of the pathogen fungi (Guo et al., 2019; Bazghaleh et al., 2020; Halifu et al., 2020; Figure 1A). *Trichoderma* has strong adaptability to the environment (Köhl et al., 2019; Morán-Diez et al., 2019; Pescador et al., 2022; Xu et al., 2022). Through its rapid growth and reproduction, it can seize nutrients and space near the plant rhizosphere, consume oxygen in the air, and weaken the growth of plant pathogenic fungi (Basińska-Barczak et al., 2020; Oszust et al., 2020; Panchalingam et al., 2022). The growth rate of *Trichoderma* is much faster than that of plant-pathogenic fungi; therefore, it can effectively inhibit the growth of plant-pathogenic fungi (Mohiddin et al., 2021). After entering the soil for 24 h, *Trichoderma* can quickly adsorb to the roots of crops for propagation, and the hyphae quickly wrap the roots of crops to form a protective layer, protect the roots of crops from the invasion of pathogens, and kill the nearby pathogens. Risoli et al. (2022) found that the growth rate of *T. harzianum* was 2.0 to 4.2 times faster than that of *B. cinerea*. *Trichoderma* mycelium competed with *Fusarium graminearum* by clinging, twining, inter-penetration, and other mechanisms, which caused the mycelium of *F. graminearum* to deform and eventually disappear (Dugassa et al., 2021). *Trichoderma* can capture water and nutrients, occupy space, and consume oxygen, etc. through rapid growth and reproduction, to weaken and exclude the gray mold pathogen in the same habitat (Herrera-Téllez et al., 2019).

Mycoparasitism of *Trichoderma*

Mycoparasitism is one of the important mechanisms in the biological control of *Trichoderma* (Figure 1B). *Trichoderma* can parasitize about 18 genera of *Pythium*, *Phytophthora*, *Rhizoctonia*, and *Peronospora*. They directly invade or wound the mycelium, causing the pathogen cells to expand, deform, shorten, become round, shrink the protoplasm, and break the cell wall. *Trichoderma* TM can invade the hyphae of *Sclerotinia sclerotiorum*, attach to and wrap around the hyphae of pathogenic fungi, and break the hyphae of *S. sclerotiorum* until it disintegrates (Shaw et al., 2016). Risoli et al. (2022) found that *Trichoderma* can form putrescence in a specific environment, which has a mycoparasitic effect on *Botrytis cinerea*. It forms a large number of branches and sexual structures after entering the host hyphae, thus inhibiting the appearance of grape *B. cinerea* symptoms (Aswani et al., 2022). *Trichoderma* can degrade the cell wall of pathogenic fungi by secreting chitin-degrading enzymes, so as to better invade the interior

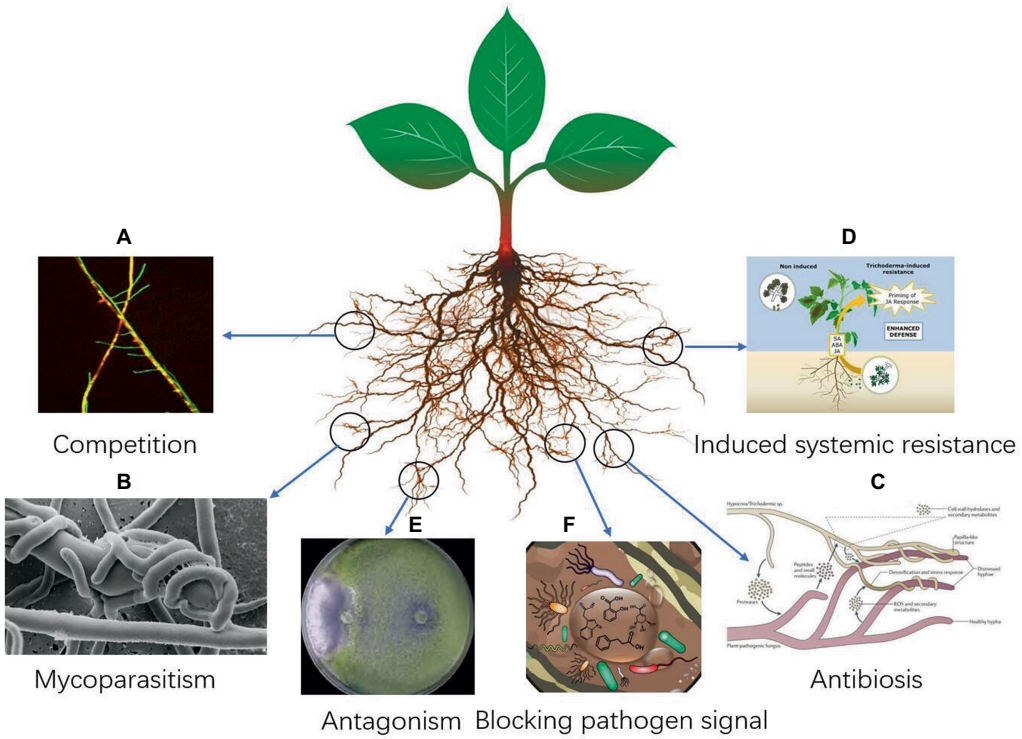

FIGURE 1
(A–F) Schematic diagram of the mechanism of action of *Trichoderma* in plant fungal disease control (Martínez-Medina et al., 2013; Lamdan et al., 2015; Morán-Diez et al., 2020; Manzar et al., 2022; Tamizi et al., 2022).

of pathogenic fungi. *Trichoderma* mycelium hyperparasitized *Fusarium graminearum* by clinging, twining, inter-penetration, and other mechanisms, which caused the mycelium of *F. graminearum* to deform and eventually disappear (Tian et al., 2018). Chitinase secreted by *T. harzianum* plays an important role in promoting cell wall dissolution, mycelial autolysis, chitin assimilation, fungal parasitism, and inhibiting spore germination, mycelial growth, and spore formation (Saravanakumar et al., 2017). *T. koningiopsis* can invade the hyphae of *Sclerotinia sclerotiorum*, attach to and wrap around the hyphae of pathogenic fungi, and break the hyphae of *S. sclerotiorum* until it disintegrates (Shaw et al., 2016).

Antibiosis effect of *Trichoderma*

Antibiosis mainly refers to the ability of *Trichoderma* to inhibit the growth of plant pathogenic fungi by secreting antagonistic substances (Kottb et al., 2015; Izquierdo-García et al., 2020; Morán-Diez et al., 2020; Shobha et al., 2020; El-Hasan et al., 2022; Figure 1C). *Trichoderma* can produce hundreds of antimicrobial secondary metabolites, including trichomycin, gelatinomycin, chlorotrichomycin, and antibacterial peptides (Maruyama et al., 2020). These secondary metabolites can act as antibacterial agents, promote plant growth, and provide rich materials for the development of agricultural antibiotics (Nawrocka et al., 2018). Naglot et al. (2015) found that the metabolites of *T. viride* had a significant inhibitory effect on the wilt-specific form of *F. oxysporum*, with an inhibition rate of 54.81%. Manganiello et al. (2018) found that the volatile secondary metabolites secreted by *T. viride* TG050 609 can cause the mycelium of *P. nicotianae* to grow irregularly, break, or even dissolve, proving that *T. viride* has an antibiosis effect on *P. nicotianae*. In addition, most *Trichoderma* strains can produce antimicrobial substances such as pentaibols, which can inhibit a variety of plant pathogenic fungi and can also cooperate with cell wall-degrading enzymes on pathogenic fungi to effectively inhibit their growth (Debode et al., 2018; Mayo-Prieto et al., 2019; Kovács et al., 2021; Martínez-Salgado et al., 2021; Tamizi et al., 2022). Some studies have shown that some *Trichoderma* spp. can produce volatile metabolites, which can inhibit the growth of colonies to varying degrees, and some of them can inhibit the growth of colonies by more than 80% (Navazio et al., 2007; Vos et al., 2015; Samuelian et al., 2016; Marik et al., 2019; Thambugala et al., 2020; Kong et al., 2022; Li M. et al., 2022).

In recent years, research on the genome, transcriptome, proteome, and metabolome of *Trichoderma* has developed rapidly (Zhang Y. et al., 2022). Genome and EST sequencing, and microarray and microarray based expression profiling have become important tools for exploring *Trichoderma* genes and studying the mechanism of action (Tamizi et al., 2022). In genomics research, a cDNA library of *T. harzianum* EST has been constructed, and multiple new genes have been identified (Ferreira Filho et al., 2020). The researchers completed the genome sequencing of *T. reesei*, *T. virens*, and *T. atroviride*. Rubio et al. (2014) used high-density oligonucleotide (HDO) microarray technology and bioinformatics analysis to detect and analyze: after 20 h of interaction between T. hamatum T7 and tomato, there were 200 differentially expressed genes, of which 166 were up-regulated and 34 were down-regulated; 43.14% of genes are related to molecular function, 56.86% are related to biological processes, and 32.0% are related to cell component formation. Shoresh and Harman (2010) identified the changes of 27 endochitinase genes and 4 exochitinase genes in maize after interaction between *T. harzianum* T22 and maize using proteomic methods and EST libraries and discovered a new specific chitinase. Chen et al. (2021) used proteomic techniques to identify proteins related to resistance to root rot in maize, among which chitinase, SOD, isoflavone reductase, and PR protein are associated with resistance to root rot in maize seedlings.

Induced systemic resistance of *Trichoderma*

Trichoderma can induce host plants to produce defense responses. While inhibiting the growth and reproduction of pathogenic fungi, it can also induce crops to produce self-defense systems to obtain local or systemic disease resistance (Figure 1D). *Trichoderma*-induced plant disease resistance is achieved through two approaches: one is to regulate the plant disease resistance response by regulating elicitors or effectors; second, the cell wall-degrading enzyme produced by *Trichoderma* releases oligosaccharides that can induce plant resistance (Gomes et al., 2015). At present, there are more than 10 elicitors of *Trichoderma* that induce plant resistance, including Sm1, QID74 hydrophobic protein, chitin-degrading enzyme, MRSP1, xylanase, cellulase, endopolygalacturonase, sucrase, and antibacterial peptides. These substances are mainly derived from five *Trichoderma* species: *T. asperellum*, *T. viride*, *T. atroviride*, and *T. harzianum* (Karimi Aghcheh et al., 2013; Lamdan et al., 2015; Ngo et al., 2021; Matas-Baca et al., 2022; Zaid et al., 2022; Zhu et al., 2022). Saravanakumar et al. (2016) found that the activities of peroxidase (POD) and phenylalanine ammonia lyase (PAL) of corn seeds coated with *Trichoderma* increased significantly, and the plants were resistant to curvularia leaf spot of corn.

Antagonism of *Trichoderma*

The antagonism of *Trichoderma* is often considered the result of simultaneous or sequential action of more than two mechanisms (Saravanakumar et al., 2016; Sui et al., 2022; Figures 1E,F). Based on multiple mechanisms, *Trichoderma* has synergistic capabilities (Alonso-Ramírez et al., 2014; Moreno-Ruiz et al., 2020; Stracquadanio et al., 2020; Alukumbura et al., 2022; Chung et al., 2022; Kappel et al., 2022). Jogaiah et al. (2018) found that the synergistic use of *T. harzianum* and fungicides can effectively inhibit tomato gray mold, and the inhibition rate was higher than that of both fungicides alone. Zhang et al. (2017) found that the fermentation metabolites of *T. viride* CCTCC-SWB0199 and brassinolide in a certain proportion had a higher effect on the control of tomato gray mold than when the two were applied separately. Jogaiah et al. (2018) found that the biocontrol effect of *Trichoderma* spp. against plant pathogens fungi are often the result of a combination of multiple mechanisms, and different strains have different emphasis on biocontrol mechanisms. Monfil and Casas-Flores (2014) used transcriptology and metabolomics to study the tripartite interactions of *Arabidopsis*, *Trichoderma*, and *Pseudomonas syringae* tomato varieties. The results showed that the treatment of *Arabidopsis* roots with *Trichoderma* for 48 h induced more than 300 gene expression changes in the roots, but the changes in leaf genes were different from those in the roots (Monfil and Casas-Flores, 2014). *Trichoderma* induces the differential expression of host plant genes, mainly at the level of quantity (Viterbo et al., 2005; Malmierca et al., 2012; Park et al., 2019). A metabolomics study found that 27 compounds were related to induced resistance in *Arabidopsis thaliana* (Monfil and Casas-Flores, 2014). The biocontrol effect of *Trichoderma* on plant pathogenic fungi is often the result of multiple mechanisms, and different strains have different biocontrol mechanisms (De Zotti

et al., 2020; Cai et al., 2021; Ji et al., 2021; Ruangwong et al., 2021b; Figure 1).

Application and mechanism of action of *Trichoderma* in plant nematode disease control

Application of *Trichoderma* in the control of plant nematodes

At present, the reported *Trichoderma* with nematicidal activity mainly includes *T. longibrachiatum*, *T. viride*, *T. harzianum*, *T. Hamatum*, *T. atroviride,* and *T. koningii* (Zhu et al., 2022). The fermentation broth of *T. longibrachiatum* T6 has a strong lethal effect on the eggs and second-instar larvae of cereal cyst nematodes in wheat (Zhu et al., 2022). The relative inhibition rate of the two concentrated fermentation broths on egg hatching was 46.47%, and the corrected mortality rate for the second-instar larvae was 44.45% (Sokhandani et al., 2016). Microscopic observation showed that the fermentation liquid of *T. longibrachiatum* T6 could digest the contents of nematode eggs and body cavities of the second instar larvae (Zhu et al., 2022). Khan et al. (2020) used inducers to make *T. koningiopsis* UFSMQ40 produced fermentation broth containing a large amount of chitinase, and its lethal rate to root-knot nematodes of South China and Java was 90.4 and 63.2%, respectively. Baazeem et al. (2021) analyzed the transcriptional activity of chi18-5 and chi18-12 genes of *T. harzianum* FB10 in *Trichoderma* egg parasitism. Compared to the control, the expression of chi18-5 and chi18-12 genes during parasitism increased significantly, indicating that the chitinase content increased, which could provide favorable conditions for egg cleavage (Baazeem et al., 2021).

Mechanism of *Trichoderma* resistance to nematode disease

The mechanism by which *Trichoderma* inhibits nematode disease remains unclear. Some studies suggest that the serine protease pr1 of *Trichoderma* has similar biochemical characteristics to the protein Pr1 of nematicidal fungi, so it has a certain nematode inhibition effect (Forghani and Hajihassani, 2020). The antimicrobial peptides produced by *Trichoderma* also have nematicidal effects (Fan et al., 2020).

Mycoparasitism effect of *Trichoderma*

Trichoderma mycoparasitism is an important mechanism for controlling nematodes and includes identification, contact, entanglement, penetration, and parasitism (Li et al., 2020; Figure 2). *Trichoderma* mycelium penetrates the eggshell or cuticle of larvae and adults of nematodes, colonizes, absorbs nutrients from nematodes, and causes nematode death (Marraschi et al., 2019). *Trichoderma* mycoparasitic nematode processes involve the production and co-secretion of various degrading enzymes (Moo-Koh et al., 2022). The induction of *Trichoderma* activities of β-1, 3-glucanase, chitinase, and protease are increased, which can enhance the immunity of plants to nematodes (Poveda et al., 2020). The hyperparasitic process is mainly regulated by heterotrimeric G protein, cAMP, and MAPK motif signals, and secretes extracellular chitinase, glucanase, xylanase, cellulase, and protease, among which chitinase and protease are particularly important and can degrade the cyst, egg, larva, and adult body wall of nematodes (Li et al., 2020). *Trichoderma* secretes glucosidases NAG1 and NAG2, which act on the extracellular and self-cell walls, respectively, and their main function is to degrade chitin so that they can protect their cell walls from degradation during the process of hyperparasitism (Poveda et al., 2020).

Antibiosis effect of *Trichoderma*

Trichoderma can inhibit the growth and reproduction of nematodes by secreting antagonistic substances (Moo-Koh et al., 2022). *Trichoderma* produces a variety of secondary metabolites, including trichomycin, gliotoxin, viridin, antibacterial peptide, β-1, 3-glucanase, chitinase, polypeptides, polyketones, butyrolactones, sesquiterpene heptadecarboxylic acid, terpenes, and some volatile substances (hydrocarbons, alcohols, furans, aldehydes, alkanes, olefins, esters, aromatic compounds, heterocyclic compounds, and various terpenoids) (Kappel et al., 2020). Contina et al. (2017) reported for the first time that *T. harzianum* ThzID1-M3 labeled with GFP significantly inhibited the reproduction of potato cyst nematodes, with a cyst decline rate of 60%. The inhibition rates of the fermentation broth of *T. hamatum* HZ-9 and *T. virens* HZ-L9 on the hatching of soybean cyst nematode eggs were 80.6 and 79.4%, respectively (Contina et al., 2017). The secondary metabolites produced by the same *Trichoderma* species in different media have different effects on nematode resistance (Forghani and Hajihassani, 2020). The inhibition rate of *T. viride* secondary metabolites on wheat medium and solid medium on egg hatching of southern root knot nematode was 71.6 and 67.3%, respectively (Baazeem et al., 2021). Baazeem et al. (2021) detected and analyzed the *T. hamatum* FB10 secondary metabolite nematicidal active ingredient; thirteen kinds of chemical substances were obtained, including 6-amyl-α-pyranone. The inhibition rate of egg hatching of *Meloidogyne incognita* was 78.26%.

Toxicity effect of *Trichoderma*

Trichoderma produces toxic secondary metabolites that directly come into contact with nematodes, which is an important direct biological control mechanism (Khan et al., 2020). It has been found that the toxic secondary metabolites produced by *Trichoderma* are divided into two categories, one is small molecules and volatile substances, including aromatic compounds, polyketides, butenolactones, and terpenoids, etc.; the other is macromolecular metabolites, including peptides, enzymes, etc. (Khan et al., 2020). It has been reported that the main nematicidal substances isolated from *Trichoderma* are trichodermin, acetic acid, gliotoxin, and peptide cyclosporin A (Fan et al., 2020). Meanwhile, Moo-Koh et al. (2022) used GC–MS to detect and analyze the nematicidal active components of *Trichoderma* TUV-13 strain and obtained more than 40 chemical components, among which of which the main alkanes are the most, in addition to organic acids, esters, ketones, steroids, and other organic compounds. Li et al. (2020) summarized and analyzed the secondary

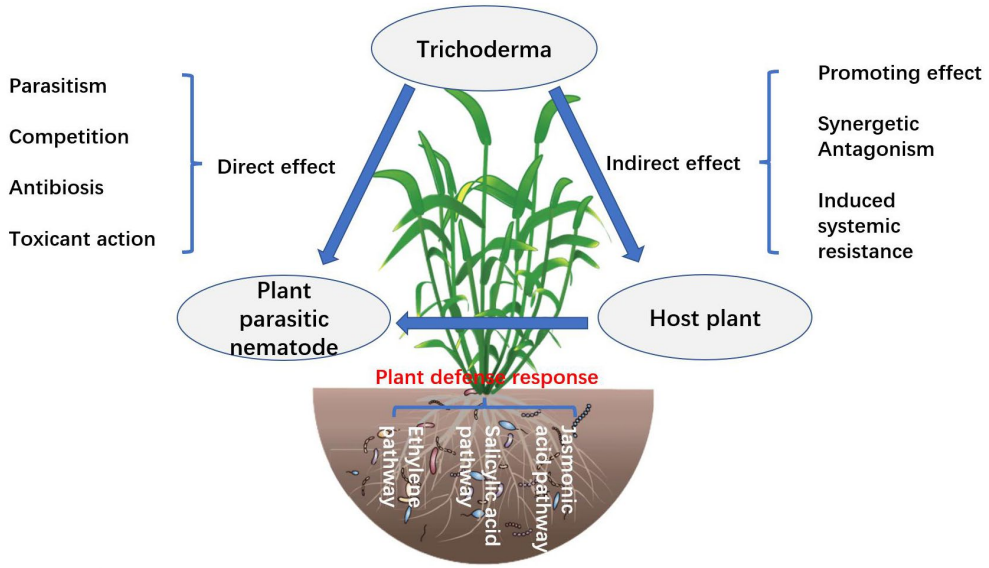

FIGURE 2
Schematic diagram of the mechanism of action of *Trichoderma* in plant nematode disease control (Sokhandani et al., 2016; Forghani and Hajihassani, 2020; Khan et al., 2020).

metabolites and activities of 20 species of *Trichoderma*, including *T. aureoviride*, *T. arundinaceum*, *T. brevicompactum*, *T. citrinoviride*, *T. gamsii*, *T. polysporum*, *T. saturnisporum*, *T. spirale*, *T. cremeum*, *T. pesudokoningii*, and *T. lignorum*. There were 390 non-volatile secondary metabolites, among which wickerol A, harziandione, trichodermin, and cyclonerodiol exhibited nematicidal activity (Khan et al., 2020). The *T. virens* B3 fermentation broth has strong toxic activity against cereal cyst nematodes, and the killing rate is as high as 86.2% (Forghani and Hajihassani, 2020). The fermentation broth can maintain good stability for a long time. The fermentation broth of *T. citrinoviride* , *T. harzianum* , *T. acroviride*, and *T. koningiopsis* had a strong toxic effect on the southern root-knot nematode J2, with a mortality rate of more than 85% (Du et al., 2020).

Induced resistance effect of *Trichoderma*

Induced resistance is the response of plants to stress, which is stimulated by external factors. *Trichoderma*-colonized plant roots cause physiological and metabolic changes and produce a variety of secondary metabolites that act as elicitors (Al-Hazmi and TariqJaveed, 2016). At present, there are more than 20 elicitors produced by *Trichoderma* that induce plant resistance, including antitoxins, polypeptides, lipopeptides, cellulases, hydrophobic proteins, non-toxic gene proteins, terpenoids, phenol derivatives, glycosidic ligands, and flavonoids (Pocurull et al., 2020). These secondary metabolites induce plant defense responses and promote plant growth. The interaction between *Trichoderma* and plants increases the synthesis of defense-related enzymes and substances. *T. hamatum* can induce the activities of phenylalanine ammonia lyase (PAL), polyphenol oxidase (PPO), and peroxidase (POD), which are related to tobacco defense reaction, to increase significantly (Al-Hazmi and TariqJaveed, 2016). In tomatoes treated with *T. harzianum*, the control effect against *M. incognita* was 61.88%. Further studies have shown that the levels of reactive oxygen species (ROS), superoxide (O^{2-}), hydrogen peroxide (H_2O_2), and malondialdehyde (MDA) in tomatoes were significantly increased, and the defense-related genes PAL, C4H, 4CL, CAD, LPO, CCOMT, Tpx1, and G6PDH were upregulated, thus inducing the defense response of tomatoes to *M. incognita* (Pocurull et al., 2020). Plant-induced resistance mainly involves signal transduction pathways such as those of salicylic acid (SA), jasmonic acid (JA), and ethylene (ET). In the interaction between *Trichoderma* and Arabidopsis, tomato, and cucumber, JA, SA, and ET contents increased to varying degrees, indirectly improving plant resistance (Hinterdobler et al., 2021). This process is also related to activating chitinase and glucanase activities and inhibiting the plant antioxidant enzyme system. The expression of ETR1 and LOX1 genes of jasmonic acid and the ethylene signal pathway increased significantly in *T. asperellum* DQ-1 irrigated tomato, which enhanced tomato resistance (Agbessenou et al., 2022). Some volatile secondary metabolites of *Trichoderma* are important elicitors that induce plant resistance (Al-Hazmi and TariqJaveed, 2016). The volatile substances produced by *T. harzianum* and *T. asperellum* act as elicitors to stimulate the up-regulated expression of Arabidopsis-induced resistance-related transcription factor MYB72, which triggers a JA-regulated defense response (Agbessenou et al., 2022). At present, the interaction mechanisms and signal transduction pathways between *Trichoderma* volatile secondary metabolites and plants have not been thoroughly studied. The active substances produced by *Trichoderma* are recognized by plants, thus activating the signal transduction pathway and inducing the production of plant system resistance. The microbial determinants recognized by microorganisms are called microbe-associated molecular patterns (MAMPs) (Baazeem et al., 2021). After *Trichoderma* infects plant roots, it releases a variety of MAMPs to activate immune response

(MTI), thus inducing plant systemic resistance (ISR) (Li X. et al., 2022). Abdelkhalek et al. (2022) showed that *T. hamatum* strain Th23 promotes tomato growth and induces systemic resistance against tobacco mosaic virus.

Application and mechanism of action of *Trichoderma* in promoting crop growth and repairing environment

Application of *Trichoderma* in promoting plant growth and repairing environment

Trichoderma can produce plant growth stimulators, such as indoleacetic acid (IAA) and harzianolide, to promote the development and growth of plant roots by secreting phytase and ferritin to promote the absorption of P and Fe by plants; decomposes soil organic matter; increases the supply of soil nutrients; improves crop photosynthetic efficiency; improves plant height, stem diameter, and other agronomic traits; and increases production (Lombardi et al., 2020a). Many studies have shown that most *Trichoderma* spp. can produce bioactive substances and have antagonistic effects on plant-pathogenic fungi and plant-pathogenic nematodes (Şesan et al., 2020; Abdelkhalek et al., 2022; Organo et al., 2022; Rao et al., 2022). Bioactive substances, including secondary metabolites and cell wall-degrading enzymes, can effectively improve the resistance of crops, reduce plant diseases, and promote plant growth (Domínguez et al., 2016; Viriyasuthee et al., 2019; Jaiswal et al., 2020; Tseng et al., 2020).

Trichoderma can improve soil nutrient availability and utilization efficiency. The aboveground biomass of cucumber seedlings inoculated with *Trichoderma* MF-2 increased by 39.07%, with a significant growth-promoting effect, and an increased number of beneficial microorganisms in the soil (Singh et al., 2019; Ye et al., 2020). Different *Trichoderma* strains had different degrees of antagonism to *F. oxysporum*, and the combination of *Trichoderma* wettable powder treatment significantly increased banana yield (Samuelian, 2016; Bubici et al., 2019; Damodaran et al., 2020). Li et al. (2020) found that the biocontrol agent *Trichoderma* GYXM-1p1 strain had a strong growth-promoting effect through pot cultivation. After treatment with this strain, the root length, plant height, root fresh weight, dry weight, total fresh weight, and total dry weight of cabbage plants were significantly improved compared to the water control ($p < 0.05$), and the total fresh weight and total dry weight of cabbage plants were increased by 417. 60% and 762. 69%, respectively, compared with water control. Ruan et al. (Intana et al., 2021; Nuangmek et al., 2021) found that the application of nitrogen fertilizer with *Trichoderma* promoted the quality of muskmelon. After the application of *Trichoderma*, the soluble sugar content of muskmelon fruit increases significantly, improving the quality of muskmelon. The application of *Trichoderma* can increase the SPAD value of chlorophyll in peanut leaves, improve the main agronomic traits of peanuts, significantly increase the activity of protective enzymes in peanut roots, stems, and leaves, and reduce the content of MDA (Kovács et al., 2021; Al-Askar et al., 2022). When 1.5 kg/666.7 m^{-2} was applied, the number of pods per plant, pod weight, seed kernel weight, 100 fruit quality, 100 fruit kernel quality, and yield per plant of peanut increased by 24.63, 20.22, 14.10, 4.86, 7.63, and 12.85%, respectively, compared with the control (Al-Askar et al., 2022).

Mechanism of *Trichoderma* in promoting plant growth and repairing environment

Trichoderma can promote plant growth, produce substances that can promote plant growth, improve the solubility of nutrients in the soil, and improve plant rhizosphere microecology, thereby promoting plant absorption and growth (Karuppiah et al., 2019a; Kakabouki et al., 2021; Marra et al., 2021; Figure 3). *Trichoderma* plant interactions can not only induce resistance but also improve the resistance of plants to abiotic stress factors (salt, high temperature, UV). Treatment of cucumber seeds with *T. asperellum* T203 improved the plant's salt tolerance, and the activities of Mn/Cu SOD and catalase (CAT), and significantly reduced ascorbic acid in the plant (Illescas et al., 2022). *Trichoderma* can significantly enhance the Na^+ efflux from the root system of *Lycium barbarum* and its transport to the upper ground, ensure K^+ absorption and maintain the ion balance in the plant, thus reducing the damage of PSII caused by ion toxicity and oxidative stress, protecting photosynthetic pigments, maintaining the photosynthetic performance of *L. barbarum* under salt stress, and reducing biomass loss (Brotman et al., 2013).

The synthesis of plant growth hormones, such as IAA, ABA, ET, GA, and CK is the main mechanism of *Trichoderma* (Karuppiah et al., 2019b; Wang et al., 2021; Degani et al., 2021b; Agbessenou et al., 2022). *T. asperellum* induced cucumber to produce IAA, GA, and ABA to promote growth (Liu H. et al., 2022). The height, stem diameter, soluble sugar content, and absorption rate of available nitrogen of tomato seedlings treated with *T. asperellum* were significantly increased, and the expression of tomato hormone signal transduction-related genes JAR1, MYC2, NPR1, PR1, and GH3 was significantly increased (Rawal et al., 2022). Another study showed that *T. asperellum* can upregulate the expression of xylanase genes in poplar and has a significant growth-promoting effect (Karuppiah et al., 2019b). *T. harzianum* regulates tricarboxylic acid cycle (TAC) and hexose monophosphate pathway (HMP) to promote tomato growth by enhancing succinate dehydrogenase and glucose-6-phosphate dehydrogenase activities (Manganiello et al., 2018). *Trichoderma* produces acidic substances that can dissolve insoluble trace elements in soil and provide more nutrition to plants (Samuelian, 2016). *T. asperellum* can transform insoluble phosphate in the soil into effective phosphorus and promote the absorption and utilization of cucumbers (Karuppiah et al., 2021; Figure 3). *T. koningiopsis* can produce organic acids that dissolve insoluble tricalcium phosphate under high alkaline stress and can also produce alkaline phosphatase under drought stress to solubilize phosphorus and improve the utilization of nutrients by plants (You et al., 2022). Many experiments have verified that *Trichoderma* promotes plant growth (Mayo et al., 2015; Bononi et al., 2020; Lombardi et al., 2020b; Swain et al., 2021; Velasco et al., 2021; Bridžiuvienė et al., 2022; Joo and Hussein, 2022; Li X. et al., 2022); under complex field production conditions, the mechanism by which *Trichoderma* promotes plant growth requires more systematic research.

Conclusion and future perspectives

At present, chemical control is the main method used for plant disease control and is achieved by spraying pesticides and fungicides. Although the effect of chemical control is good and helpful in

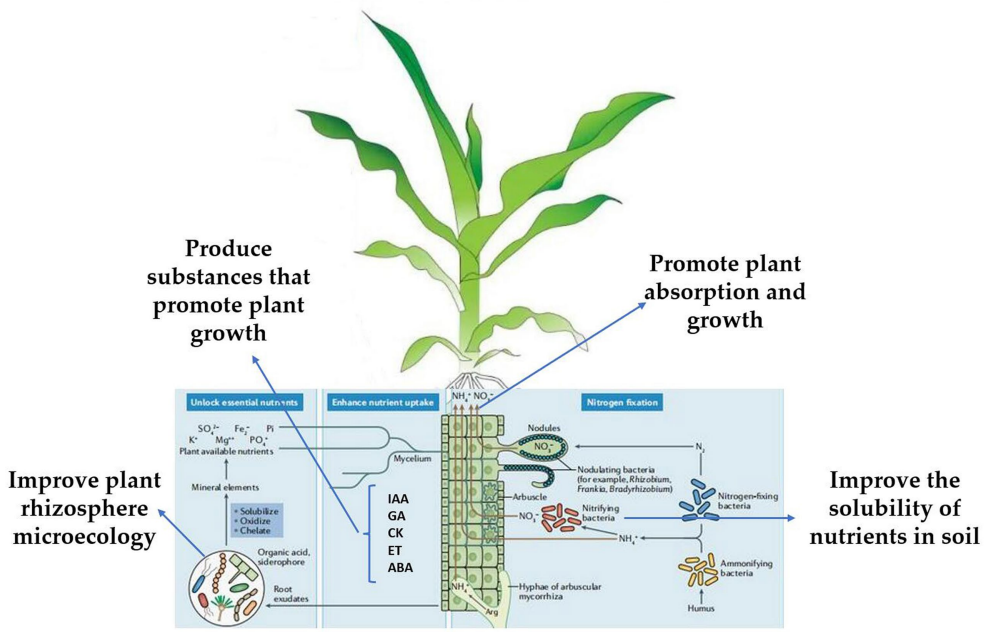

FIGURE 3
Schematic diagram of the mechanism of action of *Trichoderma* in promoting crop growth and repairing the environment (Jaiswal et al., 2020; Lombardi et al., 2020a; Şesan et al., 2020; Karuppiah et al., 2021).

increasing agricultural production, the unscientific use of chemical pesticides has caused serious pollution to the environment and enhanced pathogens' resistance to and chemical pesticides. Several experiments have proven that *Trichoderma* has good biological control effects and can reduce the use of chemical pesticides. However, there are still few biocontrol agents against *Trichoderma* on the market, and more effective and suitable strains need to be found to join the biocontrol team (Nieto-Jacobo et al., 2017; Fiorentino et al., 2018; López et al., 2019; Nawrocka et al., 2019; Poveda et al., 2019; Cabral-Miramontes et al., 2022). Although *Trichoderma* has great prospects for agricultural applications, there are still some problems in the development and utilization of *Trichoderma* (Rubio et al., 2014; Zhang et al., 2018; Phoka et al., 2020; Santos et al., 2020; Wang H. et al., 2022). Because the spore preparation of *Trichoderma* is generally a living fungal preparation, which is often affected by various natural factors such as humidity, temperature, soil acidity, alkalinity, and the soil microbial community when it is applied in the field, the field test performance is unstable, and the biological control effect is weakened. In addition, the shelf life of biological control agents is relatively short, and some microorganisms must be stored at low temperatures to ensure the concentration of live microorganisms when they are applied.

There are still several problems to be solved in the application of *Trichoderma* in the biological control of plant diseases (Caruso et al., 2020; He et al., 2020; Boamah et al., 2021; González-López et al., 2021). The first is to explore and produce efficient strains, which can be screened through genetic engineering technology to produce *Trichoderma* biocontrol-engineered strains that are resistant to chemical pesticides and low temperatures. At the same time, it is necessary to develop effective *Trichoderma* agents suitable for use with various application methods to enhance the control effect and improve the processing technology of *Trichoderma* agents to extend the shelf life of biological control agents. Second, exploring the combined effects of *Trichoderma* spp. and other microorganisms is necessary. The development of Pesticides with volatile and non-volatile secondary metabolites secreted by *Trichoderma* as the main active ingredient will be the focus of future research and the development of new Pesticides. To improve the quality of *Trichoderma* biopesticides, in addition to monitoring traditional indicators such as pH, dissolved oxygen, and temperature in the fermentation process, it is also necessary to monitor its correlation with the yield of antagonistic substances at the level of the cell metabolic flow, genome, proteome, and metabolome (Mulatu et al., 2021). However, it is necessary to establish more scientific quality standards for *Trichoderma* products *in vivo*, such as increasing the content of antagonistic substances or activity indicators (Niu et al., 2020). The development of new dosage forms, such as cell microcapsules, water-in-oil emulsions, and other protective dosage forms, should be strengthened, and the molecular mechanism of chlamydospore production should be further studied (Table 1).

With further study of transgenic *Trichoderma*, a prospective study on the biological and environmental safety of transgenic *Trichoderma* should be conducted (Li et al., 2021). At present, the balance regulation of *Trichoderma* colonizing host and plant immune response, long-distance and trans-growth period transduction mechanism of systematically induced plant disease resistance and its defense signals, identification of *Trichoderma* elicitors to recognize plant targets or receptors, and mechanism of *Trichoderma*-induced plant endophytic microbiome to synergistically stimulate plant immune response has become an international research topic of interest. Studies on miRNA regulation of *Trichoderma* colonization host process and plant

TABLE 1 The main biological function of common species of *Trichoderma*.

Name of species	Major function	Reference
T. harzianum	Induced systemic resistance to fungi disease and increased plant productivity; Nematode resistance; Improved plant growth and root architecture.	Saravanakumar et al. (2016), Poveda et al. (2019), Coppola et al. (2019)
T. asperellum	Antifungal activities; Plant growth promotion; Stress resistance; Enrich soil fertility	Wang H. et al. (2022), AL-Askar et al. (2021), Degani et al. (2021b)
T. asperelloides	Antifungal activities; Plant growth promotion; Stress resistance	Ruangwong et al. (2021a), Phoka et al. (2020), Rawal et al. (2022)
T. atroviride	Fungistatic activity, plant growth promotion; Antifungal and antibacterial activities; Plant growth promotion and nutrient assimilation; Induced systemic defense responses; Stress resistance	Coppola et al. (2019), Zhang C. et al. (2022), González-López et al. (2021), Leal et al. (2021), Nawrocka et al. (2019)
T. hamatum	Nematode resistance; Increased plant productivity; Antibacterial and antifungal activities; Plant growth promoting	Li X. et al. (2022), Velasco et al. (2021), Baazeem et al. (2021)
T. virens	Antifungal activities; Plant growth promotion	Jogaiah et al. (2018), Halifu et al. (2020)
T. viride	Antifungal activities; Enhanced root development; Nematode resistance; Stress resistance	Al-Hazmi and TariqJaveed, (2016), Naglot et al. (2015), He et al. (2020)
T. longibrachiatum	Antifungal activities; Improve salt resistance; Nematode resistance; Plant growth promotion; Induced systemic defense responses	Ngo et al. (2021), Boamah et al. (2021), AL-Askar et al. (2022), Degani et al. (2021b), Yuan et al. (2019)
T. ghanense	Plant growth promotion; Enrich soil fertility	Bridžiuvienė et al., 2022
T. tomentosum	Plant growth promotion; Enrich soil fertility	Bridžiuvienė et al. (2022)
T. volatiles	Induced systemic resistance	Pescador et al. (2022)
T. velutinum	Plant growth promotion	Mayo-Prieto et al. (2019)
T. phayaoense	Antifungal activities; improve plant growth and root architecture	Nuangmek et al. (2021)
T. koningiopsis	Antifungal activities; Plant growth promotion	Ruangwong et al. (2021b), You et al. (2022)
T. citrinoviride	Antifungal activities; Nematode resistance	Park et al. (2019), Fan et al. (2020)
T. reesei	Antifungal activities	Hinterdobler et al. (2021)
T. gamsii	Antifungal activities; Affected herbivore feeding behavior	Alukumbura et al. (2022), Zhou et al. (2018), Di Marco et al. (2022)
T. aggressivum	Fungal diseases biological control	Sánchez-Montesinos et al. (2021)
T. atrobrunneum	Nematode resistance	Hernández et al. (2018)
T. afroharzianum	Plant growth promotion	Kappel et al. (2022)
T. bissettii	Antifungal activities	Chung et al. (2022)
T. parareesei	Improve plant quality	Rubio et al. (2014)
T. lignorum	Nematode resistance	Daza et al. (2019)
T. taxi	Antifungal activities	Chen et al. (2021)
T. strigosellum	Nematode resistance; Plant growth promotion	Batista et al. (2021)
T. hebeiensis	Antifungal activities; Plant growth promotion	Swain et al. (2021)
T. erinaceum	Antifungal activities; Plant growth promotion	Swain et al. (2021)

immune response, and the regulation mechanism of cross-border miRNA transduction between *Trichoderma*, plants, and pathogenic microorganisms are emerging. The combination design or co-culture technology of *Trichoderma* and other microorganisms has become key for tapping new metabolites with specific functions of microorganisms, broadening the target spectrum of microbial metabolites, and developing new biopesticides and biostimulants based on metabolites (Wang Y. et al., 2022). It is expected to become a new direction for the development of macromolecular biopesticides by molecular construction or modification of the *Trichoderma* multi-stimulator fusion protein and the development of new plant immune-activating protein pesticides. At present, it is urgent to reveal the synergistic interactions among *Trichoderma*, plants, and pathogenic microorganisms in induced disease resistance on a cross-genome scale, develop *Trichoderma* and other microbial symbiotic agents that can cure both diseases and pests, and develop new biostimulator products based on *Trichoderma* metabolites.

Compared with single-life biocontrol fungi, compound biocontrol fungi can better avoid the problems of weak adaptability to the environment, narrow range of disease resistance, and insufficient control effect. At present, there are many preparations

containing different kinds of *Trichoderma*, which are being used in sustainable agricultural crops, but the application of these preparations is still expensive, and not available to all farmers. The application of compatible or affinity multiple microorganisms for compounding has become a trend in the development of biocontrol agents. *Trichoderma* can form alliances with a variety of microorganisms such as bacteria and fungi to directly or indirectly improve the ability of plants to prevent and control diseases. The following aspects may be the main research focus of *Trichoderma* as a biocontrol fungus in the future: the molecular mechanism of the specific interaction between *Trichoderma* and plants; Molecular basis of plant immunity induced by *Trichoderma*; Improvement of *Trichoderma* fermentation process; Establishing diversified application technology models of *Trichoderma*. The commercial application of biocontrol *Trichoderma* depends largely on the stress resistance (such as high temperature, drying, ultraviolet radiation, etc.) and storage resistance (more than 1 year at normal temperature) of the *Trichoderma* agent. At present, there are two main technologies. One is to reduce the acidity and regulate the utilization of oxygen to induce *Trichoderma* to produce stress-resistant chlamydospores, and the other is to add some chemical additives (such as copper) to the inoculum. How the effectors produced by *Trichoderma* interact with plant cell receptors has become the key to revealing the mechanism of *Trichoderma* inducing plant immunity. With the deepening of the research on transgenic *Trichoderma*, prospective research on the biological and environmental safety of transgenic *Trichoderma* should be carried out.

Author contributions

MZ and XY: software. KZ and MZ: data curation. XY: writing – original draft preparation. JR, JC, and KZ: writing, review, and editing. All authors read and agreed to the published version of the manuscript.

Funding

This research was supported by the National Science Foundation of China (32161143005 and 32160669) and the Guizhou Science and Technology Support Program ([2020]1Y125).

Conflict of interest

The authors declare that the research was conducted in the absence of any commercial or financial relationships that could be construed as a potential conflict of interest.

Publisher's note

References

Abbas, A., Mubeen, M., Zheng, H., Sohail, M. A., Shakeel, Q., Solanki, M. K., et al. (2022). *Trichoderma* spp. genes involved in the biocontrol activity against *Rhizoctonia solani*. *Front. Microbiol.* 13:884469. doi: 10.3389/fmicb.2022.884469

Abdelkhalek, A., Al-Askar, A. A., Arishi, A. A., and Behiry, S. I. (2022). *Trichoderma hamatum* strain Th23 promotes tomato growth and induces systemic resistance against tobacco mosaic virus. *J. Fungi* 8:228. doi: 10.3390/jof8030228

Agbessenou, A., Akutse, K. S., Yusuf, A. A., and Khamis, F. M. (2022). The endophyte *Trichoderma asperellum* M2RT4 induces the systemic release of methyl salicylate and (Z)-jasmone in tomato plant affecting host location and herbivory of *Tuta absoluta*. *Front. Plant Sci.* 13:860309. doi: 10.3389/fpls.2022.860309

Al-Askar, A. A., Rashad, E. M., Moussa, Z., Ghoneem, K. M., Mostafa, A. A., Al-Otibi, F. O., et al. (2022). A novel endophytic *Trichoderma longibrachiatum* WKA55 with biologically active metabolites for promoting germination and reducing mycotoxinogenic fungi of peanut. *Front. Microbiol.* 13:772417. doi: 10.3389/fmicb.2022.772417

Al-Askar, A. A., Saber, W., Ghoneem, K. M., Hafez, E. E., and Ibrahim, A. A. (2021). Crude citric acid of *Trichoderma asperellum*: tomato growth promotor and suppressor of *Fusarium oxysporum* f. sp. *lycopersici*. *Plants* 10:222. doi: 10.3390/plants10020222

Alfiky, A., and Weisskopf, L. (2021). Deciphering *Trichoderma*-plant-pathogen interactions for better development of biocontrol applications. *J. Fungi* 7:61. doi: 10.3390/jof7010061

Al-Hazmi, A. S., and TariqJaveed, M. (2016). Effects of different inoculum densities of *Trichoderma harzianum* and *Trichoderma viride* against *Meloidogyne javanica* on tomato. *Saudi J. Biol. Sci.* 23, 288–292. doi: 10.1016/j.sjbs.2015.04.007

Alonso-Ramírez, A., Poveda, J., Martín, I., Hermosa, R., Monte, E., and Nicolás, C. (2014). Salicylic acid prevents *Trichoderma harzianum* from entering the vascular system of roots. *Mol. Plant Pathol.* 15, cc doi: 10.1111/mpp.12141

Al-Surhanee, A. A. (2022). Protective role of antifusarial eco-friendly agents (*Trichoderma* and salicylic acid) to improve resistance performance of tomato plants. *Saudi J. Biol. Sci.* 29, 2933–2941. doi: 10.1016/j.sjbs.2022.01.020

Alukumbura, A. S., Bigi, A., Sarrocco, S., Fernando, W., Vannacci, G., Mazzoncini, M., et al. (2022). Minimal impacts on the wheat microbiome when *Trichoderma gamsii* T6085 is applied as a biocontrol agent to manage fusarium head blight disease. *Front. Microbiol.* 13:972016. doi: 10.3389/fmicb.2022.972016

Álvarez-García, S., Mayo-Prieto, S., Gutiérrez, S., and Casquero, P. A. (2020). Self-inhibitory activity of *Trichoderma* soluble metabolites and their antifungal effects on *Fusarium oxysporum*. *J. Fungi* 6:176. doi: 10.3390/jof6030176

Andrade-Hoyos, P., Silva-Rojas, H. V., and Romero-Arenas, O. (2020). Endophytic *Trichoderma* species isolated from *Persea americana* and *Cinnamomum verum* roots reduce symptoms caused by *Phytophthora cinnamomi* in avocado. *Plan. Theory* 9:1220. doi: 10.3390/plants9091220

Aswani, R., Roshmi, T., and Radhakrishnan, E. K. (2022). Induction of plant defense response by endophytic microorganisms. In *Biocontrol Mechanisms of Endophytic Microorganisms*. Academic Press. 89–115.

Baazeem, A., Almanea, A., Manikandan, P., Alorabi, M., Vijayaraghavan, P., and Abdel-Hadi, A. (2021). In vitro antibacterial, antifungal, nematocidal and growth promoting activities of *Trichoderma hamatum* FB10 and its secondary metabolites. *J. Fungi* 7:331. doi: 10.3390/jof7050331

Bardin, M., Ajouz, S., Comby, M., Lopez-Ferber, M., Graillot, B., Siegwart, M., et al. (2015). Is the efficacy of biological control against plant diseases likely to be more durable than that of chemical pesticides? *Front. Plant Sci.* 6:566. doi: 10.3389/fpls.2015.00566

Basińska-Barczak, A., Błaszczyk, L., and Szentner, K. (2020). Plant cell wall changes in common wheat roots as a result of their interaction with beneficial fungi of *Trichoderma*. *Cells* 9:2319. doi: 10.3390/cells9102319

Bazghaleh, N., Prashar, P., Woo, S., and Vandenberg, A. (2020). Effects of lentil genotype on the colonization of beneficial *Trichoderma* species and biocontrol of aphanomyces root rot. *Microorganisms* 8:1290. doi: 10.3390/microorganisms8091290

Batista, K. O. M., Silva, D. V., Nascimento, V. L., and de Souza, D. J. (2021). Effects of *Trichoderma strigosellum* in eucalyptus urophylla development and leaf-cutting ant behavior. *J Fungi* 8:15.

Boamah, S., Zhang, S., Xu, B., Li, T., and Calderón-Urrea, A. (2021). *Trichoderma longibrachiatum* (TG1) enhances wheat seedlings tolerance to salt stress and resistance to *Fusarium pseudograminearum*. *Front. Plant Sci.* 12:741231. doi: 10.3389/fpls.2021.741231

Bononi, L., Chiaramonte, J. B., Pansa, C. C., Moitinho, M. A., and Melo, I. S. (2020). Phosphorus-solubilizing *Trichoderma* spp. from Amazon soils improves soybean plant growth. *Sci. Rep.* 10:2858. doi: 10.1038/s41598-020-59793-8

Bridžiuvienė, D., Raudonienė, V., Švedienė, J., Paškevičius, A., Baužienė, I., Vaitonis, G., et al. (2022). Impact of soil chemical properties on the growth promotion ability of *Trichoderma ghanense*, *T. tomentosum* and their complex on Rye in different land-use systems. *J. Fungi* 8:85. doi: 10.3390/jof8010085

Brotman, Y., Landau, U., Cuadros-Inostroza, Á., Tohge, T., Fernie, A. R., Chet, I., et al. (2013). *Trichoderma*-plant root colonization: escaping early plant defense responses and activation of the antioxidant machinery for saline stress tolerance. *PLoS Pathog.* 9:e1003221. doi: 10.1371/journal.ppat.1003221

Bubici, G., Kaushal, M., Prigigallo, M. I., Gómez-Lama Cabanás, C., and Mercado-Blanco, J. (2019). Biological control agents against *Fusarium* wilt of Banana. *Front. Microbiol.* 10:616. doi: 10.3389/fmicb.2019.00616

Cabral-Miramontes, J. P., Olmedo-Monfil, V., Lara-Banda, M., Zúñiga-Romo, E. R., and Aréchiga- Carvajal, E. T. (2022). Promotion of plant growth in arid zones by selected *Trichoderma* spp. strains with adaptation plasticity to alkaline pH. *Biology* 11:1206. doi: 10.3390/biology11081206

Cai, X., Zhao, H., Liang, C., Li, M., and Liu, R. (2021). Effects and mechanisms of symbiotic microbial combination agents to control tomato *Fusarium* crown and root rot disease. *Front. Microbiol.* 12:629793. doi: 10.3389/fmicb.2021.629793

Carro-Huerga, G., Compant, S., Gorfer, M., Cardoza, R. E., Schmoll, M., Gutiérrez, S., et al. (2020). Colonization of *Vitis vinifera* L. by the endophyte *Trichoderma* sp. strain T154: biocontrol activity against *Phaeoacremonium minimum*. *Front. Plant Sci.* 11:1170. doi: 10.3389/fpls.2020.01170

Caruso, G., El-Nakhel, C., Rouphael, Y., Comite, E., Lombardi, N., Cuciniello, A., et al. (2020). *Diplotaxis tenuifolia* (L.) DC. Yield and quality as influenced by cropping season, protein hydrolysates, and *Trichoderma* applications. *Plan. Theory* 9:697. doi: 10.3390/plants9060697

Chen, J., Zhou, L., Din, I. U., Arafat, Y., Li, Q., Wang, J., et al. (2021). Antagonistic activity of *Trichoderma* spp. against *Fusarium oxysporum* in rhizosphere of radix pseudostellariae triggers the expression of host defense genes and improves its growth under long-term monoculture system. *Front. Microbiol.* 12:579920. doi: 10.3389/fmicb.2021.781826

Chung, D., Kwon, Y. M., Lim, J. Y., Bae, S. S., Choi, G., and Lee, D. S. (2022). Characterization of chitinolytic and antifungal activities in marine-derived *Trichoderma bissettii* strains. *Mycobiology* 50, 244–253. doi: 10.1080/12298093.2022.2105509

Contina, J. B., Dandurand, L. M., and Knudsen, G. R. (2017). Use of GFP-tagged *Trichoderma harzianum* as a tool to study the biological control of the potato cyst nematode *Globodera pallida*. *Appl. Soil Ecol.* 115, 31–37. doi: 10.1016/j.apsoil.2017.03.010

Coppola, M., Diretto, G., Digilio, M. C., Woo, S. L., Giuliano, G., Molisso, D., et al. (2019). Transcriptome and metabolome reprogramming in tomato plants by *Trichoderma harzianum* strain T22 primes and enhances defense responses against aphids. *Front. Physiol.* 10:745.

Damodaran, T., Rajan, S., Muthukumar, M., Gopal, R., Yadav, K., Kumar, S., et al. (2020). Biological management of banana Fusarium wilt caused by *Fusarium oxysporum* f. sp. cubense tropical race 4 using antagonistic fungal isolate CSR-T-3 (*Trichoderma reesei*). *Front. Microbiol.* 11:595845. doi: 10.3389/fmicb.2020.595845

Daza, F. F. F., Roman, G. R., Rodriguez, M. V., Vargas, I. A. G., Heano, H. C., Cereda, M. P., et al. (2019). Spores of *Beauveria bassiana* and *Trichoderma lignorum* as a bioinsecticide for the control of atta cephalotes. *Biol Res.* 52:51.

De Zotti, M., Sella, L., Bolzonello, A., Gabbatore, L., Peggion, C., Bortolotto, A., et al. (2020). Targeted amino acid substitutions in a *Trichoderma* Peptaibol confer activity against fungal plant pathogens and protect host tissues from *Botrytis cinerea* infection. *Int. J. Mol. Sci.* 21:7521. doi: 10.3390/ijms21207521

Debbi, A., Boureghda, H., Monte, E., and Hermosa, R. (2018). Distribution and genetic variability of *Fusarium oxysporum* associated with tomato diseases in Algeria and a biocontrol strategy with indigenous *Trichoderma* spp. *Front. Microbiol.* 9:282. doi: 10.3389/fmicb.2018.00282

Debode, J., De Tender, C., Cremelie, P., Lee, A. S., Kyndt, T., Muylle, H., et al. (2018). *Trichoderma*- inoculated miscanthus straw can replace peat in strawberry cultivation, with beneficial effects on disease control. *Front. Plant Sci.* 9:213. doi: 10.3389/fpls.2018.00213

Degani, O., and Dor, S. (2021). *Trichoderma* biological control to protect sensitive maize hybrids against late wilt disease in the field. *J. Fungi* 7:315. doi: 10.3390/jof7040315

Degani, O., Khatib, S., Becher, P., Gordani, A., and Harris, R. (2021a). *Trichoderma asperellum* secreted 6-pentyl-α-pyrone to control *Magnaporthiopsis maydis*, the maize late wilt disease agent. *Biology* 10:897. doi: 10.3390/biology10090897

Degani, O., Rabinovitz, O., Becher, P., Gordani, A., and Chen, A. (2021b). *Trichoderma longibrachiatum* and *Trichoderma asperellum* confer growth promotion and protection against late wilt disease in the field. *J. Fungi* 7:444. doi: 10.3390/jof7060444

Di Marco, S., Metruccio, E. G., Moretti, S., Nocentini, M., Carella, G., Pacetti, A., et al. (2022). Activity of *Trichoderma asperellum* strain ICC 012 and *Trichoderma gamsii* strain ICC 080 toward diseases of esca complex and associated pathogens. *Front. Microbiol.* 12:813410. doi: 10.3389/fmicb.2021.813410

Domínguez, S., Rubio, M. B., Cardoza, R. E., Gutiérrez, S., Nicolás, C., Bettiol, W., et al. (2016). Nitrogen metabolism and growth enhancement in tomato plants challenged with *Trichoderma harzianum* expressing the *Aspergillus nidulans* acetamidase *amdS* gene. *Front. Microbiol.* 7:1182. doi: 10.3389/fmicb.2016.01182

Druzhinina, I. S., Chenthamara, K., Zhang, J., Atanasova, L., Yang, D., Miao, Y., et al. (2018). Massive lateral transfer of genes encoding plant cell wall-degrading enzymes to the mycoparasitic fungus *Trichoderma* from its plant- associated hosts. *PLoS Genet.* 14:e1007322. doi: 10.1371/journal.pgen.1007322

Du, F. Y., Ju, G. L., Xiao, L., Zhou, Y. M., and Wu, X. (2020). Sesquiterpenes and cyclodepsipeptides from marine-derived fungus *Trichoderma longibrachiatum* and their antagonistic activities against soil-borne pathogens. *Mar. Drugs* 18:165. doi: 10.3390/md18030165

Dugassa, A., Alemu, T., and Woldehawariat, Y. (2021). In-vitro compatibility assay of indigenous *Trichoderma* and *Pseudomonas* species and their antagonistic activities against black root rot disease (*Fusarium solani*) of faba bean (*Vicia faba* L.). *BMC Microbiol.* 21:115. doi: 10.1186/s12866-021-02181-7

El-Hasan, A., Walker, F., Klaiber, I., Schöne, J., Pfannstiel, J., and Voegele, R. T. (2022). New approaches to manage Asian soybean rust (*Phakopsora pachyrhizi*) using *Trichoderma* spp. or their antifungal secondary metabolites. *Meta* 12:507. doi: 10.3390/metabo12060507

Fan, H., Yao, M., Wang, H., Zhao, D., Zhu, X., Wang, Y., et al. (2020). Isolation and effect of *Trichoderma citrinoviride* Snef1910 for the biological control of root-knot nematode, *Meloidogyne incognita*. *BMC Microbiol.* 20:299. doi: 10.1186/s12866-020-01984-4

Ferreira Filho, J. A., Horta, M. A. C., Dos Santos, C. A., Almeida, D. A., Murad, N. F., Mendes, J. S., et al. (2020). Integrative genomic analysis of the bioprospection of regulators and accessory enzymes associated with cellulose degradation in a filamentous fungus (*Trichoderma harzianum*). *BMC Genomics* 21:757. doi: 10.1186/s12864-020-07158-w

Filizola, P., Luna, M., de Souza, A. F., Coelho, I. L., Laranjeira, D., and Campos-Takaki, G. M. (2019). Biodiversity and phylogeny of novel *Trichoderma* isolates from mangrove sediments and potential of biocontrol against *Fusarium* strains. *Microb. Cell Factories* 18:89. doi: 10.1186/s12934-019-1108-y

Fiorentino, N., Ventorino, V., Woo, S. L., Pepe, O., De Rosa, A., Gioia, L., et al. (2018). *Trichoderma*-based biostimulants modulate rhizosphere microbial populations and improve N uptake efficiency, yield, and nutritional quality of leafy vegetables. *Front. Plant Sci.* 9:743. doi: 10.3389/fpls.2018.00743

Fontana, D. C., de Paula, S., Torres, A. G., de Souza, V., Pascholati, S. F., Schmidt, D., et al. (2021). Endophytic fungi: biological control and induced resistance to phytopathogens and abiotic stresses. *Pathogens* 10:570. doi: 10.3390/pathogens10050570

Forghani, F., and Hajihassani, A. (2020). Recent advances in the development of environmentally benign treatments to control root-knot nematodes. *Front. Plant Sci.* 11:1125. doi: 10.3389/fpls.2020.01125

Girma, A. (2022). In vitro biocontrol evaluation of some selected *Trichoderma* strains against the root pathogen *Fusarium oxysporum* of hot pepper (*Capsicum annum* L.) in Bure Woreda, Ethiopia. *Int. J. Microbiol.* 2022:1664116. doi: 10.1155/2022/1664116

Gomes, E. V., Costa, M., de Paula, R. G., de Azevedo, R. R., da Silva, F. L., Noronha, E. F., et al. (2015). The Cerato-Platanin protein Epl-1 from *Trichoderma harzianum* is involved in mycoparasitism, plant resistance induction and self-cell wall protection. *Sci. Rep.* 5:17998. doi: 10.1038/srep17998

González-López, M., Jijón-Moreno, S., Dautt-Castro, M., Ovando-Vázquez, C., Ziv, T., Horwitz, B. A., et al. (2021). Secretome analysis of *Arabidopsis-Trichoderma atroviride* interaction unveils new roles for the plant glutamate: Glyoxylate aminotransferase GGAT1 in plant growth induced by the fungus and resistance against *Botrytis cinerea*. *Int. J. Mol. Sci.* 22:6804. doi: 10.3390/ijms22136804

Guo, Y., Ghirardo, A., Weber, B., Schnitzler, J. P., Benz, J. P., and Rosenkranz, M. (2019). *Trichoderma* species differ in their volatile profiles and in antagonism toward ectomycorrhiza *Laccaria bicolor*. *Front. Microbiol.* 10:891. doi: 10.3389/fmicb.2019.00891

Guzmán-Guzmán, P., Alemán-Duarte, M. I., Delaye, L., Herrera-Estrella, A., and Olmedo-Monfil, V. (2017). Identification of effector- like proteins in *Trichoderma* spp. and role of a hydrophobin in the plant-fungus interaction and mycoparasitism. *BMC Genet.* 18:16. doi: 10.1186/s12863-017-0481-y

Halifu, S., Deng, X., Song, X., Song, R., and Liang, X. (2020). Inhibitory mechanism of *Trichoderma virens* ZT05 on *Rhizoctonia solani*. *Plan. Theory* 9:912. doi: 10.3390/plants9070912

Haouhach, S., Karkachi, N., Oguiba, B., Sidaoui, A., Chamorro, I., Kihal, M., et al. (2020). Three new reports of *Trichoderma* in Algeria: *T. atrobrunneum*, (South) *T. longibrachiatum* (South), and *T. afroharzianum* (Northwest). *Microorganisms* 8:1455. doi: 10.3390/microorganisms8101455

Harman, G. E. (2000). Myths and dogmas of biocontrol changes in perceptions derived from research on *Trichoderma harzinum* T-22. *Plant Dis.* 84, 377–393. doi: 10.1094/PDIS.2000.84.4.377

Harman, G., Khadka, R., Doni, F., and Uphoff, N. (2021). Benefits to plant health and productivity from enhancing plant microbial symbionts. *Front. Plant Sci.* 11:610065. doi: 10.3389/fpls.2020.610065

He, C., Wang, W., and Hou, J. (2020). Plant performance of enhancing licorice with dual inoculating dark septate endophytes and *Trichoderma viride* mediated via effects on root development. *BMC Plant Biol.* 20:325. doi: 10.1186/s12870-020-02535-9

Hernández, J. A., Cazapal-Monteiro, C. F., Arroyo, F. L., Silva, M. I., Palomero, A. M., Paz-Silva, A., et al. (2018). Biological control of soil transmitted helminths (STHs) in a zoological park by using saprophytic fungi. *Biol Control*, 122, 24–30.

Herrera-Téllez, V. I., Cruz-Olmedo, A. K., Plasencia, J., Gavilanes-Ruíz, M., Arce-Cervantes, O., Hernández-León, S., et al. (2019). The protective effect of *Trichoderma asperellum* on tomato plants against *Fusarium oxysporum* and *Botrytis cinerea* diseases involves inhibition of reactive oxygen species production. *Int. J. Mol. Sci.* 20:2007. doi: 10.3390/ijms20082007

Hinterdobler, W., Li, G., Spiegel, K., Basyouni-Khamis, S., Gorfer, M., and Schmoll, M. (2021). *Trichoderma reesei* isolated from Austrian soil with high potential for biotechnological application. *Front. Microbiol.* 12:552301. doi: 10.3389/fmicb.2021.552301

Illescas, M., Morán-Diez, M. E., Martínez de Alba, Á. E., Hermosa, R., and Monte, E. (2022). Effect of *Trichoderma asperellum* on wheat plants' biochemical and molecular responses, and yield under different water stress conditions. *Int. J. Mol. Sci.* 23:6782. doi: 10.3390/ijms23126782

Intana, W., Kheawleng, S., and Sunpapao, A. (2021). *Trichoderma asperellum* T76-14 released volatile organic compounds against postharvest fruit rot in muskmelons (*Cucumis melo*) caused by *Fusarium incarnatum*. *J. Fungi* 7:46. doi: 10.3390/jof7010046

Intana, W., Wonglom, P., Suwannarach, N., and Sunpapao, A. (2022). *Trichoderma asperelloides* PSU-P1 induced expression of pathogenesis-related protein genes against gummy stem blight of muskmelon (*Cucumis melo*) in field evaluation. *J. Fungi* 8:156. doi: 10.3390/jof8020156

Izquierdo-García, L. F., González-Almario, A., Cotes, A. M., and Moreno-Velandia, C. A. (2020). *Trichoderma virens* Gl006 and *Bacillus velezensis* Bs006: a compatible interaction controlling *Fusarium* wilt of cape gooseberry. *Sci. Rep.* 10:6857. doi: 10.1038/s41598-020-63689-y

Jaiswal, A. K., Mengiste, T. D., Myers, J. R., Egel, D. S., and Hoagland, L. A. (2020). Tomato domestication attenuated responsiveness to a beneficial soil microbe for plant growth promotion and induction of systemic resistance to foliar pathogens. *Front. Microbiol.* 11:604566. doi: 10.3389/fmicb.2020.604566

Ji, S., Liu, Z., and Wang, Y. (2021). *Trichoderma*-induced ethylene responsive factor MsERF105 mediates defense responses in *Malus sieversii*. *Front. Plant Sci.* 12:708010. doi: 10.3389/fpls.2021.708010

Jogaiah, S., Abdelrahman, M., Tran, L. P., and Ito, S. I. (2018). Different mechanisms of *Trichoderma virens*-mediated resistance in tomato against *Fusarium* wilt involve the jasmonic and salicylic acid pathways. *Mol. Plant Pathol.* 19, 870–882. doi: 10.1111/mpp.12571

Joo, J. H., and Hussein, K. A. (2022). Biological control and plant growth promotion properties of volatile organic compound-producing antagonistic *Trichoderma* spp. *Front. Plant Sci.* 13:897668. doi: 10.3389/fpls.2022.897668

Kakabouki, I., Tataridas, A., Mavroeidis, A., Kousta, A., Karydogianni, S., Zisi, C., et al. (2021). Effect of colonization of *Trichoderma harzianum* on growth development and CBD content of hemp (*Cannabis sativa* L.). *Microorganisms* 9:518. doi: 10.3390/microorganisms9030518

Kappel, L., Kosa, N., and Gruber, S. (2022). The multilateral efficacy of chitosan and *Trichoderma* on sugar beet. *J. Fungi* 8:137. doi: 10.3390/jof8020137

Kappel, L., Münsterkötter, M., Sipos, G., Escobar Rodriguez, C., and Gruber, S. (2020). Chitin and chitosan remodeling defines vegetative development and *Trichoderma* biocontrol. *PLoS Pathog.* 16:e1008320. doi: 10.1371/journal.ppat.1008320

Karimi Aghcheh, R., Druzhinina, I. S., and Kubicek, C. P. (2013). The putative protein methyltransferase LAE1 of *Trichoderma atroviride* is a key regulator of asexual development and mycoparasitism. *PLoS One* 8:e67144. doi: 10.1371/journal.pone.0067144

Karuppiah, V., Sun, J., Li, T., Vallikkannu, M., and Chen, J. (2019a). Co-cultivation of *Trichoderma asperellum* GDFS1009 and *Bacillus amyloliquefaciens* 1841 causes differential gene expression and improvement in the wheat growth and biocontrol activity. *Front. Microbiol.* 10:1068. doi: 10.3389/fmicb.2019.01068

Karuppiah, V., Vallikkannu, M., Li, T., and Chen, J. (2019b). Simultaneous and sequential based co-fermentations of *Trichoderma asperellum* GDFS1009 and *Bacillus amyloliquefaciens* 1841: a strategy to enhance the gene expression and metabolites to improve the bio-control and plant growth promoting activity. *Microb. Cell Fact.* 18:185. doi: 10.1186/s12934-019-1233-7

Karuppiah, V., Zhixiang, L., Liu, H., Vallikkannu, M., and Chen, J. (2021). Co-culture of Vel1-over- expressed *Trichoderma asperellum* and *Bacillus amyloliquefaciens*: an eco-friendly strategy to hydrolyze the lignocellulose biomass in soil to enrich the soil fertility, plant growth and disease resistance. *Microb. Cell Factories* 20:57. doi: 10.1186/s12934-021-01540-3

Khan, R., Najeeb, S., Mao, Z., Ling, J., Yang, Y., Li, Y., et al. (2020). Bioactive secondary metabolites from *Trichoderma* spp. against phytopathogenic bacteria and root-knot nematode. *Microorganisms* 8:401. doi: 10.3390/microorganisms8030401

Köhl, J., Kolnaar, R., and Ravensberg, W. J. (2019). Mode of action of microbial biological control agents against plant diseases: relevance beyond efficacy. *Front. Plant Sci.* 10:845. doi: 10.3389/fpls.2019.00845

Kong, W. L., Ni, H., Wang, W. Y., and Wu, X. Q. (2022). Antifungal effects of volatile organic compounds produced by *Trichoderma koningiopsis* T2 against *Verticillium dahliae*. *Front. Microbiol.* 13:1013468. doi: 10.3389/fmicb.2022.1013468

Kottb, M., Gigolashvili, T., Großkinsky, D. K., and Piechulla, B. (2015). *Trichoderma volatiles* effecting Arabidopsis: from inhibition to protection against phytopathogenic fungi. *Front. Microbiol.* 6:995. doi: 10.3389/fmicb.2015.00995

Kovács, C., Csótó, A., Pál, K., Nagy, A., Fekete, E., Karaffa, L., et al. (2021). The biocontrol potential of endophytic *Trichoderma* fungi isolated from Hungarian grapevines. Part I. isolation, identification and in vitro studies. *Pathogens* 10:1612. doi: 10.3390/pathogens10121612

Kubicek, C. P., Steindorff, A. S., Chenthamara, K., Manganiello, G., Henrissat, B., Zhang, J., et al. (2019). Evolution and comparative genomics of the most common *Trichoderma* species. *BMC Genomics* 20:485. doi: 10.1186/s12864-019-5680-7

Lamdan, N. L., Shalaby, S., Ziv, T., Kenerley, C. M., and Horwitz, B. A. (2015). Secretome of *Trichoderma* interacting with maize roots: role in induced systemic resistance. *Mol. Cell. Proteomics* 14, 1054–1063. doi: 10.1074/mcp.M114.046607

Lazazzara, V., Vicelli, B., Bueschl, C., Parich, A., Pertot, I., Schuhmacher, R., et al. (2021). *Trichoderma* spp. volatile organic compounds protect grapevine plants by activating defense-related processes against downy mildew. *Physiol. Plant.* 172, 1950–1965. doi: 10.1111/ppl.13406

Leal, C., Richet, N., Guise, J. F., Gramaje, D., Armengol, J., Fontaine, F., et al. (2021). Cultivar contributes to the beneficial effects of *Bacillus subtilis* PTA-271 and *Trichoderma atroviride* SC1 to protect grapevine against *Neofusicoccum parvum*. *Front. Microbiol.* 12:726132. doi: 10.3389/fmicb.2021.726132

Li, N., Alfiky, A., Wang, W., Islam, M., Nourollahi, K., Liu, X., et al. (2018). Volatile compound- mediated recognition and inhibition between *Trichoderma* biocontrol agents and *Fusarium oxysporum*. *Front. Microbiol.* 9:2614. doi: 10.3389/fmicb.2018.02614

Li, X., Leng, J., Yu, L., Bai, H., Li, X., Wisniewski, M., et al. (2022). Efficacy of the biocontrol agent *Trichoderma hamatum* against *Lasiodiplodia theobromae* on macadamia. *Front. Microbiol.* 13:994422. doi: 10.3389/fmicb.2022.994422

Li, W. C., Lin, T. C., Chen, C. L., Liu, H. C., Lin, H. N., Chao, J. L., et al. (2021). Complete genome sequences and genome-wide characterization of *Trichoderma* biocontrol agents provide new insights into their evolution and variation in genome organization, sexual development, and fungal-plant interactions. *Microbiol. Spectr.* 9:e0066321. doi: 10.1128/Spectrum.00663-21

Li, J., Philp, J., Li, J., Wei, Y., Li, H., Yang, K., et al. (2020). *Trichoderma harzianum* inoculation reduces the incidence of Clubroot disease in Chinese cabbage by regulating the rhizosphere microbial community. *Microorganisms* 8:1325. doi: 10.3390/microorganisms8091325

Li, M., Ren, Y., He, C., Yao, J., Wei, M., and He, X. (2022). Complementary effects of dark septate endophytes and *Trichoderma* strains on growth and active ingredient accumulation of *Astragalus mongholicus* under drought stress. *J. Fungi* 8:920. doi: 10.3390/jof8090920

Liu, H., Hao, D., Li, Y., Wang, X., and Chen, J. (2022). Approaches for the establishment of optimized co-culture system of multiple *Trichoderma* strains for culture metabolites highly effective in cucumber growth promotion. *Front. Microbiol.* 13:1020077. doi: 10.3389/fmicb.2022.1020077

Liu, Y., He, P., He, P., Munir, S., Ahmed, A., Wu, Y., et al. (2022). Potential biocontrol efficiency of *Trichoderma* species against oomycete pathogens. *Front. Microbiol.* 13:974024. doi: 10.3389/fmicb.2022.974024

Lombardi, N., Caira, S., Troise, A. D., Scaloni, A., Vitaglione, P., Vinale, F., et al. (2020a). *Trichoderma* applications on strawberry plants modulate the physiological processes positively affecting fruit production and quality. *Front. Microbiol.* 11:1364. doi: 10.3389/fmicb.2020.01364

Lombardi, N., Salzano, A. M., Troise, A. D., Scaloni, A., Vitaglione, P., Vinale, F., et al. (2020b). Effect of *Trichoderma* bioactive metabolite treatments on the production, quality, and protein profile of strawberry fruits. *J. Agric. Food Chem.* 68, 7246–7258. doi: 10.1021/acs.jafc.0c01438

López, A. C., Alvarenga, A. E., Zapata, P. D., Luna, M. F., and Villalba, L. L. (2019). *Trichoderma* spp. from Misiones, Argentina: effective fungi to promote plant growth of the regional crop *Ilex paraguariensis* St. Hil. *Mycology* 10, 210–221. doi: 10.1080/21501203.2019.1606860

Mahmoud, G. A., Abdel-Sater, M. A., Al-Amery, E., and Hussein, N. A. (2021). Controlling *Alternaria cerealis* MT808477 tomato phytopathogen by *Trichoderma harzianum* and tracking the plant physiological changes. *Plan. Theory* 10:1846. doi: 10.3390/plants10091846

Malmierca, M. G., Cardoza, R. E., Alexander, N. J., McCormick, S. P., Hermosa, R., Monte, E., et al. (2012). Involvement of *Trichoderma trichothecenes* in the biocontrol activity and induction of plant defense-related genes. *Appl. Environ. Microbiol.* 78, 4856–4868. doi: 10.1128/AEM.00385-12

Manganiello, G., Nicastro, N., Caputo, M., Zaccardelli, M., Cardi, T., and Pane, C. (2021). Functional hyperspectral imaging by high-related vegetation indices to track the wide-spectrum *Trichoderma* biocontrol activity against soil-borne diseases of baby-leaf vegetables. *Front. Plant Sci.* 12:630059. doi: 10.3389/fpls.2021.630059

Manganiello, G., Sacco, A., Ercolano, M. R., Vinale, F., Lanzuise, S., Pascale, A., et al. (2018). Modulation of tomato response to *Rhizoctonia solani* by *Trichoderma harzianum* and its secondary metabolite harzianic acid. *Front. Microbiol.* 9:1966. doi: 10.3389/fmicb.2018.01966

Manzar, N., Kashyap, A. S., Goutam, R. S., Rajawat, M. V. S., Sharma, P. K., Sharma, S. K., et al. (2022). *Trichoderma*: advent of versatile biocontrol agent, its secrets and insights into mechanism of biocontrol potential. *Sustainability* 14:12786. doi: 10.3390/su141912786

Marik, T., Tyagi, C., Balázs, D., Urbán, P., Szepesi, Á., Bakacsy, L., et al. (2019). Structural diversity and bioactivities of peptaibol compounds from the longibrachiatum clade of the filamentous fungal genus *Trichoderma*. *Front. Microbiol.* 10:1434. doi: 10.3389/fmicb.2019.01434

Marra, R., Lombardi, N., Piccolo, A., Bazghaleh, N., Prashar, P., Vandenberg, A., et al. (2021). Mineral biofortification and growth stimulation of lentil plants inoculated with *Trichoderma* strains and metabolites. *Microorganisms* 10:87. doi: 10.3390/microorganisms10010087

Marraschi, R., Ferreira, A., da Silva Bueno, R. N., Leite, J., Lucon, C., Harakava, R., et al. (2019). A protocol for selection of *Trichoderma* spp. to protect grapevine pruning wounds against *Lasiodiplodia theobromae*. *Braz. J. Microbiol.* 50, 213–221. doi: 10.1007/s42770-018-0029-y

Martínez-Medina, A., Fernández, I., Sánchez-Guzmán, M. J., Jung, S. C., Pascual, J. A., and Pozo, M. J. (2013). Deciphering the hormonal signalling network behind the systemic resistance induced by *Trichoderma harzianum* in tomato. *Front. Plant Sci.* 4:206. doi: 10.3389/fpls.2013.00206

Martínez-Salgado, S. J., Andrade-Hoyos, P., Parraguirre Lezama, C., Rivera-Tapia, A., Luna-Cruz, A., and Romero-Arenas, O. (2021). Biological control of charcoal rot in peanut crop through strains of *Trichoderma* spp., in Puebla, Mexico. *Plan. Theory* 10:2630. doi: 10.3390/plants10122630

Maruyama, C. R., Bilesky-José, N., de Lima, R., and Fraceto, L. F. (2020). Encapsulation of *Trichoderma harzianum* preserves enzymatic activity and enhances the potential for biological control. *Front. Bioeng. Biotechnol.* 8:225. doi: 10.3389/fbioe.2020.00225

Matas-Baca, M. Á., Urías García, C., Pérez-Álvarez, S., Flores-Córdova, M. A., Escobedo- Bonilla, C. M., Magallanes-Tapia, M. A., et al. (2022). Morphological and molecular characterization of a new autochthonous *Trichoderma* sp. isolate and its biocontrol efficacy against *Alternaria* sp. Saudi. *J. Biol. Sci.* 29, 2620–2625. doi: 10.1016/j.sjbs.2021.12.052

Mayo, S., Gutiérrez, S., Malmierca, M. G., Lorenzana, A., Campelo, M. P., Hermosa, R., et al. (2015). Influence of *Rhizoctonia solani* and *Trichoderma* spp. in growth of bean (*Phaseolus vulgaris* L.) and in the induction of plant defense-related genes. *Front. Plant Sci.* 6:685. doi: 10.3389/fpls.2015.00685

Mayo-Prieto, S., Marra, R., Vinale, F., Rodríguez-González, Á., Woo, S. L., Lorito, M., et al. (2019). Effect of *Trichoderma velutinum* and *Rhizoctonia solani* on the metabolome of bean plants (*Phaseolus vulgaris* L.). *Int. J. Mol. Sci.* 20:549. doi: 10.3390/ijms20030549

Mohiddin, F. A., Padder, S. A., Bhat, A. H., Ahanger, M. A., Shikari, A. B., Wani, S. H., et al. (2021). Phylogeny and optimization of *Trichoderma harzianum* for Chitinase production: evaluation of their antifungal behaviour against the prominent soil borne Phyto-pathogens of temperate India. *Microorganisms* 9:1962. doi: 10.3390/microorganisms9091962

Monfil, V. O., and Casas-Flores, S. (2014). Molecular mechanisms of biocontrol in *Trichoderma* spp. and their applications in agriculture. *Biotechnol. Biol. Trichoderma* 8:447. doi: 10.1016/B978-0-444-59576-8.00032-1

Moo-Koh, F. A., Cristóbal-Alejo, J., Andrés, M. F., Martín, J., Reyes, F., Tun-Suárez, J. M., et al. (2022). In vitro assessment of organic and residual fractions of nematicidal culture filtrates from thirteen tropical *Trichoderma* strains and metabolic profiles of most-active. *J. Fungi* 8:82. doi: 10.3390/jof8010082

Morán-Diez, M. E., Carrero-Carrón, I., Rubio, M. B., Jiménez-Díaz, R. M., Monte, E., and Hermosa, R. (2019). Transcriptomic analysis of *Trichoderma atroviride* overgrowing plant-wilting *Verticillium dahliae* reveals the role of a new M14 metallocarboxypeptidase CPA1 in biocontrol. *Front. Microbiol.* 10:1120. doi: 10.3389/fmicb.2019.01120

Morán-Diez, M. E., Tranque, E., Bettiol, W., Monte, E., and Hermosa, R. (2020). Differential response of tomato plants to the application of three *Trichoderma* species when evaluating the control of *Pseudomonas syringae* populations. *Plan. Theory* 9:626. doi: 10.3390/plants9050626

Moreno-Ruiz, D., Lichius, A., Turrà, D., Di Pietro, A., and Zeilinger, S. (2020). Chemotropism assays for plant symbiosis and mycoparasitism related compound screening in *Trichoderma atroviride*. *Front. Microbiol.* 11:601251. doi: 10.3389/fmicb.2020.601251

Mulatu, A., Alemu, T., Megersa, N., and Vetukuri, R. R. (2021). Optimization of culture conditions and production of bio-fungicides from *Trichoderma* species under solid-state fermentation using mathematical modeling. *Microorganisms* 9:1675. doi: 10.3390/microorganisms9081675

Naglot, A., Goswami, S., Rahman, I., Shrimali, D. D., Yadav, K. K., Gupta, V. K., et al. (2015). Antagonistic potential of native *Trichoderma viride* strain against potent tea fungal pathogens in north East India. *Plant Pathol. J.* 31, 278–289. doi: 10.5423/PPJ.OA.01.2015.0004

Navazio, L., Baldan, B., Moscatiello, R., Zuppini, A., Woo, S. L., Mariani, P., et al. (2007). Calcium- mediated perception and defense responses activated in plant cells by metabolite mixtures secreted by the biocontrol fungus *Trichoderma atroviride*. *BMC Plant Biol.* 7:41. doi: 10.1186/1471-2229-7-41

Nawrocka, J., Gromek, A., and Małolepsza, U. (2019). Nitric oxide as a beneficial signaling molecule in *Trichoderma atroviride* TRS25- induced systemic defense responses of cucumber plants against *Rhizoctonia solani*. *Front. Plant Sci.* 10:421. doi: 10.3389/fpls.2019.00421

Nawrocka, J., Małolepsza, U., Szymczak, K., and Szczech, M. (2018). Involvement of metabolic components, volatile compounds, PR proteins, and mechanical strengthening in multilayer protection of cucumber plants against *Rhizoctonia solani* activated by *Trichoderma atroviride* TRS25. *Protoplasma* 255, 359–373. doi: 10.1007/s00709-017-1157-1

Ngo, M. T., Nguyen, M. V., Han, J. W., Park, M. S., Kim, H., and Choi, G. J. (2021). In vitro and in vivo antifungal activity of *Sorbicillinoids* produced by *Trichoderma longibrachiatum*. *J. Fungi* 7:428. doi: 10.3390/jof7060428

Nieto-Jacobo, M. F., Steyaert, J. M., Salazar-Badillo, F. B., Nguyen, D. V., Rostás, M., Braithwaite, M., et al. (2017). Environmental growth conditions of *Trichoderma* spp. affects Indole acetic acid derivatives, volatile organic compounds, and plant growth promotion. *Front. Plant Sci.* 8:102. doi: 10.3389/fpls.2017.00102

Niu, B., Wang, W., Yuan, Z., Sederoff, R. R., Sederoff, H., Chiang, V. L., et al. (2020). Microbial interactions within multiple-strain biological control agents impact soil-borne plant disease. *Front. Microbiol.* 11:585404. doi: 10.3389/fmicb.2020.585404

Nuangmek, W., Aiduang, W., Kumla, J., Lumyong, S., and Suwannarach, N. (2021). Evaluation of a newly identified endophytic fungus, *Trichoderma phayaoense* for plant growth promotion and biological control of gummy stem blight and wilt of muskmelon. *Front. Microbiol.* 12:634772. doi: 10.3389/fmicb.2021.634772

Organo, N. D., Granada, S., Pineda, H., Sandro, J. M., Nguyen, V. H., and Gummert, M. (2022). Assessing the potential of a *Trichoderma*-based compost activator to hasten the decomposition of incorporated rice straw. *Sci. Rep.* 12:448. doi: 10.1038/s41598-021-03828-1

Oszust, K., Cybulska, J., and Frąc, M. (2020). How do *Trichoderma* genus fungi win a nutritional competition battle against soft fruit pathogens? A report on niche overlap nutritional potentiates. *Int. J. Mol. Sci.* 21:4235. doi: 10.3390/ijms21124235

Panchalingam, H., Powell, D., Adra, C., Foster, K., Tomlin, R., Quigley, B. L., et al. (2022). Assessing the various antagonistic mechanisms of *Trichoderma* strains against the brown root rot pathogen *Pyrrhoderma noxium* infecting heritage fig trees. *J. Fungi* 8:1105. doi: 10.3390/jof8101105

Park, Y. H., Chandra Mishra, R., Yoon, S., Kim, H., Park, C., Seo, S. T., et al. (2019). Endophytic *Trichoderma citrinoviride* isolated from mountain-cultivated ginseng (*Panax ginseng*) has great potential as a biocontrol agent against ginseng pathogens. *J. Ginseng Res.* 43, 408–420. doi: 10.1016/j.jgr.2018.03.002

Pescador, L., Fernandez, I., Pozo, M. J., Romero-Puertas, M. C., Pieterse, C., and Martínez- Medina, A. (2022). Nitric oxide signalling in roots is required for MYB72-dependent systemic resistance induced by *Trichoderma* volatile compounds in *Arabidopsis*. *J. Exp. Bot.* 73, 584–595. doi: 10.1093/jxb/erab294

Phoka, N., Suwannarach, N., Lumyong, S., Ito, S. I., Matsui, K., Arikit, S., et al. (2020). Role of volatiles from the endophytic fungus *Trichoderma asperelloides* PSU-P1 in biocontrol potential and in promoting the plant growth of *Arabidopsis thaliana*. *J. Fungi* 6:341. doi: 10.3390/jof6040341

Pocurull, M., Fullana, A. M., Ferro, M., Valero, P., Escudero, N., Saus, E., et al. (2020). Commercial formulates of *Trichoderma* induce systemic plant resistance to *Meloidogyne incognita* in tomato and the effect is additive to that of the Mi-1.2 resistance gene. *Front. Microbiol.* 10:3042. doi: 10.3389/fmicb.2019.03042

Pollard-Flamand, J., Boulé, J., Hart, M., and Úrbez-Torres, J. R. (2022). Biocontrol activity of *Trichoderma* species isolated from grapevines in British Columbia against botryosphaeria dieback fungal pathogens. *J. Fungi* 8:409. doi: 10.3390/jof8040409

Poveda, J., Abril-Urias, P., and Escobar, C. (2020). Biological control of plant-parasitic nematodes by filamentous fungi inducers of resistance: *Trichoderma*, Mycorrhizal and Endophytic Fungi. *Front. Microbiol.* 11:992. doi: 10.3389/fmicb.2020.00992

Poveda, J., Hermosa, R., Monte, E., and Nicolás, C. (2019). *Trichoderma harzianum* favours the access of *arbuscular mycorrhizal* fungi to non-host Brassicaceae roots and increases plant productivity. *Sci. Rep.* 9:11650. doi: 10.1038/s41598-019-48269-z

Rao, Y., Zeng, L., Jiang, H., Mei, L., and Wang, Y. (2022). *Trichoderma atroviride* LZ42 releases volatile organic compounds promoting plant growth and suppressing Fusarium wilt disease in tomato seedlings. *BMC Microbiol.* 22:88. doi: 10.1186/s12866-022-02511-3

Rashmi, S., Maurya, S., and Upadhyay, R. S. (2016). The improvement of competitive saprophytic capabilities of *Trichoderma* species through the use of chemical mutagens. *Braz. J. Microbiol.* 47, 10–17. doi: 10.1016/j.bjm.2015.11.003

Rawal, R., Scheerens, J. C., Fenstemaker, S. M., Francis, D. M., Miller, S. A., and Benitez, M. S. (2022). Novel *Trichoderma* isolates alleviate water deficit stress in susceptible tomato genotypes. *Front. Plant Sci.* 13:869090. doi: 10.3389/fpls.2022.869090

Rees, H. J., Drakulic, J., Cromey, M. G., Bailey, A. M., and Foster, G. D. (2022). Endophytic *Trichoderma* spp. can protect strawberry and privet plants from infection by the fungus *Armillaria mellea*. *PLoS One* 17:e0271622. doi: 10.1371/journal.pone.0271622

Risoli, S., Cotrozzi, L., Sarrocco, S., Nuzzaci, M., Pellegrini, E., and Vitti, A. (2022). *Trichoderma*-induced resistance to *Botrytis cinerea* in *Solanum* species: a meta-analysis. *Plan. Theory* 11:180. doi: 10.3390/plants11020180

Ruangwong, O. U., Pornsuriya, C., Pitija, K., and Sunpapao, A. (2021a). Biocontrol mechanisms of *Trichoderma koningiopsis* PSU3-2 against postharvest anthracnose of chili pepper. *J. Fungi* 7:276. doi: 10.3390/jof7040276

Ruangwong, O. U., Wonglom, P., Suwannarach, N., Kumla, J., Thaochan, N., Chomnunti, P., et al. (2021b). Volatile organic compound from *Trichoderma asperelloides* TSU1: impact on plant pathogenic fungi. *J. Fungi* 7:187. doi: 10.3390/jof7030187

Rubio, M. B., Quijada, N. M., Pérez, E., Domínguez, S., Monte, E., and Hermosa, R. (2014). Identifying beneficial qualities of *Trichoderma parareesei* for plants. *Appl. Environ. Microbiol.* 80, 1864–1873. doi: 10.1128/AEM.03375-13

Samuelian, S. (2016). Potential of *Trichoderma harzianum* for control of banana leaf fungal pathogens when applied with a food source and an organic adjuvant. *3 Biotech* 6:8. doi: 10.1007/s13205-015-0327-0

Samuels, G. J., Dodd, S. L., Lu, B. S., Petrini, O., Schroers, H. J., and Druzhinina, I. S. (2006). The *Trichoderma koningii* aggregate species. *Stud. Mycol.* 56, 67–133. doi: 10.3114/sim.2006.56.03

Sánchez-Montesinos, B., Santos, M., Moreno-Gavíra, A., Marín-Rodulfo, T., Gea, F. J., and Diánez, F. (2021). Biological control of fungal diseases by *Trichoderma aggressivum* f. *europaeum* and its compatibility with fungicides. *J. Fungi* 7:598. doi: 10.3390/jof7080598

Santos, M., Santos, L., Costa, D., Vieira, T. A., and Lustosa, D. C. (2020). *Trichoderma* spp. on treatment of *Handroanthus serratifolius* seeds: effect on seedling germination and development. *Heliyon* 6:e04044. doi: 10.1016/j.heliyon.2020.e04044

Saravanakumar, K., Fan, L., Fu, K., Yu, C., Wang, M., Xia, H., et al. (2016). Cellulase from *Trichoderma harzianum* interacts with roots and triggers induced systemic resistance to foliar disease in maize. *Sci. Rep.* 6:35543. doi: 10.1038/srep35543

Saravanakumar, K., Li, Y., Yu, C., Wang, Q. Q., Wang, M., Sun, J., et al. (2017). Effect of *Trichoderma harzianum* on maize rhizosphere microbiome and biocontrol of Fusarium stalk rot. *Sci. Rep.* 7:1771. doi: 10.1038/s41598-017-01680-w

Şesan, T. E., Oancea, A. O., Ştefan, L. M., Mănoiu, V. S., Ghiurea, M., Răut, I., et al. (2020). Effects of foliar treatment with a *Trichoderma* plant biostimulant consortium on *Passiflora caerulea* L. yield and quality. *Microorganisms* 8:123. doi: 10.3390/microorganisms8010123

Shaw, S., Le Cocq, K., Paszkiewicz, K., Moore, K., Winsbury, R., de Torres Zabala, M., et al. (2016). Transcriptional reprogramming underpins enhanced plant growth promotion by the biocontrol fungus *Trichoderma hamatum* GD12 during antagonistic interactions with *Sclerotinia sclerotiorum* in soil. *Mol. Plant Pathol.* 17, 1425–1441. doi: 10.1111/mpp.12429

Shobha, B., Lakshmeesha, T. R., Ansari, M. A., Almatroudi, A., Alzohairy, M. A., Basavaraju, S., et al. (2020). Mycosynthesis of ZnO nanoparticles using *Trichoderma* spp. isolated from rhizosphere soils and its synergistic antibacterial effect against *Xanthomonas oryzae* pv. *oryzae*. *J. Fungi* 6:181. doi: 10.3390/jof6030181

Shoresh, M., and Harman, G. E. (2010). Differential expression of maize chitinases in the presence or absence of *Trichoderma harzianum* strain T22 and indications of a novel exo-endo-heterodimeric chitinase activity. *BMC Plant Biol.* 10, 136–111. doi: 10.1186/1471-2229-10-136

Singh, B. N., Dwivedi, P., Sarma, B. K., Singh, G. S., and Singh, H. B. (2019). A novel function of N-signaling in plants with special reference to *Trichoderma* interaction influencing plant growth, nitrogen use efficiency, and cross talk with plant hormones. *3 Biotech* 9:109. doi: 10.1007/s13205-019-1638-3

Sokhandani, Z., Moosavi, M. R., and Basirnia, T. (2016). Optimum concentrations of *Trichoderma longibrachiatum* and cadusafos for controlling *Meloidogyne javanica* on Zucchini plants. *J. Nematol.* 48, 54–63. doi: 10.21307/jofnem-2017-009

Stracquadanio, C., Quiles, J. M., Meca, G., and Cacciola, S. O. (2020). Antifungal activity of bioactive metabolites produced by *Trichoderma asperellum* and *Trichoderma atroviride* in liquid medium. *J. Fungi* 6:263. doi: 10.3390/jof6040263

Sui, L., Li, J., Philp, J., Yang, K., Wei, Y., Li, H., et al. (2022). *Trichoderma atroviride* seed dressing influenced the fungal community and pathogenic fungi in the wheat rhizosphere. *Sci. Rep.* 12:9677. doi: 10.1038/s41598-022-13669-1

Sun, J., Karuppiah, V., Li, Y., Pandian, S., Kumaran, S., and Chen, J. (2022). Role of cytochrome P450 genes of *Trichoderma atroviride* T23 on the resistance and degradation of dichlorvos. *Chemosphere* 290:133173. doi: 10.1016/j.chemosphere.2021.133173

Sun, R. Y., Liu, Z. C., Fu, K., Fan, L., and Chen, J. (2012). *Trichoderma* biodiversity in China. *J. Appl. Genet.* 53, 343–354. doi: 10.1007/s13353-012-0093-1

Swain, H., Adak, T., Mukherjee, A. K., Sarangi, S., Samal, P., Khandual, A., et al. (2021). Seed biopriming with *Trichoderma* strains isolated from tree bark improves plant growth, antioxidative defense system in Rice and enhance straw degradation capacity. *Front. Microbiol.* 12:633881. doi: 10.3389/fmicb.2021.633881

Tamizi, A. A., Mat-Amin, N., Weaver, J. A., Olumakaiye, R. T., Akbar, M. A., Jin, S., et al. (2022). Genome sequencing and analysis of *Trichoderma* (Hypocreaceae) isolates exhibiting antagonistic activity against the papaya dieback pathogen, *Erwinia mallotivora*. *J. Fungi* 8:246. doi: 10.3390/jof8030246

Thambugala, K. M., Daranagama, D. A., Phillips, A., Kannangara, S. D., and Promputtha, I. (2020). Fungi vs. fungi in biocontrol: an overview of fungal antagonists applied against fungal plant pathogens. *Front. Cell. Infect. Microbiol.* 10:604923. doi: 10.3389/fcimb.2020.604923

Tian, Y., Tan, Y., Liu, N., Yan, Z., Liao, Y., Chen, J., et al. (2016). Detoxification of deoxynivalenol via glycosylation represents novel insights on antagonistic activities of *Trichoderma* when confronted with *Fusarium graminearum*. *Toxins* 8:335. doi: 10.3390/toxins8110335

Tian, Y., Tan, Y., Yan, Z., Liao, Y., Chen, J., De Boevre, M., et al. (2018). Antagonistic and detoxification potentials of *Trichoderma* isolates for control of zearalenone (ZEN) producing *Fusarium graminearum*. *Front. Microbiol.* 8:2710. doi: 10.3389/fmicb.2017.02710

Tilocca, B., Cao, A., and Migheli, Q. (2020). Scent of a killer: microbial volatilome and its role in the biological control of plant pathogens. *Front. Microbiol.* 11:41. doi: 10.3389/fmicb.2020.00041

Tseng, Y. H., Rouina, H., Groten, K., Rajani, P., Furch, A., Reichelt, M., et al. (2020). An endophytic *Trichoderma* strain promotes growth of its hosts and defends against pathogen attack. *Front. Plant Sci.* 11:573670. doi: 10.3389/fpls.2020.573670

Tyśkiewicz, R., Nowak, A., Ozimek, E., and Jaroszuk-Ściseł, J. (2022). *Trichoderma*: the current status of its application in agriculture for the biocontrol of fungal phytopathogens and stimulation of plant growth. *Int. J. Mol. Sci.* 23:2329. doi: 10.3390/ijms23042329

Velasco, P., Rodríguez, V. M., Soengas, P., and Poveda, J. (2021). *Trichoderma hamatum* increases productivity, glucosinolate content and antioxidant potential of different leafy *brassica* vegetables. *Plan. Theory* 10:2449. doi: 10.3390/plants10112449

Vicente, I., Baroncelli, R., Morán-Diez, M. E., Bernardi, R., Puntoni, G., Hermosa, R., et al. (2020). Combined comparative genomics and gene expression analyses provide insights into the terpene synthases inventory in *Trichoderma*. *Microorganisms* 8:1603. doi: 10.3390/microorganisms8101603

Viriyasuthee, W., Jogloy, S., Saksirirat, W., Saepaisan, S., Gleason, M. L., and Chen, R. S. (2019). Biological control of Alternaria leaf spot caused by *Alternaria* spp. in Jerusalem artichoke (*Helianthus tuberosus* L.) under two fertilization regimes. *Plan. Theory* 8:463. doi: 10.3390/plants8110463

Viterbo, A., Harel, M., Horwitz, B. A., Chet, I., and Mukherjee, P. K. (2005). *Trichoderma* mitogen-activated protein kinase signaling is involved in induction of plant systemic resistance. *Appl. Environ. Microbiol.* 71, 6241–6246. doi: 10.1128/AEM.71.10.6241-6246.2005

Vos, C. M., De Cremer, K., Cammue, B. P., and De Coninck, B. (2015). The toolbox of *Trichoderma* spp. in the biocontrol of *Botrytis cinerea* disease. *Mol. Plant Pathol.* 16, 400–412. doi: 10.1111/mpp.12189

Wang, Y., Chen, H., Ma, L., Gong, M., Wu, Y., Bao, D., et al. (2022). Use of CRISPR-Cas tools to engineer *Trichoderma* species. *Microb. Biotechnol.* 15, 2521–2532. doi: 10.1111/1751-7915.14126

Wang, R., Liu, C., Jiang, X., Tan, Z., Li, H., Xu, S., et al. (2022). The newly identified *Trichoderma harzianum* partitivirus (ThPV2) does not diminish spore production and biocontrol activity of its host. *Viruses* 14:1532. doi: 10.3390/v14071532

Wang, H., Zhang, R., Duan, Y., Jiang, W., Chen, X., Shen, X., et al. (2021). The endophytic strain *Trichoderma asperellum* 6S-2: an efficient biocontrol agent against apple replant disease in China and a potential plant-growth-promoting fungus. *J. Fungi* 7:1050. doi: 10.3390/jof7121050

Wang, H., Zhang, R., Mao, Y., Jiang, W., Chen, X., Shen, X., et al. (2022). Effects of *Trichoderma asperellum* 6S-2 on apple tree growth and replanted soil microbial environment. *J. Fungi* 8:63. doi: 10.3390/jof8010063

Xu, H., Yan, L., Zhang, M., Chang, X., Zhu, D., Wei, D., et al. (2022). Changes in the density and composition of rhizosphere pathogenic *Fusarium* and beneficial *Trichoderma* contributing to reduced root rot of intercropped soybean. *Pathogens* 11:478. doi: 10.3390/pathogens11040478

Ye, L., Zhao, X., Bao, E., Li, J., Zou, Z., and Cao, K. (2020). Bio-organic fertilizer with reduced rates of chemical fertilization improves soil fertility and enhances tomato yield and quality. *Sci. Rep.* 10:177. doi: 10.1038/s41598-019-56954-2

You, J., Li, G., Li, C., Zhu, L., Yang, H., Song, R., et al. (2022). Biological control and plant growth promotion by volatile organic compounds of *Trichoderma koningiopsis* T-51. *J. Fungi* 8:131. doi: 10.3390/jof8020131

Yuan, M., Huang, Y., Ge, W., Jia, Z., Song, S., Zhang, L., et al. (2019). Involvement of jasmonic acid, ethylene and salicylic acid signaling pathways behind the systemic resistance induced by *Trichoderma longibrachiatum* H9 in cucumber. *BMC Genomics* 20:144. doi: 10.1186/s12864-019-5513-8

Zaid, R., Koren, R., Kligun, E., Gupta, R., Leibman-Markus, M., Mukherjee, P. K., et al. (2022). Gliotoxin, an immunosuppressive fungal metabolite, primes plant immunity: evidence from *Trichoderma virens*-tomato interaction. *MBio* 13:e0038922. doi: 10.1128/mbio.00389-22

Zhang, J., Chen, J., Liu, Z., Guan, S., Li, J., Zhang, C., et al. (2017). Evaluation of the combined use of *Trichoderma atroviride* metabolite and brassinolide in the promotion of vegetable growth and control of *Botrytis cinere*. *J. Shanghai Jiaotong Univ.* 35, 1–7. doi: 10.3969/J.ISSN.1671-9964.2017.05.001

Zhang, S., Gan, Y., Liu, J., Zhou, J., and Xu, B. (2020). Optimization of the fermentation media and parameters for the bio-control potential of *Trichoderma longibrachiatum* T6 against nematodes. *Front Microbiol.* 11:574601.

Zhang, F., Huo, Y., Cobb, A. B., Luo, G., Zhou, J., Yang, G., et al. (2018). *Trichoderma* biofertilizer links to altered soil chemistry, altered microbial communities, and improved grassland biomass. *Front. Microbiol.* 9:848. doi: 10.3389/fmicb.2018.00848

Zhang, C., Wang, W., Hu, Y., Peng, Z., Ren, S., Xue, M., et al. (2022). A novel salt-tolerant strain *Trichoderma atroviride* HN082102.1 isolated from marine habitat alleviates salt stress and diminishes cucumber root rot caused by *Fusarium oxysporum*. *BMC Microbiol.* 22:67. doi: 10.1186/s12866-022-02479-0

Zhang, C., Wang, W., Xue, M., Liu, Z., Zhang, Q., Hou, J., et al. (2021). The combination of a biocontrol agent *Trichoderma asperellum* SC012 and hymexazol reduces the effective fungicide dose to control *Fusarium* wilt in cowpea. *J. Fungi* 7:685. doi: 10.3390/jof7090685

Zhang, Y., Xiao, J., Yang, K., Wang, Y., Tian, Y., and Liang, Z. (2022). Transcriptomic and metabonomic insights into the biocontrol mechanism of *Trichoderma asperellum* M45a against watermelon *Fusarium* wilt. *PLoS One* 17:e0272702. doi: 10.1371/journal.pone.0272702

Zheng, H., Qiao, M., Lv, Y., Du, X., Zhang, K. Q., and Yu, Z. (2021). New species of *Trichoderma* isolated as endophytes and saprobes from Southwest China. *J. Fungi* 7:467. doi: 10.3390/jof7060467

Zhou, D., Huang, X. F., Guo, J., Dos-Santos, M. L., and Vivanco, J. M. (2018). *Trichoderma gamsii* affected herbivore feeding behaviour on arabidopsis thaliana by modifying the leaf metabolome and phytohormones. *Microb Biotechnol.* 11, 1195–1206.

Zhu, N., Zhou, J. J., Zhang, S. W., and Xu, B. L. (2022). Mechanisms of *Trichoderma longibrachiatum* T6 fermentation against *Valsa mali* through inhibiting its growth and reproduction, pathogenicity and gene expression. *J. Fungi* 8:113. doi: 10.3390/jof8020113

frontiers | Frontiers in Microbiology

TYPE Original Research
PUBLISHED 21 June 2023
DOI 10.3389/fmicb.2023.1190624

OPEN ACCESS

EDITED BY
Mina Salehi,
Tarbiat Modares University, Iran

REVIEWED BY
Siamak Farhadi,
Tarbiat Modares University, Iran
Shaohua Wu,
Yunnan University, China
Orlando Borras-Hidalgo,
Qilu University of Technology, China
Naser Safaie,
Tarbiat Modares University, Iran

*CORRESPONDENCE
Zizhong Tang
✉ 14126@sicau.edu.cn

†These authors share first authorship

RECEIVED 22 March 2023
ACCEPTED 01 June 2023
PUBLISHED 21 June 2023

CITATION
Shen N, Chen Z, Cheng G, Lin W, Qin Y, Xiao Y, Chen H, Tang Z, Li Q, Yuan M and Bu T (2023) Diversity, chemical constituents and biological activities of endophytic fungi from *Alisma orientale* (Sam.) Juzep.
Front. Microbiol. 14:1190624.
doi: 10.3389/fmicb.2023.1190624

Diversity, chemical constituents and biological activities of endophytic fungi from *Alisma orientale* (Sam.) Juzep.

Nayu Shen[1†], Zhao Chen[2†], GuiXin Cheng[1†], Wenjie Lin[1], Yihan Qin[1], Yirong Xiao[3], Hui Chen[1], Zizhong Tang[1*], Qingfeng Li[1], Ming Yuan[1] and Tongliang Bu[1]

[1]College of Life Sciences, Sichuan Agricultural University, Ya'an, China, [2]Ya'an People's Hospital, Ya'an, China, [3]Sichuan Agricultural University Hospital, Ya'an, China

The dried tuber of *Alisma orientale* (Sam.) Juzep. (AOJ) is a traditional Chinese medicine with high medicinal value. The endophytic fungi of medicinal plants are a treasure house of natural compounds. However, there is a lack of research on the diversity and biological activity of endophytic fungi of AOJ. In this study, high-throughput sequencing technology was used to study the diversity of endophytic fungi in the roots and stems of AOJ, and endophytic fungi with a high output of phenols and flavonoids were screened by chromogenic reaction, and the antioxidant and antibacterial activities and chemical constituents of crude extracts of their fermentation broth were studied. A total of 3,426 amplicon sequence variants (ASVs) belonging to 9 phyla, 27 classes, 64 orders, 152 families, and 277 genera were identified from AOJ. There were significant differences in the endophytic fungal communities of AOJ roots and stems, as well as in the endophytic fungal communities of triangular AOJ and circular AOJ. In addition, 31 strains of endophytic fungi were isolated from AOJ, of which 6 strains had good antioxidant and antibacterial activities. The crude extract of YG-2 had the strongest free radical scavenging ability and bacteriostatic ability, and its $IC_{50\ DPPH}$, $IC_{50\ ABTS}$, and $IC_{50\cdot OH}$ values were 0.009 ± 0.000 mg/mL, 0.023 ± 0.002 mg/mL, and 0.081 ± 0.006 mg/mL, respectively. The results of LC-MS showed that the main component of the crude extract of YG-2 was caffeic acid (10.12 μmol/g). Overall, the results of this study preliminarily elucidated the diversity and community composition of endophytic fungi of AOJ, indicating that AOJ endophytic fungi have abundant secondary metabolites and good antioxidant and antibacterial activities. This study provides an important reference for further research, development and utilization of AOJ endophytic fungi and a theoretical basis for the further development of the endophytic fungus YG-2 (*Chaetomium globosum*) as a source of antioxidants.

KEYWORDS

endophytic fungi, diversity, antioxidant, bacteriostatic activity, *Alisma orientale* (Sam.) Juzep., chemical constituents, high-throughput sequencing

1. Introduction

Due to factors such as respiration and radiation, free radicals are constantly produced in the body. The presence of a large number of free radicals will destroy the body's equilibrium, resulting in oxidative stress and thus damaging biomolecules (Sharma et al., 2018). Current research results show that oxygen free radicals are directly related to most diseases in the human body (Marx, 1986; Moskovitz et al., 2002; Tappel and Tappel, 2004; Tang et al., 2022). Therefore, the search for effective antioxidants has become very important research. The resistance of pathogenic bacteria to existing drugs has become a global concern, and it is urgent to find new natural effective antimicrobials (Dos Santos et al., 2015; Gu et al., 2022).

Endophytic fungi live in plants and exist in mutually beneficial symbiosis with their hosts. They can't only significantly affect the formation of metabolites in their hosts (Jia et al., 2016) but also produce the same metabolites as their hosts (Gupta et al., 2020; Li et al., 2022). Endophytes are important sources of active natural products capable of biosynthesizing medically important "phytochemicals" that were originally thought to be produced only by the host plant, and as alternative and sustainable sources, endophytes are able to produce these compounds more quickly than plants (Wen et al., 2022). Most of the active compounds isolated from endophytic fungi have antibacterial activity, and mycelium and fermentation liquid extracts can produce certain inhibitory activity against plant, animal and human pathogens (Charria-Girón et al., 2021; Gu et al., 2022). Some secondary metabolites of endophytic fungi have good antibacterial activity and have been studied for the development of new drugs (Atiphasaworn et al., 2017; Mookherjee et al., 2020; Muthukrishnan et al., 2022; Wen et al., 2022). The endophytic fungi isolated from most plants, especially medicinal plants, showed excellent antioxidant activity. Endophytic fungi isolated from medicinal plants can produce abundant bioactive secondary metabolites, such as alkaloids, terpenoids, steroids, flavonoids, quinones, isocoumarins, lignans, phenylpropanes, phenols, and lactones (Dos Santos et al., 2015; Tang et al., 2021). Moreover, these active ingredients have corresponding rich biological functions, such as antioxidant, antibacterial, antiviral, and antidiabetic activities (Muthukrishnan et al., 2022). To date, endophytic fungi with antioxidant or antibacterial activities have been isolated from medicinal plants, such as *Loranthus tanakae* Franch. and Sav, *Passiflora incarnata*, *Ocimum basilicum*, *Ligusticum chuanxiong* Hort, and *Radix Puerariae*, and many studies have shown that phenols and flavonoids rich in medicinal plants are important sources of antioxidant or antibacterial ability of endophytic fungi of medicinal plants (Atiphasaworn et al., 2017; Silva et al., 2020; Tang et al., 2021; Deng et al., 2022; Zheng et al., 2022). Zheng et al. (2022) isolated 8 endophytic fungi that produce flavonoids from the medicinal plant *Mulberry parasitica*, among which the antioxidant and antibacterial activities of *Streptomyces* ZP28 and ZM148 were higher than those of the other 6 strains. The results of LC-MS showed that the structural types of flavonoids in the extracts of ZP28 and ZM148 were mainly flavonoids and isoflavones. Li et al. (2022) isolated endophytic fungi from *Andrographis* and determined the total phenol content and total flavonoid content of strains with strong antioxidant capacity. The results showed that the extracellular extracts of the endophytic fungi AP-1 and AP-4 showed strong antioxidant activity, and the extracellular extracts of AP-1 and AP-4 had total phenol contents of 110.194 ± 11.800 μg and 101.576 ± 9.073 μg GAE/mL, respectively, And the total flavonoid contents were 87.217 ± 8.854 μg and 77.101 ± 3.510 μg RE/mL, respectively. The extraction of active ingredients from natural medicinal plants is low in efficiency, consumes plant resources and is not friendly to the ecology, while microbial fermentation has many advantages, such as easy control conditions and a short cycle time (Silva et al., 2020). The use of endophytic fungi to develop medicinal plant chemical constituents with high economic value has become a research hotspot in agriculture, medicine, industry and other fields (Ding et al., 2018; Deng et al., 2022; Zheng et al., 2022). The diversity of endophytic fungi is considered to be an important factor affecting plant productivity and health, and the diversity of the endophytic microbial community is related to plant types and organs (Wu et al., 2022). As a kind of microbial resource with broad application prospects, the diversity of plant endophytic fungi is worth exploring (Fan M. et al., 2020; Fan et al., 2022).

Alisma orientale (Sam.) Juzep. (AOJ) is a perennial herb of Alismataceae. The dried tuber of AOJ has been widely used in traditional Chinese medicine clinical compounds and Chinese patent medicine (Kim et al., 2016; Zhao et al., 2018; Feng et al., 2021). This plant has many pharmacological activities, such as diuresis and lowering blood pressure and blood lipids (Zhang L. et al., 2017; Xu et al., 2019). AOJ is rich in bioactive ingredients, such as polysaccharides, triterpenes, flavonoids, and alkaloids, which have been proven to have anti-inflammatory, antitumor, antioxidant and other activities (Zhang L. et al., 2017; Xu et al., 2019; Feng et al., 2021). AOJ is widely distributed, mainly in Sichuan, Fujian, Jiangxi, Guangxi, etc. In addition, AOJ has an annual production of approximately 8000 tons, which represents over 90% of the national total (Xin et al., 2017; Liu et al., 2020). Overall, AOJ has high economic and medicinal value. At present, research on AOJ focuses on its water extract, alcohol extract and terpenoid compounds, and research on its diuresis, anti-calculi and hypolipemia is more adequate (Liu et al., 2020). It has been reported that AOJ contains flavonoids and phenolic acids (Huang et al., 2017; Zhang L. et al., 2017). Phenolic substances and flavonoids have been proven to have strong antioxidant and antibacterial effects in several studies. However, there are few reports on AOJ phenols and flavonoids. In addition, studies on the antioxidant and antibacterial activity of AOJ are still insufficient. Moreover, as a widely used Chinese medicine, there are few reports on AOJ endophytic fungi.

Therefore, in this study, high-throughput sequencing technology and traditional culture methods were used to study the diversity of AOJ root and stem endophytic fungi. Phenols and flavonoids were used as screening criteria to obtain AOJ endophytic fungi with antioxidant and antibacterial activities. The chemical composition and antioxidant and antibacterial activities of extracts from the fermentation broth of endophytic fungi producing phenols and flavonoids were studied. This study is helpful to supplement the insufficient research on AOJ phenols and flavonoids, contribute to the preliminary description of the community diversity of AOJ endophytic fungi, contribute to the development and utilization of AOJ endophytic fungi resources,

FIGURE 1
Two kinds of *Alisma orientale* (Sam.) Juzep.

and provide a theoretical basis for the development of a new way to produce natural antioxidants and antibacterial drugs.

2. Materials and methods

2.1. Experimental materials

As shown in **Figure 1**, the stems of AOJ grow into two shapes: round and triangular. The roots and stems of AOJ that grew into triangles were denoted as SG and SJ, respectively. The roots and stems that grew into rounded AOJ were denoted as YG and YJ, respectively. Fresh whole AOJ plants were collected from a farm at Sichuan Agricultural University (Ya' an City, Sichuan Province, China). All samples were sent to the laboratory for testing immediately after collection.

2.2. High-throughput sequencing

After the samples were washed, the tissues were disinfected on the surface, frozen with liquid nitrogen, and transported to Beijing Novogene Technology Co., Ltd. on dry ice for high-throughput sequencing analysis in the ITS1-1F region (internal transcribed spacer-1-1F). Three samples were taken from each of the two kinds of AOJ roots and stems, for a total of 12 samples: Z1, three repeated round AOJ roots; Z2, three repeated round AOJ stems; Z3, three repeated triangle AOJ roots; and Z4, three repeated triangle AOJ stems.

2.3. Isolation, identification, and phylogenetic analysis of endophytic fungi

Tissue surface disinfection was improved based on the experimental methods of Rehman et al. (2022) and Sohrabi et al. (2023). The stems and roots of AOJ were rinsed with clean water for 4 h, blotted with filter paper, and transferred to a clean workbench. The AOJ tissue was washed in sterile water for 30 s, soaked in 75% ethanol for 3 min, washed in sterile water for 30 s, soaked in 2% NaClO (root for 3 min, stem for 5 min), washed in sterile water for 30 s, washed in 75% ethanol again for 30 s, washed in sterile water for 30 s, and then drained with sterile filter paper. The stems were peeled and cut into 0.5 cm^3 chunks. The skin of the root was gently scraped off with a blade and cut into small 1 cm pieces. The cut tissue pieces were placed on potato dextrose agar (PDA) medium containing 50 μg/L ampicillin sodium and kanamycin sulfate. PDA plates were cultured in an incubator at 28°C for 7–10 days. The isolated strains were stored in the Laboratory of Molecular Biology and Biochemistry, College of Life Science, Sichuan Agricultural University. The isolated endophytic fungi were sequenced by morphology and DNA sequencing, the morphology of endophytic fungi on solid medium was observed, and the morphological characteristics of the mycelia of endophytic fungi were observed by a CX23 microscope (Olympus, Tokyo, Japan). The genomic DNA of endophytic fungi was obtained by the CTAB method, and the ITS region (internal transcribed spacer region) was amplified by primers ITS1 (TCCGTAGGTGAACCTGCGG) and ITS4 (TCCTCCGCTTATTGATATGC). The amplification conditions were the same as those of Tang et al. (2021), and the PCR products were sent to Tsingke Biotechnology Co., Ltd. for sequencing. The sequencing results were compared by BLASTN, and MEGA6 software was used to construct phylogenetic trees by the neighbor joining method.

2.4. Screening of endophytic fungi producing phenols and flavonoids

Mycelia of each purified fungus were selected and placed in a 250 mL triangular bottle containing 100 mL potato dextrose broth (PDB) medium and cultured at 28°C and 120 rpm for 7 days. Whatman No. 1 filter paper was used to separate the mixture by vacuum filtration to obtain filtrate (Rehman et al., 2022). The obtained filtrate was used as a test sample, and a color reaction was used for preliminary screening of the endophytic fungi producing flavonoids and phenols. The filtrate reacted with 0.1% $FeCl_3$:0.1% $K_3[Fe(CN)_6]$ = 1:1 solution reaction (blue solution indicates it contains phenols), 1% $FeCl_3$ solution reaction (wine-red solution indicates it contains phenols) and 1 mol/L NaOH solution reaction (yellow, orange, or red solution indicates it contains flavonols).

2.5. Preparation of extracts of fermentation broth of endophytic fungi

Endophytic fungi producing phenols or flavonoids were expanded for fermentation using the culture method mentioned in Section "2.4. Screening of endophytic fungi producing phenols and flavonoids." The experimental method was modified on the basis of Tang et al. (2020) and Bora and Devi (2023), four layers of gauze were used to filter the fermentation solution, collect the filtrate, extract it three times with an equal volume of ethyl acetate, collect the ethyl acetate part, and concentrate it to 1/4 of the original volume at 45°C by rotating evaporation. After freezing-drying, the fermentation solution extract was obtained, and 200 mg/mL of the fermentation solution extract was prepared by adding dimethyl sulfolone. The samples were stored at 4°C for later use.

2.6. Determination of the total phenol content (TPC) and total flavonoid content (TFC)

The Folin–Ciocalteu (FC) method used to determine the TPC of endophytic fungal extracts was modified from the method of Minussi et al. (2003), Li et al. (2022), and Wairata et al. (2022). A standard solution of gallic acid (0.0–0.10 mg/mL) was prepared accurately with gallic acid as the standard substance. Deionized water (200 μL) was added to the EP tube in addition to 200 μL gallic acid solution and 100 μL Folinal phenol reagent. After mixing, the solution was allowed to stand for 4 min, and 200 μL of 5% Na_2CO_3 solution was added. The absorbance of the samples was measured at 760 nm after the samples were diluted to 1 mL with deionized water and reacted at room temperature for 30 min. The linear regression equation, $y = 14.303x + 0.0905$ ($R^2 = 0.9965$), was obtained by drawing the standard curve with the mass concentration (x) and absorbance (y) of the gallic acid solution. The fungal extract solution was diluted with deionized water (0.1 mg/mL), and the absorbance of the sample at 760 nm was obtained according to the steps of the standard curve. The linear regression equation was used to calculate the mass concentration of TPC in the sample solution (mg/mL). TPC is expressed in milligrams of gallic acid per gram of crude extract, i.e., mg GAE/g.

The standard curve of flavonoids was drawn by the aluminum nitrate colorimetric method (Chen et al., 2020; Zhang et al., 2023). The standard solution of rutin was 0.1 mg/mL after accurately weighing 5 mg rutin and using 70% ethanol solution to a constant volume of 50 mL. Precision suction standard solutions (0.0, 0.1, 0.2, 0.3, 0.4, and 0.5 mL) were placed in six 1.5 mL EP tubes and supplemented with 30% ethanol to 0.5 mL. Then, 30 μL 5% sodium nitrite solution was added, mixed well and allowed to stand for 6 min. Then, 30 μL 10% aluminum nitrate solution was added, mixed and allowed to stand for 6 min. Then, 0.4 mL of 4% sodium hydroxide solution was added, filled to 1 mL with deionized water, and reacted at room temperature for 15 min, and finally the absorbance was measured at 510 nm. The linear regression equation, $y = 2.3019x + 0.0025$ ($R^2 = 0.9988$) was obtained by drawing a standard curve based on the mass concentration (x) and absorbance (y) of the rutin solution. The fungal extract solution (0.1 mg/mL) was diluted with deionized water, and the absorbance of the samples at 510 nm was obtained according to the steps of the standard curve. The linear regression equation was used to calculate the mass concentration of total flavonoids in the sample solution (mg/mL). TFC was expressed in milligrams of rutin per gram of crude extract, i.e., mg RE/g.

2.7. Antioxidant activity

The fungal extracts were prepared into a series of sample solutions with a concentration gradient (0.01, 0.05, 01, 0.2, 0.3, 0.4, 0.5, 0.7, 0.9 mg/mL). The antioxidant activity of the crude extract *in vitro* was determined by four experiments, including superoxide anion, DPPH, ABTS and hydroxyl radical scavenging activity (Hou et al., 2020; Wu et al., 2020; Zhang et al., 2020; Nataraj et al., 2022). Ascorbic acid (Vc) was used as a positive control, and the experiment was repeated three times in each group.

2.7.1. 2,2-Diphenyl-1-picrylhydrazyl radical scavenging activity assay

The sample solution of 100 μL was mixed with 100 μL DPPH ethanol solution (0.2 mM), and absorbance was measured at 517 nm after reaction for 30 min at room temperature and away from light.

$$\text{Scavenging rate}(\%) = [1-(A_1-A_2)/A_0] \times 100\%$$

where A_0 is the absorbance of 100 μL DPPH plus 100 μL ethanol, A_1 is the absorbance of 100 μL DPPH plus 100 μL sample solution, and A_2 is the absorbance of 100 μL of sample solution plus 100 μ L of ethanol.

2.7.2. Hydroxyl radical scavenging activity assay

The 100 μL sample solution was added to 20 μL salicylic acid solution (6 mM), 20 μL ferrous sulfate solution (6 mM), and 20 μL hydrogen peroxide solution (6 mM). The mixture was thoroughly mixed and reacted at 37°C for 30 min. Absorbance was measured at 510 nm.

$$\text{Scavenging rate}\ (\%) = [1-(A_1-A_2)/A_0] \times 100\%$$

where A_0 is the absorbance of 100 μL deionized water plus salicylic acid solution (6 mM), ferrous sulfate solution (6 mM), and hydrogen peroxide (6 mM) each at 20 μL; A_1 is the absorbance of salicylic acid solution (6 mM), ferrous sulfate solution (6 mM), and hydrogen peroxide (6 mM) each at 20 μL plus 100 μL sample solution; and A_2 is the absorbance of 100 μL sample solution plus salicylic acid solution (6 mM), ferrous sulfate solution (6 mM), and deionized water (instead of hydrogen peroxide) each at 20 μ L.

2.7.3. Superoxide radical scavenging assay

A total of 150 μL of Tris–HCl (0.05 mol/ml, pH 8.2) and 50 μL of sample solution were added to a 96-well plate, mixed and incubated at 25°C for 30 min. Then, 20 μL of freshly prepared 25 mmol/mL ortho-pyrogallol was added, incubated at 25°C for 30 min, and 25 μL of HCl (10 mol/mL) was quickly added to terminate the reaction, and the absorbance was determined at 325 nm.

$$\text{Scavenging rate}\ (\%) = [1-(A_1-A_2)/A_0] \times 100\%$$

where A_0 is the absorbance of 50 μL deionized water after mixing the sample solution with the reaction solution, A_1 is the absorbance of the sample after reaction with the reaction solution, and A_2 is the absorbance of 20 μL deionized water mixed with sample solution instead of o-nitrophenol.

2.7.4. ABTS radical scavenging activity assay

Accurately weighed ABTS powder (78 mg) and potassium persulfate (13.2 mg) were mixed into 20 mL ultraclean water, preserved at 4°C, stored in dark for 16 h, and used as ABTS reserve solution after stability. Before the experiment, the ABTS reserve solution was diluted with anhydrous ethanol to an absorbance of 0.7 ± 0.02, which was used as the ABTS working solution. The absorbance was measured at 734 nm after 20 μL of sample solution was mixed with 180 μL of ABTS working solution and reacted at room temperature for 6 min away from light.

$$\text{Scavenging rate}(\%) = [1-(A_1-A_2)/A_0] \times 100\%$$

where A_0 is the absorbance of 180 μL ABTS plus 20 μL deionized water, A_1 is the absorbance of 180 μL ABTS plus 20 μL sample solution, and A_2 is the absorbance of 20 μL of sample liquid plus 180 μL of deionized water.

2.8. Minimal inhibitory concentration (MIC) and minimum bactericidal concentration (MBC)

The MIC and MBC of crude extracts were evaluated by the 96-well plate method (Wiegand et al., 2008; Li et al., 2016; Zhang Y. et al., 2017; Dydak et al., 2021). Luria-Bertani (LB) liquid medium (100 μL) was added to each well to dilute the crude extract solution, and then 100 μL of 10 mg/mL crude extract solution filtered through a 0.22 μm microporous membrane was added to the first well. The 100 μL mixture from the previous well was transferred to the next well, and the process was repeated to the ninth well. The 100 μL mixture from the ninth (last) well was discarded. The crude extract was diluted to 9 concentrations of 5, 2.5, 1.25, 0.625, 0.312, 0.156, 0.0781, 0.03905, and 0.15475 mg/mL. Then, 20 μL of bacterial solution (OD_{620} = 0.08–0.1, equivalent to 1×10^8 CFU/mL) was successively added to the 96-well plate. LB liquid medium with bacterial suspension and 5% DMSO (LB liquid medium preparation) with bacterial suspension were used as blank controls, and LB liquid medium without bacterial suspension was the negative control. Positive controls were 100 μg/mL streptomycin sulfate prepared with LB liquid medium and 100 μg/mL ampicillin sodium prepared with LB liquid medium. After incubation at 37°C for 24 h, the MIC value was determined by the concentration between clarification and turbidity. The 20 μL clarifying solution was transferred to an LB culture plate and cultured in a 37°C incubator for 24 h. The minimum concentration of crude extract in the medium without bacterial growth was the MBC. All experiments were repeated three times for each type of bacteria.

2.9. Detection of bioactive compounds by liquid chromatography-Mass spectrometry (LC-MS) analysis

The LC-MS (Waters, UPLC; Thermo, Q Exactive) analysis platform was used. Compounds were isolated on an ACQUITY UPLC HSS T3 column (2.1 mm 100 mm 1.8 μm). The mobile phase was 0.05% ammonium water (A)/acetonitrile (B) at a flow rate of 0.3 mL min^{-1}. The injection volume was 5 μL, and the automatic injector temperature was 4°C. The gradient elution procedure is shown in **Supplementary Table 1**. For mass spectrometry (MS) detection, ionization was performed in ESI + mode (heater temp, 300°C; sheath gas flow rate, 45 arb; Aux gas flow rate, 15 arb; sweep gas flow rate, 1 arb; spray voltage, 3.0 KV; capillary temperature, 350°C; and S-Lens RF level, 30%.) and ESI- mode (heater temp, 300°C; sheath gas flow rate, 45 arb; aux gas flow rate, 15 arb; sweep gas flow rate, 1 arb; spray voltage, 3.2 KV; capillary temperature, 350°C; and S-Lens RF level, 60%). Full scans (MS1) were performed from 70∼1050 m/z with a resolution of 70,000, and data-dependent two-stage mass spectrometry (DDMS2, TOPN = 10) was performed with a resolution of 17,500. The obtained mass spectra were analyzed with Compound Discoverer 2.0 (Thermo Scientific), and the integrated mzcloud, metlin, and hmdb databases were used to detect secondary metabolites in an untargeted method. The scanning modes were full scan (m/z 70∼1050) and data-dependent secondary mass spectrometry (dd-MS2, TopN = 10). The resolution was 70,000 (primary mass spectrometry) and 17,500 (secondary mass spectrometry). The collision mode was high-energy collision dissociation (HCD). The obtained mass spectra were analyzed using Compound Discoverer (Thermo Scientific), and the secondary metabolites were detected by non-targeted methods using the integrated mzcloud, metlin, and hmdb databases.

2.10. Data analysis

All experimental data are expressed as the mean ± SD from three independent observations. The data were analyzed by one-way analysis of variance (ANOVA) followed by Duncan's multiple range test using SPSS 27.0 software. $P < 0.05$ was used to define statistically significant differences between the control group and experimental group.

3. Results

3.1. High-throughput sequencing statistics of endophytic fungal communities in AOJ

High-throughput sequencing technology was used to study the diversity of fungi in roots and stems of AOJ with different shapes. A total of 1,221,926 raw PE reads were obtained from 12 samples by high-throughput sequencing. After quality control, the effective tags of fungal sequences in each sample ranged from 51,680 to 112,590, and a total of 3,426 amplicon sequence variants (ASVs) were identified, belonging to 9 phyla, 27 classes, 64 orders, 152 families, and 277 genera. The ASV rarefaction curves are shown in **Figure 2A**. The curves of the four groups of samples all tended to be flat, indicating that the sequencing data amount was reasonable and could represent the fungal diversity of the samples. As shown in **Figure 2B**, Z1 shared 355 ASVs with Z3, and Z2 shared 656 ASVs with Z4. The unique ASVs among all samples collected in the Z1, Z2, Z3, and Z4 groups were 375, 533, 687, and 841, respectively. These results indicated that there were significant differences in endophytic fungal communities between Z1 and Z3 and between Z2 and Z4, which might be the cause of the round and triangular shape of the stems of AOJ (Harrison et al., 2021).

3.2. Alpha diversity

There were differences in the alpha diversity index of fungal communities in the 12 samples. It can be seen from **Table 1** that the coverage index of each sample was close to 1, indicating the integrity of the tested samples; that is, the sequencing result could

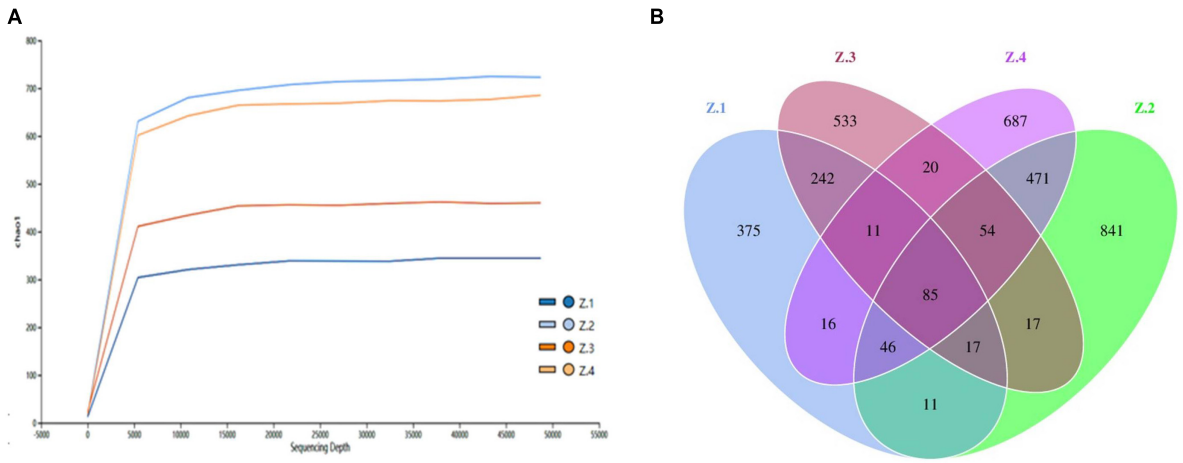

FIGURE 2
High throughput sequencing. **(A)** ASV rarefaction curves. **(B)** Venn diagram showing the number of shared and specific ASVs for each group.

TABLE 1 Alpha diversity index statistics.

Sample name	Goods coverage	Chao1	Shannon	Simpson
Z1	1.000 ± 0	368.352 ± 92.289	4.589 ± 0.661	0.860 ± 0.021
Z2	0.999 ± 0	744.586 ± 39.785	5.214 ± 0.260	0.833 ± 0.049
Z3	1.000 ± 0	489.588 ± 85.382	5.618 ± 0.180	0.935 ± 0.015
Z4	0.999 ± 0	661.080 ± 123.761	5.154 ± 0.409	0.812 ± 0.059

Values in the table are mean ± standard deviation.

reflect the real situation of the fungal community composition in the tested samples. The Chao1 index of the Z2 group was the largest, indicating that the sample community contained the largest number of low abundance species. Both the Shannon index and Simpson index of Group Z3 were the highest, indicating that the community diversity and species evenness of Group Z3 were the highest. The lowest Chao1 and Shannon indices were found in the Z1 group, indicating that this group had the fewest species with low abundance and the lowest community diversity. The Simpson index of the Z4 group was the smallest, indicating that the species uniformity of this group was the lowest.

3.3. Beta diversity

To explore beta diversity, principal coordinates analysis (PCoA) (Figure 3A) and non-metric multidimensional scaling (NMDS) (Figure 3B) were performed for AOJ samples. The sum of PCoA1 and PCoA2 was 77.19%, with Stress <0.2 in NMDS, indicating that the endophytic fungi population structure of sequenced samples had a high diversity, and NMDS could accurately reflect the degree of difference between samples. Groups Z1 and Z2 and Groups Z3 and Z4 were far apart from each other, indicating that there were significant differences in the endophytic fungal communities of the roots and stems of AOJ with two shapes. Figures 3C, D show the relative abundance of endophytes at the phylum and genus levels, respectively. The dominant phylum in the roots and stems of both AOJ types was Ascomycota (mean relative abundance was 35.46%), followed by Basidiomycota (mean relative abundance was 8.04%). The dominant genus in Z1 was *Plectosphaerella* (mean relative abundance was 9.20%). *Fusarium* was the dominant genus in Z4 (mean relative abundance was 1.17%) and a secondary dominant genus in Z1 (mean relative abundance was 4.32%) and Z3 (mean relative abundance was 3.67%). The dominant genus in Z2 was *Meyerozyma* (mean relative abundance was 6.10%). *Chaetomium* was the dominant genus in Z3 (mean relative abundance was 4.01%).

3.4. Isolation and identification of endophytic fungi

A total of 31 endophytic fungi were isolated from the roots and stems of AOJ with different shapes, including 5 and 11 strains from the roots and stems of round AOJ and 5 and 10 strains from the roots and stems of triangular AOJ. All strains were initially identified by colony morphology and microscopy (Supplementary Figures 1, 2), and molecular identification was performed by ITS-rDNA sequence analysis. The closest identified matches are listed in Table 2. The nucleotide sequences of 31 endophytic fungi were more than 98% similar to the best matched nucleotide sequences in the nucleotide database.

The most common fungi were *Bjerkandera* sp. and *Alternaria* sp., with 5 strains each, and all the endophytic fungi were divided into 17 genera. The phylogenetic tree of endophytic fungi identified from AOJ is shown in Figure 4.

3.5. Screening of polyphenol- and flavonoid-producing endophytic fungi

Chromogenic reactions were performed on 31 endophytic fungi isolated from AOJ, and the chromogenic reaction results are shown in Supplementary Figure 3. The results showed that SJ-11, YG-2, YJ-4, YJ-10, YJ-9, and SJ-2 were positive in the color

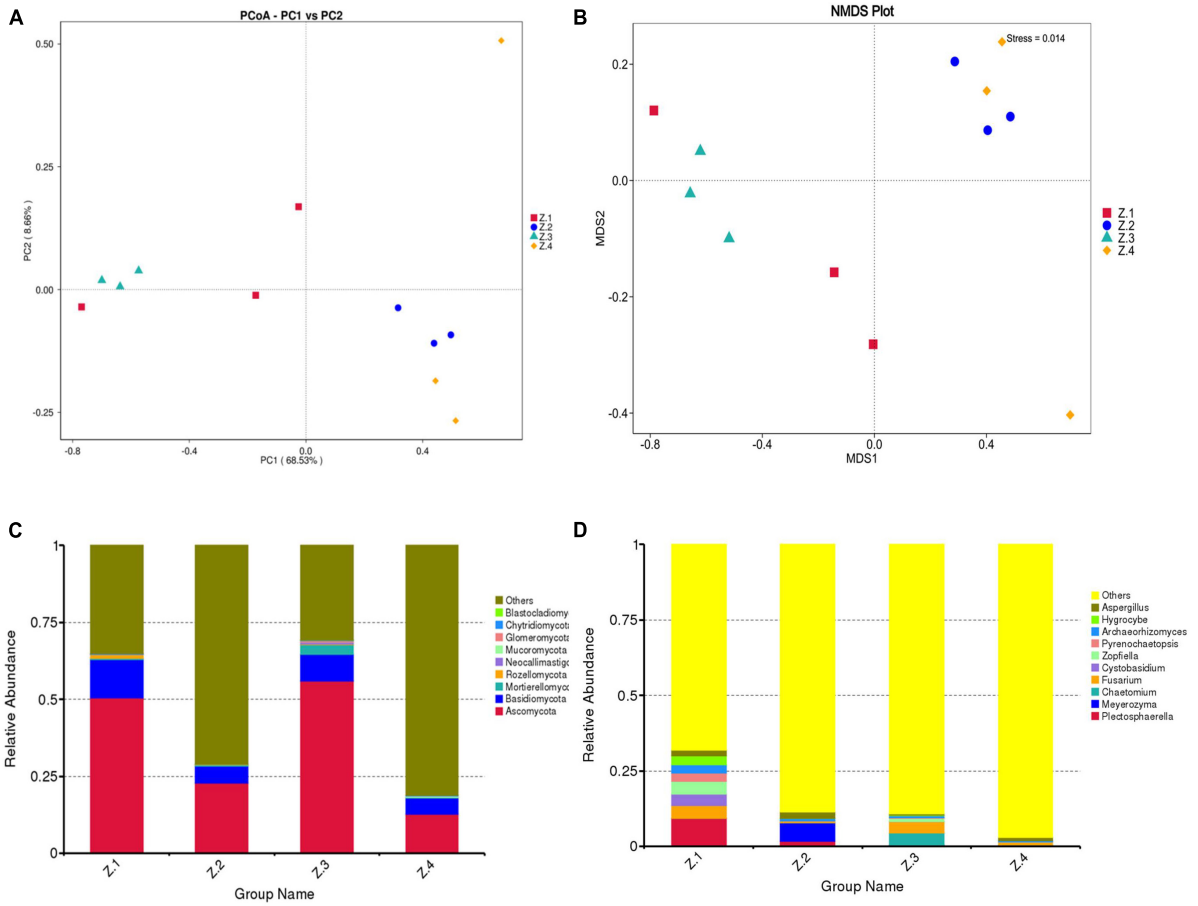

FIGURE 3
Composition of endophytic fungi in root and stem of AOJ. **(A)** Multiple sample principal coordinate analysis (PCoA) of the ASV level. **(B)** Multiple sample Non-metric multidimensional scaling (NMDS) of the ASV level. **(C)** Relative abundance of phyla in each sample. **(D)** Relative abundance of genus in each sample.

reaction of flavonoids and phenols, indicating that these 6 strains could produce flavonoids and phenolic compounds.

3.6. Determination of TPC and TFC

The Folin–Ciocalteu assay was used to measure the TPC, and the aluminum nitrate colorimetric method was used to measure the TFC. The experimental results are shown in Table 3 and Figure 5. The TPC of the fungal YG-2 extract was the highest, 348.67 ± 5.90 mg GAE/g. In addition, the extracts of fungi SJ-11, YJ-4, and YJ-9 showed higher TPC. The TPC and TFC in the extracts of SJ-2 were the lowest, 42.75 ± 0.48 mg GAE/g and 5.12 ± 1.26 mg RE/g, respectively. The JY-4 extract had the highest TFC (331.66 ± 6.93 mg RE/g).

3.7. Antioxidant activity

DPPH, ABTS, hydroxyl (·OH) radical and superoxide anion ($\cdot O_2^-$) scavenging activities were used to analyze the *in vitro* antioxidant activities of endophytic fungi crude extracts. The experimental results are shown in Table 4 and Figure 6. As shown in Figure 6, all samples showed concentration-dependent scavenging activity against all free radicals within the experimental concentration range. In DPPH, ABTS and hydroxyl radical scavenging tests, the scavenging ability of YG-2, SJ-11, YJ-4, YJ-9, YJ-10, and SJ-2 decreased gradually. Except for SJ-2, the scavenging activities of other strains on DPPH and ABTS free radicals were stronger than those on ·OH and $\cdot O_2^-$. The crude extract of YG-2 showed the strongest free radical scavenging activity, with an $IC_{50\ DPPH}$ of 0.009 ± 0.000 mg/mL, $IC_{50\ ABTS}$ of 0.023 ± 0.002 mg/mL and $IC_{50\ \cdot OH}$ of 0.081 ± 0.006 mg/mL. Significantly higher than that of other crude extracts (Table 4, $P < 0.05$). At the maximum concentration of 0.5 mg/mL, the scavenging activity of YG-2 on DPPH and ABTS was the highest (96.39 ± 0.20% and 99.82 ± 0.07%, respectively), which was close to that of the control group (96.62 ± 0.28% and 99.85 ± 0.06%, respectively). The scavenging activities of YG-2 and SJ-11 were 83.44 ± 1.05% and 85.24 ± 0.24% at 0.5 mg/mL, respectively, compared with other crude extracts. The crude extract of YJ-4 had the strongest superoxide anion scavenging activity, and its $IC_{50\cdot O2-}$ was 0.176 ± 0.01 mg/mL. The superoxide anion scavenging rate was 82.37 ± 0.99% at 0.5 mg/mL. In conclusion, the YG-2 crude extract had the strongest free radical scavenging ability, while SJ-2 had the weakest free radical scavenging ability.

3.8. Antibacterial activity

The antibacterial activity of the crude extract was evaluated by measuring the MIC and MBC values, and the results are shown in Table 5 and Supplementary Figure 4. The crude extracts from the fermentation broth of 6 strains of fungi had antibacterial effects on *Escherichia coli*, *Bacillus subtilis*, *Pseudomonas aeruginosa*, and *Staphylococcus aureus*. Among them, YG-2 had the best inhibitory effect against *S. aureus*, *B. subtilis*, *P. aeruginosa*, and *E. coli*, with MIC values of 0.625, 0.625, 1.25, and 1.25 mg/mL, respectively, indicating that YG-2 had a better inhibitory effect against gram-positive bacteria than gram-negative bacteria. However, from the point of view of minimum bactericidal concentration, SJ-11 has the best bactericidal effect, and its MBC value against *E. coli* is 2.5 mg/mL. In general, the antibacterial effect was YG-2 > SJ-11 > YJ-4 > YJ-10 > YJ-9, and SJ-2.

3.9. Liquid chromatography-Mass spectrometry

The crude extracts of fungi YG-2, SJ-11, YJ-4, and YJ-9 had high contents of total phenols and total flavonoids and had good antioxidant and antibacterial activities. LC-MS was further used to analyze the chemical constituents. The results are shown in Table 6, chromatograms of the four samples are shown in Supplementary Figure 5, and mass spectra of the main components of the four samples are shown in Supplementary Figure 6. The identified phenolic substances include non-flavonoid phenols (altenuene, phloroglucinol), flavonoids (glycitein, daidzein), phenolic acids (ferulic acid, caffeic acid), and flavonolignan (silibinin). A total of 55 compounds were identified in the YG-2 crude extract, of which caffeic acid was the main compound with a concentration of 10.12 μmol/g. The main compounds identified from the crude extracts of SJ-11 and YJ-9 were Skatole with concentrations of 5.53 μmol/g and 2.62 μmol/g, and the total compounds were 52 and 50, respectively. A total of 54 compounds were identified in the crude extract of YJ-4, of which adenine was the main compound with a concentration of 7.11 μmol/g. The results showed that the extracts of the four strains of fungi were rich in secondary metabolites with biological activity, and phenols and flavonoids were detected in all samples.

4. Discussion

With the improvement of people's living standards, the need for natural antioxidants and antibacterial drugs has become very important. The use of endophytic fungi to produce natural antioxidants and antibacterial drugs has been widely studied. It is of great significance to carry out scientific research on AOJ endophytic fungi to increase the yield potential of Chinese medicinal materials and realize the healthy cultivation of AOJ. In this study, the diversity and community structure of AOJ endophytic fungi were preliminarily described, and endophytic fungi with high phenolic production were screened. The results showed that the endophytic fungi of AOJ had strong antioxidant activity and antibacterial effects on four kinds of pathogenic bacteria, suggesting that AOJ endophytic fungi have potential as sources of antioxidants and antibacterial drugs.

TABLE 2 The homologous strains of endophyte fungi from *Alisma orientale* (Sam.) Juzep.

NO	Genus	Most closely related strain	Ident (%)	Accession.
SG-2	*Trametes* sp.	*Trametes versicolor*	99.33%	MW742530.1
SG-3	*Plectosphaerella* sp.	*Plectosphaerella oligotrophica*	99.22%	MT447499.1
SG-4	*Chaetomium* sp.	*Chaetomium globosum*	99.63%	MG885813.1
SG-5	*Bjerkandera* sp.	*Bjerkandera adusta*	99.66%	MK809422.1
SG-6	*Pseudeurotium* sp.	*Pseudeurotium* sp.	99.05%	MZ380127.1
SJ-1	*Trametes* sp.	*Trametes versicolor*	99.65%	ON319095.1
SJ-2	*Talaromyces* sp.	*Talaromyces purpureogenus.*	99.28%	ON248285.1
SJ-3	*Penicillium* sp.	*Penicillium digitatum*	98.74%	KY558584.1
SJ-4	*Botrytis* sp.	*Botrytis cinerea*	99.8%	KF533037.1
SJ-5	*Gibberella* sp.	*[Gibberella] fujikuroi var. moniliformis*	99.22%	MW405885.1
SJ-6	*Mucor* sp.	*Mucor hiemalis*	98.21%	LC515165.1
SJ-7	*Bjerkandera* sp.	*Bjerkandera fumosa*	98.5%	KX958033.1
SJ-9	*Bjerkandera* sp.	*Bjerkandera* sp.	99.16%	MT085748.1
SJ-10	*Alternaria* sp.	*Alternaria angustiovoidea*	99.45%	OM236751.1
SJ-11	*Alternaria* sp.	*Alternaria compacta*	99.63%	OM237237.1
YG-1	*Clonostachys* sp.	*Clonostachys rosea*	99.63%	MW113577.1
YG-2	*Chaetomium* sp.	*Chaetomium globosum*	99.45%	MT510030.1
YG-4	*Pleosporales* sp.	*uncultured Pleosporales*	98.61%	OM106656.1
YG-5	*Talaromyces* sp.	*Talaromyces marneffei*	98.77%	MF683085.1
YG-6	*Paraphaeosphaeria* sp.	*Paraphaeosphaeria* sp.	99.46%	MT771337.1
YJ-1	*Cladosporium* sp.	*Cladosporium cladosporioides*	99.42%	ON790391.1
YJ-3	*Bjerkandera* sp.	*Bjerkandera fumosa*	98.5%	KX958033.1
YJ-4	*Alternaria* sp.	*Alternaria* sp.	99.26%	MK037447.1
YJ-5	*Trametes* sp.	*Trametes versicolor*	99.48%	ON319098.1
YJ-6	*Botrytis* sp.	*Botrytis cinerea*	99.61%	ON566789.1
YJ-7	*Stagonosporopsis* sp.	*Stagonosporopsis cucurbitacearum*	98.82%	EF107642.1
YJ-8	*Bjerkandera* sp.	*Bjerkandera adusta*	99.66%	OK184566.1
YJ-9	*Alternaria* sp.	*Alternaria* sp.	99.44%	KX064970.1
YJ-10	*Alternaria* sp.	*Alternaria* sp.	99.62%	ON435682.1
YJ-12	*Plectosphaerella* sp.	*Plectosphaerella cucumerina*	99.41%	OM648207.1
YJ-13	*Septoriella* sp.	*Septoriella phragmitis*	99.46%	KT826679.1

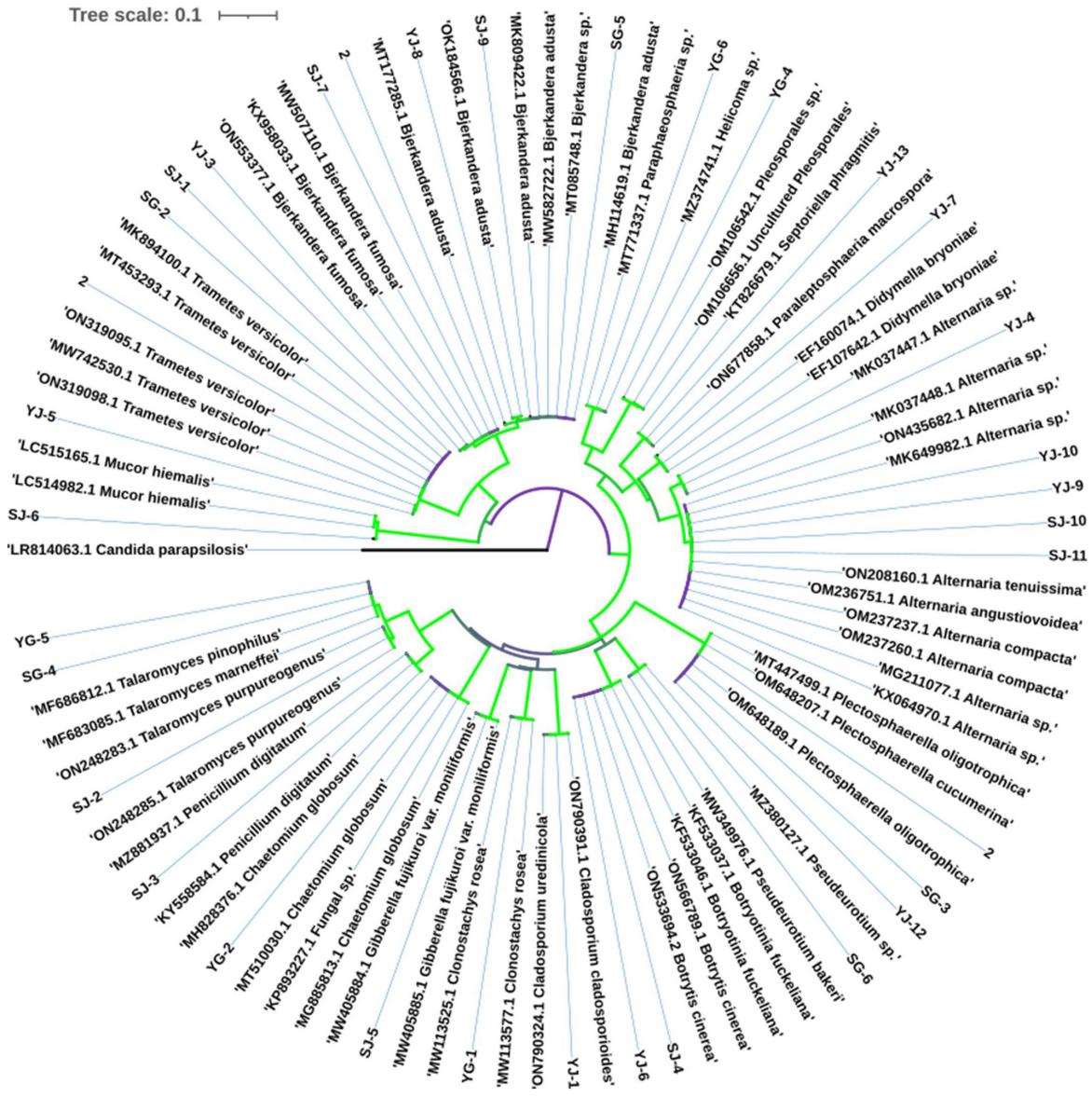

FIGURE 4
Phylogenetic tree of endophytic fungi in *Alisma orientale* (Sam.) Juzep.

TABLE 3 Total phenol and total flavonoid content.

Crude extract	TPC(mg GAE/g)	TFC(mg RE/g)
YG-2	348.67 ± 5.90^{e}	31.33 ± 2.46^{C}
SJ-11	224.21 ± 0.79^{d}	58.84 ± 1.99^{D}
YJ-4	162.30 ± 1.32^{c}	331.66 ± 6.93^{E}
YJ-9	134.77 ± 2.30^{b}	26.02 ± 2.08^{C}
YJ-10	44.57 ± 0.90^{a}	17.23 ± 1.51^{B}
SJ-2	42.75 ± 0.48^{a}	5.12 ± 1.26^{A}

$^{a-e}$ and $^{A-E}$ Significant differences between different groups ($p < 0.05$).

Endophytic fungi have mutualism with host plants, which is an important factor affecting plant productivity and health. The composition and structure of endophytic fungi are different in different plant tissues, and some endophytic fungi only exist in specific plant tissue parts. The tissue specificity of endophytic fungi is an important factor for the accumulation of bioactive substances in different tissues (Park et al., 2012; Fan S. et al., 2020). The diversity and community composition of endophytic fungi can provide new insights for the study of AOJ and endophytic fungi.

In this study, stems and roots were collected from two kinds of AOJ, and a high-throughput sequencing method overcame the problem that traditional culture could not isolate all endophytic fungi and effectively revealed the diversity and community structure of endophytic fungi in different parts of AOJ with different shapes. The Venn diagram initially revealed the ASV differences of endophytic fungi in different parts of AOJ with the same shape and in the same parts of AOJ with different shapes. There were 803, 1542, 979, and 1390 ASVs in the Z1, Z2, Z3, and Z4 groups, respectively, indicating that the

10.3389/fmicb.2023.1190624

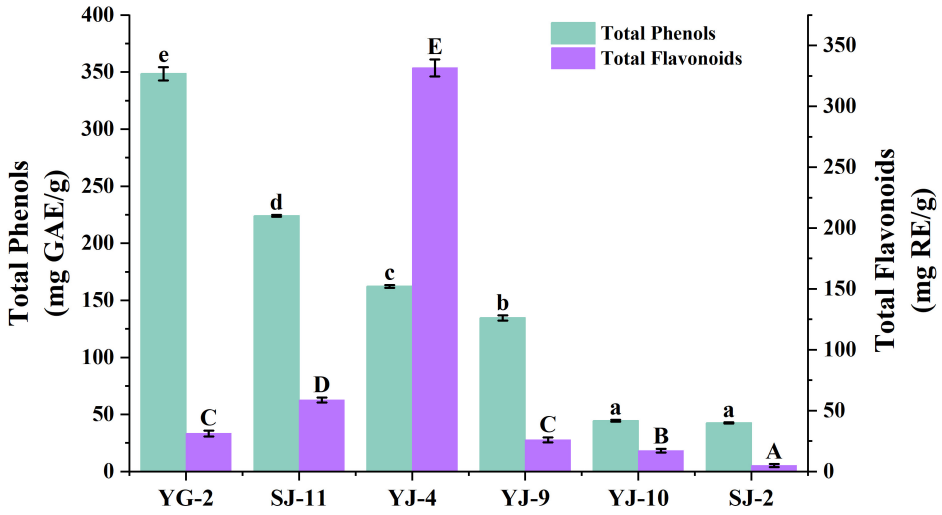

FIGURE 5
Total Phenol and Total Flavonoid Content of YG-2, SJ-11, YJ-4, YJ-9, YJ-10, and SJ-2 extracts. a–e and A–E: significant differences between different groups ($p < 0.05$).

TABLE 4 IC_{50} value from antioxidant activity *in vitro* assays of YG-2, SJ-11, YJ-4, YJ-9, YJ-10, and SJ-2 extracts.

Crude extract	IC_{50}(mg/mL)			
	DPPH	ABTS	Hydroxyl radical	Superoxide anion clearance assay
Vc	0.009 ± 0.001^{a}	0.021 ± 0.001^{a}	0.042 ± 0.003^{a}	0.119 ± 0.007^{a}
YG-2	0.009 ± 0.000^{a}	0.023 ± 0.002^{a}	0.081 ± 0.006^{a}	0.260 ± 0.030^{c}
SJ-11	0.029 ± 0.001^{b}	0.063 ± 0.006^{b}	0.153 ± 0.015^{b}	nd
YJ-4	0.144 ± 0.001^{d}	0.109 ± 0.003^{c}	0.385 ± 0.057^{d}	0.176 ± 0.017^{b}
YJ-9	0.107 ± 0.001^{c}	0.109 ± 0.003^{c}	0.236 ± 0.016^{c}	nd
YJ-10	0.186 ± 0.003^{e}	0.204 ± 0.008^{d}	0.479 ± 0.055^{e}	nd
SJ-2	0.258 ± 0.005^{f}	nd	0.252 ± 0.028^{c}	0.437 ± 0.013^{d}

$^{a-f}$ Significant differences between different groups ($p < 0.05$). nd, not detected (the result higher 0.5 mg/mL).

number of endophytic fungi in AOJ stems was greater than that in roots, which was consistent with the number of AOJ endophytic fungi isolated from traditional culture. Overall, there were significantly fewer ASVs unique to circular AOJs (908) than triangular AOJs (1519). Although the same ASVs existed in the same part of AOJ with different shapes, there were only 355 ASVs identical to Z1 and Z3 and 375 and 687 ASVs unique to Z1 and Z3, respectively. Similarly, Z2 and Z4 have 656 identical ASVs, while Z2 and Z4 have 533 and 841 unique ASVs, respectively.

Alpha diversity analysis showed that there were significant differences in the community diversity and species evenness of endophytic fungi in different groups. In the root tissue, the Shannon index and Simpson index of the circular AOJ were lower than those of the triangular AOJ, indicating that the diversity and species evenness of the endophytic fungal community in the roots of the circular AOJ were lower than those of the triangular AOJ. The results were reversed in stem tissue, and the Shannon index and Simpson index of the circular AOJ were higher than those of the triangular AOJ, indicating that the diversity and species evenness of the endophytic fungal community in the circular AOJ were higher than those in the triangular AOJ. For AOJs of both shapes, the Chao1 index of roots was lower than that of stems, indicating that there were more low-abundance species in roots than in stems in both AOJs.

In addition, the PCoA and NMDS maps in the results of beta diversity analysis indicated that the fungal communities in root and stem tissues of the two AOJs were different and divided into different communities. The results of diversity analysis showed that the dominant genus of phylum was *Ascomycota* in all the samples, and at the genus level, the dominant genus of phylum was inconsistent in all four groups. Through traditional cultivation methods, 31 endophytic fungi were isolated from AOJ, which were divided into 17 genera. *Bjerkandera* sp. and *Alternaria* sp. were the most common endophytic fungi. This result was different from the result of high-throughput sequencing, which was speculated to be because the number of isolated strains was not sufficient. To obtain more representative data on endophytic fungal diversity, multiple isolates should be used to accumulate a sufficiently large number of endophytic fungi. The reason why AOJs determine whether their stems grow round or triangular during growth is unclear. However, studies have shown that dominant endophytic fungi can have huge ecological consequences, and some studies have shown that endophytic fungi can affect the expression of host genes and thus affect plants (Harrison et al., 2021). In addition, the results of Liu et al. (2022) showed that the endophytic fungus *Epichloë bromicola* can affect the growth of host plants and has a significant effect on the plant height of *Hordeum vulgare*. Therefore, it can be hypothesized that the formation of round AOJs and triangular AOJs may be due to the existence of some endophytic fungi that affect the gene expression or growth of AOJs, and these endophytes are different in AOJ plants with two traits, which are reflected in

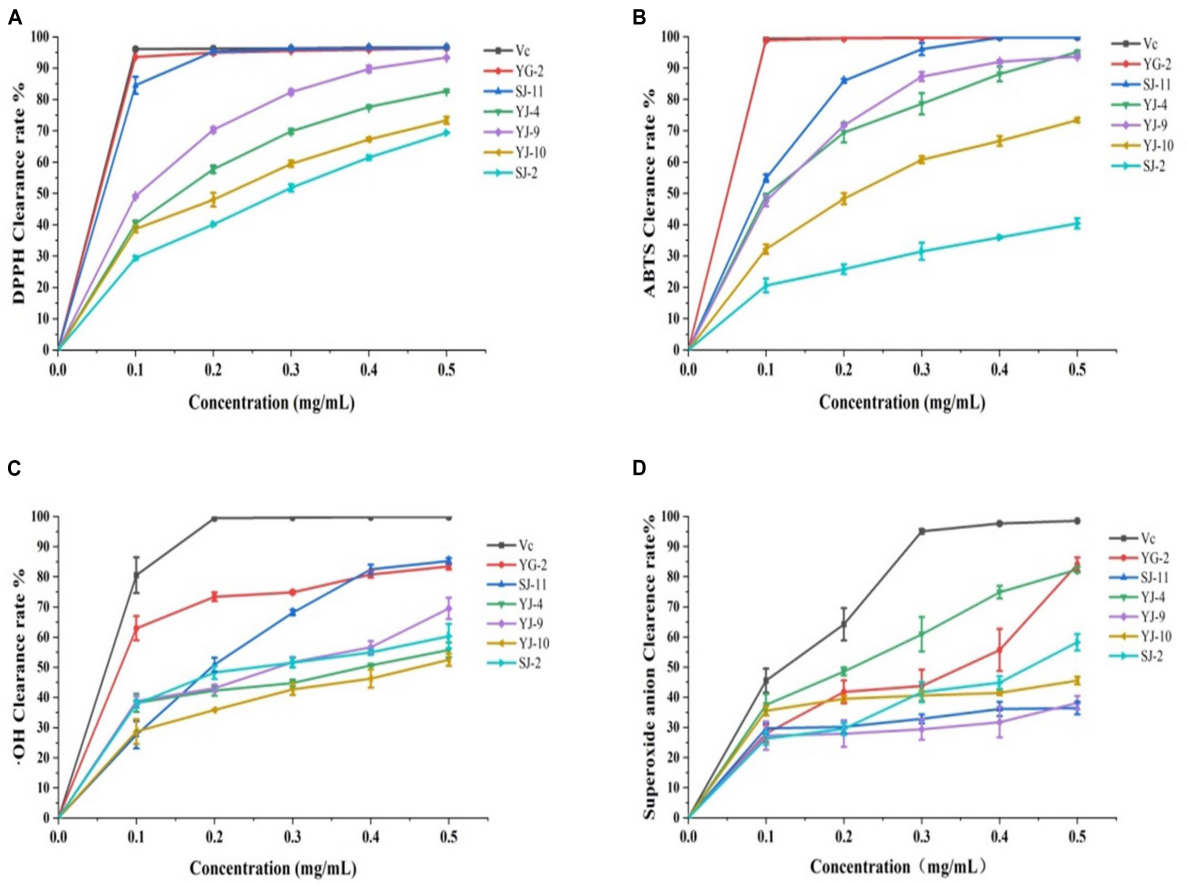

FIGURE 6
Antioxidant activity *in vitro* assays of YG-2, SJ-11, YJ-4, YJ-9, YJ-10, and SJ-2 extracts. **(A)** DPPH clearance assay; **(B)** ABTS clearance assay; **(C)** ·OH clearance assay; **(D)** superoxide anion clearance assay.

TABLE 5 Determination of MIC (mg/mL) and MBC (mg/mL) of YG-2, SJ-11, YJ-4, YJ-9, YJ-10 and SJ-2 extracts.

Crude extract	Gram-positive bacteria				Gram-negative bacteria			
	B. subtilis		*S. aureus*		*P. aeruginosa*		*E. coli*	
	MIC	MBC	MIC	MBC	MIC	MBC	MIC	MBC
YG-2	0.625	5	0.625	5	1.25	5	1.25	5
SJ-11	2.5	5	2.5	5	2.5	5	1.25	2.5
YJ-4	2.5	5	2.5	nd	2.5	nd	1.25	nd
YJ-9	5	nd	5	nd	5	nd	5	nd
YJ-10	2.5	5	2.5	5	2.5	5	2.5	5
SJ-2	5	nd	5	nd	5	nd	5	nd

nd, not detected (the result higher 5 mg/mL).

the significant difference in ASVs and the difference in dominant genera.

The six strains of fungi identified by color reaction belonged to *Talaromyces* sp. (SJ-2), *Alternaria* sp. (SJ-10, SJ-11, YJ-4, YJ-9), and *Chaetomium* sp. (YG-2). *Talaromyces purpureogenus* was isolated from brown algae by Kumari et al. (2018) showed anticancer cell proliferation and antioxidant activity. Kaul et al. (2008) revealed by GC-MS that an *Alternaria* sp. from rose is capable of producing methyl eugenol, which constitutes 1.9% of rose essential oil and is an important bioactive compound. Studies have reported that *Chaetomium* sp. is one of the most bioactive endophytic fungi, and the various metabolites involved in its production have anticancer, antibacterial, antioxidant and other properties (Fatima et al., 2016). Our results showed that the crude extracts of these six strains all contained high TPC and TFC, and the TFC of YJ-4 was higher than that of TPC. The reason why the total flavonoid content was higher than the total phenolic content was the limitation of the measurement method. To date, the Folin–Ciocalteu method is commonly used to determine the content of total phenols (Mekinić et al., 2019), and the aluminum nitrate colorimetric method and aluminum trichloride colorimetric method are commonly used to determine total flavonoids. Even if these methods are generally accepted and used, the presence of other substances in the sample may interfere with experimental results. This question has not been well addressed and has been encountered by other researchers. For example, Li et al. (2022) determined the contents of total phenol and total flavonoid in the crude extracts of endophytic fungi AP-11 and AP-12 of *Andrographis paniculata* (Burm. f.) Nees. The same methods we used, the Folin–Ciocalteu method and aluminum nitrate colorimetric method, were used, and the results showed that the TFC of the two crude extracts was greater than the TPC. The

10.3389/fmicb.2023.1190624

TABLE 6 The identification of the chemical composition of endophytic fungi extracts by LC-MS analysis.

NO	Classification	Name of identified compound	RT (min)	Formula	m/z	Adduction	Endophytic fungi (μmol/g)			
							YG-2	SJ-11	YJ-4	YJ-9
1	Flavonoid	Silibinin	5.995	$C_{25}H_{22}O_{10}$	483.128	[M + H]	0.01	nd	0.03	0.12
2	Phenol	Altenuene	5.234	$C_{15}H_{16}O_6$	293.101	[M + H]	0.01	0.07	0.01	nd
3	Flavonoid	Glycitein	4.429	$C_{16}H_{12}O_5$	285.075	[M + H]	0.31	0.01	0.10	0.03
4	Flavonoid	Daidzein	4.617	$C_{15}H_{10}O_4$	255.065	[M + H]	0.07	0.20	0.13	0.12
5	Phenol	Ferulic acid	4.336	$C_{10}H_{10}O_4$	195.065	[M + H]	0.04	0.06	0.59	0.12
6	Phenol	Caffeic acid	4.532	$C_9H_8O_4$	181.049	[M + H]	10.12	0.03	0.02	0.01
7	Phenol	Phloroglucinol	4.102	$C_6H_6O_3$	127.039	[M + H]	0.08	0.14	0.06	0.06
8	Non-phenolic	Skatole	4.261	C_9H_9N	132.080	[M + H]	0.05	5.36	0.06	2.62
9	Non-phenolic	Adenine	0.883	$C_5H_5N_5$	136.062	[M + H]	0.16	0.75	7.11	0.07
10	Non-phenolic	Cinnamic acid	4.563	$C_9H_8O_2$	149.060	[M + H]	0.03	0.15	1.32	0.14
11	Non-phenolic	LYSINE	8.904	$C_6H_{14}N_2O_2$	331.180	[2M + K]	0.61	0.00	0.01	nd
12	Non-phenolic	4-Methyl-5-thiazoleethanol	2.583	C_6H_9NOS	144.048	[M + H]	0.11	0.84	0.04	0.90
13	Non-phenolic	Kojic acid	3.362	$C_6H_6O_4$	143.034	[M + H]	0.44	0.09	1.46	0.16
14	Non-phenolic	Veratrole	6.904	$C_8H_{10}O_2$	121.065	[M + H-H_2O]	0.57	0.04	0.53	0.06
15	Non-phenolic	Hypoxanthine	1.236	$C_5H_4N_4O$	137.046	[M + H]	0.00	0.04	1.06	0.03
16	Non-phenolic	5-Hydroxyindole	1.301	C_8H_7NO	134.060	[M + H]	0.13	0.61	0.81	1.70
17	Non-phenolic	L-Norleucine	6.852	$C_6H_{13}NO_2$	132.102	[M + H]	2.49	nd	nd	nd
18	Non-phenolic	Thymine	1.719	$C_5H_6N_2O_2$	127.050	[M + H]	0.59	nd	0.20	0.01
19	Non-phenolic	4-Hydroxy-6-methyl-2-pyrone	3.54	$C_6H_6O_3$	127.039	[M+H]	0.03	0.31	4.77	0.64
20	Non-phenolic	Pyrrole-2-carboxylic acid	2.199	$C_5H_5NO_2$	112.039	[M + H]	0.03	0.51	0.05	0.72
21	Non-phenolic	Protoporphyrin IX	8.229	$C_{34}H_{34}N_4O_4$	563.274	[M + H]	0.31	nd	nd	nd
22	Non-phenolic	Carviolin	4.558	$C_{16}H_{12}O_6$	301.070	[M + H]	0.19	0.02	1.04	0.01
23	Non-phenolic	Sphingosine	8.261	$C_{18}H_{37}NO_2$	300.289	[M + H]	nd	0.05	0.02	0.51
24	Non-phenolic	Oleamide	7.897	$C_{18}H_{35}NO$	282.279	[M + H]	nd	0.00	0.85	nd
25	Non-phenolic	Pyridoxine	1.231	$C_8H_{11}NO_3$	170.081	[M + H]	0.01	0.15	0.04	0.19
26	Non-phenolic	4-Phenylbutyric acid	5.336	$C_{10}H_{12}O_2$	165.091	[M + H]	0.15	0.05	0.75	0.08
27	Non-phenolic	Arecoline	3.525	$C_8H_{13}NO_2$	156.102	[M + H]	0.03	0.20	0.10	0.25
28	Non-phenolic	Citral	8.154	$C_{10}H_{16}O$	135.117	[M + H-H_2O]	0.12	0.40	0.23	0.13
29	Non-phenolic	4-Anisic acid	5.233	$C_8H_8O_3$	153.054	[M + H]	0.29	0.07	0.05	0.08
30	Non-phenolic	3-Methoxyindole	2.758	C_9H_9NO	148.075	[M + H]	0.11	0.25	0.40	0.12
31	Non-phenolic	Gentisyl alcohol	2.731	$C_7H_8O_3$	141.054	[M + H]	0.03	0.02	0.18	0.17
32	Non-phenolic	Nicotinic acid	0.99	$C_6H_5NO_2$	124.039	[M + H]	0.32	0.03	0.20	0.05
33	Non-phenolic	Isobutyric acid	11.657	$C_4H_8O_2$	177.112	[2M + H]	0.02	0.21	0.13	0.34
34	Non-phenolic	Piperidine	4.577	$C_5H_{11}N$	86.097	[M + H]	0.08	0.02	0.75	0.02
35	Non-phenolic	Erucamide	12.868	$C_{22}H_{43}NO$	338.340	[M + H]	0.01	0.03	0.17	0.08
36	Non-phenolic	Evernic acid	4.614	$C_{17}H_{16}O_7$	333.096	[M + H]	0.11	0.03	0.05	0.05
37	Non-phenolic	Phytosphingosine	7.439	$C_{18}H_{39}NO_3$	318.300	[M + H]	0.06	0.05	0.04	0.04
38	Non-phenolic	Glutathione	7.575	$C_{10}H_{17}N_3O_6S$	308.091	[M + H]	0.15	nd	nd	nd
39	Non-phenolic	Kinetin	3.98	$C_{10}H_9N_5O$	216.088	[M + H]	0.02	0.04	0.13	0.03
40	Non-phenolic	L-Dopa	11.308	$C_9H_{11}NO_4$	198.076	[M + H]	0.10	0.01	nd	nd
41	Non-phenolic	LL-2,6-Diaminoheptanedioate	5.957	$C_7H_{14}N_2O_4$	191.106	[M + H]	0.02	0.11	0.70	0.03

(Continued)

TABLE 6 (Continued)

NO	Classification	Name of identified compound	RT (min)	Formula	m/z	Adduction	Endophytic fungi (μmol/g)			
							YG-2	SJ-11	YJ-4	YJ-9
42	Non-phenolic	4-Methoxycinnamic acid	8.818	C_{10} H_{10} O_3	179.070	[M + H]	0.03	0.01	0.40	0.08
43	Non-phenolic	6-Pentyl-2H-pyran-2-one	7.555	C_{10} H_{14} O_2	149.096	[M + H-H_2O]	0.14	0.14	0.06	0.16
44	Non-phenolic	Apocynin	6.908	C_9 H_{10} O_3	167.070	[M + H]	0.23	0.04	0.68	0.04
45	Non-phenolic	L-Phenylalanine	3.105	C_9 H_{11} N O_2	166.086	[M + H]	0.01	0.10	0.07	0.06
46	Non-phenolic	4-Coumaric acid	6.257	C_9 H_8 O_3	165.055	[M + H]	0.19	0.02	0.17	0.11
47	Non-phenolic	N-Methylanthranilic Acid	7.028	C_8 H_9 N O_2	152.070	[M + H]	nd	0.04	0.35	0.03
48	Non-phenolic	Thymol	5.068	C_{10} H_{14} O	151.112	[M + H]	0.09	0.06	0.02	0.02
49	Non-phenolic	4-Hydroxybenzoic acid	6.011	C_7 H_6 O_3	139.039	[M + H]	0.02	0.02	0.26	0.06
50	Non-phenolic	3,4-Dihydroxybenzaldehyde	4.663	C_7 H_6 O_3	139.039	[M + H]	0.14	0.04	0.14	0.10
51	Non-phenolic	Trigonelline	7.556	C_7 H_7 N O_2	138.055	[M + H]	0.00	0.04	0.01	0.11
52	Non-phenolic	4-Hydroxyindole	3.895	C_8 H_7 N O	134.060	[M + H]	0.03	0.06	0.48	0.09
53	Non-phenolic	L-Pyroglutamic acid	1.249	C_5 H_7 N O_3	130.050	[M + H]	0.06	nd	0.06	nd
54	Non-phenolic	Maltol	3.169	C_6 H_6 O_3	127.039	[M + H]	0.02	0.09	0.10	0.02
55	Non-phenolic	Uracil	1.261	C_4 H_4 N_2 O_2	113.035	[M + H]	0.01	0.01	0.15	0.05
56	Non-phenolic	Histamine	14.542	C_5 H_9 N_3	112.087	[M + H]	0.09	0.11	0.11	0.09
57	Non-phenolic	Choline	0.758	C_5 H_{13} N O	104.107	[M + H]	0.07	0.05	0.09	0.02
58	Non-phenolic	Aniline	1.231	C_6 H_7 N	94.066	[M + H]	0.03	0.06	0.02	0.09

nd, not detect.

crude extracts of the 6 strains all showed good antioxidant activity, especially YG-2, which had strong antioxidant activity *in vitro*. There was no significant difference between the crude extracts and the positive control ascorbic acid in the scavenging ability of some free radicals. To better understand the antioxidant activity of crude extracts of endophytic fungi such as YG-2, further *in vivo* antioxidant studies should be conducted.

In addition, the crude extracts of the 6 strains showed inhibitory effects on all four kinds of pathogens. MIC values were 0.625-0.5 mg/mL, and MBC values were 2.5 or 5 mg/mL. The crude extract of fungus YG-2 had the highest TPC and the best antibacterial effect, which was consistent with the results of Ju et al. (2018), whose experimental results showed that water extraction of bayberry extract had the highest TPC and antibacterial activity among four solvents. That is, the minimum MIC and MBC of the YG-2 crude extract may be due to its highest TPC. According to our results, MIC and MBC were related to the value of TPC, but the specific relationship needs to be further studied. Moreover, the main antibacterial components of different extracts were different. The antibacterial effect of extracts is not only derived from one compound but may be synergistic by many compounds (Ju et al., 2018). Our LC-MS results showed that the four crude extracts contained more than 6 phenolic compounds, including flavonoids and phenolic acids. Studies have reported that metabolites such as phenolic acids and flavonoids have antibacterial properties (Adamczak et al., 2020). Oliveira et al. (2015) showed that silibinin had a significant inhibitory effect on *E. coli*, and its MIC was 64 μg/mL. Salaheen et al. (2017) studied the antibacterial activity of phenolic acids against methicillin-resistant *Staphylococcus aureus* (MRSA), and the results showed that five phenolic acids, including caffeic acid, completely inhibited vegetative MRSA growth *in vitro*. The four crude extracts not only contain phenols such as silibinin and caffeic acid but also contain organic acids such as cinnamic acid and kojic acid. Adamczak et al. (2020) studied 6 kinds of organic acids from plants. The results showed that all 6 kinds of organic acids have antibacterial activity. In summary, the antibacterial activity of crude extracts may be closely related to phenols and organic acids, and the value of TPC was related to MIC and MBC. Our experimental results preliminarily indicated that AOJ endophytic fungal extracts have antibacterial activity, but the specific antibacterial components are still unclear and need further identification and research.

The crude extracts of four endophytic fungi with strong antioxidant and antibacterial activities were selected for preliminary chemical composition identification by LC-MS. The results of LC-MS showed that the main component of the crude extract of YG-2 was caffeic acid, which is a phenolic acid with antibacterial and antioxidant activities. The results of studies by Spagnol et al. (2019) showed that the IC_{50} value of caffeic acid clearing DPPH was 2.39 μg/mL and that of ABTS was 1.96 μg/mL, both of which were lower than that of ascorbic acid. That is, caffeic acid has better DPPH radical and ABTS radical trapping ability than ascorbic acid, showing excellent antioxidant activity (Spagnol et al., 2019). Our results showed that the IC50 value of the YG-2 crude extract in clearing DPPH and ABTS was slightly greater than or equal to that of ascorbic acid, but there was no significant difference ($p < 0.05$). Therefore, we speculate that caffeic acid is responsible for a significant portion of the antioxidant activity of YG-2, but not all of it.

In addition, the LC-MS method is suitable for the detection of substances with high polarity and has its own limitations. Although

our results are significant for the preliminary identification of chemical components in crude extracts, other methods should be added in subsequent studies to compensate for the deficiencies of a single method to better analyze and identify chemical components in crude extracts. In addition, to develop AOJ endophytic fungi for food and medical applications, especially as sources of antioxidants and antimicrobial drugs, further research is needed in the future.

5. Conclusion

In summary, this study preliminarily elaborated the diversity of endophytic fungi of AOJ, and the diversity of endophytic fungi in roots and stems of AOJ with different shapes was different. Six strains of YG-2, SJ-11, YJ-4, YJ-9, YJ-10, and SJ-2 fungi with high yields of flavonoids and phenols were isolated from AOJ. The crude extracts of endophytic fungi fermentation broth showed good antioxidant and antibacterial activities, among which the YG-2 crude extract showed the strongest antioxidant and antibacterial activity, and caffeic acid was the main component of the YG-2 crude extract. The results showed that the endophytic fungus YG-2 (*Chaetomium globosum*) had the potential to produce antioxidants.

Data availability statement

The original contributions presented in the study are included in the article/**Supplementary material**, further inquiries can be directed to the corresponding author.

Author contributions

NS, ZC, and GC performed the experiments and authored or reviewed drafts of the manuscript. YQ and WL performed the experiments. YX authored or reviewed drafts of the manuscript. ZT and HC conceived and designed the experiments and approved the final draft. QL and MY analyzed the data. TB contributed reagents, materials, and analysis tools. All authors contributed to the article and approved the submitted version.

Acknowledgments

We gratefully acknowledge financial support for this work from Enzyme Resources Sharing and Service Platform of Sichuan Province and Sichuan Province International Science and Technology Innovation cooperation Project: Isolation and physiological activities of secondary metabolites from endophytic fungi of *Conyza blinii*.

Conflict of interest

The authors declare that the research was conducted in the absence of any commercial or financial relationships that could be construed as a potential conflict of interest.

Publisher's note

All claims expressed in this article are solely those of the authors and do not necessarily represent those of their affiliated organizations, or those of the publisher, the editors and the reviewers. Any product that may be evaluated in this article, or claim that may be made by its manufacturer, is not guaranteed or endorsed by the publisher.

Supplementary material

The Supplementary Material for this article can be found online at: https://www.frontiersin.org/articles/10.3389/fmicb.2023.1190624/full#supplementary-material

References

Adamczak, A., Ozarowski, M., and Karpinski, T. M. (2020). Antibacterial activity of some flavonoids and organic acids widely distributed in plants. *J. Clin. Med.* 9:109. doi: 10.3390/jcm9010109

Atiphasaworn, P., Monggoot, S., Gentekaki, E., Brooks, S., and Pripdeevech, P. (2017). Antibacterial and antioxidant constituents of extracts of endophytic fungi isolated from *Ocimum basilicum* var. thyrsiflora leaves. *Curr. Microbiol.* 74, 1185–1193. doi: 10.1007/s00284-017-1303-1

Bora, P., and Devi, N. N. (2023). Exploration of the chemical constituents and its antioxidant, antibacterial activities of endophytic fungi isolated from the medicinal plant *Dillenia indica*. *Arch. Microbiol.* 205:67. doi: 10.1007/s00203-023-03407-0

Charria-Girón, E., Espinosa, M. C., Zapata-Montoya, A., Méndez, M. J., Caicedo, J. P., Dávalos, A. F., et al. (2021). Evaluation of the antibacterial activity of crude extracts obtained from cultivation of native endophytic fungi belonging to a tropical montane rainforest in Colombia. *Front. Microbiol* 12:16523. doi: 10.3389/fmicb.2021.716523

Chen, S., Li, X., Liu, X., Wang, N., An, Q., Ye, X. M., et al. (2020). Investigation of chemical composition, antioxidant activity, and the effects of alfalfa flavonoids on growth performance. *Oxid. Med. Cell. Longev* 2020:8569237. doi: 10.1155/2020/8569237

Deng, Y., Liu, H., Huang, Q., Tu, L., Hu, L., Zheng, B., et al. (2022). Mechanism of longevity extension of caenorhabditis elegans induced by schizophyllum commune fermented supernatant with added radix puerariae. *Front. Nutr* 9:847064. doi: 10.3389/fnut.2022.847064

Ding, C. H., Wang, Q. B, Guo, S. L., Wang, Z. Y. (2018). The improvement of bioactive secondary metabolites accumulation in *Rumex gmelini* Turcz through co-culture with endophytic fungi. *Braz. J. Microbiol.* 49, 362–369. doi: 10.1016/j.bjm.2017.04.013

Dydak, K., Junka, A., Dydak, A., Brożyna, M., Paleczny, J., Fijalkowski, K., et al. (2021). *In vitro* efficacy of bacterial cellulose dressings chemisorbed with antiseptics against biofilm formed by pathogens isolated from chronic wounds. *Int. J. Mol. Sci.* 22:3996. doi: 10.3390/ijms22083996

Fan, M., Chen, X., Luo, X., Zhang, H., Liu, Y., Zhang, Y., et al. (2020). Diversity of endophytic fungi from the leaves of *Vaccinium dunalianum*. *Lett. Appl. Microbiol.* 71, 479–489. doi: 10.1111/lam.13345

Fan, S., Miao, L., Li, H., Lin, A., Song, F., and Zhang, P. (2020). Illumina-based analysis yields new insights into the diversity and composition of endophytic fungi in cultivated *Huperzia serrata*. *PLoS One* 15:e0242258. doi: 10.1371/journal.pone.0242258

Fan, Z., Xiao, S., Hu, H., Zhang, P., Chao, J., Guo, S., et al. (2022). Endophytic bacterial and fungal community compositions in different organs of ginseng (*Panax ginseng*). *Arch. Microbiol.* 204:208. doi: 10.1007/s00203-022-02815-y

Fatima, N., Mukhtar, U., Ihsan-Ul-Haq Qazi, M. A., Jadoon, M., and Ahmed, S. (2016). Biological evaluation of endophytic fungus *chaetomium* sp. NF15 of justicia adhatoda l.: A potential candidate for drug discovery. *Jundishapur J. Microbiol.* 9:e29978. doi: 10.5812/jjm.29978

Feng, L., Liu, T. T., Huo, X. K., Tian, X. G., Wang, C., Lv, X., et al. (2021). *Alisma* genus: Phytochemical constituents, biosynthesis, and biological activities. *Phyther. Res.* 35, 1872–1886. doi: 10.1002/ptr.6933

Gu, H., Zhang, S., Liu, L., Yang, Z., Zhao, F., and Tian, Y. (2022). Antimicrobial potential of endophytic fungi from *Artemisia argyi* and bioactive metabolites from *Diaporthe* sp. AC1. *Front. Microbiol.* 13:908836. doi: 10.3389/fmicb.2022.908836

Gupta, S., Chaturvedi, P., Kulkarni, M. G., and Van Staden, J. (2020). A critical review on exploiting the pharmaceutical potential of plant endophytic fungi. *Biotechnol. Adv.* 39:107462. doi: 10.1016/j.biotechadv.2019.107462

Harrison, J. G., Beltran, L. P., Buerkle, C. A., Cook, D., Gardner, D. R., Parchman, T. L., et al. (2021). A suite of rare microbes interacts with a dominant, heritable, fungal endophyte to influence plant trait expression. *ISME J.* 15, 2763–2778. doi: 10.1038/s41396-021-00964-4

Hou, X., Huang, X., Li, J., Jiang, G., Shen, G., Li, S., et al. (2020). Extraction optimization and evaluation of the antioxidant and α-glucosidase inhibitory activity of polysaccharides from *Chrysanthemum morifolium* cv. Hangju. *Antioxidants* 9:59. doi: 10.3390/antiox9010059

Huang, Y. S., Yu, Q., Chen, Y., Cheng, M. J., and Xie, L. (2017). Phenolic constituents from *Alisma plantago-aquatica* Linnaeus and their anti-chronic prostatitis activity. *Chem. Cent. J.* 11, 9–13. doi: 10.1186/s13065-017-0350-9

Jia, M., Chen, L., Xin, H. L., Zheng, C. J., Rahman, K., Han, T., et al. (2016). A friendly relationship between endophytic fungi and medicinal plants: A systematic review. *Front. Microbiol.* 7:906. doi: 10.3389/fmicb.2016.00906

Ju, J., Yao, W., Sun, S., Guo, Y., Cheng, Y., Qiana, H., et al. (2018). Assessment of the antibacterial activity and the main bacteriostatic components from bayberry fruit extract. *Int. J. Food Prop.* 21, 1043–1051. doi: 10.1080/10942912.2018.1479861

Kaul, S., Wani, M., Dhar, K. L., and Dhar, M. K. (2008). Production and GC-MS trace analysis of methyl eugenol from endophytic isolate of *Alternaria* from Rose. *Ann. Microbiol.* 58, 443–445. doi: 10.1007/BF03175541

Kim, K. H., Song, H. H., Ahn, K. S., Oh, S. R., Sadikot, R. T., and Joo, M. (2016). Ethanol extract of the tuber of *Alisma orientale* reduces the pathologic features in a chronic obstructive pulmonary disease mouse model. *J. Ethnopharmacol.* 188, 21–30. doi: 10.1016/j.jep.2016.05.004

Kumari, M., Taritla, S., Sharma, A., and Jayabaskaran, C. (2018). Antiproliferative and antioxidative bioactive compounds in extracts of marine-derived endophytic fungus *Talaromyces purpureogenus*. *Front. Microbiol.* 9:1777. doi: 10.3389/fmicb.2018.01777

Li, L., Song, X., Yin, Z., Jia, R., Li, Z., Zhou, X., et al. (2016). The antibacterial activity and action mechanism of emodin from *Polygonum cuspidatum* against *Haemophilus parasuis* in vitro. *Microbiol. Res.* 18, 139–145. doi: 10.1016/j.micres.2016.03.008

Li, N., Xu, D., Huang, R. H., Zheng, J. Y., Liu, Y. Y., Hu, B. S., et al. (2022). A new source of diterpene lactones from *Andrographis paniculata* (Burm. f.) Nees—Two endophytic fungi of *Colletotrichum* sp. with antibacterial and antioxidant activities. *Front. Microbiol.* 13:819770. doi: 10.3389/fmicb.2022.819770

Liu, J., Wang, Z., Chen, Z., White, J. F., Malik, K., Chen, T., et al. (2022). Inoculation of Barley (Hordeum vulgare) with the Endophyte *Epichloë bromicola* affects plant growth, and the microbial community in roots and rhizosphere soil. *J. Fungi* 8:172. doi: 10.3390/jof8020172

Liu, S. S., Guo, J., Li, Z. N., Tian, S. S., Yan, L. H., and Wang, Z. M. (2020). Advances in studies on chemical compositions of *Alismatis Rhizoma* and their biological activities. *China J. Chinese Mater. Medica* 45, 1578–1595. doi: 10.19540/j.cnki.cjcmm.20190616.201

Marx, J. L. (1986). Free radicals to many diseases oxidative damage is common, and DNA. *Science* 235, 529–531.

Silva, M. H. R., Cueva-Yesquén, L. G., Júnior, S. B., Garcia, V. L., Sartoratto, A., and Angelis, D. A. (2020). Endophytic fungi from *Passiflora incarnata*: An antioxidant compound source. *Arch. Microbiol.* 202, 2779–2789. doi: 10.1007/s00203-020-02001-y

Mekinić, I. G., Skroza, D., Šimat, V., Hamed, I., Čagalj, M., and Perković, Z. P. (2019). Phenolic content of brown algae (*Pheophyceae*) species: Extraction, identification, and quantification. *Biomolecules* 9:244. doi: 10.3390/biom9060244

Minussi, R. C., Rossi, M., Bologna, L., Cordi, L., Rotilio, D., Pastore, G. M., et al. (2003). Phenolic compounds and total antioxidant potential of commercial wines. *Food Chem.* 82, 409–416. doi: 10.1016/S0308-8146(02)00590-3

Mookherjee, A., Mitra, M., Kutty, N. N., Mitra, A., and Maiti, M. K. (2020). Characterization of endo-metabolome exhibiting antimicrobial and antioxidant activities from endophytic fungus *Cercospora* sp. PM018. *South Afr. J. Bot.* 134, 264–272. doi: 10.1016/j.sajb.2020.01.040

Moskovitz, J., Yim, M. B., and Chock, P. B. (2002). Free radicals and disease. *Arch. Biochem. Biophys.* 397, 354–359. doi: 10.1006/abbi.2001.2692

Muthukrishnan, S., Prakathi, P., Sivakumar, T., Thiruvengadam, M., Jayaprakash, B., Baskar, V., et al. (2022). Bioactive components and health potential of endophytic micro-fungal diversity in medicinal plants. *Antibiotics* 11:1533. doi: 10.3390/antibiotics11111533

Nataraj, A., Govindan, S., Ramani, P., Subbaiah, K. A., Sathianarayanan, S., Venkidasamy, B., et al. (2022). Antioxidant, anti-tumour, and anticoagulant activities of polysaccharide from *Calocybe indica* (APK2). *Antioxidants* 11:1694. doi: 10.3390/antiox11091694

Oliveira, D. R., De Tintino, S. R., Flaviana, M., Morais, B., Boligon, A. A., Athayde, M. L., et al. (2015). In *Vitro* antimicrobial and modulatory activity of the natural products silymarin and silibinin. *Biomed Res. Int.* 2015:292797. doi: 10.1155/2015/292797

Park, S. U., Lim, H. S., Park, K. C., Park, Y. H., and Bae, H. (2012). Fungal endophytes from three cultivars of *Panax ginseng* meyer cultivated in Korea. *J. Ginseng Res.* 36, 107–113. doi: 10.5142/jgr.2012.36.1.107

Rehman, B., Khan, S. A., Hamayun, M., Iqbal, A., and Lee, I. J. (2022). Potent bioactivity of endophytic fungi isolated from *moringa oleifera* leaves. *Biomed Res. Int.* 2022:2461021. doi: 10.1155/2022/2461021

Salaheen, S., Peng, M., Joo, J., Teramoto, H., and Butaye, P. R. (2017). Eradication and Sensitization of methicillin resistant *Staphylococcus aureus* to methicillin with bioactive extracts of berry pomace. *Front Microbiol.* 8:253. doi: 10.3389/fmicb.2017.00253

Dos Santos, I., da Silva, L., da Silva, M., de Araújo, J., Cavalcanti Mda, S., and Lima, V. (2015). Antibacterial activity of endophytic fungi from leaves of *Indigofera suffruticosa* Miller (Fabaceae). *Front. Microbiol* 6:350. doi: 10.3389/fmicb.2015.00350

Sharma, G. N., Gupta, G., and Sharma, P. (2018). A comprehensive review of free radicals, antioxidants, and their relationship with human ailments. *Crit. Rev. Eukaryot. Gene Expr.* 28, 139–154. doi: 10.1615/CritRevEukaryotGeneExpr.2018022258

Sohrabi, M., Samsampour, D., and Bagheri, A. (2023). Molecular identification of fungal endophytes of medicinal plant *Citrullus colocynthis* (L.) schrad as a medicinal plant: Role of tissue type and sampling location on the diversity. *Mol. Biotechnol.* doi: 10.1007/s12033-022-00630-w

Spagnol, C. M., Assis, R. P., Brunetti, I. L., Isaac, V. L. B., Salgado, H. R. N., and Corrêa, M. A. (2019). In vitro methods to determine the antioxidant activity of caffeic acid. *Spectrochim. Acta A Mol. Biomol. Spectrosc.* 219, 358–366. doi: 10.1016/j.saa.2019.04.025

Tang, Z., Qin, Y., Chen, W., Zhao, Z., Lin, W., Xiao, Y., et al. (2021). Diversity, chemical constituents, and biological activities of endophytic fungi isolated from *Ligusticum chuanxiong* Hort. *Front. Microbiol.* 12:771000. doi: 10.3389/fmicb.2021.771000

Tang, Z., Qin, Y., Wang, Y., Lin, W., Wang, Q., Shen, N., et al. (2022). The endophytic fungus *Penicillium* oxalicum isolated from *Ligusticum chuanxiong* Hort possesses DNA damage-protecting potential and increases stress resistance properties in *Caenorhabditis elegans*. *Front. Pharmacol.* 13:983716. doi: 10.3389/fphar.2022.983716

Tang, Z., Wang, Y., Yang, J., Xiao, Y., Cai, Y., Wan, Y., et al. (2020). Isolation and identification of flavonoid-producing endophytic fungi from medicinal plant Conyza blinii H.Lév that exhibit higher antioxidant and antibacterial activities. *PeerJ* 2020:e8978. doi: 10.7717/peerj.8978

Tappel, A., and Tappel, A. (2004). Oxidant free radical initiated chain polymerization of protein and other biomolecules and its relationship to diseases. *Med. Hypotheses* 63, 98–99. doi: 10.1016/j.mehy.2004.01.022

Wairata, J., Fadlan, A., Setyo Purnomo, A., Taher, M., and Ersam, T. (2022). Total phenolic and flavonoid contents, antioxidant, antidiabetic and antiplasmodial activities of *Garcinia forbesii* King: A correlation study. *Arab. J. Chem.* 15:103541. doi: 10.1016/j.arabjc.2021.103541

Wen, J., Okyere, S. K., Wang, S., Wang, J., Xie, L., Ran, Y., et al. (2022). Endophytic fungi: An effective alternative source of plant-derived bioactive compounds for pharmacological studies. *J. Fungi* 8:205. doi: 10.3390/jof8020205

Wiegand, I., Hilpert, K., and Hancock, R. E. W. (2008). Agar and broth dilution methods to determine the minimal inhibitory concentration (MIC) of antimicrobial substances. *Nat. Protoc.* 3, 163–175. doi: 10.1038/nprot.2007.521

Wu, C., Wang, W., Wang, X., Shahid, H., Yang, Y., Wang, Y., et al. (2022). Diversity and communities of culturable endophytic fungi from the root holoparasite *Balanophora polyandra* Griff. and their antibacterial and antioxidant activities. *Ann. Microbiol.* 72:19. doi: 10.1186/s13213-022-01676-6

Wu, H., Li, M., Yang, X., Wei, Q., Sun, L., Zhao, J., et al. (2020). Extraction optimization, physicochemical properties and antioxidant and hypoglycemic activities of polysaccharides from roxburgh rose (*Rosa roxburghii* Tratt.) leaves. *Int. J. Biol. Macromol.* 165, 517–529. doi: 10.1016/j.ijbiomac.2020.09.198

Xin, X. L., Yu, Z. L., Tian, X. G., Wei, J. C., Wang, C., Huo, X. K., et al. (2017). Phenylpropanoid amides from *Alisma orientalis* and their protective effects against H_2O_2-induced damage in SH-SY5Y cells. *Phytochem. Lett.* 21, 46–50. doi: 10.1016/j.phytol.2017.05.027

Xu, L., Jing, M., Yang, L., Jin, L., Gong, P., Lu, J., et al. (2019). The *Alisma* and *Rhizoma* decoction abates nonalcoholic steatohepatitis-associated liver injuries in mice by modulating oxidative stress and autophagy. *BMC Complement. Altern. Med.* 19:92. doi: 10.1186/s12906-019-2488-6

Zhang, H., Zhao, J., Shang, H., Guo, Y., and Chen, S. (2020). Extraction, purification, hypoglycemic and antioxidant activities of red clover (Trifolium pratense L.) polysaccharides. *Int. J. Biol. Macromol.* 148, 750–760. doi: 10.1016/j.ijbiomac.2020.01.194

Zhang, L., Xu, W., Xu, Y. L., Chen, X., Huang, M., and Lu, J. J. (2017). Therapeutic potential of *Rhizoma Alismatis*: A review on ethnomedicinal application, phytochemistry, pharmacology, and toxicology. *Ann. N. Y. Acad. Sci.* 1401, 90–101. doi: 10.1111/nyas.13381

Zhang, X., Li, Y., Li, Y., Zhao, J., Cheng, Y., Wang, Y., et al. (2023). Changes of bioactive components and antioxidant capacity of pear ferment in simulated gastrointestinal digestion *In Vitro*. *Foods* 12:1211. doi: 10.3390/foods12061211

Zhang, Y., Wu, Y. T., Zheng, W., Han, X. X., Jiang, Y. H., Hu, P. L., et al. (2017). The antibacterial activity and antibacterial mechanism of a polysaccharide from *Cordyceps cicadae*. *J. Funct. Foods* 38, 273–279. doi: 10.1016/j.jff.2017.09.047

Zhao, X. Y., Wang, G., Wang, Y., Tian, X. G., Zhao, J. C., Huo, X. K., et al. (2018). Chemical constituents from *Alisma plantago-aquatica* subsp. *orientale* (Sam.) Sam and their anti-inflammatory and antioxidant activities. *Nat. Prod. Res.* 32, 2749–2755. doi: 10.1080/14786419.2017.1380024

Zheng, Z., Chai, S., Chen, J., Yang, H., Chang, J., and Yang, G. (2022). Isolation and identification of flavonoid-producing endophytic fungi from *Loranthus tanakae* Franch. & Sav that exhibit antioxidant and antibacterial activities. *J. Appl. Microbiol* 133, 1892–1904. doi: 10.1111/jam.15696

frontiers | Frontiers in Microbiology

TYPE Original Research
PUBLISHED 10 August 2023
DOI 10.3389/fmicb.2023.1216029

OPEN ACCESS

EDITED BY
Mina Salehi,
Tarbiat Modares University, Iran

REVIEWED BY
Siamak Farhadi,
Tarbiat Modares University, Iran
Simone Cantamessa,
Council for Agricultural Research and Economics (CREA), Italy

*CORRESPONDENCE
Stéphane Declerck
✉ stephan.declerck@uclouvain.be

†These authors have contributed equally to this work and share first authorship

RECEIVED 03 May 2023
ACCEPTED 24 July 2023
PUBLISHED 10 August 2023

CITATION
Zhao Y, Cartabia A, Garcés-Ruiz M, Herent M-F, Quetin-Leclercq J, Ortiz S, Declerck S and Lalaymia I (2023) Arbuscular mycorrhizal fungi impact the production of alkannin/shikonin and their derivatives in *Alkanna tinctoria* Tausch. grown in semi-hydroponic and pot cultivation systems.
Front. Microbiol. 14:1216029.
doi: 10.3389/fmicb.2023.1216029

Arbuscular mycorrhizal fungi impact the production of alkannin/shikonin and their derivatives in *Alkanna tinctoria* Tausch. grown in semi-hydroponic and pot cultivation systems

Yanyan Zhao[1†], Annalisa Cartabia[1†], Mónica Garcés-Ruiz[1], Marie-France Herent[2], Joëlle Quetin-Leclercq[2], Sergio Ortiz[2,3], Stéphane Declerck[1*] and Ismahen Lalaymia[1]

[1]Mycology, Earth and Life Institute, Université catholique de Louvain – UCLouvain, Louvain-la-Neuve, Belgium, [2]Pharmacognosy Research Group, Louvain Drug Research Institute (LDRI), Université catholique de Louvain – UCLouvain, Brussels, Belgium, [3]UMR 7200, Laboratoire d'Innovation Thérapeutique, Université de Strasbourg, CNRS, Strasbourg Drug Discovery and Development Institute (IMS), Illkirch-Graffenstaden, France

Introduction: *Alkanna tinctoria* Tausch. is a medicinal plant well-known to produce important therapeutic compounds, such as alkannin/shikonin and their derivatives (A/Sd). It associates with arbuscular mycorrhizal fungi (AMF), which are known, amongst others beneficial effects, to modulate the plant secondary metabolites (SMs) biosynthesis. However, to the best of our knowledge, no study on the effects of AMF strains on the growth and production of A/Sd in *A. tinctoria* has been reported in the literature.

Methods: Here, three experiments were conducted. In Experiment 1, plants were associated with the GINCO strain *Rhizophagus irregularis* MUCL 41833 and, in Experiment 2, with two strains of GINCO (*R. irregularis* MUCL 41833 and *Rhizophagus aggregatus* MUCL 49408) and two native strains isolated from wild growing *A. tinctoria* (*R. irregularis* and *Septoglomus viscosum*) and were grown in a semi-hydroponic (S-H) cultivation system. Plants were harvested after 9 and 37 days in Experiment 1 and 9 days in Experiment 2. In Experiment 3, plants were associated with the two native AMF strains and with *R. irregularis* MUCL 41833 and were grown for 85 days in pots under greenhouse conditions. Quantification and identification of A/Sd were performed by HPLC-PDA and by HPLC-HRMS/MS, respectively. *LePGT1*, *LePGT2*, and *GHQH* genes involved in the A/Sd biosynthesis were analyzed through RT-qPCR.

Results: In Experiment 1, no significant differences were noticed in the production of A/Sd. Conversely, in Experiments 2 and 3, plants associated with the native AMF *R. irregularis* had the highest content of total A/Sd expressed as shikonin equivalent. In Experiment 1, a significantly higher relative expression of both *LePGT1* and *LePGT2* was observed in plants inoculated with *R. irregularis* MUCL 41833 compared with control plants after 37 days in the S-H cultivation system. Similarly, a significantly higher relative expression of *LePGT2* in plants inoculated

with *R. irregularis* MUCL 41833 was noticed after 9 versus 37 days in the S-H cultivation system. In Experiment 2, a significant lower relative expression of *LePGT2* was observed in native AMF *R. irregularis* inoculated plants compared to the control.

Discussion: Overall, our study showed that the native *R. irregularis* strain increased A/Sd production in *A. tinctoria* regardless of the growing system used, further suggesting that the inoculation of native/best performing AMF is a promising method to improve the production of important SMs.

KEYWORDS

arbuscular mycorrhizal fungi, *Alkanna tinctoria*, semi-hydroponic cultivation system, alkannin/shikonin derivatives, native strains

1. Introduction

The hydroxynaphthoquinones (HNQs) of natural origin, and in particular the isohexenylnaphthazarins (IHNs), such as the chiral pair alkannin and shikonin (A/S), are lipophilic red pigments characterized by a wide spectrum of wound healing, antibacterial, anti-inflammatory, anticancer, and antithrombotic activities (Papageorgiou et al., 1999; Tappeiner et al., 2014). Monomeric A/S derivatives, mainly esters of the side chain hydroxyl group, have been found in the root periderm of several plants of the Boraginaceae family, including *Alkanna tinctoria* Tausch. This important medicinal plant, commonly known as alkanet or dyers' bugloss/alkanet, is found across southern Europe, northern Africa, and southwestern Asia, with a central distribution in the Mediterranean region (Valdés, 2011). Preparations made with *A. tinctoria* roots are commonly used in traditional medicine to treat wounds, burns, and ulcers, while extracted A/S are employed as active ingredients in different marketed pharmaceutical formulations (e.g., Histoplastin Red® and HELIXDERM®) as strong wound healing medicines. Root extracts are also used as cosmetics, food additives or natural dyes for staining silk (Papageorgiou et al., 2008; Malik et al., 2016).

Today, nature remains the main source of commercial A/S and their derivatives (A/Sd), despite significant efforts to synthesize these compounds over the years (Papageorgiou et al., 2008). The only successful example of shikonin scaling up from cell cultures was with *Lithospermum erythrorhizon* Siebold & Zucc. (Boraginaceae) by Mitsui Petrochemical Industries Ltd. (now Mitsui Chemicals Inc., Tokyo, Japan) in 1984 (Yazaki, 2017). Few more attempts have been made with cell suspension cultures of *Arnebia* spp. (Boraginaceae) in stirred-tank (New Brunswick Scientific Company Inc., Edison, NJ, USA) and in air-lift bioreactors, but no further commercial successes have been reported (Gupta et al., 2014; Malik et al., 2016). For *A. tinctoria*, cell tissues and root cultures have been used, but the level of A/S production remained insufficient for commercial use (Urbanek et al., 1996; Gerardi et al., 1998). Yet, these important compounds remain mostly extracted from plants grown in the wild, with a risk of extinction as already documented for other Boraginaceae spp. (e.g., *L. erythrorhizon* in Japan, *Alkanna sieheana* Rech. Fil. and *Alkanna orientalis* L. Boiss. in Turkey). Indeed, *A. tinctoria* is considered as very rare in some European countries, such as Slovakia, Bulgaria, and Hungary (Yazaki, 2017; Yaman et al., 2019; Ahmad et al., 2021). Moreover, this plant is characterized by a very low seed germination rate and its cultivation under conventional agriculture practices is hampered by several constraints (e.g., time needed for A/S production, high costs of harvesting, and exposure to biotic/abiotic stresses) (Malik et al., 2016). For these reasons, *in vitro* and *ex vitro* cultivation protocols have been developed for the propagation and preservation of this plant (Cartabia et al., 2022). In addition, hydroponic cultivation of medicinal plants has attracted the attention of the scientific community and industrial sector, as it can effectively meet the nutrients needs of the plants under controlled/stable environmental conditions (Gontier et al., 2002; Sgherri et al., 2010). Interestingly, these cultivation systems are adapted to the growth of microorganisms such as arbuscular mycorrhizal fungi (AMF) (IJdo et al., 2011; Garcés-Ruiz et al., 2017). These obligate plant symbionts, belonging to the Glomeromycota phylum, provide their hosts with nutrients (especially N and P) in exchange for carbon and lipids (Smith and Read, 2008; Chen et al., 2018). A number of studies have reported their impact on the production of secondary metabolites (SMs) in leaves, roots or fruits/tubers of different crops used as food or for medicinal purposes (Zeng et al., 2013; Avio et al., 2018; Pandey et al., 2018; Kaur and Suseela, 2020; Zhao et al., 2022). For instance, artemisinin in leaves of *Artemisia annua* L. (Chaudhary et al., 2008), caffeic acid and rosmarinic acid in shoots of *Ocimum basilicum* L. (Toussaint et al., 2007), and triterpenes and phenolics in *Dioscorea* spp. (Lu et al., 2015) were increased in AMF-colonized plants. In addition, the AMF *Rhizophagus irregularis* MUCL 41833 was shown to modulate the primary and secondary metabolites (PMs and SMs, respectively) production of *Anchusa officinalis* L. (i.e., shoot and root tissues as well as exudates in the nutrient solution), another important Boraginaceae plant, under a semi-hydroponic (S-H) cultivation system (Cartabia et al., 2021). A similar study, conducted with *A. officinalis* associated with different AMF species (*R. irregularis* MUCL 41833, *Rhizophagus intraradices* MUCL 49410, *Rhizophagus clarus* MUCL 46238, and *R. aggregatus* MUCL 49408), demonstrated that specific symbiotic associations can affect the production of

bioactive compounds differently in the same host (Tsiokanos et al., 2022).

Biosynthesis of A/Sd involves the phenylpropanoid and mevalonate pathways (Song et al., 2020). Several genes, responsible for encoding enzymes involved in the biosynthesis of shikonin, have been identified in Boraginaceae plant species (Wang et al., 2014; Wu et al., 2017; Takanashi et al., 2019). The *p*-hydroxybenzoate geranyltransferase (*PGT*) gene plays a key role in coding the enzyme catalyzing the coupling of *p*-hydroxybenzoic acid and geranyl diphosphate to produce *m*-geranyl-*p*-hydroxybenzoic acid, which is the first step in the formation of the basic carbon skeleton leading to A/Sd, and it has been cloned and characterized in cell cultures of *L. erythrorhizon* and *Arnebia euchroma* (Royle) Johnston (Yazaki et al., 2002; Singh et al., 2010). In addition, geranylhydroquinone 3″-hydroxylase (*GHQH*), an enzyme hydroxylating the isoprenoid side chain of geranylhydroquinone (GHQ), a well-known precursor of shikonin, has also been identified in *L. erythrorhizon* cell suspension cultures (Yamamoto et al., 2000). However, to our knowledge, no study has investigated the gene regulation of the biosynthesis of A/Sd in *A. tinctoria*, in particular in the presence of AMF.

In this study, the main objectives were to determine whether (1) AMF from international collection (i.e., GINCO) could enhance the production of A/Sd and whether this effect is more/less significant compared to AMF isolated from *A. tinctoria* grown in the wild; (2) AMF can modulate the expression of genes involved in the A/Sd biosynthetic pathway; (3) the production of A/Sd is affected similarly under semi-hydroponic and pot cultivation systems. To address these objectives, the quantification of A/Sd was performed through High-Performance Liquid Chromatography coupled with Photodiode Array (HPLC-PDA) detection and the related genes expression through Real-Time Quantitative Reverse Transcription PCR (RT-qPCR). Moreover, identification of the main A/Sd was performed using HPLC coupled with High-Resolution Mass Spectrometry detection (HPLC-HRMS/MS).

2. Materials and methods

2.1. Chemicals

All used organic solvents [i.e., n-hexane 97%, methanol, trifluoroacetic acid (TFA), and acetonitrile (ACN) (VWR INTERNATIONAL, Leuven, Belgium)] were HPLC/LC-MS grade. Water was purified and demineralized with a Milli-Q system manufactured by Millipore (Bedford, MA, USA). Shikonin (purity >98%) was purchased from Cayman Chemical Company (Biomol GmbH, Hamburg, Germany) and used as internal standard.

For gene expression analysis (i.e., RNA extraction) all non-disposable materials (e.g., glass materials, mortars, and pestles) were first treated with RNase AWAY™ Surface Decontaminant (Thermo Fisher Scientific™, Belgium) and 0.1% diethylpyrocarbonate (DEPC)-treated sterile water. All the reagents were prepared with sterilized (121°C for 15 min) DEPC-treated water. Reagents used in RNA extraction were the following: extraction buffer [100 mM Tris–HCl (pH 8.0), 20 mM EDTA, 1.4 M NaCl, 2% CTAB (w/v) and 2% PVP (w/v)], 2% β-mercaptoethanol (v/v), 5 M NaCl, 1.2 M NaCl, 0.38 M trisodium citrate dihydrate, chloroform, isopropanol, and 70% ethanol (stored at −20°C).

2.2. Biological materials

Rhizophagus irregularis (Błaszk, Wubet, Renker and Buscot) C. Walker and A. Schüßler as ["irregulare"] MUCL 41833 and *Rhizophagus aggregatus* (N.C. Schenck & G.S. Sm.) C. Walker MUCL 49408 were supplied by the *Glomeromycota in vitro* collection (GINCO).[1] Both AMF were mass-produced on *Zea mays* L. cv. ES Ballade (Euralis, Lescar, France) in 10 L plastic boxes containing sterilized (121°C for 15 min) lava (DCM, Grobbendonk, Belgium). Two other AMF strains (*R. irregularis* and *Septoglomus viscosum*) were isolated from *A. tinctoria* growing in a suburban pine forest, altitude 50 m of Northern Greece (Evaggelistria, Seih Sou, Thessaloniki, special collection permit obtained by the Institute of Plant Breeding and Genetic Resources, Hellenic Agricultural Organization Demeter – IPBGR, HAO Demeter). They were first trapped on *Plantago lanceolata* L. (Ecosem, Belgium) and *Medicago truncatula* Gaertn. (SARDI, Australia) to stimulate the production of numerous spores and then grown as monospores on *P. lanceolata* at the GINCO premises to obtain single species cultures (see section **Isolation and mono-species culture of AMF** in **Supplementary material**, **Supplementary Figures 1–4**, and **Supplementary Table 1**). They were finally mass-produced on *Z. mays* L. in 5 L plastic boxes containing the same sterilized lava substrate as above.

The four AMF strains were grown under greenhouse conditions at 25/18°C (day/night), a relative humidity (RH) of 38%, a photoperiod of 16 h day^{-1} and a photosynthetic photon flux (PPF) of 120 µmol m^{-2} s^{-1}.

Alkanna tinctoria unrooted *in vitro* explants (International Plant Exchange Network – IPEN – accession number GR-1-BBGK-17,5975) were provide by IPBGR, HAO Demeter (Thessaloniki, Greece). The plants were proliferated on Murashige-Skoog (MS) basal medium enriched with plant growth regulators (PGRs) and rooted on Root Culture 1 (RC1) modified medium free of ammonium nitrate (Cartabia et al., 2022). The rooted *A. tinctoria* plants were further acclimatized following different steps resulting in an optimal plant survival rate (see section "*Alkanna tinctoria* acclimatization protocol" in **Supplementary material** and **Supplementary Figure 5**). The acclimatization protocol was applied for all the experiments in order to have plants of the same age and established under identical growth conditions (first acclimatization from 2nd November 2020 to 7th December 2020 and second from 1st February 2021 to 10th March 2021).

2.3. Colonization of *A. tinctoria*

After the acclimatization phase, the plants were carefully removed from the substrate, gently washed under a stream of demineralized water, and transplanted into 1 L pots (11 × 11 × 12 cm) containing a sterilized (121°C for 15 min) substrate mixture (2 peatmoss/2 compost/1 perlite/1 quartz 0.4–0.8 mm/1 quartz 1–2 mm) (see **Supplementary Figure 5**). Total fresh weight (TFW) of the plants was evaluated before AMF inoculation.

In each experiment, plants were associated [i.e., the mycorrhizal (M) treatments] or not [i.e., the non-mycorrhizal (NM) treatments]

1 http://www.mycorrhiza.be/ginco-bel/

with AMF. For the M plants, the substrate was half mixed with the AMF-inoculum substrate above, whereas for the NM treatments, the substrate was half mixed with the same AMF-inoculum substrate above but sterilized (121°C for 15 min). The plants were grown in the substrates for two months under greenhouse conditions set at 24/22°C (day/night), RH of 50%, photoperiod of 16 h day^{-1} and LED light (lumigrow) intensity of about 220 µmol m^{-2} s^{-1}.

2.4. Experiment 1: A/Sd production and genes expression of *A. tinctoria* associated with *R. irregularis* before and after 9 and 37 days in an S-H cultivation system

In Experiment 1, the objective was to evaluate the production of A/Sd and the expression of genes involved in the biosynthetic pathways of A/Sd in *A. tinctoria* roots colonized (later abbreviated for fluency as M^{irr}) or not (NM) with *R. irregularis* MUCL 41833, before (T0) and after 9 (T1) and 37 days (T2) of growth in the S-H cultivation system. These harvesting times were based on the study of Cartabia et al. (2021), conducted with *Anchusa officinalis* (another Boraginaceae). The authors made a kinetic study (before the transfer of the plants to the S-H cultivation system and after 9 and 30 days of growth in the S-H cultivation system) on the effect of *R. irregularis* MUCL 41833 on the metabolites profile of *A. officinalis*. Interesting results were obtained at these harvesting times, and therefore were considered in the present study.

Two-month-old M^{irr} and NM plants were gently removed from the pots above and their roots cleaned with demineralized water to eliminate substrate debris (see **Supplementary Figure 5**). Six plants belonging to the M^{irr} and NM treatments were randomly harvested, and AMF root colonization assessed before (T0) transfer to the S-H cultivation system (see section "2.7. Plants biomass and AMF root colonization"). Fourteen additional plants from the M^{irr} and NM treatments were transferred to the S-H cultivation system as detailed in Cartabia et al. (2021). The plants were placed in 500 ml plastic bottles (VWR INTERNATIONAL, Leuven, Belgium), cut at the base and covered with a 100 µm size pore nylon mesh (Prosep B.V.B.A., Zaventem, Belgium) glued on the top. The bottles (called containers thereafter) were used bottom-up, filled with 32 g of perlite (KNAUF GMBH, Dortmund, Germany), covered with a superficial layer of black lava rock (1–3 mm) and wrapped in aluminum foil to avoid algae development and inhibition of shikonin production (as shikonin is sensitive to light) (Yazaki, 2017). The containers were transferred randomly in holes made in flex foam supports and were maintained in the greenhouse set at the same conditions as described above. A 90% P-impoverished modified Hoagland solution (see Garcés-Ruiz et al., 2017; and **Supplementary Table 2**) lacking ammonium nitrate (NH_4NO_3) [as NH_4^+ is an inhibitor of shikonin production (Yazaki, 2017)] was used at two different concentrations as detailed in Cartabia et al. (2021). After 7 days of acclimatization, the circulatory system was started. Each container was connected to a 1 L glass bottle covered with aluminum foil containing $Hoagland^{dil100X}$ solution. A 4.6 mm diameter black supply pipe (GARDENA®, Micro-Drip System, Ulm, Germany) connected a dropper cap fixed on the bottom of the plant container with the glass bottle, and another black pipe of the same diameter connected the glass bottle to the upper part of the plant container via a multichannel peristaltic pump (Gilson's Minipuls Evolution, France). Once the circulation started, the nutrient solution was pumped from the glass bottle into the plant container and the liquid flowed back by gravity into the bottle. Before starting with the circulation, initial flushing was performed as described in Cartabia et al. (2021). Then, four successive circulations were performed at a velocity of 7.5 ml min^{-1} for different durations: 42 h at day 9 (T1), 8 h at day 17, 24, and 31, and finally 42 h at day 37 (T2).

2.5. Experiment 2: A/Sd production and genes expression of *A. tinctoria* associated with different AMF strains after 9 days in an S-H cultivation system

In Experiment 2, the objective was to evaluate the production of A/Sd and the expression of genes involved in the biosynthetic pathways of A/Sd in *A. tinctoria* roots colonized (later abbreviated for fluency as M^{irr}, M^{aggreg}, M^{Rhiz}, and M^{Sept}) or not (NM) with *R. irregularis* MUCL 41833, *R. aggregatus* MUCL 49408, the native *R. irregularis* and *S. viscosum* and grown for 9 days in the S-H cultivation system. This harvesting time was based on the study of Tsiokanos et al. (2022) where different AMF strains were associated to *A. officinalis*, and plants were harvested after 9 days of growth in the S-H cultivation system. Interesting results were obtained following this harvesting time and therefore considered in the present study. The same procedure as in Experiment 1 was applied. Briefly, after cleaning the roots system, 2-month-old plants (six per treatment) were transferred in the S-H cultivation system, and the containers were randomly placed in the holes made in the flex foam supports. Then, after the acclimatization period of 7 days, a regular circulation was initiated and maintained at 7.5 ml min^{-1} for 42 h.

2.6. Experiment 3: A/Sd production and genes expression of *A. tinctoria* associated with different AMF strains in an 85 days pot-experiment in the greenhouse

In Experiment 3, the objective was to evaluate the production of A/Sd and the expression of genes involved in the biosynthetic pathways of A/Sd in *A. tinctoria* roots colonized (M^{irr}, M^{Rhiz}, and M^{Sept}) or not (NM) with *R. irregularis* MUCL 41833, the native *R. irregularis* and *S. viscosum* and growing for 85 days in pots under greenhouse conditions. In this Experiment, *R. aggregatus* MUCL 49408 was not considered due to inoculum limitation. Six plants per treatment were gently removed from the 1 L pots above and transplanted in 3 L pots (3 × 18.5 × 17 cm) containing a sterilized (2 × 121°C for 15 min) substrate mixture (2 peatmoss/2 compost/1 perlite/1 quartz 0.4–0.8 mm/1 quartz 1–2 mm). They received 200 ml $Hoagland^{dil200X}$ solution and were randomly moved every week until harvest. The plants were grown under the same conditions as for the S-H cultivation system in Experiments 1 and 2.

2.7. Plants biomass and AMF root colonization

For the three experiments, plants were harvested and biomass as well as AMF root colonization evaluated. In Experiment 1, plants were harvested before transfer to the S-H cultivation system (T0) and after 9 (T1) and 37 days (T2) corresponding to 57 and 94 days after AMF inoculation of the plants, respectively. In Experiment 2, they were harvested after 9 days (i.e., 79 days after AMF inoculation of the plants), and in Experiment 3, 85 days after AMF inoculation of the plants.

Whatever the experiment, shoots were separated from roots (cleaned under demineralized water and gently dried). Shoot fresh weigh (SFW) and roots fresh weight (RFW) were then measured. Root colonization was further evaluated by McGonigle et al. (1990). Roots (an approximate of 2 g fresh material) were cut into circa 1 cm length pieces and placed in 50-ml Falcon tubes. Twenty-five milliliter of KOH 10% was added to the roots before incubation at 70°C for 40 min. The KOH solution was then removed and replaced with H_2O_2 3.5% before incubation at 70°C for 5 min. The roots were then rinsed with demineralized water and HCl 1% was added for 1 min at room temperature. After discarding the solution, the roots were stained with ink 2% (Parker Blue Ink, United States) in HCl 1% (Walker, 2005) by placing the tubes at 70°C for 30 min. The roots were finally rinsed with demineralized water and kept in lactoglycerol (lactic acid/glycerol/distilled water, 1:1:1, v/v) until observation. For colonization assessment, the root fragments were placed on microscope slides and covered with 40 × 22 mm coverslips before observation under a bright field light microscope (Olympus BH2-RFCA, Japan) at ×10 magnification. Around 200 root intersections were observed for each plant in Experiments 1 and 2 and around 300 intersections for the plants in Experiment 3. The total colonization percentage (TC%) of roots (e.g., hyphae, arbuscules, and vesicles/spores), and arbuscules colonization percentage (AC%) was further calculated (McGonigle et al., 1990).

The remaining root system of each replicate was divided in two parts of around 5 g each for metabolites and gene expression analysis. Regarding the analysis of metabolites, roots were freeze-dried during 72 h and kept at −80°C before proceeding with A/Sd extraction (see section "2.8. Quantitative and qualitative analysis of A/Sd in *A. tinctoria* roots"). For analysis of gene expression, roots were transferred within 5–10 min after sampling into liquid nitrogen and kept at −80°C before proceeding with the RNA extraction (see section "2.9. Analysis of A/Sd target genes expression in *A. tinctoria* roots").

2.8. Quantitative and qualitative analysis of A/Sd in *A. tinctoria* roots

2.8.1. Standards stock solutions, calibration curves, and validation parameters

The standard stock solution of shikonin was serially diluted in HPLC-grade methanol to obtain a range of concentrations from 0.05 to 0.8 mg ml^{-1} (i.e., stock solution of 1 mg ml^{-1} of shikonin was prepared and diluted in HPLC-grade methanol to obtain the calibration solutions of 0.8, 0.6, 0.4, 0.2, 0.1, and 0.05 mg ml^{-1}). The calibration curve was made by plotting the average peak areas of three independent experiments versus the concentration of each analyte. The method was validated with three independent series of experiments based on total error and tolerance intervals (Hubert et al., 2003). Specificity was evaluated by analysis of an extract sample by HPLC-HRMS and comparison of MS^1 signals of blank, shikonin standard, and *A. tinctoria* extract at 0.8 µg ml^{-1}, respectively (see section "2.8.4. MS data treatment, organization, and dereplication"). Linear regression equation, response function, linearity (R^2), precision, trueness, accuracy, limit of detection (LOD), limit of quantification (LOQ), and stability were provided (see section "HPLC quantification: methodology validation" in **Supplementary material**, **Supplementary Figures 6, 7**, and **Supplementary Table 3**).

2.8.2. Samples preparation

For the three experiments, primary and secondary roots of *A. tinctoria* plants were freeze-dried separately and reduced into powder using liquid nitrogen, mortar and pestle. Fifty milligram of each root type was then mixed in glass test tube (labbox 10 ml neutral glass, TU04-160-100) closed with a plastic cap. Then, the total 100 mg of root material was subjected to a 20-min ultrasound-assisted extraction (two cycles), using *n*-hexane 97% (2 ml) at room temperature. The samples were finally centrifuged at 1,500 rpm for 10 min at 4°C and the supernatants of each cycle were combined and evaporated at room temperature. The extraction protocol was adapted from Bossard et al. (2022).

Prior to analysis, the plant extracts and nutrient solution residues were weighed and solubilized in methanol and were filtered through a 45-µm PTFE membrane (Whatman™, Maidstone, UK). Each sample was adjusted to the final concentration of 2 mg ml^{-1}, using methanol LCMS-grade.

2.8.3. HPLC-PDA and HPLC-HRMS/MS analysis

For the three experiments, the quantification of HNQ enantiomers (A/Sd) in their free form (not linked to sugars) was performed following the protocol of Bossard et al. (2022). For HPLC-PDA analysis, we used an Accela HPLC system (Thermo Fischer Scientific™, Bremen, Germany) coupled with a photodiode array (PDA) detector, an autosampler equipped with a conventional sample tray compartment with its cooler (set at 4°C), an injection system with a sample loop of 20 µl, and a quaternary pump, all piloted by ChromQuest software. The column used was an Alltech ALLTIME C8 250 × 4.6 mm, packed with 5 µm particles. Twenty microliter of sample was injected in full loop injection mode by the autosampler. The column was eluted at constant flow rate of 1 ml min^{-1} using a binary solvent system: solvent A, Milli-Q water 0.1% TFA and solvent B, ACN, isocratic mode (25% A: 75% B). Quantification analyses were conducted at a wavelength of 510 nm corresponding to the maximum absorption of A/Sd and their content was calculated according to the shikonin standard curve. The total shikonin equivalent production was calculated as the sum of peaks corresponding to A/Sd free forms (i.e., by integration of the different peaks identified as A/Sd-type compounds by their UV spectra) contained in the root powder, reported as mg g^{-1} root powder using the same shikonin standard curve (so not corresponding to an absolute quantification of each compound). Peaks were identified by comparing their retention

times (RT) and UV spectra with the standard chromatogram of shikonin. The chromatographic profiles were in agreement with the chemical profile reported by Bossard et al. (2022), for A/Sd obtained from *A. tinctoria* roots. In total, 18 M and 18 NM root samples (6 NM and 6 M^{irr} plants for each time harvest-T0, T1, and T2) were considered in Experiment 1, 30 root samples (6 M^{irr}, 6 M^{aggreg}, 6 M^{Rhiz}, 6 M^{Sept}, and 6 NM) in Experiment 2, and 24 root samples (6 M^{irr}, 6 M^{Rhiz}, 6 M^{Sept}, and 6 NM) in Experiment 3. All samples were analyzed in duplicates.

The HPLC-HRMS/MS analysis was performed at the end of Experiments 2 and 3 on an HPLC-PDA-HRMS system consisting of an Accela pump and PDA detector (Thermo Fisher Scientific™, Bremen, Germany) connected with a LTQ orbitrap XL mass spectrometer (Thermo Fisher Scientific™, Bremen, Germany). The instrument was controlled using a Thermo Fisher Scientific™ Xcalibur X software. The LC separation was done as reported above except for the solvent A: Milli-Q water 0.1% formic acid (FA). The chromatograms were recorded between 200 and 600 nm. HRMS analyses were realized in ESI positive and negative modes with the following inlet conditions for the positive mode: capillary temperature 250°C; sheath gas flow 10 a.u.; auxiliary gas flow 5 a.u. and sweep gas flow 5 a.u; ionization spray voltage 3 kV; capillary voltage of 15 V; tube lens voltage of 90 V. For negative mode, the only differences from the positive mode were the capillary voltage (−10 V) and tube lens voltage (−125 V). The data-dependent MS/MS events were performed on the three most intense ions detected in full scans MS. Peaks were tentatively identified by comparing their HRMS and MS/MS spectra with the literature data of A/Sd.

2.8.4. MS data treatment, organization, and dereplication

All HRMS run data (.RAW) files were treated using MZmine software suite version 2.5.3 (Pluskal et al., 2010). For mass detection at MS^1 level, the noise level was set to 1.5×10^4 for positive mode and to 8.5×10^3 for negative mode. For MS^2 detection, the noise level was set to 1. The ADAP chromatogram builder was used and set to a minimum group size of scans of 4, a minimum group intensity of 1.0×10^4, a minimum highest intensity of 1.0×10^4, and *m/z* tolerance of 8 ppm. The ADAP algorithm (wavelets) was used for chromatogram deconvolution. The intensity window signal to noise (S/N) was used as a S/N estimator with S/N ratio set at 10, a minimum feature height of 1.0×10^4, a coefficient area threshold of 25, a peak duration ranging from 0.02 to 0.8 min, and a RT wavelet range from 0.02 to 0.2 min. Isotopes were detected using the isotope peak grouper with a *m/z* tolerance of 8 ppm, a RT tolerance of 0.02 min (absolute), a maximum charge set at 1, and the representative isotope used was the most intense. Then, the aligned list peak was gap-filled with RT range of 0.05 min and *m/z* tolerance of 8 ppm. The resulting list was filtered using the peak list rows filter option to remove all the duplicates and all the features without MS^2 spectrum associated.

A molecular network was constructed from the .mgf file exported from MZmine, using the online workflow on the GNPS website (Wang et al., 2016). The precursor ion mass tolerance was set to 0.02 Da with a MS/MS fragment ion tolerance of 0.02 Da. A network was then created where edges were filtered to have a cosine of 0.7 and more than 3 matched peaks. The spectra in the network were then searched against GNPS's spectral libraries filtered under the same conditions as before. Putative identification was carried out comparing available MS/MS fragmentation patterns from the literature. Data visualization was achieved using Cytoscape 3.8.0 (Shannon et al., 2003). Peak area data from the .csv file obtained from MZmine was added to the network. Size nodes were set proportionally to the total area of each peak detected in both analyzed extracts.

2.9. Analysis of A/Sd target genes expression in *A. tinctoria* roots

2.9.1. Total RNA extraction

Frozen roots of each replicate were ground in liquid nitrogen (−196°C) with a pestle and mortar. Total RNA extraction was done on 0.2 g root material using the protocol from Xu et al. (2010) slightly modified. Main differences were in the extraction buffer composition and in the last steps of the protocol, where the pellet was washed with 70% ethanol and the total RNA was dissolved in 55 µl DEPC-treated water. Further, the total RNA was treated with TURBO DNA-free™ Kit (Thermo Fisher Scientific™, Belgium), according to the manufacturer protocol. The RNA of all samples was loaded on 1.5% agarose gel, electrophoresed to separate RNA, stained with GelRed® (Biotium, United States), and visualized under UV light to assess the integrity of ribosomal bands. Moreover, concentration of each RNA sample was measured using NanoDrop-ND 1000 UV-vis Spectrophotometer (NanoDrop® Technologies, United States) and RNA purity estimated from the A260/A280 and A260/A230 absorbance ratios. Finally, a 1 µg aliquot of total RNA was used for the first-strand cDNA synthesis according to the protocol of the Transcriptor High Fidelity cDNA Synthesis Kit (Roche, Montreal, QC, Canada). For each RNA sample, a reaction without Transcriptor High Fidelity Reverse Transcriptase (Hifi RT) enzyme was performed as a control for contamination by genomic DNA.

Five biological replicates (i.e., means of relative genes expression) for M and NM treatments at each time harvest (T0, T1, and T2) were considered in Experiment 1, six biological replicates for treatments M^{irr}, M^{aggreg}, M^{Rhiz}, M^{Sept}, and NM in Experiment 2, and six biological replicates for treatments M^{irr}, M^{Rhiz}, and NM and five for M^{Sept} in Experiment 3.

For all the experiments, tissue samples for A/Sd and molecular determinations were simultaneously collected at the same period of the day, between 9:00 and 11:00 a.m.

2.9.2. Real-time quantitative PCR

For RT-qPCR, the expression of three target genes: *LePGT1*, *LePGT2*, and *GHQH* involved in the shikonin (A/Sd) biosynthesis was analyzed (see section "Analysis of A/Sd target genes expression in *A. tinctoria* roots" in **Supplementary material** and **Supplementary Table 4**). Since no published genomic resources are available for *A. tinctoria*, a previously published primer for amplification of *LePGT1* in *Onosma paniculatum* Bur. et Franch was used, while for *PGT2* and *GHQH* new primer pairs were designed. Sequences of each gene (*LePGT2* or *GHQH*) from two phylogenetically distant Boraginaceae species (*L. erythrorhizon* and *A. euchroma*) were obtained from NCBI, aligned, and primers

generated from conserved regions (see section "Alignments used to design primers" in **Supplementary material**). The glyceraldehyde-3-phosphate dehydrogenase gene (*GAPDH*) was used as internal reference control. RT-qPCR was performed using a LightCycler® FastStart Essential DNA Green Master (Roche) in 10 μl volume of reaction formed as follows: 5 μl Master mix (or Mix SYBR 2x), 0.5 μl of each primer from the pair (10 μM), and 4 μl cDNA (dil 5x). The reaction was carried out in a Roche LightCycler® 96 System using the following parameters: 10 min at 95°C, followed by 40 (for housekeeping gene) and 50 (for target genes) cycles of denaturation (95°C, 10 s)/annealing (60°C housekeeping gene/56°C target genes, 15 s)/extension (72°C, 10 s), and finalized by a standard melting curve analysis (95°C). Reactions were performed in three replicates. Normalization was achieved for each experiment separately using the reference gene (i.e., *GAPDH*) and the "Pfaffl" method (Pfaffl, 2001).

2.10. Statistical analysis

For all the experiments, a one-way ANOVA followed by HSD Tukey *post-hoc* test ($p < 0.05$) was applied to discriminate between means for plant growth parameters (i.e., SFW, RFW, and TFW), AMF colonization (i.e., TC% and AC%), A/Sd content, and relative genes expression at different time points (Experiment 1) or different AMF treatments (Experiments 2 and 3). Moreover, in Experiment 1, differences between M and NM treatments were highlighted by pairwise comparison with Bonferroni correction ($p < 0.05$) at each harvesting time (T0, T1, and T2). For all parameters, normal distribution of residuals variance and normality was checked before analyses. Non-normal data were normalized by log10 transformation before analysis. Data analyses were performed by IBM SPSS Statistics for Windows, version 28 (IBM Corp., Armonk, N.Y., USA).

3. Results

3.1. Plants biomass and root colonization by AMF

In Experiment 1, no significant differences between harvesting times (before plants transfer to the containers-T0, and after 9-T1 and 37-T2 days of growth in the S-H cultivation system) were noticed for SFW, RFW, and TFW of plants in the M^{irr} treatment and for SFW of plants in the NM treatment. Conversely, a significantly greater RFW was noticed at T1 and T2 as compared to T0, and greater TFW at T2 compared to T0 for plants in the NM treatment. Irrespective of the harvest time, no significant difference was reported between the SFW of plants in the M^{irr} and NM treatments, while at T2, the RFW and TFW of the plants in the NM treatment was significantly greater than that in the M^{irr} treatment. In the M^{irr} treatment, a significant decrease in TC% was observed at T2 compared to T0 and T1 and in AC% at T1 and T2 compared to T0 (**Table 1**). No root colonization was observed in plants of the NM treatment.

In Experiment 2, no significant differences were observed in SFW, RFW and TFW and in TC% between the different treatments (M^{irr}, M^{aggreg}, M^{Rhiz}, M^{Sept}, and NM) after 9 days of growth of the plants in the S-H cultivation system. Conversely, a significant higher AC% was observed for the plants in the M^{Rhiz} treatment compared to those in the M^{aggreg} treatment, while intermediate values were noticed in the plants of the M^{Sept} and M^{irr} treatments (**Table 1**). No root colonization was observed in plants of the NM treatment.

In Experiment 3, no significant differences were observed in SFW and RFW of plants between the different treatments (M^{irr}, M^{Rhiz}, M^{Sept}, and NM) after 85 days of growth in pots. Similarly, no significant differences were observed for TC% between the different treatments, while a significantly higher AC% was observed for the plants in the M^{Sept} treatment compared to those of the M^{irr} treatment. Plants in the M^{Rhiz} treatment had intermediate value (**Table 2**). No root colonization was observed in plants of the NM treatment.

3.2. Alkannin/shikonin and their derivatives content

In Experiment 1, whatever the harvesting time (T0, T1, or T2) or treatment (M^{irr} or NM) no significant differences in content of A/Sd were noticed (**Table 1**).

In Experiment 2, a significant higher content of total A/Sd expressed as shikonin equivalent was observed in the plants of the M^{Rhiz} treatment compared to those in the M^{irr}, M^{agreeg}, and NM treatments, while an intermediate value was observed for the plants in the M^{Sept} treatment (**Table 1**).

In Experiment 3, a significantly higher content of shikonin, whose values were nevertheless below the LOQ (**Supplementary Table 2**), and in total A/Sd expressed as shikonin equivalent, was reported in the roots of the plants in the M^{Rhiz} treatment compared to those in the M^{irr} and NM treatments, while an intermediate value was observed for the plants in the M^{Sept} treatment (**Table 2**).

3.3. Alkannin/shikonin and their derivatives target genes expression

In Experiment 1, whatever the time of evaluation (T0, T1, or T2) or treatment (M^{irr} or NM) no significant differences were noticed in gene expression of *GHQH*. Similarly, no significant differences between harvesting times were observed in expression of *LePGT1* gene of the plants in the M^{irr} treatment and expression of *LePGT1* and *LePGT2* genes of the plants in the NM treatment. Conversely, a significantly higher expression of LePGT2 gene was observed at T2 compared to T1 for the plants in the M^{irr} treatment, while an intermediate gene expression was noticed at T0. A significant higher relative expression of both *LePGT1* and *LePGT2* genes was observed in the plants of the M^{irr} treatment compared to those in the NM treatment at T2 (**Figure 1A**).

In Experiment 2, whatever the treatment (M^{irr}, M^{aggreg}, M^{Rhiz}, M^{Sept}, and NM), no significant differences were observed in expression of *GHQH* and *LePGT1* genes. A significant lower relative expression of *LePGT2* was observed in the plants of the M^{Rhiz} treatment compared with the other treatments that did not differ among them (**Figure 1B**).

TABLE 1 Shoot, root and total fresh weights (SFW, RFW, and TFW, respectively), total colonization percentage (TC%), arbuscules colonization percentage (AC%), and total A/Sd expressed as shikonin equivalent content of *A. tinctoria* plants inoculated (M^{irr}) or not (NM) with *R. irregularis* MUCL 41833 before (T0) and after 9 (T1) and 37 (T2) days in the S-H cultivation system (Experiment 1), and of *A. tinctoria* plants inoculated (M^{irr}, M^{aggreg}, M^{Rhiz}, M^{Sept}) or not (NM) with different AMF strains (two from GINCO – *R. irregularis* MUCL 41833 and *R. aggregatus* MUCL 49408, and two isolated from wild *A. tinctoria* – *R. irregularis* and *S. viscosum*) after 9 days in the S-H cultivation system (Experiment 2).

Experiment 1							
Treatments	Time	SFW (g)	RFW (g)	TFW (g)	TC%	AC%	Total shikonin equivalent mg g^{-1} root powder
M^{irr}	T0	14 ± 2.3	10 ± 1.6	24 ± 2.4	61 ± 7 a	34 ± 4 a	3.3 ± 1.5
	T1	13 ± 2.7	10.8 ± 2.2	23.7 ± 3.6	53 ± 7 a	17 ± 5 b	1.9 ± 1.5
	T2	13 ± 1.2	12.4 ± 1.1*	25.7 ± 2*	29 ± 4 b	12 ± 3 b	2.1 ± 1
NM	T0	13.5 ± 2	7.9 ± 2.3 b	21.4 ± 3.8 b	–	–	2.5 ± 1
	T1	14.2 ± 2	11 ± 2.4 a	25.2 ± 3.7 ab	–	–	2.6 ± 1.1
	T2	13.6 ± 0.6	14 ± 1 a*	28 ± 1 a*	–	–	2.3 ± 0.7
Experiment 2							
Treatments		SFW (g)	RFW (g)	TFW (g)	TC%	AC%	Total shikonin equivalent mg g^{-1} root powder
M^{Rhiz}		9.8 ± 1	11.3 ± 1	21 ± 1.8	44 ± 7	21 ± 5 a	8.7 ± 1.3 a
M^{Sept}		11.1 ± 2	13.1 ± 2.6	24.2 ± 1	39 ± 9	17 ± 7 ab	6.8 ± 2.2 ab
M^{irr}		11.2 ± 1	12.8 ± 1.7	24.2 ± 2.4	42 ± 6	16 ± 2 ab	4.3 ± 2.1 b
M^{aggreg}		10.3 ± 5	11 ± 3.3	20 ± 5	43 ± 9	12 ± 4 b	5 ± 0.6 b
NM		10.3 ± 2	11 ± 2.1	21.5 ± 3.3	–	–	4.9 ± 1.9 b

The parameters measured are expressed as mean ± standard deviation (SD) of five replicates per treatment (M^{irr} and NM) and harvesting time (T0, T1, and T2) in Experiment 1, and 6 replicates per treatment (M^{irr}, M^{aggreg}, M^{Rhiz}, M^{Sept}, and NM) in Experiment 2. Means followed by different lowercase letters within the same column are significantly different according to HSD Tukey *post-hoc* test ($p < 0.05$) (Experiments 1 and 2). Means followed by asterisk within the same column are significantly different according to pairwise comparison with Bonferroni correction ($p < 0.05$) (Experiment 1).

TABLE 2 Shoot and root fresh weights (SFW and RFW, respectively), total colonization percentage (TC%), arbuscules colonization percentage (AC%), shikonin, and total A/Sd expressed as shikonin equivalent of *A. tinctoria* inoculated (M^{irr}, M^{Rhiz}, and M^{Sept}) or not (NM) with different AMF strains (one from GINCO – *R. irregularis* MUCL 41833, and two isolated from wild *A. tinctoria* – *R. irregularis* and *S. viscosum*) after 85 days in pots under greenhouse conditions (Experiment 3).

Treatments	SFW (g)	RFW (g)	TC%	AC%	mg shikonin g^{-1} root powder	Total shikonin equivalent mg g^{-1} root powder
M^{irr}	15.8 ± 2	13.3 ± 2.6	25 ± 6.6	4 ± 2 b	0.04 ± 0.01 b	7.2 ± 1 b
M^{Rhiz}	17.7 ± 0.6	14 ± 2.1	23 ± 16	8 ± 10 ab	0.12 ± 0.07 a	9.6 ± 0.7 a
M^{Sept}	16.3 ± 2.3	12.8 ± 1.7	25 ± 13	22 ± 11 a	0.06 ± 0.02 b	7.8 ± 1 b
NM	16.1 ± 1.3	14.4 ± 0.6	–	–	0.04 ± 0.01 b	8 ± 1 b

The parameters measured are expressed as mean ± standard deviation (SD) of six replicates per treatment (M^{irr}, M^{Rhiz}, M^{Sept}, and NM). Means followed by different lowercase letters within the same column are significantly different according to HSD Tukey *post-hoc* test ($p < 0.05$).

In Experiment 3, *LePGT2* target gene was not considered due to contamination by the primer dimer. Whatever the treatment (M^{irr}, M^{Rhiz}, M^{Sept}, and NM), no significant differences were observed in expression of *GHQH* and *LePGT1* genes (data not presented).

3.4. HPLC-HRMS/MS analysis

To better recognize the metabolites produced in *A. tinctoria* roots, the main chemical compounds were tentatively identified in Experiments 2 and 3 by performing a dereplication strategy based on HPLC-HRMS/MS analysis (Figure 2 and Tables 3, 4) and molecular network representation (Figures 3–5). These analyses were not performed in Experiment 1, since no significant differences were reported in the production of A/Sd.

In Experiment 2, the HPLC-HRMS/MS analysis was performed in positive and negative modes. However, shikonin was not detected in any root sample analyzed. Dereplication analyses of shikonin derivatives were done on positive mode to compare our results with published data available in the literature (Bossard et al., 2022). The major detected compounds were organized in two distinctive clusters: A/Sd naphthoquinones (cluster A, Figures 3A and Table 3) and lipid amides derivatives (cluster B, Figure 3B and Table 3). In cluster A, the first eluted derivative

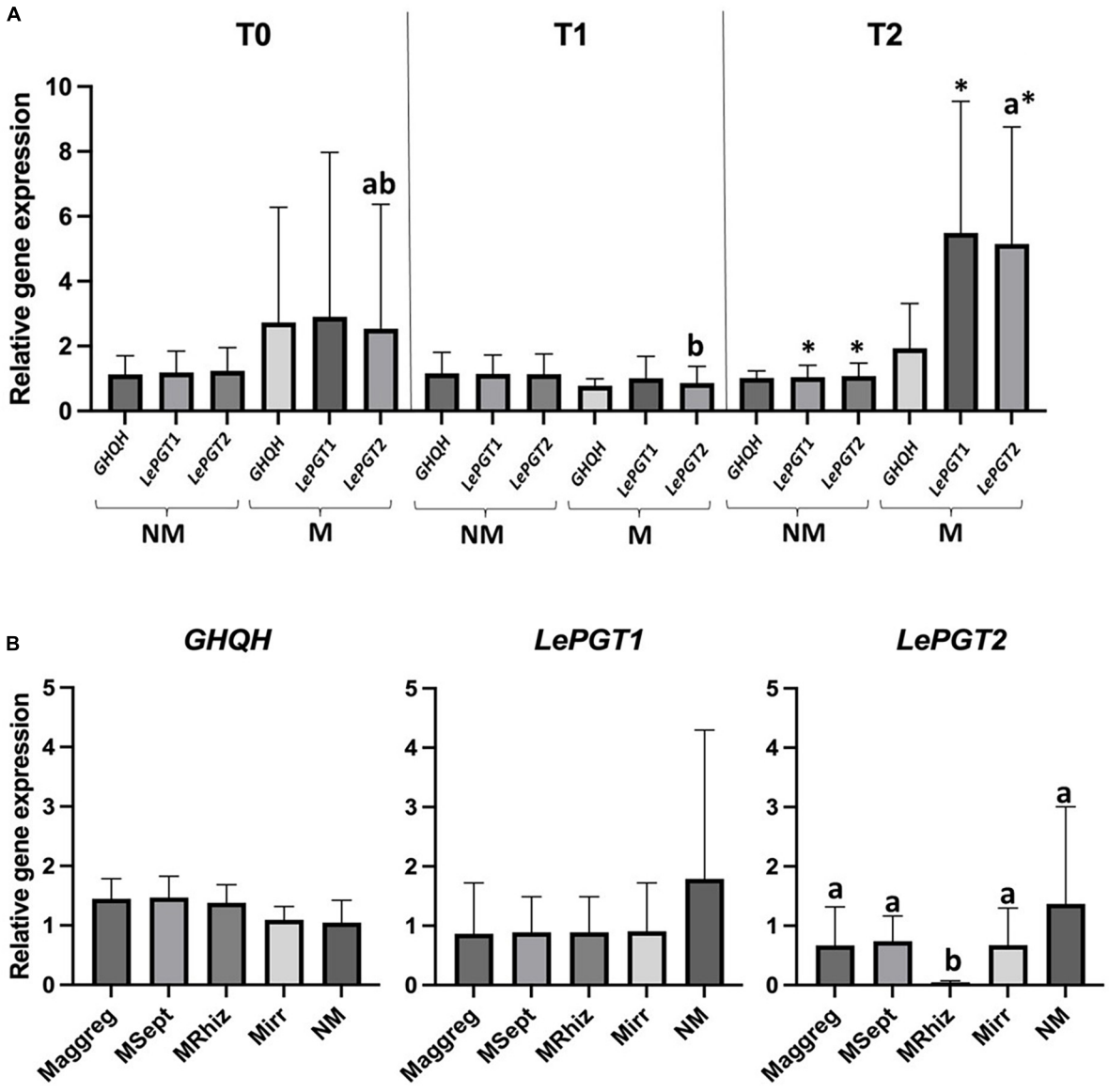

FIGURE 1
(A) Graphical representation of RT-qPCR relative genes expression analysis of *GHQH*, *LePGT1*, and *LePGT2* in *A. tinctoria* roots inoculated (M^{irr}) or not (NM) with *R. irregularis* MUCL 41833 before (T0) and after 9 (T1) and 37 (T2) days in the S-H cultivation system (Experiment 1); **(B)** graphical representation of RT-qPCR relative genes expression analysis of *GHQH*, *LePGT1*, and *LePGT2* in *A. tinctoria* roots inoculated (M^{irr}, M^{aggreg}, M^{Rhiz}, and M^{Sept}) or not (NM) with different AMF strains (two from GINCO – *R. irregularis* MUCL 41833 and *R. aggregatus* MUCL 49408, and two isolated from wild *A. tinctoria* – *R. irregularis* and *S. viscosum*) after 9 days in the S-H cultivation system (Experiment 2). Means followed by different lowercase letters within the same column are significantly different according to HSD Tukey *post-hoc* test ($p < 0.05$). Means followed by asterisk within the same column are significantly different according to pairwise comparison with Bonferroni correction ($p < 0.05$).

was putatively identified as a methylshikonin isomer (1) which gave a protonated molecular ion $[M + H]^+$ at *m/z* 303 and fragmented to *m/z* 285, 243, and 233, corresponding to the loss of a H_2O molecule, a $C_2H_4O_2$ and a C_5H_{10} fragment from the alkyl chain. Similar fragmentation pattern was observed for compound 4 with a protonated dehydrated molecular ion $[M + H\text{-}H_2O]^+$, putatively identified as a second methylshikonin derivative. Similar loss was observed for compounds 3 and 6, putatively corresponding to methyl-1′-deoxyshikonin and anhydroalkannin at *m/z* of 287 and 271, respectively. Data also indicated that the major shikonin derivative produced by the plants under these conditions was anhydroalkannin (6) (Kyogoku et al., 1973; Bai and Jin, 1994). Moreover, a group of lipid amides were also putatively detected from the *A. tinctoria* roots samples and represented in cluster B. These amides derivatives were tentatively identified as palmitoleamide (7), linoleamide (8), oleamide (9), and stearamide (10) with protonated molecular ions $[M + H]^+$ at *m/z* 254, 280, 282, and 284, presenting a loss of a fragment of *m/z* 17, corresponding to the loss of an ammoniac molecule (Divito et al., 2012). Other isomeric compounds were also detected by HPLC-HRMS/MS, but in the absence of their fragmentation patterns, putative identities were not proposed. No significant differences were noticed in the metabolites' production profile of *A. tinctoria* roots associated or not with different AMF strains (**Figure 4**).

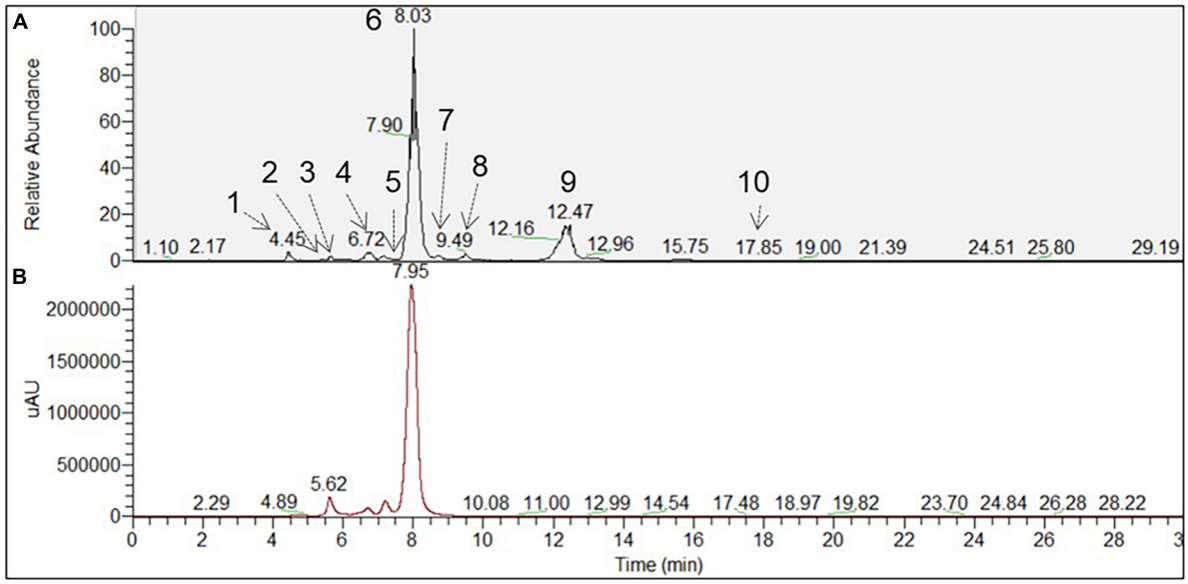

FIGURE 2
Chromatographic profile of *A. tinctoria* root samples associated with *Septoglomus viscosum* detected under **(A)** HPLC-MS (BP+) and **(B)** HPLC-PDA (510 nm). Each peak defined by a number referred to a tentative identified compound, which has been described in **Table 4**.

In Experiment 3, shikonin was detected only in negative mode and this result was corroborated by co-injection with shikonin standard solution (**Table 4**). Due to the important differences in the fragmentation spectra in positive mode of A/Sd, clusters of these compounds were not formed (**Figure 5**). In addition, the abovementioned shikonin derivatives isomers (1 and 6) were also observed as deprotonated molecular ion $[M-H]^-$ at *m/z* 301 with fragmentation signals at *m/z* 286 and 232 corresponding to the loss of a CH_3 and C_5H_9 groups, for 1, and at *m/z* 269 with fragment loss at *m/z* 251 and 241, corresponding to the loss of a H_2O and CO molecules, for 6. The deprotonated molecular ion $[M-H]^-$ of shikonin (11) was observed at *m/z* 287 with fragmentation signals at *m/z* 218 and 190, corresponding to the loss of C_5H_9 and the subsequent loss of a CO group (Liao et al., 2015). Moreover, an additional shikonin derivative was observed with a deprotonated molecular ion $[M-H]^-$ at *m/z* 329, putatively identified as acetylshikonin (13), with fragmentation loss at *m/z* 269, 251, and 241 corresponding to a McLafferty rearrangement (i.e., neutral loss of acetic acid), and the subsequent loss of a H_2O and CO molecules (Liao et al., 2015). Three others unidentified compounds (12, 14, and 15) were detected under negative ionization mode with deprotonated molecular ion $[M\text{-}H]^-$ at *m/z* 797, 1111, and 1147. However, no clusters were observed between compounds 1, 6, 11, and 13 (shikonin derivatives) and for 12, 14, and 15 (unknown compounds) because they show a low degree of similarities in their fragmentation spectra (in positive ionization mode).

Slight differences in metabolites production were observed between Experiments 2 and 3, when samples were analyzed in the same ionization mode. Nevertheless, the most important difference between the two experiments was the detection of shikonin only in Experiment 3. Analyses performed in negative mode for root samples of Experiment 2 did not show the presence of shikonin. Similarly, in Experiment 3, no significant differences were observed in the metabolites' production profile of *A. tinctoria* roots associated or not with different AMF strains, thus producing similar chromatographic profiles.

4. Discussion

In the present study, two native AMF strains isolated from *A. tinctoria* roots and two strains from GINCO were tested and compared on the production of A/Sd and on the expression of genes involved in A/Sd biosynthesis in *A. tinctoria* plants grown either in a semi-hydroponic or in a pot cultivation system. In Experiment 1, conducted only with the GINCO strain *R. irregularis* MUCL 41833, no effect was observed on the production of A/Sd, while a significantly higher relative expression of LePGT2 was observed after 37 days compared to 9 days of growth in the S-H cultivation system. Furthermore, the relative expression of *LePGT1* and *LePGT2* genes were significantly higher in the plants colonized with this AMF compared to the non-mycorrhized ones. In Experiment 2, four AMF strains (two from GINCO: *R. irregularis* MUCL 41833 and *R. aggregatus* MUCL 49408 and two isolated from *A. tinctoria*: *R. irregularis* and *S. viscosum*) were associated to *A. tinctoria* in the S-H cultivation system. The native strain *R. irregularis* significantly increased the production of A/Sd in the roots of *A. tinctoria*, although this was not accompanied by an increased expression of genes involved in the A/Sd biosynthesis pathway. In Experiment 3, the two native strains (*R. irregularis* and *S. viscosum*) and the GINCO one (*R. irregularis* MUCL 41833) were associated to *A. tinctoria* in pots. The native strain *R. irregularis* was confirmed to significantly enhance the content of shikonin and total A/Sd in *A. tinctoria* roots. However, no significant increase in relative genes expression was observed.

TABLE 3 Putative identification of major chemical constituents in *A. tinctoria* extracts from Experiment 2 (positive mode ESI).

	Code	Retention time (min)	UV	(*m/z*)	MS major ion(s)	Molecular formula	Δ ppm	Δ mDa	MS/MS fragments (*m/z*)	Putative identification
Cluster A	1	4.60	513, 272	303.1224	$[M + H]^+$	$C_{17}H_{18}O_5$	−2.80	−0.85	285.1119 243.1013 233.0442	Methylshikonin isomer I
	2	5.41	n.d.	220.1119	$[M + H]^+$	$C_{16}H_{13}N$	−3.29	−0.72	205.0883 142.0648 128.0618	*N*-phenyl-naphthylamine
	3	5.66	515, 272, 489	287.1267	$[M + H]^+$	$C_{17}H_{18}O_4$	−5.69	−1.63	219.0649 269.1168 231.0648 245.0804	*O*-methyl-1′-deoxyshikonin
	4	6.74	415, 258	285.1125 303.1228	$[M + H\text{-}H_2O]^+$ $[M + H]^+$	$C_{17}H_{18}O_5$	−0.65	−0.18	267.1012 243.0649 233.0443	Methylshikonin isomer II
	5	7.16	n.d.	403.2317	$[M + H]^+$	$C_{20}H_{34}O_8$	−3.70	−1.49	361.2221 329.1594 273.0968 213.0757	Not identified
	6	8.00	517, 484, 281	271.0955 541.1843	$[M + H]^+$ $[2M + H]^+$	$C_{16}H_{14}O_4$	−5.66	−1.53	229.0493 253.0855 165.0181 191.0338 179.0338 243.1014	Anhydroalkannin
Cluster B	7	8.76	n.d.	254.2475	$[M + H]^+$	$C_{16}H_{31}NO$	−3.50	−0.89	237.2209 219.2104	Palmitoleamide
	8	9.52	n.d.	280.2627 559.5198	$[M + H]^+$ $[2M + H]^+$	$C_{18}H_{33}NO$	−4.78	−1.34	263.2365 245.2260	Linoleamide
	9	12.33	n.d.	282.2793 563.2793	$[M + H]^+$ [2M + H] +	$C_{18}H_{35}NO$	−1.38	−0.39	265.2522 247.2417	Oleamide
	10	17.87	n.d.	284.2943	[M + H] +	$C_{18}H_{37}NO$	−3.66	−1.04	267.2267	Stearamide

Δm, mass errors; $[M - H]^+$, *m/z* of the protonated molecular ion in positive ionization mode; *m/z*, mass to charge ratio.

10.3389/fmicb.2023.1216029

10.3389/fmicb.2023.1216029

TABLE 4 Putative identification of major chemical constituents in *A. tinctoria* extracts (Experiment 3, negative mode, ESI).

Code	Retention time (min)	UV	(*m/z*)	MS major ion(s)	Molecular formula	Δ ppm	Δ mDa	MS/MS fragments (*m/z*)	Putative identification
1	4.60	513, 272.	301.1086	$[M-H]^-$	$C_{17}H_{18}O_5$	3.30	1.00	286.0847 232.0375	Methylshikonin isomer I
11	4.78	515, 274, 490	287.0934	$[M-H]^-$	$C_{16}H_{16}O_5$	5.06	1.45	218.0227 190.0273	Shikonin
12	5.26	n.d.	797.2762	$[M-H]^-$	$C_{33}H_{50}O_{22}$	5.83	4.65	527.1894	Not identified
13	5.85	516, 274, 490	329.1030	$[M-H]^-$	$C_{18}H_{18}O_6$	1.48	0.49	269.0829 251.0709 241.0865	Acetylshikonin
14	7.62	n.d.	1,111.3696	$[M-H]^-$	$C_{47}H_{68}O_{30}$	−1.90	−2.12	841.2741 571.1847 1023.3120	Not identified
15	7.98	n.d.	1,147.3676	$[M-H]^-$	$C_{50}H_{68}O_{30}$	−3.59	−4.12	877.2743 607.1854 1047.3101	Not identified
6	8.00	517, 484, 281	269.0829	$[M-H]^-$	$C_{16}H_{14}O_4$	5.63	1.52	251.0712 241.0868	Anhydroalkannin

Δm, mass errors; $[M-H]^-$, *m/z* of the deprotonated molecular in negative ionization mode; *m/z*, mass to charge ratio.

4.1. The S-H and pot cultivation systems are adequate for growth and AMF colonization of *A. tinctoria*

Whatever the growth system (S-H or pot), an increase in biomass of *A. tinctoria* was observed in the presence as well as absence of AMF. No significant difference was observed in SFW between the plants in the M and NM treatments after 9 days in the S-H cultivation system (Experiments 1 and 2) or after 85 days in the pots cultivation system (Experiment 3). However, a significantly lower RFW and TFW was reported for the plants in the M treatment compared to those in the NM treatment after 37 days in the S-H cultivation system (Experiment 1), unlike the results obtained with *A. officinalis* colonized by *R. irregularis* MUCL 41833 in the same S-H cultivation system (Cartabia et al., 2021). These results are not surprising as it has often been reported that plant growth response to AMF inoculation can vary among AMF species and that the direction (e.g., increase or decrease in plant biomass) and magnitude of the response strongly depends on the combination of plant and AMF taxa (Klironomos, 2003).

Root colonization was observed in each AMF-inoculated plant. However, colonization measured at transfer and after 9 and 37 days in the S-H cultivation system (Experiment 1), decreased steadily, probably because of damages caused to the extraradical mycelium at transfer to the S-H cultivation system with no full recovery and development within the roots throughout the experiment (Cartabia et al., 2021). It is not excluded that this is also a reason for the lower plant biomass reported at the end of Experiment 1 compared to the control, due to an imbalance between the carbon resources transported from plant to the fungus in exchange for nutrients transported from fungus to plant. Interestingly, in both Experiments 2 and 3, the total root colonization was almost similar among the AMF strains, while the percentages of arbuscules were higher in presence of the native *R. irregularis* and *S. viscosum* strains, suggesting that they were better adapted to *A. tinctoria* than the GINCO strains. This has often been reported by comparing commercial strains with local strains; the latter being more prone to rapid and effective colonization (Chenchouni et al., 2020; Wu et al., 2021). Unfortunately, this was not translated into higher plant biomass, probably because of the same justification explained above.

4.2. AMF isolated from wild *A. tinctoria* impact the production of A/Sd

The production of A/Sd was not impacted by the GINCO strain *R. irregularis* MUCL 41833 (Experiment 1), whereas a significant increase in production was observed with the native *R. irregularis* strain (Experiments 2 and 3) and an intermediate production between this strain and the GINCO strains with the other native strain *S. viscosum* (Experiment 2). Similarly, no significant effect was observed with the GINCO strains *R. irregularis* MUCL 41833 and *R. aggregatus* MUCL 49408 (Experiments 2 and 3). It cannot be ruled out that these results are related to the fungal genotypes, with the native ones being more prone to stimulate the production of A/Sd than the GINCO ones. The difference between the two native strains further suggests some degree

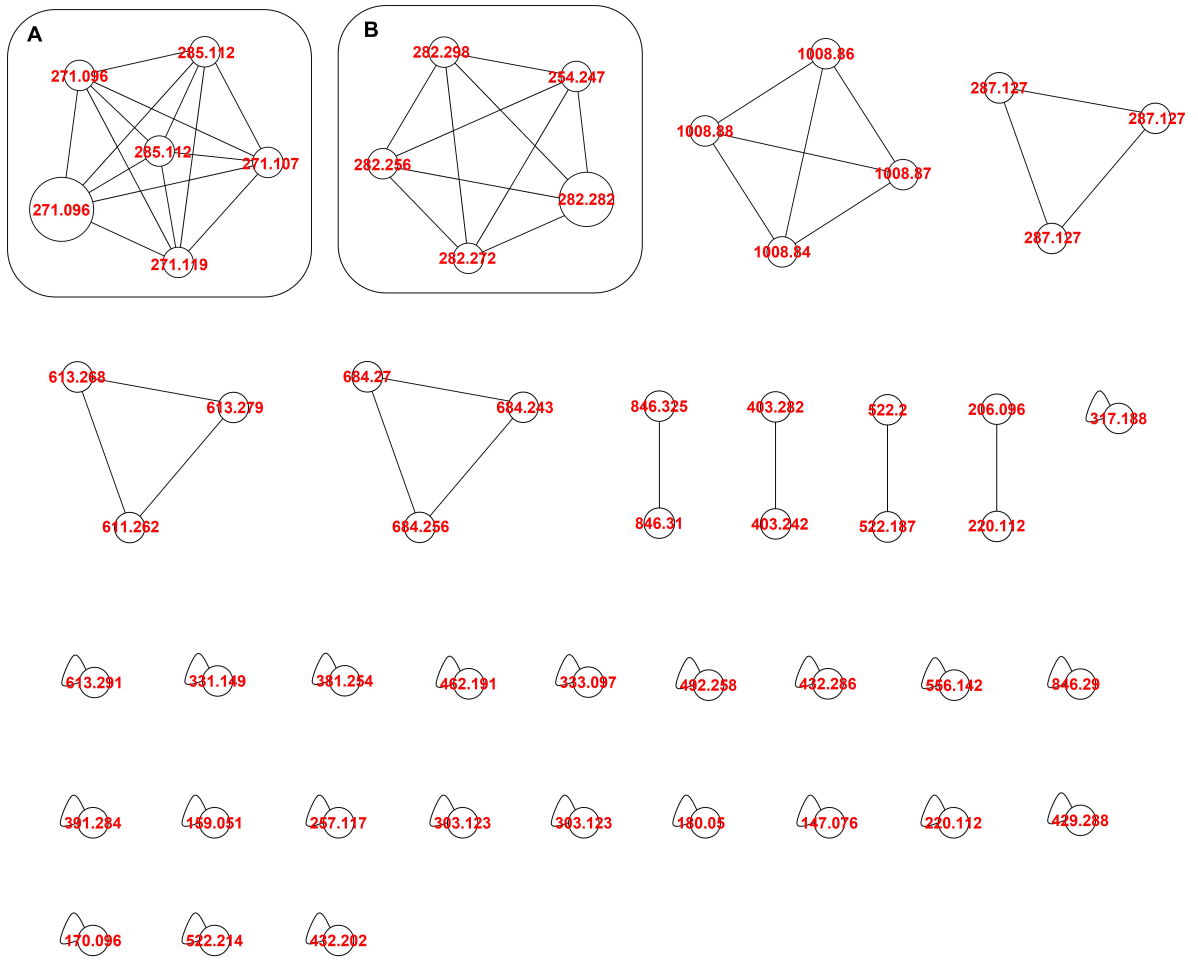

FIGURE 3
Molecular network of *A. tinctoria* root extracts obtained in Experiment 2 in positive mode. **(A)** HNQ naphthoquinone's enantiomers (A/Sd); **(B)** lipid amides. Clusters were built with a cosine of 0.7 with a minimum of 3 common ions. Size nodes are proportional to corresponding peak area.

of functional specialization. This is supported by recent studies revealing that various species/strains of AMF can induce different changes in the production of metabolites in the same plant species (Kapoor et al., 2002; Larose et al., 2002; Copetta et al., 2006; Khaosaad et al., 2006; Toussaint et al., 2007; Zubek et al., 2010). For example, Toussaint et al. (2007) showed that *Funneliformis caledonium*[2] increased rosmarinic acid and caffeic acid production in *O. basilicum*, whereas *Funneliformis mosseae* only increased caffeic acid production. In another study, Jurkiewicz et al. (2010) showed that total phenolic acids accumulation was significantly higher in the roots of *Arnica montana* L. associated with AMF collected from particular plant's natural stands (in Kurpie or in Karkonosze), while intermediate increase was observed with AMF isolated from other regions (i.e., *R. intraradices* UNIJAG PL24-1 and *R. intraradices* BEG 140 or a mixture composed of the above and of *Funneliformis geosporum* UNIJAG PL 12-2, *Septoglomus constrictum* 265-5 Walker and *F. mosseae* BEG 12). Finally, Frew (2020) reported that the inoculation with a mixture of four commercial species of AMF (*Claroideoglomus etunicatum*, *Funneliformis coronatum*, *F. mosseae*, and *R. irregularis*) had a greater effect on phenolic concentrations in *Hordeum vulgare* L. cv. "Hindmarsh" as compared to a single commercial inoculant (*R. irregularis*). Interestingly, the author also demonstrated that the effects of the commercial mixture was not different from the results obtained with a native multi-species AMF inoculant extracted from field soil. This suggested that a commercial AMF mixture provided little to no additional benefits (Frew, 2020). Conversely, several specialized compounds produced by plants may be synthesized as a chemical defense against the presence of AMF in the roots (Copetta et al., 2006). However, this defense mechanism would be likely to occur with AMF strains that have never been associated to the plant. Our native strains isolated from the wild *A. tinctoria* in their natural habitat are more adapted to the plant and are likely to have evolved as good associates. Natives *R. irregularis* and *S. viscosum* could be better adapted to the presence of A/Sd, which are characterized by different biological activities and by various effects on soil microorganisms (e.g., antifungal activities), and thus better interact with their host plants to regulate and enhance the production of these important therapeutic metabolites (Yan et al., 2019). As reported above, a significant higher AC% was observed with M^{Rhiz} and M^{Sept}

2 It is to be noticed that the species names of AMF follow the nomenclature of today not the one at the time of publication.

10.3389/fmicb.2023.1216029

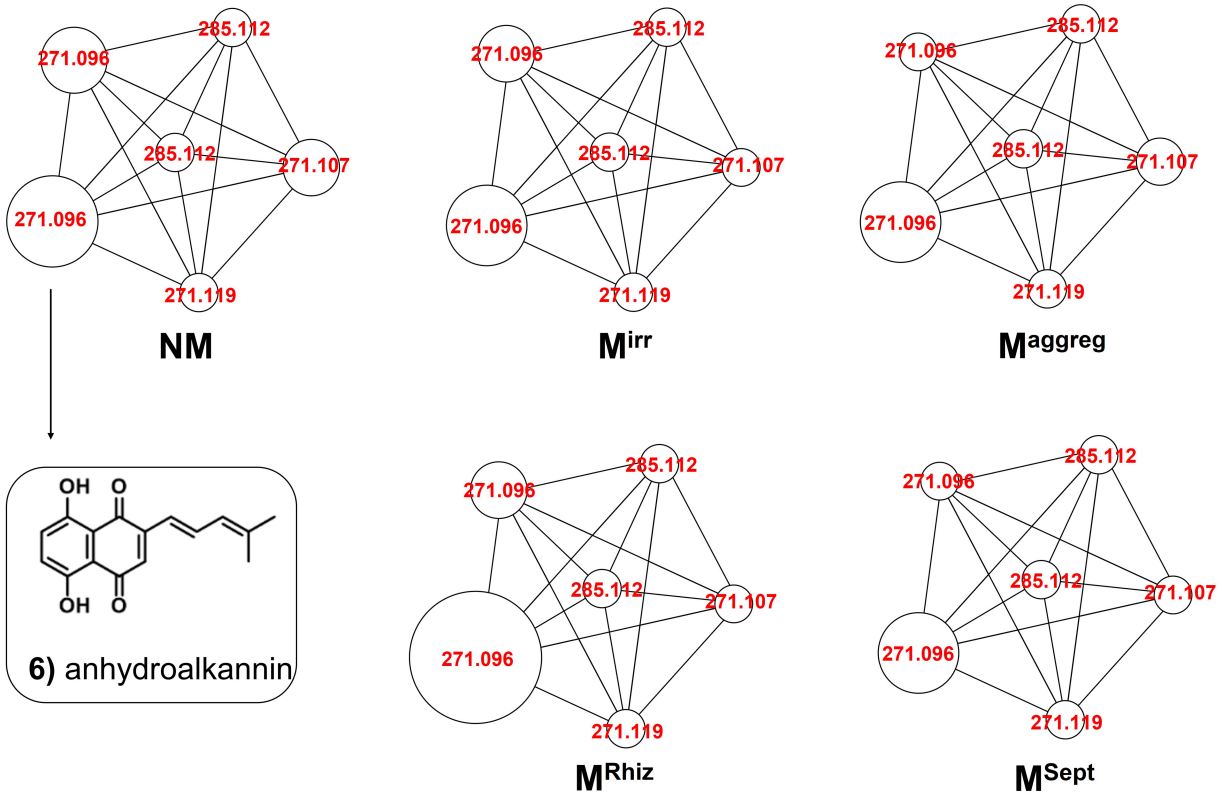

FIGURE 4
Comparative molecular networking of shikonin derivatives cluster (different nodes) between *A. tinctoria* roots inoculated or not (control) with different AMF strains (two from GINCO – *R. irregularis* MUCL 41833 and *R. aggregatus* MUCL 49408, and two isolated from wild *A. tinctoria* – *R. irregularis* and *S. viscosum*) and growing for 9 days in the S-H cultivation system (Experiment 2).

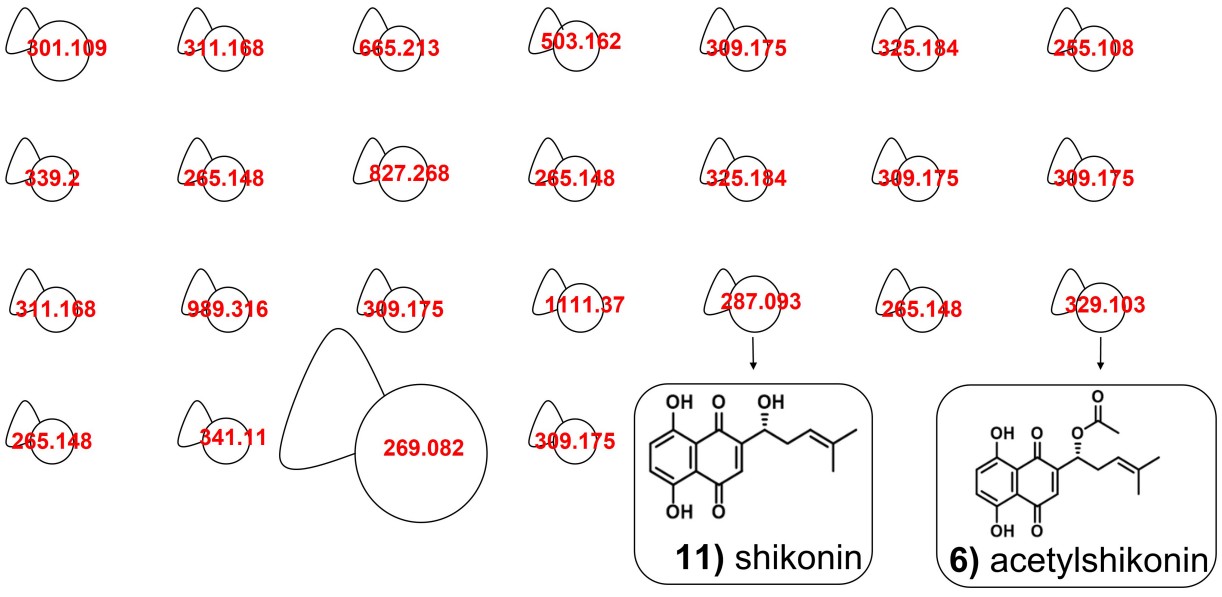

FIGURE 5
Molecular network in *A. tinctoria* root extracts obtained in Experiment 3 in negative mode. Size nodes are proportional to corresponding peak area.

treatments in Experiments 2 and 3, respectively. An increase in nutrients uptake via the arbuscules can lead to an enhanced production of precursor compounds, such as NADPH, ATP, acetyl-CoA (mevalonic acid pathway), and pyruvate glyceraldehyde and phosphate (methylerythritol-4-phosphate pathway) that are required for the biosynthesis of various SMs (e.g., terpenoids,

phenolic, and alkaloids) (Kapoor et al., 2017). In our study, a higher AC% could have led to an increase in the precursor compounds essential to produce A/Sd. However, this was not confirmed in Experiment 3, where the higher AC% in M^{Sept} treatment was not accompanied by a higher production of A/Sd. If we parallel this to plant biomass, it is well known that the response of plants to inoculation with an AMF may vary depending on the AMF species as previously reported (Klironomos, 2003). It is not excluded that similar effect is observed on metabolites production, although this needs to be demonstrated.

4.3. AMF modulate the expression of genes involved in the A/Sd biosynthetic pathway in *A. tinctoria* roots

At the end of Experiment 1, a significantly higher relative expression of *LePGT1* and *LePGT2* genes was observed in *A. tinctoria* associated with *R. irregularis* MUCL 41833 compared to the NM treatment. In addition, a significantly higher relative expression of *LePGT2* was observed in the AMF-colonized plants at day 37 compared to day 9. However, these increases were not accompanied by an enhanced production of A/Sd. Conversely, in Experiment 2, a significant lower relative expression of *LePGT2* was observed in plants associated with the native *R. irregularis* strain, compared with the other AMF and NM treatments, whereas a significantly higher production of A/Sd was observed with this strain. In both Experiments, no differences were reported for *GHQH*. In Experiment 3, no significant differences between the treatments were noted for all the genes tested (data not presented).

Although these results may seem surprising, similar outcomes were reported in the literature. For example, Wang et al. (2014) demonstrated that the application of methyl jasmonate (MeJA) on shikonin-deficient *A. euchroma* cell lines rapidly led to the overexpression of several genes involved in the biosynthesis of A/Sd, including *PGT*, but was not accompanied by a significant higher production of A/Sd. In another study, Ahmad et al. (2022b) showed a significantly higher expression of *LePGT1*, *LePGT2*, and *LeGHQH1* in *Lithospermum officinale* L. roots treated with MeJA, but no higher accumulation of total A/Sd, after eight weeks. Conversely, the same authors (Ahmad et al., 2022a) demonstrated that the bacterium *Chitinophaga* sp. strain R-73072 significantly upregulated *LePGT1* and *LePGT2*, and a cytochrome P450-LeCYP76B101 genes, resulting in a significant enhanced production of total A/Sd in *L. erythrorhizon* roots, after 2-3 weeks.

In our study, a few hypotheses can be advanced to explain why upregulation of *PGT*s was not followed by higher production of A/Sd and, conversely, why downregulation was followed by higher production of A/Sd. Firstly, it is not excluded that the duration of Experiment 1 (37 days) was too short to result in a significant increased production of A/Sd, or that the timing of plant harvesting in our experiments was not optimal (i.e., gene expression behavioral oscillations due to the plant circadian cycle) (Merrow et al., 2005). The *PGT*s regulate the first biosynthetic steps forming the basic carbon skeleton that leads to A/Sd, and therefore, it is possible that the resulting modulation of A/Sd production took longer after the upregulation of the relative expression of target *PGT* genes, as supported by Ahmad et al. (2022b), or that the genes oscillations were not timely targeted during our harvest times, as suggested by Wang et al. (2014) (**Figure 6**). Secondly, in a study by Andrade et al. (2013), a mismatch between alkaloid levels, another important SM group, and gene expression was reported in different *Catharanthus roseus* (L.) G. Don tissues. In this study, the AMF *C. etunicatum* had a greater influence (i.e., alkaloids production) in roots than in shoots, and a higher gene expression was reported in the older leaves of M plants as well as in the youngest leaves of NM plants (leaves were harvested at the same time) (Andrade et al., 2013). These results suggest a very precise phenological and spatial regulation process during alkaloid biosynthesis (Mahroug et al., 2007). Moreover, the reported influence of AMF on idioblast and laticifer density in *C. roseus* plants might have enhanced the expression of enzymes specifically located in these cells (St-Pierre et al., 1999). An increase in glandular trichome density upon mycorrhization was also linked with an enhanced concentration of another group of SMs, the terpenoids (Zhao et al., 2022). This is an interesting aspect that needs to be further verified. In fact, A/Sd compounds are sequestered as granules in the phospholipid layer and are accumulated in the apoplastic spaces, and they can be found in the cork layer of mature roots (Brigham et al., 1999; Singh et al., 2010; Tatsumi et al., 2016). A difference in A/Sd accumulation might have occurred (i.e., higher content in the primary roots as compared to the secondary roots) upon AMF colonization and might have not been fully displayed across *A. tinctoria* root samples used for our RT-qPCR analysis (i.e., no homogenous samples analyzed with mostly secondary roots utilized). Thirdly, the regulation and accumulation of SMs in plants is usually controlled by a complex network characterized by transcription factors (TFs), which promote or inhibit the expression of multiple genes involved in one or more biosynthetic pathways (Yang et al., 2012; Wu et al., 2021). Transcription factors can act alone or in combination with other TFs to modulate the expression of target genes, and also one TF can regulate the expression of multiple genes participating in one or more biosynthetic pathways (Pinson et al., 2009; Goossens et al., 2017; Hassani et al., 2020). In our study, different TFs might have regulated the target genes (*PGT*s and *GHQH*), yet the full landscape of the A/Sd biosynthesis pathway is not entirely understood, with co-expressed genes still to be identified (Suttiyut et al., 2022). Finally, even after a gene has been transcribed, its expression could still be regulated at various stages. Post transcriptional modifications changes might occur to a newly transcribed primary RNA transcript after transcription has occurred and prior to its translation into a protein.

4.4. Chemical profile of *A. tinctoria* does not markedly differ between semi-hydroponic and pot cultivation systems and in presence of different AMF

A similar chemical composition was reported in *A. tinctoria* roots associated with the different AMF and non-colonized control plants in Experiments 2 (S-H cultivation system) and 3 (pot cultivation system) (**Figures 4**, **5**) except for the detection of shikonin in Experiment 3 (**Tables 3**, **4**).

The major compound detected in both experiments was putatively identified as anhydroalkannin (6). This compound is

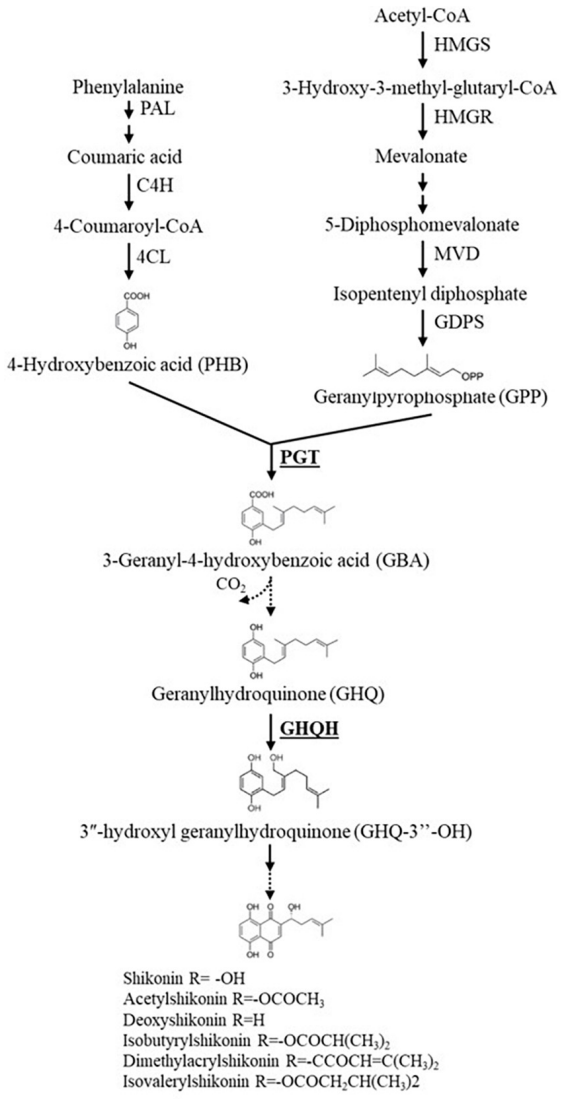

FIGURE 6
An abridged scheme of the shikonin derivatives biosynthesis pathway. The genes that were investigated in this study are reported in bold font. Single arrows represent one step reaction, while double arrows represent multiple step reactions. Dashed arrows signify undefined steps or the enzymes have not been verified yet. HMGS, 3-hydroxy-3-methylglutaryl-CoA synthase; HMGR, 3-hydroxy-3-methylglutaryl-CoA reductase; MVD, mevalonate diphosphate decarboxylase; GDPS, geranyl diphosphate synthase; PAL, phenylalanine ammonia-lyase; C4H, cinnamic acid 4-hydroxylase; 4CL, 4-coumaroyl-CoA ligase; PGT, *p*-hydroxybenzoate geranyltransferase; GHQH, geranylhydroquinone 3″-hydroxylase.

also a main product of shikonin biotransformation by several human intestinal bacteria in aerobic conditions and it was found to be less cytotoxic against a series of human tumor cell lines *in vitro*, in comparison with shikonin (Meselhy et al., 1994; Min et al., 2000). Methyl A/Sd isomers, as detected in our samples, were also identified from *Lithospermum*, *Alkanna*, and *Onosma* species. 1′-methyl shikonin was isolated and characterized from roots of *L. erythrorhizon*, exerting moderate antioxidant activity (Han et al., 2008). To the best of our knowledge, 5- or 8- O-methoxyshikonin derivatives have not yet been identified from natural sources. To better clarify the chemical composition of our samples, putative methylshikonin derivatives (1 and 4) must be purified and the methoxyl position elucidated in the structure of these isomers. In addition, in both experiments, four main lipid amides were tentatively identified as palmitoleamide (7), linoleamide (8), oleamide (9), and stearamide (10). Fatty acids amides are a group of nitrogen-containing, lipid-soluble fatty acid derivatives, which act against a variety of diseases such as cancer, bacterial infections, parasitic infection, inflammations, diabetes, and obesity (Kim et al., 2010; Tanvir et al., 2018). Further, it has been reported that fatty acid amides as oleamide from plant root exudates can participate in strong plant-microbe interactions, stimulating nitrogen metabolism in rhizospheric bacteria (Sun et al., 2016).

The data of chemical composition obtained from *A. tinctoria* growing in our cultivation systems cannot be accurately compared with data from literature (i.e., from nature, commercial samples, and/or from cell plant suspension). Indeed, the proportion and quantity of A/Sd varies depending on the level of stress and microorganisms present in the rhizosphere (Brigham et al., 1999). The influence of the cultivation systems on the production of these methoxy and anhydro A/Sd must be deeply studied to better understand their significance. Secondary metabolites' production and compositional changes have a strong correlation and association with the environment, and thus synthesized only under specific growth conditions (Peñuelas and Llusià, 1997). Variations in an environmental factor, such as light, temperature, soil water, soil fertility, and salinity, may alter the plant metabolites content (Yang et al., 2018). Indeed, many chemical and physical factors have been found to inhibit shikonin production, such as NH_4^+, 2,4-dichlorophenoxyacetic acid (a synthetic auxin), low pH, temperature higher than 28°C, and light, especially blue light (Tatsumi et al., 2016). Skoneczny et al. (2017), using a metabolomic approach profiling hydroxynaphthoquinones (HNQs) and pyrrolizidine alkaloids (PAs), demonstrated the influence of high temperatures and water withholding on the accumulation of A/Sd in *Echium plantagineum* L. Abundance of HNQs, especially deoxyshikonin, shikonin, and dimethylacrylshikonin, rapidly increased in roots exposed to elevated temperatures. Water withholding initially increased NQ abundance, but prolonged drought resulted in reduced total PAs and HNQs (Skoneczny et al., 2017). In our study, *A. tinctoria* growing in the S-H cultivation system were kept in perlite, while a mixture of peatmoss, perlite, and quartz was used in the pots experiment. Perlite is a growing medium frequently used in hydroponic cultivation system since it has a high-water retention and provide the plants' roots with strong anchor points for stability and strength. Moreover, in this system, plants received minerals by the circulating nutrient solution flowing directly through the plants' container, while in the pots it was added at constant intervals and left to be completely absorbed by the plants. Therefore, it is possible that the temperature and the water/nutrient solution retention was higher in the conventional pots than in the plant containers of the S-H cultivation system. Moreover, shikonin and A/Sd might have better accumulated in the pots, while leached out in the S-H system. Finally, plant developmental stage qualitatively and quantitatively influences primary and secondary metabolism. A recent study by Csorba et al. (2022) reported this aspect as the most important driver influencing *A. tinctoria* metabolites content, revealing a peak

content of A/Sd at the fruiting stage. In our study, plants were harvested during the vegetative growth (around five months old), and thus, might have played a role in the chemical profile reported.

5. Conclusion

For the first time, to the best of our knowledge, AMF isolated from wild-growing *A. tinctoria* were identified and applied under the cultivation systems described in this study. Native *R. irregularis* significantly increased A/Sd production in *A. tinctoria* roots, whatever the system used (S-H or pots), thus opening new perspectives toward the application of AMF in the production of these valuable therapeutic compounds in medicinal plants. A better adaptation of this indigenous strain toward its host was demonstrated, with higher arbuscules formation and production of A/Sd reported in *A. tinctoria* roots. This result suggests that the selection of the most effective AMF species (native or not; single or combinations of different AMF strains) remains a key point in studying the modulation/increase of SMs. However, the mechanisms behind AM symbiosis and their impact on the A/Sd biosynthetic pathways still need to be further clarified. Additionally, the conditions characterizing the conventional pots system seemed to be the optimal one in term of shikonin detection. Therefore, the application of the best growing conditions should be further investigated as well. Since shikonin was reported only in the pot system, the recovery of SMs can yet be conducted only in a destructive way (i.e., using the roots of *A. tinctoria*). For this reason, further studies applying S-H cultivation systems/innovative systems are required, especially for testing non-destructive ways of trapping the metabolites exudates by the roots in the circulating nutrient solution.

Data availability statement

The datasets presented in this study can be found in online repositories. The names of the repository/repositories and accession number(s) can be found in the article/**Supplementary material**.

Author contributions

YZ: isolation and identification of AMF from *A. tinctoria* plants, experimental set up, data collection, analysis and interpretation, drafting the work, commentaries, corrections, final approval, and agreement with all aspects of the work. AC: *A. tinctoria in vitro* and *ex vitro* production, experimental setup, data collection, development of protocols for the analyses and interpretation, drafting the work, commentaries, corrections, final approval, and agreement with all aspects of the work. SO: data analysis and interpretation, draft corrections, final approval, and agreement with all aspects of the work. MG-R: contribution on strain identification and assembly of AMF phylogenetic tree. M-FH: data analysis and interpretation, final approval, and agreement with all aspects of the work. JQ-L and SD: substantial contributions to the conception and design of the experiments, interpretation of the data, draft corrections, final approval, and agreement with all aspects of the work. IL: contribution to the development of the experiment, data analysis and interpretation, draft correction, and final approval and agreement with all aspects of the work. All authors contributed to the article and approved the submitted version.

Funding

YZ and AC were financially supported by the Special Research Funds (FSR) of the Université Catholique de Louvain (Belgium).

Acknowledgments

We would like to thank the Université Catholique de Louvain (Belgium) for financial support via the Special Research Funds (FSR). We would also like to thank Dr. Muhammad Ahmad and Dr. rer. nat. Eva Maria Molin from the Center for Health and Bioresources, AIT Austrian Institute of Technology GmbH (Tulln, Austria), for the design of the primers applied in the RT-qPCR analysis, the Institute of Plant Breeding and Genetic Resources, Hellenic Agricultural Organization Demeter (IPBGR, HAO Demeter), in particular Dr. Virginia Sarropoulou and Dr. Katerina Grigoriadou, for the supply of the *A. tinctoria in vitro* explants, and Dr. Nikos Krigas for the collection and botanical identification of *A. tinctoria* plants. Moreover, we thank Stéphanie Huret and Céline Bivort (Technician at UCLouvain Earth and Life Institute – Applied Microbiology – BCCM/MUCL) for the help in the RNA extraction and genes expression analysis and molecular identification of AMF, respectively, and Catherine Rasse (Statistical Methodology and Computing Service/Louvain Institute of Data Analysis and Modeling in Economics and Statistics, SMCS/LIDAM, UCLouvain) for the support in the statistical analysis. Finally, MS data were obtained at the MASSMET platform of UCLouvain.

Conflict of interest

The authors declare that the research was conducted in the absence of any commercial or financial relationships that could be construed as a potential conflict of interest.

Publisher's note

Supplementary material

The Supplementary Material for this article can be found online at: https://www.frontiersin.org/articles/10.3389/fmicb.2023.1216029/full#supplementary-material

References

Ahmad, M., Leroy, T., Krigas, N., Temsch, E. M., Weiss-Schneeweiss, H., Lexer, C., et al. (2021). Spatial and ecological drivers of genetic structure in Greek populations of *Alkanna tinctoria* (*Boraginaceae*), a polyploid medicinal herb. *Front. Plant Sci.* 12:706574. doi: 10.3389/fpls.2021.706574

Ahmad, M., Varela, A. A., Koletti, A. E., Rodić, N., Reichelt, M., Rödel, P., et al. (2022b). Dynamics of alkannin/shikonin biosynthesis in response to jasmonate and salicylic acid in *Lithospermum officinale*. *Sci Rep.* 12:17093. doi: 10.1038/s41598-022-21322-0

Ahmad, M., Varela, A. A., Koletti, A. E., Assimopoulou, A. N., Declerck, S., Schneider, C., et al. (2022a). Transcriptional dynamics of *Chitinophaga* sp. strain R-73072-mediated alkannin/shikonin biosynthesis in *Lithospermum officinale*. *Front. Microbiol.* 13:978021. doi: 10.3389/fmicb.2022.978021

Andrade, S. A. L., Malik, S., Sawaya, A. C. H. F., Bottcher, A., and Mazzafera, P. (2013). Association with arbuscular mycorrhizal fungi influences alkaloid synthesis and accumulation in *Catharanthus roseus* and *Nicotiana tabacum* plants. *Acta Physiol Plant*. 35, 867–880. doi: 10.1007/s11738-012-1130-8

Avio, L., Turrini, A., Giovannetti, M., and Sbrana, C. (2018). Designing the ideotype mycorrhizal symbionts for the production of healthy food. *Front. Plant Sci*. 9:1089. doi: 10.3389/fpls.2018.01089

Bai, G., and Jin, X. J. (1994). Chemical constituents of *Lithospermum erythrorhizon*. *Chem. Res. Chin. Univ*. 10, 263–265.

Bossard, E., Tsafantakis, N., Aligiannis, N., and Fokialakis, N. (2022). A development strategy of tailor-made natural deep eutectic solvents for the enhanced extraction of hydroxynaphthoquinones from *Alkanna tinctoria* roots. *Planta Med.* 88, 826–837. doi: 10.1055/a-1738-5648

Brigham, L. A., Michaels, P. J., and Flores, H. E. (1999). Cell-specific production and antimicrobial activity of naphthoquinones in roots of *Lithospermum erythrorhizon*. *Plant Physiol.* 119, 417–428. doi: 10.1104/pp.119.2.417

Cartabia, A., Sarropoulou, V., Grigoriadou, K., Maloupa, E., and Declerck, S. (2022). *In vitro* propagation of *Alkanna tinctoria* Tausch.: A medicinal plant of the *Boraginaceae* family with high pharmaceutical value. *Ind. Crops Prod.* 182:114860. doi: 10.1016/j.indcrop.2022.114860

Cartabia, A., Tsiokanos, E., Tsafantakis, N., Lalaymia, I., Termentzi, A., Miguel, M., et al. (2021). The arbuscular mycorrhizal fungus *Rhizophagus irregularis* MUCL 41833 modulates metabolites production of *Anchusa officinalis* L. under semi-hydroponic cultivation. *Front. Plant Sci.* 12:724352. doi: 10.3389/fpls.2021.724352

Chaudhary, V., Kapoor, R., and Bhatnagar, A. K. (2008). Effectiveness of two arbuscular mycorrhizal fungi on concentrations of essential oil and artemisinin in three accessions of *Artemisia annua* L. *Appl. Soil Ecol.* 40, 174–181. doi: 10.1016/j.apsoil.2008.04.003

Chen, M., Arato, M., Borghi, L., Nouri, E., and Reinhardt, D. (2018). Beneficial services of arbuscular mycorrhizal fungi – From ecology to application. *Front. Plant Sci.* 9:1270. doi: 10.3389/fpls.2018.01270

Chenchouni, H., Mekahlia, M. N., and Beddiar, A. (2020). Effect of inoculation with native and commercial arbuscular mycorrhizal fungi on growth and mycorrhizal colonization of olive (*Olea europaea* L.). *Sci. Hortic. Vol.* 261:108969. doi: 10.1016/j.scienta.2019.108969

Copetta, A., Lingua, G., and Berta, G. (2006). Effects of three AM fungi on growth, distribution of glandular hairs, and essential oil production in *Ocimum basilicum* L. var. Genovese. *Mycorrhiza* 16, 485–494. doi: 10.1007/s00572-006-0065-6

Csorba, C., Rodić, N., Zhao, Y., Antonielli, L., Brader, G., Vlachou, A., et al. (2022). Metabolite production in *Alkanna tinctoria* links plant development with the recruitment of individual members of microbiome thriving at the root-soil interface. *mSystems* 7, e451–e422. doi: 10.1128/msystems.00451-22

Divito, E. B., Davic, A. P., Johnson, M. E., and Cascio, M. (2012). Electrospray ionization and collision induced dissociation mass spectrometry of primary fatty acid amides. *Anal. Chem.* 84, 2388–2394. doi: 10.1021/ac203158u

Frew, A. (2020). Contrasting effects of commercial and native arbuscular mycorrhizal fungal inoculants on plant biomass allocation, nutrients and phenolics. *Plants People Planet* 3, 536–540. doi: 10.1002/ppp3.10128

Garcés-Ruiz, M., Calonne-Salmon, M., Plouznikoff, K., Misson, C., Navarrete-Mier, M., Cranenbrouck, S., et al. (2017). Dynamics of short-term phosphorus uptake by intact mycorrhizal and non-mycorrhizal maize plants grown in a circulatory semi-hydroponic cultivation system. *Front. Plant Sci.* 8:1471. doi: 10.3389/fpls.2017.01471

Gerardi, C., Mita, G., Grillo, E., Giovinazzo, G., Miceli, A., and De Leo, P. (1998). "*Alkanna tinctoria* T. (Alkanets): *In vitro* culture and the production of alkannin and other secondary metabolites," in *Medicinal and aromatic plants X, biotechnology in agriculture and forestry*, ed. Y. P. S. Bajaj (Berlin: Springer Berlin Heidelberg), doi: 10.1007/978-3-642-58833-4_2

Gontier, E., Clément, A., Tran, T. L. M., Gravot, A., Lièvre, K., Guckert, A., et al. (2002). Hydroponic combined with natural or forced root permeabilization: A promising technique for plant secondary metabolite production. *Plant Sci.* 163, 723–732. doi: 10.1016/S0168-9452(02)00171-1

Goossens, J., Mertens, J., and Goossens, A. (2017). Role and functioning of bHLH transcription factors in jasmonate signalling. *J. Exp. Bot.* 68, 1333–1347. doi: 10.1093/jxb/erw440

Gupta, K., Garg, S., Singh, J., and Kumar, M. (2014). Enhanced production of napthoquinone metabolite (shikonin) from cell suspension culture of *Arnebia* sp. and its up-scaling through bioreactor. *3 Biotech* 4, 263–273. doi: 10.1007/s13205-013-0149-x

Han, J., Weng, X. C., and Bi, K. (2008). Antioxidants from a Chinese medicinal herb – *Lithospermum erythrorhizon*. *Food Chemistry* 106, 2–10. doi: 10.1016/j.foodchem.2007.01.031

Hassani, D., Fu, X., Shen, Q., Khalid, M., Rose, J. K. C., and Tang, K. (2020). Parallel transcriptional regulation of artemisinin and flavonoid biosynthesis. *Trends Plant Sci.* 25, 466–476. doi: 10.1016/j.tplants.2020.01.001

Hubert, P., Nguyen-Huu, J. J., Boulanger, B., Chapuzet, E., Chiap, P., Cohen, N., et al. (2003). Validation des procédures analytiques quantitatives, Harmonisation des démarches. *S.T.P. Pharma Pratiq.* 13, 101–138.

IJdo, M., Cranenbrouck, S., and Declerck, S. (2011). Methods for large-scale production of AM fungi: Past, present, and future. *Mycorrhiza* 21, 1–16. doi: 10.1007/s00572-010-0337-z

Jurkiewicz, A., Ryszka, P., Anielska, T., Waligórski, P., Białońska, D., Góralska, K., et al. (2010). Optimization of culture conditions of *Arnica montana* L.: Effects of mycorrhizal fungi and competing plants. *Mycorrhiza* 20, 293–306. doi: 10.1007/s00572-009-0280-z

Kapoor, R., Anand, G., Gupta, P., and Mandal, S. (2017). Insight into the mechanisms of enhanced production of valuable terpenoids by arbuscular mycorrhiza. *Phytochem Rev.* 16, 677–692. doi: 10.1007/s11101-016-9486-9

Kapoor, R., Giri, B., and Mukerji, K. G. (2002). *Glomus macrocarpum*: A potential bioinoculant to improve essential oil quality and concentration in Dill (*Anethum graveolens* L.) and Carum (*Trachyspermum ammi* (Linn.) Sprague). *World J. Microbiol. Biotechnol.* 18, 459–463. doi: 10.1023/A:1015522100497

Kaur, S., and Suseela, V. (2020). Unraveling arbuscular mycorrhiza-induced changes in plant primary and secondary metabolome. *Metabolites* 10:335. doi: 10.3390/metabo10080335

Khaosaad, T., Vierheilig, H., Nell, M., Zitterl-Eglseer, K., and Novak, J. (2006). Arbuscular mycorrhiza alter the concentration of essential oils in oregano (*Origanum sp.*, Lamiaceae). *Mycorrhiza* 16, 443–446. doi: 10.1007/s00572-006-0062-9

Kim, K. H., Choi, S. U., Son, M. W., and Lee, K. R. (2010). Two new phenolic amides from the seeds of pharbitis nil. *Chem. Pharm Bull.* 58, 1532–1535. doi: 10.1248/cpb.58.1532

Klironomos, J. (2003). Variation in plant response to native and exotic arbuscular mycorrhizal fungi. *Ecology*. 84, 2292–2301. doi: 10.1890/02-0413

Kyogoku, K., Terayama, H., Tachi, Y., Suzuki, T., and Komatsu, M. (1973). Studies on the constituents of "shikon". I. Structure of three new shikonin derivatives and isolation of anhydroalkanin. *Shoyakugaku Zasshi*. 27, 31–36.

Larose, G., Chênevert, R., Moutoglis, P., Gagné, S., Piché, Y., and Vierheilig, H. (2002). Flavonoid levels in roots of *Medicago sativa* are modulated by the developmental stage of the symbiosis and the root colonizing arbuscular mycorrhizal fungus. *J. Plant Physiol.* 159, 1329–1339. doi: 10.1078/0176-1617-00896

Liao, M., Li, A., Chen, C., Ouyang, H., Zhang, Y., Xu, Y., et al. (2015). Systematic identification of shikonins and shikonofurans in medicinal Zicao species using ultra-high performance liquid chromatography quadrupole time of flight tandem mass spectrometry combined with a data mining strategy. *J. Chromatogr. A*. 1425, 158–172. doi: 10.1016/j.chroma.2015.11.028

Lu, F. C., Lee, C. Y., and Wang, C. L. (2015). The influence of arbuscular mycorrhizal fungi inoculation on yam (*Dioscorea* spp.) tuber weights and secondary metabolite content. *PeerJ* 3, e1266. doi: 10.7717/peerj.1266

Mahroug, S., Burlat, V., and St-Pierre, B. (2007). Cellular and sub-cellular organisation of the monoterpenoid indole alkaloid pathway in *Catharanthus roseus*. *Phytochem. Rev.* 6, 363–381. doi: 10.1007/s11101-006-9017-1

Malik, S., Bhushan, S., Sharma, M., and Ahuja, P. S. (2016). Biotechnological approaches to the production of shikonins: A critical review with recent updates. *Crit. Rev. Biotechnol.* 36, 327–340. doi: 10.3109/07388551.2014.961003

McGonigle, T. P., Miller, M. H., Evans, D. G., Fairchild, G. L., and Swan, J. A. (1990). A new method which gives an objective measure of colonization of roots by vesicular-arbuscular mycorrhizal fungi. *New Phytol.* 115, 495–501. doi: 10.1111/j.1469-8137.1990.tb00476.x

Merrow, M., Spoelstra, K., and Roenneberg, T. (2005). The circadian cycle: Daily rhythms from behaviour to genes: First in the cycles review series. *EMBO Rep*. 6, 930–935. doi: 10.1038/sj.embor.7400541

Meselhy, R. M., Shigetoshi, K., Koji, T., Masao, H., and Tsuneo, N. (1994). Biotransformation of shikonin by human intestinal bacteria. *Tetrahedron* 50, 3081–3098. doi: 10.1016/S0040-4020(01)81108-X

Min, B. S., Hattori, M., Kim, H. M., and Kim, Y. H. (2000). Cytotoxicity of shikonin metabolites with biotransformation of human intestinal bacteria. *J. Microbial. Biotechnol.* 10, 514–517.

Pandey, D. K., Kaur, P., and Dey, A. (2018). "Arbuscular mycorrhizal fungi: Effects on secondary metabolite production in medicinal plants," in *Fungi and their role in sustainable development: Current perspectives*, eds P. Gehlot and J. Singh (Singapore: Springer Singapore), doi: 10.1007/978-981-13-0393-7_28

Papageorgiou, V., Assimopoulou, A., and Ballis, A. (2008). Alkannins and shikonins: A new class of wound healing agents. *CMC* 15, 3248–3267. doi: 10.2174/092986708786848532

Papageorgiou, V. P., Assimopoulou, A. N., Couladouros, E. A., Hepworth, D., and Nicolaou, K. C. (1999). The chemistry and biology of alkannin, shikonin, and related naphthazarin natural products. *Angew Chem. Int. Ed. Engl.* 38, 270–301.

Peñuelas, J., and Llusià, J. (1997). Effects of carbon dioxide, water supply, and seasonally on terpene content and emission by *Rosmarinus officinalis*. *J. Chem. Ecol.* 23, 979–993. doi: 10.1023/B:JOEC.0000006383.29650.d7

Pfaffl, M. W. (2001). A new mathematical model for relative quantification in real-time RT-PCR. *Nucleic Acids Res.* 29, 45e–445e. doi: 10.1093/nar/29.9.e45

Pinson, B., Vaur, S., Sagot, I., Coulpier, F., Lemoine, S., and Daignan-Fornier, B. (2009). Metabolic intermediates selectively stimulate transcription factor interaction and modulate phosphate and purine pathways. *Genes Dev.* 23, 1399–1407. doi: 10.1101/gad.521809

Pluskal, T., Castillo, S., Villar-Briones, A., and Oresic, M. (2010). MZmine 2: Modular framework for processing, visualizing, and analyzing mass spectrometry-based molecular profile data. *BMC Bioinform.* 11:395. doi: 10.1186/1471-2105-11-395

Sgherri, C., Cecconami, S., Pinzino, C., Navari-Izzo, F., and Izzo, R. (2010). Levels of antioxidants and nutraceuticals in basil grown in hydroponics and soil. *Food Chem.* 123, 416–422. doi: 10.1016/j.foodchem.2010.04.058

Shannon, P., Markiel, A., Ozier, O., Baliga, N. S., Wang, J. T., Ramage, D., et al. (2003). Cytoscape: A software environment for integrated models of biomolecular interaction networks. *Genome Res.* 13, 2498–2504. doi: 10.1101/gr.1239303

Singh, R. S., Gara, R. K., Bhardwaj, P. K., Kaachra, A., Malik, S., Kumar, R., et al. (2010). Expression of 3-hydroxy-3-methylglutaryl-CoA reductase, p-hydroxybenzoate-m-geranyltransferase and genes of phenylpropanoid pathway exhibits positive correlation with shikonins content in arnebia [*Arnebia euchroma* (Royle) Johnston]. *BMC Mol. Biol.* 11:88. doi: 10.1186/1471-2199-11-88

Skoneczny, D., Weston, P. A., Zhu, X., Gurr, G. M., Callaway, R. M., Barrow, R. A., et al. (2017). Metabolic profiling and identification of shikonins in root periderm of two invasive *Echium* spp. weeds in Australia. *Molecules* 22:330. doi: 10.3390/molecules22020330

Smith, S. E., and Read, D. (2008). *Mineral nutrition, toxic element accumulation and water relations of arbuscular mycorrhizal plants*. Amsterdam: Elsevier, doi: 10.1016/B978-012370526-6.50007-6

Song, W., Zhuang, Y., and Liu, T. (2020). Potential role of two cytochrome P450s obtained from *Lithospermum erythrorhizon* in catalyzing the oxidation of geranylhydroquinone during Shikonin biosynthesis. *Phytochemistry* 175:112375. doi: 10.1016/j.phytochem.2020.112375

St-Pierre, B., Vazquez-Flota, F. A., and De Luca, V. (1999). Multicellular compartmentation of *Catharanthus roseus* alkaloid biosynthesis predicts intercellular translocation of a pathway intermediate. *Plant Cell* 11, 887–900. doi: 10.1105/tpc.11.5.887

Sun, L., Lu, Y., Kronzucker, H. J., and Shi, W. (2016). Quantification and enzyme targets of fatty acid amides from duckweed root exudates involved in the stimulation of denitrification. *J. Plant Physiol.* 198, 81–88. doi: 10.1016/j.jplph.2016.04.010

Suttiyut, T., Auber, R. P., Ghaste, M., Kane, C. N., McAdam, S. A. M., Wisecaver, J. H., et al. (2022). Integrative analysis of the shikonin metabolic network identifies new gene connections and reveals evolutionary insight into shikonin biosynthesis. *Hortic. Res.* 9:uhab087. doi: 10.1093/hr/uhab087

Takanashi, K., Nakagawa, Y., Aburaya, S., Kaminade, K., Aoki, W., Saida-Munakata, Y., et al. (2019). Comparative proteomic analysis of *Lithospermum erythrorhizon* reveals regulation of a variety of metabolic enzymes leading to comprehensive understanding of the shikonin biosynthetic Pathway. *Plant Cell Physiol.* 60, 19–28. doi: 10.1093/pcp/pcy183

Tanvir, R., Javeed, A., and Rehman, Y. (2018). Fatty acids and their amide derivatives from endophytes: New therapeutic possibilities from a hidden source. *FEMS Microbiol. Lett.* 365:fny114. doi: 10.1093/femsle/fny114

Tappeiner, J., Vasiliou, A., Ganzera, M., Fessas, D., Stuppner, H., Papageorgiou, V. P., et al. (2014). Quantitative determination of alkannins and shikonins in endemic Mediterranean *Alkanna* species: Quantitative determination of alkannins and shikonins. *Biomed. Chromatogr.* 28, 923–933. doi: 10.1002/bmc.3096

Tatsumi, K., Yano, M., Kaminade, K., Sugiyama, A., Sato, M., Toyooka, K., et al. (2016). Characterization of shikonin derivative secretion in *Lithospermum erythrorhizon* hairy roots as a model of lipid-soluble metabolite secretion from plants. *Front. Plant Sci.* 7:1066. doi: 10.3389/fpls.2016.01066

Toussaint, J.-P., Smith, F. A., and Smith, S. E. (2007). Arbuscular mycorrhizal fungi can induce the production of phytochemicals in sweet basil irrespective of phosphorus nutrition. *Mycorrhiza* 17, 291–297. doi: 10.1007/s00572-006-0104-3

Tsiokanos, E., Cartabia, A., Tsafantakis, N., Lalaymia, I., Termentzi, A., Miguel, M., et al. (2022). The metabolic profile of *Anchusa officinalis* L. differs according to its associated arbuscular mycorrhizal fungi. *Metabolites* 12:573. doi: 10.3390/metabo12070573

Urbanek, H., Bergier, K., Saniewski, M., and Patykowski, J. (1996). Effect of jasmonates and exogenous polysaccharides on production of alkannin pigments in suspension cultures of *Alkanna tinctoria*. *Plant Cell Rep.* 15, 637–641. doi: 10.1007/BF00232468

Valdés, B. (2011). *Boraginaceae in Euro+Med plantbase: The information resource for Euro-Mediterranean plant diversity*. Poltava: EuroPlus.

Walker, C. (2005). A simple blue staining technique for arbuscular mycorrhizal and other root-inhabiting fungi. *Inoculum* 56, 68–69.

Wang, M., Carver, J. J., Phelan, V. V., Sanchez, L. M., Garg, N., Peng, Y., et al. (2016). Sharing and community curation of mass spectrometry data with global natural products social molecular networking. *Nat. Biotechnol.* 34, 828–837. doi: 10.1038/nbt.3597

Wang, S., Guo, L. P., Xie, T., Yang, J., Tang, J. F., Li, X., et al. (2014). Different secondary metabolic responses to MeJA treatment in shikonin-proficient and shikonin-deficient cell lines from *Arnebia euchroma* (Royle) Johnst. *Plant Cell Tiss. Organ. Cult.* 119, 587–598. doi: 10.1007/s11240-014-0558-5

Wu, F. Y., Tang, C. Y., Guo, Y. M., Bian, Z. W., Fu, J. Y., Lu, G. H., et al. (2017). Transcriptome analysis explores genes related to shikonin biosynthesis in Lithospermeae plants and provides insights into boraginales' evolutionary history. *Sci. Rep.* 7:4477. doi: 10.1038/s41598-017-04750-1

Wu, Y. H., Wang, H., Liu, M., Li, B., Chen, X., Ma, Y. T., et al. (2021). Effects of native arbuscular mycorrhizae isolated on root biomass and secondary metabolites of *Salvia miltiorrhiza* Bge. *Front. Plant Sci.* 12:617892. doi: 10.3389/fpls.2021.617892

Xu, J., Aileni, M., Abbagani, S., and Zhang, P. (2010). A reliable and efficient method for total RNA isolation from various members of spurge family (*Euphorbiaceae*). *Phytochem. Anal.* 21, 395–398. doi: 10.1002/pca.1205

Yamamoto, H., Inoue, K., Li, S. M., and Heide, L. (2000). Geranylhydroquinone 3"-hydroxylase, a cytochrome P-450 monooxygenase from *Lithospermum* erythrorhizon cell suspension cultures. *Planta* 210, 312–317. doi: 10.1007/PL00008139

Yaman, C., Uranbey, S., Ahmed, H. A., Ozcan, S., Tugay, O., and Basalma, D. (2019). Callus induction and regeneration of *Alkanna orientalis* var. orientalis and *A. sieheana*. *Bangladesh J. Bot.* 48, 633–640. doi: 10.3329/bjb.v48i3.47941

Yan, Y., Tan, F., Miao, H., Wang, H., and Cao, Y. (2019). Effect of shikonin against *Candida albicans* biofilms. *Front Microbiol.* 10:1085. doi: 10.3389/fmicb.2019.01085

Yang, C. Q., Fang, X., Wu, X. M., Mao, Y. B., Wang, L. J., and Chen, X. Y. (2012). Transcriptional regulation of plant secondary metabolism. *F. J. Integr. Plant Biol.* 54, 703–712. doi: 10.1111/j.1744-7909.2012.01161.x

Yang, L., Wen, K. S., Ruan, X., Zhao, Y. X., Wei, F., and Wang, Q. (2018). Response of plant secondary metabolites to environmental factors. *Molecules* 23, 762. doi: 10.3390/molecules23040762

Yazaki, K. (2017). *Lithospermum erythrorhizon* cell cultures: Present and future aspects. *Plant Biotechnol.* 34, 131–142. doi: 10.5511/plantbiotechnology.17.0823a

Yazaki, K., Kunihisa, M., Fujisaki, T., and Sato, F. (2002). Geranyl diphosphate:4-Hydroxybenzoate geranyltransferase from *Lithospermum erythrorhizon*. *J. Biol. Chem.* 277, 6240–6246. doi: 10.1074/jbc.M106387200

Zeng, Y., Guo, L.-P., Chen, B.-D., Hao, Z.-P., Wang, J.-Y., Huang, L.-Q., et al. (2013). Arbuscular mycorrhizal symbiosis and active ingredients of medicinal plants: Current research status and prospectives. *Mycorrhiza* 23, 253–265. doi: 10.1007/s00572-013-0484-0

Zhao, Y., Cartabia, A., Lalaymia, I., and Declerck, S. (2022). Arbuscular mycorrhizal fungi and production of secondary metabolites in medicinal plants. *Mycorrhiza* 32, 221–256. doi: 10.1007/s00572-022-01079-0

Zubek, S., Stojakowska, A., Anielska, T., and Turnau, K. (2010). Arbuscular mycorrhizal fungi alter thymol derivative contents of *Inula ensifolia* L. *Mycorrhiza* 20, 497–504. doi: 10.1007/s00572-010-0306-6

frontiers | Frontiers in Microbiology

TYPE Original Research
PUBLISHED 30 October 2023
DOI 10.3389/fmicb.2023.1261140

OPEN ACCESS

EDITED BY
Mina Salehi,
Tarbiat Modares University, Iran

REVIEWED BY
Sathiyamoorthy Subramaniyam,
Insilicogen Inc, Republic of Korea
Kunal Singh,
Institute of Himalayan Bioresource Technology (CSIR), India
Bartholomew Saanu Adeleke,
Olusegun Agagu University of Science and Technology, Nigeria
Moslem Bahmankar,
Agricultural Research, Education and Extension Organization (AREEO), Iran

*CORRESPONDENCE
Tao Liu
✉ yantao618@126.com
Bo Cai
✉ caibo198553@163.com

RECEIVED 08 August 2023
ACCEPTED 05 October 2023
PUBLISHED 30 October 2023

CITATION
Zhang Q, Chang S, Yang Y, Xi C, Dong Y, Liu L, He Y, Liu Y, Cai B and Liu T (2023) Endophyte-inoculated rhizomes of *Paris polyphylla* improve polyphyllin biosynthesis and yield: a transcriptomic analysis of the underlying mechanism.
Front. Microbiol. 14:1261140.
doi: 10.3389/fmicb.2023.1261140

Endophyte-inoculated rhizomes of *Paris polyphylla* improve polyphyllin biosynthesis and yield: a transcriptomic analysis of the underlying mechanism

Qing Zhang[1], Sheng Chang[2], Ying Yang[2], Congfang Xi[1], Yumei Dong[1], Lufeng Liu[1], Yunchao He[3], Yu Liu[4], Bo Cai[2]* and Tao Liu[1]*

[1]National-Local Joint Engineering Research Center on Germplasm Innovation and Utilization of Chinese Medicinal Materials in Southwest China, College of Agriculture and Biotechnology, Yunnan Agricultural University, Kunming, China, [2]Center of Yunnan Zhongyan Industry Co., Ltd., Kunming, China, [3]Lushui City Katma Township People's Government Agricultural and Rural Integrated Service Center, Lushui, Yunnan, China, [4]Shenzhen TCM Hospital, Shenzhen, China

Introduction: Polyphyllin from *Paris polyphylla* var. *yunnanensis* exhibits anti-inflammatory, analgesic, antibacterial, and antiviral properties. However, the current production of polyphyllin can barely meet market demand. To improve the content of polyphyllin produced by *P. polyphylla*, two endophyte strains, *Bacillus cereus* LgD2 and *Fusarium oxysporum* TPB, were isolated from *Paris fargesii* Franch. and inoculated in the roots of *P. polyphylla*. Both symbiotic strains significantly promoted the accumulation of saponins in *P. polyphylla*.

Methods: The content of polyphyllin in rhizomes of *P. polyphylla* treated with TPB with LgD2 strain was determined using High Performance Liquid Chromatography and the expressed genes were analyzed by RNA-seq. Gene Ontology and Kyoto Encyclopedia of Genes annotations were performed on the differentially expressed genes, a clustering tree of UDP-glycosyltransferase (UGT) and cytochrome P450 (CYP450) gene families was constructed, and UGT and CYP450 involved in the biosynthesis of polyphyllin were predicted using weighted correlation network analysis (WGCNA).

Results: RNA-seq and qRT-PCR analyses showed that endophytic inoculation did not promote polyphyllin accumulation by enhancing the upstream terpene biosynthesis pathway, but probably by up-regulating the downstream CYP450 and UGT genes associated with polyphyllin biosynthesis. Genomes enrichment analyses of differentially expressed genes indicated that inoculation with LgD2 and TPB played a positive role in promoting the defense against pathogenic bacteria, enhancing the biosynthesis of carbohydrates, attenuating the process of nitrogen metabolism, and maintaining the equilibrium of the redox reaction homeostasis, potentially indirectly enhancing the polyphyllin yield of *P. polyphylla*. By combining differentially expressed genes screening, WGCNA, and phylogenetic tree analyses, 17 CYP450 and 2 UGT candidate genes involved in the biosynthesis of polyphyllin I, polyphyllin II, polyphyllin VII, polyphyllin D, and polyphyllin H were identified. These results suggest that endophytes probably effectively promote the accumulation of polyphyllin by regulating key downstream genes in biosynthetic pathways.

Discussion: This study provides a new approach for investigating the regulatory mechanisms of endophytes that promote the production and accumulation

of polyphyllin in *P. polyphylla*, providing a basis for further elucidating the mechanisms of plant-endophyte interactions.

KEYWORDS

***Paris polyphylla*, endophyte, polyphyllin biosynthesis, transcriptome, beneficial interaction**

1. Introduction

Paris polyphylla var. *yunnanensis* produces polyphyllin, which is an important ingredient used in traditional Chinese medicine, such as Gongxin, Yunnan Baiyao, Jinfu Kang Oral Liquid, and Lou Lian Capsules (Ren et al., 2020; Yan et al., 2021). Steroidal saponins, which mainly include isospirostanol-type saponins such as polyphyllin, diosgenin, and pennogenin, are important medicinal active ingredients derived from *P. polyphylla* (Thapa et al., 2022).

Polyphyllin I (PPI), polyphyllin II (PPII), polyphyllin VII (PPVII), polyphyllin H (PPH), and polyphyllin D (17-hydroxygracillin, PPD) are known to exert antitumor, anti-inflammatory, analgesic, antibacterial, antiviral, hemostatic, immune, and other therapeutic effects (Chen T. et al., 2019; Lin et al., 2021; Meng et al., 2021; Li Z. et al., 2022). For example, PPII has been reported to inhibit colorectal carcinogenesis by regulating mitochondrial fission and the activity of NF-κB pathways (Chen M. et al., 2019); PPVII exerts anti-inflammatory effects (Zhang et al., 2019), inhibits the proliferation of cell lines, and induces apoptosis and autophagy (Xiang et al., 2022); and PPH enhances blood clotting in the body and was also shown to treat acute myelogenous leukemia (Lu et al., 2018; Wen et al., 2019). Unfortunately, the slow growth and overexploitation of *P. polyphylla* have led to resource scarcity in Yunnan, resulting in domestic and international demand exceeding current supply (Negi et al., 2014). Even with widespread artificial cultivation, the amounts of active ingredients isolated from *P. polyphylla* cannot meet market demand; therefore, finding ways to increase the yield of polyphyllin in *P. polyphylla* appears to be a feasible method to counteract the imbalance in supply and demand.

Plant endophytes promote the growth and production of secondary metabolites of host plants, directly or indirectly, through various pathways (Santoyo et al., 2016; Worsley et al., 2020; Chen et al., 2021). They also produce bioactive compounds similar to the secondary metabolites of the host (Li et al., 2023). For example, the endophytic fungus *Pseudodidymocyrtis lobariellae* KL27, isolated from red buds, promotes the biosynthesis and accumulation of paclitaxel (Cao et al., 2022). Likewise, endophytes isolated from *Miquelia dentata Bedd*, produce camptothecin (Shweta et al., 2013).

An effective way for endophytes to promote the accumulation of polyphyllin in *P. polyphylla* is by enhancing the expression of genes in the polyphyllin biosynthetic pathway (Cao et al., 2022; Li Y. et al., 2022). Two pathways are involved in the biosynthesis of the terpene skeleton of polyphyllin, the cytoplasmic mevalonate (MVA) and plastidic 2-C-methyl-D-erythritol-methyl-D-erythritol-4-phosphate (MEP) pathways, among which the MVA pathway is dominant (Wang et al., 2015; Gao et al., 2020). Members of the cytochrome P450 (CYP450) and UDP-glycosyltransferase (UGT) gene superfamilies are required for the structural diversification of polyphyllin (Cheng et al., 2020), control of oxidation, and hydroxylation and glycosylation steps downstream of polyphyllin biosynthesis. Owing to the numerous members of these gene superfamilies, fully elucidating their roles in polyphyllin biosynthesis is difficult. However, RNA-seq technology can now be used to identify those gene members involved in polyphyllin biosynthesis (Cheng et al., 2020).

Despite the fact that endophytic fungi promote the growth, accumulation of secondary metabolites, and disease resistance of *P. polyphylla*, most studies have focused on growth promotion and disease resistance (Huang et al., 2009; Zhang et al., 2011; Tao et al., 2021). Few studies have investigated the effects of endophytes on the accumulation of polyphyllin in *P. polyphylla* and its mechanisms of action. *Bacillus cereus* LgD2 and *Fusarium oxysporum* TPB isolated from *Paris fargesii* Franch. play an important role in promoting the accumulation of polyphyllin (Yan et al., 2022). To further elucidate the biological mechanisms by which endophytes promote the accumulation of polyphyllin, the rhizomes of *P. polyphylla* inoculated with endophytes were subjected to RNA-seq analysis, and the candidate genes of the CYP450 and UGT superfamilies involved in the biosynthesis of polyphyllin were screened out. This study provides a theoretical basis for the regulatory role of endophytes in the accumulation of medicinal components in host plants and helps us better understand the role of CYP450s and UGTs in the postbiosynthetic modifications of polyphyllin. The findings provide a foundation for the development of biocides and *in vitro* polyphyllin biosynthesis.

2. Materials and methods

2.1. Activation and cultivation of endophytes

The endophytes *Bacillus cereus* LgD2 and *Fusarium oxysporum* TPB were isolated from *P. fargesii*, preserved in 50% glycerol, and stored at −80°C (Yan et al., 2022). Both LgD2 and TPB strains were removed and rapidly shaken at 37°C in a water bath for 10 s for activation.

The activated LgD2 bacterial solution was aspirated and inoculated in LB agar medium using the four-zone delineation method and incubated overnight at 37°C. A single colony was inoculated into 2 mL LB liquid medium (Solarbio Life Sciences, China) and incubated at 37°C for 5 h with shaking. Subsequently, 1 mL of this culture was inoculated into a triangular flask containing 500 mL liquid medium and shaken at 200 rpm at 37°C until the OD_{600} was 0.5–0.6. The culture was then centrifuged at 8.93 *g* for 5 min, and 500 mL of sterile water was added to resuspend the pellet and create a bacterial suspension (Costa Júnior et al., 2020; Liu et al., 2022).

An activated TPB mycelium was selected and inoculated into Potato Dextrose Agar medium (Solarbio Life Sciences, China) and cultured at 28°C for 5–7 days. The surface of the mycelium was rinsed with sterile water, and then filtered through four layers of sterile gauze

to obtain a spore suspension (Andrade et al., 2018; Wang et al., 2021). The spore suspension was diluted in sterile water to 1×10^7 cells/mL and kept for subsequent experiments.

2.2. Planting and endophyte inoculation of *Paris polyphylla*

On April 1, 2022, two-year-old *P. polyphylla* seedlings were purchased from Yunnan Suixitang Biotechnology Co. (China). They were planted in sterile plastic pots containing nutrient soil sterilized at 121°C for 1 h. Five plants were placed in each plastic pot and provided with 100 mL sterile water every 2–3 days. The pots were placed in the backyard greenhouse of Yunnan Agricultural University, 50% of the area of which was covered by a shade net, and its top was closed by a transparent plastic film. The strain inoculation treatments were carried out on May 1, 2022, with roots inoculated with bacterial or spore suspension every 15 dpi; five pots were inoculated for each treatment, with 50 mL of bacterial or spore suspension being poured into each pot separately. Sterile water (50 mL) was used as the control treatment. The rhizomes of *P. polyphylla* inoculated with endophyte strains three and six times (45 dpi and 90 dpi treatments) were collected on June 14, 2022 and July 29, 2022, respectively, cleaned, and immediately stored in liquid nitrogen.

2.3. RNA extraction

Three replicates of each of 45 dpi and 90 dpi rhizomes of *P. polyphylla* treated with LgD2, TPB, or sterile water (18 samples in total) were removed from liquid nitrogen and ground (0.1 g for each rhizome sample). RNA was extracted from the rhizomes of *P. polyphylla* using the HiPure HP Plant RNA Mini Kit (Guangzhou Magen Biotechnology, China) RNA integrity was assessed using 1% agarose gel electrophoresis and an Agilent 5,300 Bioanalyzer (Agilent, USA).

2.4. Library construction and sequencing

Briefly, 10 μg of total RNA of acceptable integrity, concentration, and purity was selected from each rhizome sample; 18 samples were used to construct libraries using the TruSeq Stranded mRNA LT Sample Prep Kit. Transcriptome sequencing was performed at Wuhan SeqHealth Technology Co., Ltd. (China), using an Illumina HiSeq 4,000 platform. The raw data obtained from MGISEQ-T7 sequencing were converted into sequence data using base calling (FASTQ format) to obtain the most original sequencing data file.

2.5. *De novo* transcriptome assembly and read notes

De novo transcriptome assembly and splice variant calling were performed using the Trinity software to obtain transcript sequences, with the longest transcripts as Unigenes. The SortMerna software was used to filter rRNA reads, which were error-corrected and deduplicated using the Rcorrector and fastUniq software. Data quality control was performed using fastp (version 0.23.0). Transcript splicing quality was evaluated using BUSCO (version 5.5.0).

2.6. Functional annotation and enrichment analysis

Protein sequences obtained from the Coding sequence (CDS) prediction by Unigene were annotated using the primary mission of Universal Protein Resource (UniPprot), Non-Redundant (NR), Pfam, evolutionary genealogy of genes: Non-supervised Orthologous Groups (eggNOG), Gene Ontology (GO),[1] Kyoto Encyclopedia of Genes and Genomes (KEGG),[2] and CAZYmes databases. Unigene sequences predicted without CDS were created in the NR and Rfam databases for annotation. Fragments per kilobase per million (FPKM) and read count values were calculated for each Unigene using Bowtie2 and eXpress. The absolute value of log2(FC) > 1 and value of $p < 0.05$ were used as criteria to indicate that the gene was a differentially expressed Unigene. Hierarchical clustering analysis of differentially expressed genes (DEGs) was performed to determine the expression patterns of genes among different groups and samples. GO and KEGG pathway enrichment analyses were performed for DEGs using hypergeometric distribution-based R.

2.7. Construction of phylogenetic tree

The BLAST software and Pfam databases were used to identify transcripts belonging to CYP450 and UGTs. These transcripts were then translated into protein sequences using TBtools (version 1.120). The CYP450 protein sequences of *Arabidopsis thaliana* downloaded from TAIR,[3] whereas the UGT sequences of *A. thaliana*, *Isatis tinctoria*, *Malus domestica*, *Carthamus tinctorius*, *Avena strigosa*, and *Arachis hypogaea* were downloaded from the NCBI database. A phylogenetic tree of CYP450 and UGT gene members was constructed using the maximum likelihood method (Chen et al., 2020). Phylogenetic topology was assessed using 1,000 bootstrap replicates.

2.8. Construction of gene coexpression networks

Gene co-expression networks were constructed using the weighted gene co-expression network (WGCNA) method in R software (version 3.2.2) (Langfelder and Horvath, 2008; Li et al., 2022). Genes with FPKM <1 in 90% of samples were filtered out, and the expression matrices of the top 8,000 genes were selected as input files in WGCNA for the identification of gene modules with strong co-expression. By calculating the correlation coefficients and clusters of the levels of expression of each sample, samples with low correlation or those that could not be clustered on the tree diagram were removed. The WGCNA network was constructed and modules were detected based on the phenotypic traits of polyphyllin. Candidate CYP450 and

1 http://www.geneontology.org
2 http://www.genome.jp/kegg/
3 https://www.arabidopsis.org/

UGT genes were selected from the important templates most relevant to the phenotypic data, based on edge and KME values assigned to the assumed hub genes of the polyphyllin biosynthesis network. Final visualization was performed using Cytoscape (version 3.10.0) (Doncheva et al., 2019).

2.9. Quantitative real-time fluorescence PCR (qRT-PCR)

Total RNA of acceptable purity and integrity was used for the synthesis of first-strand cDNA using the All-in-One RT 5× MasterMix (ABM, Canada) alongside the AccuRT Genomic DNA Removal Kit. The EvaGreen 2X qPCR MasterMix kit (ABM, Canada) was used to validate the levels of expression of five genes related to the steroid saponin biosynthesis pathway. Primers were designed using Primer3Plus[4] (Supplementary Table S1). The reaction system (20 μL) consisted of 10 μL of 2× SYBR Premix Ex Taq™, 2 μL cDNA template, 0.5 μL of upstream and downstream primers, and 7 μL of ddH_2O. PCR conditions were as follows: initial denaturation at 95°C for 2 min, followed by 40 cycles of denaturation at 95°C for 10 s, annealing at 60°C for 15 s, and extension at 72°C for 15 s. Four biological replicates were used for each treatment. The relative gene expression was analyzed using the $2^{-\Delta\Delta Cq}$ method and β-actin was used as the internal reference gene (Bustin et al., 2005; Nolan et al., 2006).

2.10. PPI, PPII, PPVII, PPH, and PPD content determination

According to the standard for the determination of the medicinal content of *P. polyphylla* in "Chinese Pharmacopoeia 2020 Edition," high-performance liquid chromatography (General 0512) was used to determine the content of PPI, PPII, PPVII, PPH, and PPD in *P. polyphylla*. Briefly, rhizome samples of *P. polyphylla* treated with TPB and LgD2 for 90 dpi were dried at 45°C to a constant weight, and then ground into powder using a Chinese herbal medicine pulverizer. Next, 0.5 g of powder (passed through sieve No. 3) was obtained, precisely weighed, and placed in a 50 mL volumetric flask. Then, 20 mL methanol was added to the flask, immersed for 30 min, ultrasonicated for 30 min for extraction, and cooled at 25°C. Additional methanol was used to make up for the loss of weight, and the mixture was shaken well, centrifuged at 8.93 *g* for 5 min, and then filtered through a 0.45 μm micropore filter membrane. The content of PPI, PPII, PPVII, PPH, and PPD in the solution was determined by high performance-liquid chromatography (HPLC) using a C18 column (Zorbax ODS 4.6 × 250 mm, 5 μm; Agilent Technologies, USA) at a detection wavelength of 203 nm, column temperature of 30°C, and flow rate of 1.0 mL/min. PPI, PPII, PPVII, PPH, and PPD controls were purchased from Sichuan Vicki Biotechnology Co. Ltd. (China). Appropriate amounts of PPI, PPII, PPVII, PPH, and PPD controls were obtained, precisely weighed, and mixed with methanol to obtain solutions containing 0.4 mg of each per 1 mL of methanol. For analysis, 20 μL of each of the control and test solutions were precisely aspirated, using octadecylsilane-bonded silica gel as filler and acetonitrile (solvent A) and water (solvent B) as the moving phase in a linear gradient: 0 min: 30% A; 40 min: 60% A; 41 min: 100% A; 44 min: 80% A (Yang et al., 2013; Yan et al., 2022).

2.11. Data analysis

IBM SPSS Statistics (version 25) was used to calculate the mean and standard deviation. An independent samples *t*-test was used to statistically evaluate the differences between the two treatments. *Asterisks indicate significant differences from the control group (*t*-test; $* \ p < 0.05$; $** \ p < 0.01$). The "heatmap" package in R (version 4.2.2) was used for clustering heatmap plots, whereas the "ggplot2" package was used for visualization.

3. Results

3.1. TPB and LgD2 inoculation promoted the accumulation of polyphyllin in *Paris polyphylla*

To investigate the potential effect of endophytes on polyphyllin biosynthesis in *P. polyphylla*, the content of polyphyllin in *P. polyphylla* was determined before and after treatment with TPB and LgD2. Inoculation with TPB and LgD2 led to the increased accumulation of polyphyllin in *P. polyphylla* (Supplementary Table S2). The contents of PPVII, PPD, PPH, and PPI were significantly increased by 42.77, 26.95, 21.96, and 15.27%, respectively, in the TPB treatment group. Likewise, the contents of PPVII, PPD, and PPH were significantly increased by 24, 69.38, and 19.06%, respectively, whereas the PPII content was significantly decreased by 45.97% in the LgD2 treatment group. These results indicated that inoculation with TPB or LgD2 significantly induced the biosynthesis and accumulation of polyphyllin in *P. polyphylla*.

3.2. RNA-seq assembly and annotation

To identify the intrinsic mechanism by which the TPB and LgD2 strains promote polyphyllin biosynthesis, total RNA isolated from the rhizomes of *P. polyphylla* was sequenced under different treatments using the Illumina HiSeq 4,000 platform. Eighteen sequencing libraries constructed from three biological replicates each of 45 and 90 dpi TPB-, LgD2-treated, and control rhizome samples yielded a total of 861,041,222 clean data reads. The Q30 of each sequencing data set was >95%, and 788,438,886 dedup reads were retained after UID deduplication. Accordingly, 1,329,726 contigs were obtained by assembling the dedup reads using Trinity, with an N50 of 638 bp, average length of 537.49 bp, longest read length of 16,964 bp, and average GC content of 45.11%. BUSCO analysis suggested 81% coverage and completeness for transcriptome assembly (Table 1). Then, 1,262,695 (94.96%) of these Unigenes were annotated using the KEGG, UniProt, NR, Pfam, Rfam, eggnog, and GO databases (Supplementary Table S3). The transcriptome sequence data were stored in the NCBI Short Read Archive (SRA) under the BioProject registration number PRJNA935848.

4 https://www.primer3plus.com/

TABLE 1 Summary of sequences obtained by RNA-seq analysis of *Paris polyphylla*.

Names	Number
Total of raw reads	976,402,382
Clean reads	861,041,222
Dedup reads	562,331,692
Total base	714,719,250
GC percentage (%)	45.11
Number of contigs	1,329,726
Maximum length of contigs (bp)	16,964
Minimum length of contigs (bp)	180
Average length of contigs (bp)	537.49
N50 of contigs (bp)	638
Number of Unigenes	1,038,548
Total BUSCO groups searched	2,326
Complete BUSCO (%)	81.5
Missing BUSCO (%)	12.4

3.3. Functional annotation and enrichment analysis of DEGs

DEGs were screened from plants inoculated with TPB and LgD2 strains and functional annotation was performed. Gene expression was significantly different between plants under treatment with different strains and inoculation times (Supplementary Figure S1). GO annotation of DEGs revealed that TPB treatment significantly upregulated phosphorus metabolism, protein modification, oxidation–reduction, and phosphotransferase, methyltransferase, acyltransferase, and metal ion transmembrane transporter activities, whereas nitrogen metabolism, RNA metabolism, metal ion binding, and cation binding were significantly downregulated. Additionally, LgD2 treatment upregulated oxidation–reduction processes, responses to abiotic stimuli, cellular redox homeostasis, carbohydrate and ATP biosynthesis, phosphotransferase, and UDP-glycosyltransferase activities, whereas carbohydrate metabolism, purine nucleotide metabolism, and metal and oxygen binding were downregulated (Supplementary Figure S2). KEGG pathway analysis showed that TPB treatment upregulated DEGs mainly enriched in the pathways of carbon fixation, glycolysis/gluconeogenesis, and plant-pathogen interaction in photosynthetic organisms. Conversely, downregulated DEGs were mainly enriched in the pathways of bacterial invasion of epithelial cells, pathogenic *E. coli* and *Salmonella* infections, and shigellosis. LgD2 treatment also upregulated carbon metabolism, the tricarboxylic acid (TCA) cycle, plant interactions with pathogens, *Vibrio cholerae* infection, nitrogen metabolism, oxidative phosphorylation, and other pathways (Figure 1). These analyses revealed that TPB and LgD2 treatment promoted carbohydrate accumulation and redox homeostasis, increased the levels of phosphorylation, glycosylation, and acylation, and reduced the binding capacity to metal ions and cations. In particular, plant-pathogen interactions were significantly upregulated, whereas the ability of some pathogenic bacteria for infection and bacterial invasion of epithelial cells were decreased, suggesting that endophytic inoculation may promote the defense response of *P. polyphylla* against some bacteria and pathogens.

3.4. Inoculation with TPB and LgD2 alters the terpene backbone and steroid biosynthetic pathway

The terpene backbone and steroid biosynthesis pathways are located upstream of polyphyllin biosynthesis. According to the annotation using the KEGG database, 722 Unigenes were identified as involved in "steroid biosynthesis" (ko00100), encoding 31 enzymes, and while 823 Unigenes were identified as related to "terpenoid skeleton biosynthesis" (ko00900), encoding 36 enzymes. Twenty Unigenes were highly homologous to the functional signature and DEGs under different strain treatments. More specifically, eight DEGs were present in the terpene skeleton biosynthesis pathway, whereas 12 DEGs were present in the steroid biosynthesis pathway (Figure 2).

Unexpectedly, the remaining genes, except farnesyltransferase type-1 subunit alpha (FNTA), 1-deoxy-D-xylulose-5-phosphate synthase (dxs), and TAG lipase acyltransferase (TGL4), were downregulated under strain treatment compared with those in the control. An increased number of genes and differential genes were annotated to the MVA pathway, corroborating that the MVA pathway is the main pathway for polyphyllin biosynthesis (Liu et al., 2016; Upadhyay et al., 2018). These genes were downregulated at 90 dpi, except for hydroxymethylglutaryl-CoA reductase (HMGCR), geranylgeranyl diphosphate synthase (GGPS), plant 4,4-dimethylsterol C-4alpha-methyl-monooxygenase (SMO1), and plant 4alpha-monomethylsterol monooxygenase (SMO2). Previous studies have shown that PPI, PPII, and PPD are diosgenins, whereas PPVII and PPPH are pennogenins, all of which are synthesized from cholesterol (Deng et al., 1999; Li et al., 2001). Therefore, cholesterol accumulation is key to the biosynthesis and accumulation of polyphyllin. Strain treatment did not significantly promote cholesterol biosynthesis; it had the opposite effect, showing a decreasing tendency in the levels of cholesterol over time.

To further validate the transcriptomic results, the expression of five key genes involved in polyphyllin biosynthesis was investigated. The qRT-PCR analysis revealed that the expression of four genes involved in cholesterol biosynthesis, 3-hydroxy-3-methylglutaryl coenzyme A reductase (HMGR), squalene synthase (SQS), cycloartenol synthase (CAS), and oxidosqualene cyclase (SE), was downregulated in *P. polyphylla* under TPB and LgD2 treatment. The only exceptions were the *CAS* gene at 45 dpi rhizomes under TPB treatment and the *SE* gene at 90 dpi rhizomes treated with LgD2 (Supplementary Figure S3). Overall, the genes upstream of polyphyllin biosynthesis mainly showed a trend of downregulated expression under different strain inoculations and time treatments, which was basically consistent with our RNA sequencing analysis, indicating reliable the RNA-seq results. CYP90B27 is responsible for C-22 hydroxylation in the steroidal alkaloid biosynthesis pathway, a downstream pathway in polyphyllin biosynthesis (Yin et al., 2018). The expression of the *CYP90B27* gene was upregulated in *P. polyphylla* treated with either strain at 90 dpi, which may be important for the accumulation of polyphyllin.

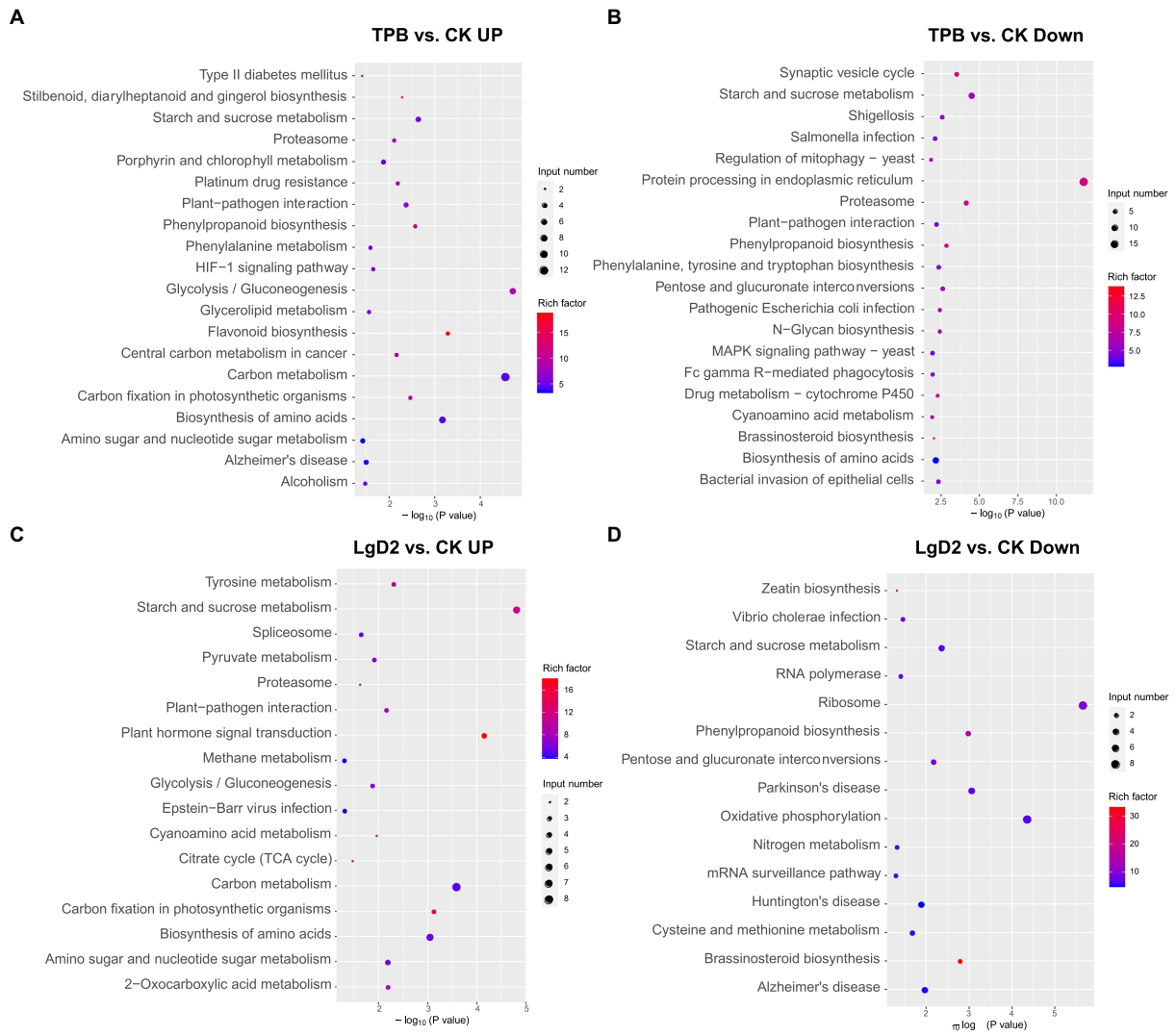

FIGURE 1
Bubble plots of KEGG functional enrichment for *Paris polyphylla* under TPB treatment, **(A)** upregulated vs. **(B)** downregulated; and *P. polyphylla* under LgD2 treatment **(C)** upregulated vs. **(D)** downregulated compared with the control. The size and color of circles in the graph indicates the number of genes and enrichment factor, respectively; a more intense color indicates more enrichment.

3.5. Phylogenetic analysis of the CYP and UGT gene families in *Paris polyphylla*

In this study, Pfam annotation and the BLAST algorithm were used to identify 257 CYP450s and 71 UGTs. Forty-five CYP450s were downloaded from the *Arabidopsis thaliana* database and used to construct a phylogenetic tree; in total, 302 CYP450s were characterized into 13 subfamilies (Figure 3A). Through phylogenetic analysis, the 257 CYP450s of *P. polyphylla* were assigned to the CYP71, CYP94, CYP81, CYP704, CYP90, CYP85, CYP86, and CYP55 families. Among them, CYP71 and CYP94 had the largest number of CYPs, followed by CYP86, CYP90, and CYP55, whereas CYP704 had the lowest number of CYP450s. Additionally, 132 UGTs of *A. thaliana*, *Isatis tinctoria*, *Malus domestica*, *Carthamus tinctorius*, *Avena strigosa*, and *Arachis hypogaea* were downloaded and used to construct a phylogenetic tree. In total, 203 UGTs were classified into 11 subfamilies (Figure 3B). The 71 UGTs of *P. polyphylla* belonged to the UGT74, UGT75, UGT85, UGT87, UGT91, UGT80, UGT71, and UGT73 families. Among them, UGT87 and UGT80 had the highest number of UGT genes, followed by UGT91, UGT74, and UGT75, whereas UGT85 had the lowest number of genes.

In total, 257 CYP450s and 71 UGTs genes were screened for differential expression and 32 CYP450s and 11 UGTs were differentially expressed between the control and TPB and LgD2 treatments. These differentially expressed CYP450s were grouped into three categories, with the most common being CYP71, followed by CYP86 and CYP94 (Figure 4A). Interestingly, genes in the first category were highly expressed in the control at 45 dpi, those in the second category were highly expressed in the control at 90 dpi, whereas those in the third category were upregulated at both 45 and 90 dpi under TPB and LgD2 treatments. Similarly, UTGs were grouped into two categories, with ten genes belonging to UGT87, whereas one was assigned to UGT80 (Figure 4B). The first class of UGTs was upregulated at 90 dpi, whereas the second class was highly expressed at 45 dpi in plants under TPB treatment. Differentially

10.3389/fmicb.2023.1261140

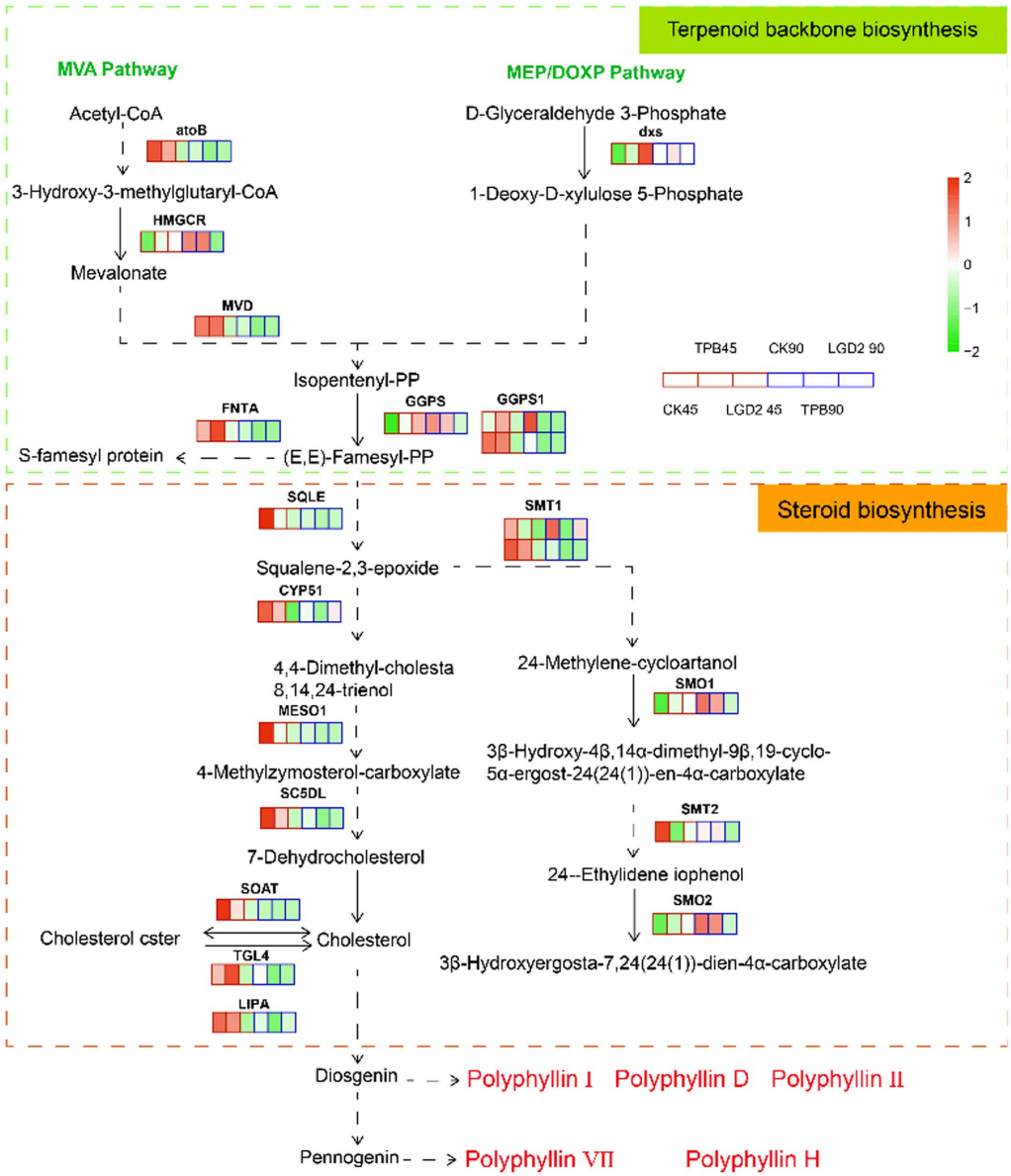

FIGURE 2
Terpene skeleton and steroid biosynthesis pathways with expression map. The heatmap highlights the expression patterns of these genes under treatment with different strains and at different times; RPKM values were used to normalize the corresponding color coding.

expressed CYP450s were both up- and down-regulated, whereas differentially expressed UGTs were mostly upregulated at different times and under different treatments.

Annotation of these CYP450 and UGT genes to the Uniprot, NR, eggNog, GO, KEGG, and CAZYmes databases (Supplementary Table S4) revealed that the functions of these differentially expressed UGTs were mainly related to the formation of glycosidic bonds (GTs), with GT1 accounting for the major part. GO annotation showed that among them, TRINITY_DN2024_c0_g1 and TRINITY_DN2707_c1_g1 belonged to the metabolic pathway of secondary metabolite biosynthesis, functioning in the transfer of hexosyl groups. Moreover, eggNOG database annotations revealed that TRINITY_DN2707_c1_g1 has a flavonol 3-O-glucosyltransferase activity. TRINITY_DN2024_c0_g1 was annotated as scopoletin glucosyltransferase-like protein in the NR database. Annotation of TRINITY_DN541052_c0_g1 and TRINITY_DN117284_c0_g1, which are differentially expressed CYP450 genes, suggested that they function as GT31 and GT1, respectively, in the CAZYmes database. NR annotations identified TRINITY_DN541052_c0_g1 as a lanosterol 14-alpha-demethylase and TRINITY_DN117284_c0_g1 as an isoflavone 2′-hydroxylase-like enzyme.

3.6. Prediction of functional genes by gene coexpression analysis and polyphyllin content

The coexpression network was constructed by inputting transcript data from *P. polyphylla* under different treatments and choosing a soft threshold, $\beta = 14$, at which $R^2 = 0.9$, indicating the successful generation of

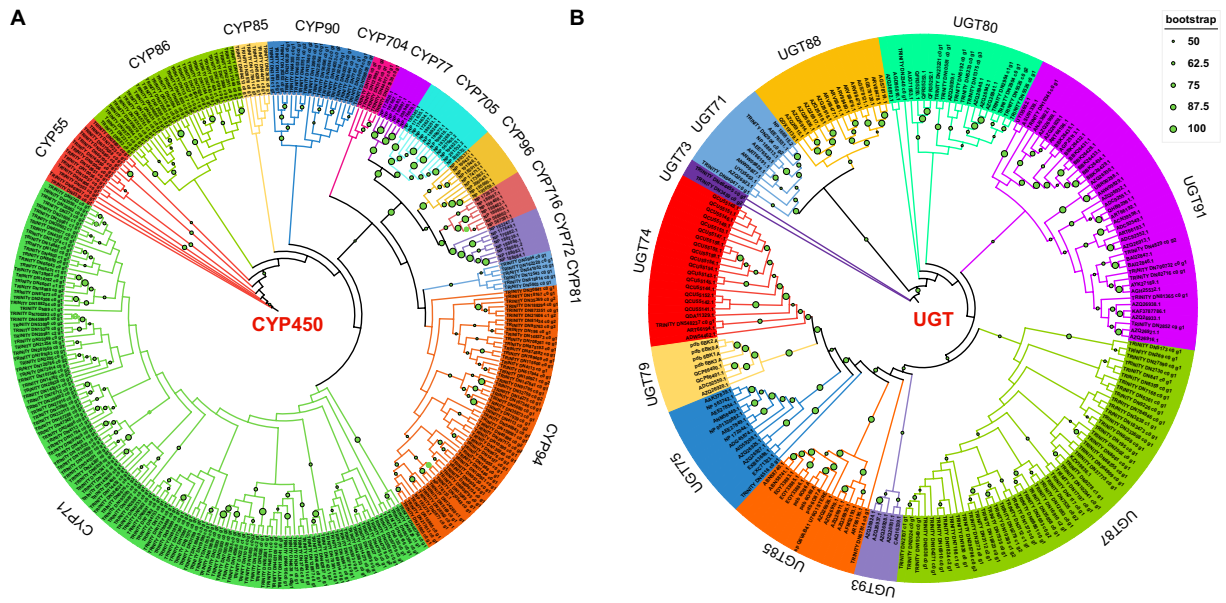

FIGURE 3
Phylogenetic tree of **(A)** CYP450s and **(B)** UGTs. Predicted amino acid sequences of CYP450s and UGTs in *P. polyphylla* were aligned with selected CYP450s and UGTs from other plant species using MUSCLE. The evolutionary history was inferred using the maximum-likelihood method. The bootstrap consensus tree inferred from 1,000 replicates represents the evolutionary history of the taxa analyzed.

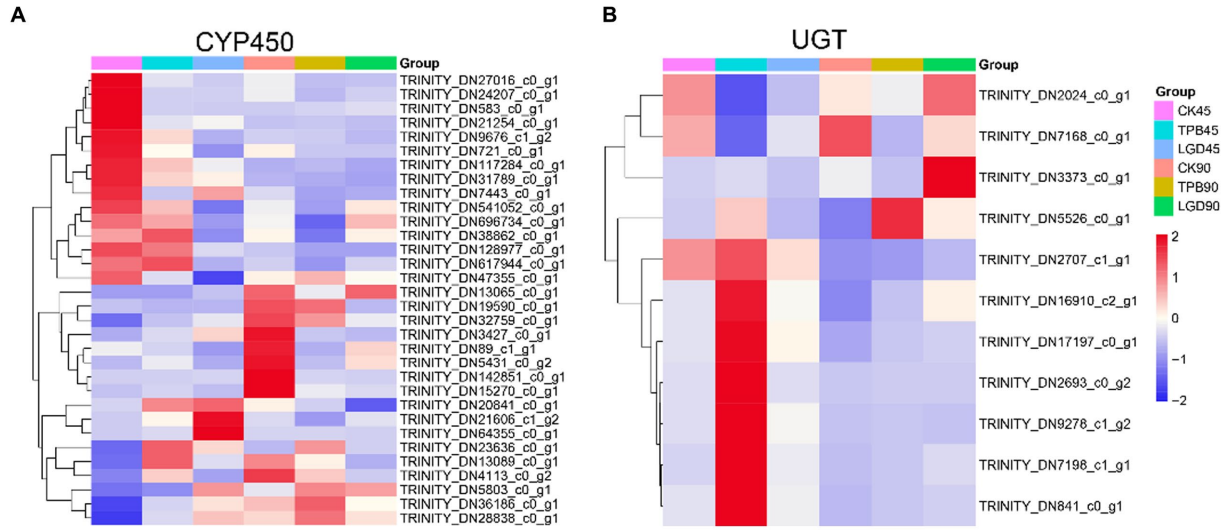

FIGURE 4
Heatmap of the expression of CYP450 **(A)** and UGT **(B)** genes in *P. polyphylla* under treatment with different strains and at different times. RPKM values were used to normalize the corresponding color coding.

the model (Figure 5A). Unigenes with similar expression patterns were clustered in the same branch, with different colors indicating different coexpression modules in the branch (Figure 5B). A threshold of 30 was chosen for each module, and the 8,000 Unigenes were divided with the highest correlation into 26 modules (Figure 5C). Then, the genes in the steroid and terpene backbone biosynthesis pathway were identified by selecting the expression modules that were significantly associated with polyphyllin content, and the correlation coefficients between the biosynthesis of polyphyllin and gene modules were calculated (Figure 6A). The closer the correlation coefficient was to one, the more similar the expression or distribution patterns of the metabolites and genes in the modules of *P. polyphylla* inoculated with different strains. Among them, PPVII and PPH were most correlated with the pink module, with correlation values of 0.75 and 0.76, respectively; PPD was most correlated with the yellow module (0.68); PPII was most correlated with the brown module (0.44); and PPI was most correlated with the light green module (0.51), indicating that the genes in the pink, yellow, brown, and light green modules were highly correlated and might be involved in polyphyllin biosynthesis. In total, 1880 genes were co-clustered with the expression modules in the four modules.

10.3389/fmicb.2023.1261140

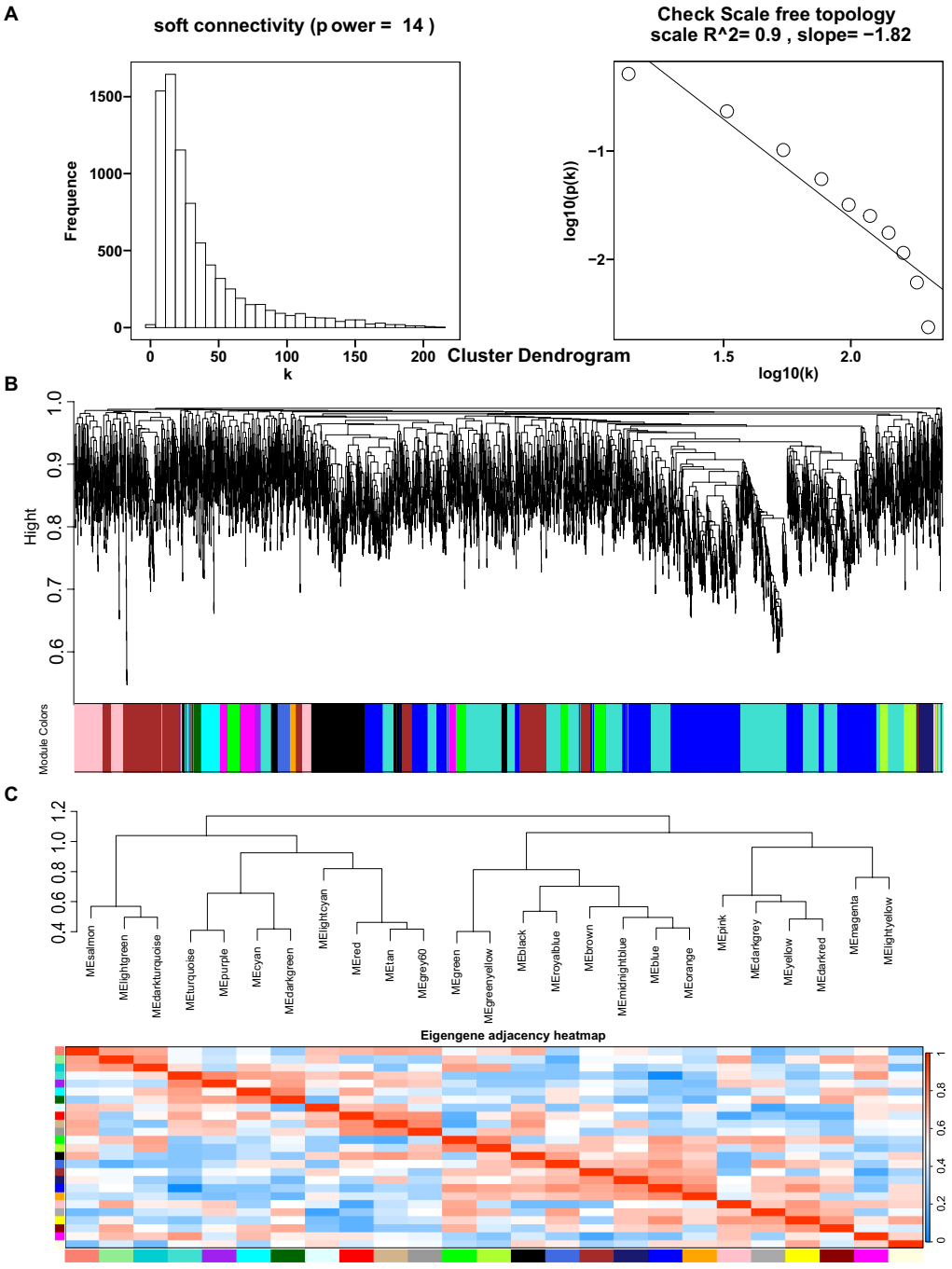

FIGURE 5
Optimal soft threshold map **(A)**, clustered dendrogram **(B)**, and eigengene adjacency heatmap **(C)** for WGCNA analysis. The hierarchical gene clustering method was used to organize the clustering tree of coexpression network modules based on the 1-tom matrix. Each module uses a different color.

Of the 1880 genes, were selected and screened those involved in the terpene skeleton and steroid biosynthesis pathways to identify genes shared in the CYP450 and UGT phylogenetic trees. Using the four prediction modules, six genes in the terpene skeleton biosynthesis pathway, six genes in the steroid biosynthesis pathway, 17 CYP450s, and 2 UGTs were identified. The clustering heatmap shows the expression patterns of these genes under different treatments (Supplementary Figure S4). The expression of these genes was upregulated under TPB and LgD2 treatment, especially that of CYP90B1, which may play a key role in promoting polyphyllin biosynthesis.

To explore the function of these CYP450 and UGT genes, these candidate genes were annotated into the Uniprot, NR, eggNog, GO, KEGG, and CAZYmes databases (Supplementary Table S5). Annotation in the CAZYmes database revealed that TRINITY_DN2002_c0_g1 and TRINITY_DN19349_c0_g1 were both GT1, whereas NR database annotation resulted in their identification as UDP-glycosyltransferase 92A1-like and UDP-glycosyltransferase

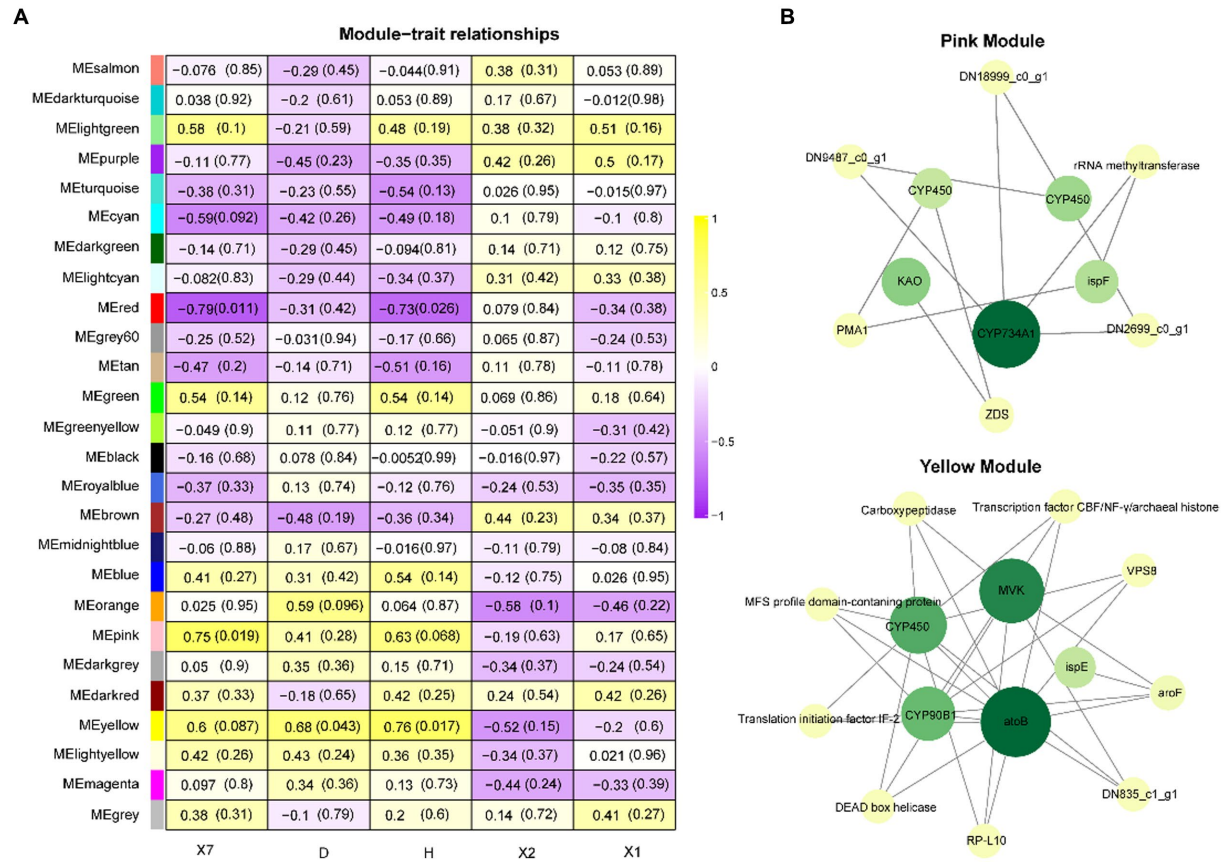

FIGURE 6
WGCNA analysis. **(A)** Heatmap of WGCNA coexpression module-trait association. The rows and columns correspond to the module of the trait genes and metabolites, respectively. Each cell contains the correlation and value of p of the gene in the module with the corresponding metabolite. **(B)** Hub gene correlation network diagram.

89B1, respectively. TRINITY_DN7787_c1_g1 was annotated to the diterpenoid biosynthesis pathway in the KEGG database and to GT31 in the CAZYmes database, and Uniprot and NR annotations revealed that this gene encodes an Ent-kaurenoic acid oxidase.

To further investigate the roles of CYP450s and UGTs in polyphyllin-related modules, the top genes with the highest weights in the pink and yellow modules were selected for network correlation analysis. CYP450, KAO, CYP734A1, and ispE play key roles in the pink module, whereas CYP450, acetyl-CoA C-acetyltransferase (atoB), 4-diphosphocytidyl-2-C-methyl-D-erythritol kinase (ispE), CYP90B1, and mevalonate kinase (MVK) play key roles in the yellow module (Figure 6B).

4. Discussion

Endophytes, such as bacteria and fungi, are microorganisms that interact with host plants. Complex microbial communities are beneficial for host nutrient supply, plant growth hormones, promotion of metabolite accumulation, and control of soil-borne and systemic pathogens (Deng and Cao, 2017; Dudeja et al., 2021; Pandey et al., 2022). Hence, endophytes have potential applications in the pharmaceutical, agricultural, and food industries because of their ability to enhance the levels of biologically active secondary metabolites in the host and produce metabolites similar to those of the host (El-Sayed et al., 2020). Endophytes can form long-term, stable, and mutually beneficial symbiotic relationships with medicinal plants, influencing the secondary metabolism of the plant and its therapeutic properties (Maggini et al., 2017). Endophytes of the genera *Fusarium*, *Nodulisporium*, *Brevundimonas*, and *Bacillus*, isolated from *Panax notoginseng*, can produce major ginsenosides (Luo et al., 2013).

Polyphyllin is the main medicinal active ingredient in the perennial medicinal plants of *P. polyphyllin* listed in the Chinese Pharmacopeia. However, owing to its slow growth, *P. polyphyllin* has a low polyphyllin content, whereas *P. fargesii*, a closely related species of the same genus, has a high polyphyllin content. Therefore, it is of great significance to isolate and screen *P. fargesii* strains to identify the specific factors that promote the accumulation of polyphyllin content in *P. polyphyllin*, and increase the accumulation of its medicinal active ingredients. The endophytes LgD2 and TPB isolated from *P. fargesii* have the potential to promote the biosynthesis of polyphyllin in *P. polyphyllin*. Although *F. oxysporum* is a pathogen of most plants and can cause wilt, root-, and foot-rot in many plant species, as a root endophyte, it can also inhibit diseases caused by vascular pathogens and pathogenic *F. oxysporum* strains owing to a long-term interactive relationship with the host plant, further protecting the host plant against root pathogens from other plant endophytes (de Lamo and Takken, 2020).

After inoculating *P. polyphylla* with TPB and LgD2 by root irrigation, the accumulation of polyphyllin in the rhizomes was significantly increased at 90 dpi (Supplementary Table S2). In addition,

TPB treatment had the strongest positive effect on pennogenins (PPVII and PPH), whereas LgD2 treatment had the strongest effect on diosgenins (PPI, PPII, and PPD). The effects of these two strains on the biosynthetic pathway of polyphyllin in *P. polyphylla* differed. Moreover, the increase in the content of PPD and decrease in that of PPII under LgD2 treatment were simultaneous, indicating that the change in the content of PPD was likely attributed to the conversion of the original PPII biosynthetic pathway.

To reveal the intrinsic mechanism of endophytic inoculation on polyphyllin biosynthesis in *P. polyphylla*, 45 dpi and 90 dpi treated *P. polyphylla* were selected for RNA-seq and qRT-PCR analysis (Yan et al., 2022). A total of 1,329,726 Unigenes were annotated from 18 sequencing libraries. Annotation and enrichment analyses of the identified DEGs showed that the activities of auxin biosynthesis, protein modification, methylation, acylation, and phosphorylation were increased in plants under TPB treatment. Methylation, UDP-glycosylation, and phosphorylation were upregulated in *P. polyphylla* under LgD2 treatment (Figure 1). In plant environments, microorganisms can interact with host plants and synthesize specific metabolites. Epigenetic modifications are key regulators of plant chromatin structure and gene expression, controlling plant growth and development, as well as responses to various environmental stresses (Wang et al., 2020). Various coenzymes catalyze redox, group transfer, and allosteric reactions. In addition, methylation, acylation, and glycosylation of secondary metabolites catalyzed by O-methyltransferases allow the modification of secondary metabolites (Cheynier et al., 2013). Endophytic bacteria upregulate protein modification, methylation, acylation, and glycosylation in plant hosts, suggesting that endophytes enhance plant resistance and may play an important role in the modification of secondary metabolites.

Both treatments enhanced the redox reactions, TCA cycle, and carbohydrate biosynthesis in *P. polyphylla* (Figure 1). Redox reactions in plants play an important role in photosynthesis. The nitrogen-fixing reaction in the photosystem is the most important part of redox reactions in plant cells and plays a crucial role in photosynthesis. The TCA cycle is the ultimate common oxidation pathway for carbohydrates, fats, and amino acids. It is the most important metabolic pathway for supplying energy to the body (Akram, 2014). As plant growth occurs through carbon fixation (Ducat and Silver, 2012), the observed increase in carbon fixation capacity implied that both strains have a facilitative effect on photosynthesis. Carbohydrates are the basis for plant biomass and yield (Chandel, 2021), and the accumulation of photosynthetic products is the result of increased photosynthetic capacity, indicating that the TPB and LgD2 strains had positive effects on the growth of *P. polyphylla*. In addition, increased plant-pathogen interactions decreased bacterial invasion in epithelial cells, and infection by pathogenic *E. coli*, *Salmonella*, and *Shigella*, suggesting that endophytic bacteria also play a role in the disease resistance and defense response of the host plant.

qRT-PCR analysis revealed that the four genes involved in cholesterol biosynthesis, HMGR, SQS, CAS, and SE, were downregulated, whereas CYP90B27, which is involved in C-22 hydroxylation, was upregulated in plants after strain treatment. RNA-seq results also revealed that the expression of Unigenes, which was annotated to the terpene skeleton and steroid biosynthesis pathways, was not increased by strain treatment, whereas an increase was mainly observed in CYP450 and UGT genes (Figures 2, 4). Hence, the increase in the content of polyphyllin in rhizomes of *P. polyphyllin* treated with TPB and LgD2 was mainly attributed to the modification of cholesterol, such as glycosylation and hydroxylation.

Many members of the CYP450 and UGT superfamilies are involved in the biosynthesis of steroids and polyphyllin and play key roles in the conversions of PPI, PPII, PPVII, PPD, and PPH. CYP716A53v2 is a protopanaxadiol 6-hydroxylase that catalyzes the production of PPT from PPD in ginseng (Park et al., 2016). CYP72A397 is an oleanolic acid 23-hydroxylase involved in the production of oleanolic acid in *Kalopanax septemlobus* (Han et al., 2018). CYP90B1 is a steroidal C-22 hydroxylase that catalyzes the early C-22 hydroxylation of various C sterols including C27, C28, and C29 (Fujita et al., 2006; Cheng et al., 2020). UGTs, which are the largest family of glycosyltransferases in higher plants that modify secondary metabolites and hormones, mediate the transfer of glycosyl residues from activated nucleotide sugars to glycosidic elements. This family of genes plays an important role in the broad diversity of species-specific plant secondary metabolites (Ross et al., 2001; Nishimura et al., 2010).

Using WGCNA, the genes of the steroidal saponin and terpene backbone biosynthesis pathways that were most significantly affected under strain treatment were selected. Combined with the phylogenetic tree, the CYP450 and UGT genes in the coexpression module, which are likely to be responsible for the differences in polyphyllin content; however, these results need further validation. To find the key CYP450 and UGT candidate genes, The screened genes were functionally annotated. Annotation to the CAZYmes database revealed that these genes mainly function as GTs (glycosidic bond formation), of which GT1 accounted for the major portion, followed by GT31. The GT1 family consists of a variety of enzymes that catalyze the monosaccharide addition of different compounds. The 11 differentially expressed screened UGTs were identified to function as GT1, of which, except for TRINITY_DN7168_c0_g1, were more highly expressed under strain treatment. The glycosylation modification of these UGTs may play a key role in the accumulation of PPI, PPII, PPVII, PPD, and PPH. Moreover, the action of TRINITY_DN7168_c0_g1 resulted in a decrease in the accumulation of PPI, PPII, PPVII, PPD, and PPH, and may be a paralogous branch for the synthesis of poliphyllin.

Under the induction of endophytes, host plants may improve the polyphyllin yield by regulating genes related to the polyphyllin biosynthesis pathway. In the present study, the transcriptomes of *B. cereus* LgD2 and *F. oxysporum* TPB-inoculated rhizomes of *P. polyphylla* were sequenced. Enrichment analysis of DEGs revealed that endophyte inoculation promoted the chemical modification of downstream metabolites and had positive effects on the growth and disease resistance of *P. polyphylla*. Phylogenetic trees and WGCNA revealed CYP450s and UGTs that may be involved in the biosynthesis of PPI, PPII, PPVII, PPD, and PPH; however, their specific functions and roles must be further validated.

5. Conclusion

This study showed that the endophytes, *B. cereus* (LgD2) and *F. oxysporum* (TPB), promote the accumulation of polyphyllin in *P. polyphylla* and facilitate beneficial plant-endophyte interactions. In addition, endophyte-plant associations increased the production of polyphyllin by enhancing the expression of CYP450s and UGTs. This study revealed the effects of *B. cereus*

and *F. Oxysporum* on plant metabolism and related regulatory processes and screened for CYPs and UGTs that affect polyphyllin biosynthesis. These findings provide a theoretical basis for improving the medicinal value of Chinese herbal medicines and help to further elucidate plant-endophyte interactions and biosynthetic pathways of polyphyllin.

Data availability statement

The data presented in this study are deposited in the NCBI Sequence Read Archive (SRA) under accession number PRJNA935848 (https://www.ncbi.nlm.nih.gov/sra/?term=PRJNA935848).

Author contributions

QZ: Writing – original draft. SC: Writing – review & editing, Formal analysis, Validation. YY: Writing – review & editing, Formal analysis, Validation. CX: Data curation, Investigation, Writing – review & editing. YD: Writing – review & editing. LL: Validation, Writing – review & editing. YH: Writing – review & editing. YL: Formal analysis, Resources, Writing – review & editing. BC: Writing – review & editing, Methodology, Resources. TL: Conceptualization, Methodology, Funding acquisition, Writing – original draft.

Funding

The author(s) declare financial support was received for the research, authorship, and/or publication of this article. This work was supported by the National Key R&D Program of China (grant no. 2021YFD1000202 and 2021YFD1601003), Key projects of Yunnan Provincial Natural Fund (grant no. 202201AS070064), Key R&D program of Yunnan Province of China (grant no. 202103AC100003), and the Research and Application of Personalized Cigarette Products (grant no. 2023CP02).

Conflict of interest

SC, YY, and BC were employed by Center of Yunnan Zhongyan Industry Co., Ltd.

The authors declare that this study received funding from Center of Yunnan Zhongyan Industry Co., Ltd. The funder was directly involved in the design, analysis and interpretation of data, writing of the article, and decision-making of the study.

Publisher's note

Supplementary material

The Supplementary material for this article can be found online at: https://www.frontiersin.org/articles/10.3389/fmicb.2023.1261140/full#supplementary-material

References

Akram, M. (2014). Citric acid cycle and role of its intermediates in metabolism. *Cell Biochem. Biophys.* 68, 475–478. doi: 10.1007/s12013-013-9750-1

Andrade, H. F., Araújo, L. C. A., Santos, B. S. D., Paiva, P. M. G., Napoleão, T. H., Correia, M., et al. (2018). Screening of endophytic fungi stored in a culture collection for taxol production. *Braz. J. Microbiol.* 49, 59–63. doi: 10.1016/j.bjm.2018.06.001

Bustin, S. A., Benes, V., Nolan, T., and Pfaffl, M. W. (2005). Quantitative real-time RT-PCR--a perspective. *J. Mol. Endocrinol.* 34, 597–601. doi: 10.1677/jme.1.01755

Cao, X., Xu, L., Wang, J., Dong, M., Xu, C., Kai, G., et al. (2022). Endophytic fungus Pseudodidymocyrtis lobariellae KL27 promotes taxol biosynthesis and accumulation in Taxus chinensis. *BMC Plant Biol.* 22:12. doi: 10.1186/s12870-021-03396-6

Chandel, N. S. (2021). Carbohydrate metabolism. *Cold Spring Harb. Perspect. Biol.* 13:568. doi: 10.1101/cshperspect.a040568

Chen, C., Chen, H., Zhang, Y., Thomas, H. R., Frank, M. H., He, Y., et al. (2020). TBtools: an integrative toolkit developed for interactive analyses of big biological data. *Mol. Plant* 13, 1194–1202. doi: 10.1016/j.molp.2020.06.009

Chen, Y., Hu, B., Xing, J., and Li, C. (2021). Endophytes: the novel sources for plant terpenoid biosynthesis. *Appl. Microbiol. Biotechnol.* 105, 4501–4513. doi: 10.1007/s00253-021-11350-7

Chen, T., Lin, J., Tang, D., Zhang, M., Wen, F., Xue, D., et al. (2019). Paris saponin H suppresses human hepatocellular carcinoma (HCC) by inactivation of Wnt/β-catenin pathway *in vitro* and *in vivo*. *Int. J. Clin. Exp. Pathol.* 12, 2875–2886.

Chen, M., Ye, K., Zhang, B., Xin, Q., Li, P., Kong, A. N., et al. (2019). Paris Saponin II inhibits colorectal carcinogenesis by regulating mitochondrial fission and NF-κB pathway. *Pharmacol. Res.* 139, 273–285. doi: 10.1016/j.phrs.2018.11.029

Cheng, Y., Liu, H., Tong, X., Liu, Z., Zhang, X., Li, D., et al. (2020). Identification and analysis of CYP450 and UGT supergene family members from the transcriptome of *Aralia elata* (Miq.) seem reveal candidate genes for triterpenoid saponin biosynthesis. *BMC Plant Biol.* 20:214. doi: 10.1186/s12870-020-02411-6

Cheynier, V., Comte, G., Davies, K. M., Lattanzio, V., and Martens, S. (2013). Plant phenolics: recent advances on their biosynthesis, genetics, and ecophysiology. *Plant Physiol. Biochem.* 72, 1–20. doi: 10.1016/j.plaphy.2013.05.009

Costa Júnior, P. S. P., Cardoso, F. P., Martins, A. D., Teixeira Buttrós, V. H., Pasqual, M., Dias, D. R., et al. (2020). Endophytic bacteria of garlic roots promote growth of micropropagated meristems. *Microbiol. Res.* 241:126585. doi: 10.1016/j.micres.2020.126585

de Lamo, F. J., and Takken, F. L. W. (2020). Biocontrol by fusarium oxysporum using endophyte-mediated resistance. *Front. Plant Sci.* 11:37. doi: 10.3389/fpls.2020.00037

Deng, Z., and Cao, L. (2017). Fungal endophytes and their interactions with plants in phytoremediation: a review. *Chemosphere* 168, 1100–1106. doi: 10.1016/j.chemosphere.2016.10.097

Deng, S., Yu, B., Hui, Y., Yu, H., and Han, X. (1999). Synthesis of three diosgenyl saponins: dioscin, polyphyllin D, and balanitin 7. *Carbohydr. Res.* 317, 53–62. doi: 10.1016/s0008-6215(99)00066-x

Doncheva, N. T., Morris, J. H., Gorodkin, J., and Jensen, L. J. (2019). Cytoscape StringApp: network analysis and visualization of proteomics data. *J. Proteome Res.* 18, 623–632. doi: 10.1021/acs.jproteome.8b00702

Ducat, D. C., and Silver, P. A. (2012). Improving carbon fixation pathways. *Curr. Opin. Chem. Biol.* 16, 337–344. doi: 10.1016/j.cbpa.2012.05.002

Dudeja, S. S., Suneja-Madan, P., Paul, M., Maheswari, R., and Kothe, E. (2021). Bacterial endophytes: molecular interactions with their hosts. *J. Basic Microbiol.* 61, 475–505. doi: 10.1002/jobm.202000657

El-Sayed, A. S. A., El-Sayed, M. T., Rady, A., Zein, N., Enan, G., Shindia, A., et al. (2020). Exploiting the biosynthetic potency of Taxol from fungal endophytes of conifers plants; genome mining and metabolic manipulation. *Molecules* 25:3000. doi: 10.3390/molecules25133000

Fujita, S., Ohnishi, T., Watanabe, B., Yokota, T., Takatsuto, S., Fujioka, S., et al. (2006). Arabidopsis CYP90B1 catalyses the early C-22 hydroxylation of C27, C28 and C29 sterols. *Plant J.* 45, 765–774. doi: 10.1111/j.1365-313X.2005.02639.x

Gao, X., Zhang, X., Chen, W., Li, J., Yang, W., Zhang, X., et al. (2020). Transcriptome analysis of Paris polyphylla var. yunnanensis illuminates the biosynthesis and accumulation of steroidal saponins in rhizomes and leaves. *Phytochemistry* 178:112460. doi: 10.1016/j.phytochem.2020.112460

Han, J. Y., Chun, J. H., Oh, S. A., Park, S. B., Hwang, H. S., Lee, H., et al. (2018). Transcriptomic analysis of Kalopanax septemlobus and characterization of KsBAS, CYP716A94 and CYP72A397 genes involved in Hederagenin Saponin biosynthesis. *Plant Cell Physiol.* 59, 319–330. doi: 10.1093/pcp/pcx188

Huang, Y., Zhao, J., Zhou, L., Wang, M., Wang, J., Li, X., et al. (2009). Antimicrobial compounds from the endophytic fungus fusarium sp. Ppf4 isolated from the medicinal plant Paris polyphylla var. yunnanensis. *Nat. Prod. Commun.* 4, 1455–1458.

Langfelder, P., and Horvath, S. (2008). WGCNA: an R package for weighted correlation network analysis. *BMC Bioinformat.* 9:559. doi: 10.1186/1471-2105-9-559

Li, Z., Wen, W., Qin, M., He, Y., Xu, D., and Li, L. (2022). Biosynthetic mechanisms of secondary metabolites promoted by the interaction between endophytes and plant hosts. *Front. Microbiol.* 13:928967. doi: 10.3389/fmicb.2022.928967

Li, Z., Xiong, K., Wen, W., Li, L., and Xu, D. (2023). Functional endophytes regulating plant secondary metabolism: current status, prospects and applications. *Int. J. Mol. Sci.* 24:1153. doi: 10.3390/ijms24021153

Li, B., Yu, B., Hui, Y., Li, M., Han, X., and Fung, K. P. (2001). An improved synthesis of the saponin, polyphyllin D. *Carbohydr. Res.* 331, 1–7. doi: 10.1016/s0008-6215(01)00014-3

Li, Y., Zhao, J., Chen, H., Mao, Y., Yang, Y., Feng, L., et al. (2022). Transcriptome level reveals the triterpenoid Saponin biosynthesis pathway of Bupleurum falcatum L. *Genes (Basel)* 13:2237. doi: 10.3390/genes13122237

Lin, X., Gajendran, B., Varier, K. M., Liu, W., Song, J., Rao, Q., et al. (2021). Paris Saponin VII induces apoptosis and cell cycle arrest in Erythroleukemia cells by a mitochondrial membrane signaling pathway. *Anti Cancer Agents Med. Chem.* 21, 498–507. doi: 10.2174/1871520620666200615134039

Liu, J. Q., Chen, S. M., Zhang, C. M., Xu, M. J., Xing, K., Li, C. G., et al. (2022). Abundant and diverse endophytic bacteria associated with medicinal plant *Arctium lappa* L. and their potential for host plant growth promoting. *Antonie Van Leeuwenhoek* 115, 1405–1420. doi: 10.1007/s10482-022-01785-x

Liu, T., Li, X., Xie, S., Wang, L., and Yang, S. (2016). RNA-seq analysis of Paris polyphylla var. yunnanensis roots identified candidate genes for saponin synthesis. *Plant Divers.* 38, 163–170. doi: 10.1016/j.pld.2016.05.002

Lu, Q., He, Y., Wang, Y., Gao, L., Zheng, Y., Zhang, Z., et al. (2018). Saponins from Paris forrestii (Takht.) H. Li display potent activity against acute myeloid leukemia by suppressing the RNF6/AKT/mTOR signaling pathway. *Front. Pharmacol.* 9:673. doi: 10.3389/fphar.2018.00673

Luo, S. L., Dang, L. Z., Li, J. F., Zou, C. G., Zhang, K. Q., and Li, G. H. (2013). Biotransformation of saponins by endophytes isolated from Panax notoginseng. *Chem. Biodivers.* 10, 2021–2031. doi: 10.1002/cbdv.201300005

Maggini, V., De Leo, M., Mengoni, A., Gallo, E. R., Miceli, E., Reidel, R. V. B., et al. (2017). Plant-endophytes interaction influences the secondary metabolism in *Echinacea purpurea* (L.) Moench: an *in vitro* model. *Sci. Rep.* 7:16924. doi: 10.1038/s41598-017-17110-w

Meng, M., Yue, Z., Chang, L., Liu, Y., Hu, J., Song, Z., et al. (2021). Anti-rheumatoid arthritic effects of Paris Saponin VII in human rheumatoid arthritis fibroblast-like Synoviocytes and adjuvant-induced arthritis in rats. *Front. Pharmacol.* 12:683698. doi: 10.3389/fphar.2021.683698

Negi, J. S., Bisht, V. K., Bhandari, A. K., Bhatt, V. P., Singh, P., and Singh, N. (2014). Paris polyphylla: chemical and biological prospectives. *Anti Cancer Agents Med. Chem.* 14, 833–839. doi: 10.2174/1871520614666140611101040

Nishimura, Y., Tokimatsu, T., Kotera, M., Goto, S., and Kanehisa, M. (2010). Genome-wide analysis of plant UGT family based on sequence and substrate information. *Genome Inform.* 24, 127–138. doi: 10.1142/9781848166585_0011

Nolan, T., Hands, R. E., and Bustin, S. A. (2006). Quantification of mRNA using real-time RT-PCR. *Nat. Protoc.* 1, 1559–1582. doi: 10.1038/nprot.2006.236

Pandey, S. S., Jain, R., Bhardwaj, P., Thakur, A., Kumari, M., Bhushan, S., et al. (2022). Plant probiotics – endophytes pivotal to plant health. *Microbiol. Res.* 263:127148. doi: 10.1016/j.micres.2022.127148

Park, S. B., Chun, J. H., Ban, Y. W., Han, J. Y., and Choi, Y. E. (2016). Alteration of *Panax ginseng* saponin composition by overexpression and RNA interference of the protopanaxadiol 6-hydroxylase gene (CYP716A53v2). *J. Ginseng Res.* 40, 47–54. doi: 10.1016/j.jgr.2015.04.010

Ren, X., Zhu, Y., Xie, L., Zhang, M., Gao, L., and He, H. (2020). Yunnan Baiyao diminishes lipopolysaccharide-induced inflammation in osteoclasts. *J. Food Biochem.* 44:e13182. doi: 10.1111/jfbc.13182

Ross, J., Li, Y., Lim, E., and Bowles, D. J. (2001). Higher plant glycosyltransferases. *Genome Biol.* 2:Reviews3004. doi: 10.1186/gb-2001-2-2-reviews3004

Santoyo, G., Moreno-Hagelsieb, G., Orozco-Mosqueda Mdel, C., and Glick, B. R. (2016). Plant growth-promoting bacterial endophytes. *Microbiol. Res.* 183, 92–99. doi: 10.1016/j.micres.2015.11.008

Shweta, S., Bindu, J. H., Raghu, J., Suma, H. K., Manjunatha, B. L., Kumara, P. M., et al. (2013). Isolation of endophytic bacteria producing the anti-cancer alkaloid camptothecine from Miquelia dentata Bedd. (Icacinaceae). *Phytomedicine* 20, 913–917. doi: 10.1016/j.phymed.2013.04.004

Tao, L., Qiuhong, L., Fuqiang, Y., Shuhui, Z., Suohui, T., and Linyuan, F. (2021). Plant growth-promoting activities of bacterial endophytes isolated from the medicinal plant pairs polyphylla var. yunnanensis. *World J. Microbiol. Biotechnol.* 38:15. doi: 10.1007/s11274-021-03194-0

Thapa, C. B., Paudel, M. R., Bhattarai, H. D., Pant, K. K., Devkota, H. P., Adhikari, Y. P., et al. (2022). Bioactive secondary metabolites in Paris polyphylla Sm. and their biological activities: a review. *Heliyon* 8:e08982. doi: 10.1016/j.heliyon.2022.e08982

Upadhyay, S., Jeena, G. S., Shikha, , and Shukla, R. K. (2018). Recent advances in steroidal saponins biosynthesis and *in vitro* production. *Planta* 248, 519–544. doi: 10.1007/s00425-018-2911-0

Wang, X., Chen, D., Wang, Y., and Xie, J. (2015). De novo transcriptome assembly and the putative biosynthetic pathway of steroidal sapogenins of *Dioscorea composita*. *PLoS One* 10:e0124560. doi: 10.1371/journal.pone.0124560

Wang, W., Liu, Y., You, L., Sun, M., Qu, C., Dong, X., et al. (2020). Inhibitory effects of Paris saponin I, II, VI and VII on HUVEC cells through regulation of VEGFR2, PI3K/AKT/mTOR, Src/eNOS, PLCγ/ERK/MERK, and JAK2-STAT3 pathways. *Biomed. Pharmacother.* 131:110750. doi: 10.1016/j.biopha.2020.110750

Wang, G. K., Yang, J. S., Huang, Y. F., Liu, J. S., Tsai, C. W., Bau, D. T., et al. (2021). Culture separation, identification and unique anti-pathogenic Fungi capacity of endophytic Fungi from Gucheng *Salvia Miltiorrhiza*. *In Vivo* 35, 325–332. doi: 10.21873/invivo.12263

Wen, F., Chen, T., Yin, H., Lin, J., and Zhang, H. (2019). *In vitro* effects on thrombin of Paris Saponins and *in vivo* hemostatic activity evaluation of Paris fargesii var. brevipetala. *Molecules* 24:1420. doi: 10.3390/molecules24071420

Worsley, S. F., Newitt, J., Rassbach, J., Batey, S. F. D., Holmes, N. A., Murrell, J. C., et al. (2020). Streptomyces endophytes promote host health and enhance growth across plant species. *Appl. Environ. Microbiol.* 86:1053. doi: 10.1128/aem.01053-20

Xiang, Y. C., Peng, P., Liu, X. W., Jin, X., Shen, J., Zhang, T., et al. (2022). Paris saponin VII, a hippo pathway activator, induces autophagy and exhibits therapeutic potential against human breast cancer cells. *Acta Pharmacol. Sin.* 43, 1568–1580. doi: 10.1038/s41401-021-00755-9

Yan, X. X., Pan, Q. D., Sun, H. Y., Gao, L., Yang, R., and Yang, L. X. (2021). Traditional use of Paris polyphylla and its active components. *Zhongguo Zhong Yao Za Zhi* 46, 6343–6352. doi: 10.19540/j.cnki.cjcmm.20210901.101

Yan, D., Wang, X., Xi, C., Zi, S., and Liu, T. (2022). Isolation and identification of symbiotic strains in Paris fargesii Franch that promote disease resistance. *Front. Agron.* 4:1028. doi: 10.3389/fagro.2022.1021028

Yang, D. Z., Yin, X. X., Ong, C. N., and Tang, D. Q. (2013). Multidimensional information-based HPLC technologies to evaluate traditional Chinese medicine. *J. Chromatogr. Sci.* 51, 716–725. doi: 10.1093/chromsci/bmt057

Yin, Y., Gao, L., Zhang, X., and Gao, W. (2018). A cytochrome P450 monooxygenase responsible for the C-22 hydroxylation step in the Paris polyphylla steroidal saponin biosynthesis pathway. *Phytochemistry* 156, 116–123. doi: 10.1016/j.phytochem.2018.09.005

Zhang, C., Li, C., Jia, X., Wang, K., Tu, Y., Wang, R., et al. (2019). *In vitro* and *in vivo* anti-inflammatory effects of Polyphyllin VII through downregulating MAPK and NF-κB pathways. *Molecules* 24:875. doi: 10.3390/molecules24050875

Zhang, Y., Zhao, J., Wang, J., Shan, T., Mou, Y., Zhou, L., et al. (2011). Chemical composition and antimicrobial activity of the volatile oil from fusarium tricinctum, the endophytic fungus in Paris polyphylla var. yunnanensis. *Nat. Prod. Commun.* 6, 1759–1762. doi: 10.1177/1934578X1100601146

frontiers | Frontiers in Microbiology

TYPE Review
PUBLISHED 08 December 2023
DOI 10.3389/fmicb.2023.1280258

OPEN ACCESS

EDITED BY
Mina Salehi,
Tarbiat Modares University, Iran

REVIEWED BY
Debdulal Banerjee,
Vidyasagar University, India
Nakkeeran S.,
Tamil Nadu Agricultural University, India
Tariq Mukhtar,
Pir Mehr Ali Shah Arid Agriculture University, Pakistan

*CORRESPONDENCE
Shafaq Rasool
shafaq.rasool@smvdu.ac.in

†These authors have contributed equally to this work

RECEIVED 19 August 2023
ACCEPTED 21 November 2023
PUBLISHED 08 December 2023

CITATION
Bhardwaj M, Kailoo S, Khan RT, Khan SS and Rasool S (2023) Harnessing fungal endophytes for natural management: a biocontrol perspective.
Front. Microbiol. 14:1280258.
doi: 10.3389/fmicb.2023.1280258

Harnessing fungal endophytes for natural management: a biocontrol perspective

Mansavi Bhardwaj†, Swadha Kailoo†, Rabiya Tabbassum Khan†, Sofia Sharief Khan† and Shafaq Rasool*

Molecular Biology Laboratory, School of Biotechnology, Shri Mata Vaishno Devi University, Katra, Jammu and Kashmir, India

In the ever-evolving realm of agriculture, the convoluted interaction between plants and microorganisms have assumed paramount significance. Fungal endophytes, once perceived as mere bystanders within plant tissues, have now emerged as dynamic defenders of plant health. This comprehensive review delves into the captivating world of fungal endophytes and their multifaceted biocontrol mechanisms. Exploring their unique ability to coexist with their plant hosts, fungal endophytes have unlocked a treasure trove of biological weaponry to fend off pathogens and enhance plant resilience. From the synthesis of bioactive secondary metabolites to intricate signaling pathways these silent allies are masters of biological warfare. The world of fungal endophytes is quite fascinating as they engage in a delicate dance with the plant immune system, orchestrating a symphony of defense that challenges traditional notions of plant-pathogen interactions. The journey through the various mechanisms employed by these enigmatic endophytes to combat diseases, will lead to revelational understanding of sustainable agriculture. The review delves into cutting-edge research and promising prospects, shedding light on how fungal endophytes hold the key to biocontrol and the reduction of chemical inputs in agriculture. Their ecological significance, potential for bioprospecting and avenues for future research are also explored. This exploration of the biocontrol mechanisms of fungal endophytes promise not only to enrich our comprehension of plant-microbe relationships but also, to shape the future of sustainable and ecofriendly agricultural practices. In this intricate web of life, fungal endophytes are indeed the unsung heroes, silently guarding our crops and illuminating a path towards a greener, healthier tomorrow.

KEYWORDS

fungal endophyte, biocontrol mechanism, secondary metabolites, sustainable agriculture, bioactive potential

1 Introduction

In the realm of agriculture and plant health management, the quest for sustainable and environmentally friendly alternatives to conventional methods has never been more pressing. The exponential growth of the global population, along with the ever-escalating demands for food production, places immense pressure on our agricultural systems. In this view, the health of cultivated plants is crucial for many economic sectors because plants not only offer food for the inhabitants, but also critical items like wood, textiles, medicines, and bioenergy, among others. Plant diseases are to blame for production losses that are both large in terms of quantity

and quality, costing businesses a lot of money, and occasionally having disastrous social effects (Savary et al., 2019). On a global scale, plant illnesses can result in losses of up to 16%, and studies have already shown that pathogens and, more precisely, conducted cultivations are the targets of losses (Savary et al., 2019). Without a doubt, diseases have the capacity to cause losses, and the severity of those losses may vary depending on the climate, microbes, and the aggressiveness of the disease-causing agent. For ages, numerous methods have been exploited to increase food production, many of which are unsustainable since they pose risks to the environment (Sahu and Mishra, 2021). According to this assumption, reducing these eco-threats and investigating potential endophytic microbes will aid in achieving an ecosystem that is stable and will enable the cultivation of pathogen-free plants for increased crop output. In this context, endophytic fungi have emerged as an intriguing and promising class of microorganisms that hold the potential to revolutionize modern agriculture (Sharma and Singh, 2021). In nature, both plants and microbes live in relationships among themselves, which in turn can affect the overall growth and development of plants. Endophytic microbes are an intriguing collection of organisms that are linked to diverse parts and tissues of plants. The association of these microbes with plants can be facultative or obligate and causes no harm to their host. On the other hand, these endophytes exhibit intricate relationships with their host plants, including antagonism and mutualism (Parker, 1995). One such widely acknowledged interaction of mutualism or symbiosis involves the interaction of medicinal plants and their associated endophytes. These endophytes are known to produce certain secondary metabolites of immense pharmacological importance (Elgorban et al., 2019). Fungal endophytes have gained a lot of attention from taxonomists, mycologists, ecologists, chemists, and evolutionary biologists over the last three decades (Saikkonen, 2007). They actually represent a diverse array of fungi that establish mutualistic relationships within the tissues of plants, all while evading the conventional signs of diseases or distress that are typically associated with pathogenic fungi. This intriguing class of microorganisms has remained hidden allies of the plant kingdom for centuries performing their roles quietly and unobtrusively. However, recent decades have witnessed a surge of research interest in these cryptic microorganisms, revealing their profound influence on plant growth, development, and resistance to abiotic and biotic stresses. The remarkable attribute of these fungi lies in their ability to form mutualistic associations with a wide range of plant species without causing overt symptoms of disease, setting them apart from their pathogenic counterparts (Saikkonen, 2007). Approximately 5% of the estimated million fungal species on earth have been described, which is a very tiny percentage (Panda and Sujogya., 2013). They are being studied due to their ability to boost plant health; for example, in *Musa* spp., *Piriformospora indica* has been found to induce resistance against *Fusarium oxysporium* f. sp. *cubense* (Cheng et al., 2020). These endophytes can affect the host plant's biochemistry, physiology, distribution, and ecology, and their persistence has been known for the past 100 years. The effect of the association of endophytic fungi, on plant growth and immunity against pathogens greatly depends on the site of the colonization and the secondary metabolites produced by the endophytes (Yu et al., 2018). Several studies have shown that the presence of microbes in the plant endosphere affects the plant's response to environmental stimuli and can regulate plant diseases (Zhang et al., 2020). Reports have shown that endophytic fungi have the potential to maintain plant health and can be engineered to integrate into crop breeding (Liu et al., 2018). An interesting fact about Rhizospheric microbes/fungi living in the proximity of root endosphere is that they can modify their morphology rapidly and can colonize the plant tissues, thus becoming endophytic microbe/ fungi (Abedinzadeh et al., 2019). It is interesting to note that data has demonstrated how endophytic fungi can colonize and infiltrate internal plant tissue (endosphere) from their external root environment (rhizosphere), establishing endophytic microbial communities (Vishwas, 2011). When compared to non-symbiotic plants, endophytes can strongly and quickly stimulate and activate the host plant's stress response (Wu et al., 2018). As already stated above, plant pathogens have always been the first threat to food security in our world, and in most cases, the available tools were insufficient to effectively manage them. *Phytophthora infestans*, the first ever plant pathogen reported in tomato and other related cultivars, is still responsible for their reduced production. A lot of different hosts and most strains make it harder to use non-host crops and resistant cultivars. The use of chemically synthesized. Pesticides is not always that effective or applicable, both in terms of cost and method of application. On the other hand, security is expected not only in terms of food production but also in quality and overall impact on the environment (Lechenet et al., 2017). Plants can support a microbial community in the rhizosphere and even recruit some in adverse conditions. A fresh perspective on biological control, particularly through endophytes, offers innovative biotechnological methods of managing plant diseases and a unique viewpoint on the relationship between microbes and plants (Tena, 2018). As biocontrol agents, endophytic fungi, during their entire life cycle, protect the host plants from infections as they easily adjust to adverse environmental conditions (Xie et al., 2018). Interaction between endophytes and their host plants improves plant growth and protects the plant from harmful effects, e.g., by helping in developing resistance against pathogens, aiding in resistance mechanisms like phytoremediation, increasing the crop yield, etc. (Saikkonen et al., 2004). In this interaction, both endophytes and hosts benefit as the plant provides protection, nutrition, and shelter to them. Endophytes, on the other hand, assist their hosts by stimulating their growth, development, and adaptation (Killham, 1994). When the plant gets attacked by a disease pathogen, the host defense system gets activated, and protection against disease occurs mainly by minimizing the level of infection as well as masking and reducing the pathogen's growth (Jia et al., 2016). Endophytes have helped their host plants by enhancing their growth and developing resistance against pathogens in the course of co-existence and evolution. This results in the establishment of special interactions such as mutualism, neutralism, and antagonism between the host plant and its endophytes (Jia et al., 2016). Due to their efficacy as biocontrol agents against several plant infections, the screening of endophytic fungi have recently increased, as reported (Abaya et al., 2021). Endophytic fungi that live in different plant compartments generally encourage plant growth in a variety of direct and indirect ways (Adeleke et al., 2022). In the direct mechanism, endophytes control different plant hormones such as auxins and cytokinins and improve the availability of soil nutrients through nitrogen fixation, siderophore production, phosphorus, and iron solubilization, whereas in the indirect mechanism, endophytes produce various volatile compounds like hydrogen cyanide, enzymes, and antibiotics that cease pathogen activity and promote systemic resistance in plants (Selim et al., 2018).

It has been suggested that endophytic ecological occupation and phytoalexin synthesis caused by fungal endophytes may be the primary mechanisms by which plants protect themselves from diseases. This review paper embarks on an exploration of the multifaceted world of endophytic fungi, focusing on their extraordinary biocontrol mechanisms and their potential applications in sustainable agriculture. As the global community seeks innovative solutions to address challenges such as crop diseases, pests, and the adverse effects of climate change, endophytic fungi stand as nature's hidden allies, offering a treasure trove of mechanisms that can be harnessed to combat these pressing issues. As one traverse the complex landscape of endophytic fungi and their biocontrol mechanisms, it becomes evident that these enigmatic organisms hold the key to a sustainable and resilient agricultural future. This review aims to spark more research and new ideas by shedding light on their many different strategies and the environmental factors that make them successful. This will help us learn more about these hidden allies and how important they are to global food security (Figure 1).

2 Direct mechanism against plant pathogens

Endophytes have been the subject of recent research, which has shown that they can improve host defense against diseases and lessen the ecological harm that pathogenic microorganisms can cause (Arnold et al., 2003). Most of these investigations involved the assessment of the survival rate of plants in the presence and absence of fungal endophytes or *in vitro* coculture of fungal endophytes and phytopathogens. Although some studies suggest that endophytes may reduce the effects of plant-pathogen damage, the current understanding of the precise regulation of endophytes, pathogens, and plants is still in the beginning stages (Mejía et al., 2008). The direct mechanism employed by endophytes for the protection of plants against phytopathogens involves direct antagonistic measures such as antibiosis, competitive exclusion of phytopathogens, parasitism and elucidation of pathogen virulence (Köhl et al., 2019). Endophytes can exert antibiosis by secreting allelochemicals like bacteriocins, lipopeptides, biosurfactants, enzymes that break down cell walls, antibiotics, and volatile chemicals that interfere with phytopathogen metabolism and hence stop pathogen development (Raymaekers et al., 2020). Additionally, competition between the endophytes and the pathogens for nutrition and space also plays a role in the reduction of pathogenic infection in plants. Secretion of enzymes like pectinases and chitinases also inhibits the virulence of pathogen by interfering with factors responsible for pathogenicity in phytopathogens (Wang et al., 2022). However, the direct interactions between endophytic fungi and phytopathogens are complicated and species-specific in nature (Gouda et al., 2016).

2.1 Antibiotics production from endophytes

Studies throughout the decades have shown that endophytes are central to plant protection against pathogens (Barkodia et al., 2018). During the direct interaction between endophytes and pathogens, endophytes produce antibiotics to suppress the pathogens and protect the plant from the damage caused by pathogens (Fadiji and Babalola, 2020). Endophytes produce certain secondary metabolites that have antimicrobial properties like antifungal, antibacterial, etc. (Palanichamy et al., 2018). These antimicrobials have a strong inhibitory action on plant pathogens. A single class of endophytes is capable of producing a variety

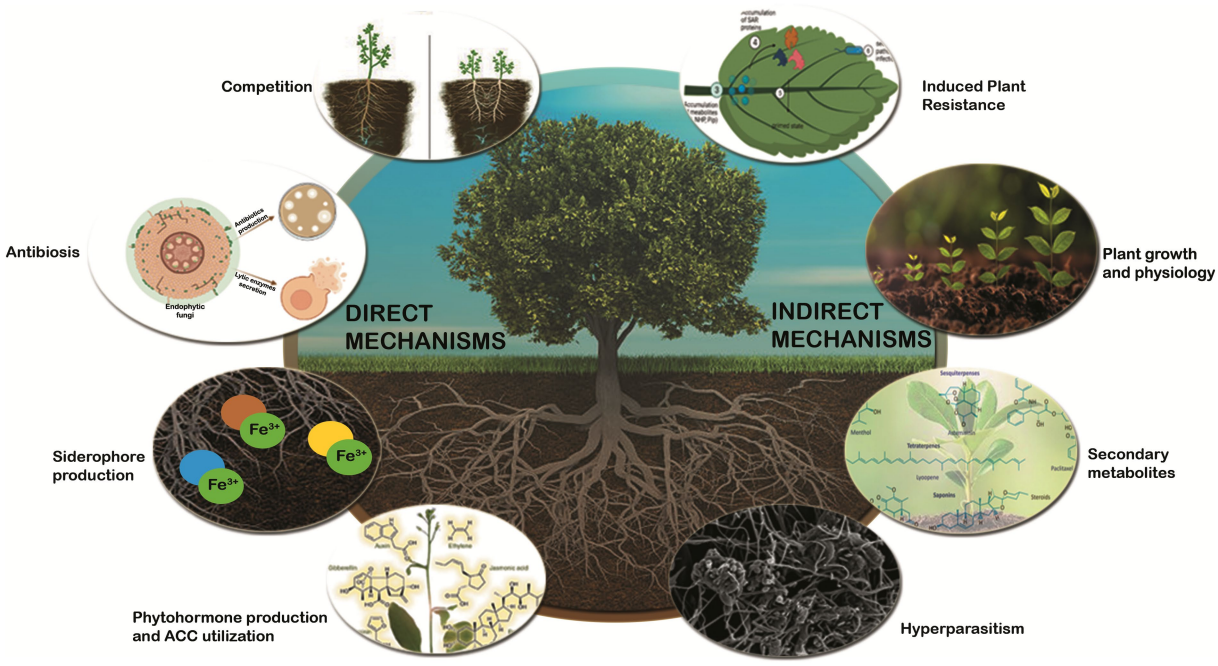

FIGURE 1
Schematic representation of defense mechanisms used by endophytic fungi for plant protection against phytopathogens.

of bioactive agents (antibiotics) such as aromatic compounds, terpenoids, polypeptides, and terpenoids (Balla et al., 2021). Antimicrobials synthesized by some endophytic fungi are listed in Table 1.

2.2 Secretion of lytic enzymes

Lytic enzyme secretions play a significant role in plant protection from pathogens, particularly when it comes to endophytic microorganisms. Most microbes produce lytic enzymes that aid in the hydrolysis of polymers (Tripathi et al., 2008). Endophytic fungi create a symbiotic relationship with plants when they colonize the internal tissues of plants; this interaction is advantageous to both the plant and the fungus. As pathogens attempt to invade the plant, the fungal endophytes parasitize pathogenic hyphae in various ways, including twisting, coiling, perforation of the pathogenic hyphae, and secretion of cell wall-degrading enzymes leading to lysis and inhibition of pathogens (Waghunde et al., 2017). By degrading the cell walls of pathogens, the lytic enzymes limit the ability of the pathogens to invade and propagate within the plant, effectively enhancing the plant's natural defense mechanisms. This mechanism not only provides immediate protection but also primes the plant's immune system for induced systemic resistance (ISR), leading to long-lasting and robust defense responses against potential future pathogen attacks (Fadiji and Babalola, 2020; Trivedi et al., 2020). In lieu of chemical pesticides, the use of lytic enzymes produced by endophytic fungi offers a sustainable and environmentally benign method of plant protection, encouraging healthier and more resilient crops. Despite their involvement in mycoparasitism, these lytic enzymes also contribute to cell wall reformation and recycling during active fungal growth, as well as during aging and autolysis (Kumari and Srividhya, 2020). Endophytic fungi have a variety of enzymes such as hemicellulases,1,3-glucanases, chitinases and cellulases, that break down different types of materials (Haran et al., 1996). It has been reported that in *Trichoderma* species, a number of enzymes are directly involved in the breakdown of the cell wall of pathogenic fungi for the utilization of pathogenic fragments (Rajesh et al., 2016). Mycolytic enzymes like 1,3-glucanase or chitinase produced by *Trichoderma asperellum* have the potential to degrade the cell walls of phytopathogens. A respective increase in enzymatic activity and transcripts of 1,3, glucanase, and chitinase enzymes in cultures induced by pathogens has been observed in banana wilt affected plantations (Win et al., 2021). Biocontrol of root-knot nematodes by endophytic fungi showed elevated activity of genes encoding enzymes like glucanase and chitinase and downregulation of genes encoding antioxidant enzymes during the stimulation of the immune system of

TABLE 1 List of antimicrobials produced by endophytic fungi for plant protection.

S. no.	Endophyte	Antimicrobial compound	Plant pathogen inhibited	Reference
1	*Acremonium zeae*	Pyrrocidines A, Pyrrocidines B	*Fusarium verticillioides, Aspergillus flavus*	Wicklow and Poling (2008)
2	*Ampelomyces* spp.	3-O-Methylalaternin, Altersolanol A	*Staphylococcus aureus, Enterococcus faecalis* and *S. epidermidis*	Wen et al. (2023)
3	*Cladosporium* spp.	Brefeldin A	*Trichophyton, Candida albicans,* and *Aspergillus niger*	Akram et al. (2023)
4	*Colletotrichum gloeosporioides*	Methanol	*Escherichia coli, Pseudomonas aeruginosa*	Wang et al. (2021)
5	*Daldinia concentrica*	Volatile organic compounds	*Aspergillus niger, Penicillium digitatum, and Botrytis cinerea*	Lugtenberg et al. (2016)
6	*Gliocladium* spp.	Volatile organic compounds like 1-butanol, 3-methyl-, phenylethyl alcohol and acetic acid, 2-phenylethyl ester,	*Pythium ultimum* and *Verticillum dahlia*	Lugtenberg et al. (2016)
7	*Muscodor albus*	Aciphyllene, Tetrohydofuran, 2-butanone, 2-methyl furan	*Stachybotrys chartarum*	Saxena et al. (2015)
8	*Phomopiscassiae*	Cadinane sesquiterpenes derivatives	*Cladosporium sphaerospermum* and *Cladosporium cladsporioides*	Gao et al. (2010)
9	*Periconia* spp.	Fusicoccane diterpenes	*Salmonella typhimurium, Staphylococcus aureus, Klebsiella pneumoniae,* and *Bacillus subtilis,*	Azhari and Supratman (2021)
10	*Paraconiothyrium* spp.	Taxol/ Paclitaxel	*Heterobasidion annosum, Phaeolus schweinitzii and Perenniporia subacida*	Talbot (2015)
11	*Pestalotiopsis microspora*	Torreyanic acid	---	Ding et al. (2009)
12	*Penicillium* spp.	Penicitroamide	*Erwinia carotovora sub* sp. *Carotovora*	Deshmukh et al. (2022)
13	*Trichoderma* spp.	Trichodecenins, Trichorovins, Trichocellins, Trichorzianins A and B, Trichorzins, HA and MA, Tricholongins BI and BII Longibrachinsa	*Rhizoctonia solani, Botrytis cinerea, Phytophthora cinnamomi, Pythium irregulare, Pythium middletonii, Sclerotinia sclerotiorum, Fusarium oxysporum, Bipolaris sorokiniana*	Sood et al. (2020)
14	*Verticillium* spp.	Massariphenone ergosterol peroxide	*Pyricularia oryzae* P-2b	Rani et al. (2017)

plants in response to pathogens (Molinari and Leonetti, 2019). Although enzymes lack the ability to act as antagonizing agents independently, but they augment the antagonistic activity of other agents and pathways when merged together. Similarly, the pectinase enzyme has also been reported to help reduce pathogenesis in plants (Fadiji and Babalola, 2020).

2.3 Production of phytohormones

Phytohormones of endophytic fungi play a crucial role in plant protection, enhancing defense responses and resistance to pathogens through complex interactions with the plant (Fadiji and Babalola, 2020). The context of plant protection, the secretion of phytohormones by endophytic fungi trigger a sequence of defense mechanisms in the host plant. In response to environmental cues, endophytic fungi that have formed a symbiotic relationship with plants release phytohormones such as auxins, cytokinins, gibberellins, indole acetic acid, and jasmonic acid that act as potent signaling molecules (Baron and Rigobelo, 2022). The two phytohormones, Jasmonic acid (JA) and Salicylic acid (SA) are important defense signaling molecules that regulate the defense responses of plants against disease-causing microbes (Shi et al., 2020). Systemic acquired resistance (SAR) and biotrophic pathogen defense are both impacted by Salicylic acid, which in turn is regulated by the activation of Pathogenesis-related (PR) genes. Localized programmed cell death, a fallout of the hypersensitive response caused by the two phytohormones, jasmonic acid and salicylic acid inhibits the spread of pathogens and protects against stress (Lahlali et al., 2022). These proteins and compounds act as an immediate response to pathogen attack, hindering the progress of invading pathogens and limiting their growth (Rashad et al., 2020). When pattern recognition receptors (PRRs) recognize the pathogens, Jasmonic acid (JA) and Salicylic acid (SA) have the potential to enhance the activity of the enzymes in the phenylpropane pathway of plants resulting in the production of phenolic compounds (such as flavonoids, lignin, coumarins, and tannins), triggering pathogen-associated molecular pattern (PAMP)-triggered immunity (PTI), a robust defense response in plants (Franco-Orozco et al., 2017). Jasmonic acid and ethylene (ET), mainly produced during induced systemic resistance (ISR), are considered important for defense against necrotrophic diseases and beneficial for interactions between plants and pathogens (Li et al., 2019). The phenomenon of JA/ET-dependent systemic resistance has been seen in various plant-associated microorganisms, including Trichoderma asperellum, Penicillium sp., and the endophyte *Serendipita indica*. But in other pathosystems, *S. indica* produced resistance without relying on the JA/ET route, while *T. asperellum* coupled with plants triggered resistance in an SA-dependent manner. This suggests that the roles of phytohormones and their potential interactions are complicated, and the use of a microorganism on the plant is expected to alter the entire hormone profile rather than solely altering the levels of individual hormones. Plant defense signaling pathways have been identified and compounds act as an immediate response to pathogen attack, hindering the progress of invading pathogens and limiting their growth (Rashad et al., 2020). When pattern recognition receptors (PRRs) recognize the pathogens, jasmonic acid (JA) and salicylic acid (SA) have the potential to enhance the activity of the enzymes in the phenylpropane pathway of plants, resulting in the production of phenolic compounds (such as flavonoids, lignin, coumarins, and tannins), triggering pathogen-associated molecular pattern (PAMP)-triggered immunity (PTI), a robust defense response in plants (Bhattacharya et al., 2010). Jasmonic acid and ethylene (ET), mainly produced during induced systemic resistance (ISR), are considered important for defense against necrotrophic diseases and beneficial for interactions between plants and pathogens (Ghozlan et al., 2020). Plant defense signaling pathways have been found to involve ethylene (ET) and abscisic acid (ABA), while auxin, gibberellic acid (GA), cytokinin (CK), brassinosteroids, and peptide hormones may also be involved (Li et al., 2019). Furthermore, ethylene and jasmonic acid also initiate the synthesis of secondary metabolites, including volatile organic compounds (VOCs) and phytoalexins. VOCs can serve as signaling molecules to attract beneficial microorganisms, such as predatory insects or microbes that feed on plant pests, to further enhance plant protection. On the other hand, phytoalexins are antimicrobial compounds that are directly involved in the inhibition of pathogen growth and proliferation within the tissues of plants (Latz et al., 2018). A study conductedal on the functional role of *Trichoderma atroviride* fungi in controlling the pathogenic activity of *Fusarium verticillioides* in maize showed the involvement of this endophytic fungi in the synthesis of phytohormones such as salicylic acid, abscisic acid (ABA) and jasmonic acid (Agostini et al., 2019). Similarly, Ren and Dai also found that the interaction between *Gilmaniella* spp. and endophytic fungi *Atractylodes lancea* led to increased production of jasmonic acid along -with the production of various volatile antimicrobial compounds such as eudesmol, atractylone, atractylodin and hinesol (Ren and Dai, 2012). Together, ethylene, Jasmonic acid, and salicylic acid create a hormonal response network that is coherent and keeps the plant's defense mechanisms in place like production of compounds like ethylene and jasmonic acid in response to agents like *Penicillium* spp., *Serendipita indica* and *Trichoderma asperellum* to activate systemic resistance is crucial in avoiding host-pathogen inhabitation or activation of salicylic acid dependent systemic resistance pathway in plants inhabited by *Trichoderma asperellum* (Latz et al., 2018). These hormonal responses generated between the endophytic fungi and phytopathogens are extremely complicated and involves cross communication and multiple events between plants and the host endophytic fungi (Adeleke et al., 2022; Figure 2).

Moreover, phytohormones influence the establishment of induced systemic resistance (ISR) in the plant. Induced Systemic Resistance entails getting the plant's immune system ready to react more quickly to future pathogen attacks. This priming effect allows the plant to mount a quicker and more robust defense, effectively protecting it from potential pathogen threats (Baron and Rigobelo, 2022). Despite significant advances in research on signal transmission in induced resistance, there is still a lacuna in allocating roles to each hormone in signal transduction, particularly in complex systems. As a result, there is a need to strengthen a plant's defense systems and use it as a biomarker to detect induced resistance (Latz et al., 2018). Overall, the secretion of phytohormones by endophytic fungi in plant protection is a finely tuned mechanism that involves a network of signaling pathways and defense responses. By modulating the plant's hormonal balance, endophytic fungi contribute to a heightened state of preparedness against pathogen attacks, leading to improved plant health, resilience, and reduced reliance on chemical pesticides. Harnessing the potential of plant phytohormones from endophytic fungi offers a sustainable and eco-friendly approach to plant protection, benefiting both agricultural productivity and environmental health (Waghunde et al., 2017; Figure 3).

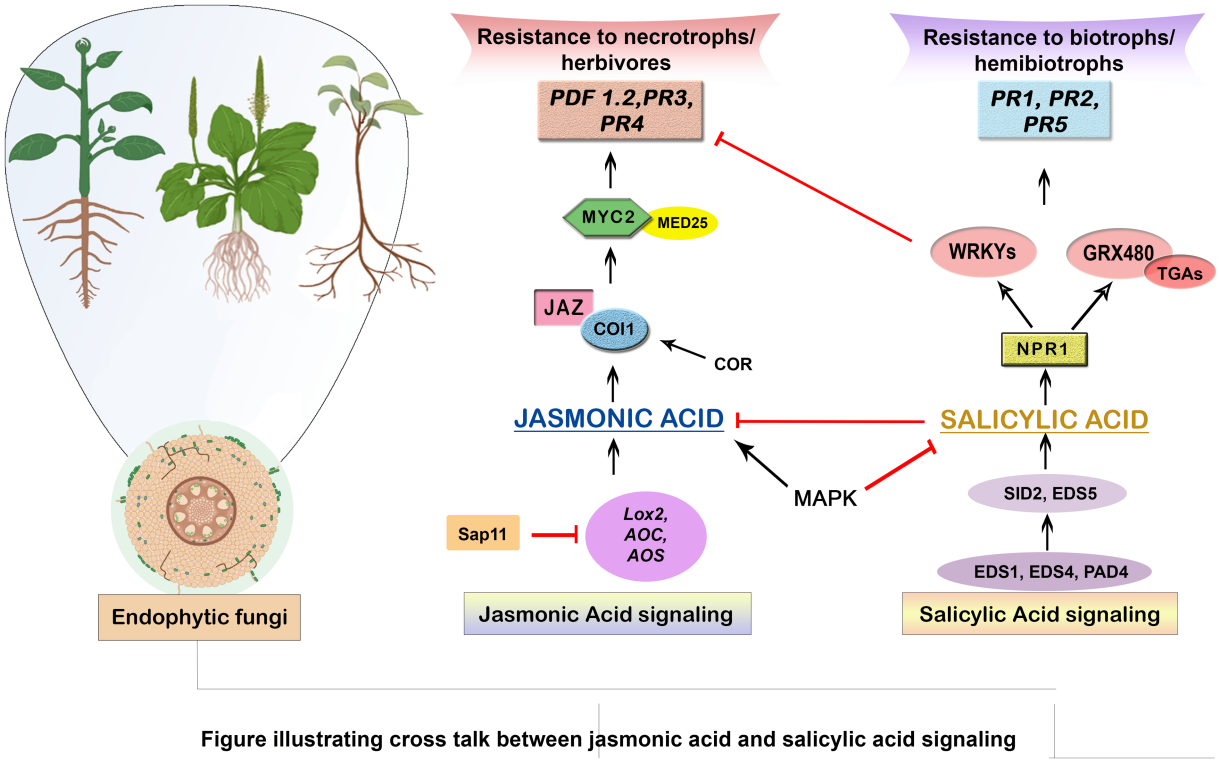

FIGURE 2
Illustrating cross talk between Jasmonic acid and Salicylic acid signaling. This schematic diagram depicts the intricate interplay between two key plant defense signaling pathways, Jasmonic acid (JA) and Salicylic acid (SA), in response to various biotic and abiotic stressors. The crosstalk between these signaling pathways plays a pivotal role in shaping a plant's response to different types of threats.

2.3.1 Volatile and non-volatile compounds of fungal endophytes

The metabolites produced by the endophytic fungi are primarily of two kinds: Volatile compounds and Non-Volatile Compounds (Santra and Banerjee, 2023). Volatile compounds can be defined as low molecular weight hydrophobic organic molecules with a high vapor pressure. Volatile organic compounds (VOC) are the name for the volatile metabolites that endophytic fungi produce. These volatile compounds can easily cross the cell membrane of the plant thus playing a vital role in soil ecosystem. The majority of VOC can be categorized into five different classes namely: Benzenoid compounds, Terpenoids, Amino acid derivatives, Fatty acid derivatives and Phenylpropanoids. These are mostly antibiotic in nature (Kaddes et al., 2019). The non-volatile metabolites produced by endophytic fungi comprise a wide range of chemically different compounds such as peptides, polyketides, steroids, enzymes, alkaloids, amino acids, hormones etc. (Singh and Kumar, 2023). Both VOC and non-volatile metabolites have a wide role in agriculture and help in plant protection against biotic and abiotic stress (Singh and Kumar, 2023). Some of the examples are shown below in Table 2.

2.3.2 Role of volatile and non-volatile compounds in post-harvest disease management

The role of endophytic bioactive compounds in plant growth, defense, and sustainable agriculture has been well documented in literature (Santra and Banerjee, 2023). The post-harvest loss of crop plants due to pathogens or physiological conditions is high, especially in the case of fruits and vegetables. With the growing resistance of phytopathogens to traditional anti-pathogenic agents like fungicides, pesticides or insecticides etc., and the effects of such substances have shifted the focus towards more sustainable options. The use of alternative approaches such as low temperatures, irradiation, essential oils, salt, antagonistic microorganisms etc. for post-harvest protection of crop plants has been documented (Youssef et al., 2022) The use of endophytic fungi as a biocontrol agent for both pre- and post-harvest protection of crop plants has emerged as a viable alternative for various chemical compounds like pesticides, insecticides, herbicides etc. (Kumar et al., 2021). Fungal endophytes such as members of genera *Muscodor*, *Xylaria*, *Trichoderma*, *Fusarium* etc. are known to produce a large number of volatile compounds with the potential of post-harvest crop protection (Macías-Rubalcava and Garrido-Santos, 2022). The volatile compounds produced by the endophytic fungi can be applied as fumigation agents, for creating controlled atmospheric storage or as inhibitors of hormones that promotes the ripening of the stored crop. Volatile compounds such as esters, alcohol hydrocarbons, lipids, ketones acids, etc. are more suitable, effective, and ecologically sustainable for the management of post-harvest pathogens due to their long-distance antagonistic action scale, resulting in direct penetration at spatial scales, e.g., volatiles of *M. albus* (also known as Mycofumigation,), volatiles of *Oxyporus latemarginatus*, volatiles of *Nodulisporium* which inhibits 12 different

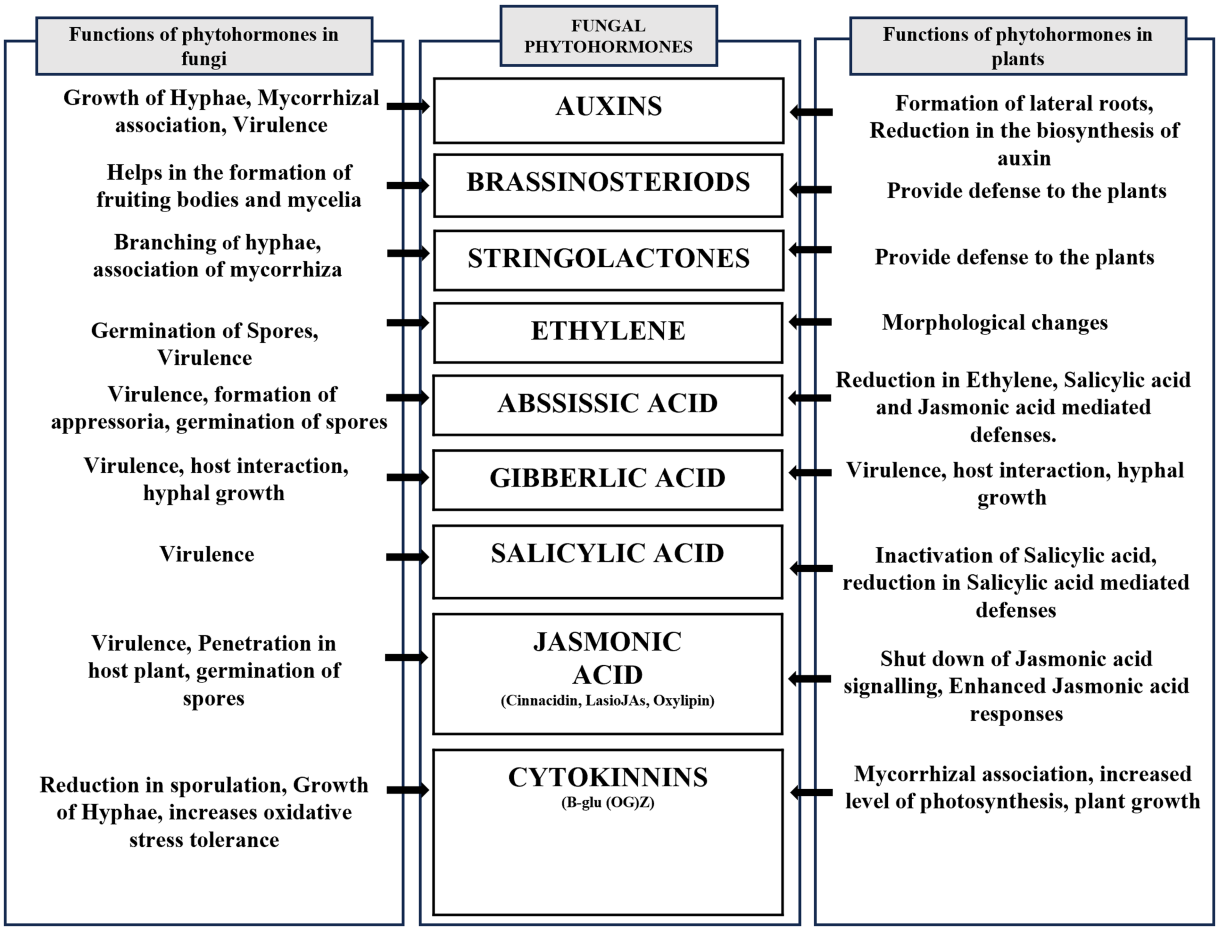

FIGURE 3
Illustrating phytohormones produced by endophytic fungi. This schematic diagram depicts different phytohormones produced by endophytic fungi and their role both in endophytic fungi and their host.

pathogens (Naik, 2018) Similarly, many non-volatile compounds produced by endophytic fungi are exploited for their potential of controlling the post-harvest pathogens. Compounds like ergot alkaloids produced by *Clavicipitaceae* have antimicrobial and pesticidal properties that are effective against a number of post-harvest pathogens (Florea et al., 2017). Resorcyclic acid lactones produced by *Penicillium* spp., Zopfiellin produced by *Zopfiella* spp. Chaetoglobosins are produced by *Chaetomium* spp. are the examples of non-volatile compounds that possess antimicrobial properties. Other compounds like aflavinines produced by *Aspergillus* spp., Indole-Diterpenes produced by *Clavicipitaceae*, Harzianic acid produced by *Trichoderma* have anti-fungal properties, Peramine produced by *Epichloë*, Tetramic Acid Derivatives produced by different genus of endophytic fungi posses' properties such as insecticidal, fungicidal and antimicrobials thus, promoting crop protection post-harvest by providing defense against the phytopathogenic (Song et al., 2021). The role of volatile and non-volatile compound in post-harvest plant protection is paramount. Use of these compounds not only help in post-harvest disease management of the crops but also offer a sustainable agriculture practice. These compounds offer multifaceted solutions that address the complex challenge of controlling pathogens and extending the shelf life of harvested crops.

2.4 Phosphate solubilization

For the growth and development of plants, phosphorus is a crucial nutrient. However, in most soils, phosphorus is present in insoluble forms like phosphate rocks or mineral complexes. This renders it less available to plants, limiting their growth and overall health (Johan et al., 2021). Endophytic fungi have evolved the ability to solubilize phosphorus from these insoluble forms into soluble forms that the plant can readily absorb. This is achieved through the secretion of organic acids, which are powerful chelators capable of breaking down complex phosphate compounds. One of the primary organic acids produced by endophytic fungi is gluconic acid. This acid is particularly effective in dissolving phosphorus compounds in the soil. When the endophytes release gluconic acid into the plant's rhizosphere, it reacts with the insoluble phosphorus, converting it into soluble phosphate ions. These soluble phosphate ions become more available for uptake by the plant's root system (Etesami et al., 2021). Phosphate solubilization by endophytic fungi is a crucial process that aids in protecting plants from pathogens. By facilitating phosphorus uptake, endophytic fungi contribute to improved plant health and vigor (Baron and Rigobelo, 2022) and healthy plants are better equipped to defend themselves against pathogens. When a plant is well-nourished with an ample supply of phosphorus, it can allocate more energy and

TABLE 2 List of volatile and non-volatile compounds produced by fungal endophytes and their role in plant protection.

Type of metabolite	Metabolite	Examples	Producer endophyte	Activity of the metabolite	Reference
	Terpenes	Azadirachtin A & B, Camptothecin, Penicimonoterpene, Sabinene, Geraniol	*Eupenicillium parvum; Fusarium solani, Penicillium chrysogenum Phomopsis* spp., *C. elatior Sw.*	Biopesticide, Antifungal	Kilani-Morakchi et al. (2021)
Volatile organic compounds	Phenols	Phenol, 4-[2-(methylamino) ethyl]-, 6-Nitro-3-chlorophenol, Phenol, 2,4,6-tri-tert-butyl-	*Curvularia* spp.	Antifungal	Santra and Banerjee (2023)
	Fatty acid derivatives	1-octen-3-ol and 3-octanone	*Muscodor* spp.	Fungicides, Pesticides, Phytotoxicity, Insecticides	Plaszkó et al. (2020)
	Alcohol	1-butanol, phenethyl alcohol, 1- propanol, isobutyl alcohol, 2- methyl-1-butanol, cyclohex-3-en-1- ol	*Phomopsis* spp. *Muscudor* CZ-620	Antifungal	Kaddes et al. (2019)
	Ketone	Acetone	*Phomopsis* spp.	Antifungal	Kaddes et al. (2019)
	Amino-acid derivative	Bactobolin & Actinobolin	*C. elatior Sw.*	Antifungal/defe nse against phytopathogen	Santra and Banerjee (2023)
	Seco-sativene sesquiterpeno id	Helminthosporic acid, Cochliobolin F, Helminthosporal acid, and Drechslerine B	*Cochliobolus sativus*	Phytotoxicity against phytopathogens	Macías-Rubalcava and Garrido-Santos (2022)
Non-volatile compounds	Hormones	Gibberellins, Indole acetic acid	*Penicillium funiculosum* LHL06, *Penicillium* spp. CBRF65	Bioremediation, Plant growth promotion	Badenoch-Jones et al. (1984)
	Enzymes	Glutathione S-transferase	*Penicillium funiculosum* LHL06	Bioremediation	Badenoch-Jones et al. (1984)
	β-resorcylic acid derivatives	de-O-methyllasiodiplodin,14-hydroxy-de-O-methyllasiodiplodin, ethyl 2,4-dihydroxy 6-(8-hydroxyheptyl) benzoate	*Lasiodiplodia theobromae* strain GC-22	Phytotoxicity against phytopathogens	Macías-Rubalcava and Garrido-Santos (2022)
	Other Natural organic compounds	Isocoumarins	*Phomopsis prunorum*	Phytotoxicity against phytopathogens	
		Chromenone and derivatives	*Daldinia eschscholtzii*	Phytotoxicity against phytopathogens	
		Rhizoperemophilanes,1α- hydroxyhydroisofukinon, PR-toxin dimethyl acetal	*Rhizopycnis vagum*	Phytotoxicity against phytopathogens	
		Fumigaclavine A, Fumigaclavine B, and Fumigaclavine C	*Aspergillus oryzae*	Resistance against phytopathogens	
		Mycotoxin deoxynivalenol	*Enterobacter* spp.	Resistance against phytopathogens	Etesami et al. (2021)
		Glomalin	*Glomus* spp.	Increased nutrient uptake,	Etesami et al. (2021)
		Siderophores	*Aspergillus* spp., *Pseudomonas* spp., *Paracoccidioides* spp. *Saccharomyces cerevisiae, Gliocladium virens, Rhodothamus chamaecistus*	Increased iron acquisition from soil and more availability of iron, resistance against phytopathogens	Silva et al. (2020)
		Harzianum A	*Trichoderma harzianum*	Fungicides, resistance against phytopathogens and biostimulants	Khan et al. (2023)

10.3389/fmicb.2023.1280258

resources toward its defense mechanisms. The mechanisms employed by endophytic fungi for phosphate solubilization can be categorized into acidification, enzyme activity, and ion exchange (Sharma et al., 2013). Phosphate solubilization by acidification involves the secretion of organic acids like citric acid, oxalic acid, malic acid, gluconic acid etc. into the rhizosphere. These organic acids act as chelating agents for the binding of metal ions present in the soil to facilitate the release of bound phosphate, thus making them available for plant uptake. Fungal strains such as *Trichoderma viride*, *Trichoderma harzianum*, *Trichoderma vixens*, and *Trichoderma longibrachiatum* have been reported for phosphate solubilization by acidification (Elhaissoufi et al., 2022). Many endophytic fungi such as *Penicillium* and *Aspergillus* have been shown to produce various enzymes like phosphatases and phytases which are capable of hydrolyzing the organic phosphate compounds present in soil and converting insoluble phosphate into soluble inorganic phosphate (Chaudhary et al., 2022). Other than these two mechanisms, endophytic fungi can also exchange metal cations present in the rhizosphere with phosphates, thus effectively releasing soluble phosphates into the surrounding soil (El Hassan, 2017). Endophytic fungi provide an additional source of phosphorus to the plants by solubilizing phosphate, thus enhancing their nutrient uptake and promoting overall growth and health. This increased nutrient availability makes the plants more resistant to pathogenic attacks in several ways such, as enhanced plant growth, and induced systemic resistance like phosphate-solubilizing endophytic fungi can trigger systemic resistance in plants. They can stimulate the plant's defense mechanisms and produce various secondary metabolites that act as natural biopesticides, thereby protecting the plant from pathogenic attacks. Overall, phosphate solubilization by endophytic fungi is a multifaceted mechanism that contributes significantly to plant protection against pathogens. These beneficial fungi play a vital role in promoting plant health and crop productivity while reducing the need for chemical fertilizers and pesticides, making them essential components of sustainable agriculture practices.

2.5 Siderophore production

For all eukaryotes and almost all prokaryotes, iron is a crucial nutrient, since it is necessary for metabolic function. Availability of iron in two different oxidation states, i.e., ferric (Fe^{3+}) and ferrous (Fe^{2+}), helps in serving iron both as a cofactor and a catalyst in basic metabolic processes. Despite being one of the metals with the highest abundance on Earth, iron has a low bioavailability due to the fact that iron forms a highly insoluble compound ferric hydroxides in the presence of oxygen (Expert, 1999). Overall, a sufficient supply of iron is necessary for survival. Various species have created controlled systems to maintain homeostasis between sufficient uptake of iron and preventing iron toxicity to avoid cell damage. In plants, animals, and bacteria, iron with high-affinity forms complex with glycoproteins such as lactoferrin or transferrin. Iron is stored intracellularly in ferritin (Arosio and Levi, 2002). Before recent times, little was known about the role of iron in interactions between fungi and their hosts as well as the general regulatory mechanisms that control iron homeostasis. Reductive iron assimilation and Siderophore-mediated iron uptake are the two major systems used by fungi for iron uptake (Oide et al., 2006). Microbes produce siderophores, which are low molecular weight, essentially ferric-specific ligands, as scavenging agents to counteract low iron stress (Sid = Iron, Phores = Bearers; Korat et al., 2001). Except for Lactobacilli, *Candida albicans, Cryptococcus neoformans*, *Saccharomyces cerevisiae* all other aerobic and facultative anaerobic microorganisms are known to produce siderophores, which function as iron chelates (Loper and Buyer, 1991). Siderophores are thought to be the result of Fe^{2+} being simultaneously oxidized to Fe^{3+} and precipitated as ferric hydroxide as an evolutionary reaction to the presence of O2 in the atmosphere (Winkelmann and Drechsel, 2008). Variety of siderophores produced by fungi have been classified mainly into five major classes (a) fusigens, (b) coprogens, (c) ferrichromes, (d) rhodotorulic acid, and (e) rhizoferrin (Chincholkar et al., 2000). Some of the fungal siderophores are enlisted in Table 3.

The extraordinarily high affinity of siderophores for ferric ions is the most notable characteristic of Siderophores (Askwith et al., 1996). When competing for nutrients in the soil, the ability to exploit siderophores produced by different microbes is a significant selection advantage. The most significant biotechnological importance of siderophores is in the plant's rhizosphere, where they nourish the plant with iron, act as a first line of defense against parasites that invade the roots, and aid in the removal of hazardous metals from contaminated soil (Matzanke et al., 1987). Studying the opportunistic human pathogen *Aspergillus fumigatus* led to the initial discovery of the function of fungal siderophores in illness (Sindhu et al., 1997). *In vitro* removal of iron from transferrin by siderophores was linked to the survival of pathogen in human serum (Hissen et al., 2004). Another example of role of fungal siderophores can be seen in *Candida albicans*, a non-siderophore producing yeast. *Candida albicans* requires Ferrichrome-type siderophores along with Arn1p/Sit1p, a siderophore transporter, for invasion and penetration of its host epithelia (Heymann et al., 2002). The discovery that the metabolic byproduct of the biosynthetic pathway involving the NPS6 gene, encoding a non-ribosomal peptide synthase from *Cochliobolus heterostrophus*, a phytopathogenic fungus, recognized the role of Siderophores in fungal virulence towards plants (Oide et al., 2007). Many studies on NPS6 gene demonstrated its role in virulence to

TABLE 3 List of reported siderophores produced by various endophytic fungi.

S. no.	Siderophore	Reported from	References
1.	Alterobactin	*Alteromonas luteoviolaces*	Sayyed et al. (2013)
2.	Asperchrome A, B & C	*Aspergillus orhraceus*	Sayyed et al. (2013)
3.	Coprogen	*Curvularia lunata*	Yuan et al. (2001)
4.	Canadaphore	*Helmenthosporium carbonum*	Sayyed et al. (2013)
5.	Ferrichrome A	*Ustilago sphaerogena*	Yuan et al. (2001)
6.	Ferrichrome	*Ustilago maydis*	Yuan et al. (2001)
7.	Ferricrocin & Hyperferricrocin	*Aspergillus fumigatus*	Schrettl et al. (2007)
8.	Rhizoferrin	*Rhizopus microsporus*	Yuan et al. (2001)
9.	Rhodotorulic acid	*Rhodotorula piliminae*	Johnson (2008)
10.	Triacetyl- fusarinine C	*Aspergillus fumigatus*	Schrettl et al. (2007)

maize against H_2O_2 hypersensitivity and to be broadly conserved among the filamentous ascomycetes (Lee et al., 2005). Beyond virulence, fungal siderophores also serve to maintain the mutualistic symbiotic relationships between grass and endophytes. The grass symbiont *Epichloe festucae* uses the NRPS gene sidN to make a new extracellular siderophore that looks like fusarinine-type siderophores. These helpful fungi are never free-living; instead, they are restricted to the intercellular spaces (apoplast) of leaf sheaths and blades, where they do not spread disease. On the other hand, Mycorrhizal fungi frequently create advantageous symbiosis with the roots of terrestrial plant communities, which benefit plant nutrition, including the uptake of micronutrients (Johnson, 2008). Also, these fungi have been found to produce hydroxamate siderophores, and it is believed that siderophore-mediated iron uptake is crucial for the acquisition of iron by the host plant (Haselwandter et al., 2006). Thus, the production of siderophores is a potent strategy employed by various fungal endophytes to grab iron from the environment. Both extracellular and intracellular siderophores play an essential role in numerous fungal-host interactions.

2.6 1-Aminocyclopropane-1-carboxylate utilization

Plant hormones take an active role in symbiotic, defensive, and developmental processes. Ethylene (ET), a gaseous plant hormone that is easily absorbed by plant tissues and has effects even in extremely low quantities, is at the center of these activities (Van de Poel et al., 2015). Some studies have explored the impact of ethylene on the cell division and the finding indicates that ethylene can exert contrasting effects on the cell cycle depending on the specific tissue as well as internal and external stimuli. During the development of the apical hook, ethylene drives cell division in the subepidermal layers, most likely working in conjunction with auxins (Van de Poel et al., 2015). In addition to controlling several aspects of plant growth and development, Ethylene also engages in microbial defense and symbiotic programs which affect overall microbial assembly (Desbrosses and Stougaard, 2011). Moreover, ACC (1-Aminocyclopropane-1-carboxylate) a major precursor of ethylene is a non-proteinogenic α-amino acid that has been reported to play an important role in regulating numerous plant developmental and defense responses. The production of ethylene precursor is mainly regulated at all the major levels (transcription, post-transcription, translation, and post-translation; Lee et al., 2017). The molecule is produced from S' adenosyl methionine (SAM) in a reaction catalyzed by an enzyme ACC-synthase, releasing MTA (5-methylthioadenosine). Through a series of biochemical reactions, the released MTA is reconverted to methionine to renew the stack of available methionine (Bennett, 2003). Being localized in the cytosol, ACS is one of the members of the Pyridoxal phosphate (PLP) dependent enzymes that uses vitamin B6 as a co-factor for its enzymatic activity (Boller et al., 1979). MACC (malonyl-ACC; Amrhein et al., 1981), GACC (γ-glutamyl-ACC; Martin et al., 1995) and JA-ACC (Jasmonyl-ACC; Staswick and Tiryaki, 2004) are three different conjugates of ACC namely suggesting a complex overall biochemical regulation of ACC pool with eventual effects on the production of ethylene and other developmental and physiological processes. Apart from these conjugates produced in different mechanisms, another distinctive way to metabolize ACC (1-Aminocyclopropane-1-carboxylate) is the deamination of ACC. Initially, ACC deaminase was first reported in bacteria. Many reports suggested that some plant growth-promoting bacteria have the potential to process the plant-based ACC using the ACC deaminase enzyme into ammonia and α-ketoglutarate (Honma and Smmomura, 1978). Being multimeric with an approximate subunit molecular mass of 35-42 kDa (Ullah et al., 2019), ACC deaminase is a sulfhydryl enzyme that requires pyridoxal 5'-phosphate (PLP) for its enzymatic activity (Kushwaha et al., 2020). The cleavage of ACC to ammonia and α-ketoglutarate catalyzed by the enzyme ACC deaminase was discovered in 1978 (Ullah et al., 2019). Following X-ray crystallographic studies, the enzyme ACC deaminase folds into two domains, each of which has an open twisted α/β structure resembling the β-subunit of the tryptophan synthase (Husen et al., 2008). This PLP-dependent enzyme has a low affinity for ACC with a 1.5-15 mM reported Km value (Hontzeas et al., 2004). Many studies have shown that the root exudates contain an explicit amount of ACC that might attract ACC deaminase harboring microorganisms and set up Rhizospheric interaction (Glick et al., 2007). Interaction with the root environment is a must to access the plant-based ACC by the plant growth-promoting microbes containing ACC deaminase enzyme (Payment et al., 2011). Apart from bacterial species, fungi are also exploited for their ACC deaminase activity. Even though the functional principles of the bacterial and fungal ACC deaminase are substantially the same, their structures differ due to sequence variations. Comparison of AcdS gene sequences of various fungal and bacterial strains have shown that approximately 70-90% sequence similarity was shown by the fungal strains with that of bacterial AcdS gene rather than with the fungal gene sequence. *Schizosaccharomyces pombe* 972 h, *Clavispora lusitaniae* ATCC 42720, *Cyberlindnera saturnus* are some of the major examples of fungal strains with higher sequence similarity with bacterial AcdS rather than fungal. It has been hypothesized that horizontal gene transfer is responsible for the transfer of genes from Proteobacteria to the above-mentioned fungal strains (Nascimento et al., 2014) Furthermore, the isolated fungal ACC Deaminase genes similar to Proteobacteria mainly belong to classes Ascomycota and Basidiomycota (Gravel et al., 2007).

2.7 Competition with pathogens

In the rhizosphere and phyllosphere of plants, competitive exclusion, a frequent phenomenon, controls the population of a wide range of species (Sikora et al., 2007). In some circumstances, the biological control of root diseases and nematodes is also a result of competition for nutrients and space. Therefore, when several inoculants are required for efficient pest management, the "first-come, first-serve" aspect of colonization and the idea of survival of the fittest are the major factors that could affect the efficacy of biological control (Backman and Sikora, 2008). Because nutrients in soils are typically in scarce supply and difficult to acquire, competition for resources such as oxygen, nutrients, etc. is the active demand between soil-inhabiting microorganisms including pathogens and non-pathogens, and is a key mechanism for the management of diseases that are carried by soil (Stoytcheva, 2011). Due to competition for scarce nutrients and the fact that starvation is a significant and frequent cause of microbiological death, fungal phytopathogens may be biologically controlled (Eisendle et al., 2004). If the requirements

both in terms of nutrients, oxygen, space of endophytic fungi, and the disease-causing pathogens are similar, then only competition will occur among them. Species of *Fusarium* and *Pythium*, soil-borne pathogens that infect plants through mycelial contact are more prone to competition than those that invade through infection threads (Van Dijk and Nelson, 2000).

2.7.1 Competition for Iron

Iron is the most abundant element on Earth and an essential nutrient for microorganisms. Though it is the fourth largest mineral found abundantly on our planet it is not readily available to microorganisms. As it gets oxidized easily, it is mainly available in the form of ferric ions that cannot be directly utilized due to its extremely low solubility (Neilands et al., 1987). This in turn leads to competition among microorganisms. One of the biological controls for both bacterial and fungal phytopathogens is the fight for iron nutrition (McMorran et al., 2001). Several studies have indicated that the concentration of iron in the soil is notably lower than the necessary level for microbial growth. Siderophores, known as iron chelators, are low molecular weight molecules that bind to ferric ions dueto their high affinity for iron with Kd values ranging from 10^{-20} to 10^{-50} (Castignetti and Smarrelli, 1986). Thus, siderophore-producing microbial strains have a selective advantage over the non-producing strains, including disease-causing microorganisms. This results in the inhibition of the growth of pathogens in their immediate proximity due to iron limitation (O'Sullivan and O'Gara, 1992). It has been found that the rhizosphere biological control agents protect plants from pathogens generally by colonization resulting in the consumption of already available substrates in their surroundings. This makes disease-causing microorganisms or pathogens difficult to grow. Siderophores are produced by a wide range of Plant Growth Promoting Rhizobacteria such as *Serratia* (Berg et al., 2005), *Bacillus* (Yu et al., 2011), *Pseudomonas* (Elad and Baker, 1985) and many more playing major roles in suppressing soil-borne disease-causing pathogens. Based on the ligands, siderophores are mainly classified as carboxylates, phenolates (Catecholates), or hydroxamates (Winkelmann and Drechsel, 2008). Enterobactin, Siderochelin A, Ferrocins, Pyoverdines, Acinetobactin, Cepabactin are among the major examples of bacterial siderophores whereas Ferrichromes, Coprogens, Rhodotorulic Acid, Fusigens and Rhizoferrins are the typical examples of siderophores produces by fungal strains (Winkelmann and Drechsel, 2008). Among these Siderophores, Catecholates are exclusively produced by bacteria but hydroxamate siderophores are produced both by bacteria and fungi (Cox et al., 1981). Many studies revealed that the fungal phytopathogens have a lower affinity for iron as compared to Plant Growth Promoting Rhizobacteria (PGPRs) and thus overpower the fungal phytopathogens for iron (Schippers et al., 2003). In such a case, *Pythium and Fusarium* species are more prone to competition for iron as they cause infection through mycelial contact, from other microbes associated with soil and plants than those species that germinate directly on plant surfaces (Pal and Gardener, 2006). By analyzing the siderophore mutants, the role of siderophores in biocontrol either alone or in combination with other metabolites such as antibiotics has also been studied (Buysens et al., 1994). Many factors are responsible for affecting the overall capability of siderophores such as properties of soil, type of plant, type of siderophore, type of microbial strain, and type of disease-causing pathogens (Glick and Bashan, 1997). The plant diseases caused by various pathogens such as *Fusarium oxysporum*, *Rhizoctonia solani*, *Pseudomonas* sp., *Alternaria* sp. etc. are suppressed by siderophores in numerous reports (Sahu and Sindhu, 2011). This overall suggests that to overpower the soil-borne disease-causing pathogens, competition for iron and other mineral ions is one of the major mechanisms, however, siderophores only may not be able to suppress the disease in any case.

2.7.2 Competition for niches

In the biocontrol mechanism of fungal endophytes, competition for niches is how different fungal endophytes fight for space and resources inside a plant host in order to become dominant and use their biocontrol effects against pathogenic fungi. It has long been understood that niche complementarities may play a significant role in a species' ability to coexist (Backman and Sikora, 2008). The endosphere and the rhizosphere are the complex ecosystems that play a significant role in supporting the overall growth and development of the plants. A wide variety of microorganisms, including fungi, are heavily concentrated in the rhizosphere, the soil environment around plant roots, and the endosphere, which consists of the internal tissues of plants. The two fungal groups—endophytes and plant pathogenic fungi—represent opposing forces in this ecosystem, competing with one another for the little resources and ecological niches available (Oszust et al., 2020). In the endosphere and rhizosphere, competition for resources and space can be fierce, and it is influenced by a number of important variables. First, competition may arise from direct hostility between the two fungal species, which frequently takes the form of mycoparasitism, the direct use of resources, or the synthesis of antimicrobial substances. For instance, the well-known mycoparasitic properties of the endophyte *Trichoderma* allow it to actively attack and parasitize pathogenic fungi such as *Rhizoctonia solani,* thereby lessening their detrimental effects on plant health (Howell, 2003). It has also been discovered that fungi in the genus *Trichoderma* have an ecological niche that is most similar to that of *Colletotrichum* spp., hence excluding the latter phytopathogenic species (Oszust et al., 2020). *Trichoderma* spp. is assumed to be tough competitors that drive out slower-growing diseases since they are discovered as being particularly quick colonists (Tyśkiewicz et al., 2022). Based on an *in vitro* experiment, Oszust et al. (2020) discovered that *Trichoderma* spp. nutritionally outcompeted *Botrytis* sp., *Verticillium* spp., and *Phytophthora* spp. According to Morandi et al., the non-pathogenic endophyte *Clonostachys rosea* inhibited the growth and sporulation capability of *B. cinerea* to regulate it (Morandi et al., 2000). Second, in moderating the conflict between plant diseases and endophytes, plant host selection is essential. Certain plants have the ability to actively attract or encourage the growth of particular endophytes, which benefit them and restrict harmful fungus. In order to give endophytes a competitive edge, this procedure may involve the release of root exudates that specifically favor advantageous fungus. Moreover, the outcome of the rivalry between the two fungal groups can also be determined by their spatial distribution. The vascular system and intercellular gaps are two examples of the particular niches that endophytic fungi frequently occupy within plant tissues (Faeth, 2002). Due to the possibility that they have distinct preferred areas for colonization, this spatial separation can reduce direct competition with plant pathogenic fungus. On the other hand, direct interactions between endophytes and pathogenic fungi are more likely to occur in the rhizosphere, which is the interface between plant roots and soil.

Researchers and agricultural scientists are interested in understanding these interactions because they can impact the efficacy of using biocontrol endophytes as a sustainable alternative. By studying the competition for niches among fungal endophytes and their interactions with pathogens and the host plant, they can develop strategies with pathogens and the host plant to enhance the biocontrol potential of specific endophytes, and improve plant disease management practices.

3 Indirect mechanisms of plant protection

To survive in harsh environments like famine, salt stress, and cold, plants use a variety of strategies. Some of the biochemical and morphological changes that can be seen right away are the formation of phytoalexins, the death of cells, and the hypersensitive response. Kiraly et al., found that long-term evolution can lead to both non-specific (generic) and specific (pathogen-specific) resistance (Kiraly et al., 2007). Plants with non-specific resistance can protect themselves from a broad range of diseases, but plants with particular resistance can avoid getting sick from just one or a few infections. Endophytes produce secondary metabolites and have improved resistance, which strengthens the plant's defense system.

3.1 Induced plant resistance

Several research have examined how plants respond to disease and parasite invasions for more than 20 years, utilizing several categories. Systemic acquired resistance (SAR) and induced systemic resistance (ISR) are the two types of resistance that researchers are most interested in. ISR is regulated by ethylene or jasmonic acid, which is produced by some non-pathogenic rhizobacteria and not connected to the accumulation of pathogenesis-related (PR) proteins. Salicylic acid mediates SAR, which is a result of pathogen infections and is linked to the production of PR proteins (Tripathi et al., 2008). Invading cells are directly lysed by these PR proteins' many enzymes, like chitinases and 1, 3-glucanases, which also strengthen cell wall borders and increase resistance to cell death and infection (Gao et al., 2010). ISR generated by endophytes has also been associated with increased expression of genes involved in disease. The ISR process does not directly kill the virus or restrict it. Instead, it strengthens the plants' natural physical or chemical barriers (Van Loon et al., 1998). ISR and SAR frequently have an antagonistic action that controls the signaling at the cellular level. When SA and JA have an antagonistic effect on biotrophic or necro pathogens, and vice versa, there is upstream and downstream signaling between them (Syed Ab Rahman et al., 2018). For instance, *Blumeria graminis* f. spp. *Tritici*, which causes powdery mildew in wheat, is controlled by *Bacillus subtilis* by inducing disease resistance via the SA-dependent signaling pathway (Xia et al., 2022). The non-expression of the pathogenesis-related genes 1 (NPR1 and NPR3/4), which eventually trigger an antagonistic response via SAR through priming and reveal resistance against secondary infections, is crucially regulated by the pathogenesis-related gene 1 (PR1; Ding et al., 2009). By preventing *Botrytis cinerea's* spore germination and mycelium growth through the ISR method of resistance, *Burkholderia* species (BE17 and BE24) shield grapevine from the grey mold disease (Lahlali et al., 2022). *Trichoderma* spp. AA2 and *Pseudomonas fluorescens* PFS are the most powerful antagonists of *Ralstonia* spp., which causes bacterial wilt in tomatoes by generating ISR in the plant.

3.2 Stimulation of plant secondary metabolites

Secondary metabolites are bioactive substances that have an important function in ecological interactions, competition, and defensive signaling (Liu et al., 2018). The production of secondary metabolites via a metabolic exchange, which exhibits a complicated regulatory response, is necessary for the formation of microbial contact. These interactions may be competitive, parasitic, mutualistic, hostile, or mutualistic. The most recent advances in imaging mass spectrometry (IMS) technology have been employed to investigate the diverse roles played by mold metabolites in microbial interactions. The growth of phytopathogens is regulated by the antibacterial and antifungal activities of secondary metabolites. While under biotic stress, plants can create secondary metabolites on their own or in collaboration with other endophytes to manage stress and mount defenses (Ludwig-Müller, 2015). To safeguard plants and enhance crop quality, endophytic secondary metabolites are employed as a biocontrol agent. Whereas microorganisms create homogeneous, high-quality metabolites with the highest efficacy in terms of their biocontrol potential, plants produce bioactive molecules that are inadequate and variable in quality (Lugtenberg et al., 2016). An example of plant secondary metabolite stimulation by endophytic fungi is the production of loline (an alkaloid) in the leaves of fescue grasses by endophytic fungus *Neotyphodium* spp. and *Epichloë* spp., which protects the leaves from herbivores. The interaction between endophytic fungus *Neotyphodium coenophialum* and its host plant is another example of plant secondary metabolite stimulation. *Neotyphodium coenophialum* protects its host plants from aphids the key carriers of viruses, e.g., protection of *Festuca arundinacea* against *Rhopalosiphum padi* also inhibit the spread of viruses (Alam et al., 2021).

3.3 Hyperparasites and predation

Hyperparasites are another means by which endophytes protect their host ecologically. In this approach, recognized pathogens or their zoospores are immediately attacked by endophytes (Tripathi et al., 2008) By twisting and piercing the hyphae of the pathogens and creating lyase, which dissolves the pathogen's cell wall, endophytic fungi trap the pathogens. This sort of interaction among fungi is frequently seen. Hyper parasitism in bacteria has only occasionally been documented. A predatory bacterium called *Bdellovibrio bacteriovorus* has the peculiar ability to exploit the cytoplasm of other Gram-negative bacteria as food (McNeely et al., 2017). Over 30 fungal species, including *Cladosporium uredinicola* against *Puccinia violae* and *Alternaria alternata* against *Puccinia striiformis* f. spp. *tritici*, reported by Zheng et al. to exhibit hyper parasitism against rust pathogens (Jia et al., 2016). The reduction of plant pathogens through microbial predation is another technique. The majority of endophytes show their predatory traits in nutrient-poor environments. For

example, fungal endophytes isolated from *Taxillus chinensis* produce cell wall-degrading enzymes that promote the dissolution and relaxation of the cell wall between the host and *Taxillus chinensis* (Wu et al., 2021).

3.4 Fungal endophytes as biocontrol agents

Endophytes are described as microorganisms (bacteria or fungal) that are found living in tissue, plant organs, and seeds of almost all vascular plants (Caruso et al., 2022). The interaction between the endophyte and the host plant during their association has proven to be beneficial rather than harmful for both interacting organisms. These benefits are always based on the interaction between endophytes and the host plants (Kamana et al., 2016). Many novel bioactive compounds like antibiotics, antimycotics, antineoplastics, etc. are endophytic products (Shukla et al., 2014). The agro-industry relies heavily on the use of agrochemicals for controlling phytopathogens. This excessive use of chemicals in the agricultural industry has resulted in the development of resistant phytopathogens. The endophytes play an important in maintaining the health of the host plant (Wu et al., 2021). These endophytes can be exploited as a biocontrol agent in the agro-industry. Biocontrol agents (BCA) are described as living organisms or their products that can fight against plant diseases or pests via direct antagonistic action (Xia et al., 2022). Many endophytes are being exploited as BCA as they are effective in controlling plant diseases and can help attain sustainable agriculture. The endophytic fungi that act as biocontrol agents against different phytopathogens are summarized in Table 4.

3.5 Protection against leaf-cutting ants

Endophytic fungi play a pivotal role in safeguarding plants from the destructive foraging of leaf cutting ants. These mutualistic fungal endophytes, which commonly inhabit plant tissues, establish intricate associations with their host plants. One of their primary mechanisms of protection lies in the production of secondary metabolites, such as alkaloids and mycotoxins, which serve as potent deterrents against herbivores, including leaf-cutting ants (White and Torres, 2010). By secreting these chemical compounds, endophytic fungi effectively shield their host plants, rendering them unpalatable or toxic to the ants. This protective alliance not only benefits the plants by reducing

TABLE 4 Summarized list of endophytic fungi that act as biocontrol agents against various phytopathogens.

S. no.	Endophytic fungi	Phytopathogen activity	References
1.	*Aspergillus niger*	*Colletotrichum acutatum*	Landum et al. (2016)
2.	*Anthrinium* sp.	*Colletotrichum acutatum*	Landum et al. (2016)
3.	*Amphirosellinia nigrospora*	*Ralstonia solanacearum, Magnaporthe oryzae*	Nguyen et al. (2019)
4.	*Aureobasidium pullulans*	*Fusarium oxysporum f.* spp. *Herbemontis*	Adeleke et al. (2022)
5.	*Aporospora terricola,*	*Fusarium oxysporum f.* spp. *Herbemontis*	Adeleke et al. (2022)
6.	*Aspergillus flavus*	*Mycotoxigenic Aspergillus*	Camiletti et al. (2018)
7.	*Bjerkandera adusta*	*Fusarium oxysporum f.* spp. *Herbemontis, Colletotrichum gloeosprioides*	Adeleke et al. (2022)
8.	*Beauveria bassiana*	*Parasitic Nematodes, Botrytis cinerea, Alternaria alternate, Macrosiphum euphorbiae, Tribolium confusum*	Gautam and Avasthi (2019)
9.	*Colletotrichum boninense*	*Fusarium oxysporum f.* spp. *Herbemontis,*	Adeleke et al. (2022)
10.	*Clonostachys rosea*	*Fusarium culmorum, Botrytis cinerea, Nematodes, Sclerotinia sclerotiorum*	Dubey et al. (2020)
11.	*Conidia prior*	*Puccinia triticina, P. hordei*	Wilson et al. (2020)
12.	*Colletotrichum gloeosporioides*	*Fusarium oxysporum, Fusarium culmorum, Sphaceloma* sp., *Sordariomycetes, Glomerella* spp.	Adeleke et al. (2022)
13.	*Diaporthe citri*	*Fusarium solani, Glomerella* spp., *Moniliophthora perniciosa*	Santos et al. (2019)
14.	*Epicoccum nigrum*	*Colletotrichum acutatum, Gibberella, Haematonectria, Fusarium graminearum*	Ogórek et al. (2020)
15.	*Flavodon flavus*	*Alternaria* spp., *Glomerella* sp., *Fusarium culmorum,*	Adeleke et al. (2022)
16.	*Fusarium oxysporum*	*Pythium ultimum, Verticillium dahlia*	Fadiji and Babalola (2020)
17.	*Lecanicillium lecanii*	*Thrips, Whitefly, Aphid, Macrosiphum euphorbiae (Thomas), Scales, Mealybugs*	Reddy (2020)
18.	*Metarhizium anisopliae*	Parasitic Nematodes, *Protaetia brevitarsis seulensis*	Gautam and Avasthi (2019)
19.	*Purpureocillium lilacinum*	*Parasitic nematodes and insects*	Wang et al. (2016)
20.	*Paenibacillus polymyxa*	*Aspergillus aculeatus*	Liu et al. (2018)
21.	*Piriformospora indica*	*Golovinomyces orontii*	Grabka et al. (2022)
22.	*Rosellinia bunodes*	*Bacillus subtilis, Staphylococcus aureus*	Becker and Stadler (2020)
23.	*Serendipita herbamans*	*Fusarium oxysporum*	Sefloo et al. (2021)
25.	*Trichoderma viride*	*Penicillium digitatum, Phytophthora nicotianae, Rhizoctoniasolani*	Fontana et al. (2021)
26.	*Xylaria feejeensis*	*Alternaria tomatophila*	Brooks et al. (2022)

herbivore-induced damage but also highlights the fascinating interplay between plants and their endophytic partners in the intricate web of ecological relationships.

3.5.1 Hypocreales endophytes in coffee plants

Fungal endophytes belonging to the order Hypocreales have been discovered in coffee plants, producing mycotoxins that deter leaf cutting ants. The presence of these endophytes in the coffee plants was demonstrated in a study conducted by Mejia et al. in the year 2008 (Mejía et al., 2008).

3.5.2 Trichoderma species

Certain Trichoderma species are endophytic fungi that have been shown to protect plants from various pests, including leaf-cutting ants. These endophytes can produce antifungal and insecticidal compounds that deter herbivores. Studies like Lo et al. (2015) have highlighted their potential in biocontrol (Yao et al., 2023).

3.5.3 Clavicipitaceous endophytes in grasses

Clavicipitaceous fungal endophytes, such as *Neotyphodium* and *Epichloe* species are known to form mutualistic associations with grasses. They can produce alkaloids, like ergot alkaloids, that deter herbivores including leaf-cutting ants (Saikkonen et al., 2004).

These examples highlight the diverse array of fungal endophytes and their crucial role in protecting plants from leaf-cutting ants through various mechanisms, including the production of chemical compounds and mutualistic associations.

4 Conclusive remarks

In light of the aforementioned explanation, endophytic fungi mostly use direct and indirect approaches to combat disease-causing pathogens. The management and treatment of plant diseases are extremely important for sustainable agriculture. In order to prevent adverse impacts on the environment and human health, national rules are becoming harsher when it comes to regulating and authorizing new pesticides. The demand for organic and safe foods is growing daily. It is therefore vital to look for novel control strategies that ensure food safety and lessen these adverse consequences. To keep the harm caused by herbivores or pathogens at manageable levels for farmers, a worldwide strategy that considers all of the aforementioned issues must be devised. In this regard, with emerging applications in agriculture, endophytes present a very intriguing subject of study. Undoubtedly, a variety of endophytic fungi can be exploited for the treatment of various plant diseases and as a substitute for available biocontrol agents against phytopathogens. These fungal endophytes are also a good source of beneficial bioactive substances for plants. However, not much attention has been paid to how important it is for biotechnology that endophytic fungi make beneficial metabolites that help control plant diseases. In recent times, biologically active compound producing and plant growth promoting endophytes have drawn more interest from researchers since they are potential sources of novel drugs and eco-friendly plant protectors. Among all identified possible biocontrol agents, members of the genus *Trichoderma* have received extensive investigation; however, there are many other comparably potent endophytic fungal families that have not been adequately investigated and explored. These biocontrol organisms have a significant impact on agriculture and the overall environment. Molecular identification of microbes which are being exploited as biocontrol agents and biological characterization of bioactive chemicals produced by them is essential for understanding their antagonistic mechanisms.

5 Future prospects

The future prospects of biocontrol mechanisms involving fungal endophytes in sustainable agriculture appear exceptionally promising. As the world grapples with the growing need for environment friendly and resilient farming practices, fungal endophytes stand out as a valuable ally. These fungi possess the ability to bolster crop health and protect against pests and pathogens, reducing the reliance on chemical pesticides. As the understanding of the intricate interactions between fungal endophytes and plants deepens, can expect the development of specialized, genetically optimized strains that offer even greater efficacy. This could lead to substantial reductions in agriculture's environmental footprint while simultaneously increasing crop yields and food security. Moreover, the potential of fungal endophytes to enhance soil health and nutrient cycling holds promise for sustainable agriculture in the long term. With ongoing research and innovation, the integration of fungal endophytes into agricultural practices is likely to play a pivotal role in shaping a more sustainable and resilient future for global food production. Future research is required for better understanding of antagonistic behavior of these endophytic fungi to propagate them as environmentally friendly tools for managing phytopathogens naturally.

Author contributions

MB: Writing – original draft. SKa: Writing – original draft. RK: Writing – original draft. SKh: Conceptualization, Writing – original draft, Writing – review & editing. SR: Supervision, Writing – review & editing.

Funding

The author(s) declare that no financial support was received for the research, authorship, and/or publication of this article.

Acknowledgments

We are thankful for all the support from Shri Mata Vaishno Devi University, Katra, J&K, India.

Conflict of interest

The authors declare that the research was conducted in the absence of any commercial or financial relationships that could be construed as a potential conflict of interest.

Publisher's note

References

Abaya, A., Xue, A., and Hsiang, T. (2021). Selection and screening of fungal endophytes against wheat pathogens. *Biol. Control* 154:104511. doi: 10.1016/J.BIOCONTROL.2020.104511

Abedinzadeh, M., Etesami, H., and Alikhani, H. A. (2019). Characterization of rhizosphere and endophytic Bacteria from roots of maize (*Zea Mays* L.) plant irrigated with wastewater with biotechnological potential in agriculture. *Biotechnol. Rep.* 21:e00305. doi: 10.1016/J.BTRE.2019.E00305

Adeleke, B. S., Ayilara, M. S., Akinola, S. A., and Babalola, O. O. (2022). Biocontrol mechanisms of endophytic fungi. *Egyp. J. Biol. Pest Control.* 32:46. doi: 10.1186/s41938-022-00547-1

Agostini, R. B., Postigo, A., Rius, S. P., Rech, G. E., Campos-Bermudez, V. A., and Vargas, W. A. (2019). Long-lasting primed state in maize plants: salicylic acid and steroid signaling pathways as key players in the early activation of immune responses in silks. *Mol. Plant-Microbe Interact.* 32, 90–106. doi: 10.1094/MPMI-07-18-0208-R/ASSET/IMAGES/LARGE/MPMI-07-18-0208-R_F7.JPEG

Akram, S., Ahmed, A., He, P., He, P., Liu, Y., Wu, Y., et al. (2023). Uniting the role of endophytic fungi against plant pathogens and their interaction. *J. Fungi* 9:72. doi: 10.3390/jof9010072

Alam, B., Lǐ, J., Gě, Q., Khan, M. A., Gōng, J., Mehmood, S., et al. (2021). Endophytic fungi: from Symbiosis to secondary metabolite communications or vice versa? *Front. Plant Sci.* 12:791033. doi: 10.3389/fpls.2021.791033

Amrhein, N., Schneebeck, D., Skorupka, H., Tophof, S., and Stöckigt, J. (1981). Identification of a major metabolite of the ethylene precursor 1-aminocyclopropane-1-carboxylic acid in higher plants. *Naturwissenschaften* 68, 619–620. doi: 10.1007/BF00398617

Arnold, A. E., Mejía, L. C., Kyllo, D., Rojas, E. I., Maynard, Z., Robbins, N., et al. (2003). Fungal endophytes limit pathogen damage in a tropical tree. *Proc. Natl. Acad. Sci.* 100, 15649–15654. doi: 10.1073/pnas.2533483100

Arosio, P., and Levi, S. (2002). Ferritin, iron homeostasis, and oxidative damage. *Free Radic. Biol. Med.* 33, 457–463. doi: 10.1016/S0891-5849(02)00842-0

Askwith, C. C., De Silva, D., and Kaplan, J. (1996). Molecular biology of Iron acquisition in *Saccharomyces Cerevisiae*. *Mol. Microbiol.* 20, 27–34. doi: 10.1111/j.1365-2958.1996.tb02485.x

Azhari, A., and Supratman, U. (2021). The chemistry and pharmacology of fungal genus Periconia: a review. *Sci. Pharm.* 89:34. doi: 10.3390/scipharm89030034

Backman, P. A., and Sikora, R. A. (2008). Endophytes: an emerging tool for biological control. *Biol. Control* 46, 1–3. doi: 10.1016/J.BIOCONTROL.2008.03.009

Badenoch-Jones, J., Summons, R. E., Rolfe, B. G., and Letham, D. S. (1984). Phytohormones, rhizobium mutants, and nodulation in legumes. IV. Auxin metabolites in pea root nodules. *J. Plant Growth Regul.* 3, 23–39. doi: 10.1007/BF02041989

Balla, A., Silini, A., Cherif-Silini, H., Bouket, A. C., Moser, W. K., Nowakowska, J. A., et al. (2021). The threat of pests and pathogens and the potential for biological control in forest ecosystems. *Forests* 12:1579. doi: 10.3390/f12111579

Barkodia, M., Joshi, U., Wati, L., and Rami, N. V. (2018). Endophytes: a hidden treasure inside plant. *Int. J. Chem. Stud.* 6, 1660–1665.

Baron, N. C., and Rigobelo, E. C. (2022). Endophytic fungi: a tool for plant growth promotion and sustainable agriculture. *Mycology* 13, 39–55. doi: 10.1080/21501203.2021.1945699

Becker, K., and Stadler, M. (2020). Recent progress in biodiversity research on the xylariales and their secondary metabolism. *J. Antibiot.* 74, 1–23. doi: 10.1038/s41429-020-00376-0

Bennett, J. (2003). Protein phosphorylation in green plant chloroplasts. *Annu. Rev. Plant Physiol. Plant Mol. Biol.* 42, 281–311. doi: 10.1146/ANNUREV.PP.42.060191.001433

Berg, G., Krechel, A., Ditz, M., Sikora, R. A., Ulrich, A., and Hallmann, J. (2005). Endophytic and ectophytic potato-associated bacterial communities differ in structure and antagonistic function against plant pathogenic fungi. *FEMS Microbiol. Ecol.* 51, 215–229. doi: 10.1016/j.femsec.2004.08.006

Bhattacharya, A., Sood, P., and Citovsky, V. (2010). The roles of plant phenolics in defence and communication during agrobacterium and rhizobium infection. *Mol. Plant Pathol.* 11, 705–719. doi: 10.1111/j.1364-3703.2010.00625.x

Boller, T., Herner, R. C., and Kende, H. (1979). Assay for and enzymatic formation of an ethylene precursor, 1-aminocyclopropane-1-carboxylic acid. *Planta* 145, 293–303. doi: 10.1007/BF00454455

Brooks, S., Klomchit, A., Chimthai, S., Jaidee, W., and Bastian, A. C. (2022). *Xylaria feejeensis*, SRNE2BP a fungal endophyte with biocontrol properties to control early blight and fusarium wilt disease in tomato and plant growth promotion activity. *Curr. Microbiol.* 79, 1–15. doi: 10.1007/S00284-022-02803-X/FIGURES/5

Buysens, Saskia, Poppe, Joseph, and Höfte, Monica. (1994). "Role of Siderophores in plant growth stimulation and Antigonism by Pseudomonas Aeruginosa 7NSK2." Improving plant productivity with rhizosphere Bacteria (MH. Ryder, PM. Stephens, GD. Bowen, Eds.). - Proceedings of the Third International Workshop on Plant Growth-Promoting Rhizobacteria Adelaide, Australia, March 7-11, 139-141. Available at: http://hdl.handle.net/1854/LU-247535.

Camiletti, B. X., Moral, J., Asensio, C. M., Torrico, A. K., Lucini, E. I., de la Paz Giménez-Pecci, M., et al. (2018). Characterization of argentinian endemic *Aspergillus flavus* isolates and their potential use as biocontrol agents for mycotoxins in maize. *Phytopathology* 108, 818–828. doi: 10.1094/PHYTO-07-17-0255-R

Caruso, D. J., Palombo, E. A., Moulton, S. E., and Zaferanloo, B. (2022). Exploring the promise of endophytic fungi: a review of novel antimicrobial compounds. *Microorganisms* 10:1990. doi: 10.3390/microorganisms10101990

Castignetti, D., and Smarrelli, J. (1986). Siderophores, the iron nutrition of plants, and nitrate reductase. *FEBS Lett.* 209, 147–151. doi: 10.1016/0014-5793(86)81100-0

Chaudhary, P., Agri, U., Chaudhary, A., Kumar, A., and Kumar, G. (2022). Endophytes and their potential in biotic stress management and crop production. *Front. Microbiol.* 13:933017. doi: 10.3389/FMICB.2022.933017/BIBTEX

Cheng, C., Li, D., Qi, Q., Sun, X., Anue, M. R., David, B. M., et al. (2020). The root endophytic fungus serendipita indica improves resistance of banana to *Fusarium oxysporum* f. Sp. Cubense tropical race 4. *Eur. J. Plant Pathol.* 156, 87–100. doi: 10.1007/s10658-019-01863-3

Chincholkar, S B, Chaudhari, B L, Talegaonkar, S K, and Kothari, R M. (2000). "Microbial Iron chelators: a tool for sustainable agriculture." Biocontrol Potential and Their Exploration in Crop Disease Management 1: 49–70.

Cox, C. D., Rinehart, K. L., Moore, M. L., and Cook, J. C. (1981). Pyochelin: novel structure of an Iron-chelating growth promoter for *Pseudomonas Aeruginosa*. *Proc. Natl. Acad. Sci.* 78, 4256–4260. doi: 10.1073/pnas.78.7.4256

Desbrosses, G. J., and Stougaard, J. (2011). Root nodulation: a paradigm for how plant-microbe symbiosis influences host developmental pathways. *Cell Host Microbe* 10, 348–358. doi: 10.1016/j.chom.2011.09.005

Deshmukh, S. K., Dufossé, L., Chhipa, H., Saxena, S., Mahajan, G. B., and Gupta, M. K. (2022). Fungal endophytes: a potential source of antibacterial compounds. *J. Fungi* 8:164. doi: 10.3390/jof8020164

Dijk, K.Van, and Nelson, E. B.. (2000). "Fatty acid competition as a mechanism by which *Enterobacter Cloacae* suppresses *Pythium Ultimum* sporangium germination and damping-off." *Appl. Environ. Microbiol.* 66: 5340–5347. doi: 10.1128/AEM.66.12.5340-5347.2000

Ding, G., Li, Y., Shaobin, F., Liu, S., Wei, J., and Che, Y. (2009). Ambuic acid and torreyanic acid derivatives from the endolichenic fungus *Pestalotiopsis* Sp. *J. Nat. Prod.* 72, 182–186. doi: 10.1021/np800733y

Dubey, M., Vélëz, H., Broberg, M., Jensen, D. F., and Karlsson, M. (2020). LysM proteins regulate fungal development and contribute to hyphal protection and biocontrol traits in *Clonostachys rosea*. *Front. Microbiol.* 11:520051. doi: 10.3389/FMICB.2020.00679/BIBTEX

Eisendle, M., Oberegger, H., Buttinger, R., Illmer, P., and Haas, H. (2004). Biosynthesis and uptake of siderophores is controlled by the PacC-mediated ambient-PH regulatory system in *Aspergillus nidulans*. *Eukaryot. Cell* 3, 561–563. doi: 10.1128/EC.3.2.561-563.2004

Elad, Y., and Baker, R. (1985). Influence of trace amounts of cations and siderophore-producing pseudomonads on chlamydospore germination of *Fusarium oxysporum*. *Phytopathology* 75, 1047–1052. doi: 10.1094/Phyto-75-1047

Elgorban, A. M., Bahkali, A. H., Al Farraj, D. A., and Abdel-Wahab, M. A. (2019). Natural products of *Alternaria* Sp., an endophytic fungus isolated from *Salvadora persica* from Saudi Arabia. *Saudi J. Biol. Sci.* 26, 1068–1077. doi: 10.1016/j.sjbs.2018.04.010

Elhaissoufi, W., Ghoulam, C., Barakat, A., Zeroual, Y., and Bargaz, A. (2022). Phosphate bacterial solubilization: a key rhizosphere driving force enabling higher P use efficiency and crop productivity. *J. Adv. Res.* 38, 13–28. doi: 10.1016/J.JARE.2021.08.014

Etesami, H., Jeong, B. R., and Glick, B. R. (2021). Contribution of arbuscular mycorrhizal Fungi, phosphate–solubilizing bacteria, and silicon to P uptake by plant. *Front. Plant Sci.* 12:699618. doi: 10.3389/fpls.2021.699618

Expert, D. (1999). Withholding and exchanging Iron: interactions between *Erwinia* Spp. and their plant hosts. *Annu. Rev. Phytopathol.* 37, 307–334. doi: 10.1146/annurev.phyto.37.1.307

Fadiji, A. E., and Babalola, O. O. (2020). Elucidating mechanisms of endophytes used in plant protection and other bioactivities with multifunctional prospects. *Front. Bioeng. Biotechnol.* 8:467. doi: 10.3389/fbioe.2020.00467

Faeth, S. H. (2002). Fungal endophytes: common host plant symbionts but uncommon mutualists. *Integr. Comp. Biol.* 42, 360–368. doi: 10.1093/icb/42.2.360

Florea, S., Panaccione, D. G., and Schardl, C. L. (2017). Ergot alkaloids of the family clavicipitaceae. *Phytopathology* 107, 504–518. doi: 10.1094/PHYTO-12-16-0435-RVW

Fontana, D. C., de Paula, S., Torres, A. G., Moura, V. H., de Souza, S., Pascholati, F., et al. (2021). Endophytic fungi: biological control and induced resistance to phytopathogens and abiotic stresses. *Pathogens* 10:570. doi: 10.3390/pathogens10050570

Franco-Orozco, B., Berepiki, A., Ruiz, O., Gamble, L., Griffe, L. L., Wang, S., et al. (2017). A new proteinaceous pathogen-associated molecular pattern (PAMP) identified in ascomycete fungi induces cell death in solanaceae. *New Phytol.* 214, 1657–1672. doi: 10.1111/nph.14542

Gao, F.-K., Dai, C.-C., and Liu, X.-Z. (2010). Mechanisms of fungal endophytes in plant protection against pathogens. *Afr. J. Microbiol. Res.* 4, 1346–1351.

Gautam, Ajay Kumar, and Avasthi, Shubhi. (2019). "Fungal endophytes: potential biocontrol agents in agriculture." Role of plant growth promoting microorganisms in sustainable agriculture and nanotechnology, January, 241–283.

Ghozlan, M. H., EL-Argawy, E., Tokgöz, S., Lakshman, D. K., Mitra, A., Ghozlan, M. H., et al. (2020). Plant defense against necrotrophic pathogens. *Am. J. Plant Sci.* 11, 2122–2138. doi: 10.4236/ajps.2020.1112149

Glick, B. R., and Bashan, Y. (1997). Genetic manipulation of plant growth-promoting bacteria to enhance biocontrol of phytopathogens. *Biotechnol. Adv.* 15, 353–378. doi: 10.1016/S0734-9750(97)00004-9

Glick, Bernard R., Cheng, Zhenyu, Czarny, Jennifer, and Duan, Jin. (2007). "Promotion of plant growth by ACC deaminase-producing soil bacteria." New perspectives and approaches in plant growth-promoting rhizobacteria research, 329–339.

Gouda, S., Das, G., Sen, S. K., Shin, H. S., and Patra, J. K. (2016). Endophytes: a treasure house of bioactive compounds of medicinal importance. *Front. Microbiol.* 7:219261. doi: 10.3389/FMICB.2016.01538/BIBTEX

Grabka, R., D'entremont, T. W., Adams, S. J., Walker, A. K., Tanney, J. B., Abbasi, P. A., et al. (2022). Fungal endophytes and their role in agricultural plant protection against pests and pathogens. *Plan. Theory* 11:384. doi: 10.3390/plants11030384

Gravel, V., Antoun, H., and Tweddell, R. J. (2007). Growth stimulation and fruit yield improvement of greenhouse tomato plants by inoculation with *Pseudomonas Putida* or *Trichoderma atroviride*: possible role of indole acetic acid (IAA). *Soil Biol. Biochem.* 39, 1968–1977. doi: 10.1016/j.soilbio.2007.02.015

Haran, S., Schickler, H., and Warburg, O. (1996). Molecular mechanisms of lytic enzymes involved in the biocontrol activity of 1 Trichoderma Harzianum R-hydrolytic enzymes of *Trichoderma harzianum* involved in mycoparasitism. *Microbiology* 142. Baker, 2321–2331. doi: 10.1099/00221287-142-9-2321

Hassan, S. E. D. (2017). Plant growth-promoting activities for bacterial and fungal endophytes isolated from medicinal Plant of *Teucrium polium* L. *J. Adv. Res.* 8, 687–695. doi: 10.1016/j.jare.2017.09.001

Haselwandter, K., Passler, V., Reiter, S., Schmid, D. G., Nicholson, G., Hentschel, P., et al. (2006). Basidiochrome - a novel siderophore of the orchidaceous mycorrhizal fungi *Ceratobasidium* and *Rhizoctonia* Spp. *Biometals* 19, 335–343. doi: 10.1007/s10534-006-6986-x

Heymann, P., Gerads, M., Schaller, M., Dromer, F., Winkelmann, G., and Ernst, J. F. (2002). The siderophore Iron transporter of *Candida Albicans* (Sit1p/Arn1p) mediates uptake of ferrichrome-type siderophores and is required for epithelial invasion. *Infect. Immun.* 70, 5246–5255. doi: 10.1128/IAI.70.9.5246-5255.2002

Hissen, A. H. T., Chow, J. M. T., Pinto, L. J., and Moore, M. M. (2004). Survival of *Aspergillus Fumigatus* in serum involves removal of Iron from transferrin: the role of siderophores. *Infect. Immun.* 72, 1402–1408. doi: 10.1128/IAI.72.3.1402-1408.2004

Honma, M., and Smmomura, T. (1978). Metabolism of 1-Aminocyclopropane-1-carboxylic acid. *Agric. Biol. Chem.* 42, 1825–1831. doi: 10.1080/00021369.1978.10863261

Hontzeas, N., Zoidakis, J., Glick, B. R., and Abu-Omar, M. M. (2004). Expression and characterization of 1-aminocyclopropane-1-carboxylate deaminase from the rhizobacterium *Pseudomonas Putida* UW4: a key enzyme in bacterial plant growth promotion. *Biochim. Biophysica Acta Prot. Proteomics* 1703, 11–19. doi: 10.1016/j.bbapap.2004.09.015

Howell, C. R. (2003). Mechanisms employed by *Trichoderma* species in the biological control of plant diseases: the history and evolution of current concepts. *Plant Dis.* 87, 4–10. doi: 10.1094/PDIS.2003.87.1.4

Husen, E., Wahyudi, A. T., Suwanto, A., and Saraswati, R. (2008). Prospective use of 1-aminocyclopropane-1-carboxylate deaminase-producing bacteria for plant growth promotion and defense against biotic and abiotic stresses in peat-soil-agriculture. *Microbiol Indonesia* 2:2. doi: 10.5454/MI.2.3.2

Jia, M., Chen, L., Xin, H. L., Zheng, C. J., Rahman, K., Han, T., et al. (2016). A friendly relationship between endophytic fungi and medicinal plants: a systematic review. *Front. Microbiol.* 7:179220. doi: 10.3389/FMICB.2016.00906/BIBTEX

Johan, P. D., Ahmed, O. H., Omar, L., and Hasbullah, N. A. (2021). Phosphorus transformation in soils following co-application of charcoal and wood ash. *Agronomy* 11:2010. doi: 10.3390/agronomy11102010

Johnson, L. (2008). Iron and Siderophores in fungal–host interactions. *Mycol. Res.* 112, 170–183. doi: 10.1016/j.mycres.2007.11.012

Kaddes, A., Fauconnier, M.-L., Sassi, K., Nasraoui, B., and Jijakli, M.-H. (2019). Endophytic fungal volatile compounds as solution for sustainable agriculture. *Molecules* 24:1065. doi: 10.3390/molecules24061065

Kamana, S., Hemalatha, K., Chandanavineela, K., Kalyani, P., and Hemalatha, V. (2016). Endophytic fungi: as source of bioactive compound. *World J. Pharm. Pharm. Sci.* 5, 1026–1040.

Khan, R., Mujeebur, Z. H., Ahamad, F., and Haniph Shah, M. (2023). "Nematode problems in Rice and their sustainable management" in *Nematode diseases of crops and their sustainable management*. eds. M. Rahman Khan and M. Quintanilla (Academic Press, Cambridge, Massachusetts, United States: Elsevier), 133–166.

Kilani-Morakchi, S., Morakchi-Goudjil, H., and Sifi, K. (2021). Azadirachtin-based insecticide: overview, risk assessments, and future directions. *Front Agron.* 3:676208. doi: 10.3389/fagro.2021.676208

Killham, K. (1994). *Soil ecology*. Oxford Academic, Oxford, United Kingdom: Cambridge University Press.

Kiraly, L., Barna, B., and Király, Z. (2007). Plant resistance to pathogen infection: forms and mechanisms of innate and acquired resistance. *J. Phytopathol.* 155, 385–396.

Köhl, J., Kolnaar, R., and Ravensberg, W. J. (2019). Mode of action of microbial biological control agents against plant diseases: relevance beyond efficacy. *Front. Plant Sci.* 10:454982. doi: 10.3389/FPLS.2019.00845/BIBTEX

Korat, K., Dave, B. P., and Dube, H. C. (2001). Detection and chemical characterization of siderophores produced by certain fungi. *Indian J. Microbiol.* 41, 87–92.

Kumar, Ajay, Zhimo, Yeka, Biasi, Antonio, Salim, Shoshana, Feygenberg, Oleg, Wisniewski, Michael, et al. (2021). "Endophytic microbiome in the Carposphere and its importance in fruit physiology and pathology." 73–88.

Kumari, N., and Srividhya, S. (2020). "Secondary metabolites and lytic tool box of Trichoderma and their role in plant health" in *Molecular aspects of plant beneficial microbes in agriculture*. eds. V. Sharma, R. Salwan and L. K. Tawfeeq Al-Ani (Amsterdam: Elsevier), 305–320.

Kushwaha, P., Kashyap, P. L., Bhardwaj, A. K., Kuppusamy, P., Srivastava, A. K., and Tiwari, R. K. (2020). Bacterial endophyte mediated plant tolerance to salinity: growth responses and mechanisms of action. *World J. Microbiol. Biotechnol.* 36, 1–16. doi: 10.1007/S11274-020-2804-9/FIGURES/2

Lahlali, R., Ezrari, S., Radouane, N., Kenfaoui, J., Esmaeel, Q., El Hamss, H., et al. (2022). Biological control of plant pathogens: a global perspective. *Microorganisms*. MDPI 10:596. doi: 10.3390/microorganisms10030596

Landum, M. C., do Rosário Félix, M., Alho, J., Garcia, R., Cabrita, M. J., Rei, F., et al. (2016). Antagonistic activity of fungi of *Olea Europaea* L. against *Colletotrichum acutatum*. *Microbiol. Res.* 183, 100–108. doi: 10.1016/J.MICRES.2015.12.001

Latz, M. A. C., Jensen, B., Collinge, D. B., and Jørgensen, H. J. L. (2018). Endophytic fungi as biocontrol agents: elucidating mechanisms in disease suppression. *Plant Eco. Diversity* 11, 555–567. doi: 10.1080/17550874.2018.1534146

Lechenet, M., Dessaint, F., Py, G., Makowski, D., and Munier-Jolain, N. (2017). Reducing pesticide use while preserving crop productivity and profitability on arable farms. *Nat. Plants* 3, 1–6. doi: 10.1038/nplants.2017.8

Lee, H. Y., Chen, Y. C., Kieber, J. J., and Yoon, G. M. (2017). Regulation of the turnover of ACC synthases by phytohormones and heterodimerization in *Arabidopsis*. *Plant J.* 91, 491–504. doi: 10.1111/tpj.13585

Lee, B. N., Kroken, S., Chou, D. Y. T., Barbara Robbertse, O. C., Yoder, , and Turgeon, G. (2005). Functional analysis of all nonribosomal peptide synthetases in cochliobolus heterostrophus reveals a factor, NPS6, involved in virulence and resistance to oxidative stress. *Eukaryot. Cell* 4, 545–555. doi: 10.1128/EC.4.3.545-555.2005

Li, N., Han, X., Feng, D., Yuan, D., and Huang, L. J. (2019). Signaling crosstalk between salicylic acid and ethylene/jasmonate in plant defense: do we understand what they are whispering? *Int. J. Mol. Sci.* 20:671. doi: 10.3390/ijms20030671

Liu, Y., Bai, F., Li, T., and Yan, H. (2018). An endophytic strain of genus Paenibacillus isolated from the fruits of noni (*Morinda Citrifolia* L.) has antagonistic activity against a Noni's pathogenic strain of genus aspergillus. *Microb. Pathog.* 125, 158–163. doi: 10.1016/J.MICPATH.2018.09.018

Lo, C-T, Nelson, E. B., and Harman, G. E. (2015). Improved biocontrol efficacy of Trichoderma harzianum 1295-22 for foliar phases of turf diseases by use of spray applications. *Plant Dis.* 81, 1132–1138.

Loper, J. E., and Buyer, J. S. (1991). Siderophores in microbial interactions on plant surfaces. *Mol. Plant-Microbe Interact.* 4, 5–13. doi: 10.1094/MPMI-4-005

Ludwig-Müller, J. (2015). Plants and endophytes: equal Partners in secondary metabolite production? *Biotechnol. Lett.* 37, 1325–1334. doi: 10.1007/s10529-015-1814-4

Lugtenberg, B. J. J., Caradus, J. R., and Johnson, L. J. (2016). Fungal endophytes for sustainable crop production. *FEMS Microbiol. Ecol.* 92:fiw194. doi: 10.1093/femsec/fiw194

Macías-Rubalcava, M. L., and Garrido-Santos, M. Y. (2022). Phytotoxic compounds from endophytic fungi. *Appl. Microbiol. Biotechnol.* 106, 931–950. doi: 10.1007/s00253-022-11773-w

Martin, M. N., Cohen, J. D., and Saftner, R. A. (1995). A new 1-aminocyclopropane-1-carboxylic acid-conjugating activity in tomato fruit. *Plant Physiol.* 109, 917–926. doi: 10.1104/pp.109.3.917

Matzanke, B. F., Bill, E., Trautwein, A. X., and Winkelmann, G. (1987). Role of siderophores in Iron storage in spores of *Neurospora crassa* and *Aspergillus ochraceus*. *J. Bacteriol.* 169, 5873–5876. doi: 10.1128/jb.169.12.5873-5876.1987

McMorran, B. J., Shantha Kumara, H. M. C., Sullivan, K., and Lamont, I. L. (2001). Involvement of a transformylase enzyme in siderophore synthesis in *Pseudomonas Aeruginosa*. *Microbiology* 147, 1517–1524. doi: 10.1099/00221287-147-6-1517

McNeely, D., Chanyi, R. M., Dooley, J. S., Moore, J. E., and Koval, S. F. (2017). Biocontrol of Burkholderia cepacia complex bacteria and bacterial phytopathogens by Bdellovibrio bacteriovorus. *Can. J. Microbiol.* 63, 350–358.

Mejía, L. C., Rojas, E. I., Maynard, Z., Sunshine Van Bael, A., Arnold, E., Hebbar, P., et al. (2008). Endophytic fungi as biocontrol agents of *Theobroma Cacao* pathogens. *Biol. Control* 46, 4–14. doi: 10.1016/j.biocontrol.2008.01.012

Molinari, S., and Leonetti, P. (2019). Bio-control agents activate plant immune response and prime susceptible tomato against root-knot nematodes. *PLoS One* 14:e0213230. doi: 10.1371/journal.pone.0213230

Morandi, M. A. B., Sutton, J. C., and Maffia, L. A. (2000). Effects of host and microbial factors on development of *Clonostachys rosea* and control of *Botrytis cinerea* in rose. *Eur. J. Plant Pathol.* 106, 439–448. doi: 10.1023/A:1008738513748

Naik, B. S. (2018). Volatile hydrocarbons from endophytic fungi and their efficacy in fuel production and disease control. *Egyp. J. Biol. Pest Control* 28:69. doi: 10.1186/s41938-018-0072-x

Nascimento, F. X., Rossi, M. J., Soares, C. R. F. S., McConkey, B. J., and Glick, B. R. (2014). New insights into 1-aminocyclopropane-1-carboxylate (ACC) deaminase phylogeny, evolution and ecological significance. *PLoS One* 9:e99168. doi: 10.1371/JOURNAL.PONE.0099168

Neilands, J B, Konopka, K, Schwyn, B, Coy, M, Francis, R T, Paw, B H, et al. (1987). "*Comparative biochemistry of microbial Iron assimilation, Iron transport in microbes, plants and animals* (G. Winkelmann, HelmD. van Der and JB Neilands, Eds.)." VCH, Weinheim, Germany.

Nguyen, H. T., Kim, S., Yu, N. H., Park, A. R., Yoon, H., Bae, C. H., et al. (2019). Antimicrobial activities of an oxygenated cyclohexanone derivative isolated from *Amphirosellinia nigrospora* JS-1675 against various plant pathogenic bacteria and fungi. *J. Appl. Microbiol.* 126, 894–904. doi: 10.1111/jam.14138

O'Sullivan, D. J., and O'Gara, F. (1992). Traits of fluorescent *Pseudomonas* Spp. involved in suppression of plant root pathogens. *Microbiol. Rev.* 56, 662–676. doi: 10.1128/mr.56.4.662-676.1992

Ogórek, R., Przywara, K., Piecuch, A., Cal, M., Lejman, A., and Matkowski, K. (2020). Plant–fungal interactions: a case study of Epicoccoum Nigrum link. *Plan. Theory* 9:1691. doi: 10.3390/plants9121691

Oide, S., Krasnoff, S. B., Gibson, D. M., and Gillian Turgeon, B. (2007). Intracellular Siderophores are essential for ascomycete sexual development in heterothallic *Cochliobolus heterostrophus* and homothallic *Gibberella zeae*. *Eukaryot. Cell* 6, 1339–1353. doi: 10.1128/EC.00111-07

Oide, S., Moeder, W., Krasnoff, S., Gibson, D., Haas, H., Yoshioka, K., et al. (2006). NPS6, encoding a nonribosomal peptide synthetase involved in siderophore-mediated iron metabolism, is a conserved virulence determinant of plant pathogenic. *Plant Cell* 18, 2836–2853. doi: 10.1105/tpc.106.045633

Oszust, K., Cybulska, J., and Frąc, M. (2020). How do Trichoderma genus Fungi Win a nutritional competition battle against soft fruit pathogens? A report on niche overlap nutritional potentiates. *Int. J. Mol. Sci.* 21:4235. doi: 10.3390/ijms21124235

Pal, K. K., and Gardener, B McSpadden. (2006). "Biological control of plant pathogens." The Plant Health Instructor.

Palanichamy, P., Krishnamoorthy, G., Kannan, S., and Marudhamuthu, M. (2018). Bioactive potential of secondary metabolites derived from medicinal plant endophytes. *Egyp. J. Basic Appl. Sci.* 5, 303–312. doi: 10.1016/J.EJBAS.2018.07.002

Panda, K., and Sujogya. (2013). Endophytic fungi with great promises: a review bio-prospecting of wild mushrooms view project insights into new strategies to combat biofilms view project. *J. Adv. Pharm. Educ. Res.* 3, 152–170.

Parker, M. A. (1995). Plant fitness variation caused by different mutualist genotypes. *Ecology* 76, 1525–1535. doi: 10.2307/1938154

Payment, P., Berte, A., Prévost, M., Ménard, B., and Barbeau, B. (2011). Occurrence of pathogenic microorganisms in the Saint Lawrence River (Canada) and comparison of health risks for populations using it as their source of drinking water. *Can. J. Microbiol.* 46, 565–576. doi: 10.1139/W00-022

Plaszkó, T., Szűcs, Z., Kállai, Z., Csoma, H., Vasas, G., and Gonda, S. (2020). Volatile organic compounds (VOCs) of endophytic Fungi growing on extracts of the host, horseradish (*Armoracia Rusticana*). *Meta* 10:451. doi: 10.3390/metabo10110451

Rahman, S. A., Farhana, S., Singh, E., Pieterse, C. M. J., and Schenk, P. M. (2018). Emerging microbial biocontrol strategies for plant pathogens. *Plant Sci.* 267, 102–111. doi: 10.1016/J.PLANTSCI.2017.11.012

Rajesh, R. W., Shelake Rahul, M., and Ambalal, N. S. (2016). Trichoderma: a significant fungus for agriculture and environment. *Afr. J. Agric. Res.* 11, 1952–1965. doi: 10.5897/AJAR2015.10584

Rani, R., Sharma, D., Chaturvedi, M., and Yadav, J. P. (2017). Antibacterial activity of twenty different endophytic fungi isolated from *Calotropis procera* and time kill assay. *Clin. Microbiol. Open Access*. 6:1000280. doi: 10.4172/2327-5073.1000280

Rashad, Y., Aseel, D., and Hammad, S. (2020). Phenolic compounds against fungal and viral plant diseases. *Plant Phenolics Sustain. Agric.* 1, 201–219. doi: 10.1007/978-981-15-4890-1_9

Raymaekers, K., Ponet, L., Holtappels, D., Berckmans, B., and Cammue, B. P. A. (2020). Screening for novel biocontrol agents applicable in plant disease management – a review. *Biol. Control* 144:104240. doi: 10.1016/J.BIOCONTROL.2020.104240

Reddy, S. G. E. (2020). *Lecanicillium Spp. for the management of aphids, whiteflies, thrips, scales and mealy bugs*. London, UK: IntechOpen.

Ren, C. G., and Dai, C. C. (2012). Jasmonic acid is involved in the signaling pathway for fungal endophyte-induced volatile oil accumulation of *Atractylodes lancea* plantlets. *BMC Plant Biol.* 12, 1–11. doi: 10.1186/1471-2229-12-128/FIGURES/5

Sahu, P. K., and Mishra, S. (2021). Effect of hybridization on endophytes: the Endo-microbiome dynamics. *Symbiosis* 84, 369–377. doi: 10.1007/s13199-021-00760-w

Sahu, G. K., and Sindhu, S. S. (2011). Disease control and plant growth promotion of green gram by siderophore producing *Pseudomonas* Sp. *Res. J. Microbiol.* 6, 735–749. doi: 10.3923/jm.2011.735.749

Saikkonen, K. (2007). Forest structure and fungal endophytes. *Fungal Biol. Rev.* 21, 67–74. doi: 10.1016/j.fbr.2007.05.001

Saikkonen, K., Wäli, P., Helander, M., and Faeth, S. H. (2004). Evolution of endophyte-plant symbioses. *Trends Plant Sci.* 9, 275–280. doi: 10.1016/j.tplants.2004.04.005

Santos, C. M. D., Ribeiro, A. D. S., Garcia, A., Polli, A. D., Polonio, J. C., Azevedo, J. L., et al. (2019). Enzymatic and antagonist activity of endophytic fungi from *Sapindus Saponaria* L. (sapindaceae). *Acta Biol. Colombiana* 24, 322–330. doi: 10.15446/abc.v24n2.74717

Santra, H. K., and Banerjee, D. (2023). Antifungal activity of volatile and non-volatile metabolites of endophytes of Chloranthus Elatior sw. *Front. Plant Sci.* 14:1156323. doi: 10.3389/fpls.2023.1156323

Savary, S., Willocquet, L., Pethybridge, S. J., Esker, P., Mcroberts, N., and Nelson, A. (2019). The global burden of pathogens and pests on major food crops. *Nature* 3, 430–439. doi: 10.1038/s41559-018-0793-y

Saxena, S., Meshram, V., and Kapoor, N. (2015). Muscodor Tigerii Sp. Nov.-volatile antibiotic producing endophytic fungus from the northeastern Himalayas. *Ann. Microbiol.* 65, 47–57. doi: 10.1007/s13213-014-0834-y

Sayyed, R. Z., Chincholkar, S. B., Reddy, M. S., Gangurde, N. S., and Patel, P. R. (2013). "Siderophore producing PGPR for crop nutrition and Phytopathogen suppression" in *Bacteria in agrobiology: Disease management*. ed. D. K. Maheshweri (Berlin, Heidelberg: Springer Berlin Heidelberg), 449–471.

Schippers, B., Bakker, A. W., and Bakker, P. A. H. M. (2003). Interactions of deleterious and beneficial rhizosphere microorganisms and the effect of cropping practices. *Ann. Rev.* 25, 339–358. doi: 10.1146/ANNUREV.PY.25.090187.002011

Schrettl, M., Bignell, E., Kragl, C., Sabiha, Y., Loss, O., Eisendle, M., et al. (2007). Distinct roles for intra- and extracellular Siderophores during *Aspergillus Fumigatus* infection. *PLoS Pathog.* 3:e128. doi: 10.1371/journal.ppat.0030128

Sefloo, G., Negar, S. S., and Hage-Ahmed, K. (2021). The bioprotective effect of root endophytic Serendipita Herbamans against fusarium wilt in tomato and its impact on root traits are determined by temperature. *Rhizosphere* 20:100453. doi: 10.1016/J.RHISPH.2021.100453

Selim, K. A., Elkhateeb, W. A., Tawila, A. M., El-Beih, A. A., Abdel-Rahman, T. M., El-Diwany, A. I., et al. (2018). Antiviral and antioxidant potential of fungal endophytes of Egyptian medicinal plants. *Fermentation* 4:49. doi: 10.3390/fermentation4030049

Sharma, S. B., Sayyed, R. Z., Trivedi, M. H., and Gobi, T. A. (2013). Phosphate solubilizing microbes: sustainable approach for managing phosphorus deficiency in agricultural soils. *Springerplus* 2, 1–14. doi: 10.1186/2193-1801-2-587/FIGURES/3

Sharma, Pooja, and Singh, Surendra Pratap. (2021). "Role of the endogenous fungal metabolites in the plant growth improvement and stress tolerance." Fungi bio-prospects in sustainable agriculture, environment and nano-technology: volume 3: fungal metabolites, functional genomics and nano-technology, January, 381–401.

Shi, X., Qin, T., Liu, H., Wu, M., Li, J., Shi, Y., et al. (2020). Endophytic fungi activated similar defense strategies of *Achnatherum sibiricum* host to different trophic types of pathogens. *Front. Microbiol.* 11:1607. doi: 10.3389/fmicb.2020.01607

Shukla, S. T., Habbu, P. V., Kulkarni, V. H., Jagadish, K. S., Pandey, A. R., and Sutariya, V. N. (2014). Endophytic microbes: a novel source for biologically/pharmacologically active secondary metabolites. *Asian J. Pharmacol. Toxicol.* 2, 1–16.

Sikora, R. A., Schäfer, K., and Dababat, A. A. (2007). Modes of action associated with microbially induced in planta suppression of plant-parasitic nematodes. *Australas. Plant Pathol.* 36, 124–134. doi: 10.1071/AP07008

Silva, M. G., Santana, J., de Curcio, M., Silva-Bailão, G., Lima, R. M., Tomazett, M. V., et al. (2020). Molecular characterization of siderophore biosynthesis in Paracoccidioides Brasiliensis. *IMA Fungus* 11:11. doi: 10.1186/s43008-020-00035-x

Sindhu, S S, Suneja, S, and Dadarwal, K R. (1997). "Plant growth promoting rhizobacteria and their role in improving crop productivity." Biotechnological approaches in soil microorganisms for sustainable crop production. 149–191.

Singh, V. K., and Kumar, A. (2023). Secondary metabolites from endophytic fungi: production, methods of analysis, and diverse pharmaceutical potential. *Symbiosis* 90, 111–125. doi: 10.1007/s13199-023-00925-9

Song, H. C., Qin, D., Liu, H. Y., Dong, J. Y., You, C., and Wang, Y. M. (2021). Resorcylic acid lactones produced by an endophytic *Penicillium ochrochloron* strain from Kadsura Angustifolia. *Planta Med.* 87, 225–235. doi: 10.1055/a-1326-2600

Sood, M., Kapoor, D., Kumar, V., Sheteiwy, M. S., Ramakrishnan, M., Landi, M., et al. (2020). Trichoderma: the 'secrets' of a multitalented biocontrol agent. *Plan. Theory* 9:762. doi: 10.3390/plants9060762

Staswick, P. E., and Tiryaki, I. (2004). The Oxylipin signal Jasmonic acid is activated by an enzyme that conjugates it to isoleucine in Arabidopsis. *Plant Cell* 16, 2117–2127. doi: 10.1105/tpc.104.023549

Stoytcheva, M. (2011). *Pesticides in the modern world: Pesticides use and management*. London, UK: BoD–Books on Demand.

Talbot, N. J. (2015). Plant immunity: a little help from fungal friends. *Curr. Biol.* 25, R1074–R1076. doi: 10.1016/j.cub.2015.09.068

Tena, G. (2018). Recruiting microbial bodyguards. *Nat. Plants* 4:857. doi: 10.1038/s41477-018-0308-5

Tripathi, S., Kamal, S., Sheramati, I., Oelmuller, R., and Varma, A. (2008). "Mycorrhizal Fungi and other root endophytes as biocontrol agents against root pathogens" in *Mycorrhiza: state of the art, genetics and molecular biology, eco-function, biotechnology, eco-physiology, structure and systematics (third edition)*. ed. A. Varma (Berlin, Heidelberg: Springer), 281–306.

Trivedi, P., Leach, J. E., Tringe, S. G., Sa, T., and Singh, B. K. (2020). Plant–microbiome interactions: from community assembly to plant health. *Nat. Rev. Microbiol.* 18, 607–621. doi: 10.1038/s41579-020-0412-1

Tyśkiewicz, R., Nowak, A., Ozimek, E., and Jaroszuk-Ściseł, J. (2022). 'Trichoderma: the current status of its application in agriculture for the biocontrol of fungal phytopathogens and stimulation of plant growth', *J. Mol. Sci.* 23:2329. doi: 10.3390/IJMS23042329

Ullah, A., Nisar, M., Ali, H., Hazrat, A., Hayat, K., Keerio, A. A., et al. (2019). Drought tolerance improvement in plants: an endophytic bacterial approach. *Appl. Microbiol. Biotechnol.* 103, 7385–7397. doi: 10.1007/S00253-019-10045-4

Van de Poel, B., Smet, D., and Van Der Straeten, D. (2015). Ethylene and hormonal cross talk in vegetative growth and development. *Plant Physiol.* 169, 61–72. doi: 10.1104/pp.15.00724

Van Loon, L. C., Bakker, P. A. H. M., and Pieterse, C. M. J. (1998). "Systemic resistance induced by rhizosphere bacteria." *Annu. Rev. Phytopathol.* 36, 453–483. doi: 10.1146/annurev.phyto.36.1.453

Vishwas, Mohite Bhavana. (2011). "A review: Natural products from plant associated endophytic Fungi wound healing agents of plant origin view project Nephroprotective plants view project." Available at: https://www.researchgate.net/publication/258884981.

Waghunde, Rajesh Ramdas, Shelake, Rahul Mahadev, Shinde, Manisha S., and Hayashi, Hidenori. (2017). "Endophyte microbes: a weapon for plant health management." 303–25.

Wang, G., Liu, Z., Lin, R., Li, E, Mao, Z., Ling, J., et al. (2016). Biosynthesis of antibiotic leucinostatins in bio-control fungus purpureocillium lilacinum and their inhibition on phytophthora revealed by genome mining. *PLOS Pathogens.* 12:e1005685. doi: 10.1371/journal.ppat.1005685

Wang, Y. J., Deering, A. J., and Kim, H. J. (2021). Effects of plant age and root damage on internalization of Shiga toxin-producing *Escherichia coli* in leafy vegetables and herbs. *Horticulturae* 7:68. doi: 10.3390/horticulturae7040068

Wang, Y., Pruitt, R. N., Nürnberger, T., and Wang, Y. (2022). Evasion of plant immunity by microbial pathogens. *Nat. Rev. Microbiol.* 20, 449–464. doi: 10.1038/s41579-022-00710-3

Wen, J., Okyere, S. K., Wang, J., Huang, R., Wang, Y., Liu, L., et al. (2023). Endophytic Fungi isolated from *Ageratina Adenophora* exhibits potential antimicrobial activity against multidrug-resistant *Staphylococcus Aureus*. *Plan. Theory* 12:650. doi: 10.3390/plants12030650

White, J. F., and Torres, M. S. (2010). Is plant endophyte-mediated defensive mutualism the result of oxidative stress protection? *Physiol. Plant.* 138, 440–446. doi: 10.1111/j.1399-3054.2009.01332.x

Wicklow, D. T., and Poling, S. M. (2008). Antimicrobial activity of Pyrrocidines from Acremonium Zeae against endophytes and pathogens of maize. *Phytopathology* 99, 109–115. doi: 10.1094/PHYTO-99-1-0109

Wilson, A., Cuddy, W. S., Park, R. F., Harm, G. F. S., Priest, M. J., Bailey, J., et al. (2020). Investigating Hyperparasites as potential biological control agents of rust pathogens on cereal crops. *Australas. Plant Pathol.* 49, 231–238. doi: 10.1007/s13313-020-00695-8

Win, T. T., Bo, B., Malec, P., Khan, S., and Pengcheng, F. (2021). Newly isolated strain of trichoderma asperellum from disease suppressive soil is a potential bio-control agent to suppress fusarium soil borne fungal phytopathogens. *J. Plant Pathol.* 103, 549–561. doi: 10.1007/s42161-021-00780-x

Winkelmann, G., and Drechsel, H. (2008). "Microbial Siderophores" in *Biotechnology, second, completely revised edition, volume 7: Products of secondary metabolism*. eds. H. J. Rehm and G. Reed (Hoboken, New Jersey, United States: Wiley), 199–246.

Wu, W., Chen, W., Liu, S., Jianjun, W., Zhu, Y., Qin, L., et al. (2021). Beneficial relationships between endophytic Bacteria and medicinal plants. *Front. Plant Sci.* 12:646146. doi: 10.3389/FPLS.2021.646146/BIBTEX

Wu, Y. Y., Zhang, T. Y., Zhang, M. Y., Cheng, J., and Zhang, Y. X. (2018). An endophytic Fungi of *Ginkgo Biloba* L. produces antimicrobial metabolites as potential inhibitors of FtsZ of *Staphylococcus Aureus*. *Fitoterapia* 128, 265–271. doi: 10.1016/J.FITOTE.2018.05.033

Xia, Y., Liu, J., Chen, C., Mo, X., Tan, Q., He, Y., et al. (2022). The multifunctions and future prospects of endophytes and their metabolites in plant disease management. *Microorganisms* 10:1072. doi: 10.3390/microorganisms10051072

Xie, J., Ying Ying, W., Zhang, T. Y., Zhang, M. Y., Peng, F., Lin, B., et al. (2018). New antimicrobial compounds produced by endophytic Penicillium Janthinellum isolated from Panax Notoginseng as potential inhibitors of FtsZ. *Fitoterapia* 131, 35–43. doi: 10.1016/J.FITOTE.2018.10.006

Yao, X., Guo, H., Zhang, K., Zhao, M., Ruan, J., and Chen, J. (2023). Trichoderma and its role in biological control of plant fungal and nematode disease. *Front. Microbiol.* 14:1160551. doi: 10.3389/fmicb.2023.1160551

Youssef, K., Ippolito, A., and Roberto, S. R. (2022). Editorial: post-harvest diseases of fruit and vegetable: methods and mechanisms of action. *Front. Microbiol.* 13:900060. doi: 10.3389/fmicb.2022.900060

Yu, X., Ai, C., Xin, L., and Zhou, G. (2011). The Siderophore-producing bacterium, *Bacillus Subtilis* CAS15, has a biocontrol effect on fusarium wilt and promotes the growth of pepper. *Eur. J. Soil Biol.* 47, 138–145. doi: 10.1016/j.ejsobi.2010.11.001

Yu, J., Ying, W., He, Z., Li, M., Zhu, K., and Gao, B. (2018). Diversity and antifungal activity of endophytic fungi associated with *Camellia oleifera* 46, 85–91. doi: 10.1080/12298093.2018.1454008,

Yuan, W. M., Gentil, G. D., Budde, A. D., and Leong, S. A. (2001). Characterization of the *Ustilago Maydis* Sid2 gene, encoding a multidomain peptide Synthetase in the Ferrichrome biosynthetic gene cluster. *J. Bacteriol.* 183, 4040–4051. doi: 10.1128/JB.183.13.4040-4051.2001

Zhang, L., Zhang, W., Li, Q., Cui, R., Wang, Z., Yao Wang, Y., et al. (2020). Deciphering the root Endosphere microbiome of the desert plant Alhagi Sparsifolia for drought resistance-promoting Bacteria. *Appl. Environ. Microbiol.* 86:e02863-19. doi: 10.1128/AEM.02863-19

Frontiers in Microbiology

Explores the habitable world and the potential of microbial life

The largest and most cited microbiology journal which advances our understanding of the role microbes play in addressing global challenges such as healthcare, food security, and climate change.

Discover the latest Research Topics

See more →

Frontiers

Avenue du Tribunal-Fédéral 34
1005 Lausanne, Switzerland
frontiersin.org

Contact us

+41 (0)21 510 17 00
frontiersin.org/about/contact